



UNIVERSITÀ
DEGLI STUDI
DI PADOVA

Università degli Studi di Padova

Department of Industrial Engineering

Ph.D. COURSE IN: Industrial Engineering

CURRICULUM: Chemical and Environmental Engineering

SERIES: XXXII

**NOVEL EXPERIMENTAL AND MODELLING APPROACHES FOR THE RISK
ASSESSMENT OF PERFLUOROALKYL ACIDS (PFAAs)**

Thesis written with the financial contribution of the Fondazione Cariparo.

Coordinator: Prof. Paolo Colombo

Supervisor: Prof. Luca Palmeri

Co-Supervisor: Dr. Alberto Barausse

Ph.D. student: Andrea Gredelj

Summary

Per- and polyfluoroalkyl substances (PFASs) are a group of anthropogenic chemicals, widely used for many industrial and commercial purposes. The extremely strong C-F bond provides PFASs with high chemical and thermal stability. Consequently, PFASs are persistent, bioaccumulative and ubiquitously present in environmental matrices worldwide. Under environmental conditions, through changes of the non-fluorinated parts of a molecule, PFAS precursors can be transformed into perfluoroalkyl acids (PFAAs), regarded as their final transformation product. PFAAs are acidic surfactants, whose properties principally differ depending on their perfluoroalkyl chain length and their terminal polar group. Short-chain PFAAs are widely employed as alternatives for the regulated and restricted long-chain PFAAs, based on the assumption of lower bioaccumulation potential and toxicity in animals. However, they are as persistent as their long-chain homologues, highly soluble, less sorptive to solids, very mobile with water and highly bioaccumulative in plants.

The aim of this research thesis is addressing the data and research gaps to assist ecological and human health risk assessment of the perfluoroalkyl acids, with a special focus on their short-chain alternatives. PFAAs exhibit an untypical behavior when compared to other groups of neutral organic pollutants. Their affinity for proteins and phospholipid membranes makes the common risk assessment approaches, mainly relying on the partitioning in storage lipids, inapplicable. Hence, the objectives of this thesis were to address data gaps and provide new insights regarding the fate and behavior of PFAAs, from 1) the ecological risk assessment point of view and 2) in terrestrial (agronomic) ecosystems, as the main pathway of PFAAs into the terrestrial food webs. An additional focus was put on the major PFAS contamination case in the Veneto Region, Northern Italy.

The first part of the thesis concentrates on existing ecological risk assessment methodologies and proposes a new method for deriving the ecological risk thresholds of micro-contaminants, which is applied to two legacy long-chain PFAAs, PFOA and PFOS, two short chain PFAAs, PFBA and PFBS, as their common substitutes, and two well studied emerging contaminants (LAS and triclosan) for comparison. The newly proposed methodology is based on the ecological and chemicals fate model AQUATOX (USEPA), applied to aquatic ecosystem of the Po, the largest Italian river with a significant pollutants burden (including PFAAs). By the use of AQUATOX, ecological relationships between organisms were included as well as the sublethal effects of chemicals, resulting in indirect toxicity effects leading to ecological threshold values that usually differed from the ones derived by regulated methodologies.

The second part of the thesis concentrates on simulating the transfer of nine PFAAs from pre-contaminated soil and irrigation water to a model crop, the red chicory, by a combination of greenhouse plant uptake experiments, laboratory soil-sorption tests and plant uptake models. The experimental set-up includes various exposure media: soil and water, separately and in synergy, as well as a soilless (hydroponic) system. The experimental results emphasized the significance of irrigation water as exposure media, leading to a potentially higher plant uptake of PFAAs, and the uncertainty in the use of hydroponically derived plant uptake factors for risk assessment. The semi-empirical plant uptake model for PFAAs, based on inter-compartmental PFAAs distribution in red chicory, soil-water partitioning and plant-specific measured data was successfully applied to other crops and provided new mechanistic insights into the complex uptake processes. Finally, a modelling framework consisting of crop models connected to simple pharmacokinetic models for farm animals, was developed and applied in the dietary exposure of the Veneto population to long- and short-chain PFAAs.

Sommario

Le sostanze per- e polifluoroalchiliche (PFASs) sono un gruppo di sostanze chimiche antropogeniche, usate estensivamente nell'industria. Grazie al legame C-F molto forte, i PFASs sono caratterizzati da una elevata stabilità chimica e termica. Di conseguenza sono persistenti, bioaccumulativi e onnipresenti nell'ambiente. Sotto condizioni ambientali, tramite il cambiamento delle parti non-fluorurati nelle molecole, i precursori del PFAS si trasformano in acidi perfluoroalchilici (PFAAs). I PFAAs sono acidi tensioattivi e le loro proprietà si differenziano in base alla lunghezza della catena perfluoroalchilica ed al gruppo polare. Le catene corte di PFAAs vengono impiegate al posto delle catene più lunghe con l'assunzione per cui siano potenzialmente meno bioaccumulative e meno tossici negli animali. Tuttavia, esse sono molto persistenti, ed altamente solubili. Inoltre sono meno assorbite nei solidi, molto mobili in acqua ed estremamente bioaccumulative nelle piante.

Lo scopo di questa tesi consiste nell'analisi dei dati per la valutazione del rischio degli PFAAs, con maggior attenzione per le catene più corte. I PFAAs mostrano un comportamento non tipico rispetto ad altri gruppi di inquinanti organici neutri. La loro affinità per le proteine e le membrane fosfolipidi rende la valutazione del rischio convenzionale, basato sulla ripartizione dello stoccaggio nei lipidi, inapplicabile. Perciò, questa tesi focalizzerà l'attenzione sulle mancanze nella ricerca e fornirà nuovi approfondimenti per comprendere il comportamento degli PFAAs, iniziando da 1) la valutazione del rischio dal punto di vista ecologico e 2) nell'ecosistema terrestre, come la via principale dei PFAAs nella rete alimentare terrestre, con un'attenzione particolare sull'inquinamento dei PFAAs nella Regione del Veneto (Nord Italia).

La prima parte della tesi focalizzerà l'attenzione sulle metodologie esistenti per la valutazione del rischio ecologico e proporrà un nuovo metodo per derivare le soglie ecologiche di microinquinanti, applicato per due PFAAs di catene lunghe, PFOA e PFOS, due PFAAs di catene corte, PFBA e PFBS, come i loro sostituti, e due inquinanti emergenti (LAS e triclosan) al fine di eseguire un confronto. La metodologia proposta è basata sul modello ecologico AQUATOX (USEPA), applicato sull'ecosistema acquatico del Po, il fiume italiano più grande e con il maggior inquinamento. Usando il modello AQUATOX, sono state incluse relazioni ecologiche tra gli organismi, così come gli effetti chimici indiretti e sub-letali. I risultati sono valori di soglia ecologica diversi da quelli calcolati usando metodologie convenzionali.

La seconda parte della tesi concentra l'attenzione sulla simulazione del trasferimento di nove tipi di PFAAs da suolo e acqua pre-contaminati alla pianta, radichio, con una combinazione di esperimenti in serra, prove in laboratorio per l'assorbimento del suolo e modelli per l'assorbimento nelle piante. L'esperimento include vari modi di esposizione: acqua e suolo, separatamente e in sinergia, così come un sistema idroponico. I risultati hanno evidenziato la valenza dell'acqua come il metodo di esposizione più importante, ed una incertezza dell'uso dei fattori di bioaccumulazione derivati da esperimenti idroponici per la valutazione del rischio. Il modello semi-empirico dell'assorbimento degli PFAAs, basato sulla distribuzione inter-compartimentale degli PFAAs nel radichio, ripartizione tra acqua e suolo e parametri delle piante, è stato applicato su colture diverse e ha fornito nuovi approfondimenti del processo di assorbimento molto complesso. In fine, un quadro modellistico consistente di modelli di colture, insieme ad un modello farmacocinetico per animali d'allevamento, è stato applicato per valutare l'esposizione della popolazione del Veneto ai PFAAs di catena corta e lunga.

Table of Contents

Summary	I
Sommario	II
Chapter 1	1
1. Introduction and background.....	1
1.1. Aims and scope of the thesis	2
1.2. Background	3
1.2.1. Per- and polyfluoroalkyl substances (PFASs): terminology, applications and main physico-chemical properties.....	3
1.2.2. PFAAs exposure, risks and existing regulations.....	6
1.3. Thesis organization.....	13
1.4. References	16
Chapter 2.....	26
2. Deriving predicted no-effect concentrations (PNECs) for emerging contaminants in the river Po, Italy, using three approaches: assessment factor, species sensitivity distribution and AQUATOX ecosystem modelling	26
2.1. Introduction.....	28
2.2. Materials and Methods.....	30
2.2.1. Study area: the River Po and its biota.....	30
2.2.2. Assessed contaminants	30
2.2.3. Deriving PNECs with Assessment Factors.....	32
2.2.4. Deriving PNECs using Species Sensitivity Distribution	32
2.2.5. Deriving PNECs using AQUATOX	33
2.2.6. Deriving ecologically-safe thresholds using AQUATOX	34
2.3. Results and Discussion.....	36
2.3.1. Assessment Factor method	36
2.3.2. SSD method	37
2.3.4. AQUATOX model	38
2.3.5. Comparison of the methods.....	40
2.3.6. Advantages and disadvantages of the methods.....	45
2.4. Conclusions	47
2.5. References:	49
Chapter 3.....	55
3. Uptake and translocation of perfluoroalkyl acids (PFAA) in red chicory (<i>Cichorium intybus</i> L.) under various treatments with pre-contaminated soil and irrigation water	55
3.1. Introduction.....	57

3.2.	Materials and methods.....	58
3.2.1.	Chemical reagents and materials.....	58
3.2.2.	Experimental set-up.....	59
3.2.3.	Soil-water partition coefficients	60
3.2.4.	Chemical analyses of crop tissues, soil and irrigation water.....	61
3.2.5.	Data analyses.....	61
3.2.6.	Quality assurance and control.....	62
3.3.	Results and discussion	63
3.3.1.	Inter-compartmental distribution of PFAAs.....	63
3.3.2.	Bioconcentration factors	64
3.3.3.	Effects of different treatments on PFAAs bioavailability and bioaccumulation	66
3.3.4.	Sulfonates vs. carboxylates	67
3.3.5.	Vertical distribution of PFAAs in soil and soil-water partitioning	68
3.4.	Conclusions	71
3.5.	References	73
Chapter 4.....		77
4.	Model-based analysis of the uptake of perfluoroalkyl acids (PFAAs) from soil into plants	77
4.1.	Introduction.....	79
4.2.	Methodology	80
4.2.1.	Perfluoroalkyl acids.....	80
4.2.2.	Experimental data.....	81
4.2.3.	Model description.....	82
4.2.4.	Model calibration.....	83
4.2.5.	Plant parameters and model parametrization.....	85
4.2.6.	Applying the modeling approach to other crops	85
4.2.7.	Statistical evaluation of the results.....	85
4.3.	Results and discussion	85
4.3.1.	Modeling results and measurements	85
4.3.2.	R values	86
4.3.3.	Partitioning.....	88
4.3.4.	Other crops.....	89
4.4.	Conclusions	90
4.5.	References:	92
Chapter 5.....		97
5.	Uptake and translocation of perfluoroalkyl acids (PFAAs) in hydroponically grown red chicory (<i>Cichorium intybus</i> L.): PFAAs toxicity, comparison with the soil experiment and bioavailability implications.....	97

5.1.	Introduction.....	99
5.2.	Materials and methods.....	101
5.2.1.	Materials and chemicals	101
5.2.2.	Experiment set-up.....	101
5.2.3.	Chemical analyses of chicory tissues and nutrient solution.....	102
5.2.4.	Plant parameters	102
5.2.5.	Quality control and data analyses	102
5.2.6.	Comparison with the soil experiment	103
5.3.	Results and discussion	104
5.3.1.	Plants growth and phytotoxic effects.....	104
5.3.2.	PFAAs uptake, bioaccumulation and translocation	106
5.3.3.	Uptake in hydroponics vs. uptake from soil	110
5.4.	Conclusions	111
5.5.	References	112
Chapter 6	117
6.	Predicting the human exposure to perfluoroalkyl acids (PFAAs) through diet: A case of the Veneto Region, Italy.....	117
6.1.	Introduction.....	119
6.2.	Materials and methods.....	121
6.2.1.	Consumption data.....	121
6.2.2.	Measured water concentrations and scenarios	121
6.2.3.	Crops model methodology	122
6.2.4.	Models for estimation of concentrations in meat, milk and eggs.....	122
6.2.5.	Validation of the crop modelling framework with measured data.....	126
6.3.	Results and discussion	127
6.3.1.	Daily dietary intake of PFAAs under various scenarios	127
6.3.2.	Crop modelling framework validation	130
6.3.3.	Exposure estimation for the vulnerable groups	132
6.3.4.	Five years irrigation scenario	133
6.3.5.	Characterization of the risk	134
6.4.	Conclusions	135
6.5.	References	136
Chapter 7	145
7.	Conclusions	145
7.1.	Major findings and their significance	146
7.2.	Future perspectives and further research.....	148

Appendices	150
APPENDIX 1: Supplementary information for Chapter 2	151
APPENDIX 2: Supplementary information for Chapter 3	194
APPENDIX 3: Supplementary information for Chapter 4	218
APPENDIX 4: Supplementary information for Chapter 5	235
APPENDIX 5: Supplementary information for Chapter 6	243

Chapter 1

Introduction and background

1.1. Aims and scope of the thesis

Per- and polyfluoroalkyl substances (PFASs) are a wide group of man-made industrial chemicals, containing at least one perfluoroalkyl moiety ($C_nF_{2n+1}-$) (Buck et al., 2011). They are employed in vast variety of industrial and commercial applications, due to their unique properties, extreme stability and, frequently, surfactant nature (Buck et al., 2011; Kempisty et al., 2018; Krafft and Riess, 2015a). The same properties are what also makes PFASs very persistent in the environment. Due to high mobility of some compounds, many PFASs are ubiquitously present in water, soil, air, sediments, biota and human tissues (Krafft and Riess, 2015b). Perfluorinated molecular parts of PFASs are not degradable under environmental conditions and environmental (bio)transformations are limited to non-fluorinated functional groups, eventually transforming them to perfluoroalkyl acids (PFAAs) (Brendel et al., 2018). The aim of this research thesis is addressing the data and research gaps to assist ecological and human health risk assessment of perfluoroalkyl acids (PFAAs).

Since the legacy PFAAs - PFOS and PFOA - were regulated and phased out in many countries, precursors of short-chain PFAAs have been used as some of their substitutes (Cousins et al., 2019). However, these non-regulated PFAAs are found to be as environmentally persistent as PFOS and PFOA (Brendel et al., 2018; Wang et al., 2015) and were found to bioaccumulate in plants (Ghisi et al., 2019). They are very mobile (with water) and can be infiltrated to the groundwater or transported on the long distances (Zhao et al., 2012). Consequently, a particular attention all the way thought this work has been put on short-chain PFAAs.

In 2013, a large-scale contamination with perfluoroalkyl acids (PFAAs) was discovered in the Veneto region, Northern Italy, as a consequence of the emissions from a fluorochemical plant in the province of Vicenza, which have caused the contamination of surface water, groundwater and drinking water (Mastrantonio et al., 2018; WHO, 2016). Hence, this research also aims to address this concrete issue while providing the data, insights and approaches applicable to other similar cases of PFAS contamination worldwide.

PFAAs are almost entirely ionized at environmental pH, they are not accumulating in storage lipids, but have strong affinity to proteins and phospholipid membranes (Ng and Hungerbühler, 2014). Consequently, usual methods to determine or predict partition coefficients (i.e. based on the octanol-water partition and distribution coefficient, K_{OW} and D_{OW}) are not applicable for the modelling of PFAAs bioaccumulation, emphasizing the need for media-specific partitioning measurements (Droge, 2019). Additionally, almost all studies addressing environmental behavior and fate of PFAAs are having human health risk in their focus, rather than ecological risks or risk to ecosystems themselves. Having all these in mind, two main focuses are put upfront as research scopes: 1) Effects of PFAAs on the aquatic ecosystems as a whole with the means provided by ecological models, and with the main aim of deriving new protective ecological thresholds; 2) Bioaccumulation of PFAAs in edible crops, with all the aspects affecting their bioavailability and behavior in agricultural ecosystems, considering that the ingestion of food and water is regarded as the main pathway of human exposure to PFAAs.

In conclusion, this works aims to improve current knowledge of PFAAs behavior and fate in both terrestrial (agricultural) and aquatic ecosystems and to help decision makers in the Veneto Region in managing the PFAA health risk issues, but also to serve as an example of holistic approach to micro-contaminant management for the other international areas suffering from PFAAs contamination problems.

1.2. Background

1.2.1. Per- and polyfluoroalkyl substances (PFASs): terminology, applications and main physico-chemical properties

Per- and polyfluoroalkyl substances (PFASs) are a group of anthropogenic, highly fluorinated aliphatic substances containing at least one perfluoroalkyl moiety $-C_nF_{2n+1}$ (Buck et al., 2011; DeWitt et al., 2018). They contain multiple C-F bonds, the strongest known single bond in organic chemistry (Krafft and Riess, 2015b), which is essentially providing PFASs with their exceptional stability and resistance to thermal and (bio)chemical degradation (Xiao, 2017a). The group of PFASs includes perfluoroalkyl acids (PFAAs), their precursors and number of surfactants and fluoropolymers (Buck et al., 2011; Dewitt, 2015; Wang et al., 2017). Figure 1-1 is showing the main PFASs classification, groups and representative individual compounds. Most of PFASs are surfactants, with variety of polar groups attached to fluorinated carbon chain, having both hydrophilic and lipophilic properties (Kempisty et al., 2018). The unique combination of properties, as the surfactant nature of some of them and great thermal and chemical stability, made PFASs irreplaceable in many industrial applications (Wang et al., 2017; Xiao, 2017a). Commercial application of PFASs started in 1950s, developing vast number of molecules for the immense number of applications: cosmetics, fire-fighting foams, food contact materials, household products (e.g. Teflon®), inks, medical devices, oil production, mining, pesticides, textile (e.g. Goretex®), leather and apparel (Krafft and Riess, 2015b; Loos et al., 2008; Wang et al., 2017). At the moment, more than 4700 individual PFASs and their mixtures have been present on the market (Cousins et al., 2019). However, wide use of PFASs (and consequently - many possible emission sources), together with their persistence and stability, caused some of them to be ubiquitously present in the environment (water, soil, sediments, wildlife, and humans) (Cheng and Ng, 2018).

Substances containing the perfluoroalkyl moiety have a potential to be transformed abiotically or biotically, through changes in the non-fluorinated part of the molecule, into perfluoroalkyl acids (PFAAs), regarded as their final transformation product (Brendel et al., 2018; Buck et al., 2011; Ghisi et al., 2019). PFAAs are highly persistent group of PFASs, low weight ionizing surfactants differing among group in their perfluoroalkyl chain length and their terminal polar group (consequently forming carboxylic (PFCAs), sulfonic (PFSAs), sulfinic, phosphonic (PFPAAs), and phosphinic (PFPIAs) perfluoroalkyl acids) (Wang et al., 2017). The most commonly used and environmentally detected PFAAs are perfluorooctane sulfonic acid (PFOS) and perfluorooctanoic acid (PFOA) (Cheng and Ng, 2018). After realization that bioaccumulation and, likely, health risks are lowering with the decrease in perfluoroalkyl chain length, PFAAs were formally divided into long- and short- chain PFAAs. PFCAs with 7 or more and PFSAs with 6 or more fluorinated carbons are considered long-chain PFAAs (Eschauzier et al., 2013; Krafft and Riess, 2015a, 2015a; Valsecchi et al., 2015). Concerns have been raised about the environmental and health risk of long-chain perfluorocarboxylic and perfluorosulfonic acids in the early 2000s, leading to phase-out of PFOS (and its related compounds) and PFOA by the 3M company, their major manufacturer (Buck et al., 2011). Since then, regulatory measures have been undertaken, leading to restrictions and regulations of long-chain PFAAs (Chapter 1.2.2.), resulting with the shift of production towards unregulated alternatives, many of them being short-chain PFAAs and their precursors (Brendel et al., 2018).

Short-chain PFAAs (and their precursors) were assumed to have lower bioaccumulation potential, improved environmental properties and were considered as “safe” alternatives for long-chain PFAAs (Brendel et al., 2018; Dewitt, 2015; Kempisty et al., 2018). Half-lives of short-chain PFAAs in animals and humans are remarkably shorter. However, short-chain PFAAs are as persistent as the long-

chain ones and, due to the production shift, they are widely present in the environment (Brendel et al., 2018). Compared to long-chain PFAAs, less research initiative has been committed to the environmental fate and toxicity of their short-chain homologues (Dewitt, 2015). Recent research efforts have emphasized their higher mobility in the environmental matrices (e.g. soil and groundwater (McLachlan et al., 2019)), the higher bioaccumulation in plants (including crops) (Ghisi et al., 2019) and the lower efficiency of removal (purification) techniques for their elimination from drinking water (Cousins et al., 2016), all being a strong motivation for higher attention to short-chain PFAAs in this thesis. A list of employed PFAAs in the thesis is given in Table 1-1.

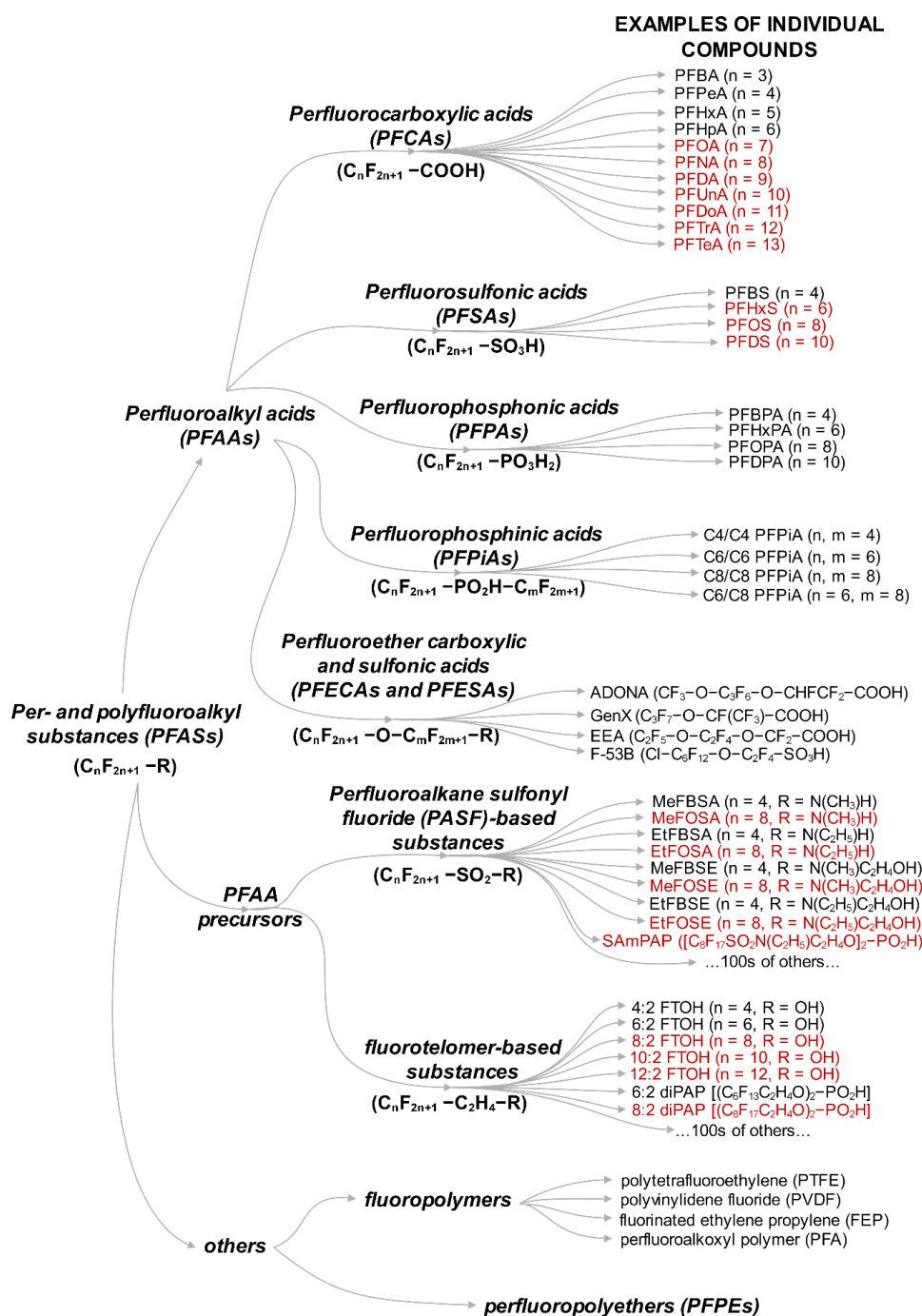


Figure 1-1. Classification of PFASs, main groups and individual compounds. PFASs in red are restricted under national/regional/global regulatory or voluntary frameworks (accepted and modified from Wang et al. (2017))

Table 1-2. A list of investigated PFAAs with relevant physico-chemical properties and structures (Smith et al., 2016)

Abbreviation	Chemical (common) name	No. of perfluorinated carbons	CAS number	Molar mass (g/mol)	Dissociation constant (pKa)	Water solubility (g/L)	Structure
Perfluoroalkyl carboxylates/Perfluoroalkyl carboxylic acids (PFCAs)							
PFBA	Perfluorobutanoic acid	3	375-22-4	214.04	-0.2 to 0.7	miscible	
PFPeA	Perfluoropentanoic acid	4	2706-90-3	264.05	-0.06	112.6	
PFHxA	Perfluorohexanoic acid	5	307-24-4	314.05	-0.13	21.7	
PFHpA	Perfluoroheptanoic acid	6	375-85-9	364.06	-0.15	4.2	
PFOA	Perfluorooctanoic acid	7	335-67-1	414.07	~0.5 ¹	3.4 to 9.5	
PFNA	Perfluorononanoic acid	8	375-95-1	464.08	-0.17	9.5	
PFDA	Perfluorodecanoic acid	9	335-76-2	514.08	-0.17	9.5	
Perfluoroalkyl sulfonates/Perfluoroalkyl sulfonic acids (PFSAs)							
PFBS	Perfluorobutane sulfonic acid	4	375-73-5	300.1	-6.0 to -5.0	46.2 to 56.6	
PFOS	Perfluorooctane sulfonic acid	8	1763-23-1	500.13	-6.0 to -2.6	0.52 to 0.57	

¹(Johansson et al., 2017)

1.2.2. PFAAs exposure, risks and existing regulations

1.2.2.1. *Main sources and emissions*

Direct emissions of PFAAs to the environment occur through their whole life-cycle (from the production through the use to their disposal) or indirectly through the transformation of precursors which is frequently overlooked (Krafft and Riess, 2015a; Prevedouros et al., 2006; Wang et al., 2015). The manufacturing facilities of fluorochemicals are the greatest point sources of PFAAs and their precursors (Prevedouros et al., 2006; Valsecchi et al., 2015). Until today, contamination hot-spots around fluorochemical industry have been detected worldwide: from the most known Minnesota and West Virginia cases discovered in 2000s in the USA, caused by 3M and DuPont fluorochemical companies, to European cases in Dordrecht, Netherlands, Antwerp, Belgium and Veneto Region, Italy (Dauwe et al., 2007; Goldenman et al., 2019; WHO, 2016). Production sites using PFASs in the manufacture of consumer goods and products are another major source of PFAS emissions (e.g. tanneries, textile industry, metal plating industry, paper industry), together with the use of PFAS as surfactants and coatings (e.g. professional cleaning) (Goldenman et al., 2019). Many cases of local hot-spot contamination are caused by the application of aqueous film-forming foams (AFFFs), used in extinguishing of the petroleum-based fires (Kempisty et al., 2018). AFFF contamination cases are usually located near airports and military bases (Borg and Hakansson, 2012; Gobelius et al., 2017), fire-fighting training facilities (Gewurtz et al., 2014) or can be connected to fire accidents (Munoz et al., 2017). The use phase of some products containing PFASs can be a significant source of PFAAs to the environment or it can cause direct human exposure, e.g. the use of stain-repelling products, water-repelling textiles, cosmetics or PFAS-treated food contact materials (Cousins et al., 2019; Goldenman et al., 2019; Trier et al., 2011). These products can be disposed or washed-out into wastewater (and consequently end up in municipal wastewater treatment plants and sewage sludge) or on landfills, where they pose another possible source to the environment (primarily surface- and groundwater, but also atmosphere in the case of volatile precursors) (Ahrens et al., 2011; Eriksson et al., 2017; Hamid et al., 2018).

1.2.2.2. *Environmental fate and behavior*

Perfluoroalkyl acids are often regarded as “forever chemicals” due to their resistance to biodegradation and chemical transformation under normal environmental conditions and their consequent extreme persistence (Pelch et al., 2019; Smith et al., 2016). PFAAs are primarily emitted to surface waters, water being the largest reservoir of PFAAs in the environment and the most important transport media (Mclachlan and Holmstro, 2007; Zareitalabad et al., 2013; Valsecchi et al., 2015). They are highly water soluble, considering the presence of a hydrophilic carboxylic or sulfonic group in their molecules, their solubility decreasing with the chain length increase (Smith et al., 2016). PFAAs are dissociated under environmentally relevant pHs, and as ions (anions) they have negligible vapor pressure (Ding and Peijnenburg, 2013a). However, their precursors (e.g. PAPs, FTOHs, FASAs) are volatile and can undergo long-range atmospheric transport (LRAT). In the atmosphere, they can also be transformed into PFAAs and end up in remote areas (e.g. Antarctic) as a result of wet and dry deposition (Ahrens and Bundschuh, 2014; Zhao et al., 2012). Being ionic, PFCAs and PFSAAs are globally transported by ocean currents, reported as their main pathway to regions where they are not emitted (González-Gaya et al., 2019; Zhao et al., 2012). In general, PFAAs are distributing from source areas to the global environment by advection, dispersion, dilution and burial processes; deep oceans and sediment burial being considered as their final sink (Cousins et al., 2016; Prevedouros et al., 2006).

Mobility of PFAAs in water will be influenced by their sorption capacity to soils, sediments or sewage sludge (Zareitalabad et al., 2013). A sorption to soils and sediments can eliminate the portion of

PFAAs from the aqueous phase, permanently or temporarily, causing retardation of their transport and lowering of their velocity relative to water (Smith et al., 2016). Sorption of PFCAs and PFSAs to soil and sediments (commonly described with K_d , soil-water partition coefficient) does not exclusively depend on the organic carbon content (%OC) and cannot be normalized to the soil OC for the modelling purposes (Y. Li et al., 2018), as usually applied for neutral organic contaminants. In some cases, long chain PFAA's K_d s were significantly correlated with the OC content (Y. Li et al., 2018; Milinovic et al., 2015), but short chain PFAAs generally did not (F. Li et al., 2018; Zhu et al., 2014). K_d s for different soils (and sediments) are varying significantly (e.g. between 0.1 and > 3000 L/kg for PFOS) (Zareitalabad et al., 2013), but their sorption capacity is found to decrease with the chain length decrease (Higgins and Luthy, 2006; McLachlan et al., 2019; Sepulvado et al., 2011; Vierke et al., 2014). Considering the amphiphilic nature and ionized form of PFAAs in water, their interactions with sorbents are governed also by electrostatic interactions, ion exchange and hydrogen bonding and cannot be attributed to only one soil property as the organic matter or hydrophobic interactions of their perfluoroalkyl chain (Campos Pereira et al., 2018; Du et al., 2014; F. Li et al., 2018; Y. Li et al., 2018).

The partitioning of PFAAs between solids and water is particularly relevant from the aspect of their infiltration to subsurface and groundwater contamination and it depends on the characteristics of soil or sediment and physico-chemicals properties of different PFAAs (mainly chain length and polar group) (Lutz Ahrens et al., 2011; McLachlan et al., 2019; Sepulvado et al., 2011; Vierke et al., 2014). Short chain PFAAs, particularly PFBA, PFBS and PFPeA are found to sorb only weakly to soils and sediments (McLachlan et al., 2019; Vierke et al., 2014), the sorption of sulfonates being generally stronger than of the carboxylates (Higgins and Luthy, 2006). Consequently, due to their high mobility and persistence, infiltration and diffusion with water would occur and result with the generation of large, persistent contamination plumes of short-chain PFAAs in the groundwater (Brusseu, 2018; Cousins et al., 2016). Short-chain PFAAs are frequently detected in groundwater samples worldwide and considering groundwater is often a primary source of drinking water, drinking water contamination has been a frequent cause of public concerns (Brendel et al., 2018; Cousins et al., 2016; Mastrantonio et al., 2018). Furthermore, contaminated surface or groundwater, when used for irrigation, can be a significant cause of soil contamination and consequently a source of PFAAs into terrestrial (agricultural) ecosystems (Liu et al., 2017, 2016).

1.2.2.3. Bioaccumulation, human exposure and toxicity

PFAAs are detected in biota worldwide, showing bioaccumulation potential in animals, humans and plants, and biomagnification in both aquatic and terrestrial ecosystems (Ding and Peijnenburg, 2013a; Falk et al., 2019; Ghisi et al., 2019; Ng and Hungerbühler, 2014). In animal and human body, bioaccumulation increases with the chain length increase and is higher for PFSAs than PFCAs of the same chain length (Krafft and Riess, 2015a). Long- and short-chain PFAAs were originally distinguished with the assumption of short-chain PFAAs having a lower bioaccumulation potential and being less persistent and toxic compared to their long-chain homologues (Buck et al., 2011). In general, long-chain PFAAs have been studied more extensively, particularly PFOS and PFOA, while data on the toxicity and bioaccumulation of short-chain PFAAs are still inconsistent and much less abundant (Smith et al., 2016).

Short-chain PFAAs have much shorter serum elimination half-lives than long-chain PFAAs, ranging from a couple of days (e.g. 1.2 - 6.3 days for PFBA (Chang et al., 2008) and 25.8 days for PFBS (Olsen et al., 2009) in occupationally exposed humans) to several years for PFOS, PFHxS and PFOA (5.4, 8.5 and 3.8 years in fluorochemical factory workers, respectively (Olsen et al., 2007)). There are uncertainties in accumulation processes and also acute and chronic toxicity effects

considering the variations of bioaccumulation and toxicity response in different species and between genders (Krafft and Riess, 2015a; Sznajder-Katarzyńska et al., 2019). Bioaccumulation factors (BCFs) for aquatic animals (as the ratio between the PFAA concentration in an organism and in water) were in an order of thousands for PFOS, e.g. 3100 L/kg in the blood of rainbow trout (Martin et al., 2003) and between 274 and 41600 L/kg in liver of fishes from the Tokyo Bay (Taniyasu et al., 2003). BCFs for PFOA in fish are lower (e.g. 12 L/kg in a liver or the rainbow trout (Martin et al., 2003) and according to the “B” criterion for bioaccumulation ($BCF_{fish} \geq 2000$ L/kg) under EU REACH Directive (Registration, Evaluation, Authorisation and Restriction of Chemicals), PFCAs of 7 perfluorinated carbons or less are not considered bioaccumulative (Conder et al., 2008; Cousins et al., 2016; Ding and Peijnenburg, 2013a). However, due to long half-lives in (some) mammals and in humans, its omnipresence in human blood of the general population and evidence that PFOA biomagnifies across food chains (having biomagnification factor, BMF, higher than 1) it was considered that, according to a weight of evidence approach, PFOA still fulfills the “B” criterion for bioaccumulation (ECHA, 2014; Smith et al., 2016).

It has been shown that due to their amphiphilic properties and surfactant behavior, in animals and humans PFAAs do not accumulate in adipose tissues as neutral hydrophobic chemicals, but are showing affinity to proteins (e.g. serum albumin) and phospholipid membranes (Ding and Peijnenburg, 2013a; Ng and Hungerbühler, 2014). Consequently, protein-rich tissues and blood are their main distribution compartments, while liver, lung and kidney represent the main target organs (Ding and Peijnenburg, 2013a; Krafft and Riess, 2015a). The main clearance route for PFAAs is through urinary excretion for human and other mammalian species, while in fish they can also be eliminated via respiratory system, making the elimination much more efficient in fish (ATSDR, 2018; Cousins et al., 2016).

The presence of PFAAs has been confirmed in the breast milk of lactating mothers, umbilical cord blood and in seminal plasma (Jian et al., 2018; Sznajder-Katarzyńska et al., 2019). PFAAs can be transferred from a mother to her fetus by the trans-placental passage and to infants by the breast milk (Cariou et al., 2015). This transfer is also chain length and polar head dependent, again long-chain PFSAAs accumulating the most in mother’s blood serum, milk and umbilical cord blood (PFOS, PFOA, PFHxS and PFNA dominating) (Cariou et al., 2015). However, the major exposure pathway of PFAAs to humans is through the consumption of contaminated food and water (Vestergren and Cousins, 2009a). The exposure (mainly to neutral PFAA precursors) can also occur through the outdoor and indoor air and via house dust ingestion (Fromme et al., 2009) or through the migration of PFAAs from the food contact materials or PTFE cookware (Trier et al., 2011; Winkens et al., 2017).

A large number of epidemiological studies associated PFAAs (mainly PFOS and PFOA) with various health adverse effects in humans: pregnancy-induced hypertension/pre-eclampsia and increased risk of fertility decrease, decreased birth weight and size, liver damage and liver hypertrophy, liver cancer, increases in the serum lipids (total cholesterol and low-density lipoprotein cholesterol), effects on the immune system functioning (atrophy of thymus and spleen, suppressed antibody responses) and endocrine system (increased risk of thyroid disease), induction of adverse neurobehavioral reactions, obesity and tumor formation (ATSDR, 2018; Sznajder-Katarzyńska et al., 2019).

1.2.2.4. Bioaccumulation in crops

The uptake of chemicals by plants is the main route for their entrance into terrestrial ecosystems (Trapp and Matthies, 1998). The studies of PFAAs uptake into crops are still mostly limited to PFOS and PFOA (Ghisi et al., 2019), and few studies performed with PFAAs mixtures have revealed a

strong chain length, crop and soil type dependency (Blaine et al., 2013, 2014c; Krippner et al., 2015). As opposed to long-chain perfluoroalkyl sulfonates that are the most bioaccumulative PFAAs in animals and humans, short-chain PFAAs are found to be highly bioaccumulative in aerial plant parts, PFBA and PFPeA being the dominant compounds (Ghisi et al., 2019). Edible crops, and particularly vegetables, have been identified as important food category contributing to human dietary exposure to PFAAs (Felizeter et al., 2014; McLachlan et al., 2019). A root uptake is the main uptake pathway for PFAAs into plants and considering PFAAs are in ionic state and, hence, not volatile, gaseous deposition or volatilization loss are not expected to occur (Blaine et al., 2014a; Stahl et al., 2009; Trapp, 2007). With high mobility (and low sorption affinity) of short-chain PFAAs and their relatively small molecular size, transport from roots to aerial parts through xylem (transpiration stream) is being considered as the main uptake mechanism (Felizeter et al., 2014).

Several studies that have been conducted so far, examine the root uptake of PFAAs from soil (Blaine et al., 2013, 2014a; Krippner et al., 2015; Stahl et al., 2009; Wen et al., 2014) or hydroponic solution (Felizeter et al., 2012, 2014; Müller et al., 2016). Agricultural soil contamination with PFAAs can be a consequence of the biosolids amendment (Blaine et al., 2013), addition of the sewage sludge (Bizkarguenaga et al., 2016) or irrigation with the contaminated water (Blaine et al., 2014b; Liu et al., 2017, 2019).

Hydroponic studies (Felizeter et al., 2012, 2014; Müller et al., 2016) have shown the clear pattern of long-chain PFAAs retention in roots and transport of short-chain PFAAs upwards to aerial plant compartments (shoots and fruits). However, this root accumulation pattern was not visible in the soil uptake studies, generally uptake being either inclined towards short-chain PFAAs or showing no chain length dependency (Blaine et al., 2014b; Wen et al., 2014). Sorption in soil has a significant impact on the bioavailability of PFAAs in pore water and their uptake to roots. Nevertheless, soil-water distribution coefficients (K_{ds}) are reported for growing media only in the plant uptake study of (Blaine et al., 2014b), where they were based only on a single-point batch test. In the same study, authors researched an effect of organic carbon content (0.4, 2 and 6 %OC) on the PFAAs uptake from reclaimed water into lettuce, where the highest uptake of PFBA and PFPeA was not achieved from the soil with the lowest %OC of 0.4%, but from the soil with 2% OC. The same study also indicated that, when delivered with the irrigation water (opposed to the biosolids amendment), PFAAs uptake could be higher. In general, there are variations between the uptake studies regarding the PFAAs exposure concentration dependency, growth media, soils and biosolids characteristics, species and plants varieties. The soil-water-crop interactions are complex and further research is needed to clarify the roles of different influential factors (Blaine et al., 2013; Ghisi et al., 2019; Navarro et al., 2017; Lei Xiang et al., 2018).

1.2.2.5. PFAAs modelling

Multi-media mass-balance environmental modelling is a popular approach applied to quantify environmental fate of chemicals, from their sources, transport, phase partitioning, transformation and degradation (MacLeod et al., 2010). The environment is represented as the series of interconnected homogeneous or well-mixed compartments, such as hydrosphere (e.g. lake, river), lithosphere (e.g. soils, sediments, suspended solids), atmosphere or biota, and where organic chemical partitions between various phases, it is being transported or degraded, depending on the environmental parameters and its physico-chemical properties (Mackay, 2001). The persistence, bioaccumulation and toxicity, together with the chemical's quantity and its environmental distribution, are the key parameters for evaluation of the substance's potential to pose a risk and cause harm (Mackay, 2001). For the risk assessment of chemicals, key descriptor for chemical "hydrophobicity" and its preferential partitioning into lipids, organics or fats is octanol-water partition coefficient (K_{ow} , for the

neutral species) or octanol-water distribution coefficient (D_{OW} , for ionized species at the certain pH) (Droge, 2019; Mackay, 2001). Octanol is an excellent surrogate for natural organic matter in soils and sediments, lipids or fats and plant waxes and, therefore, correlations are usually developed between octanol-water and other partition coefficients (e.g. soil-water, root-water etc.) (Mackay, 2001). However, K_{OW} cannot be experimentally determined for ionic surfactants as PFASs, while quantitative structure-activity relationship models (QSARs) based on molecular fragments cannot be properly calibrated because of the lack of experimental data (Conder et al., 2008; Droge, 2019). Nevertheless, this traditional equilibrium partitioning approach applicable for lipophilic organic chemicals, cannot be applied for PFASs bioaccumulation, due to their affinity for proteins and phospholipid membranes rather than the lipids (Conder et al., 2008; Ng and Hungerbühler, 2014).

1.2.2.6. Current regulations and standards

Current PFAAs regulatory actions and restrictions are directed mostly on PFOS and PFOA, their precursors and their long-chain homologues. The changes in PFASs production and restrictions started when global presence of PFOS in wildlife and human serum was reported (DeWitt et al., 2018; Giesy and Kannan, 2001; Hansen et al., 2001); afterwards 3M, the main manufacturer, ceased the production of PFOS and POSF related chemistry in 2002 (3M, 2000). In the same year, Organization for Economic Co-operation and Development (OECD), classified PFOS as a persistent, bioaccumulative and toxic (PBT) (OECD, 2002; Sznajder-Katarzyńska et al., 2019).

In 2009, POSF, PFOS and its salts were added to Annex B of the Stockholm Convention on Persistent Organic Pollutants (POPs), restricting its production and use (UNEP, 2009). The European Commission added PFOS to the List of priority substances, identifying it as a “priority hazardous substance”, through Directive 2013/39/EC (The European Parliament and the Council of the European Union, 2013), with an annual average concentration of 0.65 ng/L as the Environmental Quality Standard (EQS) for inland surface water (freshwater). From June 2013, PFOA has been on the Candidate List of substances of very high concern for Authorisation, in accordance with the REACH regulation, as a PBT (persistent, bioaccumulative and toxic) and CMR (carcinogenic, mutagenic and toxic for reproduction) substance, but there are still no established environmental thresholds (ECHA, 2013). In 2017, two other PFASs entered this list, Nonadecafluorodecanoic acid (PFDA) and its sodium and ammonium salts (ECHA, 2017a), and Perfluorohexane-1-sulphonic acid (PFHxS) and its salts (ECHA, 2017b), while PFOA and its salts entered the Restricted list (ECHA, 2017c). In 2018, long-chain perfluorocarboxylic acids (PFNA, PFDA, PFUnDA, PFDoDA, PFTTrDA, PFTDA, their salts and precursors) are officially identified as the substances of very high concern and are added to the Candidate list (ECHA/SEAC/RAC, 2018). The most recent addition to REACH Candidate list is a GenX chemical (2,3,3,3-Tetrafluoro-2-(heptafluoropropoxy) propanoic acid), from July 2019 (ECHA, 2019).

According to the European Food Safety Agency (EFSA) (EFSA, 2008), tolerable daily intakes (TDIs) were established in 2008 to 150 $\text{ngkg}_{\text{BW}}^{-1}\text{d}^{-1}$ for PFOS and 1500 $\text{ngkg}_{\text{BW}}^{-1}\text{d}^{-1}$ for PFOA. In 2018, EFSA Panel on Contaminants in the Food Chain (CONTAM), proposed the thresholds of 13 $\text{ng kg}_{\text{BW}}^{-1}\text{week}^{-1}$ for PFOS and 6 $\text{ngkg}_{\text{BW}}^{-1}\text{week}^{-1}$ for PFOA (EFSA CONTAM, 2018). The United States Environmental Protection Agency established the oral non-cancer reference doses (RfDs) of 20 $\text{ngkg}_{\text{BW}}^{-1}\text{d}^{-1}$ for both PFOS and PFOA (USEPA, 2016a, 2016b). Recommended TDIs from the Food Standards Australia New Zealand agency are set to 20 $\text{ngkg}_{\text{BW}}^{-1}\text{d}^{-1}$ for PFOS and 160 $\text{ngkg}_{\text{BW}}^{-1}\text{d}^{-1}$ for PFOA (FSANS, 2017). Currently, there are no uniform drinking water regulatory thresholds in the EU or USA, but different countries and states are proposing and implementing their own standards. However, EU Drinking water Directive 98/83/EC is under the revision and thresholds of 0.1 $\mu\text{g/l}$ for individual PFAS and 0.5 $\mu\text{g/l}$ for PFASs in total are proposed (Council of the European Union, 2018).

In 2016, US EPA released a lifetime health advisory of 70 ng/L for PFOA and PFOS, individually or combined, but it is not enforceable (Cordner et al., 2019; US Government/USEPA, 2016) and is currently working towards establishing standards for the drinking water and groundwater cleanup (USEPA, 2019).

There is not any regulation currently in force for short-chain PFAAs or their precursors, despite of their high production, wide application and persistence comparable to their long-chain homologues, and, consequently, frequent detection in the environmental matrices worldwide (Brendel et al., 2018; DeWitt et al., 2018).

1.2.2.7. Ecological risk assessment

Ecological risk assessment for chemicals stands for the assessment of risk posed by the presence of anthropogenically released chemicals on theoretically all living organisms in different environmental ecosystems. It includes hazard identification, dose (concentration) – response (effect) assessment, exposure assessment and risk characterization. The effects assessment involves estimation of the Predicted No-Effect Concentration (PNEC), exposure assessment calculation of the Predicted Environmental Concentration (PEC), while the Risk Quotient (RQ), PEC/PNEC ratio, represents the way of conventional risk characterization (European Commission, 2003; Fairman et al., 1998). Risk quotient (RQ) methodology, where RQ is calculated as the ratio of Measured Environmental Concentration (MEC) and PNEC of the substance of interest has been widely used to estimate the risk posed by micropollutants to the environment. If RQ exceeds 1, it is assumed that adverse effects on ecosystem populations are mostly likely to occur. On the contrary, if RQ is less than 1, the risk for ecosystems should be negligible (Thomaidi et al., 2017; Wright-Walters et al., 2011). At the European level, standardized environmental risk assessment is implemented in the REACH (REACH, EC, 2006) and through the Environmental Quality Standards Directive, a daughter directive of the Water Framework Directive (Directive 2000/60/EC (European Community, 2000)), providing the consistent approach of estimating ecological threshold (PNEC) in aquatic (freshwater) ecosystems (ECHA, 2008; European Commission, 2011). Based on this regulations, PNECs can be derived using three approaches: deterministic approach based on the assessment factors (AFs), probabilistic approach using species sensitivity distribution (SSD) modeling and by using the results from model ecosystem and field studies (European Commission, 2011). The AF and SSD methods are more commonly applied, as there are guidelines for their application (ECHA, 2008; European Commission, 2011), both methods depending on the quality and quantity of ecotoxicological data available.

In EU, environmental standards are currently set only for PFOS, as already mentioned in Chapter 1.2.2.6., with an annual average concentration (AA-EQS) of 0.65 ng/L for inland surface water (freshwater) and 0.13 ng/L for coastal and transitional waters (The European Parliament and the Council of the European Union, 2013). The same Directive (2013/39/EC) set the Maximum Allowable Concentration EQS (MAC-EQS) on 38 µg/L for freshwater and 7.2 µg/L for coastal and transitional waters. The threshold was also set for the concentration in biota (for secondary poisoning) on 9.1 µg/kg (European Commission Subgroup on Review of the Priority Substances List, 2011; The European Parliament and the Council of the European Union, 2013). Environment Canada derived Federal Environmental Quality Guidelines (FEQGs) for PFOS with the aim of identifying the benchmarks for aquatic ecosystem intended to protect all aquatic life forms for indefinite period of exposure. The FEQGs were set on 6.8 µg/L for the surface water, 9.4 mg/kg_{ww} for the fish tissue, and 4.6 and 8.2 µg/kg_{ww} for the piscivorous mammals and birds, respectively (Environment and Climate Change Canada, 2018). Generally, much more regulatory attention is currently being put on human health standards; it mainly concentrates on PFOS as the individual compound and is mostly

based on aquatic species and ecosystems. However, high bioconcentration and persistence of PFAAs and their ubiquitous presence in wildlife suggest for the need of comprehensive ecological risk assessments (McCarthy et al., 2017).

1.2.2.8. The Veneto Region contamination case

In 2013, a large-scale contamination of surface water, groundwater and drinking water was discovered in the Veneto Region, Northern Italy, caused by emissions from a fluorochemical plant that was producing PFASs since 1968 (Ingelido et al., 2018; WHO, 2016). Veneto is situated in the Po valley and is one of the greatest Italian agronomic producers, accounting for 10% of national production and being responsible for 38% of Veneto's gross domestic product (WHO, 2016). Italy, including Veneto, has the highest use of water for agricultural purposes in Europe, with about 50% of it being surface- and groundwater (Nicoletto et al., 2017).

More than 120'000 citizens, living in 21 municipalities (in the provinces of Vicenza, Verona and Padova), were drinking water contaminated with PFASs for years. The contamination was discovered after water sampling across European large rivers had been performed under the European PERFORCE project and when the highest concentrations of PFOA were measured in the Po River (Loos et al., 2008; McLachlan et al., 2007). A further research across Italian river basins discovered the "hot spot" in the river Brenta basin (Ingelido et al., 2018; Valsecchi et al., 2015). The Brenta River originates from the lakes of the South Tirol and inflows into the northern Adriatic Sea, south of the Venice lagoon. It receives the waters of the Bacchiglione and Fratta-Gorzone rivers, collecting the wastewater effluents of textile and tannery industries and also fluorochemical factory (Valsecchi et al., 2015). One of the contamination pathways was also infiltration into the groundwater, considering the high permeability of subsurface and shallow pebble and gravel alluvial aquifer, contaminating an area of 150 km² (Figure 1-2). The groundwater is the main source of drinking water, so some wells were closed and Granular Activated Carbon (GAC) filters were installed (2013) and Italian drinking water standards were derived and put into force in 2014 (PFOS: ≤ 30 ng/L; PFOA: ≤ 500 ng/L; other PFAS: ≤ 500 ng/L) (WHO, 2016; Zaggia et al., 2016).

Regular monitoring of wastewater, surface water, groundwater and spring water is performed by Regional Environmental Protection Agency (ARPAV), reporting the presence of PFCAs (from 3 to 13 fluorinated carbon atoms) and PFSAAs (PFBS, PFHxS, PFHpS and PFOS), Perfluoro 2-Propoxy-Propanoic Acid (GenX), cC6O4 ammonium salt (CAS 329238-24-6, a complex mixture of C₃F₆ClO-[CF₂CF(CF₃)O]_n-[CF(CF₃)O]_m, n = 1-4, m = 0-2), 4:2 FTS, 6:2 FTS and 8:2 FTS (ARPAV, 2018a, 2018b). PFOA is the most frequently detected and most abundant compound, in concentrations up to 20 µg/L in the groundwater, 3.4 µg/L in surface waters and 7.9 µg/L in spring waters of the Vicenza province, with measured peaks of PFOA up to 700 µg/L in industrially contaminated wells in the area (ARPAV, 2018b). Even though the most abundant PFAA in the groundwater is PFOA, short-chain PFAAs are significantly contributing to the total PFAAs load, PFBA, PFBS, PFHxA and PFPeA being the most significant compounds after PFOA (ARPAV, 2018a).

The biomonitoring of serum concentrations (Ingelido et al., 2018) and ecological mortality study (Mastrantonio et al., 2018) were performed for the Veneto population living in the area of contaminated municipalities, and high serum concentrations were correlated to consumption of contaminated drinking water. Maximum detected serum PFOA concentration in exposed population was 754.5 ng/g, while 13.8 ng/g was the median value, followed by the concentrations of PFOS (max 70.27 and median 8.7 ng/g) and PFHxS (max 43.4 and median 2.9 ng/g) (Ingelido et al., 2018). Ecological mortality study associated high exposure to PFAAs in contaminated provinces with higher mortality for some causes of death. Statistical significance was found between the exposure to PFAAs and diabetes, cerebrovascular diseases, myocardial infarction and Alzheimer's disease in

both sexes. In females, statistically higher risk of breast and kidney cancer and Parkinson disease were observed as well (Mastrantonio et al., 2018).

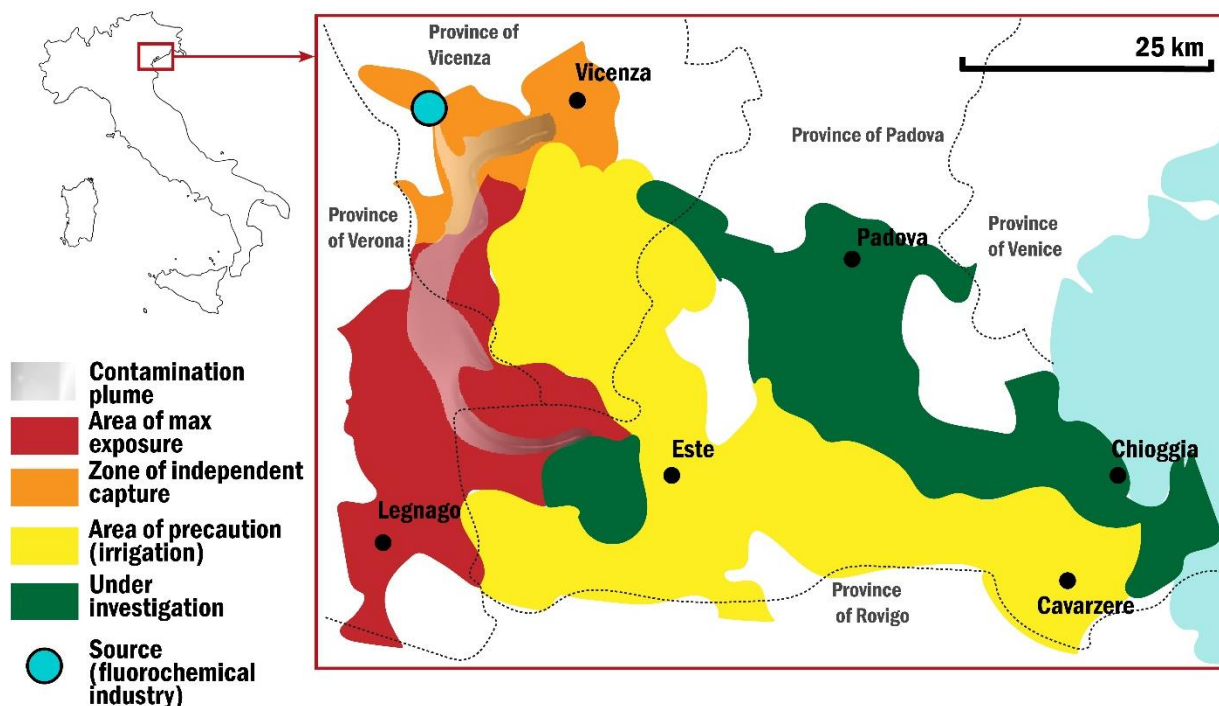


Figure 1-2. The areas of the Veneto Region impacted by PFAAs contamination: 1) the red area includes 21 municipalities with contaminated aqueducts, 2) the orange area, where private wells were contaminated, but the water from the public supply system was clean 3) the yellow area including the network of environmental control systems for surface- and groundwater 4) the green area, where PFAAs were detected in the environmental matrices, but requires further investigation 5) contamination plume (marked in grey) of the contaminated wastewater from the fluorochemical plant into the groundwater (accepted and modified from (WHO, 2016)).

1.3. Thesis organization

The thesis is organized in seven chapters and five appendices. **Chapter 1** includes research aims and scope and introductory and background information for all of the research work presented in **Chapters 2-6**. **Chapters 2-6** consist of published, submitted or prepared papers which are delivered in a form of research publication. Appendices 1-5 are including the supplementary materials of papers/chapters. **Chapter 7** includes the summary of findings, overall conclusions and the recommendations for future work. The summary of chapters is briefly delivered in the following text.

Chapter 2, entitled “*Deriving predicted no-effect concentrations (PNECs) for emerging contaminants in the river Po, Italy, using three approaches: assessment factor, species sensitivity distribution and AQUATOX ecosystem modelling*”, by Andrea Gredelj, Alberto Barausse, Laura Grechi and Luca Palmeri, has been published in *Environment International* (Gredelj et al., 2018). Andrea Gredelj collected the ecotoxicological data, performed the simulations and calculations and drafted the manuscript. In the paper, two regulated methods are used for deriving ecological thresholds and one novel method is proposed, based on the AQUATOX ecological and chemicals fate model, for four PFAAs (PFBA, PFBS, PFOA and PFOS) and two already well-researched emerging contaminants (LAS and triclosan). Apart from the new methodology development and thresholds proposal, modelling results are used to examine indirect and sublethal effects of the chemicals.

Chapter 3, entitled “*Uptake and translocation of perfluoroalkyl acids (PFAA) in red chicory (Cichorium intybus L.) under various treatments with pre-contaminated soil and irrigation water*”, by Andrea Gredelj, Carlo Nicoletto, Sara Valsecchi, Claudia Ferrario, Stefano Polesello, Roberto Lava, Francesca Zanon, Alberto Barausse, Luca Palmeri, Laura Guidolin and Marco Bonato, was published in *Science of the Total Environment* (Gredelj et al., 2019a). Andrea Gredelj designed the study, planned the experiments, implemented and guided the greenhouse and laboratory experimental work and took the leading role in elaboration of the results and writing the manuscript. The crop uptake study was performed in a greenhouse, with red chicory as a model crop, exposed to nine perfluoroalkyl acids through 12 treatments with pre-contaminated (spiked) soil, spiked irrigation water or their combination. Bioaccumulation potential was investigated under different exposure conditions and in different crop compartments (head, leaves and roots). PFAAs in-soil mobility was examined through the sampling of pots by depth and within the laboratory batch experiments for soil-water partitioning. This is a first comprehensive study taking into account two delivery media, soil- and plant-specific PFAAs partitioning and is bringing new insights to the fate of PFAAs in simulated agricultural ecosystem.

Chapter 4, entitled “*Model-based analysis of the uptake of perfluoroalkyl acids (PFAAs) from soil into plants*” by Andrea Gredelj, Fabio Polesel and Stefan Trapp, was accepted for publication in *Chemosphere* (Gredelj et al., 2019b). Andrea Gredelj measured and calculated crop specific parameters (i.e. for growth and transpiration) and performed calculations and simulations. Andrea Gredelj and Stefan Trapp evaluated the standard plant uptake model (Trapp, 2015; Trapp and Matthies, 1995) performance and modified it for PFAA’s specific behavior. This study uses measured uptake data for nine PFAAs into red chicory and derived soil-water distribution coefficients, as reported in Chapter 3, and plant-specific data that was measured and calculated for the purpose. A new parameter was introduced to explain the slow transfer of PFAAs across root epidermis biomembranes, based on red chicory, and it was successfully implemented for other crops. The transfer of PFAAs to aerial plant parts was successfully explained by the combination of the parameter for slow uptake, soil-water partition coefficients and root-to-soil empirical bioconcentration factors.

Chapter 5, entitled “*Uptake and translocation of perfluoroalkyl acids (PFAAs) in hydroponically grown red chicory (Cichorium intybus L.): PFAAs toxicity, comparison with the soil experiment and bioavailability implications*” is in preparation for submission to a peer-reviewed journal. Andrea Gredelj and Carlo Nicoletto designed the hydroponic set-up. Andrea Gredelj performed calculations and initial results evaluation and drafted the manuscript. In this study, red chicory was grown in the hydroponic tanks with increasing concentrations of PFAA mixtures. PFAAs toxicity effects were assessed by the measurements of chlorophyll a (indirectly), roots length, transpiration volume and plants biomass. Bioaccumulation in various plant compartments and PFAAs transfer to aerial plant parts were compared with the results obtained in the soil uptake experiments (Chapter 3).

Chapter 6, entitled “*Predicting the human exposure to perfluoroalkyl acids (PFAAs) through diet: The case of the Veneto Region, Italy*” is in preparation for submission to a peer-reviewed journal. Andrea Gredelj designed the introduced modelling framework, performed all the simulations and drafted the manuscript. In this work, one-compartment steady-state pharmacokinetic models for farm animals are integrated with the crop uptake models for nine PFAAs (Chapter 4) into the modelling framework for predicting the human exposure to PFAAs through terrestrial (agricultural) food web. Human exposure was predicted for the Veneto Region through the integration with regional food consumption data and exposure scenarios were developed based on measured aquatic concentrations (surface- and groundwater). Additionally, crop models’ connections with irrigation

water were validated by multi-compartmental concentrations measured around a Chinese fluorochemical plant (Liu et al., 2019, 2016).

1.4. References

- 3M, 2000. Phase-out plan for POSF-based products. Maplewood, Minnesota.
- Ahrens, L., Bundschuh, M., 2014. Fate and effects of poly- and perfluoroalkyl substances in the aquatic environment: A review. *Environ. Toxicol. Chem.* 33, 1921–1929. <https://doi.org/10.1002/etc.2663>
- Ahrens, L., Shoeib, M., Harner, T., Lee, S.C., Guo, R., Reiner, E.J., 2011. Wastewater treatment plant and landfills as sources of polyfluoroalkyl compounds to the atmosphere. *Env. Sci Technol* 45.
- Ahrens, Lutz, Yeung, L.W.Y., Taniyasu, S., Lam, P.K.S., Yamashita, N., 2011. Partitioning of perfluorooctanoate (PFOA), perfluorooctane sulfonate (PFOS) and perfluorooctane sulfonamide (PFOSA) between water and sediment. *Chemosphere* 85, 731–737. <https://doi.org/10.1016/j.chemosphere.2011.06.046>
- ARPAV, 2018a. Contaminazione da PFAS Azioni ARPAV (PFAS contamination actions of the Regional Environmental Protection Agency of Veneto). Padova.
- ARPAV, 2018b. Concentrations of the Perfluoroalkyl substances in the waters of Veneto region, Open data on PFASs monitoring, from 02/07/2013 to 20/09/2018 [WWW Document]. URL <http://www.arpa.veneto.it/dati-ambientali/open-data/idrosfera/concentrazione-di-sostanze-perfluoroalchiliche-pfas-nelle-acque-prelevate-da-arpav> (accessed 11.25.18).
- ATSDR, 2018. Toxicological Profile for Polyfluoroalkyls - draft for Public Comment. Atlanta.
- Bizkarguenaga, E., Zabaleta, I., Mijangos, L., Iparraguirre, A., Fernández, L.A., Prieto, A., Zuloaga, O., 2016. Uptake of perfluorooctanoic acid, perfluorooctane sulfonate and perfluorooctane sulfonamide by carrot and lettuce from compost amended soil. *Sci. Total Environ.* <https://doi.org/10.1016/j.scitotenv.2016.07.010>
- Blaine, A.C., Rich, C.D., Hundal, L.S., Lau, C., Mills, M.A., Harris, K.M., Higgins, C.P., 2013. Uptake of perfluoroalkyl acids into edible crops via land applied biosolids: Field and greenhouse studies. *Environ. Sci. Technol.* 47, 14062–14069. <https://doi.org/10.1021/es403094q>
- Blaine, A.C., Rich, C.D., Sedlacko, E.M., Hundal, L.S., Kumar, K., Lau, C., Mills, M.A., Harris, K.M., Higgins, C.P., 2014a. Perfluoroalkyl acid distribution in various plant compartments of edible crops grown in biosolids-amended soils. *Environ. Sci. Technol.* 48, 7858–7865. <https://doi.org/10.1021/es500016s>
- Blaine, A.C., Rich, C.D., Sedlacko, E.M., Hyland, K.C., Stushnoff, C., Dickenson, E.R. V., Higgins, C.P., 2014b. Perfluoroalkyl Acid Uptake in Lettuce (*Lactuca sativa*) and Strawberry (*Fragaria ananassa*) Irrigated with Reclaimed Water. *Environ. Sci. Technol.* 48, 14361–14368. <https://doi.org/10.1021/es504150h>
- Borg, D., Hakansson, H., 2012. Environmental and Health Risk Assessment of Perfluoroalkylated and Polyfluoroalkylated Substances (PFASs) in Sweden.
- Brendel, S., Fetter, É., Staude, C., Vierke, L., Biegel-Engler, A., 2018. Short-chain perfluoroalkyl acids: environmental concerns and a regulatory strategy under REACH. *Environ. Sci. Eur.* 30, 9. <https://doi.org/10.1186/s12302-018-0134-4>

- Brusseu, M.L., 2018. Assessing the potential contributions of additional retention processes to PFAS retardation in the subsurface. *Sci. Total Environ.* 613–614, 176–185. <https://doi.org/10.1016/j.scitotenv.2017.09.065>
- Buck, R.C., Franklin, J., Berger, U., Conder, J.M., Cousins, I.T., de Voogt, P., Jensen, A.A., Kannan, K., Mabury, S.A., van Leeuwen, S.P., 2011. Perfluoroalkyl and polyfluoroalkyl substances in the environment: Terminology, classification, and origins. *Integr. Environ. Assess. Manag.* 7, 513–541. <https://doi.org/10.1002/ieam.258>
- Campos Pereira, H., Ullberg, M., Kleja, D.B., Gustafsson, J.P., Ahrens, L., 2018. Sorption of perfluoroalkyl substances (PFASs) to an organic soil horizon – Effect of cation composition and pH. *Chemosphere* 207, 183–191. <https://doi.org/10.1016/j.chemosphere.2018.05.012>
- Cariou, R., Veyrand, B., Yamada, A., Berrebi, A., Zalko, D., Durand, S., Pollono, C., Marchand, P., Leblanc, J.C., Antignac, J.P., Le Bizec, B., 2015. Perfluoroalkyl acid (PFAA) levels and profiles in breast milk, maternal and cord serum of French women and their newborns. *Environ. Int.* 84, 71–81. <https://doi.org/10.1016/j.envint.2015.07.014>
- Chang, S.C., Das, K., Ehresman, D.J., Ellefson, M.E., Gorman, G.S., Hart, J.A., Noker, P.E., Tan, Y.M., Lieder, P.H., Lau, C., Olsen, G.W., Butenhoff, J.L., 2008. Comparative pharmacokinetics of perfluorobutyrate in rats, mice, monkeys, and humans and relevance to human exposure via drinking water. *Toxicol. Sci.* 104, 40–53. <https://doi.org/10.1093/toxsci/kfn057>
- Cheng, W., Ng, C.A., 2018. Predicting Relative Protein Affinity of Novel Per- and Polyfluoroalkyl Substances (PFASs) by An Efficient Molecular Dynamics Approach. *Environ. Sci. Technol.* 52, 7972–7980. <https://doi.org/10.1021/acs.est.8b01268>
- Conder, J.M., Hoke, R.A., De Wolf, W., Russell, M.H., Buck, R.C., 2008. Are PFCAs bioaccumulative? A critical review and comparison with regulatory criteria and persistent lipophilic compounds. *Environ. Sci. Technol.* 42, 995–1003. <https://doi.org/10.1021/es070895g>
- Cordner, A., De La Rosa, V.Y., Schaidler, L.A., Rudel, R.A., Richter, L., Brown, P., 2019. Guideline levels for PFOA and PFOS in drinking water: the role of scientific uncertainty, risk assessment decisions, and social factors. *J. Expo. Sci. Environ. Epidemiol.* 29, 157–171. <https://doi.org/10.1038/s41370-018-0099-9>
- Council of the European Union, 2018. Proposal for a DIRECTIVE OF THE EUROPEAN PARLIAMENT AND OF THE COUNCIL on the quality of water intended for human consumption (recast). Brussels.
- Cousins, I.T., Goldenman, G., Herzke, D., Lohmann, R., Miller, M., Ng, C.A., Patton, S., Scheringer, M., Trier, X., Vierke, L., Wang, Z., DeWitt, J.C., 2019. The concept of essential use for determining when uses of PFASs can be phased out. *Environ. Sci. Process. Impacts.* <https://doi.org/10.1039/c9em00163h>
- Cousins, I.T., Vestergren, R., Wang, Z., Scheringer, M., McLachlan, M.S., 2016. The precautionary principle and chemicals management: The example of perfluoroalkyl acids in groundwater. *Environ. Int.* 94, 331–340. <https://doi.org/10.1016/j.envint.2016.04.044>

- Dauwe, T., Van de Vijver, K., De Coen, W., Eens, M., 2007. PFOS levels in the blood and liver of a small insectivorous songbird near a fluorochemical plant. *Environ. Int.* 33, 357–361. <https://doi.org/10.1016/j.envint.2006.11.014>
- DeWitt, J., Berger, U., Miller, M., Green, C., Huang, J., Perkola, N., Vierke, L., Higgins, C., Buser, A.M., Lindstrom, A.B., Boucher, J.M., Lau, C.S., Knepper, T., Liu, J., Wang, Z., Herzke, D., Ahrens, L., Hung, H., Cousins, I., van der Jagt, K., Bopp, S.K., Fletcher, T., Leinala, E., Scheringer, M., Småstuen Haug, L., Borg, D., Ritscher, A., Valsecchi, S., Shi, Y., Ohno, K., Trier, X., Bintein, S., 2018. Zürich Statement on Future Actions on Per- and Polyfluoroalkyl Substances (PFASs). *Environ. Health Perspect.* 126, 084502. <https://doi.org/10.1289/ehp4158>
- Dewitt, J.C., 2015. *Toxicological Effects of Perfluoroalkyl and Polyfluoroalkyl Substances, Molecular and Integrative Toxicology.* Springer International Publishing, Cham. <https://doi.org/10.1007/978-3-319-15518-0>
- Ding, G., Peijnenburg, W.J.G.M., 2013. Physicochemical Properties and Aquatic Toxicity of Poly- and Perfluorinated Compounds. *Crit. Rev. Environ. Sci. Technol.* 43, 598–678. <https://doi.org/10.1080/10643389.2011.627016>
- Droge, S.T.J., 2019. Membrane-Water Partition Coefficients to Aid Risk Assessment of Perfluoroalkyl Anions and Alkyl Sulfates. *Environ. Sci. Technol.* 53, 760–770. <https://doi.org/10.1021/acs.est.8b05052>
- Du, Z., Deng, S., Bei, Y., Huang, Q., Wang, B., Huang, J., Yu, G., 2014. Adsorption behavior and mechanism of perfluorinated compounds on various adsorbents-A review. *J. Hazard. Mater.* 274, 443–454. <https://doi.org/10.1016/j.jhazmat.2014.04.038>
- ECHA/SEAC/RAC, 2018. Opinion on an Annex XV dossier proposing restrictions on PFNA, PFDA, PFUnDA, PFTTrDA, PFTDA; their salts and precursors. Helsinki.
- ECHA, 2019. Inclusion of Substances of Very High Concern in the Candidate List for eventual inclusion in Annex XIV. Helsinki.
- ECHA, 2017a. Inclusion of substances of very high concern in the Candidate List for eventual inclusion in Annex XIV (Decision of the European Chemicals Agency), PFDA. Helsinki.
- ECHA, 2017b. Inclusion of substances of very high concern in the Candidate List for eventual inclusion in Annex XIV (Decision of the European Chemicals Agency), PFHxS. Helsinki.
- ECHA, 2017c. One new substance added to the Candidate List, several entries updated [WWW Document]. ECHA/PR/17/14. URL <https://echa.europa.eu/-/one-new-substance-added-to-the-candidate-list> (accessed 10.6.17).
- ECHA, 2014. ANNEX XV Restriction report proposal for a restriction (PFOA). Helsinki.
- ECHA, 2013. Member state committee support document for identification of pentadecafluorooctanoic acid (PFOA) as a substance of very high concern because of its CMR and PBT properties.
- ECHA, 2008. Guidance on information requirements and chemical safety assessment Chapter R.10: Characterisation of dose [concentration] - response for environment.

- EFSA, 2008. Perfluorooctane sulfonate (PFOS), perfluorooctanoic acid (PFOA) and their salts Scientific Opinion of the Panel on Contaminants in the Food chain. *EFSA J.* 6, 1–131. <https://doi.org/10.2903/j.efsa.2008.653>
- EFSA CONTAM, 2018. Risk to human health related to the presence of perfluorooctane sulfonic acid and perfluorooctanoic acid in food. *EFSA J.* 16, 284. <https://doi.org/10.2903/j.efsa.2018.5194>
- Environment and Climate Change Canada, 2018. Federal Environmental Quality Guidelines Perfluorooctane Sulfonate (PFOS).
- Eriksson, U., Haglund, P., Kärrman, A., 2017. Contribution of precursor compounds to the release of per- and polyfluoroalkyl substances (PFASs) from waste water treatment plants (WWTPs). *J. Environ. Sci.* 61, 80–90. <https://doi.org/10.1016/j.jes.2017.05.004>
- Eschauzier, C., Raat, K.J., Stuyfzand, P.J., Voogt, P. De, 2013. Perfluorinated alkylated acids in groundwater and drinking water: Identification, origin and mobility. *Sci. Total Environ.* 460, 477–485. <https://doi.org/10.1016/j.scitotenv.2013.04.066>
- European Commission, 2011. Common Implementation Strategy for the Water Framework Directive (2000/60 /EC) Guidance Document No. 27 Technical Guidance For Deriving Environmental Quality Standards. <https://doi.org/10.2779/43816>
- European Commission, 2006. Regulation (EC) No 1907/2006 - REACH. European Union.
- European Commission, 2003. Technical Guidance Document on Risk Assessment in support of Commission Directive 93/67/EEC on Risk Assessment for new notified substances, Commission Regulation (EC) No 1488/94 on Risk Assessment for existing substances, and Directive 98/8/EC of the Euro. Ispra.
- European Commission Subgroup on Review of the Priority Substances List, 2011. EQS dossier for PFOS.
- European Community, 2000. Directive 2000/60/EC. Official Journal of the European Communities, European Union. <https://doi.org/10.1039/ap9842100196>
- Fairman, R., Mead, C.D., Williams, P.W., 1998. Chapter 6: Ecological Risk Assessment, in: *Environmental Risk Assessment: Approaches, Experiences and Information Sources*. Copenhagen: European Environment Agency, 1998., Copenhagen.
- Falk, S., Stahl, T., Fliedner, A., Rüdell, H., Tarricone, K., Brunn, H., Koschorreck, J., 2019. Levels, accumulation patterns and retrospective trends of perfluoroalkyl acids (PFAAs) in terrestrial ecosystems over the last three decades. *Environ. Pollut.* 246, 921–931. <https://doi.org/10.1016/j.envpol.2018.12.095>
- Felizeter, S., McLachlan, M.S., De Voogt, P., 2014. Root uptake and translocation of perfluorinated alkyl acids by three hydroponically grown crops_supp. *J. Agric. Food Chem.* 62, 3334–3342. <https://doi.org/10.15713/ins.mmj.3>
- Felizeter, S., McLachlan, M.S., De Voogt, P., 2012. Uptake of perfluorinated alkyl acids by hydroponically grown lettuce (*Lactuca sativa*). *Environ. Sci. Technol.* 46, 11735–11743. <https://doi.org/10.1021/es302398u>

- Fromme, H., Tittlemier, S.A., Volkel, W., Wilhelm, M., Twardella, D., 2009. Perfluorinated compounds---exposure assessment for the general population in western countries. *Int J Hyg Env. Heal.* 212.
- FSANS, 2017. Consolidated Report - Perfluorinated chemicals in food .
- Gewurtz, S.B., Bhavsar, S.P., Petro, S., Mahon, C.G., Zhao, X., Morse, D., Reiner, E.J., Tittlemier, S.A., Braekevelt, E., Drouillard, K., 2014. High levels of perfluoroalkyl acids in sport fish species downstream of a firefighting training facility at Hamilton International Airport, Ontario, Canada. *Environ. Int.* 67, 1–11. <https://doi.org/10.1016/j.envint.2014.02.005>
- Ghisi, R., Vamerali, T., Manzetti, S., 2019. Accumulation of perfluorinated alkyl substances (PFAS) in agricultural plants: A review. *Environ. Res.* 169, 326–341. <https://doi.org/10.1016/j.envres.2018.10.023>
- Giesy, J.P., Kannan, K., 2001. Global distribution of perfluorooctane sulfonate in wildlife. *Environ. Sci. Technol.* 35, 1339–1342. <https://doi.org/10.1021/es001834k>
- Gobelius, L., Lewis, J., Ahrens, L., 2017. Plant Uptake of Per- and Polyfluoroalkyl Substances at a Contaminated Fire Training Facility to Evaluate the Phytoremediation Potential of Various Plant Species. *Environ. Sci. Technol.* 51, 12602–12610. <https://doi.org/10.1021/acs.est.7b02926>
- Goldenman, G., Fernandes, M., Holland, M., Tugran, T., Nordin, A., Schoumacher, C., McNeill, A., 2019. The cost of inaction: A socioeconomic analysis of environmental and health impacts linked to exposure to PFAS. Copenhagen. <https://doi.org/10.1787/9789264111905-graph12-en>
- González-Gaya, B., Casal, P., Jurado, E., Dachs, J., Jimenez, begona, 2019. Vertical Transport and Sinks of Perfluoroalkyl Substances in the Global Open Ocean. *Environ. Sci. Process. Impacts.* <https://doi.org/10.1039/c9em00266a>
- Gredelj, A., Barausse, A., Grechi, L., Palmeri, L., 2018. Deriving predicted no-effect concentrations (PNECs) for emerging contaminants in the river Po, Italy, using three approaches: Assessment factor, species sensitivity distribution and AQUATOX ecosystem modelling. *Environ. Int.* 119, 66–78. <https://doi.org/10.1016/j.envint.2018.06.017>
- Gredelj, A., Nicoletto, C., Valsecchi, S., Ferrario, C., Polesello, S., Lava, R., Zanon, F., Barausse, A., Palmeri, L., Guidolin, L., Bonato, M., 2019a. Uptake and translocation of perfluoroalkyl acids (PFAA) in red chicory (*Cichorium intybus L.*) under various treatments with pre-contaminated soil and irrigation water. *Sci. Total Environ.* <https://doi.org/10.1016/j.scitotenv.2019.134766>
- Gredelj, A., Polesel, F., Trapp, S., 2019b. Model-based analysis of the uptake of per- and polyfluoroalkyl acids (PFAAs) from soil into plants. Accepted for publication in *Chemosphere*
- Hamid, H., Li, L.Y., Grace, J.R., 2018. Review of the fate and transformation of per- and polyfluoroalkyl substances (PFASs) in landfills. *Environ. Pollut.* 235, 74–84. <https://doi.org/10.1016/j.envpol.2017.12.030>
- Hansen, K.J., Clemen, L.A., Ellefson, M.E., Johnson, H.O., 2001. Compound-specific, quantitative characterization of organic fluorochemicals in biological matrices. *Environ. Sci. Technol.* 35, 766–770. <https://doi.org/10.1021/es001489z>

- Higgins, C.P., Luthy, R.G., 2006. Sorption of perfluorinated surfactants on sediments. *Environ. Sci. Technol.* 40, 7251–7256. <https://doi.org/10.1021/es061000n>
- Ingelido, A.M., Abballe, A., Gemma, S., Dellatte, E., Iacovella, N., Angelis, G. De, Zampaglioni, F., Marra, V., Miniero, R., Valentini, S., Russo, F., Vazzoler, M., Testai, E., Felip, E. De, 2018. Biomonitoring of per fluorinated compounds in adults exposed to contaminated drinking water in the Veneto Region, Italy. *Environ. Int.* 110, 149–159. <https://doi.org/10.1016/j.envint.2017.10.026>
- Jian, J.M., Chen, D., Han, F.J., Guo, Y., Zeng, L., Lu, X., Wang, F., 2018. A short review on human exposure to and tissue distribution of per- and polyfluoroalkyl substances (PFASs). *Sci. Total Environ.* 636, 1058–1069. <https://doi.org/10.1016/j.scitotenv.2018.04.380>
- Johansson, J.H., Yan, H., Berger, U., Cousins, I.T., 2017. Water-to-air transfer of branched and linear PFOA: Influence of pH, concentration and water type. *Emerg. Contam.* 3, 46–53. <https://doi.org/10.1016/j.emcon.2017.03.001>
- Kempisty, D.M., Xing, Y., Racz, L., 2018. *Perfluoroalkyl Substances in the Environment: Theory, Practice and Innovation*, Environmental and occupational health series. CRC Press, Boca Raton. <https://doi.org/10.1201/9780429487125>
- Krafft, M.P., Riess, J.G., 2015a. Per- and polyfluorinated substances (PFASs): Environmental challenges. *Curr. Opin. Colloid Interface Sci.* 20, 192–212. <https://doi.org/10.1016/j.cocis.2015.07.004>
- Krafft, M.P., Riess, J.G., 2015b. Selected physicochemical aspects of poly- and perfluoroalkylated substances relevant to performance, environment and sustainability-Part one. *Chemosphere* 129, 4–19. <https://doi.org/10.1016/j.chemosphere.2014.08.039>
- Krippner, J., Falk, S., Brunn, H., Georgii, S., Schubert, S., Stahl, T., 2015. Accumulation Potentials of Perfluoroalkyl Carboxylic Acids (PFCAs) and Perfluoroalkyl Sulfonic Acids (PFSA) in Maize (*Zea mays*). *J. Agric. Food Chem.* 63, 3646–3653. <https://doi.org/10.1021/acs.jafc.5b00012>
- Li, F., Fang, X., Zhou, Z., Liao, X., Zou, J., Yuan, B., Sun, W., 2018. Adsorption of perfluorinated acids onto soils: Kinetics, isotherms, and influences of soil properties. *Sci. Total Environ.* 649, 504–514. <https://doi.org/https://doi.org/10.1016/j.scitotenv.2018.08.209>
- Li, Y., Oliver, D.P., Kookana, R.S., 2018. A critical analysis of published data to discern the role of soil and sediment properties in determining sorption of per and polyfluoroalkyl substances (PFASs). *Sci. Total Environ.* 628–629, 110–120. <https://doi.org/10.1016/j.scitotenv.2018.01.167>
- Liu, Z., Lu, Y., Shi, Y., Wang, P., Jones, K., Sweetman, A.J., Johnson, A.C., Zhang, M., Zhou, Y., Lu, X., Su, C., Sarvajayakesavaluc, S., Khan, K., 2017. Crop bioaccumulation and human exposure of perfluoroalkyl acids through multi-media transport from a mega fluorochemical industrial park, China. *Environ. Int.* 106, 37–47. <https://doi.org/10.1016/j.envint.2017.05.014>
- Liu, Z., Lu, Y., Song, X., Jones, K., Sweetman, A.J., Johnson, A.C., Zhang, M., Lu, X., Su, C., 2019. Multiple crop bioaccumulation and human exposure of perfluoroalkyl substances around a mega fluorochemical industrial park, China: Implication for planting optimization and food safety. *Environ. Int.* 127, 671–684. <https://doi.org/10.1016/j.envint.2019.04.008>

- Liu, Z., Lu, Y., Wang, T., Wang, P., Li, Q., Johnson, A.C., Sarvajayakesavalu, S., Sweetman, A.J., 2016. Risk assessment and source identification of perfluoroalkyl acids in surface and ground water: Spatial distribution around a mega-fluorochemical industrial park, China. *Environ. Int.* 91, 69–77. <https://doi.org/10.1016/j.envint.2016.02.020>
- Loos, R., Locoro, G., Huber, T., Wollgast, J., Christoph, E.H., Jager, A. De, Gawlik, B.M., Hanke, G., Umlauf, G., 2008. Analysis of perfluorooctanoate (PFOA) and other perfluorinated compounds (PFCs) in the River Po watershed in N-Italy. *Chemosphere* 71, 306–313. <https://doi.org/10.1016/j.chemosphere.2007.09.022>
- Mackay, D., 2001. *Multimedia Environmental Models: The Fugacity Approach*, Second Edition. Lewis Publishers, Boca Raton, Florida. <https://doi.org/10.1201/9781420032543>
- MacLeod, M., Scheringer, M., McKone, T.E., Hungerbuhler, K., 2010. The state of multimedia mass-balance modeling in environmental science and decision-making. *Environ. Sci. Technol.* 44, 8360–8364. <https://doi.org/10.1021/es100968w>
- Martin, J.W., Mabury, S.A., Solomon, K.R., Muir, D.C.G., 2003. Bioconcentration and tissue distribution of perfluorinated acids in Rainbow trout (*Oncorhynchus mykiss*). *Environ. Toxicol. Chem.* 22, 196–204. <https://doi.org/10.1002/etc.5620220126>
- Mastrantonio, M., Bai, E., Uccelli, R., Cordiano, V., Screpanti, A., Crosignani, P., 2018. Drinking water contamination from perfluoroalkyl substances (PFAS): an ecological mortality study in the Veneto Region, Italy. *Eur. J. Public Health* 28, 180–185. <https://doi.org/10.1093/eurpub/ckx066>
- McCarthy, C., Kappleman, W., DiGuseppi, W., 2017. Ecological Considerations of Per- and Polyfluoroalkyl Substances (PFAS). *Curr. Pollut. Reports* 3, 289–301. <https://doi.org/10.1007/s40726-017-0070-8>
- McLachlan, M.S., Felizeter, S., Klein, M., Kotthoff, M., De Voogt, P., 2019. Fate of a perfluoroalkyl acid mixture in an agricultural soil studied in lysimeters. *Chemosphere* 223, 180–187. <https://doi.org/10.1016/j.chemosphere.2019.02.012>
- McLachlan, M.S., Holmstro, K.E., Reth, M., Berger, U., 2007. Riverine Discharge of Perfluorinated Carboxylates from the European Continent. *Environ. Sci. Technol.* 41, 7260–7265. <https://doi.org/10.1021/es071471p>
- Milinic, J., Lacorte, S., Vidal, M., Rigol, A., 2015. Sorption behaviour of perfluoroalkyl substances in soils. *Sci. Total Environ.* 511, 63–71. <https://doi.org/10.1016/j.scitotenv.2014.12.017>
- Müller, C.E., Lefevre, G.H., Timofte, A.E., Hussain, F.A., Sattely, E.S., Luthy, R.G., 2016. Competing mechanisms for perfluoroalkyl acid accumulation in plants revealed using an Arabidopsis model system. *Environ. Toxicol. Chem.* 35, 1138–1147. <https://doi.org/10.1002/etc.3251>
- Munoz, G., Desrosiers, M., Duy, S.V., Labadie, P., Budzinski, H., Liu, J., Sauvé, S., 2017. Environmental Occurrence of Perfluoroalkyl Acids and Novel Fluorotelomer Surfactants in the Freshwater Fish *Catostomus commersonii* and Sediments Following Firefighting Foam Deployment at the Lac-Mégantic Railway Accident. *Environ. Sci. Technol.* 51, 1231–1240. <https://doi.org/10.1021/acs.est.6b05432>
- Navarro, I., de la Torre, A., Sanz, P., Porcel, M.Á., Pro, J., Carbonell, G., Martínez, M. de los Á., 2017. Uptake of perfluoroalkyl substances and halogenated flame retardants by crop plants

- grown in biosolids-amended soils. *Environ. Res.* 152, 199–206. <https://doi.org/10.1016/j.envres.2016.10.018>
- Ng, C.A., Hungerbühler, K., 2014. Bioaccumulation of perfluorinated alkyl acids: Observations and models. *Environ. Sci. Technol.* 48, 4637–4648. <https://doi.org/10.1021/es404008g>
- Nicoletto, C., Maucieri, C., Sambo, P., 2017. Effects on Water Management and Quality Characteristics of Ozone Application in Chicory Forcing Process: A Pilot System. *Agronomy* 7, 29. <https://doi.org/10.3390/agronomy7020029>
- OECD, 2002. Hazard Assessment of PFOS and its salts, ENV/JM/RD(2002)17/FINAL.
- Olsen, G.W., Burriss, J.M., Ehresman, D.J., Froehlich, J.W., Seacat, A.M., Butenhoff, J.L., Zobel, L.R., 2007. Half-Life of Serum Elimination of Perfluorooctanesulfonate, Perfluorohexanesulfonate, and Perfluorooctanoate in Retired Fluorochemical Production Workers. *Environ. Health Perspect.* 115, 1298–1305. <https://doi.org/10.1289/ehp.10009>
- Olsen, G.W., Chang, S.C., Noker, P.E., Gorman, G.S., Ehresman, D.J., Lieder, P.H., Butenhoff, J.L., 2009. A comparison of the pharmacokinetics of perfluorobutanesulfonate (PFBS) in rats, monkeys, and humans. *Toxicology* 256, 65–74. <https://doi.org/10.1016/j.tox.2008.11.008>
- Pelch, K.E., Reade, A., Wolffe, T.A.M., Kwiatkowski, C.F., 2019. PFAS health effects database: Protocol for a systematic evidence map. *Environ. Int.* 130. <https://doi.org/10.1016/j.envint.2019.05.045>
- Prevedouros, K., Cousins, I.T., Buck, R.C., Korzeniowski, S.H., 2006. Sources, fate and transport of perfluorocarboxylates. *Environ. Sci. Technol.* 40, 32–44. <https://doi.org/10.1021/es0512475>
- Sepulvado, J.G., Blaine, A.C., Hundal, L.S., Higgins, C.P., 2011. Occurrence and fate of perfluorochemicals in soil following the land application of municipal biosolids. *Environ. Sci. Technol.* 45, 8106–8112. <https://doi.org/10.1021/es103903d>
- Smith, J.W.N., Beuthe, B., Dunk, M., Demeure, S., Carmona, J.M.M., Medve, A., Spence, M.J., Pancras, T., Schrauwen, G., Held, T., Baker, K., Ross, I., Slenders, H., 2016. Environmental fate and effects of poly- and perfluoroalkyl substances (PFAS). Brussels.
- Stahl, T., Heyn, J., Thiele, H., Huther, J., Failing, K., Georgii, S., Brunn, H., 2009. Carryover of perfluorooctanoic acid (PFOA) and perfluorooctane sulfonate (PFOS) from soil to plants. *Arch. Environ. Contam. Toxicol.* 57.
- Sznajder-Katarzyńska, K., Surma, M., Cieślak, I., 2019. A Review of Perfluoroalkyl Acids (PFAAs) in terms of Sources, Applications, Human Exposure, Dietary Intake, Toxicity, Legal Regulation, and Methods of Determination. *J. Chem.* 2019. <https://doi.org/10.1155/2019/2717528>
- Taniyasu, S., Kannan, K., Horii, Y., Hanari, N., Yamashita, N., 2003. A survey of perfluorooctane sulfonate and related perfluorinated organic compounds in water, fish, birds, and humans from Japan. *Environ. Sci. Technol.* 37, 2634–2639. <https://doi.org/10.1021/es0303440>
- The European Parliament and the Council of the European Union, 2013. Directive 2013/39/EC. Official Journal of the European Communities, European Union. <https://doi.org/http://dx.doi.org/http://eur-lex.europa.eu/legal-content/EN/TXT/?uri=celex:32013L0039>

- Thomaidi, V.S., Matsoukas, C., Stasinakis, A.S., 2017. Risk assessment of triclosan released from sewage treatment plants in European rivers using a combination of risk quotient methodology and Monte Carlo simulation. *Sci. Total Environ.* 603–604, 487–494. <https://doi.org/10.1016/j.scitotenv.2017.06.113>
- Trapp, S., 2015. Calibration of a plant uptake model with plant- and site-specific data for uptake of chlorinated organic compounds into radish. *Environ. Sci. Technol.* 49, 395–402. <https://doi.org/10.1021/es503437p>
- Trapp, S., 2007. Fruit tree model for uptake of organic compounds from soil and air. *SAR QSAR Environ. Res.* 18, 367–387. <https://doi.org/10.1080/10629360701303693>
- Trapp, S., Matthies, M., 1998. *Chemodynamics and Environmental Modeling, An introduction.* Springer-Verlag Berlin Heidelberg, Berlin Heideberg.
- Trapp, S., Matthies, M., 1995. Generic One-Compartment Model for Uptake of Organic Chemicals by Foliar Vegetation. *Environ. Sci. Technol.* 29, 2333–2338. <https://doi.org/10.1021/es00009a027>
- Trier, X., Granby, K., Christensen, J.H., 2011. Polyfluorinated surfactants (PFS) in paper and board coatings for food packaging. *Environ. Sci. Pollut. Res.* 18, 1108–1120. <https://doi.org/10.1007/s11356-010-0439-3>
- UNEP, 2009. Report of the Conference of the Parties of the Stockholm Convention on Persistent Organic Pollutants on the work of its fourth meeting, Stockholm Convention on Persistent Organic Pollutants. Geneva.
- US Government/USEPA, 2016. Lifetime Health Advisories and Health Effects Support Documents for Perfluorooctanoic Acid and Perfluorooctane Sulfonate.
- USEPA, 2019. EPA's Per- and Polyfluoroalkyl Substances (PFAS) Action Plan.
- USEPA, 2016a. Drinking Water Health Advisory for perfluorooctanoic acid (PFOA). Washington DC.
- USEPA, 2016b. Drinking Water Health Advisory for Perfluorooctane Sulfonate (PFOS). Washington DC.
- Valsecchi, S., Rusconi, M., Mazzoni, M., Viviano, G., Pagnotta, R., Zaghi, C., Serrini, G., Polesello, S., 2015. Occurrence and sources of perfluoroalkyl acids in Italian river basins. *Chemosphere* 129, 126–134. <https://doi.org/10.1016/j.chemosphere.2014.07.044>
- Vestergren, R., Cousins, I.T., 2009. Tracking the pathways of human exposure to perfluorocarboxylates. *Environ. Sci. Technol.* 43, 5565–5575. <https://doi.org/10.1021/es900228k>
- Vierke, L., Möller, A., Klitzke, S., 2014. Transport of perfluoroalkyl acids in a water-saturated sediment column investigated under near-natural conditions. *Environ. Pollut.* 186, 7–13. <https://doi.org/10.1016/j.envpol.2013.11.011>
- Wang, Z., Cousins, I.T., Scheringer, M., Hungerbuehler, K., 2015. Hazard assessment of fluorinated alternatives to long-chain perfluoroalkyl acids (PFAAs) and their precursors: Status quo, ongoing challenges and possible solutions. *Environ. Int.* 75, 172–179. <https://doi.org/10.1016/j.envint.2014.11.013>

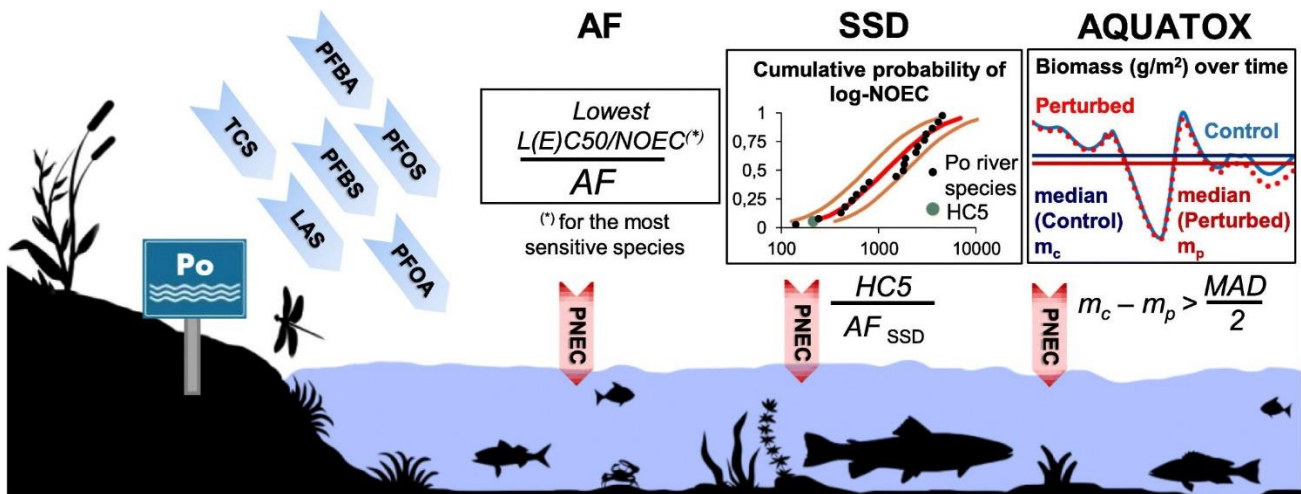
- Wang, Z., Dewitt, J.C., Higgins, C.P., Cousins, I.T., 2017. A Never-Ending Story of Per- and Polyfluoroalkyl Substances (PFASs)? *Environ. Sci. Technol.* 51, 2508–2518. <https://doi.org/10.1021/acs.est.6b04806>
- Wen, B., Li, L., Zhang, H., Ma, Y., Shan, X.Q., Zhang, S., 2014. Field study on the uptake and translocation of perfluoroalkyl acids (PFAAs) by wheat (*Triticum aestivum* L.) grown in biosolids-amended soils. *Environ. Pollut.* 184, 547–554. <https://doi.org/10.1016/j.envpol.2013.09.040>
- WHO, 2016. Keeping our water clean: the case of water contamination in the Veneto Region, Italy. AREAGRAPHICA SNC DI TREVISAN GIANCARLO & FIGLI, Venice, Italy.
- Winkens, K., Vestergren, R., Berger, U., Cousins, I.T., 2017. Early life exposure to per- and polyfluoroalkyl substances (PFASs): A critical review. *Emerg. Contam.* 3, 55–68. <https://doi.org/10.1016/j.emcon.2017.05.001>
- Wright-Walters, M., Volz, C., Talbott, E., Davis, D., 2011. An updated weight of evidence approach to the aquatic hazard assessment of Bisphenol A and the derivation a new predicted no effect concentration (PNEC) using a non-parametric methodology. *Sci. Total Environ.* 409, 676–685. <https://doi.org/10.1016/j.scitotenv.2010.07.092>
- Xiang, L., Chen, L., Yu, L.-Y., Yu, P.-F., Zhao, H.-M., Mo, C.-H., Li, Y.-W., Li, H., Cai, Q.-Y., Zhou, D.-M., Wong, M.-H., 2018. Genotypic variation and mechanism in uptake and translocation of perfluorooctanoic acid (PFOA) in lettuce (*Lactuca sativa* L.) cultivars grown in PFOA-polluted soils. *Sci. Total Environ.* 636, 999–1008. <https://doi.org/10.1016/j.scitotenv.2018.04.354>
- Xiao, F., 2017. Emerging poly- and perfluoroalkyl substances in the aquatic environment: A review of current literature. *Water Res.* 124, 482–495. <https://doi.org/10.1016/j.watres.2017.07.024>
- Zaggia, A., Conte, L., Falletti, L., Fant, M., Chiorboli, A., 2016. Use of strong anion exchange resins for the removal of perfluoroalkylated substances from contaminated drinking water in batch and continuous pilot plants. *Water Res.* 91, 137–146. <https://doi.org/10.1016/j.watres.2015.12.039>
- Zareitalabad, P., Siemens, J., Hamer, M., Amelung, W., 2013. Perfluorooctanoic acid (PFOA) and perfluorooctanesulfonic acid (PFOS) in surface waters, sediments, soils and wastewater - A review on concentrations and distribution coefficients. *Chemosphere* 91, 725–732. <https://doi.org/10.1016/j.chemosphere.2013.02.024>
- Zhao, Z., Xie, Z., Möller, A., Sturm, R., Tang, J., Zhang, G., Ebinghaus, R., 2012. Distribution and long-range transport of polyfluoroalkyl substances in the Arctic, Atlantic Ocean and Antarctic coast. *Environ. Pollut.* 170, 71–77. <https://doi.org/10.1016/j.envpol.2012.06.004>
- Zhu, Z., Wang, T., Wang, P., Lu, Y., Giesy, J.P., 2014. Perfluoroalkyl and polyfluoroalkyl substances in sediments from South Bohai coastal watersheds, China. *Mar. Pollut. Bull.* 85, 619–627. <https://doi.org/10.1016/j.marpolbul.2013.12.042>

Chapter 2

Deriving predicted no-effect concentrations (PNECs) for emerging contaminants in the river Po, Italy, using three approaches: assessment factor, species sensitivity distribution and AQUATOX ecosystem modelling

Andrea Gredelj^a, Alberto Barausse^a, Laura Grechi^a, Luca Palmeri^a

^a Environmental Systems Analysis Lab (LASA) research group, Department of Industrial Engineering, University of Padova, via Marzolo 9, 35131 Padova, Italy



Reproduced with permission from:

Environment International, 2018

Volume 119, October 2018, Pages 66-78

DOI: <https://doi.org/10.1016/j.envint.2018.06.017>

© 2018 Elsevier Ltd.

Chapter summary:

Over the past decades, per- and poly-fluoroalkyl substances (PFASs) found in environmental matrices worldwide have raised concerns due to their toxicity, ubiquity and persistence. A widespread pollution of groundwater and surface waters caused by PFASs in Northern Italy has been recently discovered, becoming a major environmental issue, also because the exact risk for humans and nature posed by this contamination is unclear. Here, the Po River in Northern Italy was selected as a study area to assess the ecological risk posed by perfluoroalkyl acids (PFAAs), a class of PFASs, considering the noticeable concentration of various PFAAs detected in the Po waters over the past years. Moreover, the Po has a large environmental and socio-economic importance: it is the largest Italian river and drains a densely inhabited, intensely cultivated and heavily industrialized watershed. Predicted no-effect concentrations (PNECs) were derived using two regulated methodologies, assessment factors (AFs) and species sensitivity distribution (SSD), which rely on published ecotoxicological laboratory tests. Results were compared to those of a novel methodology using the mechanistic ecosystem model AQUATOX to compute PNECs in an ecologically-sound manner, i.e. considering physical, chemical, biological and ecological processes in the river. The model was used to quantify how the biomasses of the modelled taxa in the river food web deviated from natural conditions due to varying inputs of the chemicals. PNEC for each chemical was defined as the lowest chemical concentration causing a non-negligible yearly biomass loss for a simulated taxon with respect to a control simulation. The investigated PFAAs were Perfluorooctanoic acid (PFOA) and Perfluorooctanesulfonic acid (PFOS) as long-chained compounds, and Perfluorobutanoic acid (PFBA) and Perfluorobutanesulfonic acid (PFBS) as short-chained homologues. Two emerging contaminants, Linear Alkylbenzene Sulfonate (LAS) and triclosan, were also studied to assess the performance of the three methodologies for chemicals whose ecotoxicology and environmental fate are well-studied. The most precautionary approach was the use of AFs generally followed by SSD and then AQUATOX, except for PFOS, for which AQUATOX yielded a much lower PNEC compared to the other approaches since, unlike the other two methodologies, it explicitly simulates sublethal toxicity and indirect ecological effects. Our findings highlight that neglecting the role of ecological processes when extrapolating from laboratory tests to ecosystems can result in under-protective threshold concentrations for chemicals. Ecosystem models can complement existing laboratory-based methodologies, and the use of multiple methods for deriving PNECs can help to clarify uncertainty in ecological risk estimates.

2.1. Introduction

Pollution is a major threat to aquatic ecosystems worldwide, impacting water quality and biodiversity and reducing the provision of ecosystem services which valuably contribute to human wellbeing (Duraiappah et al., 2005). Ecological risk assessment (ERA), the estimation of the risk posed by the presence of human-released chemicals to living organisms in ecosystems, is a fundamental step to guide management and inform policy towards sustainable solutions for mitigation of this threat. The basic steps of ERA include hazard identification, effects assessment, exposure assessment and risk characterization, where the main goal of the effects assessment is setting a safe threshold for the concentration of chemicals (Predicted No-effect Concentration, or PNEC), below which no adverse effect on ecosystem structure and functions are expected (De Laender et al., 2013; European Commission, 2003).

The foundation for ERA in the European Union is represented by several standardized procedures adopted for protecting ecosystems. The guidance for the implementation of the REACH (Registration, Evaluation, Authorisation and Restriction of Chemicals) regulation (REACH, EC, 2006), adopted to improve the protection of human health and environment from the risk posed by chemicals, and the Technical Guidance For Deriving Environmental Quality Standards as part of Common Implementation Strategy for implementation of the Water Framework Directive 2000/60/EC (European Community, 2000), provide a consistent approach to estimate ecologically-safe thresholds in aquatic ecosystems (ECHA, 2008; European Commission, 2011). Based on the abovementioned European regulations, PNECs can be derived in three manners: a deterministic approach based on the use of coefficients called assessment factors (AFs), a statistical approach based on the so-called species sensitivity distribution (SSD), and results from model ecosystems and field studies (European Commission, 2011). The most common approach is the use of assessment factors, where threshold exposure concentrations measured in the laboratory for individual species are extrapolated to populations in real-world ecosystems by dividing them by AFs, whose value depends on the amount and quality of available toxicity data (European Commission, 2011; Lei et al., 2010; Meli et al., 2014). When there is a sufficient amount of ecotoxicological data available for different taxa, the species sensitivity distribution (SSD) method is used instead (European Commission, 2011; Valsecchi et al., 2017). SSD is a cumulative probability distribution fitted to a set of toxicity thresholds for individual species of the ecosystem under the assumption that acceptable effects levels follow a certain distribution as a function of the concentration of the chemical (e.g. normal, logistic, triangle) and that the limited number of tested species is a random sample of the whole ecosystem (De Laender et al., 2013; Gao et al., 2014).

The AF and SSD methods rely on the assumption that ecosystem sensitivity to a given chemical can be related to the status of the most sensitive species, and that protecting ecosystem structure is enough to protect ecosystem functions too (Wright-Walters et al., 2011). However, population dynamics in polluted environments are not only driven by the direct toxicity effects of chemicals on single species, but also by ecological interactions between them and by the influence of abiotic factors (De Laender et al., 2007), therefore community- and ecosystem-level assessments could provide better indications of species' responses to chemicals than individual-level ones (Lulu Zhang et al., 2013). To assess ecological interactions, experimental ecosystems (microcosm, mesocosm and field enclosure studies), which can account for both direct and indirect effects of chemicals, have been used (De Laender et al., 2007, 2008a). Nevertheless, these methods are laborious, expensive and time-consuming, and the extrapolability of results to much more complex natural ecosystems, characterized by myriads of ecological interactions, remains uncertain (Lei et al., 2010; Naito et al., 2003; Lulu Zhang et al., 2013; Zhang and Liu, 2014). Considering that these methods cannot be used in the routine practice in lower tiers, there is a strong need for alternative approaches to

extrapolate single-species effects information to ecosystem-level responses (De Laender et al., 2008b). Ecological models are cost-effective alternatives for ERA of toxic chemicals, providing rapid forecasting analyses, particularly under circumstances where field experiments cannot be conducted or experimental data are lacking (which is generally the case for the contaminants of emerging concern investigated here) (Grechi et al., 2016; Lombardo et al., 2015; Naito et al., 2003; Zhang and Liu, 2014).

Although several ecological models have been developed and reviewed for use in ERA for chemicals (Galic et al., 2010; Lei et al., 2008; Naito et al., 2003), mechanistic effects modelling has not been extensively used for regulatory purposes yet because of the lack of official guidance for models choice, development and use (Galic et al., 2010; Meli et al., 2014). Among the models used in ERA (De Laender et al., 2008b; Galic et al., 2010; Lei et al., 2008; Naito et al., 2003; Pereira et al., 2017; Lulu Zhang et al., 2013), the U.S. Environmental Protection Agency's AQUATOX, an aquatic ecosystem model, is one of the relatively few comprehensive and well documented models that have been designed specifically for environmental fate and ecological impact assessment of pollutants. AQUATOX simulates both abiotic and biotic (including trophic) processes as well as lethal and sub-lethal toxicant effects, and so it can depict the propagation of these effects through food webs and ecosystems (Lei et al., 2008; Park and Clough, 2014; Zhang and Liu, 2014).

Over the past decade, serious concerns have been raised regarding the presence of per- and poly-fluoroalkyl substances (PFASs) in different environmental media, particularly water, in Northern Italy (Castiglioni et al., 2015; Loos et al., 2008; McLachlan et al., 2007; Squadrone et al., 2015; Valsecchi et al., 2017, 2015). Especially high PFAS concentrations were detected in the river Po when compared to other European rivers (McLachlan et al., 2007), confirming that the Po and its tributaries are highly polluted by different perfluoroalkyl acids (PFAAs) (Castiglioni et al., 2015; Loos et al., 2008; Valsecchi et al., 2015). Water quality management in the Po is a complex issue and matter for research, since this river crosses a densely inhabited, intensely cultivated and heavily industrialized watershed of about 71000 km², representing one of the wealthiest areas of Europe whose human activities exert multiple large pressures on its high biodiversity (Grechi et al., 2016).

This work aims to assess the ecological risk posed by a few selected unregulated and emerging contaminants in the river Po by applying three methods for deriving PNECs: AF, SSD, and a novel method based on AQUATOX modelling. ERA is carried out for four PFAAs, two long-chained (perfluorooctanesulfonic acid PFOS, perfluorooctanoic acid PFOA) and two short-chained ones (perfluorobutanesulfonic acid PFBS, perfluorobutanoic acid PFBA). The AQUATOX model used here quantitatively simulates ecosystem functioning in the final lowland section of the Po River based on the extensive use of well-documented local data, and was previously calibrated against observations (Grechi et al., 2016). The goals of this work are to compute ecologically-safe thresholds (PNECs) for emerging contaminants in the Po River applying the two classical methods and the AQUATOX-based method proposed here, and then to compare the three methods highlighting their advantages and drawbacks for deriving PNECs for emerging contaminants in rivers. To better contribute to the discussion on the tools to use for the future regulation of contaminants of emerging concern, the three ERA methods were also applied to two well-studied personal care products, linear alkylbenzene sulfonate and triclosan, which had already been investigated by Grechi et al. (2016) using the AQUATOX Po model.

2.2. Materials and Methods

2.2.1. Study area: the River Po and its biota

The Po is the longest river (652 km) in Italy, with the greatest average discharge (1470 m³ s⁻¹). It flows through the entire northern Italy, and its drainage area covers about one fourth of Italy's surface, including the main industrial and most populated areas where nearly one third of all Italian population lives (Valsecchi et al., 2015). In this study the most representative species and taxa present in the lower stretch of the Po River were considered following the selection by Grechi et al. (2016) (Table 2-1).

Table 2-1. Po River taxa considered in this study

	Po River taxa
Phytoplankton	Cyclotella Chromulina
Zooplankton	<i>Brachionus calyciflorus</i>
Macroinvertebrates	Amphipoda (<i>Echinogammarus</i>) Diptera (<i>Chironomus</i>) Oligochaeta Trichoptera (<i>Hydropsychidae</i>) Gastropoda Odonata - nymphs
Fish	Bleak (<i>Alburnus alburnus</i>) Chub (<i>Leuciscus cephalus</i>) Wels catfish (<i>Silurus glanis</i>) - adult and juvenile

The anthropogenic substances discharged to the river from its watershed exert high pressures not only on its water quality and ecological status, but also on downstream ecosystems: the Po freshwater discharge, which summed to those of other smaller Northern Italian river is about 20% of the river runoff into the whole Mediterranean Sea, carry large nutrient loads which caused severe eutrophication in the Adriatic Sea coastal zone some decades ago (Barausse et al., 2011; Vollenweider et al., 1992). The biomonitoring and ecosystem modelling efforts made for this river in the past (Grechi et al., 2016) make it an ideal study case to assess the ecological risk due to emerging contaminants such as PFAAs and to understand how the outcomes of ERA depend on the methodology chosen to quantify ecologically-safe chemicals thresholds.

2.2.2. Assessed contaminants

2.2.2.1. PFAAs

Due to their unique physico-chemical properties, PFASs have been widely used in industrial processes, but also represent a health and ecological threat because their high chemical stability and inertness make them resistant to hydrolysis, photolysis and microbial degradation, and consequently highly persistent and widespread in the environment (Squadrone et al., 2015; Valsecchi et al., 2015). PFASs have been employed from the 1950s in various industrial processes and products such as surface treatment of textiles and papers, building paints, cosmetics,

insecticides, firefighting foams and fluoropolymer production (Castiglioni et al., 2015; Valsecchi et al., 2015; P Zareitalabad et al., 2013). PFASs include thousands of chemicals, but environmental impact assessment studies mainly concentrate on perfluoroalkyl acids (PFAAs), mostly perfluoroalkylsulfonic acids (PFSAs) and perfluoroalkylcarboxylic acids (PFCAs) (Castiglioni et al., 2015; Valsecchi et al., 2015). Being primarily emitted to surface waters, water is the largest reservoir of PFAAs in the environment and the most important medium for their transport (McLachlan and Holmstro, 2007; Zareitalabad et al., 2013; Valsecchi et al., 2015).

Data on the presence of four different PFCAs in 14 major European rivers showed that the highest concentrations were detected in the river Po (McLachlan et al., 2007); further monitoring campaigns confirmed that the Po and its tributaries are highly polluted by different PFAAs, sometimes in concentrations above 6000 ng/L (the maximum reported PFAA concentration was 6480 ng/L for PFOA in Valsecchi et al., 2015) (Castiglioni et al., 2015; Loos et al., 2008; Valsecchi et al., 2015).

The European Commission recently added PFOS to the List of priority substances, identifying it as a “priority hazardous substance”, through Directive 2013/39/EC (The European Parliament and the Council of the European Union, 2013), with an annual average concentration of 0,65 ng/l as Environmental Quality Standard (EQS) for inland surface water (freshwater). From June 2013, PFOA is on the Candidate List of substances of very high concern for Authorisation, in accordance with the REACH regulation, as a PBT (persistent, bioaccumulative and toxic) and CMR (carcinogenic, mutagenic and toxic for reproduction) substance, but at the moment, there are still no established environmental thresholds (ECHA, 2013). In 2017, two other PFASs entered this list, Nonadecafluorodecanoic acid (PFDA) and its sodium and ammonium salts (ECHA, 2017a), and Perfluorohexane-1-sulphonic acid (PFHxS) and its salts (ECHA, 2017b), while PFOA and its salts entered the Restricted list (ECHA, 2017c). PFOS and PFOA have been usually detected as the main PFASs in environmental compartments worldwide through the past decades (Zareitalabad et al., 2013; Pierre and Riess, 2015; Valsecchi et al., 2017, 2015; Xiao, 2017), so their ecotoxicology and physico-chemical properties are the most researched among PFASs and they were selected as representatives of the long-chained PFAAs, while PFBA and PFBS were selected as their common short-chained industrial substitutes (Smith et al., 2016).

2.2.2.2. LAS and Triclosan

Linear alkylbenzene sulfonate (LAS) is an anionic surfactant introduced in 1964 as the readily biodegradable replacement for highly branched sulfonates. LAS is one of the most used anionic surfactant detergents, with major domestic applications and minor industrial ones, commonly found in wastewater (Oliver-Rodríguez et al., 2015).

Triclosan (TCS) is an antimicrobial agent frequently used in various personal care products, usually ending unchanged in the aquatic environment after passing through wastewater treatment plants. Contamination by TCS in surface waters has been reported worldwide as an emerging issue considering its high bioaccumulation potential to non-target organisms in aquatic environments.

Among emerging contaminants, both LAS and TCS are well-known and ubiquitous (Grechi et al., 2016; Guo and Iwata, 2017). The overall freshwater PNEC for LAS derived under REACH is 268 µg/L (ECHA, 2017d) and 843 ng/L for TCS (ECHA, 2017e). Since the AQUATOX Po model had already been used to conduct ERA for LAS and TCS (Grechi et al., 2016), both were included in this study to test the novel ecosystem modelling method for deriving PNECs and compare it to regulated methodologies.

2.2.3. Deriving PNECs with Assessment Factors

For all selected contaminants, available toxicity data were collected from the ECOTOX EPA database (U.S. EPA, 2000) and scientific literature, and then associated to the taxa found in the River Po to single out the species representative of the local aquatic ecosystem (Xu et al., 2015). Given the overall lack of toxicity data for non-standard test species, a biological read-across approach was applied: species with available toxicity data and belonging to the same taxon or living in similar natural habitats as the Po taxa, with similar size and diet, were selected in the database, then the Po taxa were assigned the same ecotoxicological endpoint values under the assumption of similar biological response to the given chemical (Grechi et al., 2016; Lombardo et al., 2015; Rand-Weaver et al., 2013). Toxicity data for all six contaminants are available in the Appendix 1 (Tables A1-1 to A1-6). Afterwards PNECs were computed following the European Technical Guidance Document (TGD) for deriving EQS, using the Annual Average Quality Standard (AA-QS_{fw,eco}) methodology (protection against the occurrence of prolonged exposure) based on direct ecotoxicity for protection of the pelagic species (equivalent to the REACH guidelines for deriving PNECs for freshwater species) (ECHA, 2008; European Commission, 2011). So, different assessment factors were used according to the availability of long- or short-term toxicity data for three different trophic levels (fish, invertebrates - preferably *Daphnia*, algae).

2.2.4. Deriving PNECs using Species Sensitivity Distribution

The four steps required for effects risk assessment with SSD include screening of toxicity data, selecting the distribution model, fitting the SSD curve, and calculating the values of hazardous concentration (HC) and PNEC to quantify the ecological risk (Gao et al., 2014). To derive PNECs with this method, the available toxicity data for Po and read-across species were analyzed and adapted to the method requirements. Ideally, the dataset for the SSD method should be statistically and ecologically representative of the community of interest and, when the problem is in the lower concentration range, the SSDs used to derive PNECs should be based on chronic ecotoxicity data, preferably no-observed effect concentrations (NOECs). Accordingly, at least eight species covering different taxonomic groups are desirable, with preferably 10-15 NOECs (Amiard and Amiard-Triquet, 2015; ECETOC, 2014; ECHA, 2008). When equivalent ecotoxicological data were available, obtained from the same test conditions on the same endpoint and species, the geometric mean was used as input for calculations (ECHA, 2008). When data were available for multiple time points, the longest time point was used (Tenbrook et al., 2010).

Since chronic toxicology studies were not available for all tested species, acute ecotoxicological data needed conversion to NOECs. Extrapolation was made by using acute-to-chronic ratios (ACRs). For LAS and triclosan, ACRs were accepted from ECETOC (2003), proposing EC50/NOEC = 2 and LC50/EC50 = 1.7 for LAS and EC50/NOEC = 2 and LC50/EC50 = 3.9 for triclosan. ACRs for PFAAs were unavailable in the literature, so they were derived according to ECETOC guidelines (ECETOC, 2003). All species with both acute and chronic ecotoxicological data available for the same PFAA were used for linear regression and the resulting slopes of 1.85 and 1.6 were used as EC50/NOEC and LC50/EC50 ratios for all PFAAs toxicity data conversions.

Both chronic and acute toxicity data were lacking for short-chained PFAAs (PFBA and PFBS), so an estimation based on interspecies correlation was made. To estimate the acute toxicity of PFAAs to untested species that were taxonomically too far for using the read-across approach, the Web-based Interspecies Correlation Estimation (ICE) model was used in the SSD mode for aquatic species (U.S. EPA, 2016a). Web-ICE estimates the acute toxicity of a chemical to a species, genus or family with no test data, by using acute ecotoxicological data available for more commonly tested surrogate

species (Raimondo et al., 2010). The outputs of the ICE model were EC50s of all species, then local or read-across species of the Po river were selected (Tables A1-7 and A1-8 in Appendix 1).

SSD curves were derived by using the lognormal statistical distribution, a simple and accepted model, allowing comparison with other studies (Gao et al., 2014; Xu et al., 2015). Curves were fitted using the SSD CADDIS generator (log-probit distribution) developed by U.S. EPA (2016b).

SSDs are used to estimate the concentration that should be protective for the most of the species in the ecosystem. PNEC values are usually taken to correspond to HC5 (5% hazard concentration), the 5th percentile of the distribution, a concentration that should protect over 95% of the species in the ecosystem (Amiard and Amiard-Triquet, 2015; European Commission, 2011; Gao et al., 2014). Although SSD modelling explicitly deals with differences in sensitivity between species, and SSDs can be constructed only when data are plentiful, HC5 should be divided by an additional AF to account for remaining uncertainties in the estimated threshold (the highest AF = 5 is the default value) (Amiard and Amiard-Triquet, 2015; ECHA, 2008; European Commission, 2011).

2.2.5. Deriving PNECs using AQUATOX

2.2.5.1. *The AQUATOX model*

US-EPA AQUATOX 3.1 (Park and Clough, 2014) is an integrated ecological and ecotoxicological process-based model intended for use in prospective ERA to predict the fate of nutrients, organic chemicals and toxicants in aquatic ecosystems and their direct and indirect effects on living organisms. In this study, the calibrated Po River AQUATOX model developed by Grechi et al. (2016) was used to predict the fate and effect of different concentrations of LAS, triclosan and PFAAs in a segment of the Po River, stretching from the closing section of the catchment to the beginning of the branching section of the delta, modeled as a continuous stirred-tank reactor. The simulated food web is depicted on Figure A1-2 (Appendix 1), and technical information about the ecosystem model parameterization are in Grechi et al. (2016). The impact of each chemical was evaluated in terms of variation of biota biomass density between control (i.e. without pollutants) and perturbed (i.e. with pollutants) model runs. To simulate PFAA behavior, the related AQUATOX sub-model (Park and Clough, 2014) was used (Section 2.2.5.3): to our knowledge, this is its first published application in a peer-reviewed international journal (but see Park et al., 2007, and Rashleigh et al., 2010).

2.2.5.2. *Parameters of the chemicals*

Input parameters for organic chemicals in AQUATOX governing their fate and partitioning include chemicals' properties (i.e. physico-chemical parameters describing fate processes such as ionization, volatilization, hydrolysis, photolysis, sorption and microbial degradation), ecotoxicity data for the modelled organisms, initial concentrations and loading from upstream. The required ecotoxicity endpoints are LC50 and EC50 (on growth and reproduction) for every consumer species, and LC50 and EC50 (on photosynthesis) for every primary producer (Park and Clough, 2014). For our purpose of simulating the constant chronic exposure to selected chemicals, the initial concentration and the inflow concentration (from upstream) were kept equal, and inflow concentration was constant during the simulation. The main physico-chemical and ecotoxicological parameters of LAS and TCS are in the Appendix 1 (Tables A1-21, A1-23 and A1-24).

2.2.5.3. *PFAA submodel*

The characteristics and environmental behavior of PFAAs distinguish them from other organic contaminants, and the increased public interest following their widespread appearance in different environmental compartments, particularly aquatic ecosystems, has led to the development of a PFAA submodel in AQUATOX. The submodel has different inputs regarding physico-chemical

parameters, e.g. it does not use the octanol-water partitioning coefficient for bioaccumulation, sorption and in-water mobility predictions, due to PFAAs non-typical lipid partitioning dynamics, their persistence to biodegradation in water or soil, and resistance to hydrolysis and photolysis (Smith et al., 2016). This resulted in a different approach for calculating sorption, biotransformation, bioaccumulation, uptake and depuration in the submodel, and in computing bioaccumulation factors through empirical equations based on chain length and type of terminal functional group. Since PFAAs do not follow the typical pattern of partitioning and accumulation into fatty tissues, but tend to bind to proteins, their kinetics calculations did not include the fraction of lipids in organisms (Martin et al., 2003; Park and Clough, 2014). Sorption is modelled through an empirical approach requiring the organic matter partition coefficient for sediments, calculated by dividing the soil organic carbon–water partitioning coefficient by the fraction of organic matter in detritus, considering that PFAAs sorption depends on the fraction of organic carbon in the sorbent (Asante-Duah, 1995; Park and Clough, 2014; Smith et al., 2016). Sorption to primary producers, simulated in AQUATOX through bioconcentration factors (BCFs) for Algae and for Macrophytes, can also be modelled empirically (Park and Clough, 2014), but in this study BCFs were taken from literature.

The physico-chemical parameters for the chosen PFAAs in AQUATOX are shown in Table A1-22 (Appendix 1). Species with available toxicity data for PFOS, PFOA, PFBS and PFBA were associated to the taxa modelled in AQUATOX; considering the scarcity of data, a read-across was performed, as well as conversions using ACR and LC50/EC50 ratios depending on data availability. Interspecies Correlation Estimation for PFBS and PFBA was used as described in Section 2.2.4. PFAAs ecotoxicological parameters for the modelled species are on Tables A1-25 to A1-28 (Appendix 1).

2.2.6. Deriving ecologically-safe thresholds using AQUATOX

To represent ecosystem seasonality, the Po River model had been stabilized and calibrated by Grechi et al. (2016) for a period of one year, so here every simulation was run for one year, with daily time steps. Moreover, a one-year simulation makes the AQUATOX methodology comparable to regulated ones, as chronic exposure is estimated there as annual average (European Commission, 2011). The objective was to develop a methodology to derive PNEC based on the biomass density ($\text{mg}_{\text{dry}}/\text{L}$ or $\text{g}_{\text{dry}}/\text{m}^2$) of each modelled taxon, by deciding what is a non-negligible biomass loss negatively affecting the corresponding population(s). The cut-off value proposed by the few available publications dealing with a similar issue (De Laender et al., 2008b, 2008c; Lei et al., 2010; Naito et al., 2003; Zhang et al., 2013; Zhang and Liu, 2014) was based on the claim of Suter (1992) that a 20% reduction is the minimum detectable difference in population biomass in the field. However, this approach can be criticized since not all populations are equally sensitive to a 20% biomass reduction (which may not affect the viability of one population, but it could lead to local extinction of another, e.g. if its biomass distribution over the year generally displays very low values except for a single, short-lived but large bloom), which is thus arbitrary. Furthermore, we see no reason to define an ecologically safe threshold of biomass change based on field detectability when using a mechanistic model that can keep track of arbitrarily small biomass changes. Therefore, we proposed an alternative methodology to derive a taxon-dependent threshold (Figure 2-1):

- 1) AQUATOX was run in control mode (with no chemicals), taken as a measure of the natural biomass oscillations of modelled organisms over the year. Simulation plots are provided on Figure A1-1 (Appendix 1);
- 2) Perturbed runs (with one chemical: LAS, TCS, PFOS, PFOA, PFBS or PFBA) were performed for gradually increasing chemical concentration, decided in accordance with previously proposed overall PNECs (ECHA, 2017d, 2017e; Valsecchi et al., 2017). Perturbed runs for LAS were from 0 (control) to 500 $\mu\text{g}/\text{L}$ with increments of 10; TCS: from 0 (control)

to 2 µg/L with increments of 0.05; PFOS: from 0 (control) to 0.01 µg/L with increments of 0.0001 and from 0.01 to 2 µg/L with increments of 0,01; PFOA: from 0 (control) to 3000 µg/L with increments of 200 and from 3000 to 6000 µg/L with increments of 100; PFBS: from 0 (control) to 10 µg/L with increments of 0.5, from 10 to 5000 µg/L with increments of 10 and from 5000 to 30000 µg/L with increments of 500; PFBA: from 0 (control) to 2000 µg/L with increments of 50;

- 3) For every run (control or perturbed), the median of daily biomass values over the year was calculated for every modelled taxon. The median was preferred to the mean as a measure of typical annual biomass, being less sensitive to the short-lived blooms characterizing several simulated taxa over the year (Legendre and Legendre, 1998) (Figure A1-1, Appendix 1);
- 4) For the control run, the median absolute deviation of daily biomass values (*MAD*) was computed as a robust measure of the natural variability of the biomass across the year. *MAD* was preferred to the standard deviation due to its insensitivity to outliers and since the yearly biomass distribution could not generally be approximated by a normal distribution (Legendre and Legendre, 1998);
- 5) The differences between the median biomass of the control (m_c) and the medians of the perturbed runs ($m_{p,i}$, for every i^{th} concentration) were calculated for every modelled taxon and compared to half of *MAD* for the control. So, the decrease in the typical biomass (represented by the median) of a taxon over the year due to the increased toxicant concentration was compared to the natural biomass variability level over the year. On the first occasion that, following an increase in toxicant concentration, the following condition was fulfilled for a taxon

$$m_c - m_{p,i} > \frac{MAD}{2} \quad (2-1)$$

the decrease in median biomass was considered larger than a natural biomass change for that taxon and, hence, significant: that concentration can be considered as the Lowest Observed Effect Concentration (LOEC). The rationale is that, for taxa with nearly-constant biomass over the year (low *MAD*), even a small biomass decrease indicates a significant deviation from usual conditions, while for naturally highly-oscillating taxa (high *MAD*), only a large biomass decrease represents a significant deviation given the characteristic variability;

- 6) Following REACH (ECHA, 2008) and TGD guidelines (European Commission, 2011), and the perspective that an ecosystem can be considered as sensitive as its most sensitive species, the LOEC of the most sensitive taxon according to the simulations was taken as the LOEC of the Po river ecosystem;
- 7) After finding LOEC, the highest concentration not fulfilling equation (2-1) was sought in the interval [LOEC - I_j , LOEC], where I_j is the increment of the j^{th} contaminant, and that highest concentration was taken as the Po ecosystem PNEC. Two conditions were applied to decide the precision in searching for PNEC. One was the limit of the detection (LOD), i.e. the current precision of the most sensitive analytical method for determining each chosen contaminant in surface water. The other was a maximum of four significant digits for PNEC.

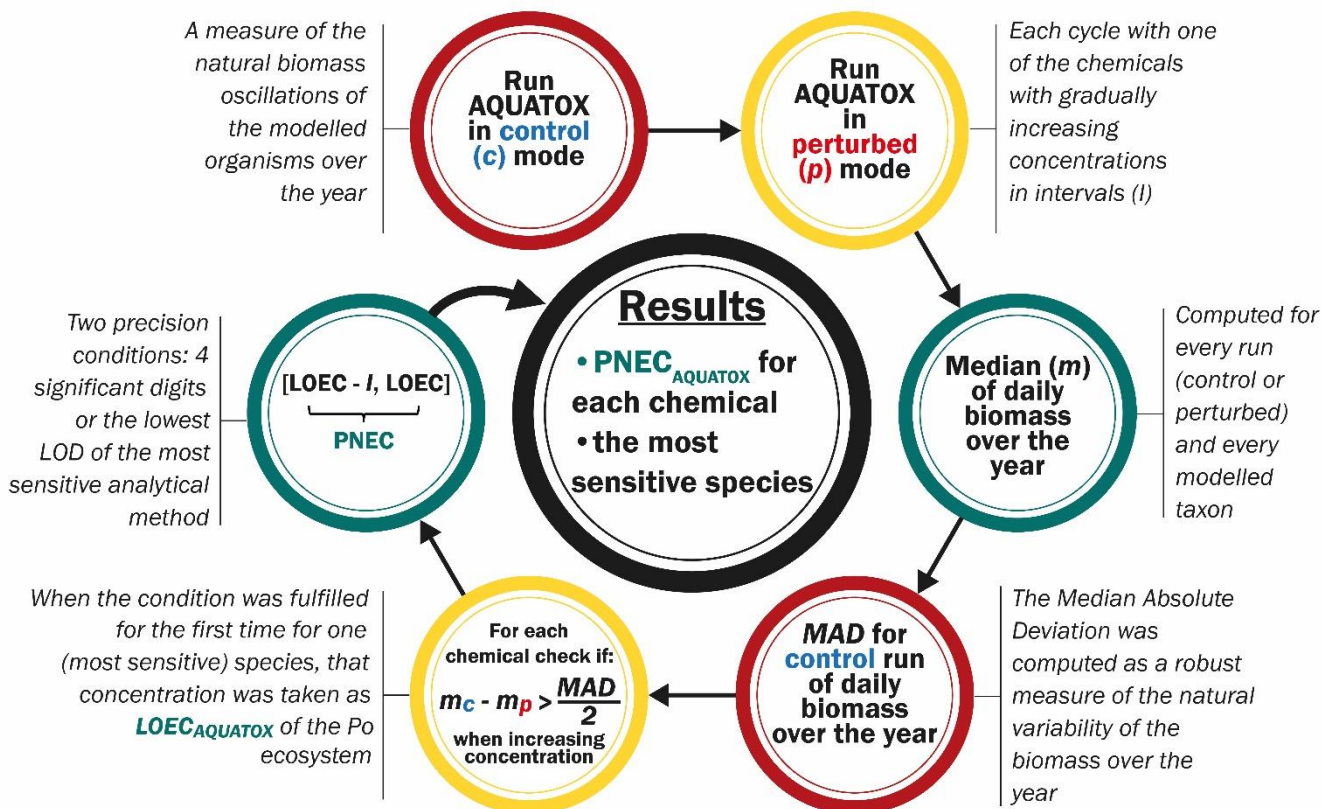


Figure 2-1. Scheme of the developed methodology for deriving PNEC through AQUATOX ecosystem modelling

2.3. Results and Discussion

2.3.1. Assessment Factor method

To derive PNEC for LAS, two long-term results (NOECs) from species representing two trophic levels (fish and/or *Daphnia* and/or algae) were available, implying the use of AF = 50. Such AF was applied to the lowest NOEC of *Cryptophycophyta* (140 µg/L), yielding PNEC = 2.8 µg/L. In comparison to the overall freshwater PNEC = 268 µg/L given by ECHA (ECHA, 2017d), the PNEC for the Po river ecosystem was two orders of magnitude stricter.

For triclosan, long-term results (NOECs) from at least three species (fish, *Daphnia*, algae) representing three trophic levels were available, leading to AF = 10. The lowest NOEC referred to *Chlamydomonas* sp. (0.015 µg/L), so PNEC in the Po was 0.0015 µg/L after dividing by AF, again stricter than the overall freshwater PNEC given by ECHA (0.843 µg/L) (ECHA, 2017e).

The same condition of three available long-term results was met for both PFOS and PFOA, so AF = 10 was applied to the lowest NOECs. For PFOS, the lowest NOEC was 49 µg/L (*Chironomus tetans*), so PNEC = 4.9 µg/L was computed for the Po. The recent PFOS EQS dossier (European Commission Subgroup on Review of the Priority Substances List, 2011) estimated a freshwater PNEC of 0.65 ng/L, and Qi et al. (2011) indicated an aquatic toxicity threshold for PFOS from 0.61-6.66 µg/L. NOEC for *Brachionus calyciflorus* was used for PFOA (4000 µg/L), leading to PNEC = 400 µg/L for the Po. The overall PNEC for freshwater derived using mesocosm studies on male plasma concentrations of the fish *Pimephales promelas* (Valsecchi et al., 2017) was 30 µg/L for PFOA, but given the uncertain ecological relevance of this endpoint and the unclear implications for

population mortality, growth or reproduction, we did not consider this test result as applicable and did not include it in Table A1-4 (Appendix 1).

Without extrapolation of results by using Interspecies Correlation Estimation, AF would have been the only feasible method for deriving PNEC for PFBS and PFBA. For PFBS, two long-term results (NOECs) from species representing two trophic levels (fish and/or *Daphnia* and/or algae) were available. However, the additional criterion that the trophic level of the NOECs includes the trophic level of the lowest acute L(E)C50 was not met: in this case, the application of AF = 100 to the lowest L(E)C50 is recommended by TGD if the lowest L(E)C50 is lower than the lowest NOEC. EC50 = 450'000 µg/L for *Danio rerio* (read-across species substitute for *Gobio gobio*) was used for deriving PNEC for PFBS in the Po, which was 4500 µg/L. The overall PNEC proposed by Valsecchi et al. (2017) for PFBS was 372 µg/L, the difference mainly coming from the use of AF = 1000 on different species. For PFBA, AF = 1000 was used, as at least one short-term L(E)C50 from each of the three trophic levels was available. There were no available long-term toxicity data for any of the Po species, and the lowest LC50 was 110000 µg/L (*Brachionus calyciflorus*), giving PNEC = 110 µg/L after dividing by AF. The same value for the overall PNEC for PFBA was proposed by Valsecchi et al. (2017).

2.3.2. SSD method

SSD curves with the corresponding HC5s are in Figure 2-2, while statistical details are in Tables A1-9 to A1-20 (Appendix 1). To derive PNECs, AF = 5 was applied to all HC5s, being no reasons to reduce AFs according to the TGD guidelines (European Commission, 2011). The resulting PNECs for the Po River ecosystem were 42.33 µg/L for LAS, 0.0026 µg/L for TCS, 15.95 µg/L for PFOS, 1065.70 µg/L for PFOA, 5665.84 µg/L for PFBS and 1417.83 µg/L for PFBA.

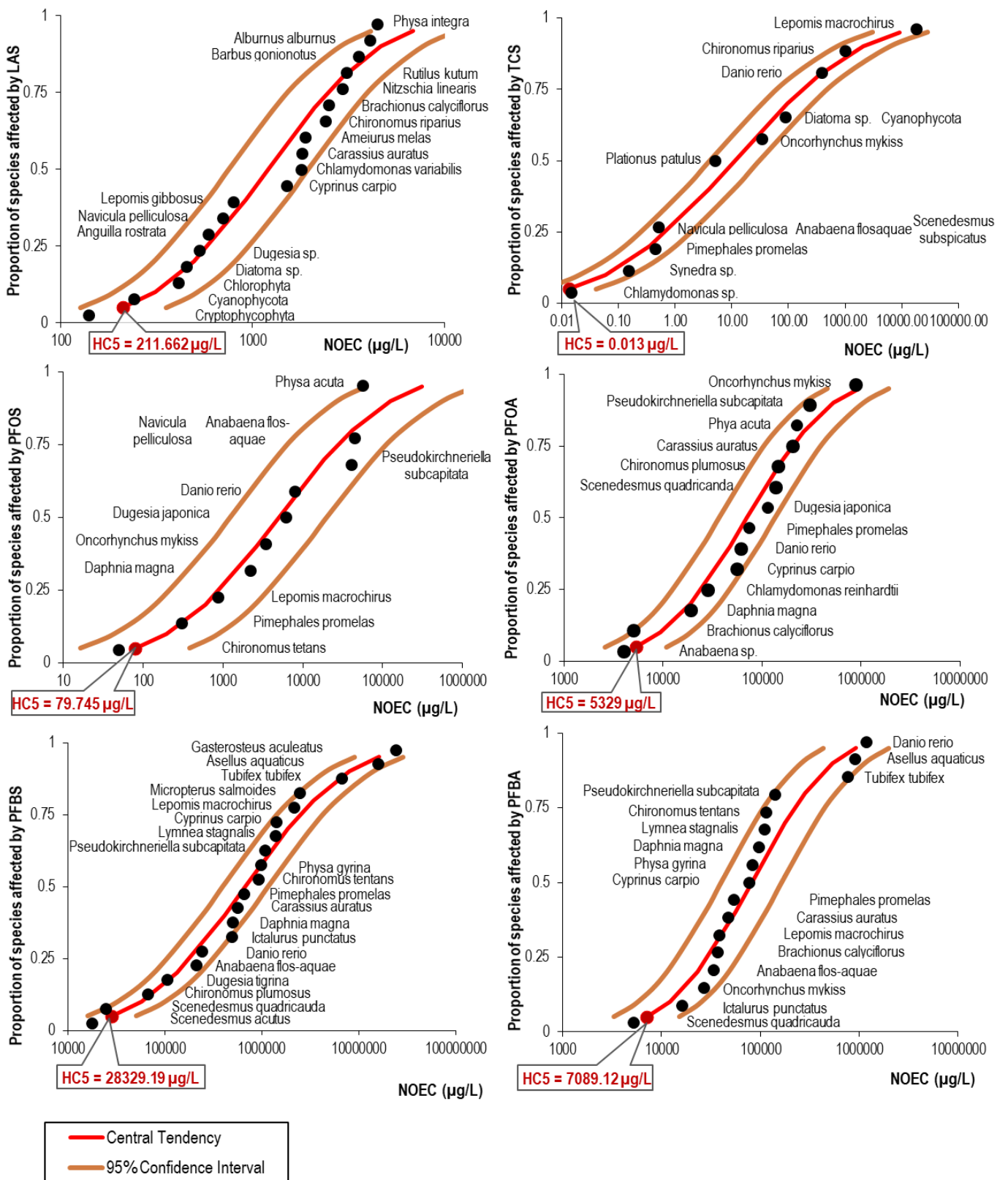


Figure 2-2. Fitted SSD curves for long-term toxicity data (NOECs) of the Po river taxa, for each contaminant

2.3.4. AQUATOX model

LOECs and PNECs for each contaminant in the Po River ecosystem determined using AQUATOX are in Table 2-2. Figure 2-3 shows the yearly biomass variations in the control and perturbed modelling scenarios for the most sensitive organisms indicated in Table 2-2. For all chemicals,

PNECs were determined with four significant digits (LODs were much lower) except PFOS, whose value was determined using the smallest known LOD, which is 0.00003 µg/L (Gallen et al., 2014).

Table 2-2. LOECs and PNECs resulting from the AQUATOX ERA methodology

	LAS	TCS	PFOS	PFOA	PFBS	PFBA
LOEC (µg/L)	190	0.30	0.0001	2600	12000	1150
PNEC (µg/L)	187.0	0.2502	0.000023	2546	11620	1102
Most sensitive taxon	Caddisfly, Trichoptera	Caddisfly, Trichoptera	Caddisfly, Trichoptera	Caddisfly, Trichoptera	Odonata	Caddisfly, Trichoptera

By modelling physical, chemical, biological and ecological processes, AQUATOX allowed us to reconstruct the fate of the chemicals in the Po ecosystem. To do this, we computed a mass balance for each chemical in the model. For all chemicals, the input to the modelled system took place through water advection from upstream, washout of the chemical mass with the outflowing water being the only loss from the system with the exception of LAS, where microbial degradation between 10–35% of the total mass loss per day occurred. Both of these model features are consistent with literature, PFAAs being resistant to degradation under environmental conditions (HERA, 2013; Smith et al., 2016), but inconsistent with laboratory experiments showing that TCS is subject to photolysis (Health Canada, 2012). The modelled mass of the chemicals in the system was computed as the difference between input and loss. Modelling results showed that more than 98% of the mass of the chemicals was dissolved in the water on every daily time step but for TCS, whose mass in the water varied between 78% and 100% as a consequence of its uptake by microalgae, up to 9% in the growing season, and of its almost- constant mass in animals ranging from 7-9% of the total mass in the system over the year. This result can be explained by the high bioaccumulation of TCS, particularly in fish (Table A1-24, Appendix 1). While BCFs were entered manually for LAS and TCS, BCFs were estimated by the chain-length and functional group dependent equations for PFAAs, and were equal for all organisms in the food web for each PFAAs. The computed BCFs were 1482 L/kg for PFOS, 4.4 L/kg for PFOA and less than 0.03 L/kg for both PFBS and PFBA, approximately correspondent to the average of the few available experimentally-derived values (Smith et al., 2016). Regarding the total modelled chemicals mass in biota, most of the TCS and LAS mass was present in the primary producers (algae), while PFAAs were almost entirely in animals, especially PFOS with almost 99%. In agreement with the used BCFs most of the total modelled mass of LAS and TCS in animals was contained in fishes, while for PFAAs most of the mass was predicted in primary and secondary consumers (i.e. Rotifers, Oligochaeta, Caddisfly, Odonata).

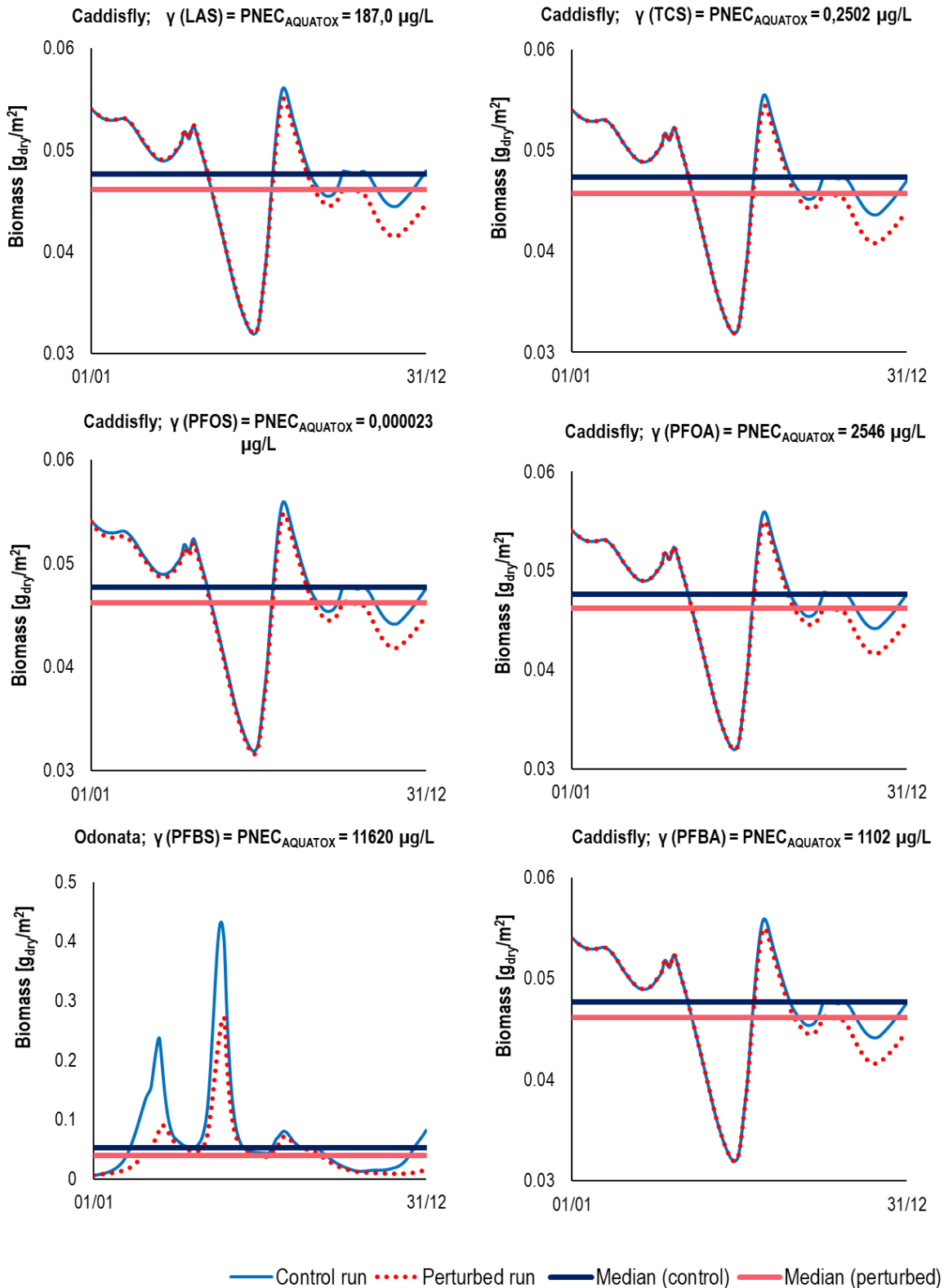


Figure 2-3. Control and perturbed biomass changes in AQUATOX over the simulated year, for contaminant concentration equal to the PNEC derived using AQUATOX.

2.3.5. Comparison of the methods

The computed PNECs differed across contaminants and depended on the methods employed to derive them (Table 2-3). The AF method always gave the lowest, most precautionary PNEC but for PFOS, for which the AQUATOX-derived PNEC was very small (the ratio of $PNEC_{AF}$ and $PNEC_{SSD}$ to $PNEC_{AQUATOX}$ was about

200000 and 700000, respectively). However, $PNEC_{SSD}$ and $PNEC_{AF}$ were generally of the same or similar order of magnitude, with their ratio ranging from 1.3–15. AQUATOX tended to give the highest, least precautionary PNEC except for PFOS, as mentioned, and PFBA, for which $PNEC_{AQUATOX}$ was slightly lower than $PNEC_{SSD}$ (for PFBA, $PNEC_{AQUATOX}:PNEC_{SSD} = 0,78$, $PNEC_{AQUATOX}:PNEC_{AF} = 10$): in all other cases, the ratio of $PNEC_{AQUATOX}$ to $PNEC_{AF}$ or $PNEC_{SSD}$ ranged from 2.6-167 and from 2-96, respectively. However, $PNEC_{AQUATOX}$ and $PNEC_{SSD}$ were generally of the same order of magnitude (the only exceptions were TCS and PFOS), unlike when comparing AQUATOX to the AF method.

Table 2-3. Comparison of the derived PNECs for all contaminants and methods

	LAS	TCS	PFOS	PFOA	PFBS	PFBA
$PNEC_{AF}$ (µg/L)	2,8	0,0015	4,9	400	4500	110
$PNEC_{SSD}$ (µg/L)	42,33	0,0026	15,95	1065,70	5665,84	1417,83
$PNEC_{AQUATOX}$ (µg/L)	187,0	0,2502	0,000023	2546	11620	1102

While it is intuitive that the AF method is the most precautionary, being based on the protection of the most sensitive species and on the use of very large factors when there is scarcity of data (particularly for chronic toxicity), there are many explanations for the other differences in the order of magnitude and (sometimes) rank of the estimated PNECs across methodologies and contaminants. One is the different data needs of the three methods: for example, extrapolation was employed to fulfill the data requirements of SSD and AQUATOX (either just as ACRs or using both ACRs and ICE for PFBS and PFBA), and consequently not entirely the same ecotoxicological data were used in all methods (sections 2.2.3, 2.2.4 and 2.2.5). Another explanation is the submodel that AQUATOX uses to model internal toxicity (Park and Clough, 2014) which may introduce additional, hard-to-assess bias in the comparison. Finally, the three methods are based on radically different assumptions: the AF and AQUATOX methods aim to protect the most sensitive species (and with it, the whole community), SSD just a major fraction of the community, and both AF and SSD methods are based on laboratory-derived toxicity data but ignore sub-lethal effects of chemicals as well as ecological interactions between species, and between species and abiotic factors (European Commission, 2011; Wright-Walters et al., 2011). AQUATOX simulates the impact of a chemical not only in terms of lethal toxicity (a direct effect), but also of sublethal toxicity (e.g. how the presence of a toxicant can impair physiological rates such as growth, consumption or reproduction) and indirect effects (Ulanowicz, 2009) triggered by the input of that chemical (e.g., predator-prey interactions). So, it simulates the mediating role of ecological processes, such as predation, which can propagate the effect of toxicity to other taxa in the ecosystem in noticeable and even counterintuitive manners (Grechi et al., 2016; Lombardo et al., 2015; Niu et al., 2016; Zhang and Liu, 2014). In AQUATOX the different toxicity modes of action of contaminants may also become relevant, as they determine which biological processes or functional groups are most impacted and how toxicity effects propagate throughout the food web (Lombardo et al., 2015). The level of aggregation of the food web modelled in AQUATOX, which does not simulate just single species, and the few taxa selected for modelling (out of the many found in the Po river) are also a potential, well-known source of bias in food web models whose impact is however difficult to quantify without complex investigations (Abarca-Arenas and Ulanowicz, 2002; Pinnegar et al., 2005; Ulanowicz, 2009).

Parallels can be drawn between our AQUATOX-based approach and traits-based approaches recently introduced into ERA (Rubach et al., 2011), proposing that the ecotoxicological effects of a chemical determining the vulnerability of a population can be linked to species traits, where a trait can be defined as a “phenotypic or ecological character of an organism, generally measured at the individual level, but often applied as the mean state of a species”. AQUATOX can simulate several ecological and ecotoxicological processes and factors, such as population growth, ingestion, trophic position and food preference, habitat choice, dispersal, toxicokinetics processes, etc. which can be

related to traits (see Rubach et al., 2011). For example, bioaccumulation modelling in AQUATOX requires mean individual wet weight and lipid fraction, which are key traits determining the sensitivity of species to the bioaccumulation of chemicals (Baird and Van den Brink, 2007; Park and Clough, 2014; Rubach et al., 2011). Thus, AQUATOX represents a tool for quantitatively testing the strength of the relationship between species traits and vulnerability to chemicals in complex, ecologically realistic conditions, keeping in mind the well-known limitations of ecological models, which are simplified descriptions of real processes and ecosystems, and whose reliability depends on the quantity and quality of input data (Jorgensen and Bendoricchio, 2001).

Field studies such as microcosms and mesocosms have been used as evidence for evaluating the accuracy of SSD and other ERA methodologies. The use of SSD should yield a more precautionary estimation of risk than field studies (Belanger et al., 2017). Since AQUATOX simulates ecological interactions and sub-lethal chemical effects which take place in riverine communities, we expect that PNECs based on field studies are closer to $PNEC_{AQUATOX}$ than to PNECs derived using SSD and AF methodologies, if the model can properly simulate the relevant features of the modelled ecosystem. For the chemicals tested in this work, PNECs based on field studies have been derived only for LAS. One work investigating C12-LAS through a 56-day experimental stream mesocosm study reported a NOEC of 0.268 mg/L (Belanger et al., 2002), this data was then normalized using QSARs resulting in $PNEC = 0.27$ mg/L (McDonough et al., 2016). The above NOEC was also used for calculating an overall freshwater $PNEC = 268$ μ g/L (NOEC/AF, with AF = 1) by ECHA (Belanger et al., 2002; ECHA, 2017d). $PNEC_{AQUATOX}$ for the Po River is indeed closer to this number in comparison to $PNEC_{AF}$ and $PNEC_{SSD}$, suggesting that our modelling approach to ERA is ecologically sound.

Although ecosystem models have been used for predicting ecologically-safe thresholds such as NOECs (De Laender et al., 2008b, 2007; Naito et al., 2003) for different pollutants in various ecosystems, to our knowledge AQUATOX was used for deriving NOECs only in Baiyangdian Lake, China (Lulu Zhang et al., 2013; Zhang and Liu, 2014), and for deriving PNECs only for three chlorophenols in Taihu Lake, China (Lei et al., 2010). Lei et al. (2010) found a PNEC rank, $PNEC_{SSD} > PNEC_{AQUATOX} > PNEC_{AF}$, not confirmed by our findings, since we report such rank only for one out of the six tested chemicals, and for four other chemicals we found $PNEC_{AQUATOX} > PNEC_{SSD} > PNEC_{AF}$. This difference is probably due to our alternative PNEC derivation methodology in AQUATOX and the fact that Lei et al. (2010) focused on a single group of chemicals. All the mentioned applications, except that of Zhang and Liu (2014), did not rely on a large amount of local ecological data or did not include a quantitative model calibration, which is a key step in ecological modelling (Jorgensen and Bendoricchio, 2001). Moreover, all these authors followed the approach based on a 20% threshold for biomass decrease, i.e. the lowest detectable biomass decrease in the field according to Suter (1992), to highlight significant impacts.

Indeed, an important issue in our comparison of ERA methodologies is that the AQUATOX estimates of PNEC also depend on the significant biomass decrease threshold defined for each taxon, which we related to its natural fluctuations. Although our choice represents an advancement with respect to the current literature, which relies on an arbitrary (in our opinion) 20% biomass decrease (De Laender et al., 2008c, 2008b; Lei et al., 2010; Naito et al., 2003; Suter, 1992; Lulu Zhang et al., 2013; Zhang and Liu, 2014), more research is needed to unambiguously define what a non-negligible biomass decrease is: other definitions are possible and their implications could be explored through comparative work. For example, from a conservation perspective it could be better to focus on the annual biomass minimum of the most sensitive species over the year, which is a better indicator of extinction risk in the case of endangered species than median biomass. In a human-centered vision, a non-negligible biomass decrease could be an ecologically significant one capable of directly or indirectly impairing the provision of the desired level of ecosystem services by the river, e.g. a fish

population decline which makes recreational fishing no longer feasible. We acknowledge that the choice of the coefficient 2 in the threshold $MAD/2$, meant to make this threshold smaller than natural fluctuations (MAD), is arbitrary too: our initial idea was to define this coefficient based on inter-calibration between the AQUATOX method and the AF and/or SSD methods, but such purpose was abandoned since AQUATOX and SSD derived PNECs were already of the same order of magnitude for 4 contaminants out of 6 and for the other 2 contaminants the difference was marked, so an inter-calibration would have simply complicated interpretation without being informative. We recommend that future studies carry out an uncertainty analysis regarding the value of such coefficient and try to define it depending on the quality of ecological/ecotoxicological parameters used to build the model (analogously to an assessment factor) and on the biology of the population under scrutiny. For example, a larger protective coefficient should be adopted for highly-variable populations tending to experience very low biomass minima and hence more prone to local extinction if impacted by a toxicant, thus linking such coefficients to population traits and stochasticity. Indeed, AQUATOX is a deterministic model, but natural populations experience stochastic variations in abundance, e.g. due to environmental variability or demographic stochasticity (Lande, 1993), which can potentially drive them to extinction even under conditions not predicted to be unfavorable by AQUATOX. Future developments of our work should explore how risk estimates change when the effect of stochasticity on population dynamics is modelled, e.g. through the built-in AQUATOX routine (Park and Clough, 2014).

In comparison to lethal toxicity, understanding the impact of sublethal toxicity and indirect effects, that are accounted for in AQUATOX unlike in the AF and SSD methods, on riverine biota dynamics is not straightforward. The interpretation of what drives biomass changes in AQUATOX is complicated by the high model complexity resulting from the large amount of parameters and simulated processes and interactions (Lombardo et al., 2015; Niu et al., 2016), and requires an in-depth and time-consuming analysis of modelling outputs, an exercise that was carried out here only for PFOS, being not the main goal of the paper. Indeed, the PNEC and LOEC derived for PFOS (Table 2-2 and Table 2-3) were several orders of magnitude smaller than those computed using the AF and SSD methods, highlighting this chemical as an interesting case. So, for PFOS, the rates of processes affecting biomass changes were computed for the most sensitive organism (Caddisfly, according to the AQUATOX methodology) using model outputs such as consumption and predation rates, poisoning rates, and others, for each daily time step (Park and Clough, 2014). In this way, we could approximately reconstruct the changes in biomass (increase or decrease) ascribable to each process over time. The weight of direct effects related to lethal toxicity on biomass variation was assessed based on the percentage of poisoned organisms, while sublethal toxicity and indirect effects were evaluated by looking at biomass variations related to consumption and predation mortality. Moreover, rates of PFOS uptake and depuration were also noted and used to support the evaluation of the direct and indirect effects. All computations were made for the control scenario as well as for a PFOS concentration equal to LOEC (Figure 2-4). At the beginning of the perturbed simulation, PFOS poisoning caused a marked decline in Caddisfly biomass, due to the rapid uptake through gills (Figure 2-3, Figure 2-4.a,b)), pointing out to a direct toxicity effect. Direct lethal effects are modelled depending on the internal toxicant concentration and on BCF, LC50 and the Weibull shape parameter as a measure of the mortality spread; all these variables and parameters strongly contributed to the mortality of Caddisfly since it has the lowest LC50 in comparison to the other organisms (particularly invertebrates), high BCF, consequently one of the highest internal concentrations in animals, and a higher Weibull shape parameter (Christensen, 1984; Park and Clough, 2014) (Appendix 1, Tables A1-21 to A1-28). Sublethal effects are modelled based on the EC50 values for growth and reproduction, also relying on the Weibull shape parameter and the internal toxicant concentration and can generate both direct effects and indirect effects on the

ecosystem through reduced predation and increased production of detritus (Park and Clough, 2014). A reduced consumption in comparison to the control, ascribable both to a lack of preys (an indirect effect of the toxicant) and to the sublethal effect of PFOS on ingestion, appeared to be the main cause of the Caddisfly biomass decrease in the perturbed simulation in summer-autumn with respect to the control, leading to reduced growth. However, a lower biomass decrease from mid-July to mid-August because of a release from predatory mortality in the perturbed simulation points out the presence of indirect effects which are beneficial for Caddisfly, a counterintuitive result already noticed in other river ecosystem simulations (De Laender et al., 2007; Grechi et al., 2016; Lombardo et al., 2015; Naito et al., 2003; Lulu Zhang et al., 2013). In conclusion, Figure 2-4 shows that PFOS can influence the population dynamics of Caddisfly, at least in the model, through both direct and indirect effects with varying intensity over the year.

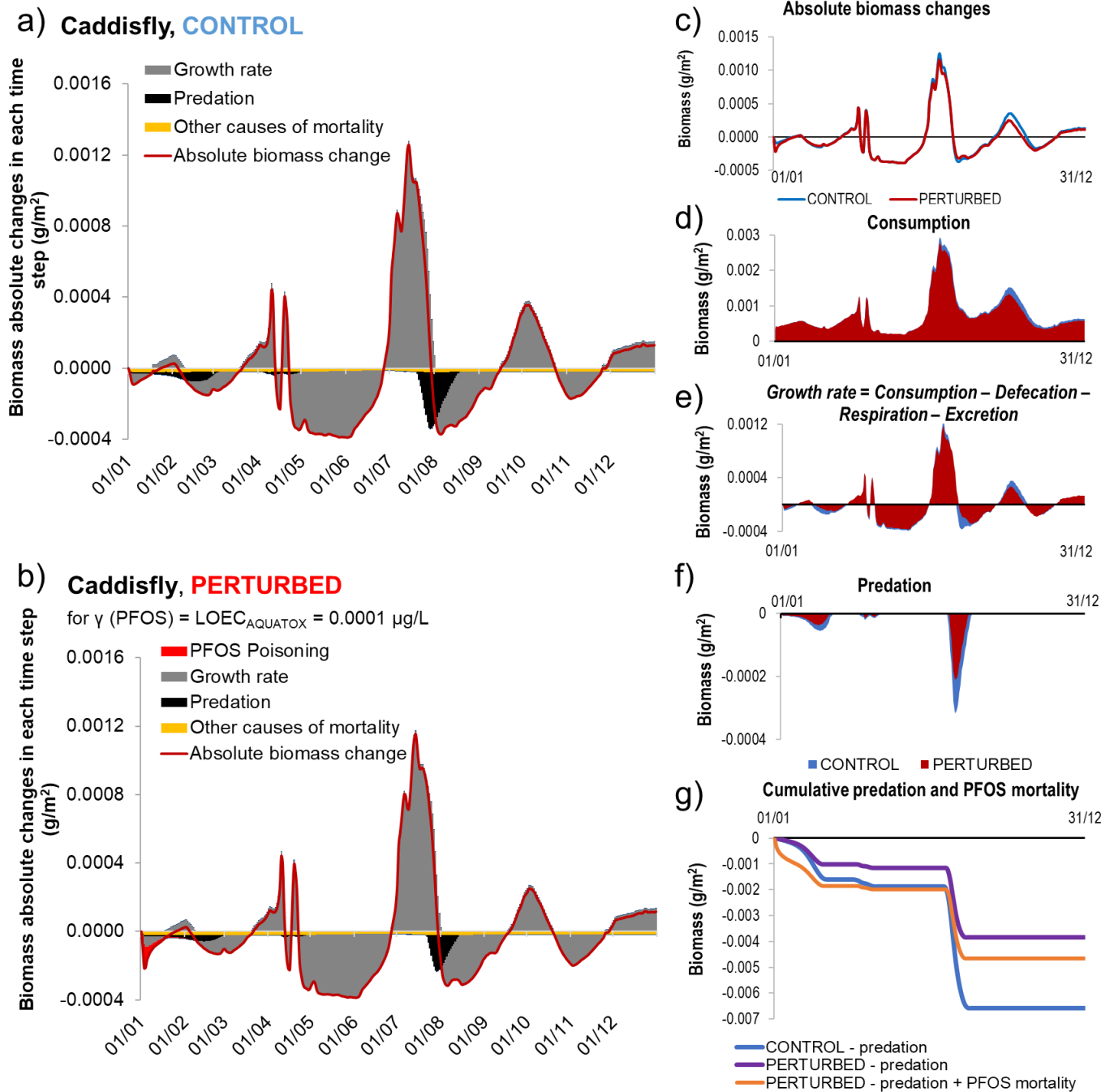


Figure 2-4. Modelled Caddisfly process rates in the control and perturbed PFOS simulations with AQUATOX. The absolute biomass change curve shows biomass differences between consecutive days (the model time step is daily) for a) control and b) perturbed simulations. The contributions of the most significant processes are shown as differently colored areas. Subplots c-f compare process rates, expressed as biomass change, for the control and perturbed simulations. Subplot g) shows the total contribution of predation-induced biomass decrease in the control scenario and of predation and PFOS poisoning in the perturbed scenario, expressed as cumulative biomass on each time step.

2.3.6. Advantages and disadvantages of the methods

Compared to the AF and SSD methods, the AQUATOX methodology proposed here has the advantage of summarizing both lethal and sublethal toxicity effects and all biomass changes resulting from indirect effects having predominance in different parts of the year, all in one criterion, which takes into account the peculiarities of the population dynamics of each taxon, measured as

biomass fluctuations over the year through the *MAD* estimator. It also has the capability of simulating the effect of chemical mixtures and of the concurrent action of multiple human stressors associated with water quality (discharges of chemicals, nutrients, organic substance, etc.). Thus, AQUATOX has the potential of being more ecologically realistic. Furthermore, it has all the advantages of ecological models as management and scientific tools (Jorgensen and Bendoricchio, 2001), such as the capability of making predictions (e.g. in the assessment of possible management scenarios), of being usable to test ecological hypotheses (e.g. cause-effect relationship regarding the input of a chemical and changes in the ecosystem), and of highlighting weaknesses in our knowledge of the studied system (e.g. the need for certain biomonitoring data; Grechi et al., 2016; Zhang and Liu, 2014), without high costs and effort. On the other hand, a good quality model requires good quality data for calibration and validation (Jorgensen and Bendoricchio, 2001), which can be challenging to find in the case of river ecosystem models and their use for ERA, limiting their application to regulatory risk assessment: river ecosystem models have high data requirement in comparison to what collected in current biomonitoring programs, especially if one aims to distinguish the impact of a chemical on biota from those of other chemicals, human pressures and natural forcings (Grechi et al., 2016; Lei et al., 2008; Lombardo et al., 2015). The potential bias on results given by food web aggregation, discussed in Section 2.3.5, should also be mentioned. In the case of the Po, the available biomonitoring data allowed Grechi et al. (2016) to construct a good quality ecosystem model which they successfully stabilized and calibrated against mean annual biomass values for food web compartments (calibration is a fundamental good practice in modelling, rarely done in AQUATOX; Lombardo et al., 2015), and then used to highlight that realistic exposure concentrations of LAS and triclosan likely have a negligible impact on riverine biota under the tested scenario (exposure to single chemicals). Also, the simulations carried out here highlighted that sublethal toxicity and ecological relationships are potentially important in the Po, e.g. they made us identify a very precautionary protective threshold concentration when modelling PFOS. On the other hand, the biomonitoring data used by Grechi et al. (2016) to construct the Po model were not of sufficient quality to faithfully reproduce all seasonal dynamics in the river ecosystem; in general, the Po model has not been validated enough to tell if its higher ecological realism translates to a more trustable ERA with respect to the AF and SSD methods in this work. A possible partial solution, beyond the scope of this paper, would be to carry out an uncertainty analysis to test the robustness of AQUATOX outputs to different model parameterizations.

Unlike ecological modelling, the AF and SSD methods have the important advantage of being standardized approaches. In particular, the AF method is well-tested, simple and applicable with limited ecotoxicological datasets, which is often the case with new chemicals. On the other hand, the estimated PNECs can show large uncertainty, since the extrapolation from the individual to the population level is being made only with a single, simplistic factor (Gao et al., 2014; Grechi et al., 2016; Lombardo et al., 2015; Meli et al., 2014), which does not consider that the standard conditions of laboratories, where toxicity data are derived, radically differ from those in the ecosystem under consideration. In natural ecosystems, environmental fluctuations and ecological interactions can exert a large influence on population dynamics, affecting their response to the input of a chemical in a complex manner and acting together with additional human stressors (including other chemicals), and also sublethal toxicity can play an important role. This issue leaves open the question whether AFs result in over- or under-protective PNECs (Meli et al., 2014). Also, the AF methodology strongly depends on the amount of available data (Belanger et al., 2017): when applying the AF method to the Po, we chose not to consider all the available ecotoxicological data for the tested chemicals, but only data for species relevant for the Po ecosystem (i.e. species found there or similar to them). It is hard to say how this choice affected the computed $PNEC_{AF}$: on the one hand, we possibly omitted previously-tested species showing high sensitivity to the tested chemicals from the analysis, on the

other hand the inclusion of more species in the analysis could have led to select less precautionary AFs (e.g., because more trophic levels would have been covered). Thus, more ecotoxicological data for species relevant for the local ecosystem are needed to make the AF methodology more reliable in the case of the Po.

Such issues apply also to SSD: although this method can provide larger statistical confidence compared to the AF method (Lei et al., 2010), as it focuses on toxicity effects on the whole community, it assumes that the sensitivity of a community can be computed from a set of independent species sensitivities obtained from single-species toxicity tests, entirely ignoring ecological interactions between species (De Laender et al., 2008a; Grechi et al., 2016; Lei et al., 2010; Naito et al., 2003). SSD requires more ecotoxicological measures than the AF method, which in addition should be statistically and ecologically representative of the investigated community, something difficult to achieve. The SSD approach used here aimed, at least, to reflect the local conditions of the Po, by fitting toxicity data only for species relevant for that ecosystem and avoiding mixing data for species which do not belong to the same community as done in regulatory applications where the SSD method is generally used for deriving an overall PNEC applicable to different ecosystems (Belanger et al., 2017). To address the drawbacks of the SSD approach, research is ongoing: for example, computing separate SSDs for reproduction, growth and mortality makes this approach more ecologically sound, avoiding the mix of different endpoints (Beaudouin and Pery, 2013), and novel approaches are being developed like field-based SSD (using field data based on population abundance and biomass), hierarchical SSD (addressing data gaps in taxa diversity through knowledge of how sensitivity relates to taxonomic distance between species) and trait-based SSD (using groupings based on traits instead of species) (Belanger et al., 2017).

2.4. Conclusions

Here, ecologically-safe thresholds for LAS, triclosan and four perfluoroalkyl acids were evaluated by deriving PNECs for the Po River ecosystem through the assessment factor method, the species sensitivity distribution and a novel methodology relying on the process-based ecosystem model AQUATOX. These methodologies sometimes provided similar results, but in other cases PNEC estimates were quite different. The case of PFOS suggests that by taking indirect ecological effects and both lethal and sublethal toxicity into account, higher risk than expected is possible: the PNEC resulting from AQUATOX is 3.6% of the accepted annual average EQS for freshwater (The European Parliament and the Council of the European Union, 2013). Thus, the use of multiple, complementary methods for PNEC derivation seems useful to clarify uncertainties in ecological risk estimates and ensure higher confidence in results. Our PNEC estimates for PFAAs could surely be improved, e.g. with the availability of more ecotoxicological data, needed to avoid ICE extrapolation, and, in the case of AQUATOX, by using measured BCFs and not those modelled using chain-length dependent equations. An ecological risk assessment for PFAAs mixtures can be implemented using AQUATOX and appears as a future logical step, given the simultaneous presence of different substances in the groundwater and surface water contamination in northern Italy.

This work shows that including ecological relationships and chemical sublethal toxicity in ERA through models can give a fuller picture of the concentration–response relationship in ecosystems, potentially resulting in a more ecologically-relevant risk assessment, provided that good quality data are available for model construction, calibration and validation, and that the uncertainty of model predictions is properly acknowledged and investigated. Ecosystem models could be a useful tool in planning mesocosm studies and for pre-evaluation in the assessment of chemical impact on ecosystems as a whole. Nonetheless, more work needs to be done to standardize modelling

approaches and provide guidelines for their application, before their full inclusion in regulatory risk assessment. Also, to satisfy the expectations of policy and decision-making and allow standardized use, ERA models should not be too complicated or provide hard-to-interpret results, two requirements which clash with the fact that ERA models should be complex enough to realistically depict a wide range of ecological scenarios.

Acknowledgements

Andrea Gredelj's PhD research was funded by the Fondazione CARIPARO's grant for foreign PhD students at the University of Padova.

2.5. References:

- Abarca-Arenas, L.G., Ulanowicz, R.E., 2002. The effects of taxonomic aggregation on network analysis. *Ecol. Modell.* 149, 285–296.
- Amiard, J., Amiard-Triquet, C., 2015. Conventional Risk Assessment of Environmental Contaminants, in: *Aquatic Ecotoxicology*. Elsevier Inc., pp. 25–49. <https://doi.org/10.1016/B978-0-12-800949-9.00002-4>
- Asante-Duah, K., 1995. Appendix C: Important fate and transport properties of environmental contaminants, in: *Management of Contaminated Site Problems*. CRC Press, Boca Raton, Florida, p. 432.
- Baird, D.J., Van den Brink, P.J., 2007. Using biological traits to predict species sensitivity to toxic substances. *Ecotoxicol. Environ. Saf.* 67, 296–301. <https://doi.org/10.1016/j.ecoenv.2006.07.001>
- Barausse, A., Michieli, A., Riginella, E., Palmeri, L., Mazzoldi, C., 2011. Long-term changes in community composition and life-history traits in a highly exploited basin (northern Adriatic Sea): The role of environment and anthropogenic pressures. *J. Fish Biol.* 79, 1453–1486. <https://doi.org/10.1111/j.1095-8649.2011.03139.x>
- Beaudouin, R., Pery, A.R., 2013. Comparison of species sensitivity distributions based on population or individual endpoints. *Env. Toxicol Chem* 32, 1173–1177. <https://doi.org/10.1002/etc.2148>
- Belanger, S., Barron, M., Craig, P., Dyer, S., Galay-Burgos, M., Hamer, M., Marshall, S., Posthuma, L., Raimondo, S., Whitehouse, P., 2017. Future needs and recommendations in the development of species sensitivity distributions: Estimating toxicity thresholds for aquatic ecological communities and assessing impacts of chemical exposures. *Integr. Environ. Assess. Manag.* 13, 664–674. <https://doi.org/10.1002/ieam.1841>
- Belanger, S.E., Bowling, J.W., Lee, D.M., LeBlanc, E.M., Kerr, K.M., McAvoy, D.C., Christman, S.C., Davidson, D.H., 2002. Integration of aquatic fate and ecological responses to linear alkyl benzene sulfonate (LAS) in model stream ecosystems. *Ecotoxicol. Environ. Saf.* 52, 150–171. <https://doi.org/10.1006/eesa.2002.2179>
- Castiglioni, S., Valsecchi, S., Polesello, S., Rusconi, M., Melis, M., Palmiotto, M., Manenti, A., Davoli, E., Zuccato, E., 2015. Sources and fate of perfluorinated compounds in the aqueous environment and in drinking water of a highly urbanized and industrialized area in Italy. *J. Hazard. Mater.* 282, 51–60. <https://doi.org/10.1016/j.jhazmat.2014.06.007>
- Christensen, E.R., 1984. Dose-response functions in aquatic toxicity testing and the Weibull model. *Water Res.* 18, 213–221. [https://doi.org/10.1016/0043-1354\(84\)90071-X](https://doi.org/10.1016/0043-1354(84)90071-X)
- De Laender, F., De Schamphelaere, K.A.C., Janssen, C.R., Vanrolleghem, P.A., 2007. An ecosystem modelling approach for deriving water quality criteria. *Water Sci. Technol.* 56, 19–27. <https://doi.org/10.2166/wst.2007.582>
- De Laender, F., De Schamphelaere, K.A.C., Vanrolleghem, P.A., Janssen, C.R., 2008a. Validation of an ecosystem modelling approach as a tool for ecological effect assessments. *Chemosphere* 71, 529–545. <https://doi.org/10.1016/j.chemosphere.2007.09.052>
- De Laender, F., De Schamphelaere, K.A.C., Vanrolleghem, P.A., Janssen, C.R., 2008b. Comparison of different toxic effect sub-models in ecosystem modelling used for ecological effect

assessments and water quality standard setting. *Ecotoxicol. Environ. Saf.* 69, 13–23. <https://doi.org/10.1016/j.ecoenv.2007.08.020>

De Laender, F., De Schampheleere, K.A.C., Vanrolleghem, P.A., Janssen, C.R., 2008c. Is ecosystem structure the target of concern in ecological effect assessments? *Water Res.* 42, 2395–2402. <https://doi.org/10.1016/j.watres.2008.01.006>

De Laender, F., Van Sprang, P., Janssen, C.R., 2013. A re-evaluation of fifteen years of European risk assessment using effect models. *Environ. Toxicol. Chem.* 32, 594–601. <https://doi.org/10.1002/etc.2098>

Duraiappah, A.K., Naeem, S., Agardy, T., Ash, N.J., Cooper, H.D., Díaz, S., Faith, D.P., Mace, G., McNeely, J. a., Mooney, H. a., Alfred A. Oteng-Yeboah, Henrique Miguel Pereira, Polasky, S., Prip, C., Reid, W. V., Samper, C., Schei, P.J., Scholes, R., Schutyser, F., Jaarsve, A. Van, 2005. Millennium Ecosystem Assessment, Ecosystems and human well-being: Current State and Trends, Volume 1. ed, Ecosystems. Island press, Washington. <https://doi.org/10.1196/annals.1439.003>

ECETOC, 2014. Estimating toxicity thresholds for aquatic ecological communities from sensitivity distributions. Amsterdam. <https://doi.org/ISSN-2078-7219-28>

ECETOC, 2003. Aquatic Hazard Assessment II, Technical Report No . 91. Brussels. <https://doi.org/ISSN-0773-8072-91>

ECHA, 2017a. Inclusion of substances of very high concern in the Candidate List for eventual inclusion in Annex XIV (Decision of the European Chemicals Agency), PFDA. Helsinki.

ECHA, 2017b. Inclusion of substances of very high concern in the Candidate List for eventual inclusion in Annex XIV (Decision of the European Chemicals Agency), PFHxS. Helsinki.

ECHA, 2017c. One new substance added to the Candidate List, several entries updated [WWW Document]. ECHA/PR/17/14. URL <https://echa.europa.eu/-/one-new-substance-added-to-the-candidate-list> (accessed 10.6.17).

ECHA, 2017d. ECHA Brief Profile: Benzenesulfonic acid, C10-13-alkyl derivs., sodium salts [WWW Document]. URL <https://echa.europa.eu/brief-profile/-/briefprofile/100.063.721> (accessed 10.6.17).

ECHA, 2017e. ECHA Brief Profile: Triclosan [WWW Document]. URL <https://echa.europa.eu/brief-profile/-/briefprofile/100.020.167> (accessed 10.6.17).

ECHA, 2013. Member state committee support document for identification of pentadecafluorooctanoic acid (PFOA) as a substance of very high concern because of its CMR and PBT properties.

ECHA, 2008. Guidance on information requirements and chemical safety assessment Chapter R.10: Characterisation of dose [concentration] - response for environment.

European Chemicals Bureau, 2003. Technical Guidance Document on Risk Assessment: Part II. Ispra.

European Commission, 2011. Common Implementation Strategy for the Water Framework Directive (2000/60 /EC) Guidance Document No. 27 Technical Guidance For Deriving Environmental Quality Standards. <https://doi.org/10.2779/43816>

- European Commission, 2006. Regulation (EC) No 1907/2006 - REACH. European Union.
- European Commission Subgroup on Review of the Priority Substances List, 2011. EQS dossier for PFOS.
- European Community, 2000. Directive 2000/60/EC. Official Journal of the European Communities, European Union. <https://doi.org/10.1039/ap9842100196>
- Galic, N., Hommen, U., Baveco, J.M.H., Brink, P.J. Van Den, 2010. Potential Application of Population Models in the European Ecological Risk Assessment of Chemicals II : Review of Models and Their Potential to Address Environmental Protection Aims. *Integr. Environ. Assess. Manag.* 6, 338–360. <https://doi.org/10.1002/ieam.68>
- Gallen, C., Baduel, C., Lai, F.Y., Thompson, K., Thompson, J., Warne, M., Mueller, J.F., 2014. Spatio-temporal assessment of perfluorinated compounds in the Brisbane River system, Australia: Impact of a major flood event. *Mar. Pollut. Bull.* 85, 597–605. <https://doi.org/10.1016/j.marpolbul.2014.02.014>
- Gao, P., Li, Z., Gibson, M., Gao, H., 2014. Ecological risk assessment of nonylphenol in coastal waters of China based on species sensitivity distribution model. *Chemosphere* 104, 113–119. <https://doi.org/10.1016/j.chemosphere.2013.10.076>
- Grechi, L., Franco, A., Palmeri, L., Pivato, A., Barausse, A., 2016. An ecosystem model of the lower Po river for use in ecological risk assessment of xenobiotics. *Ecol. Modell.* 332, 42–58. <https://doi.org/10.1016/j.ecolmodel.2016.03.008>
- Guo, J., Iwata, H., 2017. Risk assessment of triclosan in the global environment using a probabilistic approach. *Ecotoxicol. Environ. Saf.* 143, 111–119. <https://doi.org/10.1016/j.ecoenv.2017.05.020>
- Health Canada, 2012. Preliminary Assessment Report on Triclosan.
- HERA, 2013. LAS Linear Alkylbenzene Sulphonate (CAS No. 68411-30-3), Human and Environmental Risk Assessment of ingredients of Household Cleaning Products.
- Jorgensen, S.E., Bendoricchio, G., 2001. *Fundamentals of Ecological Modelling*, 3rd ed. Elsevier Ltd, Amsterdam, Netherlands.
- Lande, R., 1993. Risks of population extinction from demographic and environmental stochasticity and random catastrophes. *Am. Nat.* 142, 911–927.
- Legendre, P., Legendre, L., 1998. *Numerical ecology: second English edition, Developments in environmental modelling*. Elsevier B.V., Amsterdam.
- Lei, B., Huang, H., Jin, X., Wang, Z., 2010. Deriving the aquatic predicted no-effect concentrations (PNECs) of three chlorophenols for the Taihu Lake, China. *J. Environ. Sci. Heal. Part A* 45, 1823–1831. <https://doi.org/10.1080/10934529.2010.520495>
- Lei, B.L., Huang, S.B., Qiao, M., Li, T., Wang, Z., 2008. Prediction of the environmental fate and aquatic ecological impact of nitrobenzene in the Songhua River using the modified AQUATOX model. *J. Environ. Sci.* 20, 769–777. [https://doi.org/10.1016/S1001-0742\(08\)62125-7](https://doi.org/10.1016/S1001-0742(08)62125-7)
- Lombardo, A., Franco, A., Pivato, A., Barausse, A., 2015. Food web modeling of a river ecosystem for risk assessment of down-the-drain chemicals: A case study with AQUATOX. *Sci. Total Environ.* 508, 214–227. <https://doi.org/10.1016/j.scitotenv.2014.11.038>

- Loos, R., Locoro, G., Huber, T., Wollgast, J., Christoph, E.H., Jager, A. De, Gawlik, B.M., Hanke, G., Umlauf, G., 2008. Analysis of perfluorooctanoate (PFOA) and other perfluorinated compounds (PFCs) in the River Po watershed in N-Italy. *Chemosphere* 71, 306–313. <https://doi.org/10.1016/j.chemosphere.2007.09.022>
- Martin, J.W., Mabury, S.A., Solomon, K.R., Muir, D.C.G., 2003. Bioconcentration and tissue distribution of perfluorinated acids in Rainbow trout (*Oncorhynchus mykiss*). *Environ. Toxicol. Chem.* 22, 196–204. <https://doi.org/10.1002/etc.5620220126>
- McDonough, K., Casteel, K., Itrich, N., Menzies, J., Belanger, S., Wehmeyer, K., Federle, T., 2016. Evaluation of anionic surfactant concentrations in US effluents and probabilistic determination of their combined ecological risk in mixing zones. *Sci. Total Environ.* 572, 434–441. <https://doi.org/10.1016/J.SCITOTENV.2016.08.084>
- McLachlan, M.S., Holmstro, K.E., Reth, M., Berger, U., 2007. Riverine Discharge of Perfluorinated Carboxylates from the European Continent. *Environ. Sci. Technol.* 41, 7260–7265. <https://doi.org/10.1021/es071471p>
- Meli, M., Palmqvist, A., Forbes, V.E., Groeneveld, J., Grimm, V., 2014. Two pairs of eyes are better than one: Combining individual-based and matrix models for ecological risk assessment of chemicals. *Ecol. Modell.* 280, 40–52. <https://doi.org/10.1016/j.ecolmodel.2013.07.027>
- Naito, W., Miyamoto, K.I., Nakanishi, J., Masunaga, S., Bartell, S.M., 2003. Evaluation of an ecosystem model in ecological risk assessment of chemicals. *Chemosphere* 53, 363–375. [https://doi.org/10.1016/S0045-6535\(03\)00055-9](https://doi.org/10.1016/S0045-6535(03)00055-9)
- Niu, Z., Gou, Q., Wang, X., Zhang, Y., 2016. Simulation of a water ecosystem in a landscape lake in Tianjin with AQUATOX: Sensitivity, calibration, validation and ecosystem prognosis. *Ecol. Modell.* 335, 54–63. <https://doi.org/10.1016/j.ecolmodel.2016.05.003>
- Oliver-Rodríguez, B., Zafra-Gómez, A., Reis, M.S., Duarte, B.P.M., Verge, C., Ferrer, J.A. De, Pérez-Pascual, M., Vilchez, J.L., 2015. Wide-range and accurate modeling of linear alkylbenzene sulfonate (LAS) adsorption/desorption on agricultural soil. *Chemosphere* 138, 148–155. <https://doi.org/10.1016/j.chemosphere.2015.05.085>
- Park, R.A., Clough, J.S., 2014. Aquatox (release 3.1 plus) Modeling Environmental Fate and Ecological Effects in Aquatic Ecosystems, Volume 2: Technical Documentation. Washington DC.
- Park, R.A., Clough, J.S., Wellman, M.C., 2007. Aquatox: Modeling Fate of Toxic Organics in the Galveston Bay Ecosystem.
- Pereira, A.S., José Cerejeira, M., Daam, M.A., 2017. Ecological risk assessment of imidacloprid applied to experimental rice fields: Accurateness of the RICEWQ model and effects on ecosystem structure. *Ecotoxicol. Environ. Saf.* 142, 431–440. <https://doi.org/10.1016/j.ecoenv.2017.04.045>
- Pierre, M., Riess, J.G., 2015. Per- and poly fluorinated substances (PFASs): Environmental challenges. *Curr. Opin. Colloid Interface Sci.* 20, 192–212. <https://doi.org/10.1016/j.cocis.2015.07.004>
- Pinnegar, J.K., Blanchard, J.L., Mackinson, S., Scott, R.D., Duplisea, D.E., 2005. Aggregation and removal of weak-links in food-web models: system stability and recovery from disturbance. *Ecol. Modell.* 184, 229–248.

- Qi, P., Wang, Y., Mu, J.L., Wang, J., 2011. Aquatic predicted no-effect-concentration derivation for perfluorooctane sulfonic acid. *Environ. Toxicol. Chem.* 30, 836–842. <https://doi.org/10.1002/etc.460>
- Raimondo, S., Vivian, D.N., Barron, M.G., 2010. Web-based Interspecies Correlation Estimation (Web-ICE) for Acute Toxicity: User Manual v3.1, Epa/600/R-10/004.
- Rand-Weaver, M., Margiotta-Casaluci, L., Patel, A., Panter, G.H., Owen, S.F., Sumpter, J.P., 2013. The read-across hypothesis and environmental risk assessment of pharmaceuticals. *Environ. Sci. Technol.* 47, 11384–11395. <https://doi.org/10.1021/es402065a>
- Rashleigh, B., Park, R.A., Clough, J., Wellman, M.C., Bringolf, R., Lasier, P.J., 2010. Modeling Bioaccumulation as a Potential Route of Riverine Foodweb Exposures To PFOS, in: Joint Meeting of Carolinas and Southeast Chapters of the Society of Environmental Toxicology & Chemistry. SETAC, U.S. EPA, Athens, GA.
- Rubach, M.N., Ashauer, R., Buchwalter, D.B., De Lange, H.J., Hamer, M., Preuss, T.G., Töpke, K., Maund, S.J., 2011. Framework for traits-based assessment in ecotoxicology. *Integr. Environ. Assess. Manag.* 7, 172–186. <https://doi.org/10.1002/ieam.105>
- Smith, J.W.N., Beuthe, B., Dunk, M., Demeure, S., Carmona, J.M.M., Medve, A., Spence, M.J., Pancras, T., Schrauwen, G., Held, T., Baker, K., Ross, I., Slenders, H., 2016. Environmental fate and effects of poly- and perfluoroalkyl substances (PFAS). Brussels.
- Squadrone, S., Ciccotelli, V., Prearo, M., Favaro, L., Scanzio, T., Fogliani, C., Abete, M.C., 2015. Perfluorooctane sulfonate (PFOS) and perfluorooctanoic acid (PFOA): emerging contaminants of increasing concern in fish from Lake Varese, Italy. *Environ. Monit. Assess.* 187. <https://doi.org/10.1007/s10661-015-4686-0>
- Suter, G.W., 1992. *Ecological Risk Assessment*, I. ed. CRC Press, Boca Raton, Florida. <https://doi.org/10.1007/978-94-007-5704-2>
- Tenbrook, P.L., Palumbo, A.J., Fojut, T.L., Hann, P., Karkoski, J., Tjeerdema, R.S., 2010. The University of California-Davis Methodology for Deriving Aquatic Life Pesticide Water Quality Criteria. <https://doi.org/10.1007/978-1-4419-6883-8>
- The European Parliament and the Council of the European Union, 2013. Directive 2013/39/EC. Official Journal of the European Communities, European Union. <https://doi.org/http://dx.doi.org/http://eur-lex.europa.eu/legal-content/EN/TXT/?uri=celex:32013L0039>
- U.S. EPA, 2016a. Web-ICE v3.3 - release June 2016, Species Sensitivity Distributions - Aquatic Species [WWW Document]. URL <https://www3.epa.gov/webice/iceSSDSpecies.html?filename=as> (accessed 2.20.17).
- U.S. EPA, 2016b. CADDIS Volume 4. Data Analysis: Advanced Analyses [WWW Document]. URL <https://www.epa.gov/caddis-vol4/caddis-volume-4-data-analysis-advanced-analyses-controlling-for-natural-variability#tab-5> (accessed 2.6.17).
- U.S. EPA, 2000. ECOTOX [WWW Document]. URL <https://cfpub.epa.gov/ecotox/> (accessed 4.27.17).
- Ulanowicz, R.E., 2009. *A third window: Natural life beyond Newton and Darwin*. Templeton Foundation Press, West Conshohocken.

- Valsecchi, S., Conti, D., Crebelli, R., Polesello, S., Rusconi, M., Mazzoni, M., Preziosi, E., Carere, M., Lucentini, L., Ferretti, E., Balzamo, S., Gabriella, M., 2017. Deriving environmental quality standards for perfluorooctanoic acid (PFOA) and related short chain perfluorinated alkyl acids. *J. Hazard. Mater.* 323, 84–98. <https://doi.org/10.1016/j.jhazmat.2016.04.055>
- Valsecchi, S., Rusconi, M., Mazzoni, M., Viviano, G., Pagnotta, R., Zaghi, C., Serrini, G., Polesello, S., 2015. Occurrence and sources of perfluoroalkyl acids in Italian river basins. *Chemosphere* 129, 126–134. <https://doi.org/10.1016/j.chemosphere.2014.07.044>
- Vollenweider, R.A., Rinaldi, A., Montanari, G., 1992. Eutrophication, structure and dynamics of a marine coastal system: results of ten-year monitoring along the Emilia-Romagna coast (Northwest Adriatic Sea), in: *Marine Coastal Eutrophication*. Elsevier, pp. 63–106. <https://doi.org/10.1016/B978-0-444-89990-3.50014-6>
- Wright-Walters, M., Volz, C., Talbott, E., Davis, D., 2011. An updated weight of evidence approach to the aquatic hazard assessment of Bisphenol A and the derivation a new predicted no effect concentration (PNEC) using a non-parametric methodology. *Sci. Total Environ.* 409, 676–685. <https://doi.org/10.1016/j.scitotenv.2010.07.092>
- Xiao, F., 2017. Emerging poly- and perfluoroalkyl substances in the aquatic environment: A review of current literature. *Water Res.* <https://doi.org/10.1016/j.watres.2017.07.024>
- Xu, F., Li, Y., Wang, Y., He, W., Kong, X., Qin, N., Liu, W., Wu, W., Erik, S., 2015. Key issues for the development and application of the species sensitivity distribution (SSD) model for ecological risk assessment. *Ecol. Indic.* 54, 227–237. <https://doi.org/10.1016/j.ecolind.2015.02.001>
- Zareitalabad, P., Siemens, J., Hamer, M., Amelung, W., 2013. Perfluorooctanoic acid (PFOA) and perfluorooctanesulfonic acid (PFOS) in surface waters, sediments, soils and wastewater - A review on concentrations and distribution coefficients. *Chemosphere* 91, 725–732. <https://doi.org/10.1016/j.chemosphere.2013.02.024>
- Zhang, L., Liu, J., 2014. AQUATOX coupled foodweb model for ecosystem risk assessment of Polybrominated diphenyl ethers (PBDEs) in lake ecosystems. *Environ. Pollut.* 191, 80–92. <https://doi.org/10.1016/j.envpol.2014.04.013>
- Zhang, L., Liu, J., Li, Y., Zhao, Y., 2013. Applying AQUATOX in determining the ecological risk assessment of polychlorinated biphenyl contamination in Baiyangdian Lake, North China. *Ecol. Modell.* 265, 239–249. <https://doi.org/10.1016/j.ecolmodel.2013.06.003>

Chapter 3

Uptake and translocation of perfluoroalkyl acids (PFAA) in red chicory (*Cichorium intybus L.*) under various treatments with pre-contaminated soil and irrigation water

Andrea Gredelj^a, Carlo Nicoletto^b, Sara Valsecchi^c, Claudia Ferrario^c, Stefano Polesello^c, Roberto Lava^d, Francesca Zanon^d, Alberto Barausse^{a,e}, Luca Palmeri^a, Laura Guidolin^e, Marco Bonato^e

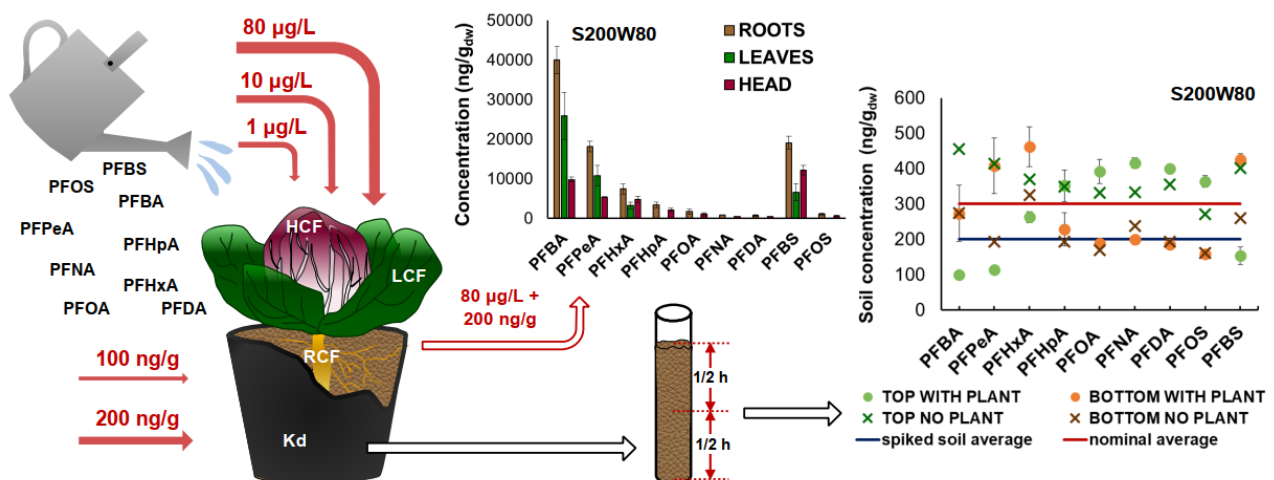
^a Department of Industrial Engineering, University of Padova, via Marzolo 9, 35131 Padova, Italy

^b Department of Agronomy, Food, Natural resources, Animals and Environment (DAFNAE), University of Padova, Viale dell'Università 16, 35020 Legnaro, Italy

^c Water Research Institute - National Research Council of Italy (IRSA-CNR), Via del Mulino 19, 20861 Brugherio (MB), Italy

^d ARPAV (Regional Environmental Agency of Veneto), Via Lissa 6, 30174 Venezia Mestre, Italy

^e Department of Biology, University of Padova, Via Bassi 58/b, 35131 Padova, Italy



Reproduced with permission from:

Science of the Total Environment, 2019

DOI: <https://doi.org/10.1016/j.scitotenv.2019.134766>

© 2019 Elsevier Ltd.

Chapter summary:

Perfluoroalkyl acids (PFAAs), particularly short-chained ones, have high potential for crop uptake, posing a threat to human health in contaminated areas. There is a scarcity of studies using contaminated water as the medium for PFAAs delivery to crops, and a lack of data on the partitioning of PFAA mixtures in growing media. In this context, a controlled experimental study was carried out in a greenhouse to investigate the uptake of a PFAA mixture into red chicory, a typical crop from a major PFAA contamination hot-spot in northern Italy, under treatments with environmentally relevant concentrations in spiked irrigation water and soil, separately and simultaneously. To our knowledge, this is the first study involving multiple exposure media and laboratory adsorption/desorption batch tests as a way of assessing the decrease in the bioavailability of PFAAs from soil. Exposure concentrations for each of the 9 utilized PFAAs were 0, 1, 10 and 80 µg/L in irrigation water and 0, 100 and 200 ng/g_{dw} in soil, combined into 12 treatments. The highest bioaccumulation was measured for PFBA in roots (maximum of 43 µg/g_{dw}), followed by leaves and heads of the chicory plants in all treatments, with the concentrations exponentially decreasing with an increasing PFAA chain length in all plant compartments. The use of irrigation water as the delivery medium increased the transport of PFAAs to the aerial chicory parts, long - chain substances in particular. Additionally, the distribution of PFAAs in the soil was assessed by depth and compared with laboratory measured soil-water equilibrium partition coefficients, revealing only partial dependency of PFAAs bioavailability on the adsorption in soil.

3.1. Introduction

Per- and polyfluoroalkyl substances (PFASs) are a wide group of anthropogenic industrial chemicals containing at least one perfluoroalkyl moiety (C_nF_{2n+1}) (Buck et al., 2011). PFASs are employed in a wide spectrum of industrial and commercial applications, from non-stick coatings to fire-fighting foams and cosmetics, due to their unique properties provided by the extreme strength of C-F bonds and their surfactant nature. Many PFASs are both hydro- and lipophobic, and they all have high chemical and thermal stability (Buck et al., 2011; Kempisty et al., 2018; Krafft and Riess, 2015a). Consequently, they are also persistent, bioaccumulative and thus ubiquitously present in the environment, wildlife and humans. Under environmental conditions, various PFASs (e.g. branched fluorotelomers) are eventually transformed to perfluoroalkyl acids (PFAAs), regarded as their final transformation product (Brendel et al., 2018). Since long-chain PFAAs, perfluorocarboxylic acids (PFCAs) with ≥ 7 fluorinated C-atoms and perfluorosulfonic acids (PFSAs) with ≥ 6 fluorinated C-atoms, were associated with toxic effects in animal studies and humans, some of them have been phased-out from the production and restricted in use (e.g. perfluorooctane sulfonic acid, PFOS, and its precursors under the Stockholm Convention, perfluorooctanoic acid, PFOA, restricted under EU REACH and long-chain PFAAs included on the EU REACH candidate list) and many national food and health authorities have established tolerable daily intakes (TDIs) (Brendel et al., 2018; DeWitt et al., 2018; Wang et al., 2017). Consequently, trends in industry shifted towards new non-regulated PFASs, many of them being short-chained, considering they were initially regarded as non-bioaccumulative and non-toxic (Brendel et al., 2018). Even though PFAAs in animals and humans accumulate progressively with increasing chain length (Ding and Peijnenburg, 2013b), this trend is found to be quite the opposite in plants, in which the shortest PFAAs accumulate the most (Blaine et al., 2014a; Felizeter et al., 2014; Krippner et al., 2015). Considering that the main uptake pathway is through the roots (Blaine et al., 2014b; McLachlan et al., 2019; Stahl et al., 2009), the contamination of agricultural soils can lead to crop contamination with PFAAs. In that way PFAAs can enter terrestrial food chains, leading to the human contamination directly or indirectly through animals fed by contaminated feed (Krippner et al., 2015). The contamination of agricultural soil with PFAAs can occur as a result of direct soil contamination, e.g. by fluorochemical industrial plants (Liu et al., 2019) or aqueous film-forming foams (Guelfo and Higgins, 2013), through the use of biosolids (Blaine et al., 2013) or contaminated irrigation water (Blaine et al., 2014b; Ghisi et al., 2019). The consumption of contaminated food and drinking water are regarded as the main pathways of human exposure (Felizeter et al., 2012; McLachlan et al., 2019).

In 2013, large-scale contamination of PFAAs was discovered in the Veneto region, Northern Italy, as a consequence of the emissions from a fluorochemical plant in the province of Vicenza (WHO, 2016). Concentrations up to 20 $\mu\text{g/L}$ (PFOA) in the groundwater, 3.4 $\mu\text{g/L}$ (PFOA) in surface waters and 7.9 $\mu\text{g/L}$ (PFOA) in spring waters of the Vicenza province were detected, with measured peaks up to 700 $\mu\text{g/L}$ of PFOA in industrially contaminated wells in the area (ARPAV, 2018b). Elevated serum PFAAs concentrations were detected in the residents of contaminated areas in Veneto, due to contaminated drinking water consumption (Ingelido et al., 2018) and associated with higher mortality levels (Mastrantonio et al., 2018). However, a comprehensive health risk assessment and research considering food consumption is still lacking. The Po valley has a strong agricultural history and is responsible for the Veneto region being one of the most significant producers of fruits, vegetables, cereals and wine in Italy and Europe (Veneto Region, 2014), making it among the most important economic sectors in the region. In general, Italy has the highest use of water for agricultural purposes in Europe, about 50% of which is in the form of surface and groundwater (Nicoletto et al., 2017).

To our knowledge, the only available study of PFAAs uptake into plants due to irrigation with contaminated water is the study of Blaine et al., in which strawberry and lettuce plants were irrigated with reclaimed water and grown in soils with varying organic carbon contents (%OC) (Blaine et al., 2014b). Studies on the uptake of PFAAs into crops are still mostly limited to PFOS and PFOA (Ghisi et al., 2019), and limited research focusing on the PFAAs mixture uptake to crops from soil has revealed a strong crop and soil type dependency (Blaine et al., 2013, 2014b; Krippner et al., 2015). The octanol-water partition coefficient, K_{ow} , is commonly used as an indicator for environmental distribution, bioavailability and toxicity of organic chemicals, but it cannot be experimentally determined due to the surfactant nature of PFAAs. Additionally, PFAAs do not accumulate in the storage lipids, but rather bind to proteins or partition to phospholipid membranes (Droge, 2019; Ng and Hungerbühler, 2014). This emphasizes the importance of PFAAs partitioning measurements on relevant sorbents in the site-specific contamination conditions (Droge, 2019). Soil sorption has a significant impact on the bioavailability of PFAAs in pore water, and then on their root uptake, but the soil-water distribution coefficients (K_d) are reported for growing media only in the plant uptake study of Blaine et al. (Blaine et al., 2014b). Their K_d s were however based only on the single-point batch test.

In this work, a typical Veneto crop - red chicory (*Cichorium intybus L.*), radicchio, was grown in a greenhouse as a model crop, under varying concentrations of the pre-contaminated soil and irrigation water corresponding to 12 different treatments, with two main goals. The first goal was to obtain a more mechanistic understanding and to systematically explore the relationship between the PFAAs chain length and uptake of chemicals from the contaminated agricultural soil and irrigation water, separately and in synergy. To reach this goal, in addition to the quantification of PFAAs distribution and mobility in the growing pots, adsorption and desorption from soil of the same PFAAs mixture were studied in laboratory batch-tests. The second goal was to measure all necessary crop-specific parameters as the growth and transpiration rates, together with the inter-compartmental PFAAs distribution, with the aim of developing a forecast model of PFAA uptake into edible crop parts under environmentally representative contamination conditions. Here, we are reporting the results of experimental work and the main conclusions on distribution and bioaccumulation of PFAAs in chicory plants and the corresponding soil under various contamination treatments.

3.2. Materials and methods

3.2.1. Chemical reagents and materials

Nine perfluoroalkyl acids (seven carboxylic and two sulfonic acids) were used through all of the experimental work (Table 3-1).

Table 3-1. A list of used PFAAs, with common abbreviations and in the increasing chain-length order

Abbreviation	Chemical (common) name	No. of perfluorinated carbons (nCF_x)	CAS number	Molar mass (g/mol)
Short - chain PFAAs				
PFBA	Perfluorobutanoic acid	3	375-22-4	214.04
PFPeA	Perfluoropentanoic acid	4	2706-90-3	264.05
PFBS	Perfluorobutane sulfonic acid	4	375-73-5	300.1
PFHxA	Perfluorohexanoic acid	5	307-24-4	314.05
PFHpA	Perfluoroheptanoic acid	6	375-85-9	364.06
Long - chain PFAAs				
PFOA	Perfluorooctanoic acid	7	335-67-1	414.07
PFNA	Perfluorononanoic acid	8	375-95-1	464.08
PFOS	Perfluorooctane sulfonic acid	8	1763-23-1	500.13
PFDA	Perfluorodecanoic acid	9	335-76-2	514.08

Non-labeled technical quality standards with a purity $\geq 96\%$ were used for all spiking purposes. Materials, reagents and labeled standards used for extraction and analyses, with details and suppliers are provided in Appendix 2 (A1-2a and A1-2b).

3.2.2. Experimental set-up

The experiment was carried out in a plastic greenhouse at Agripolis, University of Padova's experimental farm in Legnaro (45°20' N; 11°57' E), Italy, in a period of three months from August to November 2018. Red chicory plants (*Cichorium intybus* L. var. *foliosum* Hegi), Chioggia type, were grown in pots, in a loam agricultural soil typical for the area. There were twelve treatments in total, each with 5 replication plants and one no-plant blank, including the agricultural soil that was spiked with nine PFAAs (Table 3-1), each on the nominal concentrations of 100 or 200 ng/g_{dw}, while nominal concentrations in spiked irrigation water were 1, 10 and 80 µg/L. Controls with clean soil and clean water were included as well, as shown in the matrix on Figure 3-1. As shown on the figure, each treatment represents a combination of exposures to PFAAs from both irrigation water and pre-contaminated, spiked soil. The fourth experimental column was irrigated with control (clean) tap water from Agripolis, Legnaro, the same water that was used in all the other treatments after spiking to appropriate concentrations. The bottom experimental row consisted of control (clean) loam agricultural soil, the same as spiked and used in the other two treatment rows. The choice of concentrations in irrigation water was based on the measured concentrations in the ground- and surface waters in the Veneto Region database (ARPAV, 2018b) and were also representative of other similar contamination scenarios worldwide (Rumsby et al., 2010). In this case, equal nominal concentrations of PFAAs were used to simplify the interpretation, despite that environmentally measured concentrations do vary among PFAAs. Soil nominal spike concentrations were chosen on the basis of available measured PFAAs concentrations in agricultural soils with similar scenarios worldwide (Krippner et al., 2015; P Zareitalabad et al., 2013).

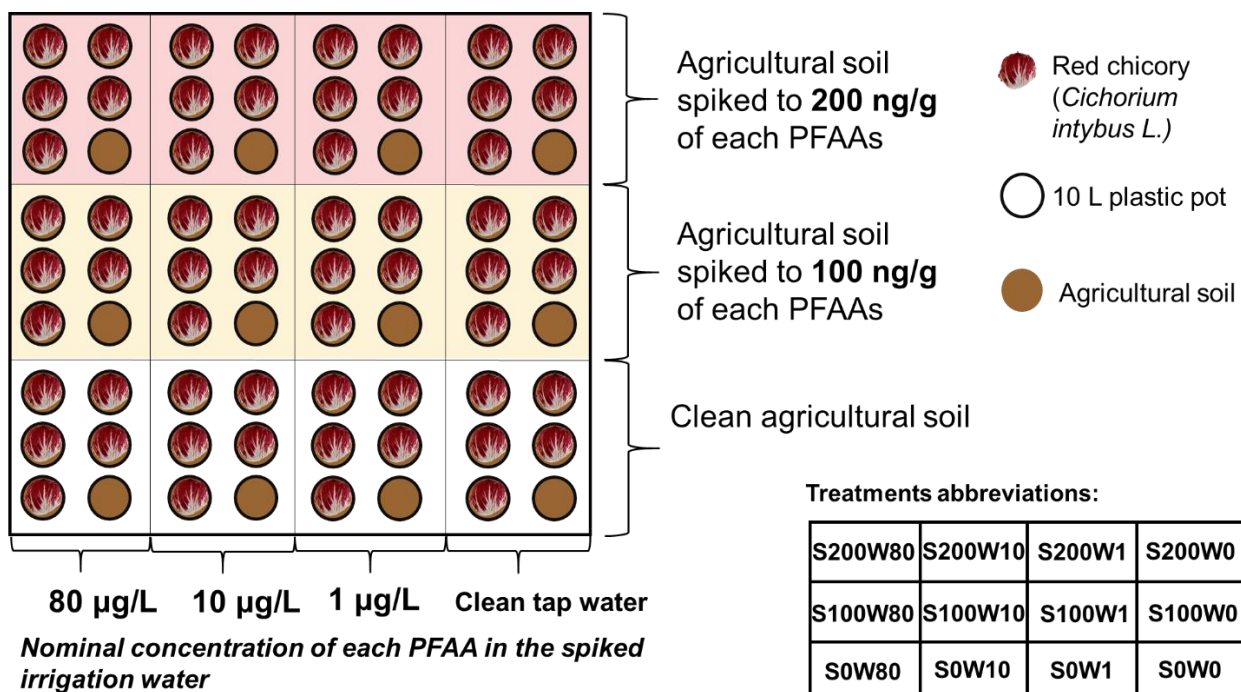


Figure 3-1. Experimental scheme of the 12 treatments. Abbreviations for each treatment were formed as: e.g. S100W80, S = "soil", 100 = nominal concentration in soil in ng/g_{dw}, W = "water", 80 = nominal concentration in irrigation water in µg/L.

Plants were pre-grown from seeds in peat nursing pots, and after four weeks and forming 3-4 true leaves, they were transferred in the prepared pots with spiked soil, previously equilibrated for 10

days. This period was chosen based on the PFAAs sorption experimental results in literature, and was therefore considered sufficient for equilibration (Guelfo and Higgins, 2013; F. Li et al., 2018). To determine spike homogeneity and actual resulting concentrations of all PFAAs, soil samples were taken immediately prior to planting the red chicory. Irrigation with contaminated water started on the 4th day of experiment and was performed manually in the equal doses per each pot, directly to soil, in an average frequency of 3 times per week and in quantities between 400 and 800 mL. Each individual water portion was weighed (A2-5), resulting with about 13.8 L of contaminated (or control) water delivered to each plant for the duration of experiment. Detailed information on the crop, cultivation conditions, soil characterization and spiking protocol are given in the A2-3 and A2-4. The growth period lasted 87 days (from transplanting) and three fully mature chicory plants were harvested per each treatment and split into roots, leaves and heads. Leaves and heads were washed with distilled water and stored in sealed plastic bags at -20°C until the extraction. Roots were thoroughly washed under a water spray for 5 minutes each, to carefully remove all remaining soil and were air dried before the extraction (water loss was accounted for by weighing). After the root harvest, soil from the corresponding pots was mixed manually to form whole-pot composite samples that were collected and stored before the extraction (sealed plastic bags at 4°C). Apart from the composite samples, vertical samples were taken with a cylindrical plastic sediment corer to determine the vertical distribution of PFAAs in the agricultural soil. Three treatments with the highest PFAAs concentration in water and/or soil were chosen for this purpose i.e corresponding to the cases with only contaminated irrigation water and clean soil (S0W80), only spiked soil and clean irrigation water (S200W0) and their combination (S200W80). Every soil core was then split into two parts, of about 10 cm in height, corresponding to the top and bottom part of the pot. In each treatment sampled with the corer, three pots in total were analyzed: two in which chicory plants were grown and one pot without a plant.

3.2.3. Soil-water partition coefficients

Adsorption and desorption equilibrium experiments were performed by a single decant-refill batch technique, by the methodology proposed in the OECD 106 guidelines (OECD, 2000). First, kinetic adsorption experiments were performed to determine the required adsorption equilibration time for each of 9 PFAAs in the same mixture as in the pot experiment and with the same agronomic soil. All batch experiments were performed in triplicates in 50 mL polypropylene (PP) centrifuge tubes, with 5 g of dry soil pre-equilibrated for 12 h with 25 ml of 0.01 M CaCl₂ and 1 g/L NaN₃ aqueous solution. After the equilibration period, all tubes, apart from the clean control samples, were spiked with 50 µL of the appropriate stock spike solution to achieve the nominal concentration of 100 µg/L of each PFAA in the kinetics test, and 1-500 µg/L in the equilibrium adsorption tests. Sacrificial samples were prepared in triplicates for every predetermined contact time in the kinetics test: 0, 2, 4, 8, 24, 48 and 72 hours. Four more time periods were interpolated, based on the result of the initial 7 points kinetics test: 15, 30, 45 and 60 minutes. After determining the required equilibration time for adsorption, triplicate sets for each isotherm point were prepared by spiking the solutions in reactors to the mass concentration of 1, 10, 100, 250 and 500 µg/L for each PFAA in a mixture. The use of adsorption-based soil-water partition coefficients (K_{ds}) for predictions of the leaching potential (and desorption) of long-chain PFAAs from soil treated with contaminated biosolids was evaluated as unreliable in (Sepulvado et al., 2011). Considering the complex processes affecting the sequestration and the irreversible sorption of long-chain PFAAs observed in (Chen et al., 2016; Zhao et al., 2016), desorption-based equilibrium partition coefficients (K_{des}) were derived as well. Subsequently, desorption tests were performed after the adsorption batch tests, by utilizing the same PP tubes; after decanting the supernatant in the adsorption experiment. A CaCl₂-NaN₃ solution was then added to the tubes until the 25 mL mark and placed back on the rotation shaker until desorption equilibrium

was reached. In addition to PFAA concentration analyses in the supernatants, the soil component was extracted and analyzed after the desorption experiment as a quality control and to determine the total recovery in all reactors. More details about chemicals, extractions, analyses and calculations for the batch adsorption/desorption tests are given in A2-2b and A2-10.

3.2.4. Chemical analyses of crop tissues, soil and irrigation water

The extraction of crop tissues (roots, leaves and heads) was carried out according to (Mazzoni et al., 2016), with a few minor modifications. Plant sample preparation procedure was based on a sonication - assisted extraction of homogenized samples with acetonitrile. All plant extracts were analysed by UHPLC-MS/MS (TSQ Quantum™ Access MAX, Thermo Scientific, USA) equipped with a Waters Acquity UPLC BEH C18 column (50x2.1 mm id, 1.7 µm particle size) by direct injection after acidification with formic acid and addition of Isotope Labelled Internal Standard mixture. Details on the procedure and the performance parameters of the analytical method are reported in the A2-1b and A2-2a.

The soil extraction protocol included oven drying at 38°C for 48h, sieving at 2 mm and milling afterwards. 10 mL (25 mL in the adsorption/desorption batch tests) of the 50:50 MeOH/H₂O (V:V) extraction solution were added to 2 g of the milled soil in the PP vials (or directly in the adsorption batch reactors), in which pH was adjusted to 9-10 by NH₄OH (1:5) aqueous solution. Samples were vortexed and then placed on a rotation shaker for a period of 65 minutes. Afterwards, they were centrifuged for 10 min at 3000 rpm (or 6000 rpm in adsorption/desorption test). Supernatants were separated by filtration through 0.2 µm filters, pH values were adjusted to 3-4 with glacial acetic acid and supernatants were then appropriately diluted for LC-MS/MS analyses. Irrigation water samples and supernatants from the adsorption/desorption tests were directly injected after appropriate dilutions. The instrument used for the soil and irrigation water analyses was a HPLC LC-30AD XR Shimadzu coupled with an API 6500 AB Sciex triple quadrupole and with a CTC PAL HTS XT autosampler, equipped with Phenomenex Kinetex Evo C18 (1.7 µm x 2.1 mm x 100 mm) and Supelco Ascentis RP-Amide (2.7 µm x 2.1 mm x 150 mm) columns for water and soil analyses, respectively. Further details of the soil and water analyses are in A2-1b and A2-2b.

3.2.5. Data analyses

3.2.5.1. Bioconcentration factors

The uptake and bioaccumulation potential of contaminants in plant tissues (roots, stem, leaves, fruits) from their environment (soil, water, air, hydroponic nutrient solution) is typically expressed as bioconcentration factor (BCF) (Torralba-Sanchez et al., 2017). Here, equilibrium bioconcentration factors were expressed on a dry weight basis as the ratio between concentration of each PFAA in chicory roots, leaves, heads (and shoots in total) and the concentration in soil:

$$BCF (g_{dw}/g_{dw}) = \frac{PFAA \text{ concentration in plant compartment } (ng/g_{dw})}{PFAA \text{ concentration in soil } (ng/g_{dw})} \quad (3-1)$$

in which BCF stands for either root concentration factor (RCF), leaves concentration factor (LCF), head concentration factor (HCF) or shoots (as the total aerial plant biomass) concentration factor (SCF), depending on the plant compartment considered. Concentration in shoots was calculated with respect to the measured concentrations and masses of heads and leaves. In this way we assumed that the only uptake pathway of PFAAs is from soil, a justified assumption since PFAAs are present as anions at the environmental pH (between 4 and 9) and, hence, they are not volatile, so atmospheric deposition or loss to air from soil could be considered negligible (Blaine et al., 2014a).

To include all PFAAs present in soil, regardless if it was delivered to soil by spiking, irrigation or both, soil concentrations $c(PFAA)_{soil}$ for the calculation of BCFs were defined as:

$$c(PFAA)_{soil}(ng/g_{dw}) = \frac{m_{soil} c(PFAA)_{spiked} + \sum_{i=1}^n V_{irr.w.,i} c(PFAA)_{irr.w.,i}}{m_{soil}} \quad (3-2)$$

in which m_{soil} is the mass of soil in the pot (g_{dw}), $c(PFAA)_{spiked}$ (ng/g_{dw}) is the measured soil concentration after spiking and equilibration, n is the total number of irrigation portions, $V_{irr.w.,i}$ (L) is the volume of i -th irrigation portion while $c(PFAA)_{irr.w.,i}$ (ng/L) is the measured concentration of PFAA in i -th irrigation treatment. Measured concentrations in spiked soil and irrigation water are given in A2-4 and A2-5.

3.2.5.2. Statistical analyses

The data are always shown as the calculated means of experimental replicates with standard error estimates. All statistical analyses were performed by SPSS Statistics, IBM statistical software. Pearson's correlation analyzes was performed to indicate the strength of individual relationship between the concentrations of every PFAA in roots, leaves and heads and its concentration in spiked soil and concentration in soil resulting from the irrigation water. Multiple regression analyzes was used for assessing the influence of the soil and water as a delivery media, because when both water and soil are used simultaneously correlation analyzes is insufficient. The analyzes was performed for each PFAA with all treatments included, having a concentration in the plant compartment as the response variable and PFAAs concentrations in spiked soil and concentration in soil resulting from the irrigation water as predictors. Concentration in soil of each PFAA originating from the irrigation water was calculated as a ratio of the mass of PFAA delivered by irrigation water and the dry soil mass, defining the least-squares regression plane as:

$$c(PFAA)_{plant\ compartment} = S c(PFAA)_{spiked} + W \frac{\sum_{i=1}^n V_{irr.w.,i} c(PFAA)_{irr.w.,i}}{m_{soil}} \quad (3-3)$$

in which S and W are regression coefficients for soil and water, respectively ($g_{dw\ soil}/g_{dw\ plant\ compartment}$). The intercept was set to 0, as the background contamination was considered negligible. Since both masses of PFAA, available from soil and available from irrigation water, were normalized to the soil mass and considering the (mostly) equal concentrations of all PFAAs per each treatment, sizes of S and W were comparable between PFAAs. Additionally, S and W are of the same order of magnitude as BCFs and as such can be considered as the partial BCFs, measuring the contribution of soil and water, respectively. Standardized regression coefficients, β_s and β_w , were then directly utilized to quantify the influence of the soil and water on the resulting concentrations in roots, leaves and heads.

Two-tailed Student's t -test was used for comparing the mean BCFs, after confirming the normality by Shapiro-Wilk test and the homogeneity of variance by Levene's test, either to compare individual PFAAs bioconcentration among treatments or to seek for differences between sulfonates and carboxylates. All correlations and statistical differences were assumed to be significant at the $p < 0.05$.

3.2.6. Quality assurance and control

All materials containing perfluoroalkyl substances (e.g. Teflon®) were avoided during the experimental phase to minimize risk of contamination. Glassware was avoided as well, knowing that some PFAAs can irreversibly bind onto glass surfaces (F. Li et al., 2018). Soil spiking efficiency was evaluated before planting by soil analyses to assess for the homogeneity of the spike. Clean control treatment was used to assess for the background PFAAs contamination or cross-contamination. Plant matrices and soil were always sampled as triplicates. Of initially 5 plants that were initially

grown per treatment, 3 pots whose plants were without noticeable degenerations and had approximately the same size and appearance were chosen for the sampling and analyses. One pot per treatment was used as the no-plant blank and was treated in the same way as the plant-containing pots. Batch reactors in the adsorption/desorption tests were always prepared and analyzed in sets of three. Two sets of experimental blanks were prepared throughout all the adsorption/desorption experiments: triplicates containing only soil and background solution as the first set of blanks for testing the background soil PFAAs contamination and another set of triplicates with only background solution, spiked with PFAAs, to test the potential PFAAs adsorption on the PP vial walls. All results are reported as the means of three values. Analytical QA/QC with details on the calibration curves, internal standards, LODs, solvent blanks, and recoveries are reported in A2-2.

3.3. Results and discussion

3.3.1. Inter-compartmental distribution of PFAAs

Figure 3-2 shows the concentration of PFAAs in the respective red chicory compartments for the three most contaminated treatments. The concentration patterns of different PFAAs were similar in 10 of 12 treatments (except the control and S0W1 in which all concentrations were <LOD), short-chain PFAA compounds accumulating the most in all the plant compartments: roots, leaves and heads. PFBA accumulated in the highest concentrations among PFAAs, but in one case (S200W80 for heads), and in some treatments (e.g. roots of S100W0, S200W0) its concentration was more than 2.5 times as high as the concentration of PFPeA, its consecutive homologue. Short-chain PFAAs (PFBA, PFPeA, PFHxA and PFBS, respectively) were the most detected PFAAs in shoots (both leaves and heads), in accordance with the findings for other crop types grown in soil (Blaine et al., 2014a; Krippner et al., 2015; Wen et al., 2014). Among the plant compartments, root concentrations were higher than expected for short-chain PFAAs (e.g. more than 40000 ng/g_{dw} of PFBA in the treatments S200W0 and S200W80), and were always higher than in the shoots, having the inverse relationship with increasing chain length. In the treatments where pre-contaminated soil was also irrigated with spiked water, the additional exposure to PFAAs via irrigation water (e.g. in S200W80) had no obvious effect on the concentration in roots; in fact, treatments S200W0 and S200W80 have almost the same resulting root concentrations. Nevertheless, irrigation evidently increased the concentrations measured in leaves and heads, where clear concentration difference can be seen between the two treatments (e.g. treatments S200W0 and S200W80 in Figure 3-2 and A2-6 for other treatments).

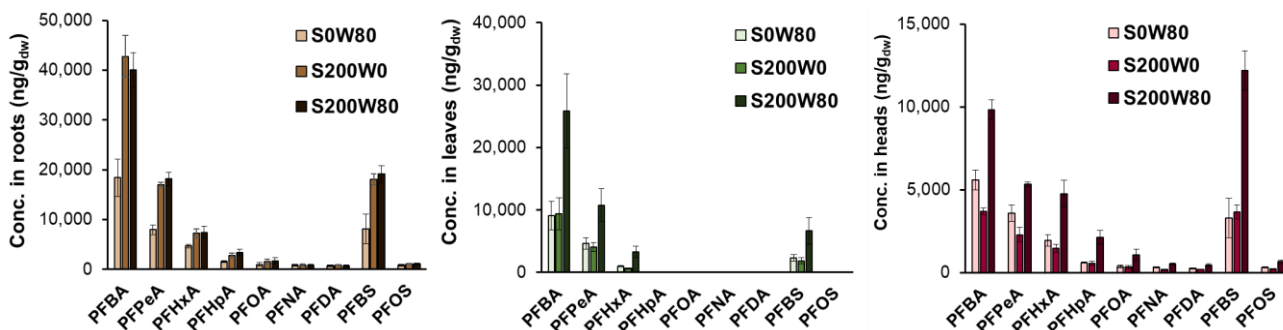


Figure 3-2 Concentration of PFAAs in radicchio compartments for the three most contaminated treatments. Means of 3 plant compartments are shown with standard error estimates.

In chicory leaves, PFHpA and all long-chain PFAAs were below LOD, even though they were regularly detected in heads i.e. the edible part. PFBA, PFPeA, PFHxA and PFBS were compounds that accumulated the highest in both leaves and heads (Figure 3-2). However, concentrations of

PFBA and PFPeA in leaves were respectively 3 and 2.4 times as high as concentrations in heads, looking at treatments average. This was in accordance with the assumption of constant transpiration rates and the passive transport of short-chain PFAAs upwards by xylem (Blaine et al., 2013; Krippner et al., 2014a) and the growing/transpiring period for heads that lasted about 30 days (1/3 of the growing cycle of 87 days). The inter-compartmental mass distributions per treatment are shown in A2-7, and, when > LOD, for all treatments and all PFAAs, PFAAs mass was mostly contained in the upper chicory parts (about 80% for PFBA, PFPeA, PFHxA and PFBS).

3.3.2. Bioconcentration factors

Root concentration factors ranged from 221 g/g_{dw} for PFBA to about 5.7 g/g_{dw} for PFNA, PFDA and PFOS (average of all treatments above LOD) and were chain length dependent, decreasing with increasing chain length (Table A2-14 in A2-8). Leaf concentration factors were also the highest for PFBA, even though lower than for the roots, with the treatments average ranging from 109.4 g/g_{dw} for PFBA to < 1 g/g_{dw} or < LOD for all of the long-chain PFAAs. Average head concentration factors of all treatments with concentrations > LOD were higher than 1 g/g_{dw} for all PFAAs, and, again, were the highest for PFBA with 38 g/g_{dw} and the lowest for PFDA with 1.4 g/g_{dw}. Our values were always lower than the BCFs reported in the greenhouse study of (Blaine et al., 2014b), who used the PFAA contaminated irrigation water and reported BCFs for PFBA in lettuce in the range from 767 to 3390 g/g_{dw} (depending on the used soil). For the lettuce (as the most similar crop to the red chicory) that was grown in the industrially impacted (biosolids amended) soil in a greenhouse (Blaine et al., 2013), resulting BCFs were 57 and 20 g/g_{dw} for PFBA and PFPeA, respectively. Our values for the red chicory are somewhere in between these values for all of the plant compartments.

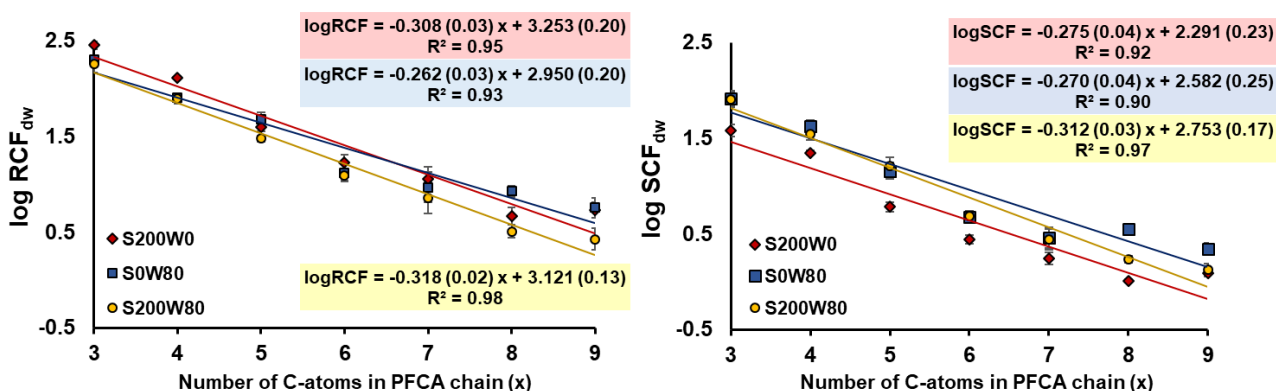


Figure 3-3. Correlations between logRCF and logSCF and number of C-atoms of the PFCAs' perfluoroalkyl chain for the three most contaminated treatments. Regression lines with slopes, intercepts and associated standard errors in brackets are shown.

For both aerial compartments, leaves and heads, chain length dependency was evident, with a decrease in accumulation as the chain length increases. Some long-chain PFAAs had concentration in leaves <LOD, but were measurable in heads. This observation could be explained by considering the time at which sampling of the leaves took place. Towards the end of the growing cycle, the oldest leaves had withered and were thereby eliminated at harvest, whilst the heads were always evaluated as a whole. It is possible that these leaves had higher overall concentrations of PFAAs due to their age and longer transpiring period. Hence, while evaluating the transport upwards between treatments and in dependency of the PFCAs chain-length, leaves and heads were assessed together as shoots, in which concentration in leaves was assumed as ½ LOD when the corresponding PFAA accumulated above LOD in the heads of all 3 replicates.

Roots and shoots concentration factors were logarithmically transformed and plotted against PFCAs' chain length (Figure 3-3). Regression lines are shown for the most contaminated treatments:

S200W0, S0W80 and S200W80, as for them all PFAAs were > LOD in roots and shoots. Both for logSCFs and logRCFs, a strong negative correlation (R^2 values greater than 0.9) with the chain length of PFCAs is evident.

For every increase in the chain length, both RCFs and SCFs decreased by about 0.2-0.6 log units (0.3 on average). RCFs of the shortest PFCAs, PFBA ($3CF_x$) and PFPeA ($4CF_x$) were significantly higher in the treatment S200W0 ($p = 0.024$ and $p = 0.001$ when compared to the treatment S200W80, respectively), despite the regression lines being similar (statistically significant differences were not observed between slopes). Additionally, the two longer PFCAs, PFNA ($8CF_x$) and PFDA ($9CF_x$) showed somewhat higher RCFs in the treatment with only contaminated water, even though it was statistically significant only for PFNA ($p = 0.035$ when compared to S200W80). On the other hand, SCFs in the treatment with only contaminated soil, S200W0, were significantly lower than the other two treatments in which contaminated irrigation water was applied to the soil (i.e. when compared with S0W80, for all PFAAs, but for PFBS, p values were < 0.05).

Studies on crop uptake of PFAA mixtures from soil have depicted the chain length dependency patterns of bioaccumulation in the aerial compartments (fruits, stems, grains, husks, etc.), but studies analyzing the root compartment in the same manner are fewer (Blaine et al., 2014a; Wen et al., 2014). To the authors' knowledge, the present study is the first one to present a strong negative correlation between root concentration factor and PFCAs' increasing chain length (Figure 3-3). However, a similar pattern of root bioaccumulation decrease with chain length increase, but less pronounced (i.e. slope was $-0.17 \log RCF/nCF_x$, compared to our $-0.31 \log RCF/nCF_x$) could be seen only for celery from (Blaine et al., 2014a). It is also significant to underline that hydroponic studies have shown an opposite chain dependency in roots, i.e. increase of the accumulation with increasing chain length of both PFCAs and PFSAs (Felizeter et al., 2014, 2012; Müller et al., 2016), while situation is more complex in soil (or biosolids) studies in which soil sorption and other soil related factors (such as leaching) influence the bioavailability. Root systems are larger (particularly the small roots and root hairs) in soil, both the soil and the root system providing more surface for PFAAs adsorption (i.e. more adsorption sites are available). In this study, the quantity of irrigation water utilized was just sufficient for growth and the irrigation was lower than usually adopted under field conditions. Additionally, pots were closed at the bottom. These factors influenced the root system development and growth and most of its biomass was discovered at the bottom of the pots whilst sampling and subsequently a high percentage of these small roots were successfully retrieved. Small roots are saturated with contaminants in the highest extent and in almost equilibrium with the soil's pore water (Trapp, 2007). In their hydroponic studies, both (Felizeter et al., 2012) and (Müller et al., 2016) hypothesized that adsorption to root surface/apoplast is likely the dominant accumulation mechanism for majority PFAAs (except for PFBA). In the kinetic experiments of (Müller et al., 2016), the shortest-chain PFAAs were irreversibly sorbed during the consequent depuration experiment. This could mean that the thorough method of cleaning and washing the roots had possibly removed those externally sorbed long-chain PFAAs, revealing the actual true uptake in roots and internally present compounds. In fact, up to 40% of the root space, the so-called "apparent free space", can be accessed by washing water without the barrier (Mc Farlane and Trapp, 1994).

The system constraints (i.e. all of the water used for irrigation was contaminated and pots were closed on the bottom) could have caused the higher BCFs than under the field conditions, considering that usually smaller BCFs were reported for the field studies (Liu et al., 2019, 2017; Wen et al., 2014). According to our knowledge, the highest field-based BCFs of 50.11 g/g_{dw} for \sum PFAA (mostly PFBA and PFOA) were calculated for the leaf blades of carrot (Liu et al., 2019) or 33.11 g/g_{dw} for the wheat grain in (Liu et al., 2017). Both the field studies of Liu et al. (Liu et al., 2019, 2017) stated that the PFAA bioaccumulation in vegetables and cereals is the result of irrigation with

contaminated water. When compared to the greenhouse experiment, due to their high mobility (McLachlan et al., 2019; Vierke et al., 2014), short-chain PFAAs could have been transported downwards and out of the root zone more freely, resulting with the lower uptake in the field conditions. Additionally, field-grown plants would receive some precipitation and not only irrigation water, which was in the study of (Liu et al., 2019) much less contaminated than the groundwater used for irrigation. This could increase the mobile PFAAs washout and also dilute the high concentrations in the pore water. The field study of (Wen et al., 2014), where the contamination of wheat resulted from the biosolids amendment, in contrary to the irrigation, reported on the grain concentration factor of 1 g/g_{dw} (for PFBA), which is significantly lower than the previously mentioned one of (Liu et al., 2017), indicating the possible impact of PFAAs delivery media in the field conditions as well.

3.3.3. Effects of different treatments on PFAAs bioavailability and bioaccumulation

Effects of different treatments were assessed through correlation and least-squares multiple regression analyses, for each PFAA and plant compartment. Regression coefficients with standard errors and p-values, standardized regression coefficients and coefficients of multiple determination (R^2) are shown in Table 3-2. PFAAs that are not listed were <LOD in the respective plant compartment for all or the majority of treatments (e.g. concentration of PFNA was not measured above LOD in 8 treatments, which was not enough to perform regression analyzes). For leaves, PFHpA, PFOA, PFNA, PFDA and PFOS were <LOD for almost all treatments, hence, they were not taken into statistical analyzes. All treatments were included in the regressions, except S100C80 that was excluded for PFDA (<LOD).

Table 3-2. Results of the correlation and multiple regression analyses per red chicory compartment and PFAA. Results of the correlation analyses are shown as Pearson's r , with ** if correlation is significant at the 0.01 level (2-tailed) and * if correlation is significant at the 0.05 level (2-tailed). Regression coefficients for soil and water ($g_{dw\ soil}/g_{dw\ plant\ compartment}$) (S and W) are shown with their standard errors (S.E.), significance level (p) at $\alpha = 0.05$ and standardized coefficients (β_s and β_w). R^2 is the coefficient of multiple determination of the linear multiple regression model.

Pearson's r			soil				water				R^2
Roots	Soil	Water	S	S.E.	p	β_s	W	S.E.	p	β_w	
PFBA	0.861**	0.352	191.51	15.62	2.4E-07	0.84	127.74	33.01	0.0031	0.26	0.96
PFPeA	0.836**	0.396	88.63	8.73	1.4E-06	0.82	53.60	15.88	0.0071	0.27	0.95
PFHxA	0.783**	0.485	32.26	3.58	4.1E-06	0.77	25.05	6.34	0.0027	0.34	0.94
PFHpA	0.821**	0.478	15.45	1.15	1.0E-07	0.79	11.42	1.99	0.0002	0.34	0.97
PFOA	0.794**	0.457	6.64	0.67	1.8E-06	0.78	6.53	1.53	0.0017	0.34	0.95
PFDA	0.794**	0.268	4.89	0.68	4.9E-05	0.84	3.17	1.61	0.0813	0.23	0.90
PFBS	0.781**	0.501	70.53	6.70	9.9E-07	0.75	77.52	14.65	0.0004	0.38	0.96
PFOS	0.721**	0.397	5.18	0.85	1.1E-04	0.76	4.14	1.64	0.0304	0.31	0.88
Leaves	Soil	Water	S	S.E.	p	β_s	W	S.E.	p	β_w	R^2
PFBA	0.688*	0.615*	75.25	8.15	3.3E-06	0.69	104.00	17.23	1.3E-04	0.45	0.95
PFPeA	0.698*	0.636*	37.80	4.20	4.2E-06	0.69	44.83	7.65	1.6E-04	0.45	0.95
PFHxA	0.613*	0.693*	7.36	1.26	1.6E-04	0.59	11.64	2.23	3.9E-04	0.53	0.92
PFBS	0.558	0.702*	14.77	2.30	7.7E-05	0.59	30.28	5.04	1.3E-04	0.55	0.93
Heads	Soil	Water	S	S.E.	p	β_s	W	S.E.	p	β_w	R^2
PFBA	0.484	0.846**	22.50	1.71	1.2E-07	0.52	60.10	3.61	1.3E-08	0.65	0.99
PFPeA	0.475	0.874**	13.16	1.07	2.4E-07	0.49	32.36	1.95	1.3E-08	0.66	0.99
PFHxA	0.444	0.859**	7.19	1.55	9.3E-04	0.40	23.12	2.75	7.5E-06	0.72	0.94
PFHpA	0.440	0.814**	3.57	0.95	3.8E-03	0.41	10.46	1.64	8.1E-05	0.70	0.90
PFOA	0.454	0.815**	1.53	0.36	1.8E-03	0.43	5.64	0.83	4.5E-05	0.69	0.92
PFDA	0.552	0.794**	1.05	0.10	3.5E-06	0.57	2.67	0.25	2.1E-06	0.61	0.97
PFBS	0.400	0.816**	16.22	5.01	8.9E-03	0.38	67.55	10.96	1.1E-04	0.72	0.89
PFOS	0.467	0.858**	1.15	0.18	7.6E-05	0.43	3.65	0.35	1.0E-06	0.71	0.96

Linear multiple regression models were a very good fit for all the PFAAs and all plant compartments (R^2 always being > 0.9) and were statistically significant in all cases except for W of PFDA in roots. For roots, Pearson's correlation coefficients were statistically significant ($p < 0.05$) for soil and were ranging between 0.7 and 0.86 for all PFAAs (in contrary to r_s for water that were between 0.35 and 0.49 and not statistically significant); implying that concentration in soil can accurately describe bioaccumulation in roots on its own. Similar to the RCFs correlated to the PFCAs chain length, correlation coefficients S and W were decreasing with the PFCAs chain-length increase, considering the higher root uptake of the short-chain PFAA. Standardized regression coefficients for soil (β_s) were constantly higher than those of water (β_w) for all PFAAs, indicating the stronger influence of soil, compared to water, on the PFAAs uptake to roots. This can be associated with the PFAAs homogeneous distribution in well mixed spiked soil and the extensive root development and branching throughout the soil, making them easily accessible. For leaves, Pearson's correlation coefficients were statistically significant for soil and water (only exception being the soil r for PFBS) and were similar for both water and soil. PFBA and PFPeA had slightly higher β_s than β_w , while they were very similar for PFHxA and PFBS, suggesting that an equal contribution of both water and soil for leaves could be the case. As described in the paragraph 3.3.2., due to the leaves withering, head is more representative compartment for the evaluation of the delivery media influence on PFAAs transport upwards. For heads, Pearson's r_s were always higher than 0.79 and were statistically significant for water, but not for soil. In agreement with the correlation results, standardized regression coefficients for water were always higher than the coefficients for soil, representing stronger dependency of the PFAAs concentration in heads on the irrigation water and amplifying the significance of PFAAs' passive transport upwards with the transpiration water. The observed effect of irrigation water in heads can also be a result of the transport of "surplus" PFAAs, delivered by irrigation, to aerial parts after the roots have already equilibrated with PFAAs in the soil pore water, an effect observed in the kinetic uptake experiment for carbofuran (ionic organic pesticide) in the bean plants (Trapp and Pussemier, 1991). In their hydroponic kinetic experiment, Müller and the coworkers (Müller et al., 2016) found for all PFCAs from $3CF_x$ to $9CF_x$ (and PFBS and PFOS) to equilibrate in the roots of *Arabidopsis* within 5 days. Equilibration of roots and pore water could be expected to some extent within the growing period of 87 days, despite of the periodical delivery of PFAAs by irrigation water (or additional desorption from soil while only clean irrigation water is used) which could lead to a state of non-equilibrium through the higher concentration of PFAAs in the pore water (i.e. increased bioavailability) and the mentioned passive transport of "surplus" PFAAs' to the shoots.

3.3.4. Sulfonates vs. carboxylates

Bioaccumulation of sulfonates and carboxylates with the same chain length was compared by means of inter-compartmental bioconcentration factors. Three representative treatments S200W0, S0W80 and S200W80 were used in the comparison between PFPeA vs. PFBS ($4CF_x$) and PFNA vs. PFOS ($8CF_x$). The accumulation of PFPeA in leaves was statistically significantly higher than the accumulation of PFBS in the treatment S200W0 ($p = 0.039$), while PFBS accumulated statistically higher than PFPeA in heads of the treatment S200W80 ($p = 0.035$). The remaining treatments have shown the same pattern (e.g. LCFs of 47.0 g/g_{dw} for PFPeA vs. 25.0 g/g_{dw} for PFBS in S200W80), even though it was not statistically significant. The comparison of the PFSA and PFCAs in roots did not show any difference in their bioaccumulation (RCFs were almost identical in the treatments S200W0 and S200W80) (A2-8), while in the hydroponic study with different crops, (Felizeter et al., 2014) noticed higher sorption of PFSA to roots. Considering the significant difference in soil sorption between PFNA and PFOS (K_{ds} of 5.11 and 93.56 L/kg, respectively, Chapter 3.3.5 and other soil sorption studies, (e.g. (McLachlan et al., 2019; Sepulvado et al., 2011)), not observed for PFPeA

and PFBS, some discrepancies in the root uptake may be expected at least for long-chain PFAAs. Here, long-chain PFCA and PFSA with $8CF_x$ did not show statistically significant differences in any of their BCFs. A different uptake of short-chain PFCA and PFSA to the upper chicory plant parts indicate the possibility for different transport mechanisms. This has already been investigated by some authors (Blaine et al., 2013; Krippner et al., 2015; Wen et al., 2014), indicating the higher uptake of PFCAs, except for the wheat grains in (Wen et al., 2014), in which PFSAs dominated. Here, the variability in uptake dependent on the treatment type was also revealed, particularly when contaminated water was involved.

3.3.5. Vertical distribution of PFAAs in soil and soil-water partitioning

Adsorption and desorption batch experiments have been carried out to derive adsorption based soil-water partition coefficients and desorption-based soil-water partition coefficients (Tables A2-16 and A2-18, A2-10). K_{ds} ranged from 0.58 L/kg for PFPeA to 93.56 L/kg for PFOS, being generally around 1 L/kg for short-chain PFAAs, very low K_{ds} indicating its high mobility and low sorption to the agricultural soil. K_{des} were derived from the linear isotherms only for long-chain PFAAs and were slightly higher than K_{ds} for PFOA, PFNA and PFDA (1.96 L/kg, 5.34 L/kg and 42.50 L/kg, respectively) and significantly lower for PFOS (59.77 L/kg). They were log-transformed and as such well correlated with the PFAAs' chain length (Figure 3-5). There was only a minor influence of the chain length increase on the K_{ds} of the shortest PFAAs, i.e. PFBA, PFPeA, PFHxA and PFBS having K_{ds} of 0.85, 0.58, 0.96 and 0.80 L/kg, respectively, already observed by (Guelfo and Higgins, 2013) and (McLachlan et al., 2019) in the agricultural soils. The increase of 0.6 and 0.8 log units was noticeable with the addition of one CF_2 group from $7CF_x$ to $8CF_x$ and from $8CF_x$ to $9CF_x$ of PFCAs. By comparing the soil sorption between PFOS and PFNA, PFCA with the same chain length ($8CF_x$), adsorption and desorption of PFOS to the agricultural soil was higher than of PFNA, with the K_d and K_{des} being larger for 1 and 1.2 log units than the ones of PFNA. Both linear and Freundlich sorption models were utilized for fitting the data of measured isotherm points (A2-10), but ultimately the K_{ds} and K_{des} of PFNA, PFDA and PFOS were derived from the linear isotherms based on only the first 3 isotherm points. Indeed, the resulting equilibrium concentration range in the soil of the pot experiments was already encompassed by these 3 points, i.e. the resulting adsorbed equilibrium concentrations in the points 4 and 5 were much higher than the pot soil range of PFNA, PFDA and PFOS (Table A2-13 and A2-10).

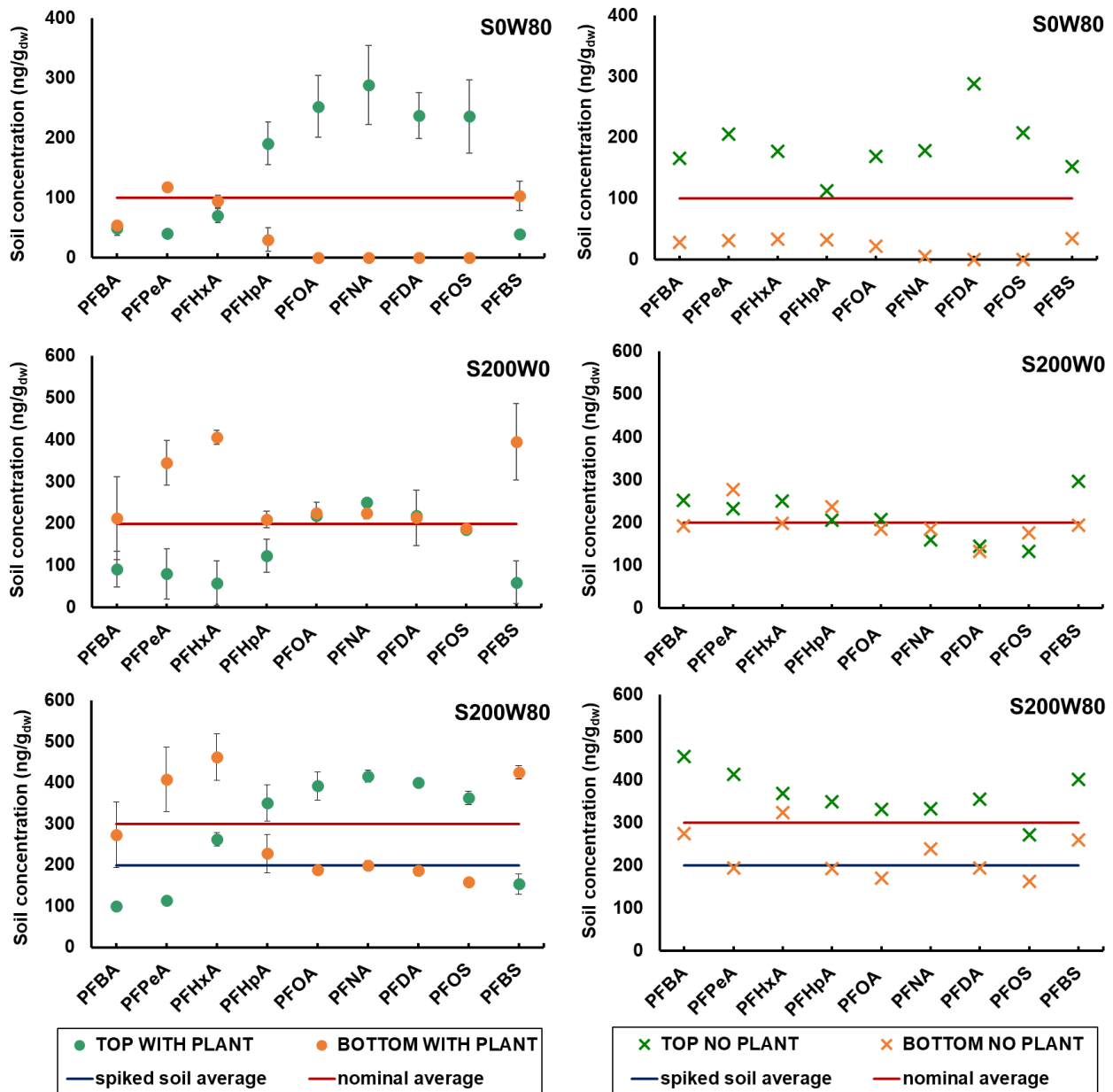


Figure 3-4. Concentrations of PFAAs in pots' top and bottom parts. Mean concentrations with standard error estimates are shown for the pots with red chicory plants ($n=2$) (full circles), while one pot per treatment was present as an empty pot ($n=1$) (crosses). Red lines indicate nominal concentrations for all PFAAs in soil (total of soil and irrigation water are accounted for), while the blue lines indicate only soil-spiked nominal concentration of the treatment S200W80.

By coring the soil, we were able to measure concentrations in the top and bottom pot parts for three significant treatments (S200W0, S0W80 and S200W80), as shown in Figure 3-4. In all treatments, a higher immobility of long-chain PFAAs can be seen, as indicated by the non-detection of long-chain PFAAs in the bottom pot halves in the S0W80 treatment, by the almost equal concentrations in both halves in the treatment S200W0 and by the visibly higher concentrations in the top part for the treatment S200W80 for about 250 ng/g_{dw} – equivalent to their concentrations in the treatment S0W80. For the shortest PFAAs (PFBA, PFPeA, PFHxA and PFBS), higher concentrations in the bottom parts were always observed, confirming their higher mobility in soil indicated by the K_d s lower than 1 L/kg. Lower concentrations than nominal for PFBA and PFPeA, observed in the treatments with contaminated irrigation water in both top and bottom soil parts could be the consequence of their high plant uptake. Total mass of PFBA in plants (the average of triplicates) was 123 μ g in

S0W80, 118 μg in S200W0 and 333 μg in S200W80, and this uptake quantity is sufficient to produce a net decrease in the measured concentrations in soil. In addition, even though pots were closed from the bottom (A2-3), leaching was sometimes observed and with the high mobility of these PFAAs in water, some losses may have occurred and be visible as lower bottom concentration. It is evident in all the treatments that PFAAs (and water) penetrate further in the pots containing plants as opposed to pots without plants, by comparing the PFAAs distribution. One reason for this could be the effect of the chicory root system which created preferential channels in the soil and another reason could be a consequence of high proportion of clay- and silt-sized particles in the Agripolis soil (A2-3), making it less permeable (during the irrigation, retaining of the water was sometimes visible in the empty pots).

Distribution coefficients between the bottom and top soil parts (K_{BT}) were calculated as the ratio of respective concentrations, in order to quantitatively assess the transport efficiency of PFAAs in the evaluated treatments. They were log-transformed and correlated to the $\log K_d$ (for S0W80), $\log K_{des}$ (for S200W0) and $\log((K_d + K_{des})/2)$ (for S200W80).

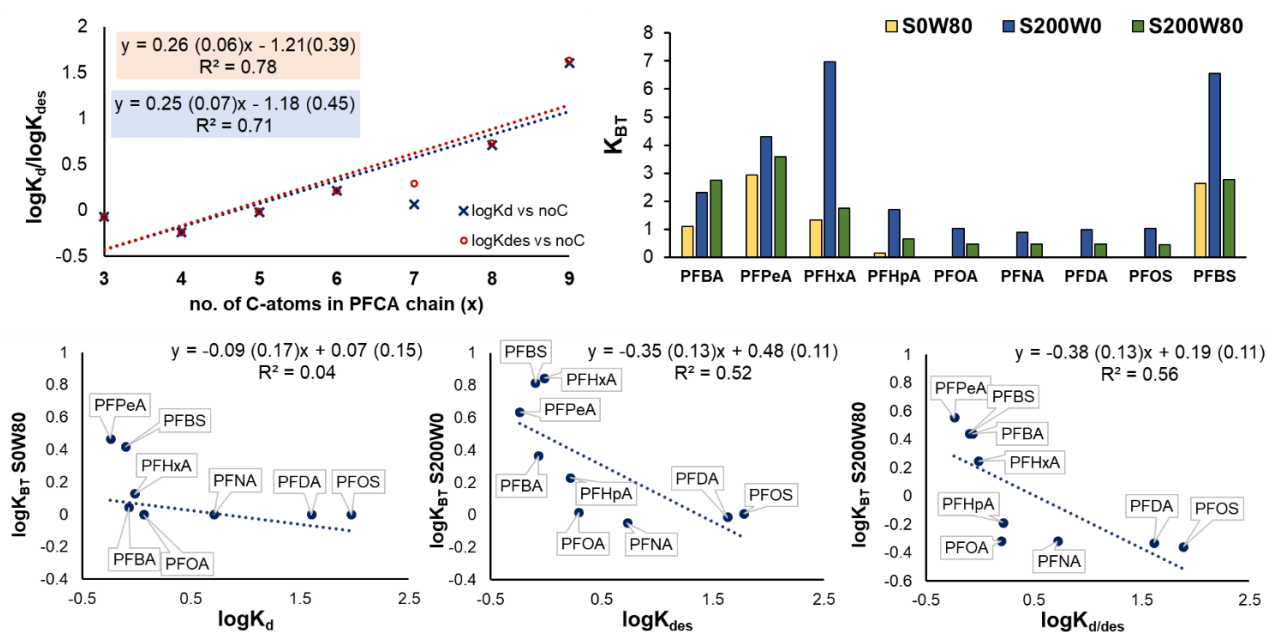


Figure 3-5. Correlations of $\log K_d/K_{des}$ with the chain-length of PFCAs (top left); bottom-to-top soil distribution coefficients (top right); correlations of assessed treatments' $\log K_d/K_{des}$ with the bottom to top soil distribution coefficients (down). Regression lines are shown with the standard errors of coefficients in the brackets and coefficients of determination.

Linear regression lines (Figure 3-5) accounted for more than 50% of the variability in the treatments S200W0 and S200W80, showing R^2 of 0.52 and 0.56, respectively. Exceptions were PFHpA and PFOA that, despite having comparably small K_d s to the shorter PFAAs, previously also shown in other agricultural soils (Blaine et al., 2014b; McLachlan et al., 2019; Milinovic et al., 2015), behaved in the same way as the longest PFAAs (PFNA, PFDA and PFOS), having very similar K_{BT} s. However, for the treatment S0W80, flat regression line indicated the total immobility of the long-chain PFAAs ($K_{BT} = 0$), underlining the significance of the PFAAs delivery media on their mobility and bioavailability, as well as the soil properties, e.g. water permeability. Moreover, soil to water ratio is always lower in the laboratory tests (here 1:5 g/mL opposed to the \approx 4:5 g/mL for the pot experiment, as the ratio of the dry soil mass and total water used for the irrigation), in which mixing of the soil in a slurry for an extended time will also affect the extrapolation of the results to more complicated (non-equilibrium) environmental situations. Hence, actual environmental conditions (surface soil type, water table and aquifer depth, plant rooting depth, root type and branching etc.) would have

significant impact on the PFAAs mobility and bioavailability. Nevertheless, laboratory derived equilibrium soil-water partition coefficients still present a valuable indication for the PFAAs behavior in different types of soil.

3.4. Conclusions

The results obtained in this study are of importance because it is the first time that both water and soil contaminated with concentrations of environmentally-relevant PFAA mixtures, were applied in a plant uptake study, with the aim of comparing the influence of delivery pathways on PFAAs bioaccumulation. Simultaneous evaluation of all treatments for the individual PFAAs has highlighted the significance of irrigation water use, resulting in a greater accumulation in the shoots, and particularly in the edible red chicory part (head). The use of contaminated water increases the uptake of long-chain PFAAs due to probable non-immediate equilibrium conditions in soil; however, the uptake of short-chain PFAAs would increase under pre-contaminated soil conditions, making it in conjunction with irrigation water a worst-case scenario (e.g. which can result from years-long irrigation of agricultural soil).

We found a clear pattern between the accumulation in roots and the chain length. It was evident that concentrations decreased with an increase in chain length, similar to the uptake pattern in aerial plant parts, but in contrast with the hydroponic experiments (Felizeter et al., 2014, 2012; Müller et al., 2016) and to the generally unclear patterns in root uptake studies with soil as the growth media (Blaine et al., 2014a; Wen et al., 2014).

Comparing the bioaccumulation of PFSAs and PFCAs with the same chain length in red chicory compartments has shown that, despite a similar uptake into the roots, significant differences and preferential uptake of PFPeA in leaves and PFBS in heads of some treatments may be a confirmation of the previous indications of different pathways for sulfonates and carboxylates. It implies that it is not only the small size of the short-chain PFAA molecules that plays a role in the PFAAs uptake to aerial crop parts, but also the functional group and delivery pathway.

Evaluation of the laboratory determined K_d / K_{des} with the measured concentrations in soil at varying depths disclosed partial applicability of such results to the realistic conditions, explaining up to 50% of PFAAs mobility in soil by K_d / K_{des} . However, predicting the uptake of PFAAs from the contaminated irrigation water, a significant problem for agriculture in contaminated areas such as Rastatt in Germany (Brendel et al., 2018) or Vicenza province in Italy, will very much depend on the water seepage through soil, as the most bioaccumulative PFAAs (i.e. 3CF_x, 4CF_x, 5CF_x) are also the ones being the most mobile in water ($K_d < 1$ L/kg).

Incorporating both the measurements of inter-compartmental PFAAs distribution in plants and soil with the adsorption/desorption in soil represents a first major step towards the modelling of PFAAs uptake into plants from soil, a challenging task given the questionable availability and applicability of the octanol-water partition coefficients and the need for media-specific partitioning measurements (Droge, 2019). Generally, further research of PFAAs uptake into crops from soil (and its soil mobility) is required to understand the most influential factors and to be able to assess the potential magnitude of PFAAs contamination in various crops (used for food or animal feed) in different environmental settings, and consequentially the possible threat for human health in and around the PFASs contamination hot-spots.

Acknowledgements:

We are grateful to Massimiliano Prenzato and Caterina Cecchinato from ARPAV Venezia for performing soil and water analyses and Fabio Biancato for the assistance with the soil samples preparation. We acknowledge the help of Francesca Corrà (UniPd, DB) and Marta Ianotta (UniPd, DAFNAE) with the plant samples preparation and the staff of DAFNAE experimental farm for the help in the greenhouse. Acknowledgements to Nicola Tormen (World Biodiversity Association) and Federico Nadaletto (Organizzazione Produttori Ortofrutticoli Veneto) for their expertise in chicory cultivation. Many thanks to Stefan Trapp (Technical University of Denmark) for his insights on contaminants plant uptake and pre-review of the text and Jacob Michael Crowe (Technical University of Denmark) for the English proofread.

Funding sources:

This work was co-funded through the LIFE programme of the European Union, Grant Agreement number LIFE16 ENV/IT/000488-Project LIFE PHOENIX. Andrea Gredelej's PhD research was funded by the Fondazione CARIPARO's grant for foreign PhD students at the University of Padova.

3.5. References

- ARPAV, 2018. Concentrations of the Perfluoroalkyl substances in the waters of Veneto region, Open data on PFASs monitoring, from 02/07/2013 to 20/09/2018 [WWW Document]. URL <http://www.arpa.veneto.it/dati-ambientali/open-data/idrosfera/concentrazione-di-sostanze-perfluoroalchiliche-pfas-nelle-acque-prelevate-da-arpav> (accessed 11.25.18).
- Blaine, A.C., Rich, C.D., Hundal, L.S., Lau, C., Mills, M.A., Harris, K.M., Higgins, C.P., 2013. Uptake of perfluoroalkyl acids into edible crops via land applied biosolids: Field and greenhouse studies. *Environ. Sci. Technol.* 47, 14062–14069. <https://doi.org/10.1021/es403094q>
- Blaine, A.C., Rich, C.D., Sedlacko, E.M., Hundal, L.S., Kumar, K., Lau, C., Mills, M.A., Harris, K.M., Higgins, C.P., 2014a. Perfluoroalkyl acid distribution in various plant compartments of edible crops grown in biosolids-amended soils. *Environ. Sci. Technol.* 48, 7858–7865. <https://doi.org/10.1021/es500016s>
- Blaine, A.C., Rich, C.D., Sedlacko, E.M., Hyland, K.C., Stushnoff, C., Dickenson, E.R. V., Higgins, C.P., 2014b. Perfluoroalkyl Acid Uptake in Lettuce (*Lactuca sativa*) and Strawberry (*Fragaria ananassa*) Irrigated with Reclaimed Water. *Environ. Sci. Technol.* 48, 14361–14368. <https://doi.org/10.1021/es504150h>
- Brendel, S., Fetter, É., Staude, C., Vierke, L., Biegel-Engler, A., 2018. Short-chain perfluoroalkyl acids: environmental concerns and a regulatory strategy under REACH. *Environ. Sci. Eur.* 30, 9. <https://doi.org/10.1186/s12302-018-0134-4>
- Buck, R.C., Franklin, J., Berger, U., Conder, J.M., Cousins, I.T., de Voogt, P., Jensen, A.A., Kannan, K., Mabury, S.A., van Leeuwen, S.P., 2011. Perfluoroalkyl and polyfluoroalkyl substances in the environment: Terminology, classification, and origins. *Integr. Environ. Assess. Manag.* 7, 513–541. <https://doi.org/10.1002/ieam.258>
- Chen, H., Reinhard, M., Nguyen, V.T., Gin, K.Y.H., 2016. Reversible and irreversible sorption of perfluorinated compounds (PFCs) by sediments of an urban reservoir. *Chemosphere* 144, 1747–1753. <https://doi.org/10.1016/j.chemosphere.2015.10.055>
- DeWitt, J., Berger, U., Miller, M., Green, C., Huang, J., Perkola, N., Vierke, L., Higgins, C., Buser, A.M., Lindstrom, A.B., Boucher, J.M., Lau, C.S., Knepper, T., Liu, J., Wang, Z., Herzke, D., Ahrens, L., Hung, H., Cousins, I., van der Jagt, K., Bopp, S.K., Fletcher, T., Leinala, E., Scheringer, M., Småstuen Haug, L., Borg, D., Ritscher, A., Valsecchi, S., Shi, Y., Ohno, K., Trier, X., Bintein, S., 2018. Zürich Statement on Future Actions on Per- and Polyfluoroalkyl Substances (PFASs). *Environ. Health Perspect.* 126, 084502. <https://doi.org/10.1289/ehp4158>
- Ding, G., Peijnenburg, W.J.G.M., 2013. Physicochemical properties and aquatic toxicity of poly- and perfluorinated compounds. *Crit. Rev. Environ. Sci. Technol.* 43, 598–678. <https://doi.org/10.1080/10643389.2011.627016>
- Droge, S.T.J., 2019. Membrane-Water Partition Coefficients to Aid Risk Assessment of Perfluoroalkyl Anions and Alkyl Sulfates. *Environ. Sci. Technol.* 53, 760–770. <https://doi.org/10.1021/acs.est.8b05052>
- Felizeter, S., McLachlan, M.S., De Voogt, P., 2014. Root uptake and translocation of perfluorinated alkyl acids by three hydroponically grown crops. *J. Agric. Food Chem.* 62, 3334–3342. <https://doi.org/10.1021/jf500674j>

- Felizeter, S., McLachlan, M.S., De Voogt, P., 2012. Uptake of perfluorinated alkyl acids by hydroponically grown lettuce (*Lactuca sativa*). *Environ. Sci. Technol.* 46, 11735–11743. <https://doi.org/10.1021/es302398u>
- Ghisi, R., Vameralli, T., Manzetti, S., 2019. Accumulation of perfluorinated alkyl substances (PFAS) in agricultural plants: A review. *Environ. Res.* 169, 326–341. <https://doi.org/10.1016/j.envres.2018.10.023>
- Guelfo, J.L., Higgins, C.P., 2013. Subsurface transport potential of perfluoroalkyl acids at aqueous film-forming foam (AFFF)-impacted sites. *Environ. Sci. Technol.* 47, 4164–4171. <https://doi.org/10.1021/es3048043>
- Ingelido, A.M., Abballe, A., Gemma, S., Dellatte, E., Iacovella, N., Angelis, G. De, Zampaglioni, F., Marra, V., Miniero, R., Valentini, S., Russo, F., Vazzoler, M., Testai, E., Felip, E. De, 2018. Biomonitoring of per fluorinated compounds in adults exposed to contaminated drinking water in the Veneto Region, Italy. *Environ. Int.* 110, 149–159. <https://doi.org/10.1016/j.envint.2017.10.026>
- Kempisty, D.M., Xing, Y., Racz, L., 2018. *Perfluoroalkyl Substances in the Environment: Theory, Practice and Innovation*, Environmental and occupational health series. CRC Press, Boca Raton. <https://doi.org/10.1201/9780429487125>
- Krafft, M.P., Riess, J.G., 2015. Per- and polyfluorinated substances (PFASs): Environmental challenges. *Curr. Opin. Colloid Interface Sci.* 20, 192–212. <https://doi.org/10.1016/j.cocis.2015.07.004>
- Krippner, J., Brunn, H., Falk, S., Georgii, S., Schubert, S., Stahl, T., 2014. Effects of chain length and pH on the uptake and distribution of perfluoroalkyl substances in maize (*Zea mays*). *Chemosphere* 94, 85–90. <https://doi.org/10.1016/j.chemosphere.2013.09.018>
- Krippner, J., Falk, S., Brunn, H., Georgii, S., Schubert, S., Stahl, T., 2015. Accumulation Potentials of Perfluoroalkyl Carboxylic Acids (PFCAs) and Perfluoroalkyl Sulfonic Acids (PFSA) in Maize (*Zea mays*). *J. Agric. Food Chem.* 63, 3646–3653. <https://doi.org/10.1021/acs.jafc.5b00012>
- Li, F., Fang, X., Zhou, Z., Liao, X., Zou, J., Yuan, B., Sun, W., 2018. Adsorption of perfluorinated acids onto soils: Kinetics, isotherms, and influences of soil properties. *Sci. Total Environ.* 649, 504–514. <https://doi.org/https://doi.org/10.1016/j.scitotenv.2018.08.209>
- Liu, Z., Lu, Y., Shi, Y., Wang, P., Jones, K., Sweetman, A.J., Johnson, A.C., Zhang, M., Zhou, Y., Lu, X., Su, C., Sarvajayakesavaluc, S., Khan, K., 2017. Crop bioaccumulation and human exposure of perfluoroalkyl acids through multi-media transport from a mega fluorochemical industrial park, China. *Environ. Int.* 106, 37–47. <https://doi.org/10.1016/j.envint.2017.05.014>
- Liu, Z., Lu, Y., Song, X., Jones, K., Sweetman, A.J., Johnson, A.C., Zhang, M., Lu, X., Su, C., 2019. Multiple crop bioaccumulation and human exposure of perfluoroalkyl substances around a mega fluorochemical industrial park, China: Implication for planting optimization and food safety. *Environ. Int.* 127, 671–684. <https://doi.org/10.1016/j.envint.2019.04.008>
- Mastrantonio, M., Bai, E., Uccelli, R., Cordiano, V., Screpanti, A., Crosignani, P., 2018. Drinking water contamination from perfluoroalkyl substances (PFAS): An ecological mortality study in the Veneto Region, Italy. *Eur. J. Public Health* 28, 180–185. <https://doi.org/10.1093/eurpub/ckx066>

- Mazzoni, M., Polesello, S., Rusconi, M., Valsecchi, S., 2016. Liquid chromatography mass spectrometry determination of perfluoroalkyl acids in environmental solid extracts after phospholipid removal and on-line turbulent flow chromatography purification. *J. Chromatogr. A* 1453, 62–70. <https://doi.org/10.1016/j.chroma.2016.05.047>
- McFarlane, C., Trapp, S., 1994. *Plant Contamination: Modeling and Simulation of Organic Chemical Processes*, 1st ed. CRC Press, Boca Raton, Florida.
- McLachlan, M.S., Felizeter, S., Klein, M., Kotthoff, M., De Voogt, P., 2019. Fate of a perfluoroalkyl acid mixture in an agricultural soil studied in lysimeters. *Chemosphere* 223, 180–187. <https://doi.org/10.1016/j.chemosphere.2019.02.012>
- Milinic, J., Lacorte, S., Vidal, M., Rigol, A., 2015. Sorption behaviour of perfluoroalkyl substances in soils. *Sci. Total Environ.* 511, 63–71. <https://doi.org/10.1016/j.scitotenv.2014.12.017>
- Müller, C.E., Lefevre, G.H., Timofte, A.E., Hussain, F.A., Sattely, E.S., Luthy, R.G., 2016. Competing mechanisms for perfluoroalkyl acid accumulation in plants revealed using an Arabidopsis model system. *Environ. Toxicol. Chem.* 35, 1138–1147. <https://doi.org/10.1002/etc.3251>
- Ng, C.A., Hungerbühler, K., 2014. Bioaccumulation of perfluorinated alkyl acids: Observations and models. *Environ. Sci. Technol.* 48, 4637–4648. <https://doi.org/10.1021/es404008g>
- Nicoletto, C., Maucieri, C., Sambo, P., 2017. Effects on Water Management and Quality Characteristics of Ozone Application in Chicory Forcing Process: A Pilot System. *Agronomy* 7, 29. <https://doi.org/10.3390/agronomy7020029>
- OECD, 2000. Test No. 106: Adsorption - Desorption Using a Batch Equilibrium Method, OECD Guideline for the Testing of Chemicals. <https://doi.org/https://doi.org/10.1787/9789264069602-en>
- Rumsby, P.C., Young, W.F., Hall, T., McLaughlin, C.L., Halden, R.U., 2010. Contaminants of Emerging Concern in the Environment: Ecological and Human Health Considerations, in: *Contaminants of Emerging Concern in the Environment: Ecological and Human Health Considerations*, ACS Symposium Series. American Chemical Society, pp. 275–296. <https://doi.org/doi:10.1021/bk-2010-1048>
- Sepulvado, J.G., Blaine, A.C., Hundal, L.S., Higgins, C.P., 2011. Occurrence and fate of perfluorochemicals in soil following the land application of municipal biosolids. *Environ. Sci. Technol.* 45, 8106–8112. <https://doi.org/10.1021/es103903d>
- Stahl, T., Heyn, J., Thiele, H., Huther, J., Failing, K., Georgii, S., Brunn, H., 2009. Carryover of perfluorooctanoic acid (PFOA) and perfluorooctane sulfonate (PFOS) from soil to plants. *Arch. Environ. Contam. Toxicol.* 57.
- Torralba-Sanchez, T.L., Kuo, D.T.F., Allen, H.E., Di Toro, D.M., 2017. Bioconcentration factors and plant–water partition coefficients of munitions compounds in barley. *Chemosphere* 189, 538–546. <https://doi.org/10.1016/j.chemosphere.2017.09.052>
- Trapp, S., 2007. Fruit tree model for uptake of organic compounds from soil and air. *SAR QSAR Environ. Res.* 18, 367–387. <https://doi.org/10.1080/10629360701303693>
- Trapp, S., Pussemier, L., 1991. Model calculations and measurements of uptake and translocation of carbamates by bean plants. *Chemosphere* 22, 327–339. [https://doi.org/10.1016/0045-6535\(91\)90321-4](https://doi.org/10.1016/0045-6535(91)90321-4)

- Veneto Region, 2014. Progress and prospects for Veneto Agriculture. [<http://statistica.regione.veneto.it/ENG/Pubblicazioni/RapportoStatistico2014/pdf/Capitolo07.pdf>]
- Vierke, L., Möller, A., Klitzke, S., 2014. Transport of perfluoroalkyl acids in a water-saturated sediment column investigated under near-natural conditions. *Environ. Pollut.* 186, 7–13. <https://doi.org/10.1016/j.envpol.2013.11.011>
- Wang, Z., Dewitt, J.C., Higgins, C.P., Cousins, I.T., 2017. A Never-Ending Story of Per- and Polyfluoroalkyl Substances (PFASs)? *Environ. Sci. Technol.* 51, 2508–2518. <https://doi.org/10.1021/acs.est.6b04806>
- Wen, B., Li, L., Zhang, H., Ma, Y., Shan, X.Q., Zhang, S., 2014. Field study on the uptake and translocation of perfluoroalkyl acids (PFAAs) by wheat (*Triticum aestivum* L.) grown in biosolids-amended soils. *Environ. Pollut.* 184, 547–554. <https://doi.org/10.1016/j.envpol.2013.09.040>
- WHO, 2016. Keeping our water clean: the case of water contamination in the Veneto Region, Italy. AREAGRAPHICA SNC DI TREVISAN GIANCARLO & FIGLI, Venice, Italy. [http://www.euro.who.int/__data/assets/pdf_file/0018/340704/FINAL_pfas-report-20170530-h1200.pdf]
- Zareitalabad, P., Siemens, J., Hamer, M., Amelung, W., 2013. Perfluorooctanoic acid (PFOA) and perfluorooctanesulfonic acid (PFOS) in surface waters, sediments, soils and wastewater - A review on concentrations and distribution coefficients. *Chemosphere* 91, 725–732. <https://doi.org/10.1016/j.chemosphere.2013.02.024>
- Zhao, L., Zhu, L., Zhao, S., Ma, X., 2016. Sequestration and bioavailability of perfluoroalkyl acids (PFAAs) in soils: Implications for their underestimated risk. *Sci. Total Environ.* 572, 169–176. <https://doi.org/10.1016/j.scitotenv.2016.07.196>

Chapter 4

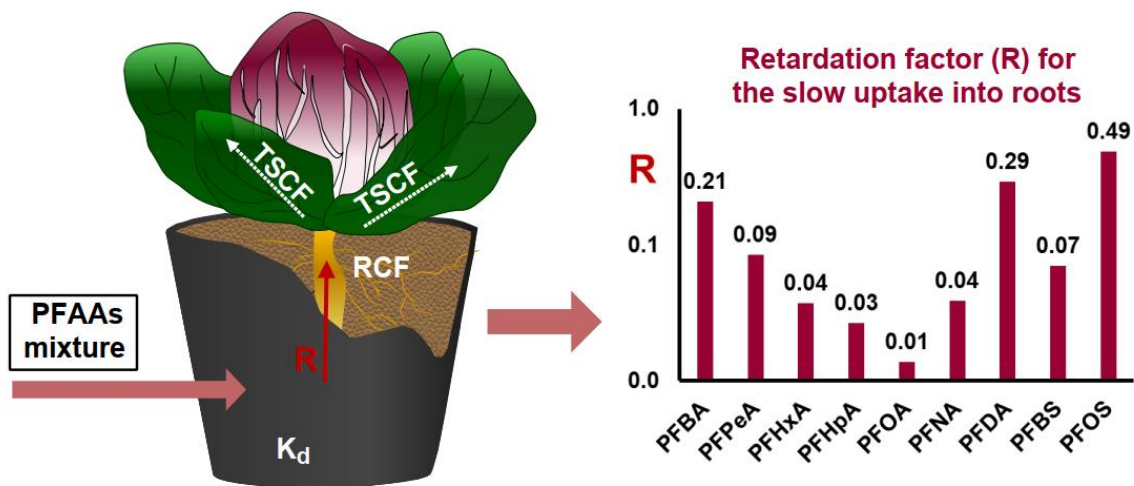
Model-based analysis of the uptake of perfluoroalkyl acids (PFAAs) from soil into plants

Andrea Gredelj^{a,b}, Fabio Polese^{a,c}, Stefan Trapp^a

^a Technical University of Denmark, Department of Environmental Engineering, Bygningstorvet 115, DK-2800 Kongens Lyngby, Denmark

^b Department of Industrial Engineering, University of Padova, via Marzolo 9, 35131 Padova, Italy

^c DHI A/S, Agern Allé 5, 2970 Hørsholm, Denmark



Reproduced with permission from:

Chemosphere, 2019

Accepted for publication

© 2019 Elsevier Ltd.

Chapter summary:

Perfluoroalkyl acids (PFAAs) bioaccumulate in crops, with uptake being particularly high for short-chain PFAAs that are constantly transported with transpiration water to aerial plant parts. Due to their amphiphilic surfactant nature and ionized state at environmental pH, predicting the partitioning behavior of PFAAs is difficult and subject to considerable uncertainty, making experimental data highly desirable. Here, we applied a plant uptake model that combines advective flux with measured partition coefficients to reproduce the set of empirically derived plant uptake and soil-partitioning data for nine PFAAs in red chicory, in order to improve the mechanistic understanding and provide new insights into the complex uptake processes. We introduced a new parameter for retarded uptake (R) to explain the slow transfer of PFAA across biomembranes of the root epidermis, which have led to low transpiration stream concentration factors (TSCFs) presented in literature so far. We estimated R values for PFAAs using experimental data derived for red chicory and used the modified plant uptake model to simulate uptake of PFAA into other crops. Results show that this semi-empirical model predicted PFAAs transport to shoots and fruits with good accuracy based on experimental root to soil concentration factors (RCF_{dw}) and soil to water partition coefficients (K_d) as well as estimated R values and plant-specific data for growth and transpiration. It can be concluded that the combination of rather low K_d with high RCF_{dw} and the absence of any relevant loss are the reason for the observed excellent plant uptake of PFAAs.

4.1. Introduction

Per- and polyfluoroalkyl substances (PFASs) are a family of anthropogenic chemicals containing at least one perfluoroalkyl moiety ($-C_nF_{2n-}$). Due to their high stability and surfactant properties of some PFASs, PFASs have been used in a variety of industrial and commercial products and processes since the 1950s (Buck et al., 2011; DeWitt et al., 2018). It is estimated that more than 4000 individual PFASs are currently present on the market (Cheng and Ng, 2018). Wide-range emissions, high thermal and (bio)chemical stability and amphiphilicity determine their persistence and ubiquitous presence in the environment, from tropical to polar areas (Chen et al., 2017; Greaves et al., 2012).

The most commonly detected (and now “historical”) PFASs in environment, wildlife and humans are perfluorooctane sulfonic acid (PFOS) and perfluorooctanoic acid (PFOA) (Cheng and Ng, 2018; Krafft and Riess, 2015a). Substances containing a perfluoroalkyl moiety have the potential to be transformed abiotically or biotically through changes in the non-fluorinated part of the molecule into perfluoroalkyl acids (PFAAs), which are regarded as their final stable transformation products (Brendel et al., 2018; Buck et al., 2011; Ghisi et al., 2019). PFAAs are acidic surfactants that, within the group, differ in perfluoroalkyl chain length and in the terminal polar group (consequently forming carboxylic, sulfonic, sulfinic, phosphonic, and phosphinic perfluoroalkyl acids). After their common detection in humans and biota, long-chain perfluorocarboxylic (PFCAs) and perfluorosulfonic (PFSAs) acids (defined as $\geq 7C$ for PFCAs, $\geq 6C$ for PFSAs) from C8 to C14 have been voluntarily phased-out by producers and are subject to the subsequent regulation (e.g. PFOS and its salts are restricted under the Stockholm Convention) (Buck et al., 2011). Precursors of short-chain PFAAs are broadly used as their alternatives (Brendel et al., 2018). Long- and short-chain PFAAs were originally distinguished with the assumption that short-chain PFAAs have a lower bioaccumulation potential and are less persistent compared to the long-chain ones (Buck et al., 2011). In animal and human body, bioaccumulation was accordingly found to steeply increase with chain length (Krafft and Riess, 2015a) and to be higher for PFSAs than PFCAs. However, recent findings have shown the opposite pattern for crops and other plants, whereby short-chain PFCAs are accumulating to a high extent in aerial plant parts (Blaine et al., 2014a; Felizeter et al., 2014; Ghisi et al., 2019). Food of plant origin was identified as an important category contributing to dietary exposure to PFAAs (D’Hollander et al., 2015; Felizeter et al., 2014; Klenow et al., 2013).

PFAAs in the environment are present in anionic form, suggesting weak adsorption to soil (Franco et al., 2009), high water solubility and negligible vapor pressure. This combination of properties, together with their extreme persistence, imposes PFAAs as good candidates for high uptake and accumulation in crops, consequently making the exposure and fate assessment for the soil-plant pathway highly needed. Sorption to soil strongly depends on the soil type and it is not fully ascribable to the soil’s organic carbon content (%OC) (Y. Li et al., 2018) but usually increases with the chain length (Guelfo and Higgins, 2013; McLachlan et al., 2019), with long-chain PFAAs adsorbing strongly to soil (McLachlan et al., 2019; Milinovic et al., 2015). Motivated by the contamination event caused by a fluorochemical plant in the Veneto Region, Northern Italy (WHO, 2016), and the significance of the area for the crop production and its extensive irrigation needs (Veneto Region, 2014), a previous study was conducted to measure uptake of 9 PFAAs into red chicory (*Cichorium intybus* L.) under simulated environmental conditions of contaminated soil and irrigation water (Gredelj et al., 2019a). Differently from previous studies on PFAAs uptake in crops (Blaine et al., 2013, 2014a, 2014c; Navarro et al., 2017; L. Xiang et al., 2018), plant-specific data and sorption to soil and roots were also measured and served as input for the plant uptake model derived here.

A widely used plant uptake model is the so-called “standard model” (Trapp, 2015, 2007; Trapp and Matthies, 1995). It combines advective fluxes into and through the plant with partition processes to

roots, stem and leaves with volatilization, degradation and dilution by growth as loss processes. Its adaption to weak acids and bases is available as well (Trapp, 2009). This basic approach has been adopted in assessment tools for contaminated soils (CSOIL (Brand et al., 2007); CLEA (Jeffries and Martin, 2009)), in chemical risk assessment (European Commission, 2003) and in sustainability assessment (dynamicroP (Fantke et al., 2011b, 2011a)). Most, if not all, of these established assessment tools require knowledge of the equilibrium partitioning between environmental compartments, in particular for adsorption to soil (K_d -value) and to plant tissue (root concentration factor RCF). Only, the estimation routines for partitioning implemented in these exposure assessment tools are strictly restricted to neutral, nonpolar chemicals (Trapp et al., 2010). PFAAs do not have typical lipid partitioning mechanisms due to their ionic state and surfactant nature, showing low storage lipid accumulation and high affinity for proteins (Cheng and Ng, 2018; Droge, 2019; Ng and Hungerbühler, 2014) and resulting in great uncertainty of both experimentally and QSAR based K_{OW} -values (Droge, 2019). Therefore, the partition coefficients cannot be estimated from structure or from physico-chemical properties, but need to be determined empirically or by inverse modeling.

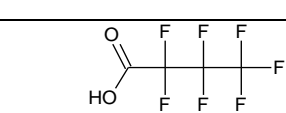
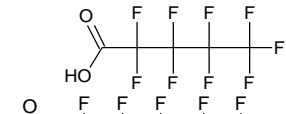

In this study, we used experimental soil-water partition coefficients and measured PFAA concentrations in red chicory grown in soil provided by (Gredelj et al., 2019a), together with plant-specific input parameters to calibrate the standard plant uptake model for PFAAs. We introduced a new parameter for retarded uptake into roots and xylem, and estimated it for all tested PFAAs. We also evaluated the relationship between the chemical structure (perfluoroalkyl acid's chain length) and root to water, root to soil and water to soil partition coefficients. The model was then applied to other experimental PFAA uptake data presented in literature to validate the modelling approach used. Overall, the outcome of our investigation allows for an improved interpretation of the experimental results and for the comparison of PFAAs with other chemicals, providing new insights into the uptake mechanisms of PFAAs into crops and being a step forward towards the prediction of the uptake of PFAAs into crops.

4.2. Methodology

4.2.1. Perfluoroalkyl acids

Physico-chemical properties of PFAAs differ with the functional group and are decreasing or increasing with the chain-length (Smith et al., 2016). A list of the PFAAs used in this study together with their names, structures and relevant physico-chemical properties is shown in Table 4-1.

Table 4-1. A list of investigated PFAAs with relevant physico-chemical properties (Smith et al., 2016)

Abbreviation	Chemical (common) name	No. of perfluorinated carbons (CF _x)	CAS number	Molar mass (g/mol)	Dissociation constant (pKa)	Structure
PFBA	Perfluorobutanoic acid	3	375-22-4	214.04	-0.2 to 0.7	
PFPeA	Perfluoropentanoic acid	4	2706-90-3	264.05	-0.06	
PFHxA	Perfluorohexanoic acid	5	307-24-4	314.05	-0.13	

PFHpA	Perfluoroheptanoic acid	6	375-85-9	364.06	-0.15	
PFOA	Perfluorooctanoic acid	7	335-67-1	414.07	~0.5 ¹	
PFNA	Perfluorononanoic acid	8	375-95-1	464.08	-0.17	
PFDA	Perfluorodecanoic acid	9	335-76-2	514.08	-0.17	
PFBS	Perfluorobutane sulfonic acid	4	375-73-5	300.1	-6.0 to -5.0	
PFOS	Perfluorooctane sulfonic acid	8	1763-23-1	500.13	-6.0 to -2.6	

¹ (Johansson et al., 2017)

4.2.2. Experimental data

Experimental uptake data for a mixture of nine PFAAs (Table 4-1) into red chicory plant compartments were taken from the study of (Gredelj et al., 2019a). Only the data from experiments with pre-contaminated soil were considered to avoid non-equilibrium conditions resulting from the use of spiked irrigation water (Blaine et al., 2014b). Briefly, uptake experiments with red chicory (*Cichorium intybus* L.) were performed in a greenhouse located in Legnaro (Italy) from August to November 2018. Plants were grown in pots containing 11 kg of agricultural soil (loam), spiked to nominal concentrations of 100 ng/g_{dw} or 200 ng/g_{dw} of each PFAA. Concentrations of PFAAs in soil were analytically determined at the beginning and at the end of experimental period of 87 days, as well as final concentrations in roots, leaves and heads of the red chicory plants.

For determination of transpiration and growth rates, the pots were weighed before every irrigation. This was also done for non-planted controls to determine evaporative losses of water. The gravimetric water content of the soil was measured at the beginning (before planting) and at the end of the experiments. Moreover, plant biomass was measured at the beginning (by weighing the seedlings before planting) and at the end of the experiments for each plant compartment. Dry matter content of plant tissue was determined by oven drying at 65 °C (72 h).

Partitioning of PFAAs between soil and water was determined by a set of batch adsorption/desorption experiments (following the standardized OECD guideline 106 (OECD, 2000)), using concentration ranges relevant for the plant uptake experiments. For the long-chain PFAAs (i.e. PFOA, PFNA, PFDA, PFOS) both adsorption and desorption-based soil-water partition coefficients were derived, $K_{d,ads}$ (L/kg) and $K_{d,des}$ (L/kg), respectively, only $K_{d,des}$ being relevant for the used treatments with the pre-contaminated soil. For the other PFAAs, concentrations of PFBA, PFPeA, PFBS and PFHxA in solution could not be quantified precisely enough in the consecutive desorption tests performed with “decant-refill” technique, due to their rather low adsorption to soil and their low concentrations in the desorption reactors (Gredelj et al., 2019a). However, considering their low K_d values and the adsorption reversibility of the short-chain PFAAs (Chen et al., 2016; Milinovic et al., 2015), $K_{d,ads}$ values were applied in uptake calculations with the short-chain PFAAs.

Data from (Gredelj et al., 2019a), including the measured PFAA concentrations in soil and plant compartments and soil-water partition coefficients are listed in the Appendix 3 (Tables A3-1 and A3-4).

4.2.3. Model description

The main purpose of the model application here is the interpretation of measured PFAA uptake data. Chemical model input parameters, specific for the investigated PFAAs, were determined either directly from the experimental data or by model calibration. This enabled us to identify plant-specific factors that influence PFAAs uptake and allowed to transfer from the red chicory experiment to other experimental results, assuming that the chemical-specific parameters remain constant and only the environmental parameters vary.

4.2.3.1. Soil

Earlier plant uptake studies with PFAAs (Bizkarguenaga et al., 2016; Blaine et al., 2014a, 2013; Navarro et al., 2017) provided measured PFAA concentrations in dry soil and bioconcentration factors on a dry weight basis as descriptors for accumulation in plants. Thus, the model was modified to accommodate for dry weight-based root to soil bioconcentration factors (RCF_{dw}) and PFAA concentration in dry soil (c_0).

The gravimetric water content w (g/g) of soil was determined by weighing the wet soil and the soil after drying in the oven at 105°C for 72 h (ASTM International, 2019). The concentration of each PFAA in the pore water c_{pw} (µg/L) of soil is then:

$$c_{pw} = \frac{c_0}{K_d + \frac{w}{\rho_{H_2O}}} \quad (4-1)$$

where c_0 is the respective concentration in dry soil (ng/g_{dw}, measured before planting), K_d (mL/g) is the soil-water distribution coefficient determined in adsorption or desorption experiments, as described, and ρ_{H_2O} (g/mL) is the density of water. w is defined as ratio of the mass of water contained in soil and mass of dry soil.

Considering K_{WS} (g/mL) as the concentration ratio between pore water c_{pw} and bulk (wet) soil concentration c_{soil} (equal to $c_0 / (1 + w)$), the pore water concentration is given as:

$$c_{pw} = K_{WS} c_{soil} = K_{WS} \frac{c_0}{1 + w} = \frac{c_0}{K_d + \frac{w}{\rho_{H_2O}}} \quad (4-2)$$

4.2.3.2. Roots and shoots

PFAAs are non-degradable and present in ionic form at environmental pH. Loss due to plant metabolism, photolysis (or other abiotic degradation processes) and volatilization can thus be safely neglected (Krafft and Riess, 2015; Liu and Avendaño, 2013). Moreover, in the case of red chicory, only the root and shoot compartments (later divided into leaves and head) need to be considered, while stem and fruits can be neglected, simplifying the model to two differential equations describing mass balances for roots and for shoots (leaves and heads), respectively.

The inflow of PFAA from soil pore water and the outflow via xylem lead to the mass balance for roots (Trapp, 2015, 2002):

$$\frac{dm_R}{dt} = R Q c_{pw} - Q c_{xy} \quad (4-3)$$

where m_R is the mass of contaminant in roots (μg), Q is the transpiration stream (L/d), c_{pw} is the concentration in pore water ($\mu\text{g/L}$) and c_{xy} is the concentration in xylem at the outflow of the root ($\mu\text{g/L}$). R is a new factor describing the retardation of uptake relative to water ($R \leq 1$, unitless) (more details are given in the section 4.2.4.).

Equation (4-3) can be modified:

- (i) by considering that $c_R = m_R/M_R$, where c_R is the concentration in roots ($\mu\text{g/kg}_{fw}$) and M_R is the mass of roots (kg),
- (ii) under the assumption of exponential plant growth and constant ratio of transpiration stream and root mass (Q/M_R), where k_R is growth dilution rate ($1/\text{d}$). The concentration in xylem at equilibrium c_{xy} is c_R/K_{RX} , where K_{RX} is the partition coefficient xylem to root (Trapp, 2007).

The differential equation for the change of concentration in roots therefore becomes:

$$\frac{dc_R}{dt} = R \frac{Q}{M_R} K_{WS} c_{soil} - \frac{Q}{M_R K_{RX}} c_R - k_R c_R \quad (4-4)$$

The steady-state solution of this differential equation is:

$$c_R = \frac{\frac{R Q}{M_R}}{\frac{Q}{K_{RX} M_R} + k_R} K_{WS} c_{soil} \quad (4-5)$$

Accordingly, the change of concentration in shoots due to the inflow from roots and with exponential growth dilution is:

$$\frac{dc_S}{dt} = \frac{Q}{M_S K_{RX}} c_R - k_S c_S \quad (4-6)$$

where c_S is the concentration of contaminant in shoots ($\mu\text{g/kg}_{fw}$), c_R is the steady-state concentration in roots ($\mu\text{g/kg}_{fw}$), k_S is the growth rate of the shoots ($1/\text{d}$) and M_S their mass (kg_{fw}). The differential equation (4-6) was solved analytically for $t = 87$ days. The reader is referred to (Legind and Trapp, 2009; Trapp, 2009, 2007), where more detailed numerical and visual descriptions of the model are provided.

4.2.4. Model calibration

According to the equations of the standard plant uptake model, all of the chemical that is taken up into the roots partitions between root tissue and xylem water. The latter fraction is translocated upwards. The chemical reaching the shoots accumulates there, as no relevant loss processes occur for PFAAs. Thus, the equation system contains only two chemical-specific parameters, namely:

The **partition coefficient K_{RX}** is describing the equilibrium concentration ratio of the chemical between root tissue and water in the xylem. Xylem solution consists of water, and for neutral compounds, K_{RX} is identical to the partition coefficient between roots and water K_{RW} (also known as root concentration factor RCF) which can be estimated from the K_{OW} (Briggs et al., 1982). For partly ionized substances, additional effects like the ion trap need to be considered (Briggs et al., 1987; Trapp, 2009). For purely ionic substances (like PFAAs), no reliable estimation method has been

provided so far. By considering root water content w_R and soil-water partition coefficient K_d (either adsorption or desorption based) it follows that the fresh-weight based partition coefficient K_{RX} (L/kg_{fw}) can be calculated as:

$$K_{RX} = RCF_{dw}(1 - w_R)(K_d + \frac{w}{\rho_{H2O}}) \quad (4-7)$$

where w_R is the water content of fresh roots, RCF_{dw} is the empirical root concentration factor, calculated as the ratio between measured root concentration of PFAA and total measured concentration in soil (accounting for all PFAA present in soil, not only the fraction that is adsorbed):

$$RCF_{dw} = \frac{PFAA \text{ concentration in roots (ng/g}_{dw})}{PFAA \text{ concentration in soil (ng/g}_{dw})} \quad (4-8)$$

The **retardation factor R** has been introduced to interpret the observed values of the transpiration stream concentration factor (TSCF), defined as the concentration ratio between xylem sap and soil pore water (Trapp and Matthies, 1995). Parameter R describes the uptake velocity of a chemical relative to the water and is thus comparable to the plant uptake factor PUF (Gourlay, 2017; Lamshoeft et al., 2018). The underlying mechanism is the difference between root permeability for a chemical and water, so R can be defined as the ratio:

$$R = \frac{P_{R,Chem}}{P_{R,H_2O}} \quad (4-9)$$

with $R \leq 1$ (advective uptake is never faster than the flow with water), where $P_{R,Chem}$ (m/s) and P_{R,H_2O} (m/s) are the root membrane permeabilities towards chemical and water, respectively. For very polar chemicals (usually ionic, PFAAs included), uptake into the root is slower than that of water, while for other chemicals R equals 1. The effect of $R < 1$ is a slower uptake and thus a lower TSCF. For example, measured water permeabilities of barley roots ranged from 0.4 to 6×10^{-9} m/s (Steudle and Peterson, 1998). The membrane permeability for neutral compounds can be estimated with satisfying accuracy from K_{OW} (Trapp, 2004):

$$\log P_{R,Chem} = \log K_{OW} - 6.7 \quad (4-10)$$

which means that only chemicals with $\log K_{OW}$ less than about -2 (log L/L) would have a membrane permeability slower than water and consequently $R < 1$. For purely ionic substances like PFAAs, such estimates are unreliable.

The TSCF (L/L) can be calculated from established empirical equations, but being also based on the K_{OW} , their applicability is restricted to neutral compounds (Briggs et al., 1982; Dettenmaier et al., 2009). Instead, TSCF can be found from the measured data as:

$$TSCF = \frac{m_s}{c_{pw} \Sigma(Q t)} \quad (4-11)$$

where m_s (μ g) is the mass of chemical in shoots at the harvest, $\Sigma(Q t)$ (L) is the total volume of the water transpired during the growth period (until the harvest) and c_{pw} (μ g/L) is the concentration of chemical in the pore water. Here, the dynamic solution of the standard uptake model equation (4-6) for shoots (including both leaves and head in the case of red chicory) was solved for $TSCF = c_{xy}/c_{pw}$:

$$TSCF = \frac{c_s}{(1 - e^{-k_s t})} \frac{M_{shoots} k_s}{C_{pw} Q} \quad (4-12)$$

The TSCF was calculated with the measured concentrations of each PFAA in shoots c_s (μ g/kg_{fw}) for $t = 87$ days.

Principally, the TSCF can also be calculated with the root model equation (Trapp, 2007):

$$TSCF = \frac{c_{xy}}{c_{pw}} = \frac{R Q}{Q + K_{RX} k_R M_R} \quad (4-13)$$

Vice versa, if the TSCF has been measured, the retardation factor can be calculated from TSCF (as was done here):

$$R = TSCF \left(1 + \frac{K_{RX}}{Q} k_R M_R \right) \quad (4-14)$$

4.2.5. Plant parameters and model parametrization

Plant-specific parameters can have a very significant impact on the uptake of chemicals into plants (Trapp, 2015). In the present study, transpiration and growth rates, together with water contents of the soil and crops were measured, providing the site-specific data set for fitting the measured PFAA concentrations in crop compartments and soil. The average transpiration coefficient (volume of water transpired per mass of the plant weight) was 35.2 L/kg_{fw}. From the measured data, average daily transpiration rate and growth rates were calculated (Text A3-1) and the input parameters are shown in Table 3-2. All data were calculated and fitted to individual plants (pots) and the results are shown as average per each treatment (initially 12 treatments, each with 5 planted pots and one empty pot that included only soil and no plant (Gredelj et al., 2019a)). As the shoot concentrations (calculated from the measured concentrations and masses of heads and leaves) were used for calculation of R values, model performance was tested for the chicory leaves and heads separately by using the determined plant specific data listed in Table A3-2.

4.2.6. Applying the modeling approach to other crops

In order to test the semi-empirical model calibrated for PFAAs uptake into red chicory, the model and the calibrated values of R were used to estimate concentrations in roots, shoots and fruits of tomato, celery, pea and radish plants. In the respective studies, soil-water partition coefficient K_d and compartmental concentrations of the same set of PFAAs were determined (Blaine et al., 2013; Blaine et al., 2014a), but no plant specific input data except time to harvest and water content of plant material were available. Accordingly, for these experimental results, model calculations were made with the default plant dataset listed in (Trapp, 2015). To evaluate the significance of using the plant specific data (Table A3-5), red chicory uptake was additionally simulated with the default parameters and compared to simulations with chicory-specific plant data.

4.2.7. Statistical evaluation of the results

The performance of model calculations was evaluated by the means of least-squares linear regression between predicted and measured concentration values in the different plant compartments for all PFAAs. With axis intercept forced to zero, the slope is a measure of the accuracy of the model simulations, while R^2 is a measure of the calculations precision. All statistical analyses were performed using the Data Analysis ToolPak from MS Excel® add-in.

4.3. Results and discussion

4.3.1. Modeling results and measurements

Figure 4-1 shows measured and calculated concentrations of PFAAs in leaves and heads of red chicory, based on chicory-specific plant data and the nominal exposure concentrations of 100 and 200 ng/g_{dw} (namely, from (Gredelj et al., 2019a), treatments S100W0 and S200W0). Data are shown from the lowest to the highest perfluoroalkyl chain length, including both PFCAs and PFSAs. For both heads and leaves, the model expectedly reproduced the trend of PFAAs distribution in leaves

and heads (R^2 -values of the regression lines between modeled and measured values being > 0.92 , Table A3-8), always overestimating concentrations for leaves (slopes of the regression line were 1.26 and 1.32 for S100W0 and S200W0, respectively, Table A3-8). Overestimated modeled concentrations could be the consequence of the oldest leaves that withered and were, therefore, not extracted and analyzed. They transpired for the longest period and probably had higher concentrations (than those actually measured in the remaining leaves) of accumulated PFAAs, as stated in (Gredelj et al., 2019a). The model performed generally better for the treatment S100W0 and performance was better for PFCAs than PFSAAs (estimation statistics improved after neglecting PFBS and PFOS from regression of modeled and measured concentrations, Table A3-8).

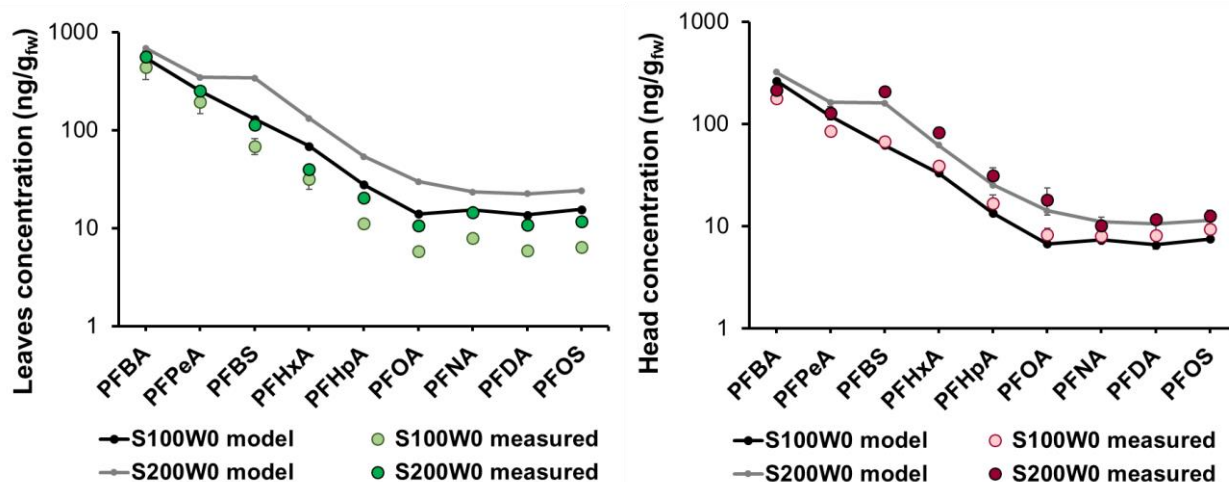


Figure 4-1 Comparison of the calculated and measured PFAA concentrations in red chicory leaves and head for two exposure concentrations. Estimated standard errors are shown for the measured data. Measured values are taken from (Gredelj et al., 2019a).

4.3.2. R values

Figure 4-2 shows the estimated R values for the two exposure concentrations used in the experiments. Values of R for PFCAs decline with chain length, from $3CF_x$ to $7CF_x$, but increase from $7CF_x$ to $9CF_x$, in an almost log-linear pattern.

Due to the relatively low K_{RX} -values, the numerical values of R are close to the values of the TSCF (Table 4-2). Except for PFOS, PFDA and PFBA, all PFAA have TSCF and R-values smaller than 0.1. Similarly, (Briggs et al., 1987) found TSCF-values of weak acids with pK_a about 3 (pK_a 2.84 to 3.7) at pH 7 (thus, about 99.99% ionized) rather constant at 0.02 to 0.05 L/L, median 0.04 L/L. This is close to the lower R values observed here, obtained for the short-chain PFAAs (except PFBA), which were between 0.01 and 0.09.

Table 4-2. Calculated values of the root-xylem partition coefficient (K_{RX}), transpiration stream concentration factor (TSCF) and their ratio ($K_{RX}/TSCF$) for all modeled PFAAs

PFAA	K_{RX} (L/kg)		TSCF (L/L)		$K_{RX}/TSCF$ (L/kg)	
	S100W0	S200W0	S100W0	S200W0	S100W0	S200W0
PFBA	13.7	20.7	0.22	0.18	62.0	116.1
PFPeA	4.18	7.27	0.09	0.08	47.5	90.8
PFBS	5.16	7.42	0.06	0.08	81.1	98.7
PFHxA	3.15	3.97	0.04	0.04	88.7	102.2
PFHpA	2.28	2.78	0.02	0.03	95.1	94.4
PFOA	1.25	1.40	0.01	0.01	93.1	98.1
PFNA	3.47	2.47	0.04	0.04	82.3	70.4

PFDA	26.6	17.5	0.29	0.26	90.5	68.3
PFOS	50.2	28.7	0.54	0.34	93.6	84.5

Trends for PFAA accumulation in shoots and roots were similar (increasing from 3CF_x to 9CF_x of PFCAs) (Gredelj et al., 2019a), implying that PFAAs substantially entering the roots (and having the highest RCF_{dw}) will also be transferred into shoots with transpiration water. Conversely, residual mass accumulated in the root cortex or the apparent free space cannot be translocated upwards and could have been lost before extraction (as explained in Gredelj et al., (2019)), considering the conclusions of (Felizeter et al., 2012) that the longest PFAAs adsorb externally to root surfaces of the lettuce grown in a hydroponic system. In addition to our hypothesis, the ratio of K_{RX}/TSCF is almost constant, usually not being the case for other chemicals. When the TSCF had been calculated from the original root model (Trapp, 2007) it gave a sigmoid curve, similarly to what had been observed by (Dettenmaier et al., 2009), with highest TSCF values for polar compounds (low K_{RX}), while low TSCF values had been calculated for strongly adsorbing lipophilic compounds (high K_{RX}) (Trapp, 2007). In other words, there was an inverse relation between adsorption to roots and translocation to shoots for neutral, lipophilic compounds. The low TSCF-values found here for PFAAs, therefore, are not originating from the adsorption to root tissue and retention within the main root, but due to their deceleration in the epidermal cell membranes, here described by the new factor R. The increase in R, observed with chain length increase above 7CF_x, may be a consequence of the pronounced surfactant nature of these PFAAs. They could have formed a film around the root cell membranes and either resided in the apparent free space (up to 40% of the root volume) (Mc Farlane and Trapp, 1994) or on the membrane surfaces, a possibility even when the cell interior is accessible for PFAAs.

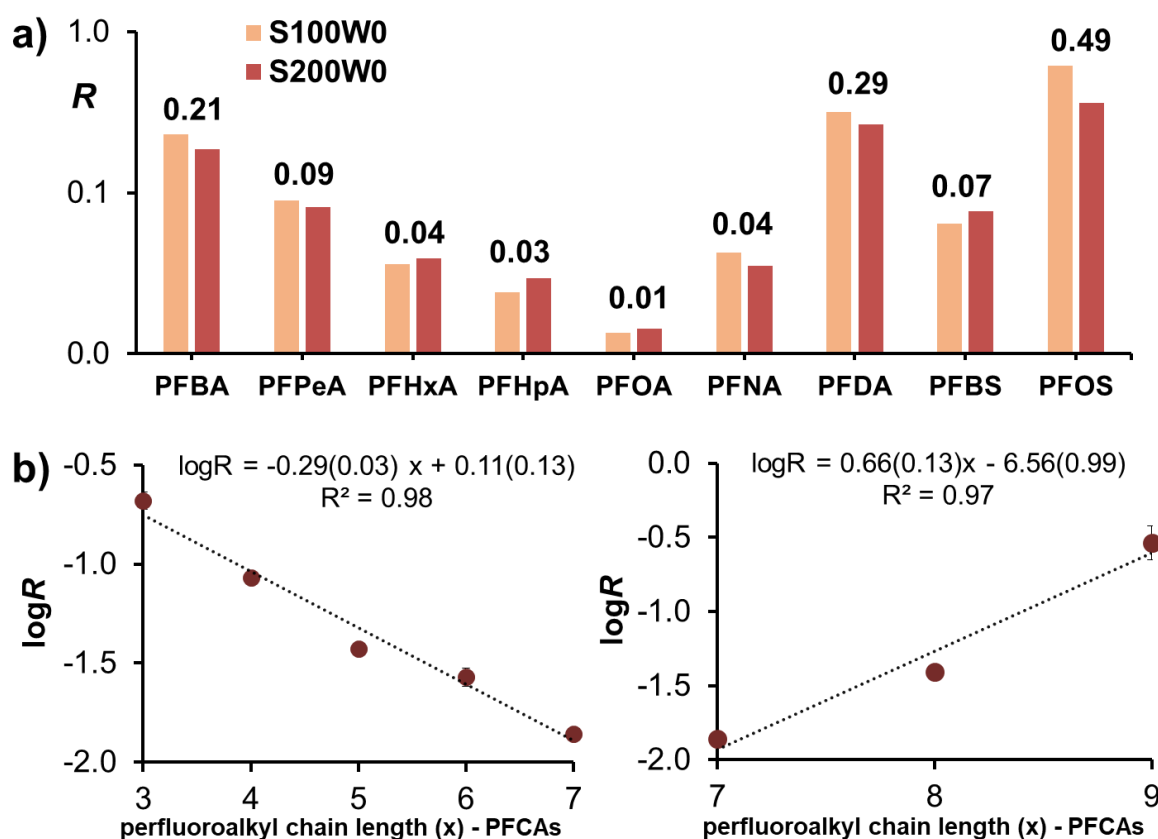


Figure 4-2. a) Calculated retardation factor (R) values for two exposure treatments. Average R-values for both treatments are shown as numerical values above the bars. b) Treatment-averaged logR in relation to PFCA chain length. Standard error estimates of two averaged treatments are shown as error bars.

4.3.3. Partitioning

The currently unknown link between the structure of PFAAs and their adsorption behavior requires experimental determination of sorption to soils, sediments or tissues (Droge, 2019). Measured K_d values of short-chain PFAAs do not correlate well with the organic carbon content (%OC) (F. Li et al., 2018; Y. Li et al., 2018; Milinovic et al., 2015; Zhu et al., 2014), and observed K_d values for PFAAs in different soils and sediments can vary significantly (e.g. between 0.1 and > 3000 L/kg for PFOS), underlining the need for experimental determination (F. Li et al., 2018; Y. Li et al., 2018). Nonetheless, to our knowledge, only one plant uptake study of PFAAs (apart from (Gredelj et al., 2019a)) included experimental determination of the K_d values of the growth medium (Blaine et al., 2014a, 2013).

The K_d values of PFCAs determined in these studies show a close relation to chain length, with almost log-linear increase with the number of carbon atoms of perfluoroalkyl chain (CF_x) (Figure 3c showing the relationship from (Gredelj et al., 2019a)). The K_d values for PFCAs with less than $6CF_x$ are below 1 L/kg, indicating very low adsorption to soil and a significant fraction of the chemical present in the soil pore water. On the contrary, RCF_{dw} values are the highest for short-chain PFCAs, being up to 260 kg/kg_{dw} (Figure 4-3 a). Attempts to correlate the RCF_{dw} to octanol-water distribution coefficient, logD (estimated using ACD/i-Lab) were unsuccessful and are not shown. Similarly, estimated adsorption to human serum albumin K_{HSA} data were unsuccessful for the prediction of the adsorption to roots. However, RCF_{dw} shows a declining and K_d an increasing trend with the chain length (Figure 4-3 bc).

The combination of comparably low adsorption to soil (K_d) and rather high partitioning into roots leads to an unusually high ratio of RCF_{dw} to K_d for the short-chain PFAAs (Figure 4-3 a). The measured ratio (average of both treatments) was from 263.5 kg/kg for PFBA to 11.4 kg/kg for PFHpA while it was lower for the long-chain PFAAs, ranging between 4.2 kg/kg (PFOA) and 0.1 kg/kg (PFOS). For other organic compounds, the opposite has been observed, i.e. adsorption to soil is typically similar or higher than adsorption to plant roots (Trapp, 1995). Usually, growth dilution and loss processes within the plant lead to concentrations below equilibrium in roots, and root-to-soil bioconcentration factors <0.01 kg/kg_{dw} have been observed for lipophilic compounds such as benzo(a)pyrene and PCBs (Trapp, 2002). Hence, the partitioning of PFAAs (PFCAs) in the soil-root environment differs very much from that of other organic compounds.

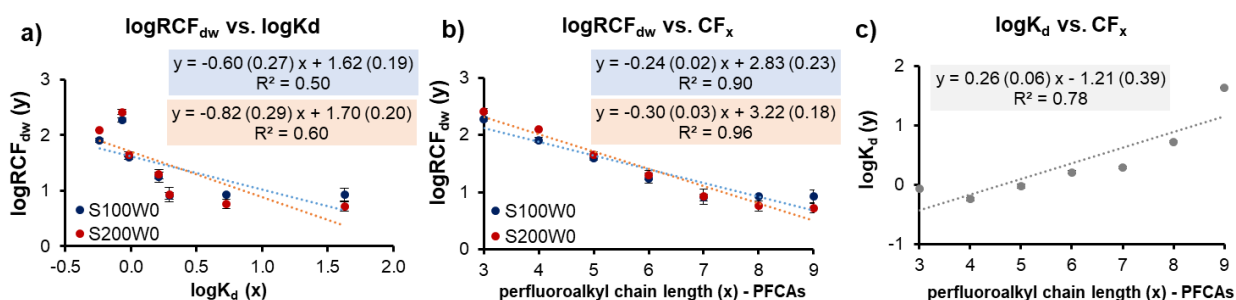


Figure 4-3. Regression analysis of logarithmically transformed dry weight-based root concentration factors ($\log RCF_{dw}$), soil-water partition coefficients ($\log K_d$) and PFCA chain length for red chicory (from Gredelj et al., (2019)). Standard error estimates ($n = 3$) are shown for measured values of RCF_{dw} . Regression lines are shown with standard errors in brackets and coefficients of determination.

4.3.4. Other crops

By adapting the plant specific input data (Tables A3-2 and A3-5), the model can be applied to other plant species when the retardation factor R of each PFAA remains the same. In order to test this assumption, the approach was applied to literature crop data-sets for PFAAs (Blaine et al., 2014a, 2013). Modeled concentrations in plant compartments of tomato, celery, pea and radish are shown in Figure 4-4, together with the measured values. Like before, measured RCF_{dw} was used to calculate K_{RX} (Eq. 4-7). For PFAAs with high K_{RX} (PFOS and PFDA), growth dilution leads to calculated root concentration somewhat below equilibrium (Table A3-9).

Concentration trends in shoots were estimated mostly accurately for all four crops, their values always being in the same order of a magnitude (slopes of the regression line between measured and modeled values ranging between 1.22 and 1.73), even though the R values were taken from the red chicory experiments and default plant data were used (Trapp, 2015). In particular, estimations were better for the short-chain PFAAs (improving of the model evaluation statistics was noticed after elimination of long-chain PFAAs, Table A3-9) and for the tomato and pea (R^2 values of 0.75 and 0.86, respectively). For radish and celery, modeled concentrations are not far from the measured ones (R^2 values of 0.78 and 0.52), despite of their overestimation (model evaluation slopes of 1.73 and 1.32) and similar trends are shown among them (e.g., lowest concentration for PFNA). Differences between measurements and simulation results could be attributed to the use of default data instead of the carefully determined plant-specific data in the case of chicory. This hypothesis was confirmed by comparing simulation results of the red chicory experiments using measured and default plant parameters sets, whereby worse model performance was observed in the latter case, with underestimation of PFOS and PFDA in roots and shoots, and overestimation in shoots for most of the other PFAAs (see Figure A3-1 and accompanying evaluation statistics). Overestimation with the default plant data for red chicory is in consistence with observations of the model performance for the other crops.

Simulation results for fruits typically overestimated measured data (Table A3-9), except for short-chain PFAAs, and exhibited the poorest fit for PFDA and PFOS. Notably, the fruit compartment is very rudimentary described in the current version of the standard plant uptake model, being identical to the leaf but with reduced water flux (this is why calculated fruit concentrations follow very closely the trend of the shoots, but about one order of magnitude lower). Complex processes that lead to phloem loading and unloading are not adequately expressed in the equations.

Interestingly, except for celery, RCF_{dw} values of these experiments show no significant correlation with the PFAA chain length (Blaine et al., 2014a) and the calibrated RCF_{dw} values are lower than those reported in (Gredelj et al., 2019a) (Figure A3-2). More data for root and soil concentrations are available for PFOS and PFOA than for the other PFAAs (Table A3-7). The experimental RCF_{dw} of PFOS found in literature ranged from < 0.1 to 8.38 kg/kg, with an average of 2.93 kg/kg (Bizkarguenaga et al., 2016; Blaine et al., 2014a; Lan et al., 2018; Navarro et al., 2017; Wen et al., 2016, 2014; Zhao et al., 2017) while for the red chicory treatments S100W0 and S200W0 they ranged from 6.14 to 11.35 kg/kg. For PFOA, experimental RCF_{dw} found in literature ranged from 0.8 to 10.34 kg/kg, with average 3.3 kg/kg (Bizkarguenaga et al., 2016; Blaine et al., 2014a; Lan et al., 2018; Navarro et al., 2017; Wen et al., 2016, 2014; Zhao et al., 2017) while the range for red chicory was from 8.10 to 10.31 kg/kg.

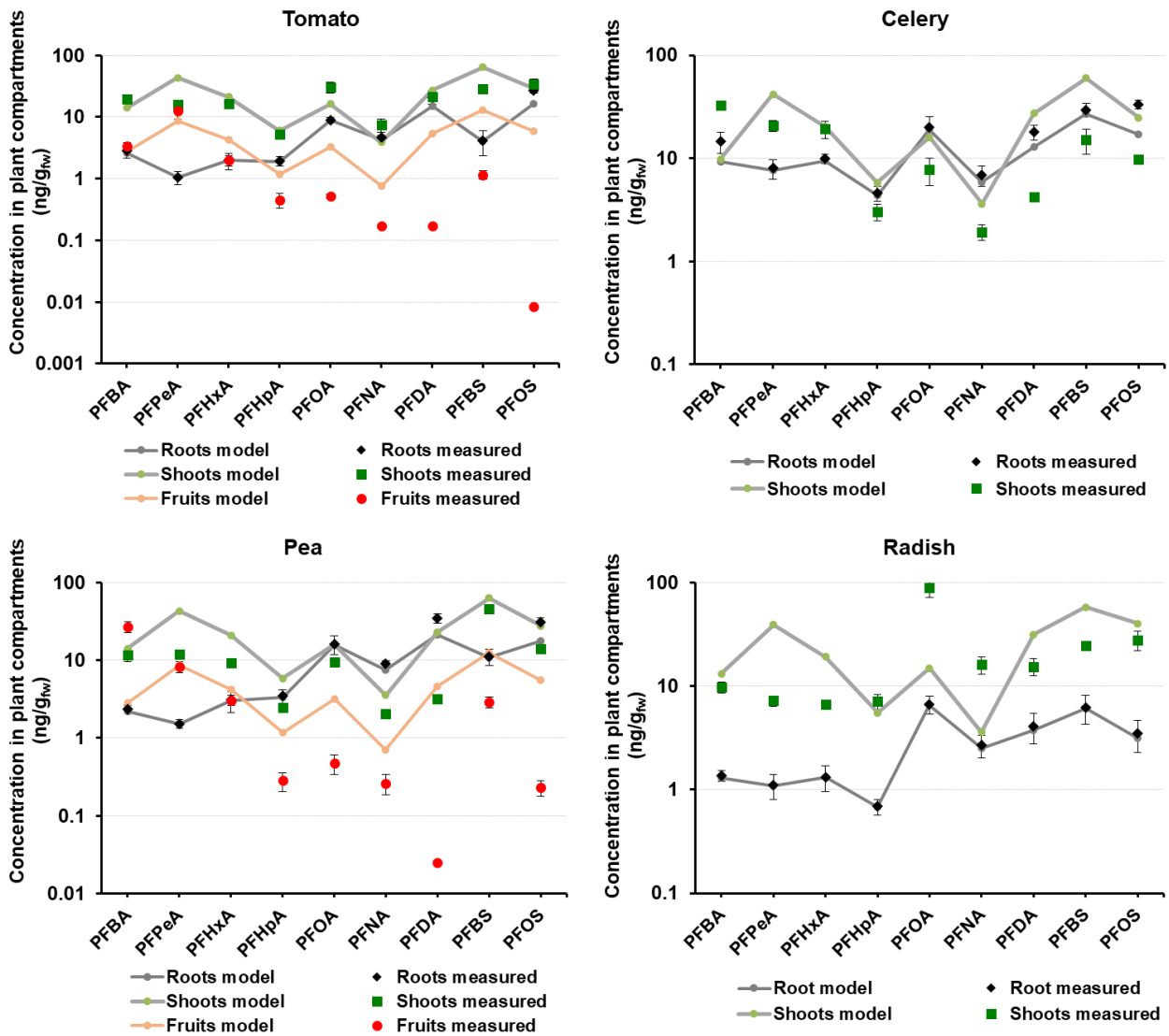


Figure 4-4. Comparison of modeled and measured PFAA concentrations in crops. Measured values are shown as means with standard errors and are taken from (Blaine et al., 2014a, 2013).

4.4. Conclusions

"Mathematical models provide a framework for understanding the cycling of compounds through environment" (Ramaswami et al., 2005). We thus applied a plant uptake model to interpret measured plant uptake data for PFAAs and gained new insights in uptake processes and accumulation mechanisms.

The high concentrations of perfluoroalkyl acids (and in particular short-chain PFAAs) in crops are neither due to rapid plant uptake, nor due to active or preferential transport, nor due to exceptionally high adsorption to plant material. We found two main reasons for the observed high accumulation potential of PFAAs in terrestrial crop plants:

i) Partition coefficients. The root-to-xylem partition coefficients K_{RX} , here derived from measured RCF_{dw} , ranged from < 1 to 54 L/kg_{fw} . The highest values were observed for the shortest PFAA ($3CF_x$, PFBA), PFDA and PFOS. At the same time, K_d values (expressing adsorption to soil) of the short-chain PFAAs are small, $< 1 \text{ L/kg}$. Thus, these PFAAs show very high bioavailability in soil and rapid

transport with water. The combination of low K_d and relatively high K_{RX} (or RCF_{dw}) is rather unusual and has not been described before. The accumulation of chemicals in roots is determined by the ratio K_{RX}/K_d , and this leads to the observed very high concentrations of short-chain PFAAs in chicory roots and consequently leaves and head. For PFOA, PFNA, PFDA and PFOS, K_d is higher than RCF_{dw} , and less accumulation in roots and shoots was accordingly observed.

ii) System dynamics. PFAAs show no rapid uptake into roots. Possibly due to their unusual chemical properties (being hydrophobic and lipophobic at the same time), their biomembrane permeability is slow, in any case slower than that of water ($R < 1$), and the retardation factor appears to be independent of the type of crop. Slow transport across biomembranes is typical for very polar or highly charged compounds. However, there are no loss processes of relevance known within the plant. Neither biotic nor abiotic degradation nor volatilization lead to a decline of chemical mass once the chemical has been taken up. The permanent transport to and within the plant with the transpiration water over time leads to very high concentrations, and no steady-state is reached. This is best seen from the solution of the underlying differential equation, $m(t) = I/k (1 - e^{-kt})$, where $m(t)$ is the mass in plant shoots at time t , I is the input (here with the transpiration water) and k is the sum of loss processes. With very small loss (k close to 0 d^{-1}), chemical mass in the shoots increases steadily as long as the chemical is transported into plant and shoots with the water taken up. Thus, considerable accumulation can be reached with longer time periods provided that the input of chemical is constant (a reasonable assumption for long-term contamination events, such as the one in the Veneto Region, Italy).

Having in mind (a) the strong affinity of PFAAs (particularly short-chain) for crop uptake through roots, (b) the long maturation period of some crops, (c) crop-dependent uptake and particularly (d) soil-type dependency as the only way for decreasing the bioavailability of PFAAs to roots through the soil sorption, research is urgently needed to improve the mechanistic understanding and allow predicting PFAAs uptake in crops, eventually leading towards more reliable human health exposure and risk assessment for these substances.

Acknowledgements

Andrea Gredelj's PhD research was funded by the Fondazione CARIPARO's grant for foreign PhD students at the University of Padova.

4.5. References:

- ASTM International, 2019. ASTM D2216, Standard Test Methods for Laboratory Determination of Water (Moisture) Content of Soil and Rock by Mass. West Conshohocken, PA. <https://doi.org/10.1520/D2216-19>
- Bizkarguenaga, E., Zabaleta, I., Mijangos, L., Iparraguirre, A., Fernández, L.A., Prieto, A., Zuloaga, O., 2016. Uptake of perfluorooctanoic acid, perfluorooctane sulfonate and perfluorooctane sulfonamide by carrot and lettuce from compost amended soil. *Sci. Total Environ.* <https://doi.org/10.1016/j.scitotenv.2016.07.010>
- Blaine, A.C., Rich, C.D., Hundal, L.S., Lau, C., Mills, M.A., Harris, K.M., Higgins, C.P., 2013. Uptake of perfluoroalkyl acids into edible crops via land applied biosolids: Field and greenhouse studies. *Environ. Sci. Technol.* 47, 14062–14069. <https://doi.org/10.1021/es403094q>
- Blaine, A.C., Rich, C.D., Sedlacko, E.M., Hundal, L.S., Kumar, K., Lau, C., Mills, M.A., Harris, K.M., Higgins, C.P., 2014a. Perfluoroalkyl acid distribution in various plant compartments of edible crops grown in biosolids-amended soils. *Environ. Sci. Technol.* 48, 7858–7865. <https://doi.org/10.1021/es500016s>
- Blaine, A.C., Rich, C.D., Sedlacko, E.M., Hyland, K.C., Stushnoff, C., Dickenson, E.R. V., Higgins, C.P., 2014b. Perfluoroalkyl Acid Uptake in Lettuce (*Lactuca sativa*) and Strawberry (*Fragaria ananassa*) Irrigated with Reclaimed Water. *Environ. Sci. Technol.* 48, 14361–14368. <https://doi.org/10.1021/es504150h>
- Brand, E., Otte, P.F., Lijzen, J.P.A., 2007. CSOIL 2000: an exposure model for human risk assessment of soil contamination. Bilthoven (NL).
- Brendel, S., Fetter, É., Staude, C., Vierke, L., Biegel-Engler, A., 2018. Short-chain perfluoroalkyl acids: environmental concerns and a regulatory strategy under REACH. *Environ. Sci. Eur.* 30, 9. <https://doi.org/10.1186/s12302-018-0134-4>
- Briggs, G.G., Bromilow, R.H., Evans, A.A., 1982. Relationships between lipophilicity and root uptake and translocation of non-ionised chemicals by barley. *Pestic. Sci.* 13, 495–504. <https://doi.org/10.1002/ps.2780130506>
- Briggs, G.G., Rigitano, R.L.O., Bromilow, R.H., 1987. Physico-chemical factors affecting uptake by roots and translocation to shoots of weak acids in barley. *Pestic. Sci.* 19, 101–112. <https://doi.org/10.1002/ps.2780190203>
- Buck, R.C., Franklin, J., Berger, U., Conder, J.M., Cousins, I.T., de Voogt, P., Jensen, A.A., Kannan, K., Mabury, S.A., van Leeuwen, S.P., 2011. Perfluoroalkyl and polyfluoroalkyl substances in the environment: Terminology, classification, and origins. *Integr. Environ. Assess. Manag.* 7, 513–541. <https://doi.org/10.1002/ieam.258>
- Chen, H., Reinhard, M., Nguyen, T.V., You, L., He, Y., Gin, K.Y.H., 2017. Characterization of occurrence, sources and sinks of perfluoroalkyl and polyfluoroalkyl substances (PFASs) in a tropical urban catchment. *Environ. Pollut.* 227, 397–405. <https://doi.org/10.1016/j.envpol.2017.04.091>
- Chen, H., Reinhard, M., Nguyen, V.T., Gin, K.Y.H., 2016. Reversible and irreversible sorption of perfluorinated compounds (PFCs) by sediments of an urban reservoir. *Chemosphere* 144, 1747–1753. <https://doi.org/10.1016/j.chemosphere.2015.10.055>

- Cheng, W., Ng, C.A., 2018. Predicting Relative Protein Affinity of Novel Per- and Polyfluoroalkyl Substances (PFASs) by An Efficient Molecular Dynamics Approach. *Environ. Sci. Technol.* 52, 7972–7980. <https://doi.org/10.1021/acs.est.8b01268>
- Dettenmaier, E.M., Doucette, W.J., Bugbee, B., 2009. Chemical hydrophobicity and uptake by plant roots. *Environ. Sci. Technol.* 43, 324–329. <https://doi.org/10.1021/es801751x>
- DeWitt, J., Berger, U., Miller, M., Green, C., Huang, J., Perkola, N., Vierke, L., Higgins, C., Buser, A.M., Lindstrom, A.B., Boucher, J.M., Lau, C.S., Knepper, T., Liu, J., Wang, Z., Herzke, D., Ahrens, L., Hung, H., Cousins, I., van der Jagt, K., Bopp, S.K., Fletcher, T., Leinala, E., Scheringer, M., Småstuen Haug, L., Borg, D., Ritscher, A., Valsecchi, S., Shi, Y., Ohno, K., Trier, X., Bintein, S., 2018. Zürich Statement on Future Actions on Per- and Polyfluoroalkyl Substances (PFASs). *Environ. Health Perspect.* 126, 084502. <https://doi.org/10.1289/ehp4158>
- Droge, S.T.J., 2019. Membrane-Water Partition Coefficients to Aid Risk Assessment of Perfluoroalkyl Anions and Alkyl Sulfates. *Environ. Sci. Technol.* 53, 760–770. <https://doi.org/10.1021/acs.est.8b05052>
- European Commission, 2003. Technical Guidance Document on Risk Assessment in support of Commission Directive 93/67/EEC on Risk Assessment for new notified substances, Commission Regulation (EC) No 1488/94 on Risk Assessment for existing substances, and Directive 98/8/EC of the Euro. Ispra.
- Fantke, P., Charles, R., Alencastro, L.F. de, Friedrich, R., Jolliet, O., 2011a. Plant uptake of pesticides and human health: Dynamic modeling of residues in wheat and ingestion intake. *Chemosphere* 85, 1639–1647. <https://doi.org/10.1016/j.chemosphere.2011.08.030>
- Fantke, P., Juraske, R., Antón, A., Friedrich, R., Jolliet, O., 2011b. Dynamic multicrop model to characterize impacts of pesticides in food. *Environ. Sci. Technol.* 45, 8842–8849. <https://doi.org/10.1021/es201989d>
- Felizeter, S., McLachlan, M.S., De Voogt, P., 2014. Root uptake and translocation of perfluorinated alkyl acids by three hydroponically grown crops. *J. Agric. Food Chem.* 62, 3334–3342. <https://doi.org/10.1021/jf500674j>
- Felizeter, S., McLachlan, M.S., De Voogt, P., 2012. Uptake of perfluorinated alkyl acids by hydroponically grown lettuce (*Lactuca sativa*). *Environ. Sci. Technol.* 46, 11735–11743. <https://doi.org/10.1021/es302398u>
- Franco, A., Fu, W., Trapp, S., 2009. Influence of soil pH on the sorption of ionizable chemicals: Modeling advances. *Environ. Toxicol. Chem.* 28, 458–464. <https://doi.org/10.1897/08-178.1>
- Ghisi, R., Vamerali, T., 2018. Accumulation of perfluorinated alkyl substances (PFASs) in agricultural plants: a review. *Environ. Res.* <https://doi.org/https://doi.org/10.1016/j.envres.2018.10.023>
- Gourlay, V., 2017. Development and application of hydroponic test systems for the determination of plant uptake factors (PUF) of xenobiotics to be used as parameters in environmental fate models. Shaker Verlag GmbH, Germany, Aachen.
- Greaves, A.K., Letcher, R.J., Sonne, C., Dietz, R., Born, E.W., 2012. Tissue-Specific Concentrations and Patterns of Perfluoroalkyl Carboxylates and Sulfonates in East Greenland Polar Bears. *Environ. Sci. Technol.* 46, 11575–11583. <https://doi.org/10.1021/es303400f>

- Gredelj, A., Nicoletto, C., Valsecchi, S., Ferrario, C., Polesello, S., Lava, R., Zanon, F., Barausse, A., Palmeri, L., Guidolin, L., Bonato, M., 2019a. Uptake and translocation of perfluoroalkyl acids (PFAA) in red chicory (*Cichorium intybus* L.) under various treatments with pre-contaminated soil and irrigation water. *Sci. Total Environ.* <https://doi.org/10.1016/j.scitotenv.2019.134766>
- Guelfo, J.L., Higgins, C.P., 2013. Subsurface transport potential of perfluoroalkyl acids at aqueous film-forming foam (AFFF)-impacted sites. *Environ. Sci. Technol.* 47, 4164–4171. <https://doi.org/10.1021/es3048043>
- Jeffries, J., Martin, I., 2009. Updated technical background to the CLEA model. Almondsbury (UK).
- Johansson, J.H., Yan, H., Berger, U., Cousins, I.T., 2017. Water-to-air transfer of branched and linear PFOA: Influence of pH, concentration and water type. *Emerg. Contam.* 3, 46–53. <https://doi.org/10.1016/j.emcon.2017.03.001>
- Krafft, M.P., Riess, J.G., 2015. Per- and polyfluorinated substances (PFASs): Environmental challenges. *Curr. Opin. Colloid Interface Sci.* 20, 192–212. <https://doi.org/10.1016/j.cocis.2015.07.004>
- Lamshoeft, M., Gao, Z., Ressler, H., Schriever, C., Sur, R., Sweeney, P., Webb, S., Zillgens, B., Reitz, M.U., 2018. Evaluation of a novel test design to determine uptake of chemicals by plant roots. *Sci. Total Environ.* 613–614, 10–19. <https://doi.org/10.1016/j.scitotenv.2017.08.314>
- Lan, Z., Zhou, M., Yao, Y., Sun, H., 2018. Plant uptake and translocation of perfluoroalkyl acids in a wheat–soil system. *Environ. Sci. Pollut. Res.* 25, 30907–30916. <https://doi.org/10.1007/s11356-018-3070-3>
- Li, F., Fang, X., Zhou, Z., Liao, X., Zou, J., Yuan, B., Sun, W., 2018. Adsorption of perfluorinated acids onto soils: Kinetics, isotherms, and influences of soil properties. *Sci. Total Environ.* 649, 504–514. <https://doi.org/https://doi.org/10.1016/j.scitotenv.2018.08.209>
- Li, Y., Oliver, D.P., Kookana, R.S., 2018. A critical analysis of published data to discern the role of soil and sediment properties in determining sorption of per and polyfluoroalkyl substances (PFASs). *Sci. Total Environ.* 628–629, 110–120. <https://doi.org/10.1016/j.scitotenv.2018.01.167>
- Liu, J., Mejia Avendaño, S., 2013. Microbial degradation of polyfluoroalkyl chemicals in the environment: A review. *Environ. Int.* 61, 98–114. <https://doi.org/10.1016/j.envint.2013.08.022>
- McLachlan, M.S., Felizeter, S., Klein, M., Kotthoff, M., De Voogt, P., 2019. Fate of a perfluoroalkyl acid mixture in an agricultural soil studied in lysimeters. *Chemosphere* 223, 180–187. <https://doi.org/10.1016/j.chemosphere.2019.02.012>
- Milinic, J., Lacorte, S., Vidal, M., Rigol, A., 2015. Sorption behaviour of perfluoroalkyl substances in soils. *Sci. Total Environ.* 511, 63–71. <https://doi.org/10.1016/j.scitotenv.2014.12.017>
- Navarro, I., de la Torre, A., Sanz, P., Porcel, M.Á., Pro, J., Carbonell, G., Martínez, M. de los Á., 2017. Uptake of perfluoroalkyl substances and halogenated flame retardants by crop plants grown in biosolids-amended soils. *Environ. Res.* 152, 199–206. <https://doi.org/10.1016/j.envres.2016.10.018>
- Ng, C.A., Hungerbühler, K., 2014. Bioaccumulation of perfluorinated alkyl acids: Observations and models. *Environ. Sci. Technol.* 48, 4637–4648. <https://doi.org/10.1021/es404008g>

- OECD, 2000. Test No. 106: Adsorption - Desorption Using a Batch Equilibrium Method, OECD Guideline for the Testing of Chemicals. <https://doi.org/https://doi.org/10.1787/9789264069602-en>
- Ramaswami, A., Milford, J.B., Small, M.J., 2005. Integrated Environmental Modeling: Pollutant Transport, Fate, and Risk in the Environment. John Wiley and Sons, Hoboken, New Jersey.
- Smith, J.W.N., Beuthe, B., Dunk, M., Demeure, S., Carmona, J.M.M., Medve, A., Spence, M.J., Pancras, T., Schrauwen, G., Held, T., Baker, K., Ross, I., Slenders, H., 2016. Environmental fate and effects of poly- and perfluoroalkyl substances (PFAS). Brussels.
- Steudle, E., Peterson, C.A., 1998. How does water get through roots? *J. Exp. Bot.* 49, 775–788. <https://doi.org/10.1093/jexbot/49.322.775>
- Trapp, S., 2015. Calibration of a plant uptake model with plant- and site-specific data for uptake of chlorinated organic compounds into radish. *Environ. Sci. Technol.* 49, 395–402. <https://doi.org/10.1021/es503437p>
- Trapp, S., 2009. Bioaccumulation of Polar and Ionizable Compounds in Plants, in: Devillers, J. (Ed.), *Ecotoxicology Modeling, Emerging Topics in Ecotoxicology: Principles, Approaches and Perspectives 2*. Springer US, Rillieux La Pape, p. 400. <https://doi.org/10.1007/978-1-4419-0197-2>
- Trapp, S., 2007. Fruit tree model for uptake of organic compounds from soil and air. *SAR QSAR Environ. Res.* 18, 367–387. <https://doi.org/10.1080/10629360701303693>
- Trapp, S., 2004. Plant Uptake and Transport Models for Neutral and Ionic Chemicals. *Environ. Sci. Pollut. Res.* 11, 33–39. <https://doi.org/10.1065/espr2003.08.169>
- Trapp, S., 2002. Dynamic root uptake model for neutral lipophilic organics. *Environ. Toxicol. Chem.* 21, 203–206. <https://doi.org/10.1002/etc.5620210128>
- Trapp, S., 1995. Model for Uptake of Xenobiotics into Plants., in: Trapp, S., McFarlane, J.C. (Eds.), *Plant Contamination: Modeling and Simulation of Organic Chemical Processes*. Lewis Publishers, Boca Raton, pp. 107–152.
- Trapp, S., Franco, A., MacKay, D., 2010. Activity-based concept for transport and partitioning of ionizing organics. *Environ. Sci. Technol.* 44, 6123–6129. <https://doi.org/10.1021/es100509x>
- Trapp, S., Matthies, M., 1995. Generic One-Compartment Model for Uptake of Organic Chemicals by Foliar Vegetation. *Environ. Sci. Technol.* 29, 2333–2338. <https://doi.org/10.1021/es00009a027>
- Veneto Region, 2014. Progress and prospects for Veneto Agriculture. [<http://statistica.regione.veneto.it/ENG/Pubblicazioni/RapportoStatistico2014/pdf/Capitolo07.pdf>]
- Wen, B., Li, L., Zhang, H., Ma, Y., Shan, X.Q., Zhang, S., 2014. Field study on the uptake and translocation of perfluoroalkyl acids (PFAAs) by wheat (*Triticum aestivum* L.) grown in biosolids-amended soils. *Environ. Pollut.* 184, 547–554. <https://doi.org/10.1016/j.envpol.2013.09.040>
- Wen, B., Wu, Y., Zhang, H., Liu, Y., Hu, X., Huang, H., Zhang, S., 2016. The roles of protein and lipid in the accumulation and distribution of perfluorooctane sulfonate (PFOS) and

perfluorooctanoate (PFOA) in plants grown in biosolids-amended soils. *Environ. Pollut.* 216, 682–688. <https://doi.org/10.1016/j.envpol.2016.06.032>

WHO, 2016. Keeping our water clean: the case of water contamination in the Veneto Region, Italy. AREAGRAFICA SNC DI TREVISAN GIANCARLO & FIGLI, Venice, Italy.

[http://www.euro.who.int/__data/assets/pdf_file/0018/340704/FINAL_pfas-report-20170530-h1200.pdf]

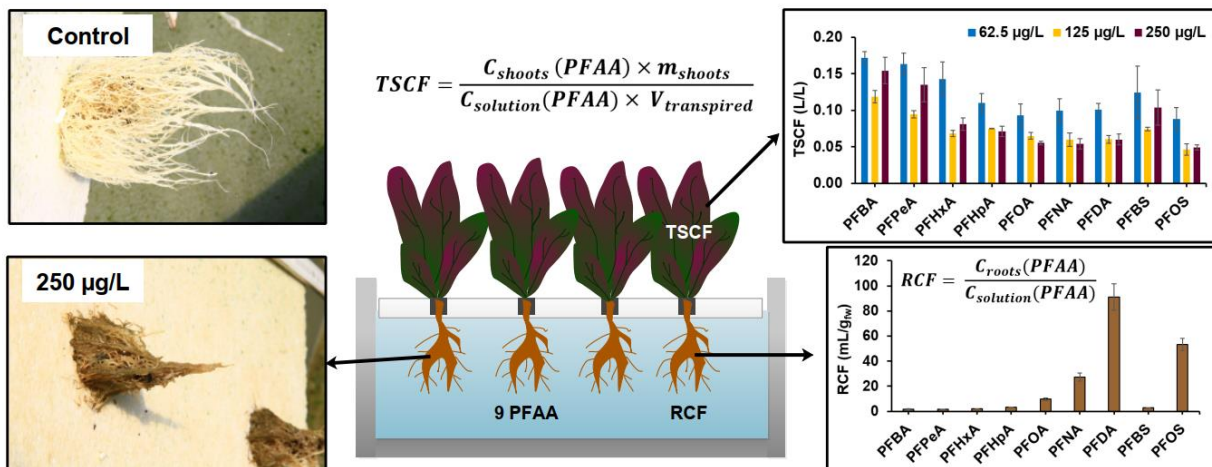
Xiang, L., Chen, L., Yu, L.-Y., Yu, P.-F., Zhao, H.-M., Mo, C.-H., Li, Y.-W., Li, H., Cai, Q.-Y., Zhou, D.-M., Wong, M.-H., 2018. Genotypic variation and mechanism in uptake and translocation of perfluorooctanoic acid (PFOA) in lettuce (*Lactuca sativa* L.) cultivars grown in PFOA-polluted soils. *Sci. Total Environ.* <https://doi.org/10.1016/j.scitotenv.2018.04.354>

Zhao, S., Fan, Z., Sun, L., Zhou, T., Xing, Y., Liu, L., 2017. Interaction effects on uptake and toxicity of perfluoroalkyl substances and cadmium in wheat (*Triticum aestivum* L.) and rapeseed (*Brassica campestris* L.) from co-contaminated soil. *Ecotoxicol. Environ. Saf.* 137, 194–201. <https://doi.org/10.1016/j.ecoenv.2016.12.007>

Zhu, Z., Wang, T., Wang, P., Lu, Y., Giesy, J.P., 2014. Perfluoroalkyl and polyfluoroalkyl substances in sediments from South Bohai coastal watersheds, China. *Mar. Pollut. Bull.* 85, 619–627. <https://doi.org/10.1016/j.marpolbul.2013.12.042>

Chapter 5

Uptake and translocation of perfluoroalkyl acids (PFAAs) in hydroponically grown red chicory (*Cichorium intybus L.*): PFAAs toxicity, comparison with the soil experiment and bioavailability implications



In preparation for publication

Chapter summary:

Short-chain perfluoroalkyl acids (PFAAs) have a high potential for plant uptake, making them possible significant contributors to the total dietary exposure to PFAAs. The plant uptake of PFAAs does not only depend on their perfluoroalkyl chain length, but also on their polar terminal group, plant species and exposure media. In this work, a plant uptake study with nine perfluoroalkyl acids (PFAAs) was carried out under the hydroponic exposure conditions. Red chicory was grown in a nutrient solution, spiked with PFAAs mixture to three different concentrations (i.e. 62.5, 125 and 250 µg/L) in a higher spectrum of concentration ranges so far employed and reported in the literature. Bioaccumulation metrics and transpiration stream concentration factors (TSCFs) were employed for the plant uptake characterization and consequent comparison with the experimental results of soil uptake experiment, previously performed with the same crop. The highest root bioconcentration factors (RCFs) were calculated for PFDA and were always decreasing with the chain length decrease. The opposite chain length dependency was present for shoots, shoots bioconcentration factors (SCFs) increasing with the chain length decrease, being the highest for PFBA and the lowest for PFOS in all the treatments. Plants from two treatments with the highest PFAAs concentrations manifested physiological changes (discoloration, inhibited roots and leaves growth), even though employed concentrations were much lower than previously published phytotoxicity thresholds. A comparison amongst RCFs and TSCFs derived from hydroponics and from the soil growth experiment showed their different magnitudes and PFAAs chain length patterns. They could not be ascribed only to soil sorption as a way for decreasing PFAAs bioavailability for plants, but also to developmental differences between the root systems formed in soil and in nutrient solution and to the potential competitive PFAAs sorption to roots in hydroponics.

5.1. Introduction

Per- and polyfluoroalkyl substances (PFASs) are a group of anthropogenic chemicals widely detected in the environment, including water matrices (Xiao, 2017a), air (Wang et al., 2015), soils and sediments (Zareitalabad et al., 2013), humans (Pérez et al., 2013), animals (Giesy and Kannan, 2001; Houde et al., 2006) and plants (Ghisi et al., 2019). Currently, there is more than 4700 individual PFASs in the market (Cousins et al., 2019), covering myriads of different applications, from industry (textile and leather industry, oil production) to consumer products as cosmetics or household products, fire-fighting foams, food contact materials, pesticides (Krafft and Riess, 2015b; Loos et al., 2008; Wang et al., 2017). All PFASs contain at least one perfluoroalkyl moiety $-C_nF_{2n+1}$ (Buck et al., 2011), the presence of extremely strong C-F bond leads to high stability and resistance to thermal and (bio)chemical degradation (Krafft and Riess, 2015b; Xiao, 2017a). Through abiotic and biotic transformations of the non-fluorinated part of molecule in the environment, PFASs will eventually end up as perfluoroalkyl acids (PFAAs), considered as their final transformation product (Brendel et al., 2018; Buck et al., 2011; Ghisi et al., 2019). PFAAs are highly persistent low weight surfactants, containing hydrophobic perfluoroalkyl chain and hydrophilic polar group, most commonly sulfonic or carboxylic (Wang et al., 2017). The most detected and, consequently, the most researched PFAAs are perfluorooctane sulfonic acid (PFOS) and perfluorooctanoic acid (PFOA) (Cheng and Ng, 2018). After the realization that bioaccumulation and toxicity of PFAAs are generally lowering with the decrease of their perfluoroalkyl chain length, PFAAs were formally divided into long- and short- chain PFAA. Long-chain PFAAs are considered to be perfluorocarboxylic acids (PFCAs) with 7 or more and perfluorosulfonic acids (PFSAs) with 6 or more fluorinated carbons (Eschauzier et al., 2013; Krafft and Riess, 2015a, 2015a; Valsecchi et al., 2015). After the phase-out of PFOS and related compounds by the major production company in 2002 (Buck et al., 2011), regulatory measures have been undertaken not only against PFOS, but also other long-chain PFAAs, resulting in the production shift towards the short-chain alternatives (Brendel et al., 2018). However, short-chain PFAAs are as persistent as their long-chain homologues and are ubiquitous in the environment as the results of historic emissions of their precursors and the production shift (Brendel et al., 2018; Cousins et al., 2016).

In contrary to the animal and human tissues, where long-chain PFAAs accumulate predominantly (Krafft and Riess, 2015a), short-chain PFAAs are found to be highly bioaccumulative in plants (Ghisi et al., 2019). In general, there is more research on PFAAs bioaccumulation and toxicity in animals than in plants (Yang et al., 2015) and more research on the long- than short - chain PFAAs (Dewitt, 2015). With diet being the main exposure pathway of PFAAs for the general population (Vestergren and Cousins, 2009b), where vegetables are considered as one of the main food categories contributing to PFASs body burden (Felizeter et al., 2014; Herzke et al., 2013), there is a need for better understanding of PFAAs behavior in plants and the effects of the biotic and abiotic factors influencing their plant uptake.

The root uptake from soil has been regarded as the main entry pathway of PFAAs into terrestrial food webs (Krippner et al., 2015; Liu et al., 2019). Considering that PFAAs are in dissociated state under the environmental pH, they are not volatile, so neither the gaseous deposition or volatilization loss are expected to occur (Blaine et al., 2014a; Stahl et al., 2009; Trapp, 2007).

Water is the main reservoir of PFAAs in the environment and the most important media for their transport (McLachlan and Holmstro, 2007; Zareitalabad et al., 2013; Valsecchi et al., 2015). The short-chain PFAAs are especially mobile with water, their affinity for sorption is low (McLachlan et al., 2019; Vierke et al., 2014) and transport from roots to aerial parts with the transpiration stream is considered as their main uptake mechanism (Felizeter et al., 2014). Transpiration occurs mainly

through the leaves, that are found to be the most significant sink for non-volatile chemicals (Trapp, 2009), including PFAAs, in plants. So far, studies about PFAAs plant uptake have researched the root uptake of PFAAs from soil (Blaine et al., 2013, 2014a; Krippner et al., 2015; Stahl et al., 2009; Wen et al., 2014) or hydroponic solution (Felizeter et al., 2014, 2012; Müller et al., 2016). For the crops grown in soil, contamination can be a result of the biosolids amendment (Blaine et al., 2013), addition of the sewage sludge (Bizkarguenaga et al., 2016) or irrigation with the contaminated water (Blaine et al., 2014b; Liu et al., 2017, 2019). PFAAs uptake to plants is affected by many factors and was shown to be concentration dependent, chain length and functional group dependent. It depends on the plant species and variety and also on the growth media (Ghisi et al., 2019).

Some vegetables are successfully cultivated in the hydroponic systems, in that case hydroponic exposure representing the realistic exposure scenario for health risk assessment through the crop consumption. However, most crops are cultivated in soil. Hydroponic studies are also conducted to investigate the contaminants behavior, translocation and phytotoxicity, as they are providing full bioavailability of tested chemical to roots (Felizeter et al., 2012). So far, hydroponic studies (Felizeter et al., 2014, 2012; Müller et al., 2016) have shown a pattern of long-chain PFAAs retention in roots and the transport of short-chain PFAAs upwards to aerial plant compartments (shoots and fruits). However, this root accumulation pattern was not visible in the soil uptake studies, generally uptake being either shifted towards short-chain PFAAs or showing no chain length dependency (Blaine et al., 2014b; Wen et al., 2014). Sorption in soil has a significant impact on the bioavailability of PFAAs in pore water and their uptake to roots, but soil to water partition coefficients have been rarely deducted and reported for the growth media (Blaine et al., 2014b; Gredelj et al., 2019a). A direct comparison of these two exposure conditions is currently lacking from the literature, i.e. there is no PFAAs uptake and translocation study considering a plant exposure to PFAAs both through the soil and the hydroponic solution, for the same plant species.

This work, motivated by the large scale PFAS contamination case of the Veneto region, one of the most agronomically developed Italian and European areas, investigates the exposure of a typical local crop, red chicory (locally known as 'radicchio'), to a mixture of nine PFAAs in a hydroponic experimental setup in a greenhouse, with the goal of better understanding PFAAs uptake and translocation in a condition of total bioavailability to chicory roots. Furthermore, results are compared to those of a recently published experiment that was conducted in the same greenhouse (Gredelj et al., 2019a) (Chapter 3), where red chicory was grown in soil and underwent various treatments with pre-contaminated soil and irrigation water, spiked with a mixture of the same nine PFAAs, to evaluate PFAAs uptake from soil by the red chicory, with a focus on inter-compartmental bioaccumulation. The emerging PFAAs vertical distribution in soil was also characterized, and a series of batch tests for determining soil-water partition coefficients was run (Gredelj et al., 2019a). The comparison of the results of this study and those presented in Chapter 3 provide a formidable occasion to shed light on the role of different exposure media – water and soil – in influencing PFAAs uptake and translocation. So, the study aims are: 1) investigating the bioaccumulation and translocation patterns of PFAAs, present in concentrations of 65.2, 125 and 250 µg/L, into the red chicory roots and shoots under hydroponics conditions; 2) their comparison with the bioaccumulation and translocation of the same PFAAs mixture when red chicory was grown in soil (Gredelj et al., 2019a); and 3) providing additional insights regarding phytotoxicity effects and assessment of their potential influence on PFAA bioaccumulation in chicory compartments.

5.2. Materials and methods

5.2.1. Materials and chemicals

Nine perfluoroalkyl acids (seven carboxylic and two sulfonic acids) were used in this experimental work: perfluorobutanoic acid (PFBA), perfluoropentanoic acid (PFPeA), perfluorohexanoic acid (PFHxA), perfluoroheptanoic acid (PFHpA), perfluorooctanoic acid (PFOA), perfluorononanoic acid (PFNA), perfluorodecanoic acid (PFDA), perfluorobutanesulfonic acid (PFBS) and perfluorooctanesulfonic acid (PFOS). Non-labeled technical quality standards with a purity $\geq 96\%$ were used for all spiking purposes. Materials, reagents and labeled standards used for extraction and analyses, with details and suppliers are provided in Annex 2 (A2-1), with the Supplementary information for Chapter 3.

5.2.2. Experiment set-up

Red chicory plants (*Cichorium inybus* L. var. *foliosum* Hegi), Chioggia type, were grown in a greenhouse in experimental hydroponic system. The greenhouse is located at Agripolis, University of Padova's experimental farm in Legnaro (45°20' N; 11°57' E), Italy and experiment took place from August to September 2018, in a period of 38 days. Plants were pre-grown from seeds in a peat nursing pots until development of 3-4 true leaves (30 days). After pre-growing period, seedlings roots were cleaned with distilled water and plants were transferred in the hydroponic tanks. The hydroponic experiment was performed in parallel with the soil uptake experiment described in Chapter 3 and is corresponding to the hypothetical worst-case scenario where PFAAs are fully bioavailable for the root uptake.

The experimental set-up included three different exposure concentrations of PFAAs mixture and a clean control, every experimental line consisting of triplicate hydroponic tanks (Figure A4-1 in Appendix 4). Each 40 L plastic tank contained four individual plants and 35 L of nutrient solution. Nutrient solutions were spiked with equal concentrations of nine PFAAs, 62.5, 125 and 250 $\mu\text{g/L}$, respectively. The concentrations were chosen with respect to the soil experiment (Chapter 3), so that total PFAAs mass in soil with nominal concentrations of 100 and 200 ng/g corresponds to the mass of PFAAs in the nutrient solution with concentrations of 125 and 250 $\mu\text{g/L}$. Twice as low concentration of 62.5 $\mu\text{g/L}$ was interpolated afterwards, also being in the concentration range of highly contaminated wastewater and groundwater in Veneto Region (ARPAV, 2018b). Total PFAAs exposure concentration was always lower than concentrations previously connected with phytotoxic effects (García-Valcárcel et al., 2014; Qu et al., 2010; Yang et al., 2015).

Apart from the clean control, three tanks without plants, for determining evaporation, were randomly accommodated between the plant-containing tanks. The tanks were filled with 35 L of half-Hoagland's nutrient solution (prepared according to (Felizeter et al., 2012)) and covered by the polystyrene floating board. Each board had four holes drilled for plants accommodation and every plant was fixed with a polypropylene sponge within the hole, in a way that only plant roots are immersed in the solution. After the accommodation of plants for 24h, nutrient solutions were spiked with the adequate quantities of PFAAs stock solution, prepared in MeOH/H₂O in 70/30 (v/v) with nominal concentration of 360 mg/L of every PFAA. More details about preparation of nutrient and spiking solution are given in the Appendix 4, Text A4-1. All hydroponic tanks were randomly placed in a greenhouse area and their places were periodically re-randomized during the experiment. After 38 days, some of the plants started to show signs of bolting, chicory heads did not form and experiment was terminated. Plants were harvested, split into roots and shoots, washed with distilled water and stored in a sealed plastic bags at -20°C until the extraction. Composite samples of four plants per tank were always prepared (unless some of the plants were dead, and they were then

excluded from sampling), for every replicate hydroponic tank. Nutrient solution was sampled from each tank after initial spiking and weekly, each time before adding water for compensation of the evapotranspiration losses. Nutrient solution samples were stored in plastic polypropylene vials at 4°C until the analyses.

5.2.3. Chemical analyses of chicory tissues and nutrient solution

The extraction of chicory roots and leaves was carried out according to (Mazzoni et al., 2016), with a few minor modifications, as already described in Chapter 3. Plant samples were prepared based on a sonication - assisted extraction of homogenized samples with acetonitrile. All plant extracts were analyzed by UHPLC-MS/MS (TSQ Quantum™ Access MAX, Thermo Scientific, USA) equipped with a Waters Acquity UPLC BEH C18 column (50x2.1 mm id, 1.7 µm particle size) by direct injection after acidification with formic acid and addition of Isotope Labelled Internal Standard mixture. The nutrient solution samples were analyzed with an HPLC LC-30AD XR Shimadzu coupled with an API 6500 AB Sciex triple quadrupole and with a CTC PAL HTS XT autosampler, equipped with Phenomenex Kinetex Evo C18 (1.7 µm x 2.1 mm x 100 mm) column for water analyses. Nutrient solution samples were directly injected after appropriate dilutions. Details on both analytical methods and instruments settings are reported in Annex 2 (A2-2), with the Supplementary information for Chapter 3.

5.2.4. Plant parameters

Plants transpiration was determined based on weighing and it was always calculated as the total transpired volume per hydroponic tank (i.e. four plants). The tanks were weighed on a weekly basis, with and without the plants-containing floating board and before and after the compensation of evapotranspiration losses. In this way, it was possible to track evaporation (from no-plant tanks), plants mass or growth and to calculate transpiration volumes through mass loss of water. PFAAs loss with volatilization was not expected, considering they are in ionic state under measured pH of the nutrient solution (6.9). The relative chlorophyll content was measured from second week of growth by chlorophyll meter (Minolta SPAD-502, Konica-Minolta, Japan), providing a non-destructive determination of relative chlorophyll content in leaves (Ling et al., 2011). Additionally, root length and number of developed true leaves were determined as the simple plant growth and development indexes.

5.2.5. Quality control and data analyses

All materials containing perfluoroalkyl substances (e.g. Teflon®) were avoided during the experimental phase to minimize risk of contamination. Glassware was avoided as well, knowing that some PFAAs can irreversibly bind to the glass surfaces (F. Li et al., 2018). All results are reported as means of the three values. Mass recoveries of total PFAAs were determined for every hydroponic tank as the ratio of PFAAs mass in plants and remaining nutrient solution opposed to the initial mass delivered by spiking. Analytical QA/QC with details on the calibration curves, internal standards, LODs, solvent blanks, and recoveries are reported in Annex 2 (A2-1), with the Supplementary information for Chapter 3.

A bioaccumulation and translocation of PFAAs were evaluated by root concentration factor (RCF), shoots concentration factor (SCF) and shoots to roots transfer factor (TF), defined as follows (Felizeter et al., 2012; Trapp, 2000):

$$RCF = \frac{C_{roots}(PFAA)}{C_{sol}(PFAA)} \quad (5-1)$$

$$SCF = \frac{C_{shoots}(PFAA)}{C_{sol}(PFAA)} \quad (5-2)$$

$$TF = \frac{C_{shoots}(PFAA)}{C_{roots}(PFAA)} \quad (5-3)$$

where $C_{roots}(PFAA)$ is the PFAA concentration in roots (ng/g_{fw}), $C_{sol}(PFAA)$ is the concentration of PFAA in the nutrient solution (ng/L), while $C_{shoots}(PFAA)$ is the concentration of PFAA in shoots (ng/g_{fw}).

Translocation of chemicals from roots to shoots by xylem (transpiration water) can be described by the transpiration stream concentration factor (TSCF), defined as the ratio between the concentration in xylem sap and concentration in the nutrient solution (or the soil pore water) (Dettenmaier et al., 2009; Trapp, 2000; Trapp and Matthies, 1995). Since the concentration in xylem is hard to measure, TSCF can be calculated from the measured data:

$$TSCF = \frac{C_{shoots}(PFAA) \times m_{shoots}}{C_{sol}(PFAA) \times V_{trans}} \quad (5-4)$$

where m_{shoots} represents a mass of shoots (g_{fw}) and V_{trans} a volume of the transpired water (L). This empirical equation considers no loss through volatilization of degradation of chemicals, a valid assumption when it comes to PFAAs (Krafft and Riess, 2015a), and also no transport back to roots by phloem (Trapp, 2000).

The data are always shown as means of experimental replicates with standard error estimates. The independent samples t-tests were performed to determine the significant differences between growth and developmental indexes (as defined in the Chapter 2.4.) in the control and exposure treatments. Shapiro-Wilk was used for testing the data normality and Levene's test for homogeneity of variance. One-way ANOVA with Tukey-HSD post-hoc test was used for comparison of the bioaccumulation factors, transfer factors and transpiration stream concentration factors between treatments. In the case of non-homogeneity of variance, Welch's ANOVA with Games-Howell post-hoc test was used instead. Regression analyses between PFAA perfluoroalkyl chain length and bioaccumulation and transfer factors were performed as well. The differences were considered as significant for $p < 0.05$. Statistical tests were performed by SPSS Statistics, IBM statistical software.

5.2.6. Comparison with the soil experiment

Root concentration factors from this experiment are compared with root concentration factors from the soil experiment (Chapter 3). For this purpose, RCFs derived on soil-concentration basis were normalized to pore water PFAA concentrations. A pore water concentration for each PFAA, C_{pw} (ng/L), was calculated as in (Gredelj et al., 2019b) (Chapter 4):

$$c_{pw} = \frac{c_0}{K_d + \frac{w}{\rho_{H_2O}}} \quad (5-5)$$

where C_0 was measured soil concentration, determined for the dry soil (ng/g_{dw}), w was the gravimetric water content in soil, K_d (L/kg) is the soil-water partition coefficient and ρ_{H_2O} (kg/L) is the density of water (Chapters 3 and 4). RCFs based on pore water concentration were then calculated according to equation (5-1), but with c_{pw} in the denominator.

In the hydroponic experiment of (Müller et al., 2016), it has been found that equilibrium between the nutrient solution and roots, for PFCAs from 3CF_x to 9CF_x and PFBS and PFOS, establishes in the roots of *Arabidopsis* within 5 days period. Equilibration of roots and pore water is expected to some extent in the soil experiment within the growing period of 87 days, as stated in (Gredelj et al., 2019a) (Chapter 3). Hence, the corresponding RCFs should not be influenced by different exposure times. It has been shown in Chapter 4 that the steady-state between the pore water and shoots will not be reached with the constant transpiration and PFAAs exposure. A different exposure times (i.e. 38 days for the hydroponic and 87 for the soil experiment) and consequent differences in total transpired volumes are thus making shoots concentration factors incomparable. Accordingly, transfer factors are not directly comparable in their magnitude either, but were used to compare PFAAs translocation patterns with the chain length. However, TSCFs can be directly compared, because TSCF accounts for the volume of transpired water at harvest, when also concentrations in shoots have been measured. For the soil-grown chicory, TSCFs were calculated by using equation (5-4), after replacing the C_{sol} (PFAA) with the C_{pw}.

5.3. Results and discussion

5.3.1. Plants growth and phytotoxic effects

The treatment concentrations were carefully chosen with respect to published studies and so far reported phytotoxicity concentration thresholds. For example, PFOS was found to be toxic to wheat seedlings up from the nutrient solution concentration of 10 mg/L in the study of (Qu et al., 2010), PFOA was found to be toxic to *Arabidopsis* from the concentration of 75 mg/L in the study of (Yang et al., 2015). The mixture of 6 PFAAs (PFBA, PFBS, PFHxA, PFHxS, PFOS and PFDA) was found to effect the growth of grass (*B. diandrus*) when each of them was present in the concentration of 1000 µg/L, according to the hydroponic study of (García-Valcárcel et al., 2014). The PFAAs mixture with total concentration of 4.64 mg/L in the nutrient solution impacted the enzymatic activities of roots and shoots of common rush (*Juncus effusus*), but did not manifest any growth related issues or visual damage to plants even in the concentrations 10 times as high as the total 4.64 mg/L (Zhang et al., 2019). The highest exposure concentration in this study resulted with total PFAAs concentration of 2.25 mg/L. However, plants from the treatments with nominal PFAA concentrations of 125 µg/L and 250 µg/L started to show signs of physiological damage from the second week of growth. They were noticeable as the leaves yellowing, delay in growth with respect to the control and browning of the root systems (as shown in Figure A4-6, Annex 4). Initially, it was not the aim of the study to investigate the toxic effects in plants, but after they were recognized, additional parameters as the relative chlorophyll content, roots length and leaves count started to be measured on a weekly basis. Series of independent samples t-tests was performed for every growth and development index, opposed to the corresponding measurement of the control for the same date. Results are shown on Figure 5-1, together with the significant p-values.

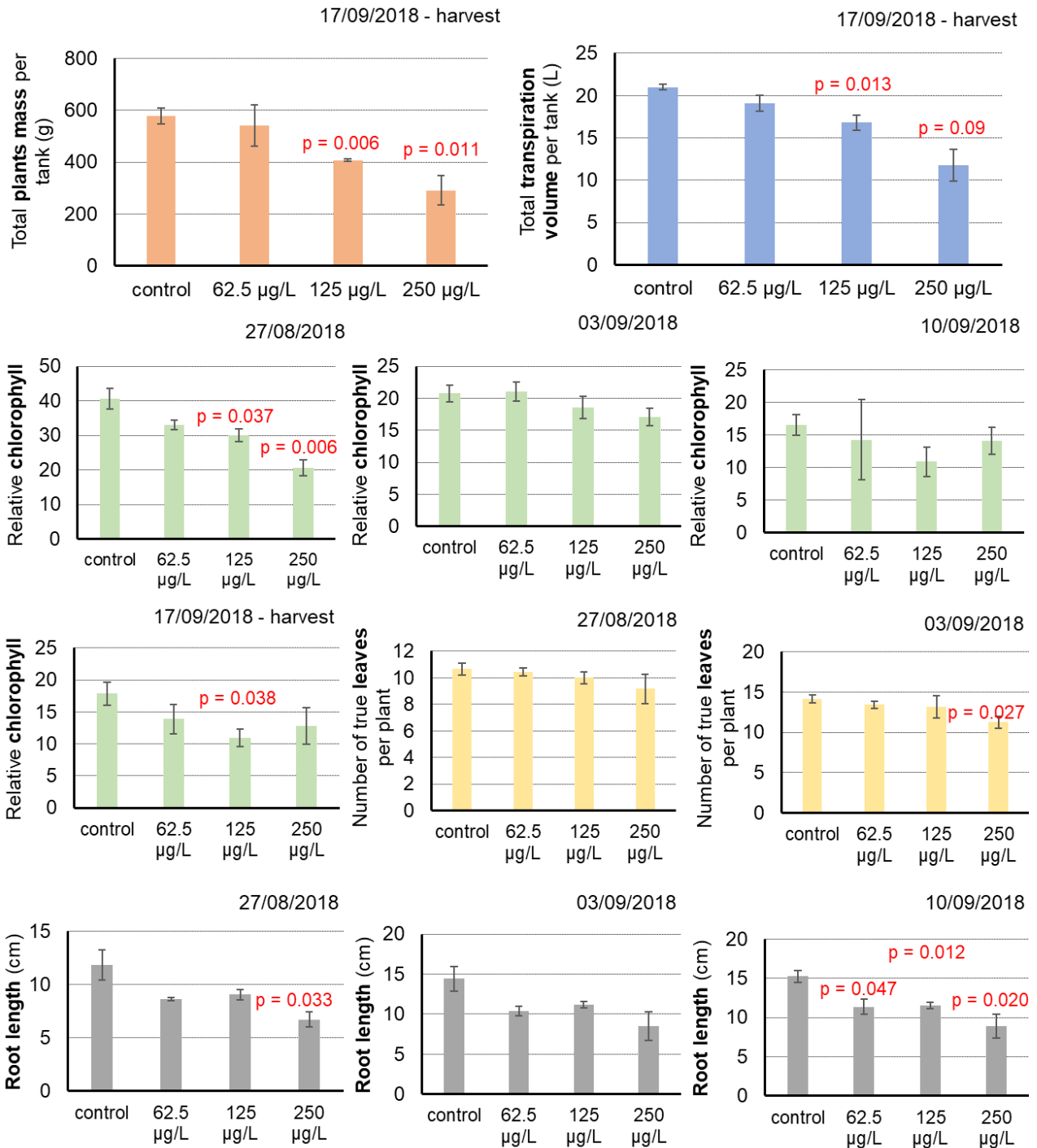


Figure 5-1. Measured growth and developmental parameters per treatments and measuring dates. Results are shown as means (n = 3) with standard error estimates. Results of statistically significant differences with control are indicated by the p-values.

Total plant growth and transpired volume were statistically significantly different from the control for treatments 125 and 250 µg/L. Transpiration volume was very well correlated with plants mass (Pearson's $r = 0.939$, $p = 0.000018$), as plant growth directly (and linearly) depends on the plant transpiration (Arkley, 1963). For these two treatments, statistical differences from the control were detected (for some dates) in the relative chlorophyll content, number of true leaves and root length. Towards the end of experiment, significantly shorter roots were detected also for the treatment with nominal concentrations of 62.5 µg/L, but it was never the case with other growth and developmental indexes. The concentration of 125 µg/L of each PFAA (1.13 mg/L of the total PFAAs) was the lowest

exposure concentration of PFAAs causing a visible damage and it was the lowest concentration of PFAAs connected with the phytotoxic effects in terrestrial plants, when compared to literature (García-Valcárcel et al., 2014; Qu et al., 2010; Yang et al., 2015; Zhang et al., 2019). It indicates that the red chicory may be more sensitive to the toxic effects of PFAAs and further research regarding the oxidative stress and enzymatic parameters (even in the lower exposure concentrations) would be useful.

5.3.2. PFAAs uptake, bioaccumulation and translocation

5.3.2.1. Measured concentrations in roots and shoots

Concentrations of PFAAs in roots and shoots of red chicory for all the treatments are shown on Figure 5-2. The highest concentrations were detected in roots, up to 23 $\mu\text{g/g}_{\text{fw}}$ for PFDA in the treatment with the nominal concentration of 250 $\mu\text{g/L}$, and were always decreasing with the chain length decrease, being only about 0.4 $\mu\text{g/g}_{\text{fw}}$ for the shortest PFAAs in the same treatment (PFBA, PFPeA and PFHxA). The opposite chain length dependency was present for shoots, concentrations increasing with the chain length decrease, reaching 1.7 $\mu\text{g/g}_{\text{fw}}$ for PFBA in the treatment with 250 $\mu\text{g/L}$ nominal concentration, always being lowest for PFOS, i.e. 0.6 $\mu\text{g/g}_{\text{fw}}$ in the same treatment. Chain length dependency, both in roots and shoots, was in accordance with other previously published hydroponic uptake studies, performed with different plant species (Felizeter et al., 2014, 2012; García-Valcárcel et al., 2014; Zhang et al., 2019; Zhao et al., 2019).

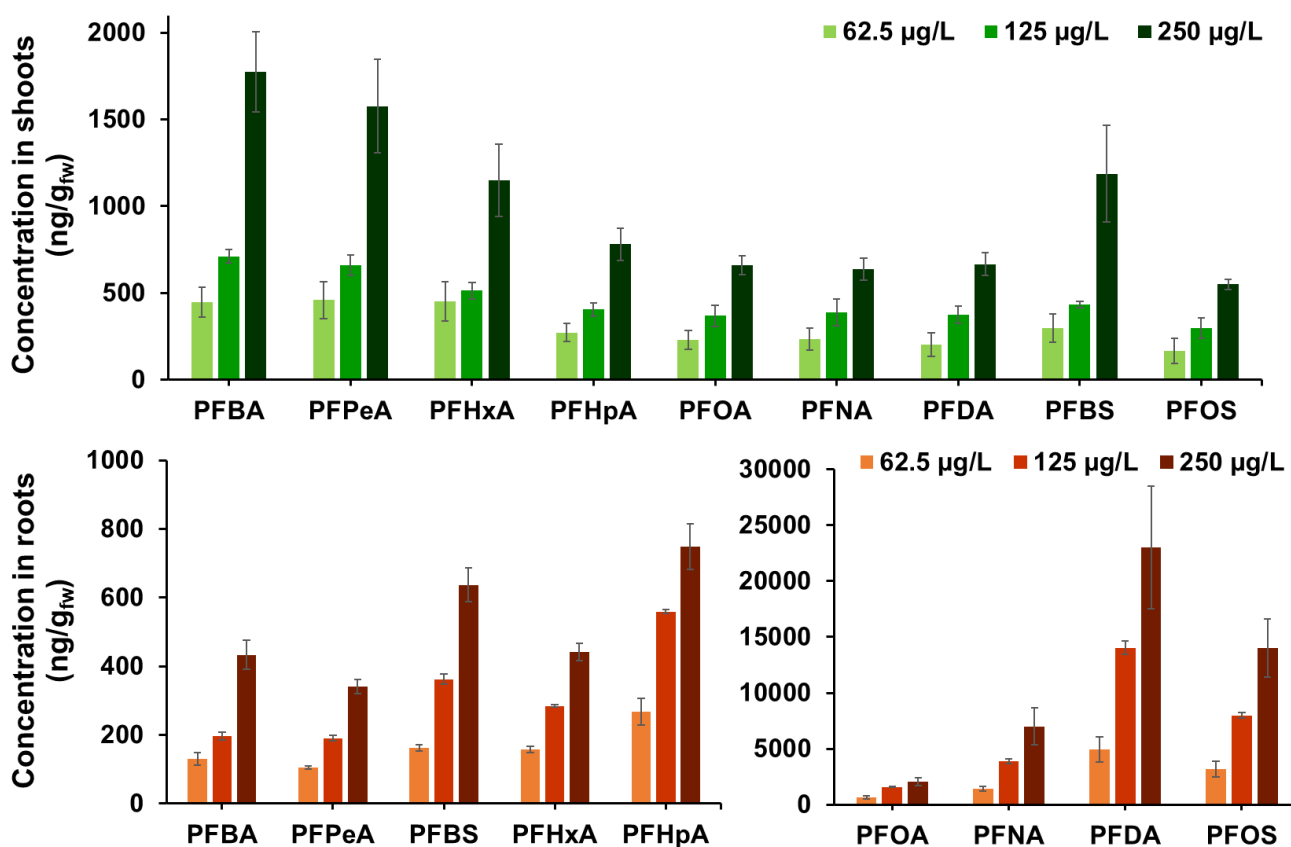


Figure 5-2. PFAA concentrations in shoots (top) and roots (bottom) in all the treatments. Error bars represent standard error estimates (n = 3).

5.3.2.2. **Bioconcentration and transfer factors**

Shoots concentration factors and shoots to roots transfer factors were not statistically different between treatments for any PFAA, implying that the PFAA bioaccumulation efficiency was not influenced by the chicory plants damage and/or concentration increase. This is in agreement with the constant transpiration coefficient of 39 L/kg_{fw} (as the ratio of the transpired water and plant biomass) and with the hypothesis of passive transport of PFAAs from roots to shoots via transpiration stream (Dettenmaier et al., 2009; Felizeter et al., 2014, 2012). As concluded by (Felizeter et al., 2012), the magnitude of PFAA root concentration factor is not only influenced by uptake into the root tissue, but also by adsorption to the root surface. Considering there were no statistical differences among treatments for RCFs as well, root damage seemingly did not affect external root sorption and uptake of PFAAs into roots. Non-linear sorption to roots, manifested as the RCFs decrease with the increase of PFAA concentration in the nutrient solution, was observed in some experiments (Felizeter et al., 2012; Müller et al., 2016). However, their highest concentrations as the ones introducing non-linearity, were lower than any of the treatments presented here, 10 µg/L (Felizeter et al., 2012) and 20 µg/L (Müller et al., 2016), respectively. Bioconcentration and transfer factors were calculated as average of the treatments, considering their independence of the exposure concentrations or plants damage, and as such, plotted against PFAA's perfluoroalkyl chain length (Figure 5-3, Table A4-6). When logarithmically transformed, RCFs, SCFs and TFs were well correlated with the perfluoroalkyl chain length of PFCAs, as shown in Figure 5-3.

Differences between BCFs and TFs of different PFAAs were assessed by one-way ANOVA (Welch's test, considering the non-homogeneity of variance indicated by Levene's test) with the Games-Howell post-hoc test. RCFs of all PFAAs were statistically significantly different ($p < 0.05$), but the RCFs of the shortest PFCAs (PFBA, PFPeA, PFHxA). Long chain PFAAs and PFHpA had very similar SCFs, statistically significantly different only from SCFs of PFBA and PFPeA. TFs of PFBA and PFPeA were not statistically significantly different, but were always statistically different to all other PFAAs. Similar to SCFs, TFs were never statistically significantly different among the PFOS, PFNA and PFDA.

When compared to results of other hydroponic studies, performed with other plant species, red chicory RCFs were in general in the same order of magnitude with lettuce from (Felizeter et al., 2012) and cabbage, zucchini and tomato from the (Felizeter et al., 2014) (Figure A4-2). However, RCF of PFNA was always about two times as low as the PFNA RCFs determined in lettuce, cabbage, zucchini and tomato. Compared to lettuce, as the most similar among the vegetables tested, RCF of PFDA was more than 2 times as low in chicory. When plotted with the increasing chain length of PFCAs, SCFs for *Arabidopsis* (Müller et al., 2016) and for lettuce (Felizeter et al., 2012) have shown the U-shaped behavior, reaching the minimum for PFHxA and further increasing from PFOA to PFDA. Here, this trend is less pronounced, SCFs reaching a minimum for PFOA, PFNA and PFDA and having almost equal SCFs for this PFAAs. The difference between these two studies and this work are the nominal exposure concentrations that were much lower, from 10 ng/L to 10 µg/L in lettuce study (Felizeter et al., 2012) and 2 µg/L in *Arabidopsis* (Müller et al., 2016). Felizeter et al. did not elaborate their SCFs, but rather TFs and TSCFs (Felizeter et al., 2012). However, they provided measured concentrations of PFAAs in lettuce shoots and nutrient solution, so they were calculated here for comparison purposes (Felizeter et al., 2012). Their study is not only convenient for the comparison with chicory because of the compartmental similarity of tested vegetables, but because of the almost equal exposure duration (40 days for lettuce and 38 days for chicory). Their lowest exposure concentration of 10 ng/L yielded the highest SCFs, between 2 and 8 times as high as for other (higher) exposure concentrations. By eliminating this concentration point, SCFs have shown less pronounced U-shape and are rather lower (Felizeter et al., 2012). It seems that the

exposure concentration magnitude affects the PFAAs uptake trend into shoots (already shown for roots in (Felizeter et al., 2012; Müller et al., 2016), as elaborated above). It could be that the concentration increase had introduced non-selectivity of the shoots bioaccumulation for long chain PFCAs, noticed here in all the treatments.

TF factors are the ratio between the concentration in shoots and concentration in roots. As such, they will account for the fraction of PFAAs externally sorbed to roots, being particularly important for long chain PFAAs (Felizeter et al., 2012; Müller et al., 2016). TF larger than one indicates higher content of chemical bioaccumulated in shoots with respect to roots. Here, this was the case for PFBA, PFPeA, PFHxA and PFBS. Transfer factor was the highest for PFPeA, as PFPeA accumulated slightly less in roots than PFBA (Figure 5-3). In lettuce, TFs higher than one were calculated only for PFBA and PFPeA (Felizeter et al., 2012). In the study of (Zhao et al., 2019), TFs for pumpkin were < 1 for all the PFAAs, but the exposure time was only 12 days, and the origin of all PFAAs was biotransformation of 6:2 fluorotelomer sulfonic acid. Almost the same values of TFs, with very similar trend were reported by (Krippner et al., 2014b) in wheat, after only 5 days of uptake, but with a similar nominal concentration in the nutrient solution of 100 $\mu\text{g/L}$ per each PFAA.

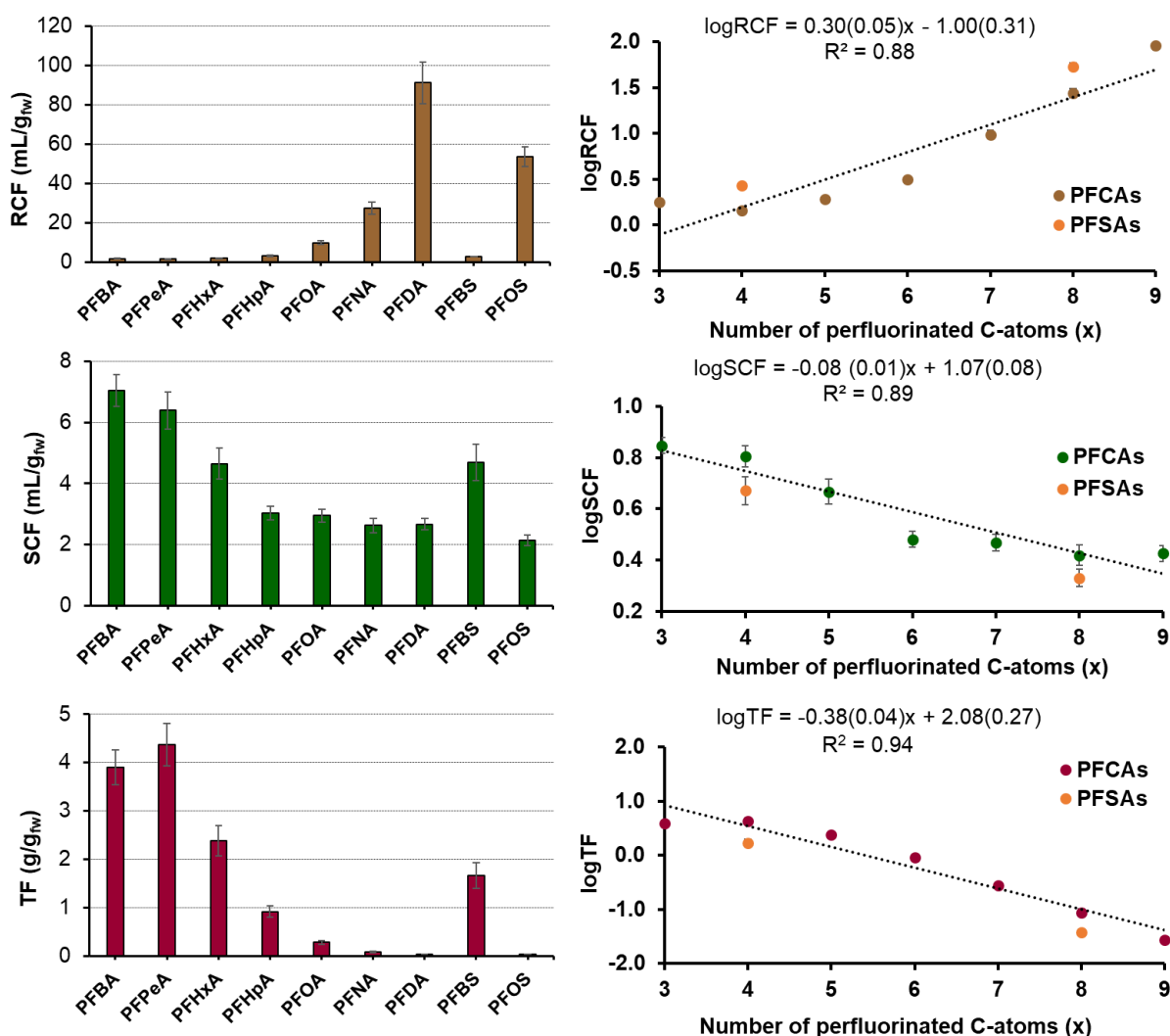


Figure 5-3. Roots and shoots concentration factors and shoots to roots transfer factors for all PFAA (left). Correlations between logRCF, logSCF, logTF and number of C-atoms of PFCAs' perfluoroalkyl chain for the average values of all treatments (right). Regression lines with slopes, intercepts and associated standard errors in brackets are shown. The error bars represent standard error estimates (n = 3).

5.3.2.3. Transpiration stream concentration factor

For all the PFAAs, transpiration stream concentration factors were always lower than 1 (Figure 5-4), indicating that the transport upwards was passive and lower than the transport of water (TSCF = 1) (Dettenmaier et al., 2009), as already hypothesized by (Felizeter et al., 2012) for PFAAs in lettuce. When compared amongst treatments, TSCFs were statistically different (higher) only for PFDA in treatment with nominal concentration of 62.5 µg/L, when compared to both treatments with higher exposure concentrations. Even when not statistically different, TSCFs of the least contaminated treatment, and only one where plants did not manifest visible toxic effects, were always higher than in the treatments with the nominal concentrations of 125 and 250 µg/L (Figure 5-4).

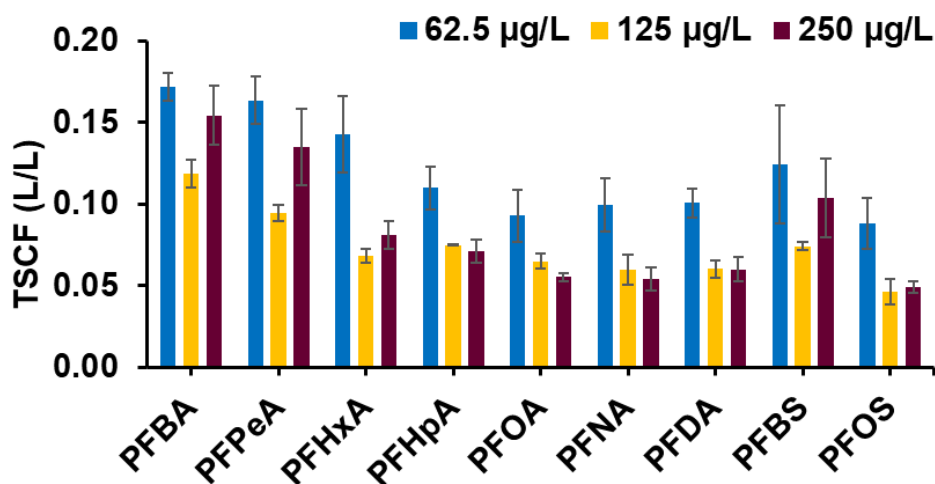


Figure 5-4. Transpiration stream concentration factors for all treatments per PFAA. The error bars represent standard error estimates ($n = 3$, except for the treatment with 62.5 µg/L exposure concentration where $n = 2$).

In treatments with nominal concentrations of 125 and 250 µg/L, roots were affected by PFAAs and manifested negative physiological changes that were visually observed (as the roots browning and changes of the root appearance, Figure A4-6) and through the significant root length decrease in comparison with the control. Considering PFAAs affinity for interfaces and surfactant nature, as already hypothesized by (Qu et al., 2010) for PFOS, in high concentrations PFOS can damage the root cell membranes and increase the root permeability. According to (Dettenmaier et al., 2009), adding the chemical in a toxic concentration level causes the apparent loss of root membrane integrity, leading to quick increase of the chemical in xylem, followed by the increase of TSCFs. Here, increase in TSCFs can be noticed with increase of the nominal concentrations from 125 to 250 µg/L for short chain PFAAs, even though TSCFs were not statistically different among treatments while evaluated by ANOVA. Short-chain PFAAs are the most efficiently transported PFAAs within the plant, their molecules are smaller and their hydrophobicity is lower, so their possibility to cross membranes is higher (Müller et al., 2016). The long chain PFAAs could have affected the increased transport of short chain PFAAs to shoots by increasing the permeability of the root membrane when their concentration was high enough (e.g. as hypothesized by (Qu et al., 2010) for PFOS concentrations ≤ 1 mg/L).

When assessed by one-way ANOVA (Welch's test) with the Games-Howell post-hoc test, TSCFs of short chain PFAAs (PFBA, PFPeA, PFHxA and PFBS) were not statistically significantly different from each other. Similarly, the long chain PFAAs (PFOS, PFOA, PFNA, and PFDA) were never statistically different among each other, but were always statistically different from PFBA and PFPeA.

The TSCFs of PFAAs, reported for lettuce (Felizeter et al., 2012), were generally in the similar magnitude, but for PFBA, for which they were much higher (0.8 L/L as opposed to the chicory treatments average TSCF of 0.15 L/L). TSCFs in cabbage and tomato were of the similar magnitude as in chicory, while zucchini showed the constant TSCFs across the different PFAAs, but in the lower magnitude (max 0.09 L/L for PFNA and not for the short chain PFAA) (Felizeter et al., 2014). The TSCFs here did not show pronounced U-shaped distribution with the chain length increase, as for the lettuce (and tomato and cabbage, but in a smaller extent) (Felizeter et al., 2014, 2012) (Figure A4-2), probably as the consequence of much higher treatment concentrations, as already explained on the basis of SCFs results in Paragraph 5.3.2.2.

5.3.3. Uptake in hydroponics vs. uptake from soil

The uptake and translocation of PFAAs from the hydroponic solution and from the soil (Chapter 3) were compared based on RCFs and TSCFs. For the soil experiment, RCFs and TSCFs were calculated separately for a different delivery media (soil and water) (Figure 5-5).

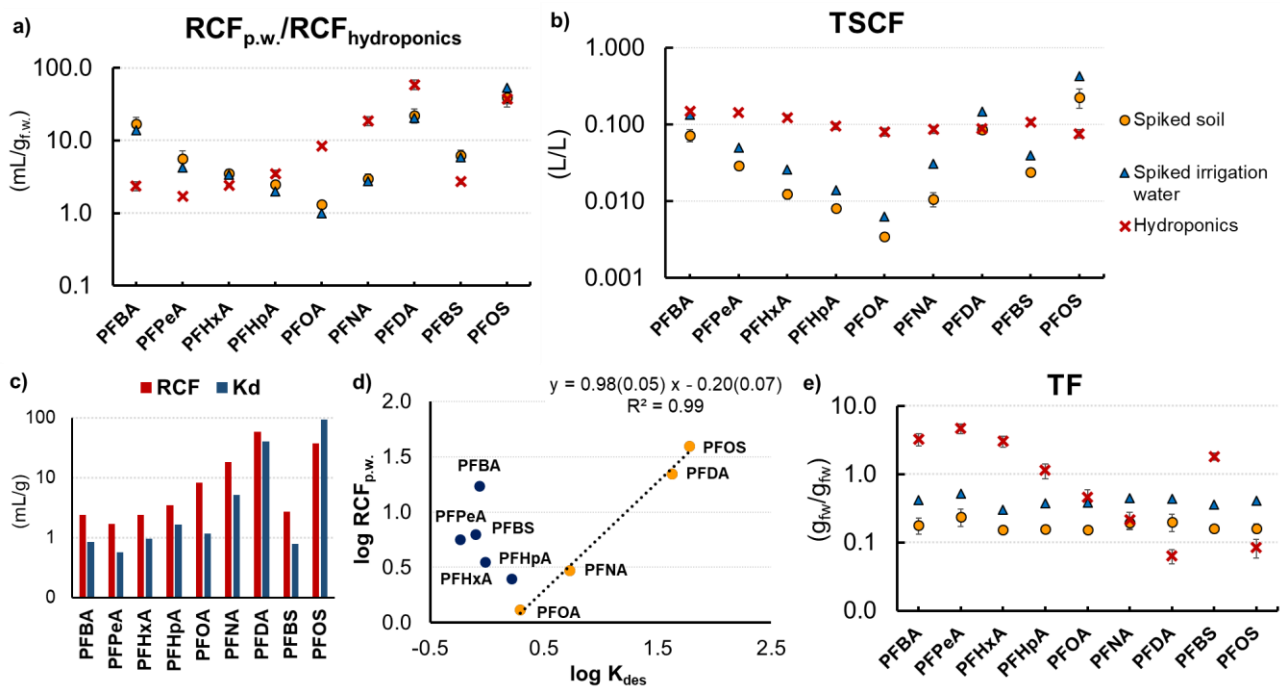


Figure 5-5. Comparison of the hydroponics and soil experiment (PFAAs delivered by irrigation water or pre-contaminated soil): a) roots concentration factors, b) transpiration stream concentration factors, c) sorption of roots (RCFs) vs. sorption to soil (K_d), d) dependency of pore water based RCFs and soil-water partitioning, e) shoots to roots transfer factors. Where shown, error bars represent the standard error estimates.

It can be clearly seen that root concentration factors differ between hydroponically grown chicory and the ones grown in soil, not only in their magnitude, but also in chain length dependency. As already stated in Chapter 3 (Gredelj et al., 2019a), root systems develop differently in the soil and in the nutrient solution. What was previously noticed by (Trapp, 2007), was also noticed here: fine roots were well produced in soil, but not in the hydroponic solution. Root system in soil was heavily branched, while this was not the case in hydroponics, subsequently resulting in higher surface area in soil. Roots development does not only affect RCFs, but also TSCFs as the measure of contaminants uptake efficiency by the transpiration water (Trapp, 2007). Trapp has found that the uptake of polar compounds depends, among other factors like transpiration stream, of the root surface, roots mass and membrane permeability (Trapp, 2007). For PFAAs, as the ionic surfactants, we have already hypothesized about their retention on the membranes of root epidermis, as described in Chapter 4. TSCFs derived from the soil experiment resulted with U-shape pattern when

plotted against the increasing chain length of PFCAs, as reported in hydroponically grown lettuce (Felizeter et al., 2012) and lettuce grown in biosolids amended soil (Blaine et al., 2013). Here, the exposure concentrations in hydroponics were much higher, as previously stated, and were also much higher than the pore water concentrations of long-chain PFAAs (i.e. between 1 and 6 µg/L for PFOS and PFDA). Almost constant TSCFs resulting from hydroponics, when compared to the TSCFs from soil, could also be from the negative influence of long chain PFAAs on the membrane integrity, noticed by (Qu et al., 2010) and as explained in the Paragraph 5.3.2.3. It is important to notice that the magnitude difference among TSCFs from hydroponics and from the soil experiment is not simply a consequence of differences in transpiration coefficient, as they were very similar (between 36 and 39 L/kg in hydroponics and between 32 and 40 L/kg, as calculated for the different plants). The other influential factor could be the competition between PFAAs in hydroponics, particularly among the highly sorbing long chain PFAAs. In the column experiment with soil, performed with PFAAs mixture, (Gellrich et al., 2012), have noticed the capability of long chain PFAAs to displace short chain PFAAs from their sorption sites. In the soil experiment with chicory, soil and root surface provide much more sorption sites than available in hydroponics, which could have resulted with the competitive sorption of PFAAs to the root surface in hydroponics (Figure 5.a). This could be seen as an increase of RCFs along the chain length and consequently in decreasing relationship of TFs with the chain length in hydroponics, as opposed to soil. When comparing the magnitude of PFAAs soil sorption with the sorption to roots (as seen on Figure 5-5.c)), PFAAs seem to sorb more to roots (fresh weight) than to dry soil. The only exception is PFOS, with the preferential sorption to soil. When RCFs are normalized to roots dry weight and K_{ds} to soil organic matter content (2.46%) (Gredelj et al., 2019a), there is an almost no difference in sorption for short chain PFAAs. The sorption of PFDA and PFOS to organic matter in soil is 10 times as high as in the roots (Table A4-5, Appendix 4), in contrary to PFOA and PFNA that sorbed strongly to the roots (e.g. as twice as high for PFOA). Hence, even when present in pore water in fairly low concentrations, PFAAs with strong affinity for the organic matter, PFDA and PFOS, will still strongly sorb also to the roots surface, which can be seen as the increase in RCF_{pw} of these compounds (Figure 5-5 a)). As shown in Figure 5-5 d), while RCF_{pw} s of short chain PFAAs do not depend on the K_{ds} (they are low, around 1), they are strongly correlated with the sorption coefficients of long-chain PFAAs.

5.4. Conclusions

This study confirms the chain length dependency patterns for PFAAs, when uptaken into roots and subsequently translocated to shoots from the nutrient solution. Long chain PFAAs were mostly retained by the surface sorption to roots, while short chain PFAAs were transported to shoots via the transpiration stream. In the given experimental set-up, PFAAs induced visible phytotoxic effects in the red chicory, in concentrations that were the lowest among so far reported in the literature. The mixture of PFAAs have caused growth inhibition of the chicory plants in two higher exposure concentrations (125 and 250 µg/L), also showing the visible root damage and yellowing of the leaves (i.e. lowering of the relative chlorophyll content). A potential increase in the root permeability under a high PFAA exposure concentration range in hydroponics was hypothesized as the reason for an almost constant TSCFs amongst PFAAs when compared to the soil experiment and also to other scientific findings resulting from the lower exposure (both through soil and nutrient solution). Additionally, developmental differences between the root systems formed in the soil and the nutrient solution, with competitive PFAAs sorption to roots in hydroponics, could be the main reasons of differences in the root concentration factors and also partially in the TSCFs. Consequently, direct extrapolation of hydroponically derived bioaccumulation and translocation factors for the human health risk assessment via dietary exposure from the agronomic ecosystems is questionable, as the PFAAs behavior very much defers when compared to soil.

5.5. References

- Arkley, R.J., 1963. Relationships between plant growth and transpiration. *Hilgardia* 34, 559–584. <https://doi.org/10.3733/hilg.v34n13p559>
- ARPAV, 2018. Concentrations of the Perfluoroalkyl substances in the waters of Veneto region, Open data on PFASs monitoring, from 02/07/2013 to 20/09/2018 [WWW Document]. URL <http://www.arpa.veneto.it/dati-ambientali/open-data/idrosfera/concentrazione-di-sostanze-perfluoroalchiliche-pfas-nelle-acque-prelevate-da-arpav> (accessed 11.25.18).
- Bizkarguenaga, E., Zabaleta, I., Mijangos, L., Iparraguirre, A., Fernández, L.A., Prieto, A., Zuloaga, O., 2016. Uptake of perfluorooctanoic acid, perfluorooctane sulfonate and perfluorooctane sulfonamide by carrot and lettuce from compost amended soil. *Sci. Total Environ.* <https://doi.org/10.1016/j.scitotenv.2016.07.010>
- Blaine, A.C., Rich, C.D., Hundal, L.S., Lau, C., Mills, M.A., Harris, K.M., Higgins, C.P., 2013. Uptake of perfluoroalkyl acids into edible crops via land applied biosolids: Field and greenhouse studies. *Environ. Sci. Technol.* 47, 14062–14069. <https://doi.org/10.1021/es403094q>
- Blaine, A.C., Rich, C.D., Sedlacko, E.M., Hundal, L.S., Kumar, K., Lau, C., Mills, M.A., Harris, K.M., Higgins, C.P., 2014a. Perfluoroalkyl acid distribution in various plant compartments of edible crops grown in biosolids-amended soils. *Environ. Sci. Technol.* 48, 7858–7865. <https://doi.org/10.1021/es500016s>
- Blaine, A.C., Rich, C.D., Sedlacko, E.M., Hyland, K.C., Stushnoff, C., Dickenson, E.R. V., Higgins, C.P., 2014b. Perfluoroalkyl Acid Uptake in Lettuce (*Lactuca sativa*) and Strawberry (*Fragaria ananassa*) Irrigated with Reclaimed Water. *Environ. Sci. Technol.* 48, 14361–14368. <https://doi.org/10.1021/es504150h>
- Brendel, S., Fetter, É., Staude, C., Vierke, L., Biegel-Engler, A., 2018. Short-chain perfluoroalkyl acids: environmental concerns and a regulatory strategy under REACH. *Environ. Sci. Eur.* 30, 9. <https://doi.org/10.1186/s12302-018-0134-4>
- Buck, R.C., Franklin, J., Berger, U., Conder, J.M., Cousins, I.T., de Voogt, P., Jensen, A.A., Kannan, K., Mabury, S.A., van Leeuwen, S.P., 2011. Perfluoroalkyl and polyfluoroalkyl substances in the environment: Terminology, classification, and origins. *Integr. Environ. Assess. Manag.* 7, 513–541. <https://doi.org/10.1002/ieam.258>
- Cheng, W., Ng, C.A., 2018. Predicting Relative Protein Affinity of Novel Per- and Polyfluoroalkyl Substances (PFASs) by An Efficient Molecular Dynamics Approach. *Environ. Sci. Technol.* 52, 7972–7980. <https://doi.org/10.1021/acs.est.8b01268>
- Cousins, I.T., Goldenman, G., Herzke, D., Lohmann, R., Miller, M., Ng, C.A., Patton, S., Scheringer, M., Trier, X., Vierke, L., Wang, Z., DeWitt, J.C., 2019. The concept of essential use for determining when uses of PFASs can be phased out. *Environ. Sci. Process. Impacts.* <https://doi.org/10.1039/c9em00163h>
- Cousins, I.T., Vestergren, R., Wang, Z., Scheringer, M., McLachlan, M.S., 2016. The precautionary principle and chemicals management: The example of perfluoroalkyl acids in groundwater. *Environ. Int.* 94, 331–340. <https://doi.org/10.1016/j.envint.2016.04.044>
- Dettenmaier, E.M., Doucette, W.J., Bugbee, B., 2009. Chemical hydrophobicity and uptake by plant roots. *Environ. Sci. Technol.* 43, 324–329. <https://doi.org/10.1021/es801751x>

- Dewitt, J.C., 2015. Toxicological Effects of Perfluoroalkyl and Polyfluoroalkyl Substances, Molecular and Integrative Toxicology. Springer International Publishing, Cham. <https://doi.org/10.1007/978-3-319-15518-0>
- Eschauzier, C., Raat, K.J., Stuyfzand, P.J., Voogt, P. De, 2013. Perfluorinated alkylated acids in groundwater and drinking water: Identification, origin and mobility. *Sci. Total Environ.* 460, 477–485. <https://doi.org/10.1016/j.scitotenv.2013.04.066>
- Felizeter, S., McLachlan, M.S., De Voogt, P., 2014a. Root uptake and translocation of perfluorinated alkyl acids by three hydroponically grown crops. *J. Agric. Food Chem.* 62, 3334–3342. <https://doi.org/10.1021/jf500674j>
- Felizeter, S., McLachlan, M.S., De Voogt, P., 2014b. Root uptake and translocation of perfluorinated alkyl acids by three hydroponically grown crops_supp. *J. Agric. Food Chem.* 62, 3334–3342. <https://doi.org/10.15713/ins.mmj.3>
- Felizeter, S., McLachlan, M.S., De Voogt, P., 2012. Uptake of perfluorinated alkyl acids by hydroponically grown lettuce (*Lactuca sativa*). *Environ. Sci. Technol.* 46, 11735–11743. <https://doi.org/10.1021/es302398u>
- García-Valcárcel, A.I., Molero, E., Escorial, M.C., Chueca, M.C., Tadeo, J.L., 2014. Uptake of perfluorinated compounds by plants grown in nutrient solution. *Sci. Total Environ.* 472, 20–26. <https://doi.org/10.1016/j.scitotenv.2013.10.054>
- Gellrich, V., Stahl, T., Knepper, T.P., 2012. Behavior of perfluorinated compounds in soils during leaching experiments. *Chemosphere* 87, 1052–1056. <https://doi.org/10.1016/j.chemosphere.2012.02.011>
- Ghisi, R., Vamerali, T., Manzetti, S., 2019. Accumulation of perfluorinated alkyl substances (PFAS) in agricultural plants: A review. *Environ. Res.* 169, 326–341. <https://doi.org/10.1016/j.envres.2018.10.023>
- Giesy, J.P., Kannan, K., 2001. Global distribution of perfluorooctane sulfonate in wildlife. *Environ. Sci. Technol.* 35, 1339–1342. <https://doi.org/10.1021/es001834k>
- Gredelj, A., Nicoletto, C., Valsecchi, S., Ferrario, C., Polesello, S., Lava, R., Zanon, F., Barausse, A., Palmeri, L., Guidolin, L., Bonato, M., 2019a. Uptake and translocation of perfluoroalkyl acids (PFAA) in red chicory (*Cichorium intybus* L.) under various treatments with pre-contaminated soil and irrigation water. *Sci. Total Environ.* <https://doi.org/10.1016/j.scitotenv.2019.134766>
- Gredelj, A., Polesel, F., Trapp, S., 2019b. Model-based analysis of the uptake of per- and polyfluoroalkyl acids (PFAAs) from soil into plants. Accepted for publication in *Chemosphere*
- Herzke, D., Huber, S., Bervoets, L., D'Hollander, W., Hajslova, J., Pulkrabova, J., Brambilla, G., De Filippis, S.P., Klenow, S., Heinemeyer, G., de Voogt, P., 2013. Perfluorinated alkylated substances in vegetables collected in four European countries; occurrence and human exposure estimations. *Environ. Sci. Pollut. Res.* 20, 7930–7939. <https://doi.org/10.1007/s11356-013-1777-8>
- Houde, M., Martin, J.W., Letcher, R.J., Solomon, K.R., Muir, D.C.G., 2006. Biological monitoring of polyfluoroalkyl substances: A review. *Environ. Sci. Technol.* 40, 3463–3473. <https://doi.org/10.1021/es052580b>

- Krafft, M.P., Riess, J.G., 2015a. Selected physicochemical aspects of poly- and perfluoroalkylated substances relevant to performance, environment and sustainability-Part one. *Chemosphere* 129, 4–19. <https://doi.org/10.1016/j.chemosphere.2014.08.039>
- Krafft, M.P., Riess, J.G., 2015b. Per- and polyfluorinated substances (PFASs): Environmental challenges. *Curr. Opin. Colloid Interface Sci.* 20, 192–212. <https://doi.org/10.1016/j.cocis.2015.07.004>
- Krippner, J., Brunn, H., Falk, S., Georgii, S., Schubert, S., Stahl, T., 2014. Effects of chain length and pH on the uptake and distribution of perfluoroalkyl substances in maize (*Zea mays*). *Chemosphere* 94, 85–90. <https://doi.org/10.1016/j.chemosphere.2013.09.018>
- Krippner, J., Falk, S., Brunn, H., Georgii, S., Schubert, S., Stahl, T., 2015. Accumulation Potentials of Perfluoroalkyl Carboxylic Acids (PFCAs) and Perfluoroalkyl Sulfonic Acids (PFSA) in Maize (*Zea mays*). *J. Agric. Food Chem.* 63, 3646–3653. <https://doi.org/10.1021/acs.jafc.5b00012>
- Li, F., Fang, X., Zhou, Z., Liao, X., Zou, J., Yuan, B., Sun, W., 2018. Adsorption of perfluorinated acids onto soils: Kinetics, isotherms, and influences of soil properties. *Sci. Total Environ.* 649, 504–514. <https://doi.org/https://doi.org/10.1016/j.scitotenv.2018.08.209>
- Ling, Q., Huang, W., Jarvis, P., 2011. Use of a SPAD-502 meter to measure leaf chlorophyll concentration in *Arabidopsis thaliana*. *Photosynth. Res.* 107, 209–214. <https://doi.org/10.1007/s11120-010-9606-0>
- Liu, Z., Lu, Y., Shi, Y., Wang, P., Jones, K., Sweetman, A.J., Johnson, A.C., Zhang, M., Zhou, Y., Lu, X., Su, C., Sarvajayakesavaluc, S., Khan, K., 2017. Crop bioaccumulation and human exposure of perfluoroalkyl acids through multi-media transport from a mega fluorochemical industrial park, China. *Environ. Int.* 106, 37–47. <https://doi.org/10.1016/j.envint.2017.05.014>
- Liu, Z., Lu, Y., Song, X., Jones, K., Sweetman, A.J., Johnson, A.C., Zhang, M., Lu, X., Su, C., 2019. Multiple crop bioaccumulation and human exposure of perfluoroalkyl substances around a mega fluorochemical industrial park, China: Implication for planting optimization and food safety. *Environ. Int.* 127, 671–684. <https://doi.org/10.1016/j.envint.2019.04.008>
- Loos, R., Locoro, G., Huber, T., Wollgast, J., Christoph, E.H., Jager, A. De, Gawlik, B.M., Hanke, G., Umlauf, G., 2008. Analysis of perfluorooctanoate (PFOA) and other perfluorinated compounds (PFCs) in the River Po watershed in N-Italy. *Chemosphere* 71, 306–313. <https://doi.org/10.1016/j.chemosphere.2007.09.022>
- Mazzoni, M., Polesello, S., Rusconi, M., Valsecchi, S., 2016. Liquid chromatography mass spectrometry determination of perfluoroalkyl acids in environmental solid extracts after phospholipid removal and on-line turbulent flow chromatography purification. *J. Chromatogr. A* 1453, 62–70. <https://doi.org/10.1016/j.chroma.2016.05.047>
- McLachlan, M.S., Felizeter, S., Klein, M., Kotthoff, M., De Voogt, P., 2019. Fate of a perfluoroalkyl acid mixture in an agricultural soil studied in lysimeters. *Chemosphere* 223, 180–187. <https://doi.org/10.1016/j.chemosphere.2019.02.012>
- McLachlan, M.S., Holmstro, K.E., Reth, M., Berger, U., 2007. Riverine Discharge of Perfluorinated Carboxylates from the European Continent. *Environ. Sci. Technol.* 41, 7260–7265. <https://doi.org/10.1021/es071471p>

- Müller, C.E., Lefevre, G.H., Timofte, A.E., Hussain, F.A., Sattely, E.S., Luthy, R.G., 2016. Competing mechanisms for perfluoroalkyl acid accumulation in plants revealed using an Arabidopsis model system. *Environ. Toxicol. Chem.* 35, 1138–1147. <https://doi.org/10.1002/etc.3251>
- Pérez, F., Nadal, M., Navarro-Ortega, A., Fàbrega, F., Domingo, J.L., Barceló, D., Farré, M., 2013. Accumulation of perfluoroalkyl substances in human tissues. *Environ. Int.* 59, 354–362. <https://doi.org/10.1016/j.envint.2013.06.004>
- Qu, B., Zhao, H., Zhou, J., 2010. Toxic effects of perfluorooctane sulfonate (PFOS) on wheat (*Triticum aestivum* L.) plant. *Chemosphere* 79, 555–560. <https://doi.org/10.1016/j.chemosphere.2010.02.012>
- Stahl, T., Heyn, J., Thiele, H., Huther, J., Failing, K., Georgii, S., Brunn, H., 2009. Carryover of perfluorooctanoic acid (PFOA) and perfluorooctane sulfonate (PFOS) from soil to plants. *Arch. Environ. Contam. Toxicol.* 57.
- Trapp, S., 2009. Bioaccumulation of Polar and Ionizable Compounds in Plants, in: Devillers, J. (Ed.), *Ecotoxicology Modeling, Emerging Topics in Ecotoxicology: Principles, Approaches and Perspectives 2*. Springer US, Rillieux La Pape, p. 400. <https://doi.org/10.1007/978-1-4419-0197-2>
- Trapp, S., 2007. Fruit tree model for uptake of organic compounds from soil and air. *SAR QSAR Environ. Res.* 18, 367–387. <https://doi.org/10.1080/10629360701303693>
- Trapp, S., 2000. Modelling uptake into roots and subsequent translocation of neutral and ionisable organic compounds. *Pest Manag. Sci.* 56, 767–778. [https://doi.org/10.1002/1526-4998\(200009\)56:9<767::AID-PS198>3.0.CO;2-Q](https://doi.org/10.1002/1526-4998(200009)56:9<767::AID-PS198>3.0.CO;2-Q)
- Trapp, S., Matthies, M., 1995. Generic One-Compartment Model for Uptake of Organic Chemicals by Foliar Vegetation. *Environ. Sci. Technol.* 29, 2333–2338. <https://doi.org/10.1021/es00009a027>
- Valsecchi, S., Rusconi, M., Mazzoni, M., Viviano, G., Pagnotta, R., Zaghi, C., Serrini, G., Polesello, S., 2015. Occurrence and sources of perfluoroalkyl acids in Italian river basins. *Chemosphere* 129, 126–134. <https://doi.org/10.1016/j.chemosphere.2014.07.044>
- Vestergren, R., Cousins, I.T., 2009. Tracking the Pathways of Human Exposure to Perfluorocarboxylates. *Environ. Sci. Technol.* 43, 5565–5575. <https://doi.org/10.1021/es900228k>
- Vierke, L., Möller, A., Klitzke, S., 2014. Transport of perfluoroalkyl acids in a water-saturated sediment column investigated under near-natural conditions. *Environ. Pollut.* 186, 7–13. <https://doi.org/10.1016/j.envpol.2013.11.011>
- Wang, Z., Dewitt, J.C., Higgins, C.P., Cousins, I.T., 2017. A Never-Ending Story of Per- and Polyfluoroalkyl Substances (PFASs)? *Environ. Sci. Technol.* 51, 2508–2518. <https://doi.org/10.1021/acs.est.6b04806>
- Wang, Z., Xie, Z., Mi, W., Möller, A., Wolschke, H., Ebinghaus, R., 2015. Neutral Poly/Per-Fluoroalkyl Substances in Air from the Atlantic to the Southern Ocean and in Antarctic Snow. *Environ. Sci. Technol.* 49, 7770–7775. <https://doi.org/10.1021/acs.est.5b00920>
- Wen, B., Li, L., Zhang, H., Ma, Y., Shan, X.Q., Zhang, S., 2014. Field study on the uptake and translocation of perfluoroalkyl acids (PFAAs) by wheat (*Triticum aestivum* L.) grown in

biosolids-amended soils. Environ. Pollut. 184, 547–554.
<https://doi.org/10.1016/j.envpol.2013.09.040>

Xiao, F., 2017. Emerging poly- and perfluoroalkyl substances in the aquatic environment: A review of current literature. *Water Res.* 124, 482–495. <https://doi.org/10.1016/j.watres.2017.07.024>

Yang, X., Ye, C., Liu, Y., Zhao, F.J., 2015. Accumulation and phytotoxicity of perfluorooctanoic acid in the model plant species *Arabidopsis thaliana*. *Environ. Pollut.* 206, 560–566. <https://doi.org/10.1016/j.envpol.2015.07.050>

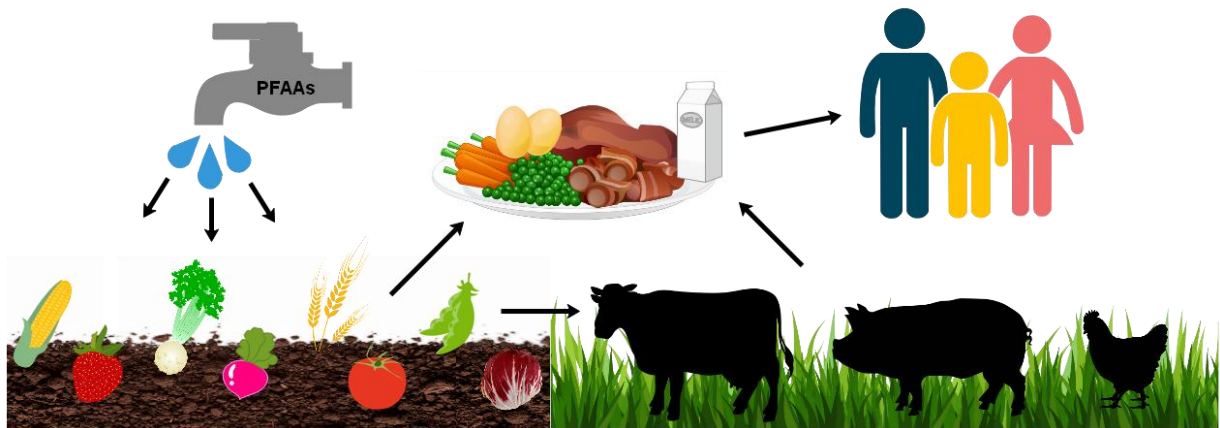
Zareitalabad, P., Siemens, J., Hamer, M., Amelung, W., 2013. Perfluorooctanoic acid (PFOA) and perfluorooctanesulfonic acid (PFOS) in surface waters, sediments, soils and wastewater - A review on concentrations and distribution coefficients. *Chemosphere* 91, 725–732. <https://doi.org/10.1016/j.chemosphere.2013.02.024>

Zhang, W., Zhang, D., Zagorevski, D. V., Liang, Y., 2019. Exposure of *Juncus effusus* to seven perfluoroalkyl acids: Uptake, accumulation and phytotoxicity. *Chemosphere* 233, 300–308. <https://doi.org/10.1016/j.chemosphere.2019.05.258>

Zhao, S., Liang, T., Zhu, L., Yang, L., Liu, T., Fu, J., Wang, B., Zhan, J., Liu, L., 2019. Fate of 6:2 fluorotelomer sulfonic acid in pumpkin (*Cucurbita maxima* L.) based on hydroponic culture: Uptake, translocation and biotransformation. *Environ. Pollut.* 252, 804–812. <https://doi.org/10.1016/j.envpol.2019.06.020>

Chapter 6

Predicting the human exposure to perfluoroalkyl acids (PFAAs) through diet: A case of the Veneto Region, Italy



In preparation for publication

Chapter summary:

Dietary intake is the main source of exposure to perfluoroalkyl acids (PFAAs) of the general population. Exposure to PFAAs through diet is usually assessed through the national food sampling (market basket) studies with often-unknown food origin. They were so far generally concentrated on PFOS and PFOA as the only PFAAs with established regulatory thresholds for the dietary intake. Food of animal origin (fish, meat, milk, eggs) has been usually regarded as the main source of these and other long chain PFAAs. It is also known that plants, including crops, can accumulate significant amounts of currently unregulated short-chain PFAAs. Here, modelling framework for the contaminated terrestrial (agricultural) ecosystem was developed for nine PFAAs, incorporating the most commonly consumed crops and farm animals and it was afterwards used for the daily dietary intake (DDI) estimations. The PFAS contamination case of Veneto Region, Northern Italy, has been used for establishment of the exposure scenarios through the monitored surface- and groundwater concentrations. PFAAs uptake into crops was based on the advective flux and partitioning plant uptake model, previously adapted for PFAAs. The animal bioaccumulation models were simple single-compartment pharmacokinetic models, parametrized for cattle, chicken and pig and were connected to the crop models via animal consumption of contaminated feeds and water. The contaminated irrigation water (either modelled as surface- or groundwater) was assumed as the only PFAAs input. The model framework was connected to the dietary intake data of North-East Italy. The calculations resulted with realistic concentrations in animal- and plant-based foods and calculated DDIs were in the range of food sampling-based daily intakes reported worldwide, with the values between the background exposure and highly contaminated areas. Five years irrigation scenario showed that with the long-term exposure to short-chain PFAAs from water, crop bioaccumulation highly exceeds the accumulation of PFOS and PFOA in the food of animal origin.

6.1. Introduction

Per- and polyfluoroalkyl substances (PFASs) are a large group of anthropogenic chemicals containing at least one perfluoroalkyl moiety (C_nF_{2n+1}) (Buck et al., 2011). They have been widely used in industrial and commercial applications since the 1950s, due to their high chemical and thermal stability provided by the strong C-F bond, and surfactant properties most of them possess (Kempisty et al., 2018; OECD/UNEP Global PFC Group, 2013). PFASs have been ubiquitously detected in environmental matrices, from water (Xiao, 2017a), soil (P Zareitalabad et al., 2013), air (Zhen Wang et al., 2015), plants (Ghisi et al., 2019), animals (Houde et al., 2006) and human tissues (Pérez et al., 2013) and have been connected with many adverse health effects in test animals and humans, such as cancer, immune system dysfunctions, liver disease, developmental and reproductive issues and hormone disruption (Pelch et al., 2019).

Fluorochemical industry is historically regarded as the most significant source of PFASs in the environment and many contamination hot-spots have been described worldwide around the industrial plants (Dauwe et al., 2007; Liu et al., 2016; Prevedouros et al., 2006; Steenland et al., 2009). Veneto Region, located in Northern Italy, is one of these contamination hot-spots, discovered in 2013, where fluorochemical plant caused large-scale contamination of surface water, groundwater and drinking water (Ingelido et al., 2018; WHO, 2016). Situated in the Po valley, the Region is one of the greatest Italian agronomic producers, accounting for the 10% of national production and is responsible for 38% of Veneto's gross domestic product (WHO, 2016). Italy, including Veneto, has the highest use of water for agricultural purposes in Europe, with about 50% of it being from surface and groundwater (Nicoletto et al., 2017).

In the general population, diet is a main source of human exposure to many organic pollutants, including perfluoroalkyl acids (PFAAs) (Papadopoulou et al., 2017; Vestergren and Cousins, 2009b; Wang et al., 2019). PFAAs detected in food can be either a consequence of environmental contamination (i.e. from the irrigation water, contaminated soil, contaminated water and feed for the livestock or aquatic bioaccumulation) (Ghisi et al., 2019; Lupton et al., 2014a; Sznajder-Katarzyńska et al., 2019; Wen et al., 2014) or contact with various food packaging items containing PFASs (Trier et al., 2011). Current research of PFAAs dietary exposure either focuses on the controlled exposure studies for farm animals (Kowalczyk et al., 2013; Lupton et al., 2014b; Numata et al., 2014; Tarazona et al., 2015) and the studies of PFAAs uptake in crops (Blaine et al., 2013, 2014c, 2014a; Krippner et al., 2015; Wen et al., 2014), or on the food sampling studies with estimations of PFAAs dietary intake (Domingo and Nadal, 2017a).

Both types of studies are mainly focused on PFOS and PFOA, the only PFASs for which regulatory threshold for the human dietary exposure are currently set (Sznajder-Katarzyńska et al., 2019). According to the European Food Safety Agency (EFSA) and their opinion from 2008 (EFSA, 2008), tolerable daily intakes (TDIs) were established to $150 \text{ ngkg}_{\text{BW}}^{-1}\text{d}^{-1}$ for PFOS and $1500 \text{ ngkg}_{\text{BW}}^{-1}\text{d}^{-1}$ for PFOA. In 2018, EFSA Panel on Contaminants in the Food Chain (CONTAM), proposed a lowering of the threshold on $13 \text{ ng kg}_{\text{BW}}^{-1}\text{week}^{-1}$ for PFOS and $6 \text{ ngkg}_{\text{BW}}^{-1}\text{week}^{-1}$ for PFOA, based on the new analytical evidences in the dietary exposure assessment (EFSA CONTAM, 2018). United States Environmental Protection Agency established the oral non-cancer reference doses (RfDs) of $20 \text{ ngkg}_{\text{BW}}^{-1}\text{d}^{-1}$ for both PFOS and PFOA (USEPA, 2016a, 2016b). Recommended TDIs from the Food Standards Australia New

Zealand agency are set to $20 \text{ ngkg}_{\text{BW}}^{-1}\text{d}^{-1}$ for PFOS and $160 \text{ ngkg}_{\text{BW}}^{-1}\text{d}^{-1}$ for PFOA (FSANS, 2017).

In the recent years, many research studies are reporting the concentrations of PFAAs in various foodstuff and estimated daily intake, mostly from European countries, showing different exposure patterns due to the differences in contamination sources and consumption habits (Domingo and Nadal, 2017a). In the majority of studies, consumption of fish and seafood was the main focus (Barbarossa et al., 2016; Domingo et al., 2012a; Hölzer et al., 2011; Munschy et al., 2013; Squadrone et al., 2014; Taylor et al., 2018; Vassiliadou et al., 2015; Wu et al., 2012; Yamada et al., 2014), while assessments of the total diets are more rare (Domingo et al., 2012b; Noorlander et al., 2011; Papadopoulou et al., 2017; Rivière et al., 2014; Vestergren et al., 2012), together with the studies reporting on the concentrations and the dietary intake of the plant based foodstuff (D'Hollander et al., 2015; Liu et al., 2019) and food coming from the terrestrial ecosystems in general (Falk et al., 2019). By looking at the total diet studies, it can be concluded that they are mostly so-called “market basket” studies, based on the sampling in the supermarkets of the one or more countries (D'Hollander et al., 2015; Heo et al., 2014; Noorlander et al., 2011; Vestergren et al., 2012). In this case, it is hard to know the exact origin of sampled food.

Long chain PFAAs, including PFOS and PFOA, are dominant PFAAs in all animal-based foodstuff, from fish and seafood to meat, liver, eggs and milk (Chen et al., 2018; Vestergren et al., 2012), while only short chain PFAAs show high bioaccumulation potential in plants (Ghisi et al., 2019). The crop root uptake from soil has been regarded as the main entry pathway of PFAAs to terrestrial food chains (Krippner et al., 2015; Liu et al., 2019). Having in mind the industrial shifts towards the “new PFAS”, including short-chain PFAAs, and much less information on their toxicity and fate in the human body and ecosystems in general, assessment of the dietary exposure, exposure through the drinking water consumption and consequent potential toxic effects is needed (Brendel et al., 2018; Cousins et al., 2016; Krafft and Riess, 2015a).

Here, a modelling framework for the dietary exposure assessment from the terrestrial ecosystem was established for PFAAs contamination hot-spot in the Veneto Region. It was composed from the semi-empirical crop uptake model developed for nine PFAA in Chapter 4 and the simple one-compartment pharmacokinetic models for farm animals, used for the estimation of PFAAs concentrations in meat (beef, pork and poultry), milk and eggs. The animal models were connected with crop uptake models through animal feed consumption. Their concentration outcomes were used for calculations of the daily dietary intakes, based on food consumption survey of the North-East Italy. A couple of assumptions were followed: 1) All consumed food was produced in the Veneto Region, 2) contaminated water (groundwater or surface water) was considered to be the only contamination source for soil and consequently animal feed and crops.

The main aim of the exposure modelling scenarios was to estimate the contributions of short and long chain PFAAs from animal and plant based foods, all coming from the same contaminated terrestrial ecosystem. Apart from the general population scenario, dietary intake was additionally estimated for children and women, as the two sensitive population categories, and compared to the general population estimations. To explore prediction capabilities of the modelling framework, crop models were also tested with the data from the well-characterized contamination hot-spot in China (Liu et al., 2019, 2017, 2016).

6.2. Materials and methods

6.2.1. Consumption data

Daily consumption data (expressed as the g of food item per kg of the body mass per day) were obtained from the national survey on food consumption in Italy (INRAN/CREA, 2010; Leclercq et al., 2009). The survey covered four main geographic areas, Veneto Region belonging to the North-East, data of which were taken for the analyses. Considering that the most of the surveyed household from the North-East area belongs to the Veneto Region, data were considered reliable enough for the purpose.

Dietary uptake was calculated for the general population, but also separately for children (3-9 years old) and adult women (18-64 years old), as the more sensitive population groups. Children are generally more sensitive to the negative effects of xenobiotics (Zeng et al., 2015) and also have a higher intake of food per body mass than adults (Legind and Trapp, 2009), resulting in higher exposure levels (EFSA, 2009). The adult women are picked as another sensitive group, due to the possibility of PFAAs to be transferred from a mother to a child through placental transfer and breast milk (Dalsager et al., 2016). Age intervals are accepted from the consumption data survey.

Daily dietary intake (DDI, $\text{ng kg}_{\text{BW}}^{-1}\text{d}^{-1}$) of each PFAA was calculated by multiplying its calculated concentrations C_i in food item i (ng g^{-1}) with its consumed quantity ($\text{consumption}_{i,g} \text{ kg}_{\text{BW}}^{-1}\text{d}^{-1}$) (Legind and Trapp, 2009):

$$DDI = \sum_i C_i \times \text{consumption}_i \quad (6-1)$$

The DDIs calculated for all foods coming from the terrestrial ecosystem were compared by currently established thresholds for the dietary consumption (EFSA, 2008). According to the European Food Safety Agency (EFSA) and their opinion from 2008, tolerable daily intakes (TDIs) were established to $150 \text{ ng kg}_{\text{BW}}^{-1}\text{d}^{-1}$ for PFOS and $1500 \text{ ng kg}_{\text{BW}}^{-1}\text{d}^{-1}$ for PFOA. In 2018, EFSA Panel on Contaminants in the Food Chain (CONTAM), proposed a lowering of the threshold on $13 \text{ kg}_{\text{BW}}^{-1}\text{week}^{-1}$ for PFOS and $6 \text{ kg}_{\text{BW}}^{-1}\text{week}^{-1}$ for PFOA, based on the new analytical evidence on the dietary exposure assessment (EFSA CONTAM, 2018). The estimated DDIs were compared both with the established ("old" TDIs) and with tolerable weekly intakes (TWIs) ("new" TWIs) currently under consideration.

6.2.2. Measured water concentrations and scenarios

The exposure scenarios were based on monitoring data of (ARPAV, 2019), continuously collected from the water matrices of the Veneto Region from 02/07/2013. The maximum concentration for nine PFAAs of interest, measured in groundwater, spring water and surface waters, as well as their average values were calculated, while wastewater influents were ignored for the purpose, as they were highly unlikely used for irrigation. Only analyses with at least one PFAA above LOD were taken into evaluation. Groundwater and spring water were evaluated together, while surface water was treated separately, all together creating four different general scenarios: regional average ground- and source waters, maximum ground- and source waters, regional average surface water and maximum concentrations in surface waters (Table 6-1). Additionally, a multiple years irrigation scenario was created, as the continuous exposure scenario with the main aim to evaluate the changes in total contribution of short chain PFAAs from (plant based) food.

Table 6-1. Measured maximum values and calculated average values of PFAAs concentrations in the Veneto Region from the period 02/07/2013 - 16/04/2019. Data on the measurement date, province and site are given for maximum values (ARPAV, 2019).

groundwater and spring water	PFBA (ng/L)	PFPeA (ng/L)	PFHxA (ng/L)	PFHpA (ng/L)	PFOA (ng/L)	PFNA (ng/L)	PFDA (ng/L)	PFBS (ng/L)	PFOS (ng/L)
average	430.4	267.1	253.2	108.1	839.2	15.8	26.7	317.2	83.6
max value	11900	7950	6310	2290	19567	81	232	6825	4610
Date:	29/09/16	29/09/16	29/09/16	29/09/16	04/07/17	21/10/15	21/05/14	17/05/18	09/10/14
Province:	Vicenza	Vicenza	Vicenza	Vicenza	Vicenza	Treviso	Vicenza	Vicenza	Verona
Site:	Sarego	Sarego	Sarego	Sarego	Sarego	Vittorio Veneto	Trissino	Sarego	Soave
surface water	PFBA (ng/L)	PFPeA (ng/L)	PFHxA (ng/L)	PFHpA (ng/L)	PFOA (ng/L)	PFNA (ng/L)	PFDA (ng/L)	PFBS (ng/L)	PFOS (ng/L)
average	108.8	56.2	55.3	23.7	163.9	109.0	11.9	125.6	20.7
max	2546	450	474	260	3417	885	37	2685	424
Date:	18/03/19	26/01/16	10/07/13	26/01/16	02/07/13	26/01/16	01/07/14	01/12/14	12/06/17
Province:	Vicenza	Verona	Vicenza	Verona	Verona	Verona	Vicenza	Verona	Vicenza
Site:	Montecchio Maggiore	Zimella	Creazzo	Zimella	Cologna Veneta	Zimella	Creazzo	Cologna Veneta	Lonigo

6.2.3. Crops model methodology

Water is the main transport media for PFAAs (McLachlan et al., 2007; Prevedouros et al., 2006), particularly the short-chain ones, and as such, it was considered as the only source of PFAAs into the modelled agricultural ecosystems and the cause of the consequential soil contamination. Leaching out of a crop rooting zone was neglected for modelling purposes, due to lack of data on the soil parameters and sufficient knowledge of PFAAs behavior for this kind of field conditions. It can be considered as the worst case scenario from the plant uptake point of view, i.e. all the PFAAs that is not sorbed to soil, is considered bioavailable to the roots. Only way of PFAAs transport to crops was by the root uptake from soil. Intercompartmental crop PFAAs concentrations were calculated with the semi-empirical model developed based on the red chicory (Chapter 4), with the crop-specific parameters from the standard plan model (Trapp, 2015), parametrized for the 1 m². The only exception was the red chicory, for which plant-specific data were available (Chapter 4). Crops selection was based on the availability of crop uptake studies for PFAAs, considering that the empirically derived root to soil concentration factors (RCFs) were needed as input data. In the case of lack of data from the adequate bioaccumulation and plant uptake studies (e.g. for potato), bioaccumulation factors were either directly used, or were extrapolated when bioaccumulation data was available only for PFOS and/or PFOA, as described in the Text A5-1 in Appendix 5.

6.2.4. Models for estimation of concentrations in meat, milk and eggs

For estimations of concentrations in beef, milk and eggs, modelling approaches for human exposure to contaminants via diet that were previously established in the regulatory context (USEPA, 2005) and/or human exposure assessment of PFASs (AECOM, 2018; Lorber and Egeghy, 2011; Vestergren and Cousins, 2009b), were applied. A first-order, one-compartment pharmacokinetic model predicting the concentration in the serum of the farm animals was used:

$$\frac{dC_{serum}}{dt} = \frac{CDI(t)}{V_d} - k_e \times C_{serum}(t) \quad (6-2)$$

Where C_{serum} (mg L^{-1}) is the concentration of contaminant in blood serum, V_d ($\text{L kg}_{\text{BW}}^{-1}$) is the apparent volume of distribution (distribution of chemical between serum/plasma and the rest of the body after oral intake), k_e (d^{-1}) is the first-order elimination rate constant and CDI ($\text{mg kg}_{\text{BW}}^{-1} \text{d}^{-1}$) is the chronic daily intake for animal.

CDI was calculated as the chronic daily intake of feed (plants), soil and water ($\text{mg kg}^{-1} \text{d}^{-1}$); C_s ($\text{mg kg}_{\text{dw}}^{-1}$), C_p ($\text{mg kg}_{\text{dw}}^{-1}$) and C_w (mg L^{-1}) are the chemical concentration in the soil, plant tissue and water consumed by an animal, respectively. IngRs refer to the ingestion rates in $\text{mg}_{\text{dw}} \text{d}^{-1}$ for soil and plants and in L d^{-1} for water, while BW is the average body weight at slaughter (AECOM, 2018; USEPA, 2005):

$$\text{CDI} = \frac{(C_s \times \text{IngR}_{i,s} + C_p \times \text{IngR}_{i,p} + C_w \times \text{IngR}_{i,w})}{\text{BW}} \quad (6-3)$$

If CDI and V_d are assumed as constant and steady state has been reached, equation can be solved as follows (Brunton et al., 2005; Lorber and Egeghy, 2011; Vestergren and Cousins, 2009b):

$$C_{\text{serum}} = \frac{\text{CDI} \times t_{1/2}}{0,693 \times V_d} \quad (6-4)$$

Where $k_e = \ln(2)/t_{1/2}$ was expressed with the well-known biological-half-life expression for elimination rate constant (Bartell, 2017). $t_{1/2}$ (d) is the serum elimination half-life, time it takes for the plasma concentration of the chemical to be reduced by 50%.

Apparent volumes of distribution (V_d) were estimated for all PFAAs as 0.2 L/kg , based on the (ATSDR, 2018) data summary for long-chained PFAAs (PFOS, PFOA and PFNA) in humans and the study of (Chang et al., 2008) performed for PFBA in rats, mice and monkeys, where its value in various animals was always close to 0.2 L/kg , typical value associated with the distribution of chemical in the extracellular space.

Concentration in animal tissue (muscle in this case) C_{tissue} (mg/kg_{fw}) was afterwards calculated by:

$$C_{\text{tissue}} = \text{TSR} \times C_{\text{serum}} \times \text{CF} \quad (6-5)$$

Where TSR is the empirical tissue/serum ratio (unitless), both tissue and chemical specific, and CF is the correction factor for the serum density ($= 0.97 \text{ L/kg}$). Elimination half-lives derived from the first-order elimination models vary significantly between species and different PFAAs (different chain-length and functional group) (ATSDR, 2018; Numata et al., 2014), but also differ with respect to dose and exposure period and route of exposure (Guruge et al., 2016). TSRs are animal-dependent, and were more functional group dependent than chain-length dependent, when series of homologues were tested (Guruge et al., 2016; Numata et al., 2014). Since half-lives were more extensively studied in humans and laboratory animals and considering the data-gaps for farm animals (Numata et al., 2014), estimations were made based on the available data. All the used parameters are listed in Table 6-2 and Table 6-3, with the explanations of estimations when necessary (either due to the lack of species- or chemical-specific data).

Table 6-2. Ingestion rates and body weight of animals modelled for human consumption. Data were accepted from (USEPA, 2005) guidelines, unless otherwise stated.

Animal:	Ingestion rates					Water (L/day)	BW (kg)
	Soil (kg _{dw} /day)	Grains (kg _{dw} /day)	Forage (kg _{dw} /day)	Silage (kg _{dw} /day)	Total plant (feed) (kg _{dw} /day)		
Cattle (beef)	0.5	0.47	8.8	2.5	11.8	70 ^a	590
Cattle (dairy)	0.4	3	13.2	4.1	20	70 ^a	630
Pig	0.37	3.3	-	1.4	5.7	20 ^b	100 ^b
Poultry	0.022	0.2	-	-	0.2	0.208 ^a	2 ^c

^a (AECOM, 2018)

^b (Almond, 1995)

^c estimated

The serum elimination half-lives $t_{1/2}$ for PFOS and PFOA in beef cattle have been obtained from (Lupton et al., 2015, 2014a, 2012), from where TSRs were calculated for cattle muscles, with the assumption of serum:plasma distribution of 1:1 for all PFAAs (ATSDR, 2018). The data for PFNA and PFDA were available only for the dairy cows (Vestergren et al., 2013), PFOA ratio between its serum elimination half-lives for dairy and beef cattle were calculated and used for data extrapolation to obtain $t_{1/2}$ also for PFNA and PFDA in beef cattle. Milk to serum ratios were calculated from (Vestergren et al., 2013). A measured data for short-chain PFAAs were not available for cattle, except for PFBS from (Kowalczyk et al., 2013), who did not detect PFBS neither in milk nor in muscle of the dairy cattle.

For pigs, elimination half-lives and TSR factors between serum and muscle were taken from (Numata et al., 2014) for PFOS, PFOA, PFHpA, PFBS and PFHxA. For other PFAAs of interest, not employed in the study of (Numata et al., 2014), serum elimination half-lives $t_{1/2}$ and TSRs were taken from (Guruge et al., 2016), in which they were determined for the microminipigs after the single dose administration.

For poultry, literature data for serum elimination half-lives and muscle to serum ratio were particularly scarce. Study of (Tarazona et al., 2015) was the most realistic, providing PFOS serum elimination half-life for adult chickens after the continuous feeding with low-contaminated diet. Another study, from (Yoo et al., 2009), provided $t_{1/2}$ for both PFOA and PFOS, but was based on subcutaneous implantation of PFAAs. Ratio of PFOS and PFOA half-lives from (Yoo et al., 2009) was used for estimation of the serum elimination half-life of PFOA, based on the $t_{1/2}$ for PFOS from the (Tarazona et al., 2015) study. In a similar way, half-life for PFDA was obtained based on the calculated PFOA/PFDA ratio from the study of (Yeung et al., 2009) assessing the accumulation and depuration of long-chain PFAAs in one-day old juvenile chickens. Considering the lack of serum elimination data for PFNA in birds, linear chain-length dependency was estimated, so $t_{1/2}$ of PFNA was calculated as the average of $t_{1/2}$ for PFOA and PFDA. Muscle to serum ratios were calculated based on the study of (Gebbinck and Letcher, 2012), where concentration of PFCAs and PFSAs were measured in the plasma and muscle of the herring gulls, considering the lack of such data for poultry. Short-chain PFAAs were not detected in bird muscles (Chu et al., 2015; Gebbinck and Letcher, 2012) and therefore, they were not considered in this estimations.

To author's knowledge, there is no presently published scientific study regarding the transfer of PFASs from birds (either from the contaminated feed or after other ways of administration) to their eggs. Consequently, concentration in chicken eggs, C_{egg} (mg/kg_{ww}) was estimated using the equation from (USEPA, 2005):

$$C_{egg} = \frac{\{\sum(F_i \times Q_{pi} \times P_i) + (Q_s \times C_s \times B_s) + (Q_w \times C_w)\} \times TF}{LR \times E_w} \quad (6-6)$$

In which, F_i is the fraction of plant type (i) grown on a contaminated soil and ingested by chicken, Q_{pi} (kg_{dw} plant/day) is the daily quantity and P_i (mg/kg) is the concentration of PFAA in the plant (i) eaten by chicken. Here, F_i was considered as 1, assuming that chicken were eating only corn grains. Value of Q_s (kg_{dw} /day) corresponds to the soil quantity eaten by chicken per day, having the PFAA concentration C_s (mg/kg) and bioavailability factor B_s (unitless and considered equal to 1). Quantity of ingested water per day is Q_w (L/day), while C_w (mg/L) is the average water concentration of PFAAs during the exposure. Value of LR is the laying rate (0.9 eggs/day), corresponding to the average number of eggs laid per day and E_w is the average weight of edible egg portion (0.0563 kg), both constant's values accepted from (AECOM, 2018). Transfer factor, TF is the ratio of PFAA concentration in fresh weight egg tissue to the contaminant intake from the feed (and water). Usually, TF is estimated based on the empirical regressions with the octanol-water partition coefficient, K_{ow} , lying on the assumption of contaminant's accumulation in the fatty tissues (Travis and Arms, 1988; USEPA, 2005), not applicable for PFAAs considering their affinity for proteins instead of the adipose tissues (Ng and Hungerbühler, 2014), and overall uncertainty of measured and estimated K_{ows} (Droge, 2019). In the absence of data, results obtained from (Australian Government - Department of Defence, 2017), reporting the percentage transfer of PFOS, PFOA and PFHxA from the drinking water consumed by chickens (as the only exposure pathway) to their eggs were accepted as the corresponding TFs. To obtain the TFs also for PFNA and PFDA, egg yolk to serum ratios were calculated from measured inter-compartmental concentrations for herring gulls from (Gebbink and Letcher, 2012) and used in extrapolation from PFOS to PFNA and PFDA. Egg yolk concentration was used since PFAAs were not detected in albumen of the herring gull eggs, result in accordance with other studies showing that long-chain PFAAs primarily accumulate in the egg yolk and not in the albumen of various bird species, including chicken (Gebbink and Letcher, 2012; Su et al., 2017; Vicente et al., 2015; Zafeiraki et al., 2016). Extrapolation was based on PFOS, considering that the amount of PFOS transferred to eggs per day was estimated to be equal to the amount of PFOS ingested by a chicken via their drinking water per day (Australian Government - Department of Defence, 2017). Comparison of PFAAs accumulation concentrations in various herring gull tissues have shown primary accumulation of PFCAs and PFSAs in egg yolks (3-fold and 17-fold higher than in the liver for PFOA and PFOS, respectively) (Gebbink and Letcher, 2012). Additionally, PFOS was found to be the most detected among all analyzed PFAAs in the home produced chicken eggs from the European studies (Su et al., 2017; Zafeiraki et al., 2016). Significant concentrations of short-chain PFAAs (compared to the concentrations of long-chain PFAAs) were found only for PFBA in the home produced chicken eggs in China (Su et al., 2017), but were negligible in other bird egg bioaccumulation studies (Gebbink and Letcher, 2012; Vicente et al., 2015; Zafeiraki et al., 2016). Consequently, short-chain PFAAs were not considered in the estimation of their bioaccumulation in chicken eggs.

Table 6-3. Toxicokinetic parameters for animals modelled for human consumption and egg transfer factors

Toxicokinetic parameters:	Cattle (beef)		Cattle (dairy)			Pig		Poultry		Egg
	t _{1/2} (day)	TSR (muscle-serum)	t _{1/2} (day)	TSR (muscle-serum)	TSR (milk-serum)	t _{1/2} (day)	TSR (muscle-serum)	t _{1/2} (day)	TSR (muscle-serum)	TF
PFBA	-	-	-	-	-	13.9 ^e	0.05 ^e	-	-	-
PFPeA	-	-	-	-	-	1.6 ^e	-	-	-	-
PFHxA	-	-	-	-	-	4.1 ^f	0.054 ^f	-	-	-
PFHpA	-	-	-	-	-	74.0 ^f	0.055 ^f	-	-	-
PFOA	0.8 ^a	0.22 ^d	1.3 ^d	0.22 ^d	0.20 ^d	236 ^f	0.061 ^f	8.46 ^g	0.10 ^k	0.45 ^l
PFNA	5.4 ^{ad}	0.16 ^d	8.7 ^d	0.16 ^d	0.08 ^d	49.5 ^e	0.050 ^e	20.10 ^j	0.05 ^k	0.35 ^m
PFDA	11.7 ^{ad}	0.12 ^d	19.0 ^d	0.12 ^d	0.08 ^d	40.8 ^e	0.100 ^e	31.74 ^{ghi}	0.07 ^k	0.95 ^m
PFOS	120.0 ^b	0.025 ^c	38.7 ^d	0.095 ^d	0.027 ^d	634 ^f	0.100 ^f	230.0 ^h	0.34 ^k	1.00 ^l
PFBS	-	-	-	-	-	43.0 ^f	0.057 ^f	-	-	-

^a (Lupton et al., 2012)

^b (Lupton et al., 2015)

^c average of the values for the low-dose steers and high dose heifers from (Lupton et al., 2015, 2014a)

^d (Vestergren et al., 2013)

^e (Guruge et al., 2016)

^f (Numata et al., 2014)

^g (Yoo et al., 2009)

^h (Tarazona et al., 2015)

ⁱ (Yeung et al., 2009)

^j estimated as the mean of PFOA and PFDA

^k (Gebbinck and Letcher, 2012)

^l (Australian Government - Department of Defence, 2017)

^m extrapolation based on (Gebbinck and Letcher, 2012) and TF (PFOS) from (Australian Government - Department of Defence, 2017)

The crop modelling framework was connected with the animal models through chronic daily intakes of plants, soil and water for animals (cattle, pig, and poultry). Water for animals was considered the same as the one used for irrigation in each scenario, while soil concentrations were set to the background concentrations measured in the Veneto soils. The only published soil concentration analyses are limited to 10 sites that were suspectedly irrigated by contaminated water, measured by the Regional Environmental Agency (ARPAV, 2018a), and were between < LOD (2 or 3 ng/g_{dw}) and 12 ng/g_{dw} for the Σ PFAAs. The corn model was used for estimation of the concentration in grains feed, forage was modelled as grass, and silage as the 50% alfalfa and 50% wheat and corn shoots (stover), as that are commonly used for the animal feed (Ghisi et al., 2019).

6.2.5. Validation of the crop modelling framework with measured data

Currently there is no available data on PFAAs concentrations, apart from PFOS and PFOA, in the foodstuff (either plant or animal based) from the Veneto Region. The least published report from the Italian National Institute of Health (ISS) (Istituto Superiore di Sanità, 2019) reports on the concentrations in various foodstuff collected from the contaminated zone in Vicenza, but only of PFOS and PFOA. Hence, data from the Chinese well-documented case of PFAAs contamination around the mega fluorochemical industrial park, covering also agricultural ecosystems, were used to validate the crops modelling performance (Liu et al., 2019, 2017, 2016). Liu et al. measured the PFCA and PFSA concentrations in various crops (grains and vegetables) and their corresponding soil in close proximity to the fluorochemical industrial plant in Huantai County, Shandong Province, China at the two agricultural sites, 300m and 1km from the plant, respectively (Liu et al., 2019). Predicted concentrations by the

model (based on the measured soil concentrations from the study and soil-water partitioning coefficient measured for the Italian agricultural soil) were compared with the measured concentrations reported by (Liu et al., 2019).

A performance of the model calculations was evaluated by the means of least-squares linear regression between modelled and measured concentration values in different plant compartments for PFCAs (3CF_x - 9CF_x). With axis intercept forced to zero, the slope is a measure of the accuracy of model simulations, while R² is a measure of the calculations precision. All statistical analyses were performed using the Data Analysis ToolPak from MS Excel® add-in.

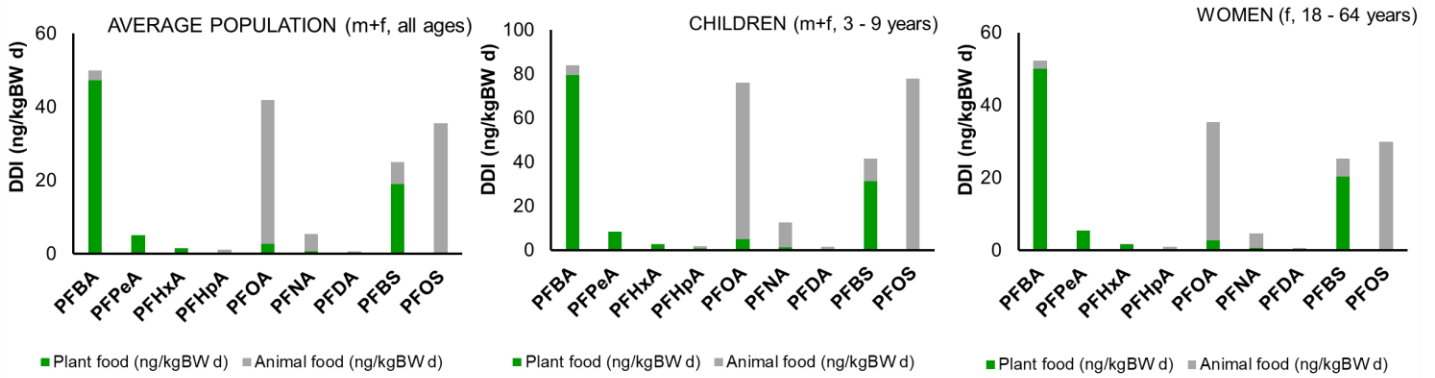
6.3. Results and discussion

6.3.1. Daily dietary intake of PFAAs under various scenarios

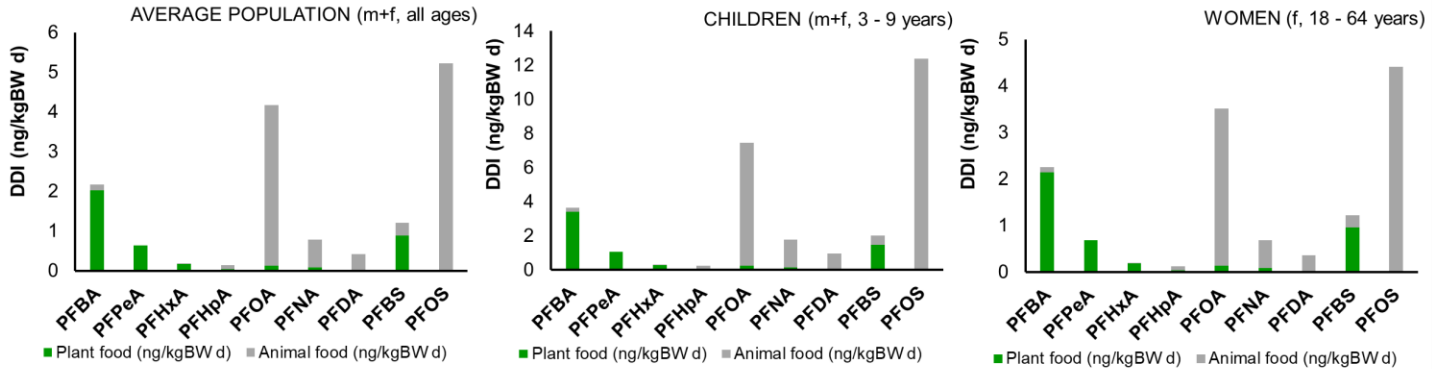
The daily dietary intakes of nine PFAAs are shown on Figure 6-1, for all of the irrigation water scenarios (average concentrations in the surface water, maximum concentrations in surface water, average concentrations in groundwater and maximum concentrations in groundwater) and population groups (average population, children (3-9 years old) and women (18-64 years old)).

In all scenarios, the highest concentrations in water were the ones of PFOA, followed by PFBA in both of the groundwater scenarios and PFBS in the surface water scenarios. Concentration of PFOS in water was about 8 times as low as concentration of PFOA in surface water (both maximum and average scenarios) and 10 and 4 times as low as PFOA in groundwater average and maximum concentrations scenarios, respectively (Table 6-1). Nonetheless, in most cases, PFOS was the most dominant PFAA in the diet, generally followed by PFOA and PFBA (Figure 1). A high DDIs of both PFOA and PFOS are the consequence of animal food intake, mainly pork, due to high pork consumption and the highest pig serum elimination half-lives for PFOS and PFOA (among the modelled animals) reported in literature (Numata et al., 2014) and used in the model. This is in accordance with the report of the Italian National Institute of Health, communicating the highest measured concentrations of PFOA and PFOS in pork meat (0.25 ng/g) and liver (2.3 ng/g) among various foodstuff sampled from the contamination zone (Istituto Superiore di Sanità, 2019). The second most important dietary source of PFOA and PFOS, according to the modelling framework, were poultry and eggs (e.g. eggs containing 10% of all PFOA daily intake for the average population and poultry meat about 40% of PFOS daily intake, both for the exposure scenario with average surface water concentrations). Eggs were characterized as the most important exposure source according to the monitoring and risk estimation study of ISS, with the second largest (after the pork liver) measured concentrations of PFOA and PFOS in eggs of 1.2 ng/g and 0.9 ng/g, respectively (Istituto Superiore di Sanità, 2019).

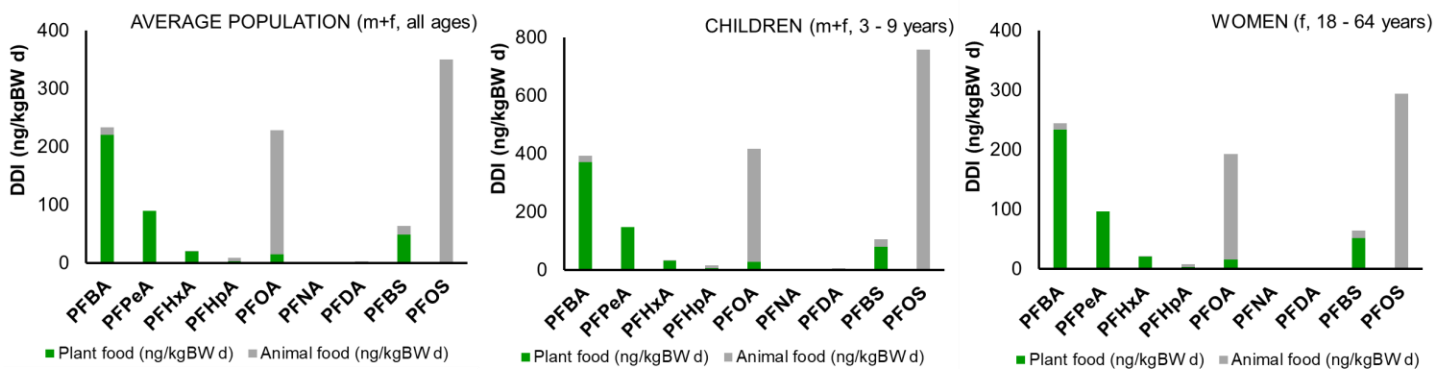
a) Maximum surface water



b) Average surface water



c) Maximum groundwater



d) Average groundwater

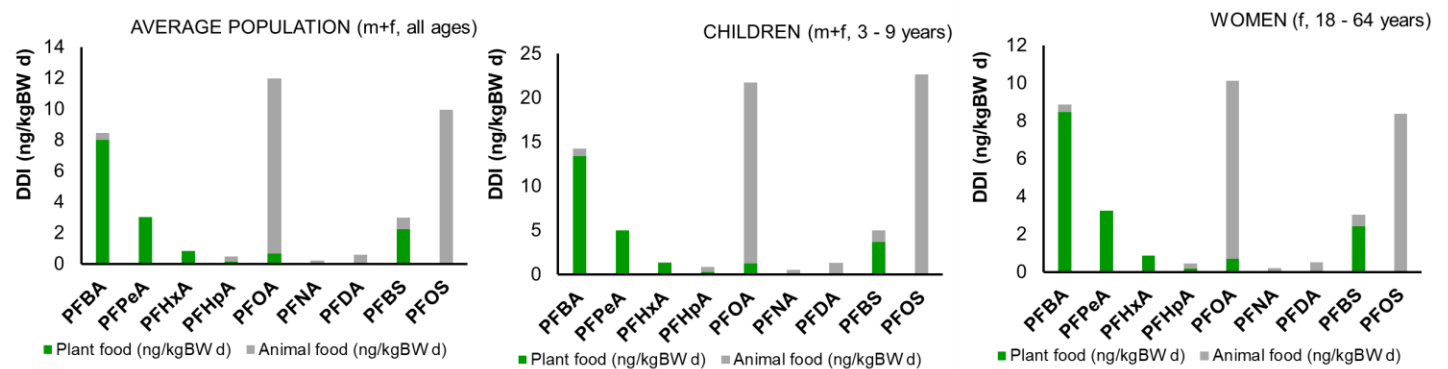


Figure 6-1. Calculated daily dietary intakes for three population groups (average population, children (3-9 years old) and women (18-64 years old) and all irrigation water scenarios: a) maximum concentrations in surface water, b) average concentrations in surface water, c) maximum concentrations in groundwater and d) average concentrations in groundwater.

As shown in Figure 6-1, magnitude of the estimated total daily dietary intakes (DDIs) varies a lot among the scenarios, from 233.1, 228.8, 63.6 and 350.4 ng kg_{BW}⁻¹ d⁻¹ for PFBA, PFOA, PFBS and PFOS for the maximum groundwater scenario, to 2.2, 4.16, 1.21 and 5.21 ng kg_{BW}⁻¹ d⁻¹ for PFBA, PFOA, PFBS and PFOS, for the average surface water scenario. Across literature, usually reported estimated daily intakes (EDIs) for PFOS and PFOA in the average adult population of different countries are around 1 ng kg_{BW}⁻¹ d⁻¹. For example, in the study of (Noorlander et al., 2011), where the analyzed foodstuff were purchased in the Dutch retail stores across the country, estimated median long-term intake of PFOS was 0.3 ng kg_{BW}⁻¹ d⁻¹ and 0.2 ng kg_{BW}⁻¹ d⁻¹ for PFOA. Similar market basket study, performed in Catalonia, Spain, estimated EDIs of 1.84 ng kg_{BW}⁻¹ d⁻¹ for PFOS and 5.05 ng kg_{BW}⁻¹ d⁻¹ for PFOA (Domingo et al., 2012b). In Norway, the median EDIs derived from a duplicate diet study were 163 pg kg_{BW}⁻¹ d⁻¹ and 86 pg kg_{BW}⁻¹ d⁻¹ for PFOS and PFOA, respectively (Papadopoulou et al., 2017). Similar estimated daily intake values were reported from other authors as well, all looking at the average exposed populations (Heo et al., 2014; Rivière et al., 2014; Vestergren et al., 2012), mostly pointing out meat, dairy and fish and/or seafood as the most contributing foods to the intake of PFOS and PFOA (Domingo and Nadal, 2017b; Rivière et al., 2014; Vestergren et al., 2012). The joint study of the four European countries, including Italy, Belgium, Czech Republic and Norway, where foodstuff of both animal and plant origin were sampled, came to the same conclusion of the average EDI being around or below 1 ng kg_{BW}⁻¹ d⁻¹ for seven different PFAAs, but stating the importance of fruits and vegetables in the dietary exposure to PFOA and some short-chain PFAAs (PFHxA and PFHxS). (D'Hollander et al., 2015; Herzke et al., 2013; Hlouskova et al., 2013; Klenow et al., 2013). However, PFBA and PFPeA, PFAAs accumulating in the most extent in crops, according to the uptake studies (e.g. (Blaine et al., 2014b, 2014a; Liu et al., 2019; Wen et al., 2014)) were not measured in vegetables (Herzke et al., 2013). Several times higher estimated daily intakes were reported for the Taiwanese general population and pregnant woman, for PFOA being as high as 85.1 ng kg_{BW}⁻¹ d⁻¹, followed by EDI for PFDA of 44.2 ng kg_{BW}⁻¹ d⁻¹ and 11.2 for PFHxA, while estimated daily intake of PFOS was much lower with 0.46 ng kg_{BW}⁻¹ d⁻¹ (Chen et al., 2018). Very high EDIs mostly resulted from the high intake of contaminated rice and contaminated pork liver. Here, DDIs resulting from the average surface water scenario could be compared to some worldwide cases of the general population exposure (e.g. Catalonia (Domingo et al., 2012b)), but are expectedly higher than the ones resulting only from the background exposure concentration levels (e.g. France (Rivière et al., 2014)).

The average groundwater scenario resulted with somewhat higher DDIs than the average surface water scenario, considering the higher average groundwater concentrations. A magnitude of the estimated DDIs among scenarios for PFBA and PFBS exactly followed water concentrations increase/decrease, i.e. DDIs for the average groundwater scenario for PFBA and PFBS were 4.0 and 2.5 times as high as for the average surface water scenario, respectively, in the exact same ratio as initial water concentrations. However, groundwater average concentrations for PFOS and PFOA, that were 4.0 and 5.1 times as high as water concentrations in the average surface water scenario, resulted with only 1.9 and 2.9 as high DDIs for PFOS and PFOA, respectively. This is the immediate consequence of the food source: PFBA and PFBS are mainly consumed with food of plant origin, where they are directly taken up with transpiration water, and, as it was shown by Blaine et al., their concentrations in plant tissues are linearly increasing with the irrigation water concentration increase (Blaine et al., 2014b). For PFOS and PFOA, whose main source is the animal-based food, DDIs are not immediately following the exposure water concentration increase, as they firstly need to pass through the animal metabolism and be translocated into the muscle tissues (or milk). In general, PFAAs DDI profiles were different for different food categories, short chain PFAAs (particularly PFBA and PFBS) being the most abundant PFAAs in plant based food

(cereals, vegetables and fruits), while, as already mentioned, long chain PFAAs were most abundant in food of animal origin (meat, milk and eggs) (Figure 6-2).

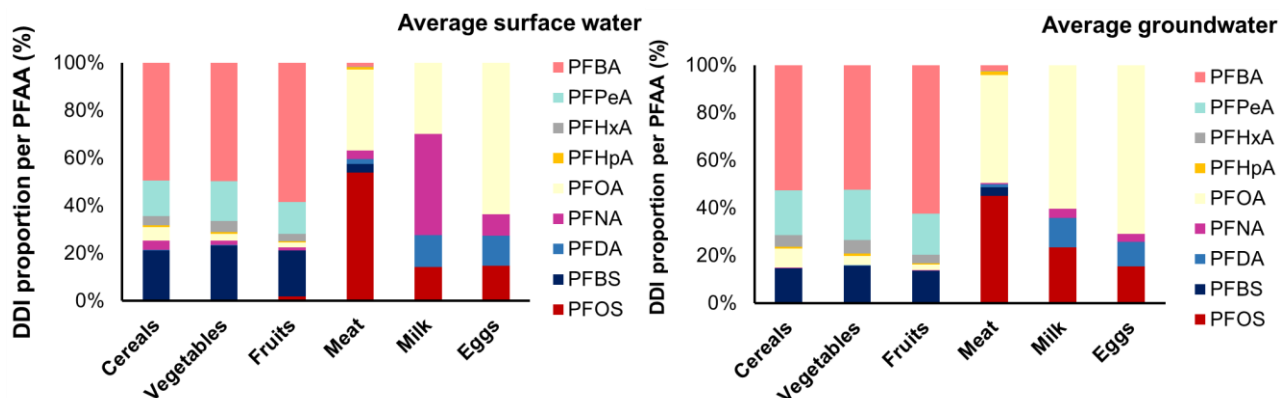


Figure 6-2. The proportions of all PFAAs in foods of plant and animal origin for two representative scenarios.

The calculated maximum groundwater and maximum surface water DDIs are considerably higher than the average scenarios (Figure 6-1). Maximum concentrations of PFAAs were for one order of a magnitude higher in groundwater (Table 6-1, Figure A5-1 and A5-2), consequently resulting with equivalently higher DDIs. Nevertheless, they were still either in line or lower of EDIs calculated for foodstuff sampled from other contaminated areas. For example, Su et al. reported on the maximum EDIs of PFBA and PFOA as high as 73.6 and 233 $\text{ng kg}_{\text{BW}}^{-1} \text{d}^{-1}$, only resulting from the consumption of contaminated eggs, home produced around the fluorochemical plant in China (Su et al., 2017). The estimated daily intake of 500 $\text{ng kg}_{\text{BW}}^{-1} \text{d}^{-1}$ of PFOS was calculated based on the total daily intake from (Wang et al., 2010), also based only on eggs consumption in the area around the fluorochemical industrial plant. According to (X. Wang et al., 2017), who have collected food concentration data of various PFAAs around the mainland China from literature, estimated total daily intake was 479 $\text{ng kg}_{\text{BW}}^{-1} \text{d}^{-1}$ for a sum of 17 PFAAs (3-13CF_x for PFCAs and 4-10CF_x for PFSA) in the low exposure scenario. Liu et al. reported EDIs calculated only on the basis of vegetables and grains consumption, for high and low exposure scenarios (i.e. grown on the field 300m and 1km from the fluorochemical plant), for PFBA being the highest and ranging between 1849 and 4.1 $\text{ng kg}_{\text{BW}}^{-1} \text{d}^{-1}$ (Liu et al., 2019). To the author's knowledge, there is currently no published data set regarding various food items originating from the same contaminated terrestrial (agricultural) ecosystem, apart from the few food items mentioned before and apart from estimations, so total validation of the modelling framework was not possible. However, it can be concluded that predicted PFAA concentrations coming from the modelling framework (and being only based on water concentrations as an input) are somewhat in range with the measured concentrations in various foods coming from the contaminated areas.

6.3.2. Crop modelling framework validation

The crop models were validated based on the published multi-media sampling study around the fluorochemical plant in Huantai County, China, reporting on the soil, water and crops concentrations from the area (Liu et al., 2019, 2017, 2016). For this purpose, five crops were selected from the study of (Liu et al., 2019) that are either of same species as the model crops or similar by the plant compartments involved (e.g. red chicory was the model representative for lettuce and the model tomato for pepper). Liu et al. (Liu et al., 2019, 2017, 2016) measured the concentrations of 12 PFAAs (PFCAs and PFSA), PFSA mainly being under the detection limit in all matrices, as they are not used in the production processes of the described fluorochemical plant. Here, results of monitoring seven PFCAs (3CF_x to 9CF_x) were used for the modelling. Firstly, PFAAs concentrations measured in the corresponding soil (0-20 cm) of each crop were used as the model input, for both sampled

fields, on 300m and 1km from the fluorochemical plant (Liu et al., 2019). Considering that the main sources of crop contamination, according to the authors of the study, were irrigation with groundwater and precipitation (Liu et al., 2019, 2017), crop model framework with irrigation water as the only source of contamination was used in the second simulation. In this second validating calculation, measured PFAA concentrations from the groundwater well G-3 (Liu et al., 2016), used for the irrigation of the field 300m from the fluorochemical plant were employed as the input water concentrations. All the crop specific data (i.e. water requirements, rooting depth, time to harvest) were left as described for the modelling framework, as these data were not available from the study of (Liu et al., 2019). They also did not report on the agricultural soil type or the site-specific soil-water partition coefficients, so the K_{ds} for the Italian agricultural soil from (Gredelj et al., 2019a) were used instead. Nevertheless, the measured soil parameters, such as pH, organic matter and organic carbon content, were similar (e.g. pH around 7.5 and OC around 1.5%, see Table S2 from (Liu et al., 2019) and Table A3-8 from Appendix 2 for the details) and this estimations were considered satisfactory for the purpose.

The first validation attempt with the measured soil concentrations as the input data resulted with under-predicting of the modelled concentrations in all the crop compartments (results not shown). This result was somehow expected, considering the high mobility of short-chain PFAAs with their high plant uptake affinity and their leaching capacity. It is probable that they leached out from the surface soil that was sampled only at harvest, behavior that was already observed for short-chain PFAAs (Gredelj et al., 2019a; McLachlan et al., 2019; Vierke et al., 2014). Additionally, according to (Hurtado et al., 2016), who studied the uptake of organic micropollutants from the irrigation water to lettuce, concentration in the soil close to roots is lower than the one in the surrounding soil because of the increased uptake of contaminants into roots. Hence, concentration in the irrigation water should be a better predictor for the accumulation of PFAAs into crops, as already stated in Chapter 3. With both approaches, using either the soil or water concentrations as input, crop models were able to accurately reproduce bioaccumulation trends among various PFAAs, taking into account both the crop affinity for short-chain PFAAs and very high concentrations measured for PFOA (Figure 6-3, validation results based on the irrigation water concentrations).

Regardless of the various approximations and simplifications, the measured field concentrations in different crop compartments (Liu et al., 2019) were reasonably well predicted with the groundwater concentrations used as input (Liu et al., 2016), modelled concentrations always being at least in the same order of a magnitude as the measured ones (Figure 6-3 and Table A5-3). It is particularly satisfactory considering the extrapolation from the greenhouse measurements that were used in the model development and parameters of different crops and soil that were employed due to the lack of data.

Even for the crops modelled as different species, but with their typical growing period (lettuce and peppers), modelled concentrations were within 13-70% of the measured ones for the most bioaccumulative PFAAs. The most underestimated concentration was for the wheat grains, which could be a consequence of the use of fruit compartment instead of grains, since there is no specific model developed for cereals yet (Legind and Trapp, 2009) and fruit compartment is being rudimentary described, as explained in Chapter 4.

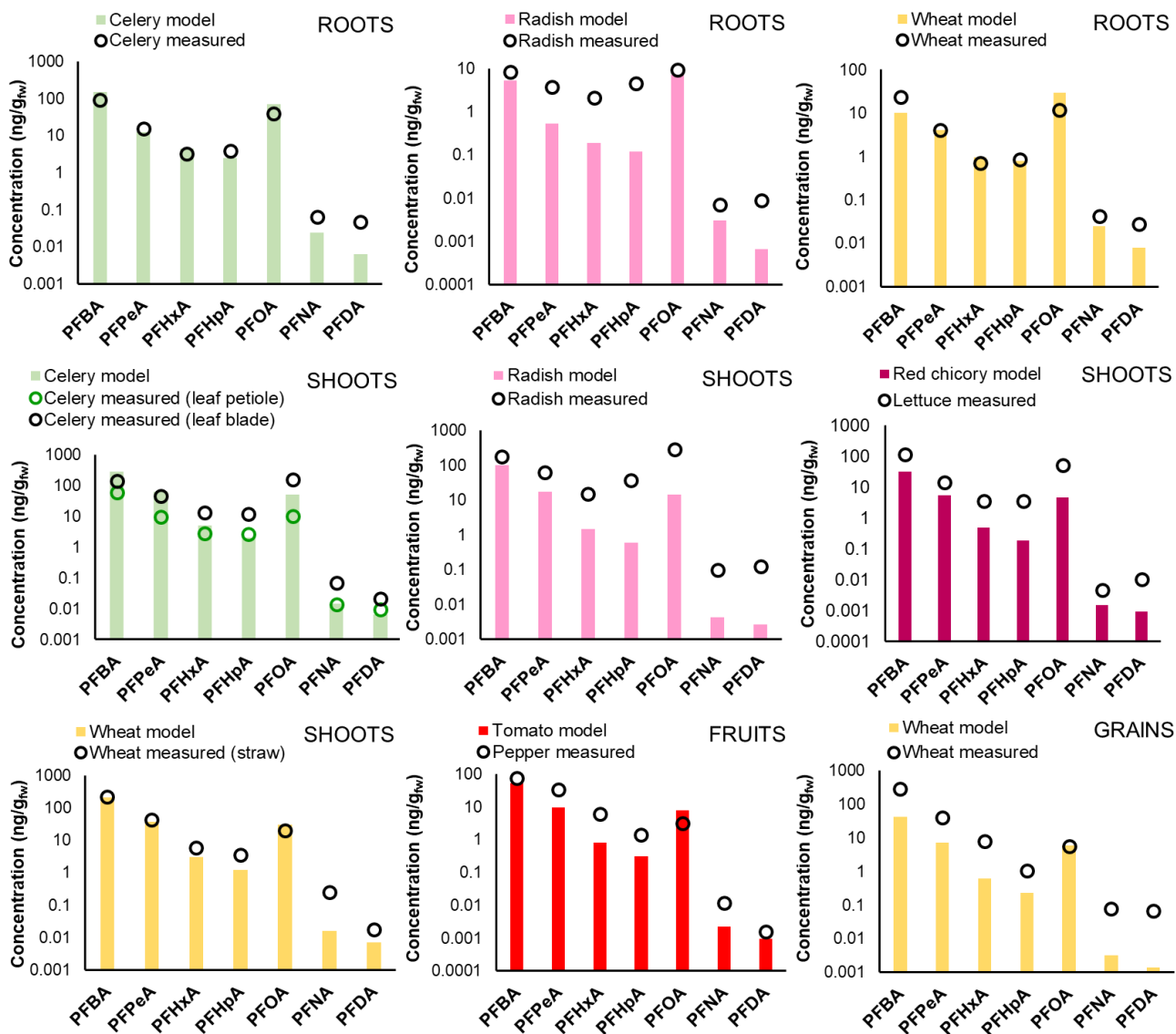


Figure 6-3. Comparison of modelled and measured PFAA concentrations for celery, radish, wheat, lettuce and peppers irrigated with groundwater (data from the field 300m from the fluorochemical plant) from (Liu et al., 2019, 2016). Concentrations are calculated to and expressed on fresh weight basis.

6.3.3. Exposure estimation for the vulnerable groups

Apart from the general population, dietary exposure was calculated also for women and children (Figure 6-1 and Figure 6-4). Exposure of woman did not differ much from the exposure of the general population. The only noticeable difference was the lower exposure to the long chain PFAAs (mostly PFOS and PFOA), 66% compared to the 70% of the total PFAAs DDI in the general population, and the higher exposure to short chain PFAAs (PFBA and PFBS). Women are generally little less exposed, due to the lower food intake (total PFAAs DDI was $14.92 \text{ ng kg}_{\text{BW}}^{-1} \text{ d}^{-1}$ in the general population and $13.45 \text{ ng kg}_{\text{BW}}^{-1} \text{ d}^{-1}$ for women, respectively).

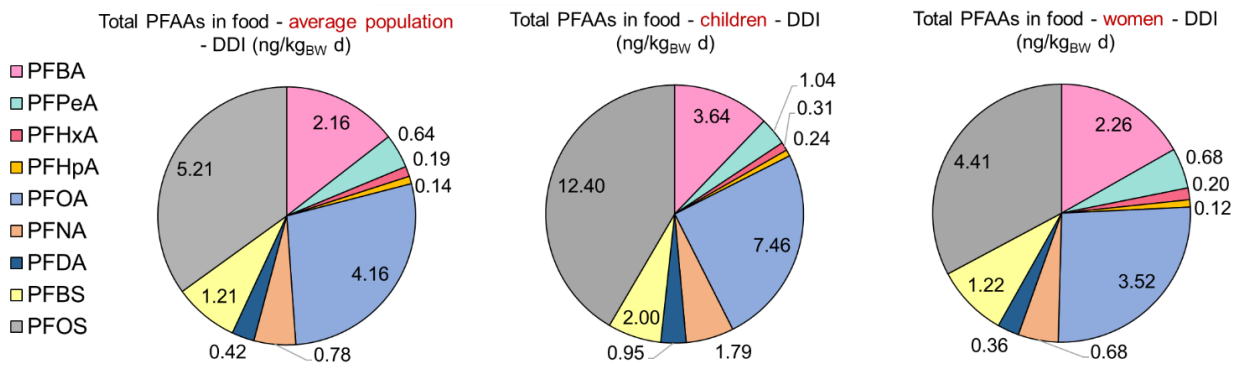


Figure 6-4. Comparison of the PFAA DDIs for the average population, children (3-9 years) and women (18-64 years) in average surface water scenario.

Children are more exposed to PFAAs, due to the higher food intake per body weight, which overall resulted with twice as high total PFAAs DDI ($29.8 \text{ ng kg}_{\text{BW}}^{-1} \text{ d}^{-1}$) than calculated for the general population. The same result could be seen in the few existing dietary intake studies that also accounted for children's diet (Domingo et al., 2012b; Heo et al., 2014; Klenow et al., 2013; Liu et al., 2019). The contribution of long and short chain PFAAs is also different in children, particularly regarding the higher exposure to PFOS, accounting for about 45% of all PFAAs in children's diet. The highest dietary exposure to PFOS for 3-6 year olds was reported from the Korean market basket study of (Heo et al., 2014). Here, higher proportion of PFOS among total modelled PFAAs can be connected with high children's consumption of poultry that is three times as high as the one in the general population.

6.3.4. Five years irrigation scenario

The regular scenarios described above were developed with the assumption of the exposure during only one growing season. However, in reality, and as it was the case with the Veneto PFAAs contamination case, years can pass by between the initial exposure and contamination discovery (WHO, 2016) and also for undertaking the regulatory, safety and clean-up measures for preventing the further human exposure (Cousins et al., 2016). Here, model was adapted for the n-th season of irrigation with contaminated water, meaning that already n-1 years have passed in the irrigation of the same land. Again, assumption of the worst-case was made with no leaching out of PFAAs root zones and the all-polluted area, without accounting for the clean animal feed and water or the irrigation water, as described before. Simulation results are shown as the comparison between the 1st and 6th irrigation season, based on the DDIs for the general population in the average groundwater scenario.

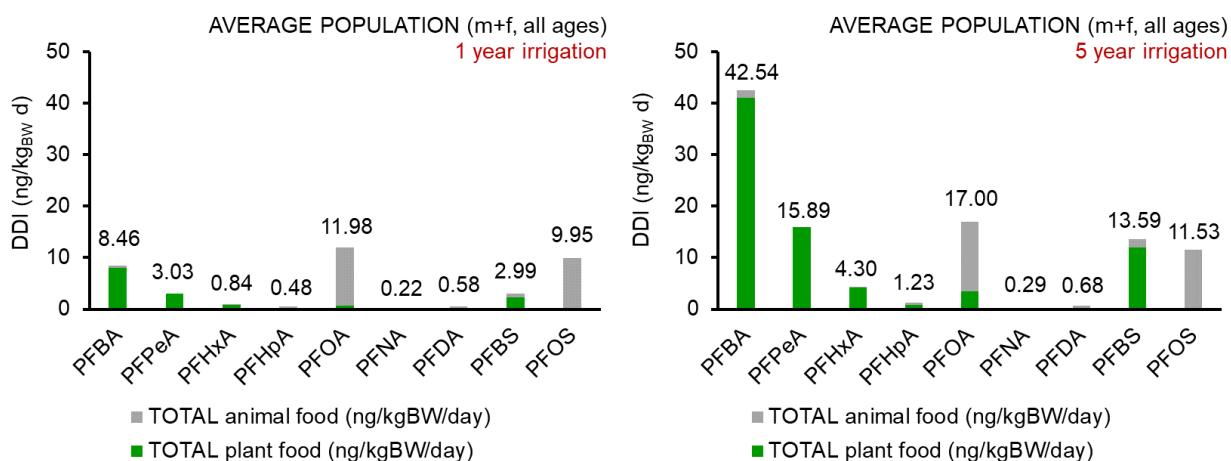


Figure 6-5. Contribution of all PFAAs to dietary intake of the general population, during the first year of irrigation and after 5 irrigation seasons.

Simulation results have shown that the prolonged irrigation with the contaminated water can result with a much higher dietary exposure to short chain PFAAs, whose proportion in the total PFAAs exposure would increase from 41% to 72%. After five years of exposure to contaminated groundwater, the total PFOA and PFOS DDIs would increase only 1.4 and 1.2 times as high as in the one year irrigation scenario, while this increase would be 5, 4.5 and 5.2 times for the same scenario for the PFBA, PFBS and PFPeA, respectively.

Even though this scenario probably is exaggerated by ignoring the short chain PFAA mobility in soil, it is not so unrealistic from the aspect of the contaminated groundwater use. In Veneto, higher concentrations of short-chain PFAAs were detected in the groundwater, compared to the surface water (ARPAV, 2019; WHO, 2016), as they remain entrapped in the closed aquifer after infiltration. The granular activated carbon (GAC) filters were installed for treating the groundwater that was used in the drinking water supply systems (WHO, 2016), but they are not efficient in removing short chain PFAAs (Ross et al., 2018). The long residence times for the groundwater, difficulties of its remediation and high water concentrations of short chain PFAAs (particularly PFBA and PFBS), as a result of the industrial substitution, together with PFAAs' extreme persistence can lead to high long term exposure to short chain PFAAs (Cousins et al., 2016). High crop bioaccumulation can be expected when the contaminated water with high short chain PFAAs content is used for the irrigation (e.g. from private wells) and consequently higher dietary intake through the food of plant origin can be expected.

6.3.5. Characterization of the risk

Results from the simulation scenarios were compared with the EFSA's current tolerable daily intake (TDI) recommendations (EFSA, 2008) of $1500 \text{ ng kg}_{\text{BW}}^{-1} \text{ d}^{-1}$ for PFOA and $150 \text{ ng kg}_{\text{BW}}^{-1} \text{ d}^{-1}$ for PFOS. The only exceedance of these TDIs was for PFOS in the maximum groundwater concentrations scenario, for all population categories (general population, women and children). PFOS TDI was exceeded more than twice for the general population and 5 times for children. However, when comparing the DDIs with new TDIs of $13 \text{ ng kg}_{\text{BW}}^{-1} \text{ week}^{-1}$ for PFOS and $6 \text{ ng kg}_{\text{BW}}^{-1} \text{ week}^{-1}$ for PFOA, currently under the evaluation in EFSA (EFSA CONTAM, 2018), every scenario would lead to TDI exceedance and conclusion of the existing risk from the dietary exposure of PFOS and PFOA through the contaminated food consumption. .

6.4. Conclusions

The modelling framework for the dietary exposure assessment of nine PFAAs was developed for the whole terrestrial (agricultural) ecosystem for the first time and was used for the dietary exposure simulations for population of the Veneto Region, one of the PFAS contamination hot spots. The crop models were successfully validated with the multi-media PFAAs concentration measurements around the fluorochemical plant from China. Crop models can reproduce PFAAs mixture ratios based on the measured concentrations in water used for irrigation and account for the uptake preferences for short-chain PFAAs. In general, model framework calculations resulted with realistic concentrations in animal- and plant- based foods and daily dietary intake was in the range between the background exposure and highly contaminated areas. The modelling framework accounts for specific dietary differences as it is based on the national survey. It also accounts for soil sorption as the main pathway of reducing PFAAs bioavailability through the use of site-specific K_d s. Nevertheless, there are limitations due to approximations that needed to be implemented, considering the scarcity of data: in animal models parameters were sometimes estimated from the other species, it considers that the steady state has been reached and assumes continuous constant exposure; for the plant models, empirical root concentration factors that are based on controlled (greenhouse) experiments have been used and extrapolated for field conditions and were sometimes used for different species than derived for. Uncertainties were also introduced through the representation of the whole food group (e.g. "other vegetables") with only one crop, leaching in soil has been neglected and so was infiltration to the groundwater and mobility of (particularly short chain) PFAAs, estimating that all of the PFAA was contained in the soil root zone after irrigation. Food consumption uncertainties always exist as well, such as individual diet preferences (e.g. vegetarianism). However, the models could be useful in estimation of the potential exposure of animals and crops and consequentially humans when only the water concentrations are known. The modelling framework can account for PFAAs mixture concentrations that are contamination area specific (i.e. different production processes produce different kind of PFAS waste or different mixtures in the AFFF spillage areas). It also pointed out a possibility of high contribution of short chain PFAAs (mainly through food of plant origin) to the total PFAAs body burden, something that is often overlooked since these PFAAs are still not regulated. Research is needed towards better mechanistic understanding of PFAAs accumulation in crops and farm animals and addressing the data gaps about PFAAs fate in agricultural soil, together with the research on the toxicity of short-chain PFAAs, which would lead to better exposure predictions and control of PFAS risks.

6.5. References

- AECOM, 2018. Human Health Risk Assessment, RAAF Base Richmond PFAS Investigation, RAAF Base Richmond PFAS Investigation. Sydney.
- Almond, G.W., 1995. HOW MUCH WATER DO PIGS NEED?, in: Proceedings of the North Carolina Healthy Hogs Seminar. p. 1.
- ARPAV, 2019. Concentrations of the Perfluoroalkyl substances in the waters of Veneto region, Open data on PFASs monitoring, from 02/07/2013 to 11/04/2019 [WWW Document]. URL <https://www.arpa.veneto.it/dati-ambientali/open-data/idrosfera/concentrazione-di-sostanze-perfluoroalchiliche-pfas-nelle-acque-prelevate-da-arpav> (accessed 9.7.19).
- ARPAV, 2018. Contaminazione da PFAS Azioni ARPAV (PFAS contamination actions of the Regional Environmental Protection Agency of Veneto). Padova.
- ATSDR, 2018. Toxicological Profile for Polyfluoroalkyls - draft for Public Comment. Atlanta.
- Australian Government - Department of Defence, 2017. PFAS in Chicken Eggs – 2017 Study Findings RAAF Base Williamstown Stage 2B Environmental Investigation.
- Barbarossa, A., Gazzotti, T., Farabegoli, F., Mancini, F.R., Zironi, E., Badiani, A., Busani, L., Pagliuca, G., 2016. Comparison of perfluoroalkyl substances contamination in farmed and wild-caught European sea bass (*Dicentrarchus labrax*). *Food Control* 63, 224–229. <https://doi.org/10.1016/j.foodcont.2015.12.011>
- Bartell, S.M., 2017. Online serum PFOA calculator for adults. *Environ. Health Perspect.* 125, 1–3. <https://doi.org/10.1289/EHP2820>
- Blaine, A.C., Rich, C.D., Hundal, L.S., Lau, C., Mills, M.A., Harris, K.M., Higgins, C.P., 2013. Uptake of perfluoroalkyl acids into edible crops via land applied biosolids: Field and greenhouse studies. *Environ. Sci. Technol.* 47, 14062–14069. <https://doi.org/10.1021/es403094q>
- Blaine, A.C., Rich, C.D., Sedlacko, E.M., Hundal, L.S., Kumar, K., Lau, C., Mills, M.A., Harris, K.M., Higgins, C.P., 2014a. Perfluoroalkyl acid distribution in various plant compartments of edible crops grown in biosolids-amended soils. *Environ. Sci. Technol.* 48, 7858–7865. <https://doi.org/10.1021/es500016s>
- Blaine, A.C., Rich, C.D., Sedlacko, E.M., Hyland, K.C., Stushnoff, C., Dickenson, E., Higgins, C.P., 2014b. *supp_Perfluoroalkyl acid uptake in lettuce (Lactuca sativa) and strawberry (Fragaria ananassa) irrigated with reclaimed water.* *Environ. Sci. Technol.* <https://doi.org/10.1021/es504150h>
- Blaine, A.C., Rich, C.D., Sedlacko, E.M., Hyland, K.C., Stushnoff, C., Dickenson, E.R. V., Higgins, C.P., 2014c. Perfluoroalkyl Acid Uptake in Lettuce (*Lactuca sativa*) and Strawberry (*Fragaria ananassa*) Irrigated with Reclaimed Water. *Environ. Sci. Technol.* 48, 14361–14368. <https://doi.org/10.1021/es504150h>
- Brendel, S., Fetter, É., Staude, C., Vierke, L., Biegel-Engler, A., 2018. Short-chain perfluoroalkyl acids: environmental concerns and a regulatory strategy under REACH. *Environ. Sci. Eur.* 30, 9. <https://doi.org/10.1186/s12302-018-0134-4>
- Brunton, L.L., Lazo, J.S., Parker, K.L., 2005. Goodman & Gilman's The pharmacological basis of therapeutics, 11th ed, The Journal of Prosthetic Dentistry. <https://doi.org/10.1036/0071422803>

- Buck, R.C., Franklin, J., Berger, U., Conder, J.M., Cousins, I.T., de Voogt, P., Jensen, A.A., Kannan, K., Mabury, S.A., van Leeuwen, S.P., 2011. Perfluoroalkyl and polyfluoroalkyl substances in the environment: Terminology, classification, and origins. *Integr. Environ. Assess. Manag.* 7, 513–541. <https://doi.org/10.1002/ieam.258>
- Chang, S.C., Das, K., Ehresman, D.J., Ellefson, M.E., Gorman, G.S., Hart, J.A., Noker, P.E., Tan, Y.M., Lieder, P.H., Lau, C., Olsen, G.W., Butenhoff, J.L., 2008. Comparative pharmacokinetics of perfluorobutyrate in rats, mice, monkeys, and humans and relevance to human exposure via drinking water. *Toxicol. Sci.* 104, 40–53. <https://doi.org/10.1093/toxsci/kfn057>
- Chen, W.L., Bai, F.Y., Chang, Y.C., Chen, P.C., Chen, C.Y., 2018. Concentrations of perfluoroalkyl substances in foods and the dietary exposure among Taiwan general population and pregnant women. *J. Food Drug Anal.* 26, 994–1004. <https://doi.org/10.1016/j.jfda.2017.12.011>
- Chu, S., Wang, J., Leong, G., Woodward, L.A., Letcher, R.J., Li, Q.X., 2015. Perfluoroalkyl sulfonates and carboxylic acids in liver, muscle and adipose tissues of black-footed albatross (*Phoebastria nigripes*) from Midway Island, North Pacific Ocean. *Chemosphere* 138, 60–66. <https://doi.org/10.1016/j.chemosphere.2015.05.043>
- Cousins, I.T., Vestergren, R., Wang, Z., Scheringer, M., McLachlan, M.S., 2016. The precautionary principle and chemicals management: The example of perfluoroalkyl acids in groundwater. *Environ. Int.* 94, 331–340. <https://doi.org/10.1016/j.envint.2016.04.044>
- D'Hollander, W., Herzke, D., Huber, S., Hajslova, J., Pulkrabova, J., Brambilla, G., De Filippis, S.P., Bervoets, L., de Voogt, P., 2015. Occurrence of perfluorinated alkylated substances in cereals, salt, sweets and fruit items collected in four European countries. *Chemosphere* 129, 179–185. <https://doi.org/10.1016/j.chemosphere.2014.10.011>
- Dalsager, L., Christensen, N., Husby, S., Kyhl, H., Nielsen, F., Høst, A., Grandjean, P., Jensen, T.K., 2016. Association between prenatal exposure to perfluorinated compounds and symptoms of infections at age 1–4 years among 359 children in the Odense Child Cohort. *Environ. Int.* 96, 58–64. <https://doi.org/10.1016/j.envint.2016.08.026>
- Dauwe, T., Van de Vijver, K., De Coen, W., Eens, M., 2007. PFOS levels in the blood and liver of a small insectivorous songbird near a fluorochemical plant. *Environ. Int.* 33, 357–361. <https://doi.org/10.1016/j.envint.2006.11.014>
- Domingo, J.L., Ericson-Jogsten, I., Perelló, G., Nadal, M., Van Bavel, B., Kärrman, A., 2012a. Human exposure to perfluorinated compounds in Catalonia, Spain: Contribution of drinking water and fish and shellfish. *J. Agric. Food Chem.* 60, 4408–4415. <https://doi.org/10.1021/jf300355c>
- Domingo, J.L., Jogsten, I.E., Eriksson, U., Martorell, I., Perelló, G., Nadal, M., Bavel, B. Van, 2012b. Human dietary exposure to perfluoroalkyl substances in Catalonia, Spain. Temporal trend. *Food Chem.* 135, 1575–1582. <https://doi.org/10.1016/j.foodchem.2012.06.054>
- Domingo, J.L., Nadal, M., 2017a. Per- and Polyfluoroalkyl Substances (PFASs) in Food and Human Dietary Intake: A Review of the Recent Scientific Literature. *J. Agric. Food Chem.* 65, 533–543. <https://doi.org/10.1021/acs.jafc.6b04683>

- Domingo, J.L., Nadal, M., 2017b. Per- and polyfluoroalkyl substances (PFASs) in food and human dietary intake: A review of the recent scientific literature. *J. Agric. Food Chem.* 65, 533–543. <https://doi.org/10.1021/acs.jafc.6b04683>
- Droge, S.T.J., 2019. Membrane-Water Partition Coefficients to Aid Risk Assessment of Perfluoroalkyl Anions and Alkyl Sulfates. *Environ. Sci. Technol.* 53, 760–770. <https://doi.org/10.1021/acs.est.8b05052>
- EFSA, 2009. General principles for the collection of national food consumption data in the view of a pan-European dietary survey. *EFSA J.* 7(12), 1–51. <https://doi.org/10.2903/j.efsa.2009.1435>. Available
- EFSA, 2008. Perfluorooctane sulfonate (PFOS), perfluorooctanoic acid (PFOA) and their salts Scientific Opinion of the Panel on Contaminants in the Food chain. *EFSA J.* 6, 1–131. <https://doi.org/10.2903/j.efsa.2008.653>
- EFSA CONTAM, 2018. Risk to human health related to the presence of perfluorooctane sulfonic acid and perfluorooctanoic acid in food. *EFSA J.* 16, 284. <https://doi.org/10.2903/j.efsa.2018.5194>
- Falk, S., Stahl, T., Fliedner, A., Rüdell, H., Tarricone, K., Brunn, H., Koschorreck, J., 2019. Levels, accumulation patterns and retrospective trends of perfluoroalkyl acids (PFAAs) in terrestrial ecosystems over the last three decades. *Environ. Pollut.* 246, 921–931. <https://doi.org/10.1016/j.envpol.2018.12.095>
- FSANS, 2017. Consolidated Report - Perfluorinated chemicals in food .
- Gebbink, W.A., Letcher, R.J., 2012. Comparative tissue and body compartment accumulation and maternal transfer to eggs of perfluoroalkyl sulfonates and carboxylates in Great Lakes herring gulls. *Environ. Pollut.* 162, 40–47. <https://doi.org/10.1016/j.envpol.2011.10.011>
- Ghisi, R., Vamerali, T., Manzetti, S., 2019. Accumulation of perfluorinated alkyl substances (PFAS) in agricultural plants: A review. *Environ. Res.* 169, 326–341. <https://doi.org/10.1016/j.envres.2018.10.023>
- Gredelj, A., Nicoletto, C., Valsecchi, S., Ferrario, C., Polesello, S., Lava, R., Zanon, F., Barausse, A., Palmeri, L., Guidolin, L., Bonato, M., 2019a. Uptake and translocation of perfluoroalkyl acids (PFAA) in red chicory (*Cichorium intybus* L.) under various treatments with pre-contaminated soil and irrigation water. *Sci. Total Environ.* <https://doi.org/10.1016/j.scitotenv.2019.134766>
- Guruge, K.S., Noguchi, M., Yoshioka, K., Yamazaki, E., Taniyasu, S., Yoshioka, M., Yamanaka, N., Ikezawa, M., Tanimura, N., Sato, M., Yamashita, N., Kawaguchi, H., 2016. Microminipigs as a new experimental animal model for toxicological studies: Comparative pharmacokinetics of perfluoroalkyl acids. *J. Appl. Toxicol.* 36, 68–75. <https://doi.org/10.1002/jat.3145>
- Heo, J.J., Lee, J.W., Kim, S.K., Oh, J.E., 2014. Foodstuff analyses show that seafood and water are major perfluoroalkyl acids (PFAAs) sources to humans in Korea. *J. Hazard. Mater.* 279, 402–409. <https://doi.org/10.1016/j.jhazmat.2014.07.004>
- Herzke, D., Huber, S., Bervoets, L., D'Hollander, W., Hajslova, J., Pulkrabova, J., Brambilla, G., De Filippis, S.P., Klenow, S., Heinemeyer, G., de Voogt, P., 2013. Perfluorinated alkylated substances in vegetables collected in four European countries; occurrence and human

exposure estimations. *Environ. Sci. Pollut. Res.* 20, 7930–7939. <https://doi.org/10.1007/s11356-013-1777-8>

- Hlouskova, V., Hradkova, P., Poustka, J., Brambilla, G., De Filipps, S.P., D'Hollander, W., Bervoets, L., Herzke, D., Huber, S., de Voogt, P., Pulkrabova, J., 2013. Occurrence of perfluoroalkyl substances (PFASs) in various food items of animal origin collected in four European countries. *Food Addit. Contam. - Part A Chem. Anal. Control. Expo. Risk Assess.* 30, 1918–1932. <https://doi.org/10.1080/19440049.2013.837585>
- Hölzer, J., Göen, T., Just, P., Reupert, R., Rauchfuss, K., Kraft, M., Müller, J., Wilhelm, M., 2011. Perfluorinated compounds in fish and blood of anglers at Lake Möhne, Sauerland area, Germany. *Environ. Sci. Technol.* 45, 8046–8052. <https://doi.org/10.1021/es104391z>
- Houde, M., Martin, J.W., Letcher, R.J., Solomon, K.R., Muir, D.C.G., 2006. Biological monitoring of polyfluoroalkyl substances: A review. *Environ. Sci. Technol.* 40, 3463–3473. <https://doi.org/10.1021/es052580b>
- Hurtado, C., Domínguez, C., Pérez-Babace, L., Cañameras, N., Comas, J., Bayona, J.M., 2016. Estimate of uptake and translocation of emerging organic contaminants from irrigation water concentration in lettuce grown under controlled conditions. *J. Hazard. Mater.* <https://doi.org/10.1016/j.jhazmat.2015.11.039>
- Ingelido, A.M., Abballe, A., Gemma, S., Dellatte, E., Iacovella, N., Angelis, G. De, Zampaglioni, F., Marra, V., Miniero, R., Valentini, S., Russo, F., Vazzoler, M., Testai, E., Felip, E. De, 2018. Biomonitoring of per fluorinated compounds in adults exposed to contaminated drinking water in the Veneto Region, Italy. *Environ. Int.* 110, 149–159. <https://doi.org/10.1016/j.envint.2017.10.026>
- INRAN/CREA, 2010. L'indagine nazionale sui consumi alimentari in Italia: INRAN-SCAI 2005-06. Rome.
- Istituto Superiore di Sanità, 2019. CONTAMINAZIONE DA SOSTANZE PERFLUOROALCHILICHE IN VENETO VALUTAZIONE DELL'ESPOSIZIONE ALIMENTARE E CARATTERIZZAZIONE DEL RISCHIO (Contamination with the perfluoroalkyl substances in Veneto Exposure through food consumption and risk characterization). Rome.
- Kempisty, D.M., Xing, Y., Racz, L., 2018. Perfluoroalkyl Substances in the Environment: Theory, Practice and Innovation, Environmental and occupational health series. CRC Press, Boca Raton. <https://doi.org/10.1201/9780429487125>
- Klenow, S., Heinemeyer, G., Brambilla, G., Dellatte, E., Herzke, D., de Voogt, P., 2013. Dietary exposure to selected perfluoroalkyl acids (PFAAs) in four European regions. *Food Addit. Contam. - Part A Chem. Anal. Control. Expo. Risk Assess.* 30, 2141–2151. <https://doi.org/10.1080/19440049.2013.849006>
- Kowalczyk, J., Ehlers, S., Oberhausen, A., Tischer, M., Fürst, P., Schafft, H., Lahrssen-Wiederholt, M., 2013. Absorption, distribution, and milk secretion of the perfluoroalkyl acids PFBS, PFHxS, PFOS, and PFOA by dairy cows fed naturally contaminated feed. *J. Agric. Food Chem.* 61, 2903–2912. <https://doi.org/10.1021/jf304680j>
- Krafft, M.P., Riess, J.G., 2015. Per- and polyfluorinated substances (PFASs): Environmental challenges. *Curr. Opin. Colloid Interface Sci.* 20, 192–212. <https://doi.org/10.1016/j.cocis.2015.07.004>

- Krippner, J., Falk, S., Brunn, H., Georgii, S., Schubert, S., Stahl, T., 2015. Accumulation Potentials of Perfluoroalkyl Carboxylic Acids (PFCAs) and Perfluoroalkyl Sulfonic Acids (PFSA) in Maize (*Zea mays*). *J. Agric. Food Chem.* 63, 3646–3653. <https://doi.org/10.1021/acs.jafc.5b00012>
- Leclercq, C., Arcella, D., Piccinelli, R., Sette, S., Le Donne, C., 2009. The Italian National Food Consumption Survey INRAN-SCAI 2005–06: main results in terms of food consumption. *Public Health Nutr.* 12, 2504–2532. <https://doi.org/10.1017/S1368980009005035>
- Legind, C.N., Trapp, S., 2009. Modeling the exposure of children and adults via diet to chemicals in the environment with crop-specific models. *Environ. Pollut.* 157, 778–785. <https://doi.org/10.1016/j.envpol.2008.11.021>
- Liu, Z., Lu, Y., Shi, Y., Wang, P., Jones, K., Sweetman, A.J., Johnson, A.C., Zhang, M., Zhou, Y., Lu, X., Su, C., Sarvajayakesavaluc, S., Khan, K., 2017. Crop bioaccumulation and human exposure of perfluoroalkyl acids through multi-media transport from a mega fluorochemical industrial park, China. *Environ. Int.* 106, 37–47. <https://doi.org/10.1016/j.envint.2017.05.014>
- Liu, Z., Lu, Y., Song, X., Jones, K., Sweetman, A.J., Johnson, A.C., Zhang, M., Lu, X., Su, C., 2019. Multiple crop bioaccumulation and human exposure of perfluoroalkyl substances around a mega fluorochemical industrial park, China: Implication for planting optimization and food safety. *Environ. Int.* 127, 671–684. <https://doi.org/10.1016/j.envint.2019.04.008>
- Liu, Z., Lu, Y., Wang, T., Wang, P., Li, Q., Johnson, A.C., Sarvajayakesavalu, S., Sweetman, A.J., 2016. Risk assessment and source identification of perfluoroalkyl acids in surface and ground water: Spatial distribution around a mega-fluorochemical industrial park, China. *Environ. Int.* 91, 69–77. <https://doi.org/10.1016/j.envint.2016.02.020>
- Lorber, M., Egeghy, P.P., 2011. Simple intake and pharmacokinetic modeling to characterize exposure of Americans to perfluorooctanoic acid, PFOA. *Environ. Sci. Technol.* 45, 8006–8014. <https://doi.org/10.1021/es103718h>
- Lupton, S.J., Dearfield, K.L., Johnston, J.J., Wagner, S., Huwe, J.K., 2015. Perfluorooctane Sulfonate Plasma Half-Life Determination and Long-Term Tissue Distribution in Beef Cattle (*Bos taurus*). *J. Agric. Food Chem.* 63, 10988–10994. <https://doi.org/10.1021/acs.jafc.5b04565>
- Lupton, S.J., Huwe, J.K., Smith, D.J., Dearfield, K.L., Johnston, J.J., 2014a. Distribution and excretion of perfluorooctane sulfonate (PFOS) in beef cattle (*bos taurus*). *J. Agric. Food Chem.* 62, 1167–1173. <https://doi.org/10.1021/jf404355b>
- Lupton, S.J., Huwe, J.K., Smith, D.J., Dearfield, K.L., Johnston, J.J., 2014b. Distribution and excretion of perfluorooctane sulfonate (PFOS) in beef cattle (*bos taurus*). *J. Agric. Food Chem.* 62, 1167–1173. <https://doi.org/10.1021/jf404355b>
- Lupton, S.J., Huwe, J.K., Smith, D.J., Dearfield, K.L., Johnston, J.J., 2012. Absorption and excretion of ¹⁴C-perfluorooctanoic acid (PFOA) in Angus cattle (*Bos taurus*). *J. Agric. Food Chem.* 60, 1128–1134. <https://doi.org/10.1021/jf2042505>
- McLachlan, M.S., Felizeter, S., Klein, M., Kotthoff, M., De Voogt, P., 2019. Fate of a perfluoroalkyl acid mixture in an agricultural soil studied in lysimeters. *Chemosphere* 223, 180–187. <https://doi.org/10.1016/j.chemosphere.2019.02.012>

- McLachlan, M.S., Holmstro, K.E., Reth, M., Berger, U., 2007. Riverine Discharge of Perfluorinated Carboxylates from the European Continent. *Environ. Sci. Technol.* 41, 7260–7265. <https://doi.org/10.1021/es071471p>
- Munsch, C., Marchand, P., Venisseau, A., Veyrand, B., Zeng, Z., 2013. Levels and trends of the emerging contaminants HBCDs (hexabromocyclododecanes) and PFCs (perfluorinated compounds) in marine shellfish along French coasts. *Chemosphere* 91, 233–240. <https://doi.org/10.1016/j.chemosphere.2012.12.063>
- Ng, C.A., Hungerbühler, K., 2014. Bioaccumulation of perfluorinated alkyl acids: Observations and models. *Environ. Sci. Technol.* 48, 4637–4648. <https://doi.org/10.1021/es404008g>
- Nicoletto, C., Maucieri, C., Sambo, P., 2017. Effects on Water Management and Quality Characteristics of Ozone Application in Chicory Forcing Process: A Pilot System. *Agronomy* 7, 29. <https://doi.org/10.3390/agronomy7020029>
- Noorlander, C.W., Van Leeuwen, S.P.J., Te Biesebeek, J.D., Mengelers, M.J.B., Zeilmaker, M.J., 2011. Levels of perfluorinated compounds in food and dietary intake of PFOS and PFOA in the Netherlands. *J. Agric. Food Chem.* 59, 7496–7505. <https://doi.org/10.1021/jf104943p>
- Numata, J., Kowalczyk, J., Adolphs, J., Ehlers, S., Schafft, H., Fuerst, P., Müller-Graf, C., Lahrssen-Wiederholt, M., Greiner, M., 2014. Toxicokinetics of Seven Perfluoroalkyl Sulfonic and Carboxylic Acids in Pigs Fed a Contaminated Diet. *J. Agric. Food Chem.* 62, 6861–6870. <https://doi.org/10.1021/jf405827u>
- OECD/UNEP Global PFC Group, 2013. Synthesis paper on per- and polyfluorinated chemicals (PFCs). *OECD Environ. Heal. Saf. Publ.* 1–58.
- Papadopoulou, E., Poothong, S., Koekkoek, J., Lucattini, L., Padilla-Sánchez, J.A., Haugen, M., Herzke, D., Valdersnes, S., Maage, A., Cousins, I.T., Leonards, P.E.G., Småstuen Haug, L., 2017. Estimating human exposure to perfluoroalkyl acids via solid food and drinks: Implementation and comparison of different dietary assessment methods. *Environ. Res.* 158, 269–276. <https://doi.org/10.1016/j.envres.2017.06.011>
- Pelch, K.E., Reade, A., Wolffe, T.A.M., Kwiatkowski, C.F., 2019. PFAS health effects database: Protocol for a systematic evidence map. *Environ. Int.* 130. <https://doi.org/10.1016/j.envint.2019.05.045>
- Pérez, F., Nadal, M., Navarro-Ortega, A., Fàbrega, F., Domingo, J.L., Barceló, D., Farré, M., 2013. Accumulation of perfluoroalkyl substances in human tissues. *Environ. Int.* 59, 354–362. <https://doi.org/10.1016/j.envint.2013.06.004>
- Prevedouros, K., Cousins, I.T., Buck, R.C., Korzeniowski, S.H., 2006. Sources, fate and transport of perfluorocarboxylates. *Environ. Sci. Technol.* 40, 32–44. <https://doi.org/10.1021/es0512475>
- Rivière, G., Sirot, V., Tard, A., Jean, J., Marchand, P., Veyrand, B., Le Bizec, B., Leblanc, J.C., 2014. Food risk assessment for perfluoroalkyl acids and brominated flame retardants in the French population: Results from the second French total diet study. *Sci. Total Environ.* 491–492, 176–183. <https://doi.org/10.1016/j.scitotenv.2014.01.104>
- Ross, I., McDonough, J., Miles, J., Storch, P., Thelakkat Kochunarayanan, P., Kalve, E., Hurst, J., S. Dasgupta, S., Burdick, J., 2018. A review of emerging technologies for remediation of PFASs. *Remediation* 28, 101–126. <https://doi.org/10.1002/rem.21553>

- Squadrone, S., Ciccotelli, V., Favaro, L., Scanzio, T., Prearo, M., Abete, M.C., 2014. Fish consumption as a source of human exposure to perfluorinated alkyl substances in Italy: Analysis of two edible fish from Lake Maggiore. *Chemosphere* 114, 181–186. <https://doi.org/10.1016/j.chemosphere.2014.04.085>
- Steenland, K., Tinker, S., Frisbee, S., Ducatman, A., Vaccarino, V., 2009. Association of perfluorooctanoic acid and perfluorooctane sulfonate with serum lipids among adults living near a chemical plant. *Am. J. Epidemiol.* 170, 1268–1278. <https://doi.org/10.1093/aje/kwp279>
- Su, H., Shi, Y., Lu, Y., Wang, P., Zhang, M., Sweetman, A., Jones, K., Johnson, A., 2017. Home produced eggs: An important pathway of human exposure to perfluorobutanoic acid (PFBA) and perfluorooctanoic acid (PFOA) around a fluorochemical industrial park in China. *Environ. Int.* 101, 1–6. <https://doi.org/10.1016/j.envint.2017.01.016>
- Sznajder-Katarzyńska, K., Surma, M., Cieślak, I., 2019. A Review of Perfluoroalkyl Acids (PFAAs) in terms of Sources, Applications, Human Exposure, Dietary Intake, Toxicity, Legal Regulation, and Methods of Determination. *J. Chem.* 2019. <https://doi.org/10.1155/2019/2717528>
- Tarazona, J. V., Rodríguez, C., Alonso, E., Sáez, M., González, F., San Andrés, M.D., Jiménez, B., San Andrés, M.I., 2015. Toxicokinetics of perfluorooctane sulfonate in birds under environmentally realistic exposure conditions and development of a kinetic predictive model. *Toxicol. Lett.* 232, 363–368. <https://doi.org/10.1016/j.toxlet.2014.11.022>
- Taylor, M.D., Beyer-Robson, J., Johnson, D.D., Knott, N.A., Bowles, K.C., 2018. Bioaccumulation of perfluoroalkyl substances in exploited fish and crustaceans: Spatial trends across two estuarine systems. *Mar. Pollut. Bull.* 131, 303–313. <https://doi.org/10.1016/j.marpolbul.2018.04.029>
- Trapp, S., 2015. Calibration of a plant uptake model with plant- and site-specific data for uptake of chlorinated organic compounds into radish. *Environ. Sci. Technol.* 49, 395–402. <https://doi.org/10.1021/es503437p>
- Travis, C.C., Arms, A.D., 1988. Bioconcentration of organics in beef, milk, and vegetation. *Environ. Sci. Technol.* 22, 271–274. <https://doi.org/10.1021/es00168a005>
- Trier, X., Granby, K., Christensen, J.H., 2011. Polyfluorinated surfactants (PFS) in paper and board coatings for food packaging. *Environ. Sci. Pollut. Res.* 18, 1108–1120. <https://doi.org/10.1007/s11356-010-0439-3>
- USEPA, 2016a. Drinking Water Health Advisory for perfluorooctanoic acid (PFOA). Washington DC.
- USEPA, 2016b. Drinking Water Health Advisory for Perfluorooctane Sulfonate (PFOS). Washington DC. <https://doi.org/10.1016/j.str.2011.03.017>
- USEPA, 2005. Human Health Risk Assessment Protocol for Hazardous Waste Combustion Facilities.
- Vassiliadou, I., Costopoulou, D., Kalogeropoulos, N., Karavoltsos, S., Sakellari, A., Zafeiraki, E., Dassenakis, M., Leondiadis, L., 2015. Levels of perfluorinated compounds in raw and cooked Mediterranean finfish and shellfish. *Chemosphere* 127, 117–126. <https://doi.org/10.1016/j.chemosphere.2014.12.081>

- Vestergren, R., Berger, U., Glynn, A., Cousins, I.T., 2012. Dietary exposure to perfluoroalkyl acids for the Swedish population in 1999, 2005 and 2010. *Environ. Int.* 49, 120–127. <https://doi.org/10.1016/j.envint.2012.08.016>
- Vestergren, R., Cousins, I.T., 2009. Tracking the Pathways of Human Exposure to Perfluorocarboxylates. *Environ. Sci. Technol.* 43, 5565–5575. <https://doi.org/10.1021/es900228k>
- Vestergren, R., Orata, F., Berger, U., Cousins, I.T., 2013. Bioaccumulation of perfluoroalkyl acids in dairy cows in a naturally contaminated environment. *Environ. Sci. Pollut. Res.* 20, 7959–7969. <https://doi.org/10.1007/s11356-013-1722-x>
- Vicente, J., Sanpera, C., García-Tarrasón, M., Pérez, A., Lacorte, S., 2015. Perfluoroalkyl and polyfluoroalkyl substances in entire clutches of Audouin's gulls from the Ebro delta. *Chemosphere* 119, S62–S68. <https://doi.org/10.1016/j.chemosphere.2014.04.041>
- Vierke, L., Möller, A., Klitzke, S., 2014. Transport of perfluoroalkyl acids in a water-saturated sediment column investigated under near-natural conditions. *Environ. Pollut.* 186, 7–13. <https://doi.org/10.1016/j.envpol.2013.11.011>
- Wang, X., Zhang, R., Zhang, H., Wang, Y., 2017. The occurrence, exposure and risk assessment of perfluoroalkyl acids in food from mainland, China. *Food Addit. Contam. - Part A Chem. Anal. Control. Expo. Risk Assess.* 34, 1990–1998. <https://doi.org/10.1080/19440049.2017.1347282>
- Wang, Y., Fu, J., Wang, T., Liang, Y., Pan, Y., Cai, Y., Jiang, G., 2010. Distribution of perfluorooctane sulfonate and other perfluorochemicals in the ambient environment around a manufacturing facility in china. *Environ. Sci. Technol.* 44, 8062–8067. <https://doi.org/10.1021/es101810h>
- Wang, Y., Liu, J., Li, J., Zhao, Y., Wu, Y., 2019. Dietary Exposure of Chinese Adults to Perfluoroalkyl Acids via Animal-Origin Foods: Chinese Total Diet Study (2005-2007 and 2011-2013). *J. Agric. Food Chem.* 67, 6048–6055. <https://doi.org/10.1021/acs.jafc.9b01108>
- Wang, Z., Xie, Z., Mi, W., Möller, A., Wolschke, H., Ebinghaus, R., 2015. Neutral Poly/Per-Fluoroalkyl Substances in Air from the Atlantic to the Southern Ocean and in Antarctic Snow. *Environ. Sci. Technol.* 49, 7770–7775. <https://doi.org/10.1021/acs.est.5b00920>
- Wen, B., Li, L., Zhang, H., Ma, Y., Shan, X.Q., Zhang, S., 2014. Field study on the uptake and translocation of perfluoroalkyl acids (PFAAs) by wheat (*Triticum aestivum* L.) grown in biosolids-amended soils. *Environ. Pollut.* 184, 547–554. <https://doi.org/10.1016/j.envpol.2013.09.040>
- WHO, 2016. Keeping our water clean: the case of water contamination in the Veneto Region, Italy. AREAGRAPHICA SNC DI TREVISAN GIANCARLO & FIGLI, Venice, Italy.
- Wu, Y., Wang, Y., Li, J., Zhao, Y., Guo, F., Liu, J., Cai, Z., 2012. Perfluorinated compounds in seafood from coastal areas in China. *Environ. Int.* 42, 67–71. <https://doi.org/10.1016/j.envint.2011.04.007>
- Xiao, F., 2017. Emerging poly- and perfluoroalkyl substances in the aquatic environment: A review of current literature. *Water Res.* 124, 482–495. <https://doi.org/10.1016/j.watres.2017.07.024>
- Yamada, A., Bemrah, N., Veyrand, B., Pollono, C., Merlo, M., Desvignes, V., Sirot, V., Oseredczuk, M., Marchand, P., Cariou, R., Antignac, J.P., Le Bizec, B., Leblanc, J.C., 2014. Perfluoroalkyl

acid contamination and polyunsaturated fatty acid composition of french freshwater and marine fishes. *J. Agric. Food Chem.* 62, 7593–7603. <https://doi.org/10.1021/jf501113j>

Yeung, L.W.Y., Loi, E.I.H., Wong, V.Y.Y., Guruge, K.S., Yamanaka, N., Tanimura, N., Hasegawa, J., Yamashita, N., Miyazaki, S., Lam, P.K.S., 2009. Biochemical responses and accumulation properties of long-chain perfluorinated compounds (PFOS/PFDA/PFOA) in juvenile chickens (*Gallus gallus*). *Arch. Environ. Contam. Toxicol.* 57, 377–386. <https://doi.org/10.1007/s00244-008-9278-3>

Yoo, H., Guruge, K.S., Yamanaka, N., Sato, C., Mikami, O., Miyazaki, S., Yamashita, N., Giesy, J.P., 2009. Depuration kinetics and tissue disposition of PFOA and PFOS in white leghorn chickens (*Gallus gallus*) administered by subcutaneous implantation. *Ecotoxicol. Environ. Saf.* 72, 26–36. <https://doi.org/10.1016/j.ecoenv.2007.09.007>

Zafeiraki, E., Costopoulou, D., Vassiliadou, I., Leondiadis, L., Dassenakis, E., Hoogenboom, R.L.A.P., van Leeuwen, S.P.J., 2016. Perfluoroalkylated substances (PFASs) in home and commercially produced chicken eggs from the Netherlands and Greece. *Chemosphere* 144, 2106–2112. <https://doi.org/10.1016/j.chemosphere.2015.10.105>

Zareitalabad, P., Siemens, J., Hamer, M., Amelung, W., 2013. Perfluorooctanoic acid (PFOA) and perfluorooctanesulfonic acid (PFOS) in surface waters, sediments, soils and wastewater - A review on concentrations and distribution coefficients. *Chemosphere* 91, 725–732. <https://doi.org/10.1016/j.chemosphere.2013.02.024>

Zeng, X.-W., Qian, Z., Emo, B., Vaughn, M., Bao, J., Qin, X.-D., Zhu, Y., Li, J., Lee, Y.L., Dong, G.-H., 2015. Association of polyfluoroalkyl chemical exposure with serum lipids in children. *Sci. Total Environ.* 512–513, 364–370. <https://doi.org/10.1016/j.scitotenv.2015.01.042>

Chapter 7

Conclusions

Understanding the transport, fate and behavior of perfluoroalkyl acids is essential for addressing the risks of these persistent, bioaccumulative and toxic contaminants. By being ionic surfactants and both hydrophobic and lipophobic within the same molecule, PFAAs exhibit an untypical behavior when compared to other groups of neutral organic pollutants. Their affinity for proteins and phospholipid membranes is what makes the common risk assessment approaches, mainly relying on the partitioning in storage lipids, inapplicable and unfeasible for PFAAs. Hence, the objectives of this thesis were to address the knowledge gaps and provide new insights regarding the fate and behavior of PFAAs, from 1) the ecological risk assessment point of view and 2) in terrestrial agronomic ecosystems, as the main pathway of PFAAs into the terrestrial food webs. Overall, the main emphasis has been put on short-chain, unregulated PFAAs, and on a PFAAs contamination case of the Veneto Region.

7.1. Major findings and their significance

In **Chapter 2**, two regulated and one newly proposed method, were used for deriving the ecological risk thresholds of two legacy long-chain PFAAs, PFOA and PFOS, two short-chain PFAAs, PFBA and PFBS, as their common substitutes and two well studied emerging contaminants (LAS and triclosan) for the comparison. The newly proposed methodology, based on the ecological and chemicals fate model AQUATOX (USEPA), revealed that, by including ecological relationships and indirect and sublethal effects of chemicals, a fuller picture of the concentration-response of PFAAs can be obtained, while compared to two regulation-based methods, assessment factor (AF) and species sensitivity distribution (SSD). For example, predicted no-effect concentration (PNEC) for PFOS, known for being both bioaccumulative and biomagnifying, resulted with a value of 3.6% of the currently accepted annual average environmental quality standard for PFOS in freshwater. This work introduced the approach that was able to provide a more complete picture in the characterization of the ecological risk thresholds for PFAAs by including ecological relationships among species of the local ecosystem and providing a possible base for the future ERA. It has the potential as the midpoint between commonly applied (regulated) conservative methods and expensive and time-consuming micro- and macrocosm studies.

Chapters 3-5 provide a combination of experimental and modelling approaches for addressing the fate of PFAAs in agronomic ecosystems, from the contaminated water and soil, in the separate and combined exposure, to their uptake in a model crop, red chicory. In **Chapter 3**, full-scale experimental setup, with the exposure of red chicory to nine PFAAs through the pre-contaminated soil, contaminated irrigation water and their combination was presented. The importance of the delivery media when assessing the PFAAs bioaccumulation in edible plants was emphasized. With water as the main transportation route of PFAAs in the environment, irrigation with the contaminated water is an important source of PFAAs to soil and to agricultural food webs, particularly in contaminated areas. The use of contaminated water increased the uptake of long-chain PFAAs into shoots, including the edible chicory part (head), while pre-contaminated soil condition increased the uptake of short-chain PFAAs, suggesting that the scenario of years-long irrigation may be the worst-case scenario. Sorption to agronomic soil was assessed with the laboratory batch tests for deriving soil to water partition coefficients and was evaluated by the measured vertical distribution of PFAAs in agricultural soil, revealing the importance of other influential factors (but solely sorption) on PFAAs mobility and bioavailability in soil (e.g. water seepage through soil). For the first time, measured inter-compartmental PFAAs concentrations in plants, soil and water were accompanied by soil-water adsorption/desorption partition coefficients and with plant-specific parameters, as the growth and transpiration, providing an essential experimental base for the modelling of PFAAs uptake into plants.

In **Chapter 4**, these experimental results were synthesized in so-called, standard plant uptake model (Trapp, 2015, 2007; Trapp and Matthies, 1995), widely used in the risk assessment of chemicals. However, being primarily developed for the neutral, non polar chemicals, the modelling approach needed to be adapted for PFAAs, by avoiding the usually-applied regressions based on octanol-water partition coefficient (K_{OW}). A new parameter (R) for the slow transfer of PFAAs through the membranes of root epidermis was introduced to explain the low values of transpiration stream concentration factors reported in literature. The bases for this modelling approach were parameter R , empirical root to soil bioconcentration factor (RCF_{dw}) and soil-water partition coefficients. This semi-empirical approach was successfully applied to other crop types and revealed new insights in uptake and bioaccumulation processes. High bioaccumulation potential of short-chain PFAAs in plants was explained in the terms of their high root to xylem partitioning in the combination with low soil sorption and also with never-establishing steady-state condition in shoots: as non-volatile ionics, short-chain PFAAs will accumulate in the aerial plant parts as long as there is a contamination source and as long as plant transpires. This makes long-maturing crops exposed in highly contaminated areas a potentially significant exposure source of PFAAs to humans. The model was able to account for the exposure pathway, soil sorption, exposure time and inter-species plant variability to some extent, providing a step forward in the human health exposure assessment through crops consumption.

Chapter 5 further expanded the insights regarding the red chicory exposure to PFAAs, by introducing the exposure scenario with nine PFAAs in a hydroponic set-up, i.e. by eliminating the effects of soil sorption on PFAAs bioavailability to roots. The hydroponic exposure of crops to PFAAs mixtures is not novelty by itself, but parallel experiments for the same crop in both soil (Chapter 3) and hydroponics were not performed until now. Additionally, in the given experimental set-up, PFAAs induced visible phytotoxic effects in red chicory, in the concentrations that were the lowest among so far reported in literature. The mixture of PFAAs caused the growth inhibition of chicory plants in two higher exposure concentrations (125 and 250 $\mu\text{g/L}$), also showing a visible root damage and leaves yellowing (i.e. the lowering of relative chlorophyll content). A potential increase in root permeability under these high PFAA exposure concentrations in hydroponic set-up was hypothesized as the reason for almost constant TSCFs amongst PFAAs, in contrary to soil experiment and also to other scientific findings resulting from lower exposure concentrations in both soil and hydroponics. Additionally, developmental differences between the root systems formed in soil and nutrient solution, with the competitive PFAAs sorption to roots in hydroponics, were speculated as the main reasons of differences in root concentration factors and also partially in TSCFs. Consequently, direct extrapolation of hydroponically derived bioaccumulation and translocation factors in the human exposure assessment via dietary intake from agronomic ecosystems is questionable, as PFAAs behavior very much differs in hydroponic when compared to soil system. Hence, the use of factors derived in hydroponic experiments could lead to the over- or under-prediction of actual exposure for some PFAAs.

Finally, in **Chapter 6**, the semi-empirical crop uptake model for PFAAs, developed in Chapter 4, was expanded for various crops and connected with single-compartment pharmacokinetic models for farm animals into hypothetical agronomic ecosystem, exposed to PFAAs via contaminated water used for irrigation and animal feed consumption. A PFAS contamination case of the Veneto Region was used for the establishment of exposure scenarios with the varying surface- and groundwater concentrations from regional 6-years monitoring campaign. The modelling framework was connected to the food intake data for North-Eastern Italian population and used for the estimations of dietary intake and contribution of short- and long-chain PFAAs to human diet, both from the food of animal and plant origin. In addition, crop models were successfully validated with the multi-media

PFAAs concentration measurements around a fluorochemical plant in China. The models were able to reproduce PFAAs ratios based on the measured concentrations of PFAAs mixtures in the water used for irrigation and account for the crop uptake preferences of short-chain PFAAs. In general, the modelling framework resulted with dietary exposure concentrations in realistic range between the measured concentrations characteristic for background exposure and the highly contaminated areas. Possibly, the models could be useful in the estimation of potential animal and crop exposure and consequentially the exposure of humans, when only water concentrations are available in a certain area. Finally, in the long-term irrigation scenario, simulations have shown that the total dietary exposure to short-chain PFAAs through crop consumption can exceed the exposure to PFOS and PFOA mainly resulting from the consumption of animal produce.

In general, there is a need for integrated approach in PFASs risk assessment, as they are a large group of chemicals that commonly persists in the environmental matrices as complex mixtures. A combination of experimental and modelling approaches applied here shows that new insights can be obtained when synthesizing measured data, data from controlled experiments and models.

7.2. Future perspectives and further research

This thesis work addresses some of the data gaps and provides new insights of the complex behavior of PFAAs, which may prove to be useful for human health and ecological risk assessment. However, there is a space for expansion and further research:

- Results from this work showed that the ecological thresholds derived with regulated, simple methods, may be too high for protecting aquatic ecosystems as a whole (i.e. as in the case of PFOS). More research towards comprehensive ecological risk assessment is needed, particularly for the PFAS mixtures and not only individual compounds, as they are commonly present in environmental matrices as mixtures. Considering the complex behavior of PFAAs, their high mobility and ubiquitous presence, generally more work is needed to protect aquatic and terrestrial species, as some PFAS are proven or suspected toxicants. Hence, more research work on the ecotoxicology of PFAS to wildlife is needed. Accounting of the indirect ecological effects and lethal and sublethal toxicity should be a way forward not only for PFAAs, but also in the general approach to the ecological risk assessment of any chemical.
- More research still needs to be carried out to construct well-validated ecosystem models robustly based on a large amount of biomonitoring data, which are currently scarce. Additionally, more work needs to be done for standardizing of the modelling approaches, as this is the only way forward for their full inclusion and application in regulatory ecological risk assessment.
- Given the high bioaccumulation potential of short-chain PFAAs in edible crops, more research is needed towards the human toxicity assessment of these compounds. Human toxicity studies are still mainly focused on PFOS, PFOA and other regulated long-chain PFASs. Considering the main production shift towards short-chain and other substitute PFAS, efforts need to be put in determining the safe exposure limits for these PFASs. For now, dietary exposure limits and drinking water thresholds are mainly given only for PFOS and PFOA.
- The hydroponic study has shown that phytotoxic effects can be manifested under concentrations lower than usually regarded as toxic to plants and when PFAAs are present as mixtures. Toxicity to plants is less studied than toxicity to animals, but can have great implications on PFAS uptake and bioaccumulation, e.g. in phytoremediation, which has shown a great potential as the elimination technique for short-chain PFAAs, both from soil and water.

- In this thesis, some mechanistic insights are given regarding the crop uptake of PFAAs from soil, either from pre-contaminated soil or via the irrigation water or from the nutrient solution. However, more research is needed to improve mechanistic understanding and allow for the prediction of PFAAs uptake to plants under any given exposure scenario. The crop-specificity is known to influence plant uptake of PFAAs and soil-specificity is known to effect sorption of PFAAs to soil, but a full understanding of underlying processes is still lacking.
- With this research implying that the use of contaminated water may result with the higher bioaccumulation of PFAAs in plant compartments, more crops should be tested under the irrigation water exposure conditions. Additionally, further experimentation, which would take into account soil permeability and leaching of short-chain PFAAs from soil, is highly needed.

References

- Trapp, S., 2015. Calibration of a plant uptake model with plant- and site-specific data for uptake of chlorinated organic compounds into radish. *Environ. Sci. Technol.* 49, 395–402. <https://doi.org/10.1021/es503437p>
- Trapp, S., 2007. Fruit tree model for uptake of organic compounds from soil and air. SAR QSAR *Environ. Res.* 18, 367–387. <https://doi.org/10.1080/10629360701303693>
- Trapp, S., Matthies, M., 1995. Generic One-Compartment Model for Uptake of Organic Chemicals by Foliar Vegetation. *Environ. Sci. Technol.* 29, 2333–2338. <https://doi.org/10.1021/es00009a027>

Appendices

APPENDIX 1: Supplementary information for Chapter 2

Deriving predicted no-effect concentrations (PNECs) for emerging contaminants in the river Po, Italy, using three approaches: assessment factor, species sensitivity distribution and AQUATOX ecosystem modeling

Andrea Gredeļj^a, Alberto Barausse^a, Laura Grechi^a, Luca Palmeri^a

^a Environmental Systems Analysis Lab (LASA) research group, Department of Industrial Engineering, University of Padova, via Marzolo 9, 35131 Padova, Italy

ECOTOXICITY DATA

In the following tables, the collected ecotoxicity data for LAS, TCS, PFOS, PFOA, PFBS and PFBA are reported. When more than one ecological threshold data were available for the same species, long-term toxicity data points were chosen.

Table A1-1. Ecotoxicology data of Po associated species for LAS

Trophic level	Po species	Selected species	Endpoint	Effect measurement	Exposure duration	Value	Unit	Reference
Algae	Diatoms							
	<i>Nitzschia</i>	<i>Nitzschia linearis</i>	LC50	Mortality	5 days	10 000	µg/L	(Patrick et al., 1968)
	<i>Diatoma</i>	<i>Diatoma sp.</i>	NOEC	Chlorophyll A concentration	4.5 days	450	µg/L	(Jørgensen and Christoffersen, 2000)
	<i>Navicula</i>	<i>Navicula Pelliculosa</i>	EC50	Abundance	96 hours	1400	µg/L	(Lewis and Hamm, 1986)
	Chlorophyceae (Green)							
	<i>Chlamydomonas sp.</i>	<i>Chlamydomonas variabilis</i>	EC50	Intoxication	240 min	3 570	µg/L	(Lundahl and Cabridenc, 1978)
		<i>Chlorophyta (Green Algae Division)</i>	NOEC	Abundance	4.5 days	410	µg/L	(Jørgensen and Christoffersen, 2000)
	Chryptophyceae							
		<i>Cryptophycophyta (Cryptomonad Division)</i>	NOEC	Chlorophyll A concentration	4.5 days	140	µg/L	(Jørgensen and Christoffersen, 2000)
	Cyanobacteria (Blue Green)							
	<i>Cyanophycota (Blue-Green Algae Phylum)</i>	NOEC	Abundance	4.5 days	240	µg/L	(Jørgensen and Christoffersen, 2000)	
Invertebrates	Rotifers							
	<i>Brachionus calyciflorus</i>	<i>Brachionus calyciflorus</i>	NOEC	reproduction	48 hours	2 500	µg/L	(Radix et al., 1999)
	Diptera							
	<i>Chironomus</i>	<i>Chironomus riparius</i>	NOEC	Emergence	24 days	2 400	µg/L	(Pittinger et al., 1989)
	Gastropoda							
	<i>Physa</i>	<i>Physa integra (Pouch Snail)</i>	EC50	Immobile	4 days	8 933	µg/L	(Arthur, 1970)
Tricladida								
<i>Dugesia sp.</i>	<i>Dugesia sp. (Turbellarian, Flatworm)</i>	LC50	Mortality	2 days	1 800	µg/L	(Lewis and Suprenant, 1983)	

	Isopoda							
	<i>Asellus aquaticus</i>	<i>Asellus</i> sp. (Aquatic Sowbug)	LC50	Mortality	2 days	270 000	µg/L	(Lewis and Suprenant, 1983)
Fishes	Ciprinides							
	<i>Alburnus alburnus alborella</i>	<i>Alburnus alburnus</i> (Bleak)	LC50	Mortality	2 days	13 900	µg/L	(Guerra and Comodo, 1972)
	<i>Cyprinus carpio</i>	<i>Cyprinus carpio</i> (Common Carp)	LC50	Mortality	4 days	5 130 ¹	µg/L	(Lopez-Zavala et al., 1975; Rehwoldt et al., 1974)
	<i>Carassius carassius</i>	<i>Carassius auratus</i> (Goldfish)	LC50	Mortality	4 days	6 169	µg/L	(Tsai and McKee, 1980)
	<i>Rutilus erythrophthalm</i>	<i>Rutilus kutum</i>	LC50	Mortality	4 days	10 455	µg/L	(Tehranifard et al., 2010)
	<i>Barbus plebejus</i>	<i>Barbus gonionotus</i> (Silver barb)	LC50	Mortality	4 days	12 144 ²	µg/L	(Eyanoer et al., 1985; Jangchudjai et al., 1987)
	Sunfishes							
	<i>Lepomis gibbosus</i>	<i>Lepomis gibbosus</i>	LC50	Mortality	4 days	2 700	µg/L	(Rehwoldt et al., 1974)
	Anguillidae							
	<i>Anguilla anguilla</i>	<i>Anguilla rostrata</i> (American Eel)	LC50	Mortality	4 days	2 000	µg/L	(Rehwoldt et al., 1974)
	Ictaluridae							
	<i>Ictalurus melas</i>	<i>Ameiurus melas</i> (Black Bullhead)	LC50	Mortality	4 days	6 400	µg/L	(Thatcher and Santner, 1966)

¹ Geometric mean of referenced equivalent results was used

² Geometric mean of referenced equivalent results was used

Table A1-2. Ecotoxicology data of Po associated species for triclosan

Trophic level	Po species	Selected species	Endpoint	Effect measurement	Exposure duration	Value	Unit	Reference	
Algae	Diatoms								
	<i>Diatoma</i>	<i>Diatoma sp.</i>	NOEC	Abundance	2 days	87.2	µg/L	(Proia et al., 2013)	
	<i>Navicula</i>	<i>Navicula pelliculosa</i>	NOEL	Abundance	4 days	0.5	µg/L	(U.S. EPA, 1992)	
	<i>Synedra</i>	<i>Synedra sp.</i>	NOEL	Biomass	< 13 days	0.15	µg/L	(Wilson et al., 2003)	
	Chlorophyceae (Green)								
	<i>Scenedesmus</i>	<i>Scenedesmus subspicatus</i>	NOEC	Biomass	4 days	0.5	µg/L	(Orvos et al., 2002)	
	<i>Chlamydomonas sp.</i>	<i>Chlamydomonas sp.</i>	NOEL	Biomass	< 13 days	0.015	µg/L	(Wilson et al., 2003)	
	Cyanobacteria (Blue Green)								
	<i>Anabaena cylindrica</i>	<i>Anabaena flosaquae</i>	NOEL	Abundance	4 days	0.5	µg/L	(U.S. EPA, 1992)	
		<i>Cyanophycota</i>	NOEC	Fluorescence	2 days	87.2	µg/L	(Proia et al., 2013)	
Invertebrates	Rotifers								
	<i>Brachionus calyciflorus</i>	<i>Plationus patulus</i> (Brachionidae family)	NOEC	Intrinsic rate of increase	6 days	5	µg/L	(Martinez Gomez, 2012)	
	Amphipoda								
	<i>Echinogammarus veneris</i>	<i>Daphnia magna</i>	NOEC	Reproduction, mortality	21 days	52.41	µg/L	(Orvos et al., 2002)	
	Diptera								
	<i>Chironomus</i>	<i>Chironomus riparius</i>	NOEC	Survival	4 days	1 000	ug/L	(Martínez-Paz et al., 2013)	
Fishes	Ciprinides								
	<i>Alburnus alburnus alborella</i>	<i>Pimephales promelas</i>	NOEC	Multiple effects reported as one result	21 days	0.45	ug/L	(Schultz et al., 2012)	
	<i>Gobio gobio</i>	<i>Danio rerio</i>	EC50	Multiple effects reported as one result	5 days	769.86	ug/L	(Padilla et al., 2012)	
	Sunfishes								
	<i>Lepomis gibbosus</i>	<i>Lepomis macrochirus</i>	NOEL	Mortality	4 days	18 000	ug/L	(U.S. EPA, 1992)	
Siluridae									
	<i>Silurus glanis</i>	<i>Oncorhynchus mykiss</i>	NOEC	Survival	61 days	34.1	ug/L	(Orvos et al., 2002)	

Table A1-3. Ecotoxicology data of Po associated species for PFOS

Trophic level	Po species	Selected species	Endpoint	Effect measurement	Exposure duration	Value	Unit	Reference
Algae	Diatoms							
	<i>Navicula</i>	<i>Navicula pelliculosa</i>	NOEC	Growth rate	96 h	44 000	µg/L	(Brooke et al., 2004; European Commission Subgroup on Review of the Priority Substances List, 2011; OECD, 2002)
	Chlorophyceae (Green)							
	<i>Ankistrodesmus</i>	<i>Pseudokirchneriella subcapitata</i>	EC50	Cell density, growth rate	96 h	75 548	µg/L	(Brooke et al., 2004; European Commission Subgroup on Review of the Priority Substances List, 2011)
	Cyanobacteria (Blue Green)							
	<i>Anabaena cylindrica</i>	<i>Anabaena flos-aquae</i>	NOEC	Growth rate	96 h	44 000	µg/L	(European Commission Subgroup on Review of the Priority Substances List, 2011; OECD, 2002)
Invertebrates	Amphipoda							
	<i>Echinogammarus veneris</i>	<i>Daphnia magna</i>	NOEC	Reproduction, Population, Growth	21 days	2 176.4	µg/L	(Ji et al., 2008)
	Diptera							
	<i>Chironomus</i>	<i>Chironomus tetans</i>	NOEC	Growth, survival	10 days	49	µg/L	(MacDonald et al., 2004)
	Gastropoda							
	<i>Physa</i>	<i>Physa acuta</i>	LC50	Mortality	96 h	165 000	µg/L	(Li, 2009)
	Tricladida							
	<i>Dugesia sp.</i>	<i>Dugesia japonica</i>	LC50	Mortality	96 h	18 000	µg/L	(Li, 2009, 2008)
Fishes	Ciprinides							
	<i>Alburnus alburnus alborella</i>	<i>Pimephales promelas</i>	NOEC	Survival	42 days	300	µg/L	(Brooke et al., 2004)
	<i>Gobio gobio</i>	<i>Danio rerio</i>	NOEC	Development	about 80 days	8 000	µg/L	(Huang et al., 2010)
	Sunfishes							
	<i>Lepomis gibbosus</i>	<i>Lepomis macrochirus</i>	NOEC	Mortality	62 days	870	µg/L	(European Commission Subgroup on Review of the Priority Substances List, 2011; OECD, 2002)
	Siluridae							
	<i>Silurus glanis</i>	<i>Oncorhynchus mykiss</i>	LC50	Mortality	96 h	10 069.8 ³	µg/L	(European Commission Subgroup on Review of the Priority Substances List, 2011; OECD, 2002)

³ Geometric mean of referenced equivalent results from (European Commission Subgroup on Review of the Priority Substances List, 2011) was used

Table A1-4. Ecotoxicology data of Po associated species for PFOA

Trophic level	Po species	Selected species	Endpoint	Effect measurement	Exposure duration	Value	Unit	Reference
Algae	Chlorophyceae (Green)							
	<i>Scenedesmus</i>	<i>Scenedesmus quadricanda</i>	EC50	Growth inhibition	96 hours	269630	µg/l	(Valsecchi et al., 2017; Yang et al., 2014)
	<i>Ankistrodesmus</i>	<i>Pseudokirchneriella subcapitata</i>	NOEC	Photosynthesis	4.5 hours	300095	µg/l	(Ding et al., 2012b)
	<i>Chlamydomonas</i> sp.	<i>Chlamydomonas reinhardtii</i>	EC50	Growth inhibition	96 hours	51900	µg/l	(Hu et al., 2014; Valsecchi et al., 2017)
	Cyanobacteria (Blue Green)							
	<i>Anabaena cylindrica</i>	<i>Anabaena</i> sp.	NOEC	Abundance	3 days	5000	µg/l	(Rodea-Palomares et al., 2012; Valsecchi et al., 2017)
Invertebrates	Rotifers							
	<i>Brachionus calyciflorus</i>	<i>Brachionus calyciflorus</i>	NOEC	Population	4 days	4000	µg/l	(Zhang et al., 2014)
	Amphipoda							
	<i>Echinogammarus veneris</i>	<i>Daphnia magna</i>	NOEC	Reproduction	21 days	18930 ⁴	µg/l	(Colombo et al., 2008; Ji et al., 2008; Li, 2010; OECD, 2008; Valsecchi et al., 2017)
	Diptera							
	<i>Chironomus</i>	<i>Chironomus plumosus</i>	LC50	Mortality	96 h	402240	µg/l	(Valsecchi et al., 2017; Yang et al., 2014)
	Gastropoda							
<i>Physa</i>	<i>Physa acuta</i>	LC50	Mortality	96 h	672000	µg/l	(Li, 2009; Valsecchi et al., 2017)	
	Tricladida							
	<i>Dugesia</i> sp.	<i>Dugesia japonica</i>	LC50	Mortality	96 h	337000	µg/l	(Li, 2009; Valsecchi et al., 2017)
Fishes	Ciprinides							
	<i>Alburnus alburnus alborella</i>	<i>Pimephales promelas</i>	NOEC	Mortality, growth, reproduction	39 days	74100	µg/l	(Oakes et al., 2004)
	<i>Cyprinus carpio</i>	<i>Cyprinus carpio</i>	NOEC	Enzyme, growth, morphology	4 days	55565	µg/l	(Kim et al., 2010)
	<i>Gobio gobio</i>	<i>Danio rerio</i>	NOEC	Multiple effects reported as one result, length	5 days	61237.2	µg/l	(Hagenaars et al., 2011)
	<i>Carassius carassius</i>	<i>Carassius auratus</i>	LC50	Mortality	96 h	606610	µg/l	(Valsecchi et al., 2017; Yang et al., 2014)
	Siluridae							
	<i>Silurus glanis</i>	<i>Oncorhynchus mykiss</i>	NOEC	Genotoxicity	14 days	871030	µg/l	(Tilton et al., 2008)

⁴ Geometric mean of referenced equivalent results was used

Table A1-5. Ecotoxicology data of Po associated species for PFBS

Trophic level	Po species	Selected species	Endpoint	Effect measurement	Exposure duration	Value	Unit	Reference
Algae	Chlorophyceae (Green)	<i>Pseudokirchneriella subcapitata</i>	NOEC	Biomass/growth inhibition	96 h	1077000	µg/l	(NICNAS, 2005; Valsecchi et al., 2017)
		<i>Ankistrodesmus</i>						
		<i>Pseudokirchneriella subcapitata</i>	EC50	Biomass/growth inhibition	96 h	2347000	µg/l	(NICNAS, 2005; Valsecchi et al., 2017)
Invertebrates	Amphipoda	<i>Daphnia magna</i>	NOEC	Reproduction/length	21 days	502000	µg/l	(NICNAS, 2005; Valsecchi et al., 2017)
		<i>Echinogammarus veneris</i>						
		<i>Daphnia magna</i>	EC50	Immobilization	96 h	2183000	µg/l	(NICNAS, 2005; Valsecchi et al., 2017)
Fishes	Ciprinides	<i>Alburnus alburnus alborella</i>	LC50	Mortality	96 h	1938000	µg/l	(NICNAS, 2005; Valsecchi et al., 2017)
		<i>Gobio gobio</i>						
			<i>Pimephales promelas</i>	LC50	Mortality and malformation effects	144 hpf	450000	µg/l
		<i>Danio rerio</i>	EC50					
	Sunfishes							
		<i>Lepomis gibbosus</i>	LC50	Mortality	96 h	6452000	µg/l	(NICNAS, 2005; Valsecchi et al., 2017)
		<i>Lepomis macrochirus</i>						

Table A1-6. Ecotoxicology data of Po associated species for PFBA

Trophic level	Po species	Selected species	Endpoint	Effect measurement	Exposure duration	Value	Unit	Reference
Algae	Chlorophyceae (Green)							
	<i>Ankistrodesmus</i>	<i>Pseudokirchneriella subcapitata</i>	EC50	Photosynthesis	4.5 h	260960	µg/l	(Ding et al., 2012b; Valsecchi et al., 2017)
Invertebrates	Rotifers							
	<i>Brachionus calyciflorus</i>	<i>Brachionus calyciflorus</i>	LC50	Mortality	24 h	110000	µg/l	(Valsecchi et al., 2017; Wang et al., 2014)
	Amphipoda							
	<i>Echinogammarus veneris</i>	<i>Daphnia magna</i>	EC50	Immobilization	48 h	180650	µg/l	(Ding et al., 2012a; Valsecchi et al., 2017)
Fishes	Ciprinides							
	<i>Gobio gobio</i>	<i>Danio rerio</i>	EC50	Mortality and malformation effects	144 hpf	2200000	µg/l	(Ulhaq et al., 2013; Valsecchi et al., 2017)

INTERSPECIES CORRELATION ESTIMATION

For the interspecies correlation estimation, the Web-ICE application developed by U.S. EPA was used for prediction of the lacking ecotoxicological thresholds for PFBS and PFBA (Raimondo et al., 2010; U.S. EPA, 2016a). The outputs of the program for both chemicals and surrogate species are given in Tables A1-7 and A1-8.

Table A1-7. Results of the interspecies correlation estimation for PFBS (Raimondo et al., 2010; U.S. EPA, 2016a) ^{a, b}

Common Name	Scientific name	Estimated Toxicity (µg/L)	95% Confidence Intervals (µg/L)	Surrogate	Degrees of Freedom (N-2)	R ²	p-value	Mean Square Error (MSE)	Cross-validation Success (%)	Taxonomic Distance	Slope	Intercept
Calanoid copepod	<i>Acartia tonsa</i>	121167.6	1095.44 - 13402389.37	Daphnid (<i>Daphnia magna</i>)	2	0.91	0.0443	0.17	50	5	0.59	1.31
Shortnose sturgeon	<i>Acipenser brevirostrum</i>	1297819.01	11483.66 - 146672223.16	Fathead minnow (<i>Pimephales promelas</i>)	3	0.92	0.0094	0.3	40	4	1.24	-1.43
Pheasantshell	<i>Actinonaias pectorosa</i>	1430087.15	43980.92 - 46500819.60	Daphnid (<i>Daphnia magna</i>)	2	0.96	0.0163	0.14	75	6	1	-0.19
Amphipod	<i>Allorchestes compressa</i>	185719.55	25907.72 - 1331330.76	Fathead minnow (<i>Pimephales promelas</i>)	3	0.96	0.0028	0.02	100	6	0.84	0.15
Threeridge	<i>Amblema plicata</i>	297908.64	99252.95 - 894175.51	Daphnid (<i>Daphnia magna</i>)	8	0.94	0.0000	0.18	90	6	0.87	-0.08
Black bullhead	<i>Ameiurus melas</i>	150681.16	1085.59 - 20914624.12	Fathead minnow (<i>Pimephales promelas</i>)	5	0.75	0.0114	0.99	57	4	0.84	0.02
Mysid	<i>Americamysis bahia</i>	210517.07	89586.76 - 494687.33	Daphnid (<i>Daphnia magna</i>)	160	0.68	0.0000	0.93	64	5	0.83	0.02
	<i>Anabaena flos-aquae</i>	394019.12	530.09 - 292873426.60	<i>Pseudokirchneriella subcapitata</i>	19	0.46	0.0006	0.74	62	7	0.83	0.27
Fowler's toad	<i>Anaxyrus fowleri</i>	117530.29	2981.98 - 4632280.01	Bluegill (<i>Lepomis macrochirus</i>)	10	0.56	0.0047	0.26	67	5	0.49	1.79
Isopod	<i>Asellus aquaticus</i>	29524286.75	1561483.65 - 558240558.22	Bluegill (<i>Lepomis macrochirus</i>)	2	0.98	0.0054	0.08	75	6	1.06	0.44
Snipefly	<i>Atherix variegata</i>	3377657.21	75.11 - 151880068253.64	Bluegill (<i>Lepomis macrochirus</i>)	2	0.91	0.0428	0.08	100	6	0.85	0.9
Vernal pool fairy shrimp	<i>Branchinecta lynchi</i>	1050941.66	344266.66 - 3208205.95	Daphnid (<i>Daphnia magna</i>)	5	0.98	0.0000	0.09	100	4	0.9	0.31
Isopod	<i>Caecidotea brevicauda</i>	93033.34	4162.19 - 2079478.44	Fathead minnow (<i>Pimephales promelas</i>)	7	0.8	0.0011	0.42	67	6	0.85	-0.2

Common Name	Scientific name	Estimated Toxicity (µg/L)	95% Confidence Intervals (µg/L)	Surrogate	Degrees of Freedom (N-2)	R ²	p-value	Mean Square Error (MSE)	Cross-validation Success (%)	Taxonomic Distance	Slope	Intercept
Isopod	<i>Caecidotea intermedia</i>	248582.98	16885.70 - 3659516.58	Fathead minnow (<i>Pimephales promelas</i>)	4	0.71	0.0345	0.27	50	6	0.63	1.50
Goldfish	<i>Carassius auratus</i>	1034400.68	567733.78 - 1884659.31	Fathead minnow (<i>Pimephales promelas</i>)	18	0.96	0.0000	0.1	95	2	0.97	0.06
White sucker	<i>Catostomus commersonii</i>	14065372.12	2535384.34 - 78029468.59	Bluegill (<i>Lepomis macrochirus</i>)	3	0.99	0.0003	0.02	100	4	1.19	-0.77
Daphnid	<i>Ceriodaphnia dubia</i>	1586267.13	795754.65 - 3162084.43	Daphnid (<i>Daphnia magna</i>)	30	0.95	0.0000	0.26	81	2	1	-0.19
Bigscale mullet	<i>Chelon macrolepis</i>	155976895	393040.47 - 61898946903.35	Fathead minnow (<i>Pimephales promelas</i>)	2	0.97	0.0114	0.05	100	4	1.51	-1.04
Midge	<i>Chironomus plumosus</i>	124286.95	6027.19 - 2562924.48	Daphnid (<i>Daphnia magna</i>)	19	0.5	0.0002	0.14	29	5	0.63	1.05
Midge	<i>Chironomus tentans</i>	1706623.9	51043.24 - 57060740.71	Daphnid (<i>Daphnia magna</i>)	7	0.79	0.0011	1.03	33	5	0.83	0.94
	<i>Chlorella pyrenoidosa</i>	10794142	15708.77 - 7417098059.17	<i>Pseudokirchneriella subcapitata</i>	17	0.59	0.0001	1.3	74	4	1.02	0.48
	<i>Chlorella vulgaris</i>	99721.84	126.92 - 78350875.40	<i>Pseudokirchneriella subcapitata</i>	16	0.43	0.003	0.96	67	4	0.72	0.38
Stonefly	<i>Claassenia sabulosa</i>	25.18	2.71 - 233.64	Fathead minnow (<i>Pimephales promelas</i>)	6	0.63	0.0182	0.22	75	6	0.33	-0.62
Amphipod	<i>Crangonyx pseudogracilis</i>	6016336.52	158655.04 - 228144686.58	Daphnid (<i>Daphnia magna</i>)	11	0.7	0.0003	0.85	54	5	0.87	1.25
Eastern oyster	<i>Crassostrea virginica</i>	125123.56	42575.26 - 367723.01	Bluegill (<i>Lepomis macrochirus</i>)	112	0.51	0	0.64	69	6	0.66	0.71
Leon springs pupfish	<i>Cyprinodon bovinus</i>	60751.99	10362.02 - 356185.71	Fathead minnow (<i>Pimephales promelas</i>)	2	0.99	0.0043	0	100	4	0.67	0.65
Sheepshead minnow	<i>Cyprinodon variegatus</i>	662684.1	228817.11 - 1919219.26	Bluegill (<i>Lepomis macrochirus</i>)	82	0.65	0	0.47	82	4	0.74	0.87
Common carp	<i>Cyprinus carpio</i>	2618974.58	459829.34 - 14916464.01	Bluegill (<i>Lepomis macrochirus</i>)	22	0.84	0	0.41	83	4	0.91	0.4

Common Name	Scientific name	Estimated Toxicity (µg/L)	95% Confidence Intervals (µg/L)	Surrogate	Degrees of Freedom (N-2)	R ²	p-value	Mean Square Error (MSE)	Cross-validation Success (%)	Taxonomic Distance	Slope	Intercept
Daphnid	<i>Daphnia pulex</i>	2071673.74	797370.19 - 5382483.75	Daphnid (<i>Daphnia magna</i>)	19	0.97	0	0.12	90	1	1.01	-0.14
	<i>Desmodesmus subspicatus</i>	8703212.98	2311730.91 - 32765888.04	<i>Pseudokirchneriella subcapitata</i>	30	0.96	0	0.31	84	4	1.10	-0.11
Flatworm	<i>Dugesia tigrina</i>	196862.33	58994.78 - 656918.70	Fathead minnow (<i>Pimephales promelas</i>)	5	0.87	0.002	0.06	100	6	0.58	1.71
	<i>Dunaliella tertiolecta</i>	11008037776	41.94 - 288865326397641 1600.00	<i>Pseudokirchneriella subcapitata</i>	5	0.7	0.0188	0.35	67	4	1.36	1.33
Oyster mussel	<i>Epioblasma capsaeformis</i>	1052177.98	1139.89 - 971209638.77	Daphnid (<i>Daphnia magna</i>)	1	0.99	0.0487	0.09	na	6	0.93	0.07
Spotfin Chub	<i>Erimonax monachus</i>	313123.03	253.99 - 386010258.81	Fathead minnow (<i>Pimephales promelas</i>)	3	0.83	0.0292	0.3	60	2	1	-0.6
Northern pike	<i>Esox lucius</i>	134203.17	116.55 - 154524732.67	Fathead minnow (<i>Pimephales promelas</i>)	2	0.92	0.0364	0.13	75	4	0.94	-0.59
Fountain darter	<i>Etheostoma fonticola</i>	264995.44	10940.56 - 6418551.03	Fathead minnow (<i>Pimephales promelas</i>)	1	0.99	0.018	0	na	4	0.96	-0.42
Greenthroat darter	<i>Etheostoma lepidum</i>	223310.88	2071.77 - 24070013.69	Fathead minnow (<i>Pimephales promelas</i>)	3	0.91	0.0114	0.13	100	4	0.93	-0.32
Indian bullfrog	<i>Euphyctis hexadactylus</i>	1908519.26	7708.11 - 472546957.99	Fathead minnow (<i>Pimephales promelas</i>)	6	0.66	0.0135	0.84	38	5	1.02	0.03
Pink shrimp	<i>Farfantepenaeus duorarum</i>	9844241.3	296786.39 - 326528060.92	Daphnid (<i>Daphnia magna</i>)	16	0.76	0	1.32	44	5	1.08	0.14
Banana prawn	<i>Fenneropenaeus merguensis</i>	4939692.64	1028.35 - 23727720281.51	Daphnid (<i>Daphnia magna</i>)	4	0.66	0.0473	0.4	67	5	0.82	1.43
Mosquitofish	<i>Gambusia affinis</i>	603304.66	61916.73 - 5878483.67	Fathead minnow (<i>Pimephales promelas</i>)	2	0.98	0.0062	0.12	100	4	0.96	-0.1
Amphipod	<i>Gammarus fasciatus</i>	968565.67	196526.47 - 4773501.88	Daphnid (<i>Daphnia magna</i>)	43	0.75	0	0.77	58	5	0.86	0.47
Amphipod	<i>Gammarus lacustris</i>	507.75	12.94 - 19909.61	Bluegill (<i>Lepomis macrochirus</i>)	19	0.23	0.0264	0.93	43	6	0.39	0.06
Amphipod	<i>Gammarus minus</i>	996264.83	34947.09 - 28401322.19	Fathead minnow (<i>Pimephales promelas</i>)	2	0.92	0.0379	0.08	75	6	0.74	1.46
Amphipod	<i>Gammarus pseudolimnaeus</i>	1371914.86	84001.85 - 22406056.26	Bluegill (<i>Lepomis macrochirus</i>)	21	0.73	0	0.9	39	6	1.01	-0.59
Amphipod	<i>Gammarus pulex</i>	1223166.44	26.24 - 57011468431.52	Daphnid (<i>Daphnia magna</i>)	2	0.92	0.0376	0.45	25	5	0.92	0.25

Common Name	Scientific name	Estimated Toxicity (µg/L)	95% Confidence Intervals (µg/L)	Surrogate	Degrees of Freedom (N-2)	R ²	p-value	Mean Square Error (MSE)	Cross-validation Success (%)	Taxonomic Distance	Slope	Intercept
Threespine stickleback	<i>Gasterosteus aculeatus</i>	44991816.84	133212.36 - 15195763581.76	Bluegill (<i>Lepomis macrochirus</i>)	3	0.95	0.0039	0.09	80	4	1.15	0
Bonytail	<i>Gila elegans</i>	70006.09	583.02 - 8405975.98	Fathead minnow (<i>Pimephales promelas</i>)	4	0.74	0.0275	0.24	67	2	0.69	0.59
Amphipod	<i>Hyalella azteca</i>	106596.01	7994.03 - 1421398.27	Daphnid (<i>Daphnia magna</i>)	22	0.67	0	1.77	50	5	0.77	0.09
Polychaete	<i>Hydroides elegans</i>	53696.08	2908.16 - 991438.17	Daphnid (<i>Daphnia magna</i>)	2	0.96	0.0182	0.01	100	6	0.49	21551.00
Channel catfish	<i>Ictalurus punctatus</i>	913541.55	382622.80 - 2181151.17	Fathead minnow (<i>Pimephales promelas</i>)	47	0.84	0	0.4	82	4	0.96	0.07
Flagfish	<i>Jordanella floridae</i>	1254994.63	652975.99 - 2412051.21	Zebrafish (<i>Danio rerio</i>)	3	0.99	0.0003	0.01	100	4	1.22	-0.8
Pinfish	<i>Lagodon rhomboides</i>	446121604.4	46118.71 - 4315481592948.98	Bluegill (<i>Lepomis macrochirus</i>)	1	0.99	0.0301	0	na	3	1.61	-2.02
Wavyrayed lampmussel	<i>Lampsilis fasciola</i>	1734897.01	995322.35 - 3024012.89	Bluegill (<i>Lepomis macrochirus</i>)	1	0.99	0.0132	0	na	6	0.92	0.09
Neosho mucket	<i>Lampsilis rafinesqueana</i>	1013863.89	28229.12 - 36413451.30	Daphnid (<i>Daphnia magna</i>)	2	0.97	0.0103	0.07	100	6	0.97	-0.2
Fatmucket	<i>Lampsilis siliquoidea</i>	386899.89	100940.66 - 1482965.49	Daphnid (<i>Daphnia magna</i>)	15	0.86	0	0.47	71	6	0.74	0.86
White heelsplitter	<i>Lasmigona complanata</i>	582306.27	197898.90 - 1713403.07	Daphnid (<i>Daphnia magna</i>)	4	0.98	0.0001	0.1	100	6	0.92	-0.07
Peppered loach	<i>Lepidocephalic thys guntea</i>	665330.19	15182.65 - 29155913.11	Fathead minnow (<i>Pimephales promelas</i>)	2	0.93	0.0324	0.09	75	3	0.88	0.43
Green sunfish	<i>Lepomis cyanellus</i>	2075663.67	488418.23 - 8821086.83	Bluegill (<i>Lepomis macrochirus</i>)	14	0.92	0	0.13	94	1	0.87	0.53
Bullfrog	<i>Lithobates catesbeianus</i>	1031437.95	322838.92 - 3295340.76	Fathead minnow (<i>Pimephales promelas</i>)	7	0.97	0	0.19	89	5	0.93	0.33
Oligochaete	<i>Lumbriculus variegatus</i>	1715610.09	393413.43 - 7481488.23	Fathead minnow (<i>Pimephales promelas</i>)	12	0.86	0	0.3	79	6	1.10	-0.47
Swamp lymnaea	<i>Lymnaea stagnalis</i>	2560420.24	820769.95 - 7987319.42	Daphnid (<i>Daphnia magna</i>)	7	0.96	0	0.19	78	6	1.01	0
Western pearlshell	<i>Margaritifera falcata</i>	735491.56	277878.60 - 1946705.59	Daphnid (<i>Daphnia magna</i>)	8	0.95	0	0.14	90	6	0.86	0.41
Washboard	<i>Megaloniaias nervosa</i>	685936.99	284034.40 - 1656523.08	Daphnid (<i>Daphnia magna</i>)	9	0.96	0	0.16	91	6	0.92	-0.02

Common Name	Scientific name	Estimated Toxicity (µg/L)	95% Confidence Intervals (µg/L)	Surrogate	Degrees of Freedom (N-2)	R ²	p-value	Mean Square Error (MSE)	Cross-validation Success (%)	Taxonomic Distance	Slope	Intercept
Inland silverside	<i>Menidia beryllina</i>	1350012.92	78788.84 - 23131890.18	Bluegill (<i>Lepomis macrochirus</i>)	5	0.89	0.0012	0.19	86	4	0.79	0.9
Atlantic silverside	<i>Menidia menidia</i>	4171166.39	229147.63 - 75927595.05	Bluegill (<i>Lepomis macrochirus</i>)	4	0.96	0.0005	0.14	83	4	1.05	-0.35
Tidewater silverside	<i>Menidia peninsulae</i>	735651.48	40777.13 - 13271730.43	Bluegill (<i>Lepomis macrochirus</i>)	3	0.97	0.0012	0.06	100	4	0.9	-0.1
Mysid	<i>Metamysidopsis insularis</i>	2460908.91	75057.97 - 80685269.47	Daphnid (<i>Daphnia magna</i>)	3	0.94	0.0057	0.18	80	5	0.86	0.93
Smallmouth bass	<i>Micropterus dolomieu</i>	10038229.74	1454.99 - 69255155389.74	Bluegill (<i>Lepomis macrochirus</i>)	1	0.99	0.0453	0.03	na	2	1.20	-0.92
Largemouth bass	<i>Micropterus salmoides</i>	4606240.52	1746261.09 - 12150217.30	Bluegill (<i>Lepomis macrochirus</i>)	34	0.92	0	0.12	97	2	1.02	-0.13
Striped mullet	<i>Mugil cephalus</i>	8135198.53	3235.97 - 20451811883.62	Bluegill (<i>Lepomis macrochirus</i>)	3	0.92	0.0093	0.09	100	4	1.06	-0.15
Cape Fear shiner	<i>Notropis mekistocholas</i>	247290.58	101.30 - 603627461.17	Fathead minnow (<i>Pimephales promelas</i>)	3	0.78	0.044	0.36	60	2	0.93	-0.3
Cutthroat trout	<i>Oncorhynchus clarkii</i>	206507.76	43816.45 - 973274.89	Fathead minnow (<i>Pimephales promelas</i>)	24	0.79	0	0.39	81	4	0.94	-0.4
Apache trout	<i>Oncorhynchus gilae</i>	84113.12	55.95 - 126437275.92	Fathead minnow (<i>Pimephales promelas</i>)	3	0.79	0.0437	0.31	60	4	0.88	-0.42
Coho salmon	<i>Oncorhynchus kisutch</i>	1380195.44	364718.78 - 5223036.41	Bluegill (<i>Lepomis macrochirus</i>)	19	0.91	0	0.17	90	4	0.91	0.07
Rainbow trout	<i>Oncorhynchus mykiss</i>	1937680.16	1415099.24 - 2653244.58	Bluegill (<i>Lepomis macrochirus</i>)	339	0.88	0	0.22	90	4	0.94	0.05
Chinook salmon	<i>Oncorhynchus tshawytscha</i>	3235054.02	259543.92 - 40322942.23	Bluegill (<i>Lepomis macrochirus</i>)	10	0.84	0	0.29	75	4	1.03	-0.34
Mozambique tilapia	<i>Oreochromis mossambicus</i>	494062.87	42039.95 - 5806336.88	Fathead minnow (<i>Pimephales promelas</i>)	10	0.78	0.0001	0.28	67	4	0.91	0.13
Nile tilapia	<i>Oreochromis niloticus</i>	2.67447E+12	322034.42 - 22211239759620780000.00	Daphnid (<i>Daphnia magna</i>)	4	0.77	0.0198	0.66	33	6	2.02	-0.4
Medaka	<i>Oryzias latipes</i>	338197.1	146284.94 - 781880.02	Zebrafish (<i>Danio rerio</i>)	2	0.98	0.0079	0	100	4	0.78	1.11
Midge	<i>Paratanytarsus dissimilis</i>	1405188.84	206150.90 - 9578205.13	Fathead minnow (<i>Pimephales promelas</i>)	10	0.8	0	0.52	75	6	0.8	1.27

Common Name	Scientific name	Estimated Toxicity (µg/L)	95% Confidence Intervals (µg/L)	Surrogate	Degrees of Freedom (N-2)	R ²	p-value	Mean Square Error (MSE)	Cross-validation Success (%)	Taxonomic Distance	Slope	Intercept
Midge	<i>Paratanytarsus parthenogeneticus</i>	4899026.96	2242845.88 - 10700898.05	Daphnid (<i>Daphnia magna</i>)	5	0.98	0	0.04	100	5	0.93	0.74
Yellow perch	<i>Perca flavescens</i>	2043203.32	496681.39 - 8405146.27	Bluegill (<i>Lepomis macrochirus</i>)	17	0.92	0	0.12	95	3	0.96	-0.05
	<i>Phaeodactylum tricornutum</i>	625499.06	49636.31 - 7882315.27	<i>Pseudokirchneriella subcapitata</i>	7	0.98	0	0.07	100	6	1	-0.62
Tadpole physa	<i>Physa gyrina</i>	1827207.58	674435.66 - 4950342.55	Daphnid (<i>Daphnia magna</i>)	7	0.96	0	0.14	89	6	0.99	-0.02
Guppy	<i>Poecilia reticulata</i>	322555.16	142458.29 - 730331.88	Fathead minnow (<i>Pimephales promelas</i>)	35	0.83	0	0.27	78	4	0.85	0.28
Water flea	<i>Pseudosida ramosa</i>	467711.03	17747.91 - 12325591.74	Daphnid (<i>Daphnia magna</i>)	4	0.87	0.0062	0.57	67	3	0.93	-0.24
Stonefly	<i>Pteronarcella badia</i>	44.71	12.64 - 158.11	Fathead minnow (<i>Pimephales promelas</i>)	8	0.7	0.0023	0.09	100	6	0.28	-0.06
Stonefly	<i>Pteronarcys californica</i>	60560.12	3024.27 - 1212696.03	Daphnid (<i>Daphnia magna</i>)	24	0.54	0	0.94	42	5	0.63	0.72
Colorado squawfish	<i>Ptychocheilus lucius</i>	184757.85	18057.87 - 1890337.11	Fathead minnow (<i>Pimephales promelas</i>)	5	0.91	0.0008	0.1	100	2	0.81	0.3
Atlantic salmon	<i>Salmo salar</i>	8989720.98	2468045.54 - 32744567.28	Bluegill (<i>Lepomis macrochirus</i>)	10	0.96	0	0.08	92	4	1.16	-0.71
Brown trout	<i>Salmo trutta</i>	5001778.84	1092325.17 - 22903245.36	Bluegill (<i>Lepomis macrochirus</i>)	14	0.93	0	0.15	94	4	1.07	-0.38
Brook trout	<i>Salvelinus fontinalis</i>	2434681.51	447690.25 - 13240569.79	Bluegill (<i>Lepomis macrochirus</i>)	20	0.87	0	0.26	82	4	0.98	-0.14
Lake trout	<i>Salvelinus namaycush</i>	159523.2	23030.89 - 1104935.37	Bluegill (<i>Lepomis macrochirus</i>)	21	0.65	0	0.3	78	4	0.66	0.78
Walleye	<i>Sander vitreus</i>	405841.92	6334.82 - 26000370.00	Bluegill (<i>Lepomis macrochirus</i>)	7	0.74	0.0027	0.23	78	3	0.78	0.44
	<i>Scenedesmus acutus</i>	33076.94	18.72 - 58440707.66	<i>Pseudokirchneriella subcapitata</i>	13	0.45	0.0058	0.78	73	4	0.71	-0.04
	<i>Scenedesmus quadricauda</i>	45554.77	434.11 - 4780391.52	<i>Pseudokirchneriella subcapitata</i>	19	0.57	0	0.65	76	4	0.7	0.18
	<i>Sellaphora seminulum</i>	15801.18	13.26 - 18817333.34	<i>Pseudokirchneriella subcapitata</i>	10	0.51	0.0082	0.47	67	7	0.63	0.14

Common Name	Scientific name	Estimated Toxicity (µg/L)	95% Confidence Intervals (µg/L)	Surrogate	Degrees of Freedom (N-2)	R ²	p-value	Mean Square Error (MSE)	Cross-validation Success (%)	Taxonomic Distance	Slope	Intercept
Daphnid	<i>Simocephalus serrulatus</i>	2309469.46	121061.87 - 44057216.37	Daphnid (<i>Daphnia magna</i>)	13	0.88	0	0.21	87	2	1	-0.03
Daphnid	<i>Simocephalus vetulus</i>	7047333.12	6114898.77 - 8121950.33	Bluegill (<i>Lepomis macrochirus</i>)	1	0.99	0.0008	0	na	6	1.14	-0.72
	<i>Skeletonema costatum</i>	1255825.68	251028.73 - 6282540.40	<i>Pseudokirchneriella subcapitata</i>	37	0.93	0	0.56	82	6	1.05	-0.59
Beaver-tail fairy shrimp	<i>Thamnocephalus platyurus</i>	1052147.68	583116.07 - 1898446.64	Daphnid (<i>Daphnia magna</i>)	9	0.98	0	0.05	91	4	0.91	0.21
Harpacticoid copepod	<i>Tigriopus japonicus</i>	555765.81	26990.20 - 11443992.09	Bluegill (<i>Lepomis macrochirus</i>)	3	0.92	0.0095	0.1	80	6	0.6	1.73
Harpacticoid copepod	<i>Tisbe battagliai</i>	5546061.3	2233.59 - 13770986007.89	Daphnid (<i>Daphnia magna</i>)	2	0.94	0.0289	0.08	100	5	0.86	1.25
Oligochaete	<i>Tubifex tubifex</i>	12317840.41	1044444.67 - 145272599.16	Daphnid (<i>Daphnia magna</i>)	9	0.87	0	0.5	45	6	0.86	1.59
Paper pondshell	<i>Utterbackia imbecillis</i>	761872.56	352748.60 - 1645505.56	Daphnid (<i>Daphnia magna</i>)	10	0.96	0	0.11	100	6	0.9	0.15
Rainbow mussel	<i>Villosa iris</i>	732541.36	36721.20 - 14613268.26	Daphnid (<i>Daphnia magna</i>)	3	0.95	0.0041	0.3	40	6	0.8	0.74
African clawed frog	<i>Xenopus laevis</i>	585187.9	6506.19 - 52633657.54	Fathead minnow (<i>Pimephales promelas</i>)	2	0.94	0.0279	0.16	100	5	0.85	0.55
Razorback sucker	<i>Xyrauchen texanus</i>	203041.5	6940.28 - 5940076.31	Fathead minnow (<i>Pimephales promelas</i>)	4	0.9	0.0037	0.12	100	3	0.88	-0.06

^a Surrogate species that were used:

Pseudokirchinella subcapitata, 96h, EC50 = 2 347 000 µg/L (NICNAS, 2005; Valsecchi et al., 2017)

Daphnia magna, 96h, EC50 = 2 183 000 µg/L (NICNAS, 2005; Valsecchi et al., 2017)

Danio rerio, 144 hpf, EC50 = 450 000 µg/L (Ulhaq et al., 2013; Valsecchi et al., 2017)

Pimephales promelas, 96 h, LC50 = 1 938 000 µg/L (EC50_{calc}=1 211 250 µg/L) (NICNAS, 2005; Valsecchi et al., 2017)

Lepomis macrochirus, 96h, LC50 = 6 452 000 µg/L (EC50_{calc}=4 032 500 µg/L) (NICNAS, 2005; Valsecchi et al., 2017)

^b Selected Po or read-across species are marked in grey

Table A1-8. Results of the interspecies correlation estimation for PFBA (Raimondo et al., 2010; U.S. EPA, 2016a) ^{a, b}

Common Name	Scientific name	Estimated Toxicity (µg/L)	95% Confidence Intervals (µg/L)	Surrogate	Degrees of Freedom (N-2)	R ²	p-value	Mean Square Error (MSE)	Cross-validation Success (%)	Taxonomic Distance	Slope	Intercept
Calanoid copepod	<i>Acartia tonsa</i>	27546.89	818.69 - 926874.56	Daphnid (<i>Daphnia magna</i>)	2	0.91	0.0443	0.17	50	5	0.59	1.31
Pheasantshell	<i>Actinonaias pectorosa</i>	117893.82	10375.50 - 1339592.67	Daphnid (<i>Daphnia magna</i>)	2	0.96	0.0163	0.14	75	6	1.00	-0.19
Amphipod	<i>Allorchestes compressa</i>	1010530.79	1439.88 - 709203708.35	Daphnid (<i>Daphnia magna</i>)	3	0.8	0.039	0.12	100	5	0.83	1.59
Threeridge	<i>Amblema plicata</i>	33491.19	14494.26 - 77386.43	Daphnid (<i>Daphnia magna</i>)	8	0.94	0	0.18	90	6	0.87	-0.08
Mysid	<i>Americamysis bahia</i>	26190.05	13539.66 - 50659.96	Daphnid (<i>Daphnia magna</i>)	160	0.68	0	0.93	64	5	0.83	0.02
	<i>Anabaena flos-aquae</i>	62828.12	214.86 - 18370999.57	<i>Pseudokirchneriella subcapitata</i>	19	0.46	0.0006	0.74	62	7	0.83	0.27
Isopod	<i>Asellus aquaticus</i>	1688689.27	85445.28 - 33374239.40	Daphnid (<i>Daphnia magna</i>)	6	0.82	0.0018	0.57	63	5	0.78	2.08
Vernal pool fairy shrimp	<i>Branchinecta lynchi</i>	111331.19	47228.89 - 262437.54	Daphnid (<i>Daphnia magna</i>)	5	0.98	0	0.09	100	4	0.90	0.31
Goldfish	<i>Carassius auratus</i>	88133.56	12248.78 - 634146.51	Daphnid (<i>Daphnia magna</i>)	24	0.38	0.0007	1.66	38	6	0.46	2.48
Daphnid	<i>Ceriodaphnia dubia</i>	128591.31	73973.41 - 223536.09	Daphnid (<i>Daphnia magna</i>)	30	0.95	0	0.26	81	2	1.00	-0.19
Midge	<i>Chironomus plumosus</i>	25431.8	2428.00 - 266382.54	Daphnid (<i>Daphnia magna</i>)	19	0.5	0.0002	1.14	29	5	0.63	1.05
Midge	<i>Chironomus tentans</i>	213323.55	13543.38 - 3360086.36	Daphnid (<i>Daphnia magna</i>)	7	0.79	0.0011	1.03	33	5	0.83	0.94
	<i>Chlorella pyrenoidosa</i>	1127433.71	4183.18 - 303860658.01	<i>Pseudokirchneriella subcapitata</i>	17	0.59	0.0001	1.3	74	4	1.02	0.48
	<i>Chlorella vulgaris</i>	20343.05	66.85 - 6190548.95	<i>Pseudokirchneriella subcapitata</i>	16	0.43	0.003	0.96	67	4	0.72	0.38
Amphipod	<i>Crangonyx pseudogracilis</i>	686220.48	42456.84 - 11091228.66	Daphnid (<i>Daphnia magna</i>)	11	0.7	0.0003	0.85	54	5	0.87	1.25
Eastern oyster	<i>Crassostrea virginica</i>	7479.63	3062.10 - 18270.09	Daphnid (<i>Daphnia magna</i>)	116	0.28	0	1.08	58	6	0.44	1.54
Sheepshead minnow	<i>Cyprinodon variegatus</i>	39577.43	16797.37 - 93251.07	Daphnid (<i>Daphnia magna</i>)	84	0.49	0	0.72	64	6	0.53	1.79

Common Name	Scientific name	Estimated Toxicity (µg/L)	95% Confidence Intervals (µg/L)	Surrogate	Degrees of Freedom (N-2)	R ²	p-value	Mean Square Error (MSE)	Cross-validation Success (%)	Taxonomic Distance	Slope	Intercept
Common carp	<i>Cyprinus carpio</i>	142003.98	9184.42 - 2195579.71	Daphnid (<i>Daphnia magna</i>)	23	0.44	0.0002	1.78	36	6	0.68	1.54
Daphnid	<i>Daphnia pulex</i>	163539.64	76014.15 - 351845.20	Daphnid (<i>Daphnia magna</i>)	19	0.97	0	0.12	90	1	1.01	-0.14
	<i>Desmodesmus subspicatus</i>	765635.57	236105.07 - 2482783.70	<i>Pseudokirchneriella subcapitata</i>	30	0.96	0	0.31	84	4	1.10	-0.11
	<i>Dunaliella tertiolecta</i>	546535161	19.80 - 15085447859383654.00	<i>Pseudokirchneriella subcapitata</i>	5	0.7	0.0188	0.35	67	4	1.36	1.33
Oyster mussel	<i>Epioblasma capsaeformis</i>	101749.36	353.67 - 29272676.30	Daphnid (<i>Daphnia magna</i>)	1	0.99	0.0487	0.09	na	6	0.93	0.07
Indian bullfrog	<i>Euphlyctis hexadactylus</i>	3973757.17	2584.69 - 6109324024.24	Daphnid (<i>Daphnia magna</i>)	6	0.56	0.0309	1.09	50	6	0.98	1.43
Pink shrimp	<i>Farfantepenaeus duorarum</i>	666970.83	40762.14 - 10913314.95	Daphnid (<i>Daphnia magna</i>)	16	0.76	0	1.32	44	5	1.08	0.14
Banana prawn	<i>Fenneropenaeus merguensis</i>	625551.63	938.58 - 416919278.14	Daphnid (<i>Daphnia magna</i>)	4	0.66	0.0473	0.4	67	5	0.82	1.43
Amphipod	<i>Gammarus fasciatus</i>	110879.44	31526.96 - 389959.83	Daphnid (<i>Daphnia magna</i>)	43	0.75	0	0.77	58	5	0.86	0.47
Amphipod	<i>Gammarus pseudolimnaeus</i>	129073.93	10591.79 - 1572923.94	Daphnid (<i>Daphnia magna</i>)	19	0.72	0	0.95	43	5	0.93	0.19
Amphipod	<i>Gammarus pulex</i>	123460.58	16.90 - 901491938.32	Daphnid (<i>Daphnia magna</i>)	2	0.92	0.0376	0.45	25	5	0.92	0.25
Amphipod	<i>Hyalella azteca</i>	15306.14	1881.31 - 124528.79	Daphnid (<i>Daphnia magna</i>)	22	0.67	0	1.77	50	5	0.77	0.09
Polychaete	<i>Hydroides elegans</i>	15660.88	1715.29 - 142985.60	Daphnid (<i>Daphnia magna</i>)	2	0.96	0.0182	0.01	100	6	0.49	1.59
Channel catfish	<i>Ictalurus punctatus</i>	30136.97	10300.78 - 88171.64	Daphnid (<i>Daphnia magna</i>)	72	0.38	0	1.29	41	6	0.45	2.06
Flagfish	<i>Jordanella floridae</i>	8724620.03	3349828.52 - 22723251.10	Zebrafish (<i>Danio rerio</i>)	3	0.99	0.0003	0.01	100	4	1.22	-0.80
Neosho mucket	<i>Lampsilis rafinesqueana</i>	88213.95	6496.87 - 1197761.00	Daphnid (<i>Daphnia magna</i>)	2	0.97	0.0103	0.07	100	6	0.97	-0.20
Fatmucket	<i>Lampsilis siliquoidea</i>	60389.6	21121.48 - 172663.25	Daphnid (<i>Daphnia magna</i>)	15	0.86	0	0.47	71	6	0.74	0.86

Common Name	Scientific name	Estimated Toxicity (µg/L)	95% Confidence Intervals (µg/L)	Surrogate	Degrees of Freedom (N-2)	R ²	p-value	Mean Square Error (MSE)	Cross-validation Success (%)	Taxonomic Distance	Slope	Intercept
White heelsplitter	<i>Lasmigona complanata</i>	58559.5	24032.14 - 142692.85	Daphnid (<i>Daphnia magna</i>)	4	0.98	0.0001	0.1	100	6	0.92	-0.07
Bluegill	<i>Lepomis macrochirus</i>	71577.48	46826.63 - 109410.71	Daphnid (<i>Daphnia magna</i>)	288	0.62	0	0.8	57	6	0.66	1.33
Bullfrog	<i>Lithobates catesbeianus</i>	205962.69	36119.86 - 1174440.59	Daphnid (<i>Daphnia magna</i>)	9	0.86	0	0.9	55	6	0.99	0.10
Swamp lymnaea	<i>Lymnaea stagnalis</i>	205657.52	85779.08 - 493069.14	Daphnid (<i>Daphnia magna</i>)	7	0.96	0	0.19	78	6	1.01	0.00
Western pearlshell	<i>Margaritifera falcata</i>	86215.14	41064.60 - 181008.70	Daphnid (<i>Daphnia magna</i>)	8	0.95	0	0.14	90	6	0.86	0.41
Washboard	<i>Megaloniaias nervosa</i>	68359.73	34324.06 - 136145.08	Daphnid (<i>Daphnia magna</i>)	9	0.96	0	0.16	91	6	0.92	-0.02
Mysid	<i>Metamysidopsis insularis</i>	288261.04	20609.26 - 4031897.62	Daphnid (<i>Daphnia magna</i>)	3	0.94	0.0057	0.18	80	5	0.86	0.93
Coho salmon	<i>Oncorhynchus kisutch</i>	12073.34	844.56 - 172593.03	Daphnid (<i>Daphnia magna</i>)	18	0.34	0.0062	1.41	45	6	0.48	1.52
Rainbow trout	<i>Oncorhynchus mykiss</i>	50068.9	31860.01 - 78684.68	Daphnid (<i>Daphnia magna</i>)	316	0.54	0	0.99	53	6	0.65	1.27
Chinook salmon	<i>Oncorhynchus tshawytscha</i>	16220.67	1639.83 - 160449.20	Daphnid (<i>Daphnia magna</i>)	11	0.51	0.0055	0.9	54	6	0.56	1.22
Mozambique tilapia	<i>Oreochromis mossambicus</i>	174806.6	15882.35 - 1923981.11	Daphnid (<i>Daphnia magna</i>)	9	0.75	0.0005	0.33	82	6	0.57	2.19
Nile tilapia	<i>Oreochromis niloticus</i>	17227323479	82864.41 - 3581521590875229.00	Daphnid (<i>Daphnia magna</i>)	4	0.77	0.0198	0.66	33	6	42768.00	-0.40
Medaka	<i>Oryzias latipes</i>	1166596.64	331110.44 - 4110253.11	Zebrafish (<i>Danio rerio</i>)	2	0.98	0.0079	0	100	4	0.78	1.11
Midge	<i>Paratanytarsus dissimilis</i>	150542.89	5160.27 - 4391847.50	Daphnid (<i>Daphnia magna</i>)	8	0.41	0.0441	1.96	50	5	0.57	2.17
Midge	<i>Paratanytarsus parthenogeneticus</i>	472919.11	263967.02 - 847274.34	Daphnid (<i>Daphnia magna</i>)	5	0.98	0	0.04	100	5	0.93	0.74
	<i>Phaeodactylum tricorutum</i>	68361.57	6687.51 - 698810.09	<i>Pseudokirchneriella subcapitata</i>	7	0.98	0	0.07	100	6	1.00	-0.62
Tadpole physa	<i>Physa gyrina</i>	154587.33	71859.19 - 332556.51	Daphnid (<i>Daphnia magna</i>)	7	0.96	0	0.14	89	6	0.99	-0.02

Common Name	Scientific name	Estimated Toxicity (µg/L)	95% Confidence Intervals (µg/L)	Surrogate	Degrees of Freedom (N-2)	R ²	p-value	Mean Square Error (MSE)	Cross-validation Success (%)	Taxonomic Distance	Slope	Intercept
Fathead minnow	<i>Pimephales promelas</i>	99297.98	59343.81 - 166151.92	Daphnid (<i>Daphnia magna</i>)	177	0.54	0	0.88	63	6	0.60	1.81
Guppy	<i>Poecilia reticulata</i>	34981.88	5699.95 - 214691.79	Daphnid (<i>Daphnia magna</i>)	39	0.22	0.0016	1.63	49	6	0.38	2.51
Water flea	<i>Pseudosida ramosa</i>	45738.31	4093.12 - 511099.63	Daphnid (<i>Daphnia magna</i>)	4	0.87	0.0062	0.57	67	3	0.93	-0.24
Stonefly	<i>Pteronarcys californica</i>	12308.08	1096.41 - 138167.53	Daphnid (<i>Daphnia magna</i>)	24	0.54	0	0.94	42	5	0.63	0.72
	<i>Scenedesmus acutus</i>	6862.03	10.74 - 4382111.48	<i>Pseudokirchneriella subcapitata</i>	13	0.45	0.0058	0.78	73	4	0.71	-0.04
	<i>Scenedesmus quadricauda</i>	9731.23	173.98 - 544275.85	<i>Pseudokirchneriella subcapitata</i>	19	0.57	0	0.65	76	4	0.70	0.18
	<i>Sellaphora seminulum</i>	3907.97	8.37 - 1823310.32	<i>Pseudokirchneriella subcapitata</i>	10	0.51	0.0082	0.47	67	7	0.63	0.14
Daphnid	<i>Simocephalus serrulatus</i>	186649.6	16689.90 - 2087373.68	Daphnid (<i>Daphnia magna</i>)	13	0.88	0	0.21	87	2	1.00	-0.03
	<i>Skeletonema costatum</i>	124998.88	30135.81 - 518476.78	<i>Pseudokirchneriella subcapitata</i>	37	0.93	0	0.56	82	6	1.05	-0.59
Beaver-tail fairy shrimp	<i>Thamnocephalus platyurus</i>	107369.76	67549.84 - 170663.11	Daphnid (<i>Daphnia magna</i>)	9	0.98	0	0.05	91	4	0.91	0.21
Harpacticoid copepod	<i>Tisbe battagliai</i>	641344.54	1254.19 - 327956892.60	Daphnid (<i>Daphnia magna</i>)	2	0.94	0.0289	0.08	100	5	0.86	1.25
Oligochaete	<i>Tubifex tubifex</i>	1422835.04	204185.12 - 9914824.09	Daphnid (<i>Daphnia magna</i>)	9	0.87	0	0.5	45	6	0.86	1.59
Paper pondshell	<i>Utterbackia imbecillis</i>	80252.93	44648.90 - 144248.42	Daphnid (<i>Daphnia magna</i>)	10	0.96	0	0.11	100	6	0.90	0.15
Rainbow mussel	<i>Villosa iris</i>	98080.19	8882.83 - 1082957.16	Daphnid (<i>Daphnia magna</i>)	3	0.95	0.0041	0.3	40	6	0.80	0.74

^a Surrogate species that were used:

Pseudokirchinella subcapitata, 4,5 h, EC50 = 260 960 µg/L (Ding et al., 2012b; Valsecchi et al., 2017)

Daphnia magna, 48h, EC50 = 180 650 µg/L (Ding et al., 2012a; Valsecchi et al., 2017)

Danio rerio, 144 hpf, EC50 = 2 200 000 µg/L (Ulhaq et al., 2013; Valsecchi et al., 2017)

^b Selected Po or read-across species are marked in grey

SSD DATA

SSD curves were developed by fitting NOECs data to linearized log-normal (log-probit) distribution with the U.S. EPA SSD CADDIS generator (U.S. EPA, 2016b). Background statistical data for all contaminants from the generator are given here in Tables A1-9 to A1-20.

Table A1-9. Fitted log-probit distribution model for LAS

Taxa	Exposure as NOEC [$\mu\text{g/L}$]	Proportion	Rank	Probit	Probit Predicted	Difference ²
<i>Cryptophycophyta</i>	140.00	0.026315789	1	3.06206849	2.9643572	0.0095475
<i>Cyanophycota</i>	240.00	0.078947368	2	3.58781242	3.4739385	0.01296727
<i>Chlorophyta</i>	410.00	0.131578947	3	3.88104162	3.98023135	0.0098386
<i>Diatoma sp,</i>	450.00	0.184210526	4	4.10056509	4.06824145	0.00104482
<i>Dugesia sp,</i>	529.41	0.236842105	5	4.2835025	4.22189113	0.00379596
<i>Anguilla rostrata</i>	588.24	0.289473684	6	4.44507706	4.32150165	0.01527088
<i>Navicula Pelliculosa</i>	700.00	0.342105263	7	4.59327575	4.48596161	0.01151632
<i>Lepomis gibbosus</i>	794.12	0.394736842	8	4.73300587	4.60522826	0.01632712
<i>Cyprinus carpio</i>	1508.80	0.447368421	9	4.86768715	5.21204035	0.11857913
<i>Chlamydomonas variabilis</i>	1785.14	0.5	10	5	5.37104274	0.13767272
<i>Carassius auratus</i>	1814.56	0.552631579	11	5.13231285	5.38649621	0.06460918
<i>Ameiurus melas</i>	1882.35	0.605263158	12	5.26699413	5.42117461	0.02377162
<i>Chironomus riparius</i>	2400.00	0.657894737	13	5.40672425	5.65086226	0.05960337
<i>Brachionus calyciflorus</i>	2500.00	0.710526316	14	5.55492294	5.68945643	0.01809926
<i>Nitzschia linearis</i>	2941.18	0.763157895	15	5.7164975	5.84310606	0.01602973
<i>Rutilus kutum</i>	3074.95	0.815789474	16	5.89943491	5.88515647	0.00020387
<i>Barbus gonionotus</i>	3571.80	0.868421053	17	6.11895838	6.02676567	0.0084995
<i>Alburnus alburnus</i>	4088.24	0.921052632	18	6.41218758	6.15443837	0.06643465
<i>Physa integra</i>	4466.54	0.973684211	19	6.93793151	6.23810967	0.48975061

Table A1-10. Calculated values for LAS SSD curve and 95% predictive confidence interval

Proportion	Probit	Central Tendency [$\mu\text{g/L}$]	Upper prediction interval (PI) [$\mu\text{g/L}$]	Lower prediction interval (PI) [$\mu\text{g/L}$]
0,05	3.355146373	211.6617778	353.1835018	126.8482473
0,1	3.718448434	310.8352471	511.6574044	188.8344623
0,2	4.158378766	495.0149715	804.895652	304.436757
0,4	4.746652897	922.253223	1486.680174	572.1143137
0,5	5	1205.670605	1941.86154	748.5814922
0,7	5.524400513	2099.516498	3394.084461	1298.721224
0,8	5.841621234	2936.560897	4774.855779	1806.000076
0,9	6.281551566	4676.566195	7697.967794	2841.044801
0,95	6.644853627	6867.756776	11459.69014	4115.825347

Table A1-11. Fitted log-probit distribution model for TCS

Taxa	Exposure as NOEC [$\mu\text{g/L}$]	Proportion	Rank	Probit	Probit Predicted	Difference ²
<i>Chlamydomonas sp,</i>	0.015	0.038461538	1	3.231174961	3.38289005	0.023017468
<i>Synedra sp,</i>	0.15	0.115384615	2	3.801620298	3.946614979	0.021023458
<i>Pimephales promelas</i>	0.45	0.192307692	3	4.130576227	4.215580125	0.007225663
<i>Scenedesmus subspicatus</i>	0.50	0.269230769	4	4.384858895	4.241374763	0.020587696
<i>Navicula pelliculosa</i>	0.50	0.269230769	4	4.384858895	4.241374763	0.020587696
<i>Anabaena flosaquae</i>	0.50	0.269230769	4	4.384858895	4.241374763	0.020587696
<i>Plationus patulus</i>	5.00	0.5	7	5	4.805099693	0.03798613
<i>Oncorhynchus mykiss</i>	34.10	0.576923077	8	5.194028142	5.275124731	0.006576657
<i>Diatoma sp,</i>	87.20	0.653846154	9	5.395725296	5.504990395	0.011938862
<i>Cyanophycota</i>	87.20	0.653846154	9	5.395725296	5.504990395	0.011938862
<i>Danio rerio</i>	384.93	0.807692308	11	5.869423773	5.868517027	8.22189E-07
<i>Chironomus riparius</i>	1000.00	0.884615385	12	6.198379702	6.102247665	0.009241369
<i>Lepomis macrochirus</i>	18000.00	0.961538462	13	6.768825039	6.80987607	0.001685187

Table A1-12. Calculated values for TCS SSD curve and 95% predictive confidence interval

Proportion	Probit	Central Tendency [$\mu\text{g/L}$]	Upper prediction interval (PI) [$\mu\text{g/L}$]	Lower prediction interval (PI) [$\mu\text{g/L}$]
0.05	3.355146373	0.013392953	0.040253386	0.004456052
0.1	3.718448434	0.059066773	0.171051139	0.020396729
0.2	4.158378766	0.356239585	0.997994889	0.127161615
0.4	4.746652897	3.938132894	10.79234669	1.437026732
0.5	5	11.08425594	30.33949659	4.049530923
0.7	5.524400513	94.39486714	261.8758453	34.02524938
0.8	5.841621234	344.8823058	974.4534013	122.0620757
0.9	6.281551566	2080.031172	6099.683647	709.3039454
0.95	6.644853627	9173.53558	28003.97141	3005.065024

Table A1-13. Fitted log-probit distribution model for PFOS

Taxa	Exposure as NOEC [$\mu\text{g/L}$]	Proportion	Rank	Probit	Probit Predicted	Difference ²
<i>Chironomus tetans</i>	49.00	0.045454545	1	3.30937837	3.161574906	0.021845864
<i>Pimephales promelas</i>	300.00	0.136363636	2	3.903196438	3.881762615	0.000459409
<i>Lepomis macrochirus</i>	870.00	0.227272727	3	4.252141405	4.304945613	0.002788284
<i>Daphnia magna</i>	2176.40	0.318181818	4	4.527210879	4.669392925	0.020215734
<i>Oncorhynchus mykiss</i>	3401.95	0.409090909	5	4.770115882	4.846929839	0.005900384
<i>Dugesia japonica</i>	6081.08	0.5	6	5	5.077790153	0.006051308
<i>Danio rerio</i>	8000.00	0.590909091	7	5.229884118	5.186797945	0.001856418
<i>Pseudokirchneriella subcapitata</i>	40836.76	0.681818182	8	5.472789121	5.8347185	0.130992875
<i>Navicula pelliculosa</i>	44000.00	0.772727273	9	5.747858595	5.864372035	0.013575382
<i>Anabaena flos-aquae</i>	44000.00	0.772727273	9	5.747858595	5.864372035	0.013575382
<i>Physa acuta</i>	55743.24	0.954545455	11	6.69062163	5.958398467	0.53615076

Table A1-14. Calculated values for PFOS SSD curve and 95% predictive confidence interval

Proportion	Probit	Central Tendency [$\mu\text{g/L}$]	Upper prediction interval (PI) [$\mu\text{g/L}$]	Lower prediction interval (PI) [$\mu\text{g/L}$]
0.05	3.355146373	79.74531707	386.9980577	16.43242251
0.1	3.718448434	198.9176305	898.6917712	44.0286926
0.2	4.158378766	601.6868639	2546.769116	142.1515127
0.4	4.746652897	2643.371	10692.38772	653.4939087
0.5	5	5000.139037	20151.58092	1240.666451
0.7	5.524400513	18705.83471	77164.53542	4534.573433
0.8	5.841621234	41552.16257	177262.2711	9740.269054
0.9	6.281551566	125687.1516	574356.8238	27504.26115
0.95	6.644853627	313515.4678	1542866.79	63707.34606

Table A1-15. Fitted log-probit distribution model for PFOA

Taxa	Exposure as NOEC [$\mu\text{g/L}$]	Proportion	Rank	Probit	Probit Predicted	Difference ²
<i>Brachionus calyciflorus</i>	4000.00	0.035714286	1	3.197256909	3.172393102	0.000618209
<i>Anabaena sp,</i>	5000.00	0.107142857	2	3.758133208	3.314595051	0.196726097
<i>Daphnia magna</i>	18930.00	0.178571429	3	4.079177024	4.162994581	0.007025383
<i>Chlamydomonas reinhardtii</i>	28054.05	0.25	4	4.32551025	4.413685852	0.007774937
<i>Cyprinus carpio</i>	55565.00	0.321428571	5	4.536292249	4.849206868	0.097915559
<i>Danio rerio</i>	61237.20	0.392857143	6	4.728119995	4.911150044	0.033499999
<i>Pimephales promelas</i>	74100.00	0.464285714	7	4.910357649	5.032651744	0.014955846
<i>Dugesia japonica</i>	113851.35	0.535714286	8	5.089642351	5.306343844	0.046959537
<i>Chironomus plumosus</i>	135891.89	0.607142857	9	5.271880005	5.419118375	0.021679138
<i>Scenedesmus quadricanda</i>	145745.95	0.678571429	10	5.463707751	5.463730453	5.15367E-10
<i>Carassius auratus</i>	204935.81	0.75	11	5.67448975	5.680931203	4.14923E-05
<i>Phya acuta</i>	227027.03	0.821428571	12	5.920822976	5.746169632	0.030503791
<i>Pseudokirchneriella subcapitata</i>	300095.00	0.892857143	13	6.241866792	5.923986165	0.101048093
<i>Oncorhynchus mykiss</i>	871030.00	0.964285714	14	6.802743091	6.603043086	0.039880092

Table A1-16. Calculated values for PFOA SSD curve and 95% predictive confidence interval

Proportion	Probit	Central Tendency [$\mu\text{g/L}$]	Upper prediction interval (PI) [$\mu\text{g/L}$]	Lower prediction interval (PI) [$\mu\text{g/L}$]
0.05	3.355146373	5328.507177	10842.80134	2618.602687
0.1	3.718448434	9423.111676	18712.95992	4745.108954
0.2	4.158378766	18793.38263	36503.16536	9675.632985
0.4	4.746652897	47305.45575	90450.14585	24740.76877
0.5	5	70398.95063	134392.4311	36877.16793
0.7	5.524400513	160303.4489	308101.256	83405.03402
0.8	5.841621234	263710.4957	512215.8166	135769.3833
0.9	6.281551566	525942.2175	1044446.46	264843.8447
0.95	6.644853627	930093.9431	1892617.11	457078.5808

Table A1-17. Fitted log-probit distribution model for PFBS

Taxa	Exposure as NOEC [$\mu\text{g/L}$]	Proportion	Rank	Probit	Probit Predicted	Difference ²
<i>Scenedesmus acutus</i>	17879.43	0.025	1	3.040036015	3.116526348	0.005850771
<i>Scenedesmus quadricauda</i>	24624.20	0.075	2	3.560468529	3.282476506	0.077279565
<i>Chironomus plumosus</i>	67182.14	0.125	3	3.84965062	3.802849537	0.002190341
<i>Dugesia tigrina</i>	106412.07	0.175	4	4.065410709	4.04129822	0.000581412
<i>Anabaena flos-aquae</i>	212983.31	0.225	5	4.244584974	4.40105927	0.024484206
<i>Danio rerio</i>	243243.24	0.275	6	4.402239874	4.469936555	0.004582841
<i>Ictalurus punctatus</i>	493806.24	0.325	7	4.54623781	4.837052824	0.084573373
<i>Daphnia magna</i>	502000.00	0.375	8	4.681360636	4.845585172	0.026969698
<i>Carassius auratus</i>	559135.50	0.425	9	4.810881574	4.901471548	0.008206543
<i>Pimephales promelas</i>	654729.73	0.475	10	4.937293222	4.983301433	0.002116755
<i>Chironomus tentans</i>	922499.41	0.525	11	5.062706778	5.161064965	0.009674333
<i>Physa gyrina</i>	987679.77	0.575	12	5.189118426	5.19646159	5.39221E-05
<i>Pseudokirchneriella subcapitata</i>	1077000.00	0.625	13	5.318639364	5.241348404	0.005973893
<i>Lymnea stagnalis</i>	1384010.94	0.675	14	5.45376219	5.371383047	0.006786323
<i>Cyprinus carpio</i>	1415661.94	0.725	15	5.597760126	5.383106326	0.046076254
<i>Lepomis macrochirus</i>	2179729.73	0.775	16	5.755415026	5.606878278	0.022063166
<i>Micropterus salmoides</i>	2489859.74	0.825	17	5.934589291	5.675847509	0.06694731
<i>Tubifex tubifex</i>	6658292.11	0.875	18	6.15034938	6.185829939	0.00125887
<i>Asellus aquaticus</i>	15959073.92	0.925	19	6.439531471	6.639054787	0.039809554
<i>Gasterosteus aculeatus</i>	24319900.99	0.975	20	6.959963985	6.857467742	0.01050548

Table A1-18. Calculated values for PFBS SSD curve and 95% predictive confidence interval

Proportion	Probit	Central Tendency [$\mu\text{g/L}$]	Upper prediction interval (PI) [$\mu\text{g/L}$]	Lower prediction interval (PI) [$\mu\text{g/L}$]
0.05	3.355146373	28329.19357	50402.33317	15922.73925
0.1	3.718448434	57089.34017	100146.4699	32544.26006
0.2	4.158378766	133371.6988	231006.1239	77002.33115
0.4	4.746652897	414794.3846	712048.7718	241632.8604
0.5	5	676160.2796	1159674.458	394242.2984
0.7	5.524400513	1859152.251	3200881.9	1079842.118
0.8	5.841621234	3427959.062	5937388.088	1979136.812
0.9	6.281551566	8008372.883	14048336.72	4565240.534
0.95	6.644853627	16138571.77	28713195.43	9070864.282

Table A1-19. Fitting log-probit distribution model for PFBA

Taxa	Exposure as NOEC [$\mu\text{g/L}$]	Proportion	Rank	Probit	Probit Predicted	Difference ²
<i>Scenedesmus quadricauda</i>	5260.124324	0.029411765	1	3.11049004	3.153568308	0.001855737
<i>Ictalurus punctatus</i>	16290.25405	0.088235294	2	3.64829776	3.917179347	0.072297308
<i>Oncorhynchus mykiss</i>	27064.27027	0.147058824	3	3.950868602	4.260103018	0.095625924
<i>Anabaena flos-aquae</i>	33961.14595	0.205882353	4	4.179207912	4.413446843	0.054867877
<i>Brachionus calyciflorus</i>	37162.16216	0.264705882	5	4.371095782	4.47429322	0.010649711
<i>Lepomis macrochirus</i>	38690.52973	0.323529412	6	4.542148069	4.501519034	0.001650718
<i>Carassius auratus</i>	47639.76216	0.382352941	7	4.70069309	4.642075492	0.003436023
<i>Pimephales promelas</i>	53674.58378	0.441176471	8	4.85201289	4.722645463	0.016735931
<i>Cyprinus carpio</i>	76758.90811	0.5	9	5	4.964297515	0.001274667
<i>Physa gyrina</i>	83560.71892	0.558823529	10	5.14798711	5.021651544	0.015960675
<i>Daphnia magna</i>	97648.64865	0.617647059	11	5.29930691	5.126898393	0.029724697
<i>Lymnea stagnalis</i>	111166.227	0.676470588	12	5.457851931	5.214479517	0.059230132
<i>Chironomus tentans</i>	115310.027	0.735294118	13	5.628904218	5.239201874	0.151867916
<i>Pseudokirchneriella subcapitata</i>	141059.4595	0.794117647	14	5.820792088	5.375356821	0.198412577
<i>Tubifex tubifex</i>	769100.0216	0.852941176	15	6.049131398	6.52105776	0.222714492
<i>Asellus aquaticus</i>	912805.0108	0.911764706	16	6.35170224	6.636774411	0.081266143
<i>Danio rerio</i>	1189189.189	0.970588235	17	6.88950996	6.815451436	0.005484665

Table A1-20. Calculated values for PFBA SSD curve and 95% predictive confidence interval

Proportion	Probit	Central Tendency [$\mu\text{g/L}$]	Upper PI [$\mu\text{g/L}$]	Lower PI [$\mu\text{g/L}$]
0.05	3.355146373	7089.118103	15088.46712	3330.729033
0.1	3.718448434	12138.41863	25267.22515	5831.317288
0.2	4.158378766	23280.74961	47496.25617	11411.28472
0.4	4.746652897	55616.44984	111865.6672	27650.92786
0.5	5	80924.90734	162537.7305	40291.20258
0.7	5.524400513	175882.9078	355426.5083	87035.70649
0.8	5.841621234	281298.5294	573891.6161	137881.1965
0.9	6.281551566	539513.4925	1123046.527	259183.2142
0.95	6.644853627	923787.7734	1966188.352	434029.5524

AQUATOX DATA

Table A1-21. Physico-chemical parameters of LAS and TCS in the AQUATOX model (from Grechi et al., 2016)

Parameter	LAS		TCS	
	Value/Range	Notes	Value/Range	Notes
Molecular weight (g/mol)	342.4 ^a	(C _{11,6} H _{24,2})C ₆ H ₄ SO ₃ Na	289.54 ^b	C ₁₂ H ₇ Cl ₃ O ₂
Vapour pressure at 25°C (Pa)	(3-17)×10 ⁻¹³ ^a	Calculated as C ₁₂	1.8×10 ⁻⁴ ^c	Experimental data
Boiling point (°C)	637 ^a	Calculated as C ₁₂	-	-
Melting point (°C)	277 ^a	Calculated as C ₁₂	56.4 ^b	Experimental data
Octanol - water partition coefficient (logK _{ow}) (L/kg)	3.32 ^a	Calculated as C _{11,6}	4.76 ^c	Experimental data
Organic carbon - water partition coefficient K _{oc} (L/kg)	2500 ^a	Calculated as C _{11,6}	4.28 ^c	Experimental data
Water solubility (g/L)	250 ^a	Experimental data	12 ^c	In neutral form
Sorption coefficient between soil/sediment and water, K _d (L/kg)	2-300 ^a	Experimental data	1,73 ^d	Experimental data
Density (kg/L)	1.06 (relative); 0.55 (bulk) ^a	Experimental data	1550 ^b	At 22 °C
Henry's constant (Pa*m ³ /mole)	6.35×10 ⁻³ ^a	Calculated as C ₁₂	2.3×10 ⁻³ ^c	Low
Dissociation constant		Not necessary, fully anionic	8.14 ^c	Ionisable
Primary biodegradation rate in river water (1/h)	0.06 ^a	-	0.012 ^c	-
Primary biodegradation rate in bulky sediments (1/d)	0.01 ^a	-	0.001 ^c	-
Weibull shape parameter for internal toxicity	0.33 ^e		0.33 ^e	

^a HERA (2013)

^b NICNAS (2009)

^c Lyndall et al. (2010)

^d Health Canada (2012)

^e Default value from AQUATOX 3.1 plus Chemical Library (Clough, 2014)

Table A1-22. Physico-chemical input data of PFOS, PFOA, PFBS and PFBA required in the AQUATOX PFAA submodel

Parameter	PFOS	PFOA	PFBS	PFBA
	Value			
Chemical name (IUPAC)	Perfluorooctane sulphonic acid ^a	Pentadecafluorooctanoate ^c	Nonafluorobutane sulphonate ^c	Heptafluorobutanoate ^c
CAS	1763-23-1 ^a	335-67-1 ^c	375-73-5 ^c	375-22-4 ^c
Type of PFA	Sulfonate ^b	Carboxylate ^b	Sulfonate	Carboxylate
Perfluoroalkyl Chain Length	8 ^b	7 ^b	4	3
Molecular formula	C ₈ F ₁₇ SO ₃ ^a	C ₈ F ₁₅ O ₂ ^c	C ₄ F ₉ SO ₃ ^c	C ₄ F ₇ O ₂ ^c
Molecular weight (g/mol)	500 ^a	413,06 (anion) ^c	299,092 (anion) ^c	213.03 (anion) ^c
Henry's law constant (atm. m ³ /mol)	3.1581×10 ⁻⁹ ^a	3.044 ^c	8.8209×10 ⁻¹³ ^c	0.000119 ^c
K _{om} for sediments (L/kg)	290 ^b	348 ^{c, d}	150.143 ^{c, d}	144.49 ^{c, d}
BCF for Algae (L/kg)	37 ^b	14.4 ^e	3.162 ^c	3.162 ^c
BCF for Macrophytes (L/kg)	37 ^b	14.4 ^e	3.162 ^c	3.162 ^c
Weibull shape parameter for internal toxicity	3 ^b	0.33 ^b	0.33 ^b	0.33 ^b

^a European Commission Subgroup on Review of the Priority Substances List, 2011

^b Default value from AQUATOX 3.1 plus Chemical Library (Clough, 2014)

^c Valsecchi et al. (2017)

^d Calculated from the mean of K_{oc} values given in Valsecchi et al. (2017), equation for K_{om} for sediments given in (Park and Clough, 2014)

^e Mean value of the range from Vierke et al. (2012)

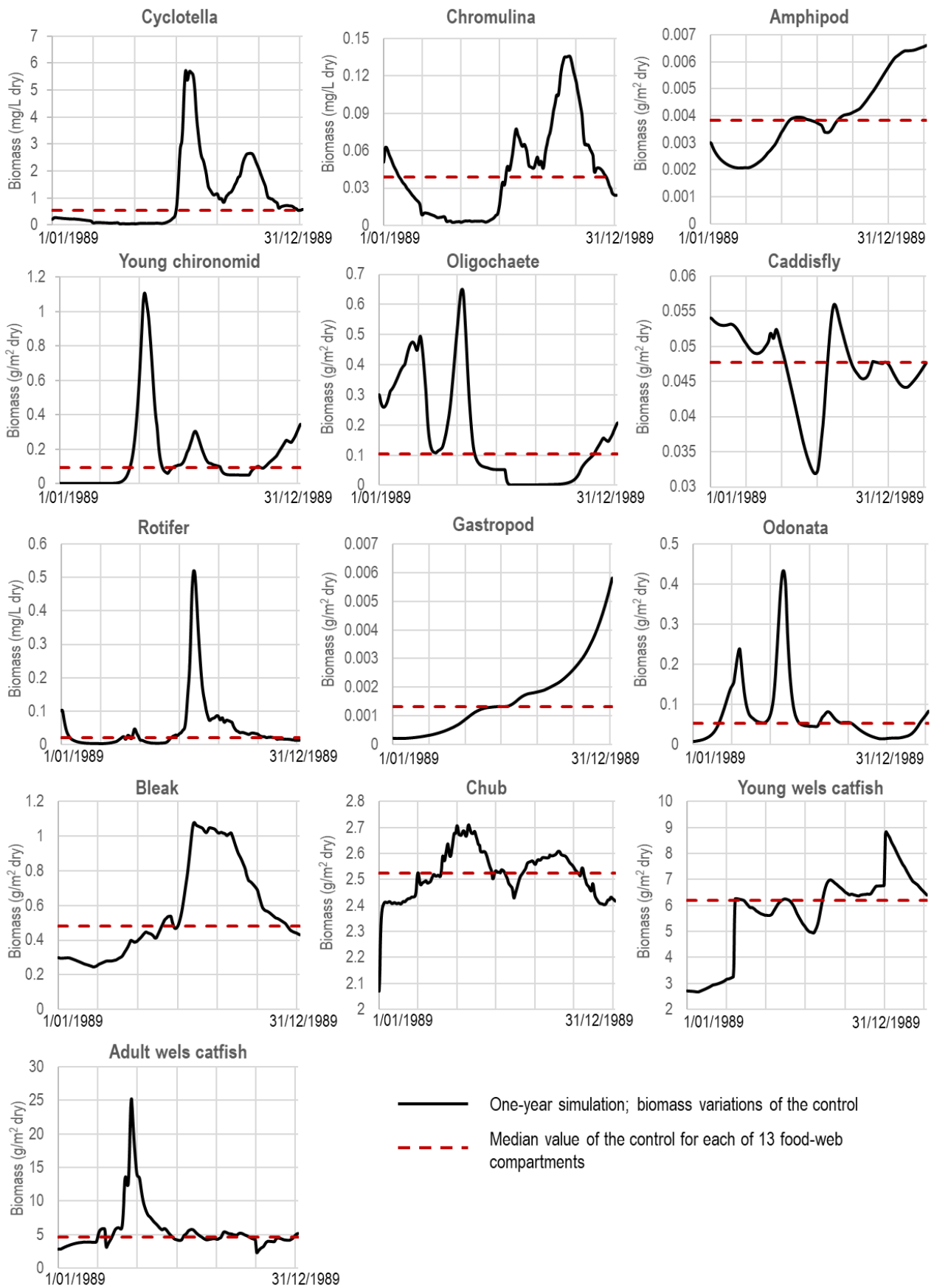


Figure A1-1. Modelled one-year AQUATOX control simulations for 13 food-web compartments

Table A1-23. LAS ecotoxicological parameters used in the model. The values in italics were calculated by AQUATOX. EC50 subscripts refer to toxicological effects on photosynthesis (photo), growth (growth) and reproduction (repro) (accepted from Grechi et al., 2016).

Model compartment	Reference species for the toxicity record	Toxicity record			Ecotoxicological parameters		
Microalgae		EC50 _{photo} (µg/L)	LC50 (µg/L)	BCF (L/kg _{dry})	k ₂ (1/d)	k ₁ (L/kg _{dry} d)	
Cyclotella (Diatom)	<i>Selenastrum capricornutum</i>	29000 ^a	290000 ^a	5450 ^a	9,6 ^a	52320	
Chromulina (Chrysophyte)	<i>Microcystis aeruginosa</i>	910 ^a	9100 ^a	5450 ^a	9,6 ^a	52320	
Model compartment	Reference species for the toxicity record	Toxicity record			Ecotoxicological parameters		
Animals		EC50 _{growth} (µg/L)	EC50 _{repro} (µg/L)	LC50 (µg/L)	BCF (L/kg _{dry})	k ₂ (1/d)	k ₁ (L/kg _{dry} d)
Brachionus (Rotifer)	<i>Brachionus calyciflorus</i>	2000 ^a	2000 ^a	3357 ^a	177 ^c	77.80 ^c	19761.2
Chironomids	<i>Chironomus riparius</i>	8000 ^a	8000 ^a	8600 ^a	100 ^d	85.91 ^c	15206.6
Trichoptera	<i>Chironomus riparius</i>	8000 ^a	8000 ^a	8600 ^a	100 ^d	85.91 ^c	15206.6
Odonata	<i>Limnodrilus hoffmeisteri</i>	1430 ^a	1430 ^a	2400 ^a	130 ^e	52.65 ^c	6844
Amphipoda	<i>Hyalella azteca</i>	1700 ^f	1700 ^f	7600 ^f	268 ^g	77.80 ^c	71103.9
Oligochaeta	<i>Curbicula</i>	610 ^a	610 ^a	1024 ^a	100 ^d	98.86 ^c	10143.3
Gastropoda	<i>Curbicula</i>	610 ^a	610 ^a	1024 ^a	100 ^d	40.77 ^c	4072.5
Bleak	<i>Pimephales promelas</i>	2400 ^a	2400 ^a	3200 ^a	296 ^h	16.94 ^c	5013.5
Chub	<i>Oreochromis niloticus</i> (NOEC = 250 µg/L) ⁱ	500 ^j	500 ^j	835 ^k	296 ^h	3.40 ^c	1006.3
Young wels catfish	<i>Lepomis macrochirus</i>	2000 ^a	2000 ^a	1670 ^a	360 ^h	3.89 ^c	1152.5
Adult wels catfish	<i>Oncorhynchus mykiss</i> (NOEC = 230 µg/L) ⁱ	460 ^j	460 ^j	770 ^k	296 ^h	1.45 ^c	429.9

^a Lombardo et al., 2015

^b Computed from average BCF_{wet} of *Curbicula*, *Elimia*, *Hyalella* (Versteeg and Rawlings, 2003)

^c Calculated using the Barber method (Park and Clough, 2014)

^d Computed from BCF_{wet} of *Curbicula* (Versteeg and Rawlings, 2003).

^e Computed from BCF_{wet} of *Elimia* (Versteeg and Rawlings, 2003)

^f ECHA, 2017

^g Computed from BCF_{wet} of *Hyalella* (Versteeg and Rawlings, 2003).

^h Computed from BCF_{wet} equal to 80 L/kg that is an average value from the study of Versteeg and Rawlings (2003) carried out on minnow (*Phimepales Promelas*).

ⁱ HERA, 2013

^j EC50/NOEC=2. The acute-chronic ratio (ACR) was chosen through expert judgement to guarantee that ACR for the chemical was as close as possible to the median value of 6 (ECETOC, 2003; Lombardo et al., 2015).

^k LC50/EC50_{growth} =1.7 (ECETOC, 2003; Lombardo et al., 2015)

Table A1-24. TCS ecotoxicological parameters used in the model. The values in italics were calculated by AQUATOX. EC50 subscripts refer to toxicological effects on photosynthesis (photo), growth (growth) and reproduction (repro) (accepted from Grechi et al., 2016)

Model compartment	Reference species for the toxicity record	Toxicity record			Ecotoxicological parameters		
Microalgae		EC50 _{photo} (µg/L)	LC50 (µg/L)		BCF (L/kg _{dry})	k ₂ (1/d)	k ₁ (L/kg _{dry} d)
Cyclotella (Diatom)	<i>Desmodesmus subspicatus</i>	1.6 ^a	16 ^a		36332	15.5 ^a	563289 ^a
Chromulina (Chrysophyte)	<i>Desmodesmus subspicatus</i>	1.6 ^a	16 ^a		36332	15.5 ^a	563289 ^a
Model compartment	Reference species for the toxicity record	Toxicity record			Ecotoxicological parameters		
Animals		EC50 _{growth} (µg/L)	EC50 _{repro} (µg/L)	LC50 (µg/L)	BCF (L/kg _{dry})	k ₂ (1/d)	k ₁ (L/kg _{dry} d)
Brachionus (Rotifer)	<i>Paramecium caudatum</i>	400 ^a	400 ^a	1544 ^a	1700 ^a	29.76 ^b	50589.3
Chironomids	<i>Chironomus tetans</i>	280 ^a	280 ^a	400 ^a	1700 ^a	3.12 ^b	5302.8
Trichoptera	<i>Chironomus tetans</i>	280 ^a	280 ^a	400 ^a	1700 ^a	2.07 ^b	3520.5
Odonata	<i>Chironomus tetans</i>	280 ^a	280 ^a	400 ^a	1700 ^a	1.96 ^b	3326.5
Amphipoda	<i>Hyalella azteca</i>	250 ^a	250 ^a	200 ^a	1700 ^a	9.62 ^b	48110.9
Oligochaeta	<i>Perna perna</i>	135 ^a	135 ^a	1260 ^a	1700 ^a	3.59 ^b	17947.5
Gastropoda	<i>Perna perna</i>	135 ^a	135 ^a	1260 ^a	1700 ^a	1.51 ^b	7540.9
Bleak	<i>Pimephales promelas</i>	67 ^a	67 ^a	260 ^a	12210 ^c	0.6 ^b	7336.4
Chub	<i>Pimephales promelas</i>	67 ^a	67 ^a	260 ^a	13365 ^c	0.12 ^b	1507.2
Young wels catfish	<i>Lepomis macrochirus</i>	96 ^a	96 ^a	370 ^a	18315 ^c	0.12 ^b	612.2
Adult wels catfish	<i>Lepomis macrochirus</i>	96 ^a	96 ^a	370 ^a	18315 ^c	0.05 ^b	263.7

^a Lombardo et al. (2015)

^b Calculated using the Barber method (Park and Clough, 2014).

^c From BCF_{lipid} for fish (Rüdel et al., 2013).

Table A1-25. PFOS ecotoxicological parameters used in the model. The values in italics were calculated by AQUATOX. EC50 subscripts refer to toxicological effects on photosynthesis (photo), growth (growth) and reproduction (repro). Calculated ACR of EC50/NOEC = 1.85 and LC50/EC50 = 1.6 were used for conversions from available data.

Model compartment	Reference species for the toxicity record	Toxicity record		Ecotoxicological parameters		
Microalgae		EC50 _{photo} (µg/L)	LC50 (µg/L)	BCF (L/kg _{dry})	k ₂ (1/d)	k ₁ (L/kg _{dry} d)
Cyclotella (Diatom)	<i>Navicula pelliculosa</i>	283000 ^a	283000 ^a	37 ^b	1.35	50
Chromulina (Chrysophyte)	<i>Isochrysis galbana</i>	37500 ^c	37500 ^c	37 ^b	1.35	50
Model compartment	Reference species for the toxicity record	Toxicity record		Ecotoxicological parameters		
Animals		EC50 _{growth} (µg/L)	EC50 _{repro} (µg/L)	LC50 (µg/L)	k ₂ (1/d)	k ₁ (L/kg _{dry} d)
Brachionus (Rotifer)	<i>Brachionus calyciflorus</i>	38625 ^d	38625 ^d	61800 ^d	5.909179267	8760.465131
Chironomids	<i>Chironomus tetans</i>	87.2 ^e	87.2 ^e	139.52 ^e	0.134282478	199.0762028
Trichoptera	<i>Chironomus tetans</i>	87.2 ^e	87.2 ^e	139.52 ^e	0.141986434	210.4974561
Odonata	<i>Enallagma cyathigerum</i>	9259.25 ^f	9259.25 ^f	14814.8 ^f	0.132133265	195.8899555
Amphipoda	<i>Daphnia magna</i>	37360 ^g	37360 ^g	130000 ^h	0.901019589	1335.777836
Oligochaeta	ICE regression	5214.11 ^b	5214.11 ^b	10428.22 ^b	0.141986434	210.4974561
Gastropoda	<i>Physa acuta</i>	103125 ⁱ	103125 ⁱ	165000 ⁱ	0.092716319	137.4536192
Bleak	<i>Pimephales promelas</i>	4700 ^j	4700 ^j	9500 ^k	0.05101631	75.63260154
Chub	<i>Primephales promelas</i>	4700 ^j	4700 ^j	9500 ^k	0.022046796	32.68477387
Young wels catfish	<i>Lepomis macrochirus</i>	4000 ^l	4000 ^l	6400 ^l	0.033004199	48.92932242
Adult wels catfish	<i>Oncorhynchus mykiss</i>	6293.6 ^m	6293.6 ^m	10069.76 ^m	0.014032096	20.80283639

^a NOEC = 44000 µg/L (Brooke et al., 2004; European Commission Subgroup on Review of the Priority Substances List, 2011; OECD, 2002)

^b Default value from AQUATOX 3.1 plus Chemical Library (Clough, 2014)

^c EC50 = 37500 µg/L (Mhadhbi et al., 2012)

^d LC50 = 61800 µg/L (Lilan Zhang et al., 2013)

^e EC50 = 87.2 µg/L (MacDonald et al., 2004)

^f NOEC = 5005 µg/L, geometric mean of the eggs and larvae test results (Bots et al., 2010)

^g Ji et al. (2008)

^h Beach et al. (2006)

ⁱ LC50 = 165000 µg/L (Li, 2009)

^j Brooke et al. (2004)

^k European Commission Subgroup on Review of the Priority Substances List (2011)

^l LC50 = 6400 µg/L (OECD, 2002)

^m LC50 = 10069.76 µg/L, geometric mean of equivalent results (European Commission Subgroup on Review of the Priority Substances List, 2011; OECD, 2002)

Table A1-26. PFOA ecotoxicological parameters used in the model. The values in italics were calculated by AQUATOX. EC50 subscripts refer to toxicological effects on photosynthesis (photo), growth (growth) and reproduction (repro). Calculated ACR of EC50/NOEC = 1.85 and LC50/EC50 = 1.6 were used for conversions from available data.

Model compartment	Reference species for the toxicity record	Toxicity record			Ecotoxicological parameters	
Microalgae		EC50 _{photo} (µg/L)	LC50 (µg/L)	BCF (L/kg _{dry})	k ₂ (1/d)	k ₁ (L/kg _{dry} d)
Cyclotella (Diatom)	<i>Scenedesmus obliquus</i>	44000 ^a	44000 ^a	14.4 ^b	0.0238	0.3423
Chromulina (Chrysophyte)	<i>Isochrysis galbana</i>	163600 ^c	163600 ^c	14.4 ^b	0.0238	0.3423
Model compartment	Reference species for the toxicity record	Toxicity record			Ecotoxicological parameters	
Animals		EC50 _{growth} (µg/L)	EC50 _{repro} (µg/L)	LC50 (µg/L)	k ₂ (1/d)	k ₁ (L/kg _{dry} d)
Brachionus (Rotifer)	<i>Brachionus calyciflorus</i>	93750 ^d	93750 ^d	150000 ^d	13.56210697	59.98285947
Chironomids	<i>Chironomus plumosus</i>	251400 ^e	251400 ^e	402240 ^e	0.548048948	2.423925952
Trichoptera	<i>Chironomus plumosus</i>	251400 ^e	251400 ^e	402240 ^e	0.325871854	1.441274994
Odonata	<i>Limnodrilus Hoffmeisteri</i>	355125 ^f	355125 ^f	568200 ^f	0.303257931	1.341257513
Amphipoda	<i>Daphnia magna</i>	365718 ^h	365718 ^h	201850 ^g	2.06792238	9.146063942
Oligochaeta	<i>Limnodrilus Hoffmeisteri</i>	355125 ^f	355125 ^f	568200 ^f	0.325871854	1.441274994
Gastropoda	<i>Physa acuta</i>	420000 ⁱ	420000 ⁱ	672000 ⁱ	0.212792433	0.94114422
Bleak	<i>Pimephales promelas</i>	137085 ^j	137085 ^j	219336 ^j	0.117087097	0.517856032
Chub	<i>Cyprinus carpio</i>	102795.25 ^k	102795.25 ^k	164472.4 ^k	0.050599414	0.223792478
Young wels catfish	<i>Pseudorasbora parva</i>	228137.5 ^l	228137.5 ^l	365020 ^l	0.075747657	0.335018818
Adult wels catfish	<i>Cyprinus carpio</i>	102795.25 ^k	102795.25 ^k	164472.4 ^k	0.032204944	0.142436913

^a EC50 = 44000 µg/L (Hu et al., 2014)

^b Mean value of a given range from (Vierke et al., 2012)

^c EC50 = 163600 µg/L (Mhadhbi et al., 2012)

^d LC50 = 150000 µg/L (Lilan Zhang et al., 2013)

^e LC50 = 251400 µg/L (Valsecchi et al., 2017; Yang et al., 2014)

^f LC50 = 568200 µg/L (Yang et al., 2014)

^g Yang et al. (2014)

^h Average of equivalent results (Colombo et al., 2008; Ding et al., 2012a; Li, 2009; OECD, 2008)

ⁱ LC50 = 672000 µg/L (Li, 2009)

^j NOEC = 74100 µg/L (Oakes et al., 2004)

^k NOEC = 55565 µg/L (Kim et al., 2010)

^l LC50 = 365020 µg/L (Yang et al., 2014)

Table A1-27. PFBS ecotoxicological parameters used in the model. The values in italics were calculated by AQUATOX. EC50 subscripts refer to toxicological effects on photosynthesis (photo), growth (growth) and reproduction (repro). Calculated ACR of EC50/NOEC = 1.85 and LC50/EC50 = 1.6 were used for conversions from available data.

Model compartment	Reference species for the toxicity record	Toxicity record			Ecotoxicological parameters	
Microalgae		EC50 _{photo} (µg/L)	LC50 (µg/L)	BCF (L/kg _{dry})	k ₂ (1/d)	k ₁ (L/kg _{dry} d)
Cyclotella (Diatom)	<i>Phaeodactylum tricornutum</i>	625499.06 ^a	625499.06 ^a	3.162 ^b	0.0021622	0.0068369
Chromulina (Chrysophyte)	<i>Selenastrum capricornutum</i>	2347000 ^c	2347000 ^c	3.162 ^b	0.0022	0.0068369
Model compartment	Reference species for the toxicity record	Toxicity record			Ecotoxicological parameters	
Animals		EC50 _{growth} (µg/L)	EC50 _{repro} (µg/L)	LC50 (µg/L)	k ₂ (1/d)	k ₁ (L/kg _{dry} d)
Brachionus (Rotifer)	<i>Acartia tonsa</i>	121167.6 ^a	121167.6 ^a	193868.16 ^a	11.25970897	1.198194069
Chironomids	<i>Chironomus tetans</i>	1706623.9 ^a	1706623.9 ^a	2730598.24 ^a	0.455008331	0.048419394
Trichoptera	<i>Chironomus tetans</i>	1706623.9 ^a	1706623.9 ^a	2730598.24 ^a	0.270549572	0.028790344
Odonata	<i>Pteronarcys californica</i>	60560.12 ^d	60560.12 ^d	96896.192 ^d	0.251774747	0.026792434
Amphipoda	<i>Daphnia magna</i>	2183000 ^e	2183000 ^e	3492800 ^e	1.716857434	0.182698185
Oligochaeta	<i>Tubifex tubifex</i>	12317840.41 ^a	12317840.41 ^a	19708544.66 ^a	0.270549572	0.028790344
Gastropoda	<i>Physa gyrina</i>	1827207.58 ^a	1827207.58 ^a	2923532.128 ^a	0.176667303	0.018799928
Bleak	<i>Pimephelas promelas</i>	1211250 ^f	1211250 ^f	1938000 ^f	0.097209574	0.010344489
Chub	<i>Pimephales promelas</i>	1211250 ^f	1211250 ^f	1938000 ^f	0.042009304	0.004470391
Young wels catfish	<i>Lepomis macrochirus</i>	4032500 ^g	4032500 ^g	6452000 ^g	0.062888205	0.006692204
Adult wels catfish	<i>Ictalurus punctatus</i>	913541.55 ^a	913541.55 ^a	1461666.48 ^a	0.026737608	0.002845264

^a EC50s are estimated with Web-ICE, ICE details are in the Table A1-7, LC50s are calculated from LC50/EC50 ratio

^b Valsecchi et al. (2017)

^c EC50 = 234700 µg/L (NICNAS, 2005)

^d EC50 is estimated with Web-ICE, calculator for Aquatic species on a surrogate species *Daphnia magna* (U.S. EPA, 2016c), LC50s are calculated from LC50/EC50 ratio

^e EC50 = 2183000 µg/L (NICNAS, 2005)

^f LC50 = 1938000 µg/L (NICNAS, 2005)

^g LC50 = 6452000 µg/L (NICNAS, 2005)

Table A1-28. PFBA ecotoxicological parameters used in the model. The values in italics were calculated by AQUATOX. EC50 subscripts refer to toxicological effects on photosynthesis (photo), growth (growth) and reproduction (repro). Calculated ACR of EC50/NOEC = 1.85 and LC50/EC50 = 1.6 were used for conversions from available data.

Model compartment	Reference species for the toxicity record	Toxicity record			Ecotoxicological parameters	
Microalgae		EC50 _{photo} (µg/L)	LC50 (µg/L)	BCF (L/kg _{dry})	k ₂ (1/d)	k ₁ (L/kg _{dry} d)
Cyclotella (Diatom)	<i>Phaeodactylum tricornutum</i>	68361.57 ^a	68361.57 ^a	3.162 ^b	8.49E-05	0.00026838
Chromulina (Chrysophyte)	<i>Selenastrum capricornutum</i>	260960 ^c	260960 ^c	3.162 ^b	0.0001	0.00026838
Model compartment	Reference species for the toxicity record	Toxicity record			0.0001	0.00026838
Animals		EC50 _{growth} (µg/L)	EC50 _{repro} (µg/L)	LC50 (µg/L)	k ₂ (1/d)	k ₁ (L/kg _{dry} d)
Brachionus (Rotifer)	<i>Brachionus calyciflorus</i>	68750 ^d	68750 ^d	110000 ^d	41.22182027	0.047035652
Chironomids	<i>Chironomus tentans</i>	213323.55 ^a	213323.55 ^a	341317.68 ^a	1.66578654	0.001900725
Trichoptera	<i>Chironomus tentans</i>	213323.55 ^a	213323.55 ^a	341317.68 ^a	0.990482602	0.001130178
Odonata	<i>Pteronarcys californica</i>	12308.08 ^a	12308.08 ^a	19692.93 ^a	0.921747923	0.001051749
Amphipoda	<i>Daphnia magna</i>	180650 ^e	180650 ^e	289040 ^e	6.285418989	0.0071719
Oligochaeta	<i>Tubifex tubifex</i>	1422835.04 ^a	1422835.04 ^a	2276536.06 ^a	0.990482602	0.001130178
Gastropoda	<i>Physa gyrina</i>	154587.33 ^a	154587.33 ^a	247339.73 ^a	0.6467794	0.000738
Bleak	<i>Pimephales promelas</i>	99297.98 ^a	99297.98 ^a	158876.79 ^a	0.355884472	0.000406078
Chub	<i>Pimephales promelas</i>	99297.98 ^a	99297.98 ^a	158876.79 ^a	0.153796157	0.000175487
Young wels catfish	<i>Lepomis macrochirus</i>	71577.48 ^a	71577.48 ^a	114523.97 ^a	0.230233864	0.000262706
Adult wels catfish	<i>Ictalurus punctatus</i>	30136.97 ^a	30136.97 ^a	48219.152 ^a	0.097886444	0.000111692

^a EC50s are estimated with Web-ICE, ICE details are in the Table A1-8, LC50s are calculated from LC50/EC50 ratio

^b Valsecchi et al. (2017)

^c EC50 = 260960 µg/L (Ding et al., 2012b)

^d LC50 = 110000 µg/L (Wang et al., 2014)

^e EC50 = 180650 µg/L (Ding et al., 2012a)

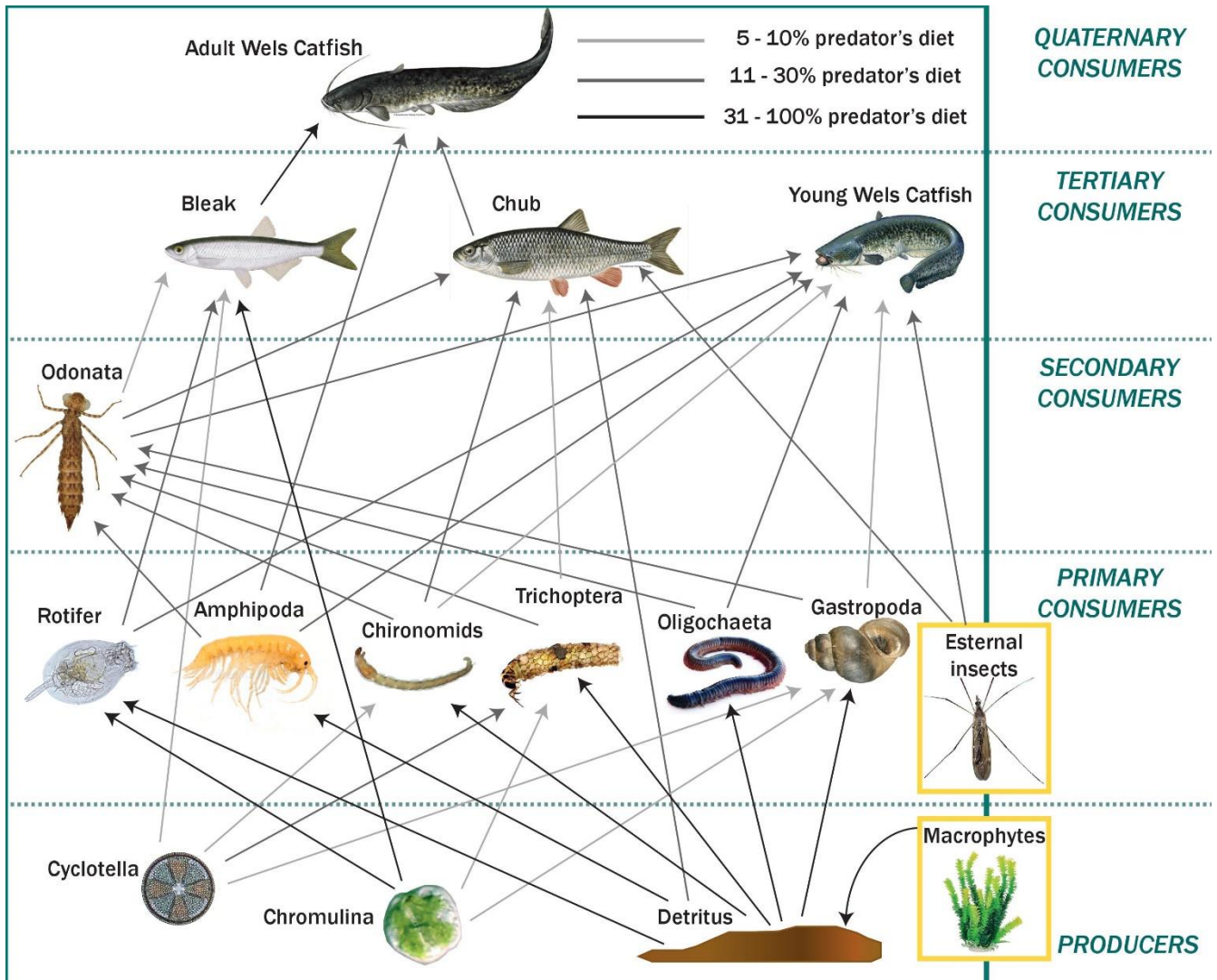


Figure A1-2. Food web scheme of the Po river (modified from Grechi et al., 2016). Arrows are going from the prey to the corresponding predator, while their shade indicates the percentage range of the predator's diet covered by the prey. If prey represented less than 5% of the predator's diet, the interaction was not shown.

References:

- Arthur, J.W., 1970. Chronic effects of linear alkylate sulfonate detergent on *Gammarus pseudolimnaeus*, *Campeloma decisum* and *Physa integra*. *Water Res.* 4, 251–257. [https://doi.org/10.1016/0043-1354\(70\)90071-0](https://doi.org/10.1016/0043-1354(70)90071-0)
- Beach, S.A., Newsted, J.L., Coady, K., Giesy, J.P., 2006. Ecotoxicological Evaluation of Perfluorooctanesulfonate (PFOS), in: Albert, L.A., de Voogt, P., Gerba, C.P., Hutzinger, O., Knaak, J.B., Mayer, F.L., Morgan, D.P., Park, D.L., Tjeerdema, R.S., Whitacre, D.M., Yang, R.S.H., Ware, G.W., Nigg, H.N., Doerge, D.R., Gunther, F.A. (Eds.), *Reviews of Environmental Contamination and Toxicology: Continuation of Residue Reviews*. Springer New York, New York, NY, pp. 133–174. https://doi.org/10.1007/0-387-32883-1_5
- Bots, J., Bruyn, L. De, Snijkers, T., den Branden, B. Van, Gossum, H. Van, 2010. Exposure to perfluorooctane sulfonic acid (PFOS) adversely affects the life-cycle of the damselfly *Enallagma cyathigerum*. *Environ. Pollut.* 158, 901–905. <https://doi.org/https://doi.org/10.1016/j.envpol.2009.09.016>
- Brooke, D., Footitt, A., Nwaogu, T.. A., 2004. Environmental Risk Evaluation Report: Perfluorooctanesulphonate (PFOS), Environment Agency.
- Clough, J.S., 2014. AQUATOX (RELEASE 3.1 plus) User's manual.
- Colombo, I., de Wolf, W., Thompson, R.S., Farrar, D.G., Hoke, R.A., L'Haridon, J., 2008. Acute and chronic aquatic toxicity of ammonium perfluorooctanoate (APFO) to freshwater organisms. *Ecotoxicol. Environ. Saf.* 71, 749–756. <https://doi.org/https://doi.org/10.1016/j.ecoenv.2008.04.002>
- Ding, G., Frömel, T., van den Brandhof, E.-J., Baerselman, R., Peijnenburg, W.J.G.M., 2012a. Acute toxicity of poly- and perfluorinated compounds to two cladocerans, *Daphnia magna* and *Chydorus sphaericus*. *Environ. Toxicol. Chem.* 31, 605–610. <https://doi.org/10.1002/etc.1713>
- Ding, G., Wouterse, M., Baerselman, R., Peijnenburg, W.J.G.M., 2012b. Toxicity of Polyfluorinated and Perfluorinated Compounds to Lettuce (*Lactuca sativa*) and Green Algae (*Pseudokirchneriella subcapitata*). *Arch. Environ. Contam. Toxicol.* 62, 49–55. <https://doi.org/10.1007/s00244-011-9684-9>
- ECETOC, 2003. Aquatic Hazard Assessment II, Technical Report No . 91. Brussels. <https://doi.org/ISSN-0773-8072-91>
- ECHA, 2017. ECHA Brief Profile: Benzenesulfonic acid, C10-13-alkyl derivs., sodium salts [WWW Document]. URL <https://echa.europa.eu/brief-profile/-/briefprofile/100.063.721> (accessed 10.6.17).
- European Commission Subgroup on Review of the Priority Substances List, 2011. EQS dossier for PFOS.
- Eyanoer, H.F., Upatham, E.S., Duangsawasdi, M., Tridech, S., 1985. Effects of water hardness and temperature on the toxicity of detergents to the freshwater fish, *Puntius gonionotus*, bleeker. *Sci. Asia* 11, 067. <https://doi.org/10.2306/scienceasia1513-1874.1985.11.067>

- Grechi, L., Franco, A., Palmeri, L., Pivato, A., Barausse, A., 2016. An ecosystem model of the lower Po river for use in ecological risk assessment of xenobiotics. *Ecol. Modell.* 332, 42–58. <https://doi.org/10.1016/j.ecolmodel.2016.03.008>
- Guerra, M., Comodo, N., 1972. Possibility of using the ichthyotoxicity test for evaluating the acceptability limits of some toxic substances in industrial effluents. *Boll. Soc. Ital. Biol. Sper.* 48, 898–901.
- Hagenaars, A., Vergauwen, L., Coen, W. De, Knapen, D., 2011. Structure–activity relationship assessment of four perfluorinated chemicals using a prolonged zebrafish early life stage test. *Chemosphere* 82, 764–772. <https://doi.org/https://doi.org/10.1016/j.chemosphere.2010.10.076>
- Health Canada, 2012. Preliminary Assessment Report on Triclosan.
- HERA, 2013. LAS Linear Alkylbenzene Sulphonate (CAS No. 68411-30-3), Human and Environmental Risk Assessment of ingredients of Household Cleaning Products.
- Hu, C., Luo, Q., Huang, Q., 2014. Ecotoxicological effects of perfluorooctanoic acid on freshwater microalgae *Chlamydomonas reinhardtii* and *Scenedesmus obliquus*. *Environ. Toxicol. Chem.* 33, 1129–1134. <https://doi.org/10.1002/etc.2532>
- Huang, H., Huang, C., Wang, L., Ye, X., Bai, C., Simonich, M.T., Tanguay, R.L., Dong, Q., 2010. Toxicity, uptake kinetics and behavior assessment in zebrafish embryos following exposure to perfluorooctanesulphonic acid (PFOS). *Aquat. Toxicol.* 98, 139–147. <https://doi.org/https://doi.org/10.1016/j.aquatox.2010.02.003>
- Jangchudjai, C., Upatham, E.S., Duangsawasdi, M., Klavanich, P., 1987. Acute toxicity of the synergism of surfactant (LAS) and copper on the freshwater fish, *Puntius gonionotus*, bleeker. *Sci. Asia* 13, 159. <https://doi.org/10.2306/scienceasia1513-1874.1987.13.159>
- Ji, K., Kim, Y., Oh, S., Ahn, B., Jo, H., Choi, K., 2008. Toxicity of perfluorooctane sulfonic acid and perfluorooctanoic acid on freshwater macroinvertebrates (*Daphnia magna* and *Moina macrocopa*) and fish (*Oryzias latipes*). *Environ. Toxicol. Chem.* 27, 2159–2168. <https://doi.org/10.1897/07-523.1>
- Jørgensen, E., Christoffersen, K., 2000. Short-term effects of linear alkylbenzene sulfonate on freshwater plankton studied under field conditions. *Environ. Toxicol. Chem.* 19, 904–911. <https://doi.org/10.1002/etc.5620190417>
- Kim, W.-K., Lee, S.-K., Jung, J., 2010. Integrated assessment of biomarker responses in common carp (*Cyprinus carpio*) exposed to perfluorinated organic compounds. *J. Hazard. Mater.* 180, 395–400. <https://doi.org/https://doi.org/10.1016/j.jhazmat.2010.04.044>
- Lewis, M.A., Hamm, B.G., 1986. Environmental modification of the photosynthetic response of lake plankton to surfactants and significance to a laboratory-field comparison. *Water Res.* 20, 1575–1582. [https://doi.org/10.1016/0043-1354\(86\)90123-5](https://doi.org/10.1016/0043-1354(86)90123-5)
- Lewis, M.A., Suprenant, D., 1983. Comparative acute toxicities of surfactants to aquatic invertebrates. *Ecotoxicol. Environ. Saf.* 7, 313–322. [https://doi.org/10.1016/0147-6513\(83\)90076-3](https://doi.org/10.1016/0147-6513(83)90076-3)

- Li, M.-H., 2010. Chronic Effects of Perfluorooctane Sulfonate and Ammonium Perfluorooctanoate on Biochemical Parameters, Survival and Reproduction of *Daphnia magna*. *J. Heal. Sci.* 56, 104–111. <https://doi.org/10.1248/jhs.56.104>
- Li, M.-H., 2009. Toxicity of perfluorooctane sulfonate and perfluorooctanoic acid to plants and aquatic invertebrates. *Environ. Toxicol.* 24, 95–101. <https://doi.org/10.1002/tox.20396>
- Li, M.-H., 2008. Effects of nonionic and ionic surfactants on survival, oxidative stress, and cholinesterase activity of planarian. *Chemosphere* 70, 1796–1803. <https://doi.org/https://doi.org/10.1016/j.chemosphere.2007.08.032>
- Lombardo, A., Franco, A., Pivato, A., Barausse, A., 2015. Food web modeling of a river ecosystem for risk assessment of down-the-drain chemicals: A case study with AQUATOX. *Sci. Total Environ.* 508, 214–227. <https://doi.org/10.1016/j.scitotenv.2014.11.038>
- Lopez-Zavala, A., de Aluja, A., Beatriz, E., Manjarrez, L., Buchmann, A., Mercado, L., Caltenco, S., 1975. The effects of the ABS, LAS and AOS detergents on fish, domestic animals and plants. *Prog. water Technol.* 7, 73–82.
- Lundahl, P., Cabridenc, R., 1978. Molecular structure—biological properties relationships in anionic surface-active agents. *Water Res.* 12, 25–30. [https://doi.org/10.1016/0043-1354\(78\)90191-4](https://doi.org/10.1016/0043-1354(78)90191-4)
- Lyndall, J., Fuchsman, P., Bock, M., Barber, T., Lauren, D., Leigh, K., Perruchon, E., Capdevielle, M., 2010. Probabilistic risk evaluation for triclosan in surface water, sediments, and aquatic biota tissues. *Integr. Environ. Assess. Manag.* 6, 419–440. https://doi.org/10.1897/IEAM_2009-072.1
- MacDonald, M.M., Warne, A.L., Stock, N.L., Mabury, S.A., Solomon, K.R., Sibley, P.K., 2004. Toxicity of perfluorooctane sulfonic acid and perfluorooctanoic acid to *Chironomus tentans*. *Environ. Toxicol. Chem.* 23, 2116–2123. <https://doi.org/10.1897/03-449>
- Martínez-Paz, P., Morales, M., Martínez-Guitarte, J.L., Morcillo, G., 2013. Genotoxic effects of environmental endocrine disruptors on the aquatic insect *Chironomus riparius* evaluated using the comet assay. *Mutat. Res. Toxicol. Environ. Mutagen.* 758, 41–47. <https://doi.org/10.1016/J.MRGENTOX.2013.09.005>
- Martinez Gomez, D.A., 2012. A survey of selected pharmaceuticals and personal care products in a binational river and their effects on a member of its zooplankton community, *Plationus patulus* (rotifera). *ETD Collect. Univ. Texas, El Paso*.
- Mhadhbi, L., Rial, D., Perez, S., Beiras, R., 2012. Ecological risk assessment of perfluorooctanoic acid (PFOA) and perfluorooctanesulfonic acid (PFOS) in marine environment using *Isochrysis galbana*, *Paracentrotus lividus*, *Siriella armata* and *Psetta maxima*. *J. Environ. Monit.* 14, 1375–1382. <https://doi.org/10.1039/C2EM30037K>
- NICNAS, 2009. Triclosan, Priority Existing Chemical Assessment Report No. 30. Sydney. <https://doi.org/ISBN: 0-9803124-4-2>
- NICNAS, 2005. Potassium Perfluorobutane Sulfonate: Hazard Assessment. *Ind. Chem. Notif. Assess. Scheme*.
- Oakes, K.D., Sibley, P.K., Solomon, K.R., Mabury, S.A., Van Der Kraak, G.J., 2004. Impact of perfluorooctanoic acid on fathead minnow (*Pimephales promelas*) fatty acyl-coa oxidase

- activity, circulating steroids, and reproduction in outdoor microcosms, *Environmental Toxicology and Chemistry*. Wiley Periodicals, Inc. <https://doi.org/10.1897/03-190>
- OECD, 2008. Substance Information Data-Sheet (SIDS), Assessment Profile for Perfluorooctanoic Acid (PFOA), Ammonium Perfluorooctanoate (APFO).
- OECD, 2002. Hazard Assessment of PFOS and its salts, ENV/JM/RD(2002)17/FINAL.
- Orvos, D.R., Versteeg, D.J., Inauen, J., Capdevielle, M., Rothenstein, A., Cunningham, V., 2002. Aquatic toxicity of triclosan. *Environ. Toxicol. Chem.* 21, 1338–1349. <https://doi.org/10.1002/etc.5620210703>
- Padilla, S., Corum, D., Padnos, B., Hunter, D.L., Beam, A., Houck, K.A., Sipes, N., Kleinstreuer, N., Knudsen, T., Dix, D.J., Reif, D.M., 2012. Zebrafish developmental screening of the ToxCast™ Phase I chemical library. *Reprod. Toxicol.* 33, 174–187. <https://doi.org/10.1016/J.REPROTOX.2011.10.018>
- Park, R.A., Clough, J.S., 2014. Aquatox (release 3.1 plus) Modeling Environmental Fate and Ecological Effects in Aquatic Ecosystems, Volume 2: Technical Documentation. Washington DC.
- Patrick, R., Scheier, A., Cairns, J., 1968. The Relative Sensitivity of Diatoms, Snails, and Fish to Twenty Common Constituents of Industrial Wastes. *Progress. Fish-Culturist* 30, 137–140. [https://doi.org/10.1577/1548-8640\(1968\)30\[137:TRSODS\]2.0.CO;2](https://doi.org/10.1577/1548-8640(1968)30[137:TRSODS]2.0.CO;2)
- Pittinger, C.A., Woltering, D.M., Masters, J.A., 1989. Bioavailability of sediment-sorbed and aqueous surfactants to *Chironomus riparius* (midge). *Environ. Toxicol. Chem.* 8, 1023–1033. <https://doi.org/10.1002/etc.5620081108>
- Proia, L., Vilches, C., Boninneau, C., Kantiani, L., Farré, M., Romaní, A.M., Sabater, S., Guasch, H., 2013. Drought episode modulates the response of river biofilms to triclosan. *Aquat. Toxicol.* 127, 36–45. <https://doi.org/10.1016/J.AQUATOX.2012.01.006>
- Radix, P., Léonard, M., Papantoniou, C., Roman, G., Saouter, E., Gallotti—Schmitt, S., Thiébaud, H., Vasseur, P., 1999. Comparison of *Brachionus calyciflorus* 2-d and microtox® chronic 22-h tests with *Daphnia magna* 21-d test for the chronic toxicity assessment of chemicals. *Environ. Toxicol. Chem.* 18, 2178–2185. <https://doi.org/10.1002/etc.5620181009>
- Raimondo, S., Vivian, D.N., Barron, M.G., 2010. Web-based Interspecies Correlation Estimation (Web-ICE) for Acute Toxicity: User Manual v3.1, Epa/600/R-10/004.
- Rehwoldt, R., Lasko, L., Shaw, C., Wirhowski, E., 1974. Toxicity study of two oil spill reagents toward Hudson river fish species. *Bull. Environ. Contam. Toxicol.* 11, 159–162.
- Rodea-Palomares, I., Leganés, F., Rosal, R., Fernández-Piñas, F., 2012. Toxicological interactions of perfluorooctane sulfonic acid (PFOS) and perfluorooctanoic acid (PFOA) with selected pollutants. *J. Hazard. Mater.* 201–202, 209–218. <https://doi.org/https://doi.org/10.1016/j.jhazmat.2011.11.061>
- Rüdel, H., Böhmer, W., Müller, M., Fliedner, A., Ricking, M., Teubner, D., Schröter-Kermani, C., 2013. Retrospective study of triclosan and methyl-triclosan residues in fish and suspended particulate matter: Results from the German Environmental Specimen Bank. *Chemosphere* 91, 1517–1524. <https://doi.org/https://doi.org/10.1016/j.chemosphere.2012.12.030>

- Schultz, M.M., Bartell, S.E., Schoenfuss, H.L., 2012. Effects of Triclosan and Triclocarban, Two Ubiquitous Environmental Contaminants, on Anatomy, Physiology, and Behavior of the Fathead Minnow (*Pimephales promelas*). *Arch. Environ. Contam. Toxicol.* 63, 114–124. <https://doi.org/10.1007/s00244-011-9748-x>
- Tehranifard, A., Fazeli, M., Yarabbi, J., 2010. Determination of LC50 of Diazinon toxin and linear anionic detergents on *Rutilus frisii kutum*, in: *WIT Transactions on Ecology and the Environment*. WIT Press, pp. 207–215. <https://doi.org/10.2495/WP100181>
- Thatcher, T.O., Santner, J.F., 1966. Acute toxicity of LAS to various fish species. *Proc. 21st Purdue Ind. Waste Conf.* 50, 996–1002.
- Tilton, S.C., Orner, G.A., Benninghoff, A.D., Carpenter, H.M., Hendricks, J.D., Pereira, C.B., Williams, D.E., 2008. Genomic Profiling Reveals an Alternate Mechanism for Hepatic Tumor Promotion by Perfluorooctanoic Acid in Rainbow Trout. *Environ. Health Perspect.* <https://doi.org/10.1289/ehp.11190>
- Tsai, C.-F., McKee, J.A., 1980. Acute Toxicity to Goldfish of Mixtures of Chloramines, Copper, and Linear Alkylate Sulfonate. *Trans. Am. Fish. Soc.* 109, 132–141. [https://doi.org/10.1577/1548-8659\(1980\)109<132:ATTGOM>2.0.CO;2](https://doi.org/10.1577/1548-8659(1980)109<132:ATTGOM>2.0.CO;2)
- U.S. EPA, 2016a. Web-ICE v3.3 - release June 2016, Species Sensitivity Distributions - Aquatic Species [WWW Document]. URL <https://www3.epa.gov/webice/iceSSDSpecies.html?filename=as> (accessed 2.20.17).
- U.S. EPA, 2016b. CADDIS Volume 4. Data Analysis: Advanced Analyses [WWW Document]. URL <https://www.epa.gov/caddis-vol4/caddis-volume-4-data-analysis-advanced-analyses-controlling-for-natural-variability#tab-5> (accessed 2.6.17).
- U.S. EPA, 2016c. Web-ICE v3.3 - release June 2016, Aquatic Species [WWW Document]. URL <https://www3.epa.gov/webice/icePredSurr.html?file=as> (accessed 4.18.17).
- U.S. EPA, 1992. Pesticide Ecotoxicity Database (Formerly: Environmental Effects Database (EEDB)), Environmental Fate and Effects Division, U.S.EPA, Washington, D.C.: EPA Office of Pesticides Program Database [WWW Document]. URL <https://cfpub.epa.gov/ecotox/> (accessed 11.12.17).
- Ulhaq, M., Carlsson, G., Örn, S., Norrgren, L., 2013. Comparison of developmental toxicity of seven perfluoroalkyl acids to zebrafish embryos. *Environ. Toxicol. Pharmacol.* 36, 423–426. <https://doi.org/https://doi.org/10.1016/j.etap.2013.05.004>
- Valsecchi, S., Conti, D., Crebelli, R., Polesello, S., Rusconi, M., Mazzoni, M., Preziosi, E., Carere, M., Lucentini, L., Ferretti, E., Balzamo, S., Gabriella, M., 2017. Deriving environmental quality standards for perfluorooctanoic acid (PFOA) and related short chain perfluorinated alkyl acids. *J. Hazard. Mater.* 323, 84–98. <https://doi.org/10.1016/j.jhazmat.2016.04.055>
- Versteeg, D.J., Rawlings, J.M., 2003. Bioconcentration and Toxicity of Dodecylbenzene Sulfonate (C12LAS) to Aquatic Organisms Exposed in Experimental Streams. *Arch. Environ. Contam. Toxicol.* 44, 237–246. <https://doi.org/10.1007/s00244-002-2017-2>
- Vierke, L., Staude, C., Biegel-Engler, A., Drost, W., Schulte, C., 2012. Perfluorooctanoic acid (PFOA) - main concerns and regulatory developments in Europe from an environmental point of view. *Environ. Sci. Eur.* 24, 16. <https://doi.org/10.1186/2190-4715-24-16>

- Wang, Y., Niu, J., Zhang, L., Shi, J., 2014. Toxicity assessment of perfluorinated carboxylic acids (PFCAs) towards the rotifer *Brachionus calyciflorus*. *Sci. Total Environ.* 491–492, 266–270. <https://doi.org/https://doi.org/10.1016/j.scitotenv.2014.02.028>
- Wilson, B.A., Smith, V.H., deNoyelles, F., Larive, C.K., 2003. Effects of Three Pharmaceutical and Personal Care Products on Natural Freshwater Algal Assemblages. *Environ. Sci. Technol.* 37, 1713–1719. <https://doi.org/10.1021/es0259741>
- Yang, S., Xu, F., Wu, F., Wang, S., Zheng, B., 2014. Development of PFOS and PFOA criteria for the protection of freshwater aquatic life in China. *Sci. Total Environ.* 470–471, 677–683. <https://doi.org/https://doi.org/10.1016/j.scitotenv.2013.09.094>
- Zhang, L., Niu, J., Li, Y., Wang, Y., Sun, D., 2013. Evaluating the sub-lethal toxicity of PFOS and PFOA using rotifer *Brachionus calyciflorus*. *Environ. Pollut.* 180, 34–40. <https://doi.org/https://doi.org/10.1016/j.envpol.2013.04.031>
- Zhang, L., Niu, J., Wang, Y., Shi, J., Huang, Q., 2014. Chronic effects of PFOA and PFOS on sexual reproduction of freshwater rotifer *Brachionus calyciflorus*. *Chemosphere* 114, 114–120. <https://doi.org/https://doi.org/10.1016/j.chemosphere.2014.03.099>

APPENDIX 2: Supplementary information for Chapter 3

Uptake and translocation of perfluoroalkyl acids (PFAA) in red chicory (*Cichorium intybus* L.) under various treatments with pre-contaminated soil and irrigation water

Andrea Gredelj^a, Carlo Nicoletto^b, Sara Valsecchi^c, Claudia Ferrario^c, Stefano Polesello^c, Roberto Lava^d, Francesca Zanon^d, Alberto Barausse^{a,e}, Luca Palmeri^a, Laura Guidolin^e, Marco Bonato^e

^a Department of Industrial Engineering, University of Padova, via Marzolo 9, 35131 Padova, Italy,

^b Department of Agronomy Food, Natural resources, Animals and Environment (DAFNAE), University of Padova, Viale dell'Università 16, 35020 Legnaro, Italy,

^c Water Research Institute - National Research Council of Italy (IRSA-CNR), Via del Mulino 19, 20861 Brugherio (MB), Italy,

^d ARPAV (Regional Environmental Agency of Veneto), Via Lissa 6, 30174 Venezia Mestre, Italy,

^e Department of Biology, University of Padova, Via Bassi 58/b, 35131 Padova, Italy

A2-1. Chemicals and materials

a) Technical standards used for spiking purposes and adsorption/desorption batch test

Table A2-1. List of perfluoroalkyl acids (PFAAs) standards used for spiking with their purity and the suppliers

Chemical	CAS	Purity	Supplier
PFBA (Perfluorobutanoic acid)	375-22-4	98.0%	Sigma Aldrich, Italy
PFPeA (Perfluoropentanoic acid)	2706-90-3	97.0%	Sigma Aldrich, Italy
PFHxA (Perfluorohexanoic acid)	307-24-4	97.0%	Sigma Aldrich, Italy
PFHpA (Perfluoroheptanoic acid)	375-85-9	99.0%	Sigma Aldrich, Italy
PFOA (Perfluorooctanoic acid)	335-67-1	96.0%	Sigma Aldrich, Italy
PFNA (Perfluorononanoic acid)	375-95-1	97.0%	Sigma Aldrich, Italy
PFDA (Perfluorodecanoic acid)	335-76-2	98.0%	Sigma Aldrich, Italy
PFBS (Perfluorobutanesulfonic acid)	375-73-5	97.0%	Sigma Aldrich, Italy
PFOS (Perfluorooctanesulfonic acid, potassium salt)	1763-23-1	98.5%	LGC Standards, Italy

Spiking solution for irrigation water was prepared by solving 90 mg (nominal mass) of each PFAAs in 250 mL of MeOH/H₂O (v/v) 70:30. Firstly, 40 mL of H₂O LC/MS grade 80 mL of MeOH (both Fluka Analytical) PFAAs were added in the volumetric flask. were then solved from longest to the shortest. Long-chain were weighted and short chain (<C₆) were added by volume directly to the flask. After that, 35 mL of ultrapure water and remaining MeOH were added and flask was shaken and sonicated for 5 min (to dissolve remaining visible amounts of PFAAs). Solution was transferred to the plastic bottle afterwards and 1 mL was taken for the analyses to validate the spiking accuracy.

Spiking solutions for soil were prepared in a similar way, as described in the A2-3.

For adsorption/desorption batch experiments additionally calcium chloride (anhydrous, granular, ≤7.0 mm, ≥93.0%) and sodium azide (BioUltra, ≥99.5%) were purchased from Sigma Aldrich. They were used as the background electrolyte (CaCl₂) and to suppress microbial activity (NaN₃). Purchased salts were used for the preparation of the aqueous solution with the concentrations of 0.01 M CaCl₂ and 1 g/L of NaN₃, which was stored and used throughout all of the sorption/desorption experiments as the aqueous phase.

Stock spike solution for adsorption/desorption tests, containing all 9 PFAAs, each in the nominal concentration of 500 mg/L, was prepared in the MeOH/H₂O (v/v) 70:30, using MeOH and H₂O LC/MS grade (Fluka Analytical), and was kept at the 4°C in the polypropylene vial. This solution was used for the further dilution and preparation of the set of five spike solutions for the batch sorption tests with the five initial concentrations in a range 1-500 µg/L (each PFAA). For dilutions, pure MeOH/H₂O 70/30 (v/v) solution was always used in order to keep the volumetric percentages of the solvents constant.

b) Analytical standards and materials

For the LC-MS/MS analyses of samples, all native PFAAs (namely: Perfluoro-*n*-butanoic acid, Perfluoro-*n*-pentanoic acid, Perfluoro-*n*-hexanoic acid, Perfluoro-*n*-heptanoic acid, Perfluoro-*n*-octanoic acid, Perfluoro-*n*-nonanoic acid, Perfluoro-*n*-decanoic, Perfluoro-*n*-undecanoic, Perfluoro-*n*-dodecanoic, Potassium perfluoro-1-butanefulfonate, Sodium perfluoro-1-hexanesulfonate and Sodium perfluoro-1-octanesulfonate) and mass-labeled (i.e.: perfluoro-

n-[¹³C₄]butanoic acid, perfluoro-*n*-[3,4,5-¹³C₃]pentanoic acid, perfluoro-*n*-[1,2-¹³C₂]hexanoic acid, Perfluoro-*n*-[1,2,3,4-¹³C₄]heptanoic acid, perfluoro-*n*-[1,2,3,4-¹³C₄]octanoic acid, Perfluoro-*n*-[1,2,3,4,5-¹³C₅]nonanoic acid, Perfluoro-*n*-[1,2-¹³C₂]decanoic, Perfluoro-*n*-[1,2-¹³C₂]undecanoic, perfluoro-*n*-[1,2-¹³C₂]dodecanoic, sodium perfluoro-1-[2,3,4-¹³C₃]butanesulfonate, sodium perfluoro-1-hexane[¹⁸O₂]sulfonate and Sodium perfluoro-1-[1,2,3,4-¹³C₄]octanesulfonate) were purchased by Wellington Laboratories with purity > 99 %. All standard solutions were stored at 4°C. All reagents were analytical reagent grade. LC-MS grade Chromasolv acetonitrile (99.7%), LC-MS grade Chromasolv methanol (99.9%) and ammonium acetate (99%) were purchased from Sigma-Aldrich (St. Louis, MO, USA). Water (<18 MΩcm resistivity) was produced by a Millipore Direct-QUV water purification system (Millipore, Bedford, MA, USA).

A2-2. Details of sample preparation and analytical methods

At harvest, red chicory plants were split in roots, external leaves and head, while representative soil samples were taken from the pot, as shown in the scheme:

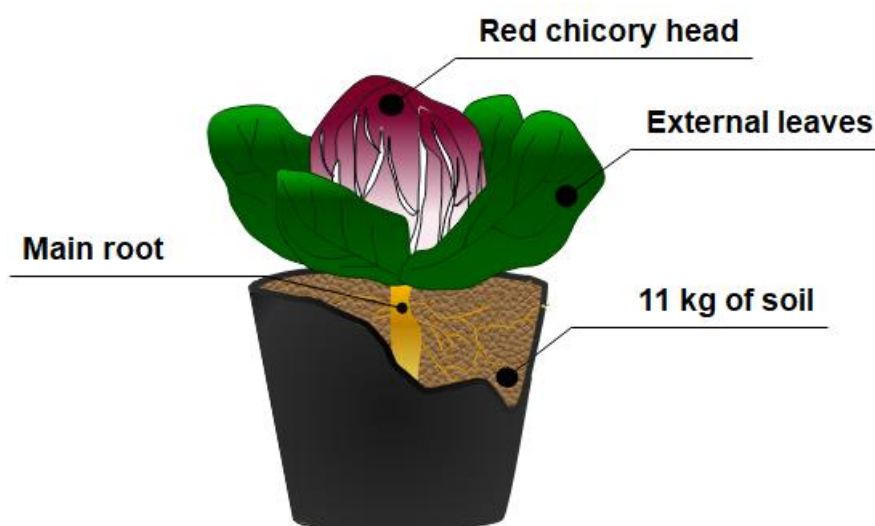


Figure A2-1. Experimental pot scheme with red chicory (radicchio) plant compartments

Symmetrical halves of every compartment were used for sample preparation for PFAAs concentrations analyzes, while the rest of the material was used for determination of dry matter content. Dry matter content was obtained by weighing samples on a fresh weight basis and after the oven drying in a PID system ventilated oven set at 65°C for 72 h.

a) Plant matrices

A sufficient portion of the uniform sample (usually ½ of every plant compartment) was homogenized by grinding in a food mixer and appropriate quantities (i.e. 0.5 g_{f.w.} of root, 0.5-5 g_{f.w.} of leaves and 1-10 g_{f.w.} of the head material) were placed into PP tubes. The extraction was then performed with the addition of 10 mL of acetonitrile, followed by vortex agitation for 30 s, sonication for 15 minutes and then centrifugation for 12 min (8000 rpm, 10°C). Finally, 2 mL of supernatant were transferred into an Eppendorf tube and stored at 4°C until the analysis. Procedural blanks were included during the analyses, and were handled in the same manner as the plant samples. 90 µL of extracts from plant sample were placed into a micro vial,

acidified by adding 10 µL of concentrated formic acid, spiked with 20 µL of the diluted SIL-IS solution (40 µg/L) and diluted to 200 µL with the addition of buffer solution (2 mM CH₃CO₂NH₄ + 5% MeOH) before the injection. All plant samples were analysed by UHPLC-MS/MS (TSQ Quantum™ Access MAX, Thermo Scientific, USA) equipped with a Waters Acquity UPLC BEH C18 column (50x2.1 mm id, 1.7 µm particle size) by direct injection (injection volume 30 µL). Calibration curves were weekly prepared using mixed standard solutions in acetonitrile. In particular, 90 µL of each standard solution were placed into a micro vial, acidified by adding 10 µL of concentrated formic acid, spiked with 20 µL of the diluted SIL-IS solution (40 µg L⁻¹) and diluted to 200 µL with the addition of buffer solution (2 mM CH₃CO₂NH₄ + 5% MeOH) before the injection. Quantification was performed by using the isotopic dilution method and calibration curves were acquired before each analytical run. Limits of detection (LOD), estimated according to the ISO 6107-2:2006 standard, are reported in Table A2-4. Reported PFAAs concentrations were corrected by subtracting the average procedural blank values above LODs.

Table A2-2. Elution gradients used by the analytical pump. Mobile phases: (A) 2 mM CH₃CO₂NH₄ + 5%MeOH; (B) MeOH.

Time (min)	Analytical pump		
	Flow (µL min ⁻¹)	A%	B%
0.00	300	95	5
2.00	300	30	70
5.50	300	10	90
10.00	300	0	100
13.00	300	0	100
14.00	300	95	5
18.50	300	95	5

Table A2-3. LC/MS/MS parameters for all target analytes and internal standards

	Target analytes	RT min	Precurs or ion (m/z)	Product ions (m/z)	Collision energy
Perfluorobutanoic acid	PFBA	2.80	212.9	168.9	11
Perfluoropentanoic acid	PFPeA	3.50	262.9	69.0 218.9	39 11
Perfluorohexanoic acid	PFHxA	3.90	312.9	119.1 268.9	22 11
Perfluoroheptanoic acid	PFHpA	4.30	362.9	169.0 318.9	18 12
Perfluorooctanoic acid	PFOA	4.60	412.9	169.0 368.9	19 13
Perfluorononanoic acid	PFNA	5.00	462.9	218.9 418.9	18 13
Perfluorodecanoic acid	PFDA	5.40	512.9	268.9 468.9	18 13
Perfluorobutane sulfonate	PFBS	3.60	298.9	80.2 99.1	44 32
Perfluorooctane sulfonate	PFOS	5.00	498.9	80.3 99.1	45 45
Perfluoro-n-[¹³C4] butanoic acid	¹³ C4-PFBA	2.80	216.9	171.9	11
Perfluoro-n-[¹³C5] pentanoic acid	¹³ C5-PFPeA	3.50	265.9	221.9	11
Perfluoro-n-[¹³C2] hexanoic acid	¹³ C2-PFHxA	3.90	314.9	269.9	11
Perfluoro-n-[¹³C4] octanoic acid	¹³ C4-PFOA	4.60	416.9	371.9	13
Perfluoro-n-[¹³C5] nonanoic acid	¹³ C5-PFNA	5.00	467.9	422.9	13
Perfluoro-n-[¹³C2] decanoic acid	¹³ C2-PFDA	5.40	514.9	469.9	13
Perfluoro-n-octane [¹³C4] sulfonate	¹³ C4-PFOS	5.00	502.9	99.1	45

Table A2-4. Limits of detection (LODs) of all target analytes estimated in plants samples according to the ISO 6107-2:2006 standard and relative recoveries

Chemical	Minimum value of LOD (maximum weight extracted= 10 g of wet samples) (ng/g_{ww.})	Maximum value of LOD (minimum weight extracted = 0.5 g of wet samples) (ng/g_{ww.})	Recovery %
PFBA	3.27	64.96	90.68
PFPeA	1.34	26.41	80.01
PFHxA	3.60	71.56	77.86
PFHpA	3.90	77.38	73.71
PFOA	2.02	40.08	69.82
PFNA	2.76	54.85	67.82
PFDA	2.06	40.81	58.41
PFBS	3.83	76.03	85.16
PFOS	2.22	44.02	73.00

b) Soil and water

The instrument used was a HPLC LC-30AD XR Shimadzu coupled with an API 6500 AB Sciex triple quadrupole and with a CTC PAL HTS XT autosampler. Acquisition and quantification were carried out with Analyst™ 1.6.3 and MULTIQUANT 3.02 software. The column used was a Phenomenex Kinetex Evo C18 (1.7 µm x 2.1 mm x 100 mm) and Supelco Ascentis RP-Amide (2.7 µm x 2.1 mm x 150 mm) for water and soil analyses, respectively. Chromatographic conditions were: 0.15 mL/min of flow for water analysis (0.3 mL/min for soil) and injection volume 80 µL with column thermostated at 40 °C.

Table A2-5. Elution gradients used by the analytical pump - **water** samples. The two eluents were: A (ultrapure water + 2mM ammonia acetate in 5% MeOH) and B (MeOH + Acetonitrile, 2:8, both LC/MS grade).

Time (min)	% A	% B
1.00	100	0
1.50	60	40
14.0	8	92
15.0	0	100
18.0	0	100
20.0	100	0
21.0	100	0

Table A2-6. Elution gradients used by the analytical pump - **soil** samples. The two eluents were: A (ultrapure water + 2mM ammonia acetate in 5% MeOH) and B (MeOH + Acetonitrile, 2:8, both LC/MS grade).

Time (min)	% A	% B
0.2	100	0
1.00	60	40
16.0	0	100
18.0	0	100
19.0	100	100
20.0	100	0

The instrumental parameters, working with ESI in negative ionization and Multiple Reaction Monitoring (MRM) acquisition mode, were: spray voltage of -4500 V, source temperature at 350 °C, ion source turbo spray curtain gas at 25 psig, ion source gas 1 at 36 psig and ion source gas 2 at 50 psig. The collision gas was nitrogen with a pressure of 9 L/min.

Calibration curves were acquired for every batch of analysis from 5 to 500 ng/L (5-200 ng/L for soils) and samples diluted accordingly. In every batch also blank, instrumental QC and process QC were injected.

The analytical procedures for aqueous and soil samples were both validated and carried out according to ISO/IEC 17025:2005. The sequence was accepted if correlation coefficients of the calibration curves were > 0.990 and requirements of internal control charts were satisfied. Recoveries were assessed using different real aqueous matrices fortified at 80 ng/L. Recoveries for every batch were all considered satisfied in the range 70-125 % for water and 35-150 % for soil. The average recoveries obtained in phase of validation of the procedures are shown in Table A2-7Table .

The LOD of the method is 5 ng/L for water and 3 µg/kg for soil, but it varied according to the dilution factors.

Table A2-7. Recoveries of all target analytes estimated in water and soil samples during the validation of procedures.

Chemical	Recovery in water (%)	Recovery in soil (%)
PFBA	95	96
PFPeA	100	92
PFHxA	96	96
PFHpA	99	92
PFOA	96	101
PFNA	98	97
PFDA	90	97
PFBS	94	93
PFOS	93	100

A2-3. Chicory cultivation and agricultural soil details

Red chicory (also “Italian chicory” or “radicchio”) seeds were obtained from Bejo Italia seed (RA), variety “Vasari F1” resistant to bolting in the high temperature. About 300 plants were seeded in the end of June 2018 in the peat nursing pots, and the most uniform looking transplants were transferred to pots on the 10th of August. Round plastic pots (Φ = 25 cm) of 10 L nominal volume were filled with 11 kg of dry soil (nominal dry mass) and on the 4th day from transplanting, plants started to receive portions of spiked water. Growing period lasted for 87 days, plants being harvested on 6th of November 2018. During the growth soil temperature ranged from the minimum 12.9°C to the maximum 34.3°C (average 22.3°C) and the greenhouse air temperature from the minimum 10.6°C to the maximum 57.5°C with the average of 26.0°C.

During the irrigation, special care was given to deliver the water only on the top soil, to avoid direct contact of contaminated water and plants. Leaching from pots was avoided by closing the bottom pot holes with the adhesive PFAS-free duct tape. However, towards the end of experiment, leaching in very small quantities was observed from some pots.

Nutrient solution (Hoagland's solution) was added three times for the duration of experiment and was delivered together with the irrigation water. Periodical treatments against insects and fungal infections were performed when needed, in order to maintain health of chicory plants. Added quantity of nutrients was equivalent to 6 mL of solutions A and B and 1 mL of 45% phosphorous acid. 5 L of each stock nutrient solution were prepared as follows:

Table A2-8. Preparation of the 5L stock nutrient solutions for soil fertilization

SOLUTION A		
Substance		Mass (g)
Iron EDTA	Fe(EDTA)	2.154
Calcium nitrate tetrahydrate	Ca(NO ₃) ₂ ×4H ₂ O	290.593
Ammonium nitrate	NH ₄ NO ₃	171.769
SOLUTION B		
Substance		Mass (g)
Magnesium sulfate heptahydrate	MgSO ₄ *7H ₂ O	121.704
Sodium molybdate dihydrate	Na ₂ MoO ₄ *2H ₂ O	0.006
Zinc Sulfate Dihydrate	ZnSO ₄ *2H ₂ O	0.038
Boric acid	H ₃ BO ₃	0.715
Cooper sulfate pentahydrate	CuSO ₄ *5H ₂ O	0.02
Manganese chloride	MnCl ₂ *4H ₂ O	0.415
Potassium sulfate	K ₂ SO ₄	130.925

Agricultural soil was analyzed for elemental content and texture characterization in the LaChi lab, University of Padova, DAFNAE, Agripolis, by the Italian's Ministry of Agriculture norm D.M. 13/09/1999 for agricultural soil chemical analyses (Table A2-9).

Table A2-9. Soil characterization

Agripolis soil - elemental analyses											
o.c.* (g/kg)	o.m.** (g/kg)	P sol*** (ppm)	Ca (ppm)	K (ppm)	Mg (ppm)	Na (ppm)	P (ppm)	N - Kjeldahl (ppm)	N-NO ₃ ⁻ (ppm)	N- NO ₂ ⁻ (ppm)	N- NH ₄ ⁺ (ppm)
14.3	24.6	1.5	70123.6	8535.5	35134.7	390.6	887.5	1457.0	24.2	0.0	3.1
Soil characterization data:											
pH	Sand (2 mm - 50 µm)	Silt (50 µm-2 µm)	Clay (< 2µm)	Fluvi-calcaric cambisoil (FAO- UNESCO, 1990)				Texture triangle (USDA):			
7.8	47%	38%	15%					Loam			

* o.c. = organic carbon content

** o.m. = organic matter content

*** P sol = total soluble potassium

A2-4. Soil spiking protocol

Spiking protocol was developed by following the recommendations given in (Northcott and Jones, 2000a, 2000b). Prior to spiking, agricultural soil was sieved with the 10 mm mesh to eliminate larger pieces, stones and debris and spread for air drying in the greenhouse for 5 days. Soil spiking was performed in steps, separately for each treatment (6 pots with 11 kg_{dw} of soil each), in total including 8 cycles of spiking with PFAAs matrix spike, that followed after 4 cycles of spiking the control soil treatments with carrier solution only. Two solutions with

appropriate PFAAs concentrations were prepared to achieve nominal concentrations in soil of 100 ng/g_{dw} and 200 ng/g_{dw} and the third one containing only solvents (methanol and ultrapure water) in the same quantity as used in the two spike solutions. Spike solutions were prepared with 70:30 volumetric ratio of methanol and ultrapure water (both HPLC grade), by dissolving 9 PFAAs in order from the longest to the shortest: PFDA, PFNA, PFOA, PFOS, PFHpA, PFHxA, PFPeA, PFBA, PFBS. Spike solutions were prepared in the concentrations of 266 mg/L (100 mL for each cycle of 66,5 kg_{dw} of soil) to achieve concentration of 200 ng/g_{dw} in soil and 133 mg/L to achieve 100 ng/g_{dw} of each PFAA in soil, respectively. Control soils were subjected to the same treatment, by spiking with 100 mL of 70:30 (V:V) methanol/ ultrapure water carrier solution. Mixing was performed with the cement mixer, which was thoroughly cleaned with the piece of paper and rinsed with tap and distilled water prior to and in between all cycles. First step included mixing the prepared 100 mL of spike solution with 25% of total soil (15 kg) for 10 minutes. After that, remaining 51.5 kg of soil was added and additionally mixed for 5 minutes. Mixer was emptied in the 6 pots included in each treatment/spiking cycle. In the following 10 days, every 2 days, soil in each pot was hand mixed for 1-2 min to ensure the air contact, methanol evaporation and PFAAs equilibration. Actual spiked concentrations and homogeneity of spiking were determined by sampling 3 pots per treatment after equilibration period and prior to planting. Composite samples of all 6 pots were taken from 4 treatments containing control soil, all measured concentrations given in the Table A2-10:

Table A2-10. Measured concentrations of PFAAs in soil after spiking and equilibration period of 10 days.

Treatment:	S0W0	S0W1	S0W10	S0W80	S100W0		S100W1		S100W10*	
(ng/g _{d.w.})					mean	st.err	mean	st.err	mean	st.err
PFBA	<0.30	<0.30	<0.30	<0.30	106.06	4.34	86.06	22.80	128.92	57.65
PFPeA	<0.30	<0.30	<0.30	<0.30	87.16	5.21	82.43	24.47	108.79	55.03
PFHxA	<0.30	<0.30	<0.30	<0.30	92.35	3.54	75.70	14.06	113.43	53.54
PFHpA	<0.30	<0.30	<0.30	<0.30	89.78	8.63	78.03	26.30	112.65	53.37
PFOA	<0.30	<0.30	<0.30	<0.30	95.25	6.45	87.50	23.13	133.02	58.87
PFNA	<0.30	<0.30	<0.30	<0.30	86.82	3.86	83.11	26.17	122.14	60.85
PFDA	<0.30	<0.30	<0.30	<0.30	87.04	6.23	83.70	22.03	138.76	74.66
PFBS	<0.30	<0.30	<0.30	<0.30	82.22	5.14	64.43	9.92	122.35	56.64
PFOS	<0.30	<0.30	<0.30	<0.30	76.21	6.32	74.35	12.08	100.95	10.64

Treatment:	S100W80		S200W0		S200W1		S200W10		S200W80	
(ng/g _{d.w.})	mean	st.err	mean	st.err	mean	st.err	mean	st.err	mean	st.err
PFBA	96.16	3.53	164.82	4.57	147.90	8.54	154.67	8.30	153.35	7.22
PFPeA	92.46	0.51	135.95	21.68	119.24	12.34	148.93	10.59	140.57	5.79
PFHxA	101.89	7.66	161.51	10.28	137.91	13.20	163.87	21.13	155.75	6.19
PFHpA	85.41	4.71	138.90	0.93	117.80	6.58	136.39	7.26	130.31	6.74
PFOA	96.17	5.75	188.36	15.80	144.61	1.90	155.79	2.10	163.08	4.43
PFNA	98.53	5.05	153.72	5.60	135.44	8.11	149.80	7.28	148.77	13.54
PFDA	90.65	2.31	157.95	3.15	129.42	11.11	152.14	15.23	159.01	3.47
PFBS	89.06	5.20	184.28	3.00	150.76	5.80	176.55	13.78	153.33	13.06
PFOS	80.15	4.69	179.93	22.64	157.05	1.69	153.81	9.91	177.29	11.42

mean = statistical mean of 3 samples per treatment; st.err. = standard error estimate, expressed as the standard deviation of concentrations in the 3 samples/square root of number of samples.

*only 2 samples were accounted for (as well as in chicory plants afterwards), due to the problems with homogeneity of the treatment's spike.

A2-5. Irrigation water

Spiked water for irrigation was prepared with the matrix spike's (A2-1.a) pre-defined doses approximately every two weeks. Every time, plastic barrels used for the irrigation were thoroughly rinsed and carefully filled with 40 L of water. After spiking with the appropriate quantities of the matrix spike, they were vigorously shaken and water was sampled for analyses. Results of the water analyses are shown in the Table A2-11. Measured concentration and quantities with the irrigation frequencies were used for calculations of the delivered quantities of each PFAA to all the pots.

Volumes and dates of each irrigation portion are given on the Figure A2-2:

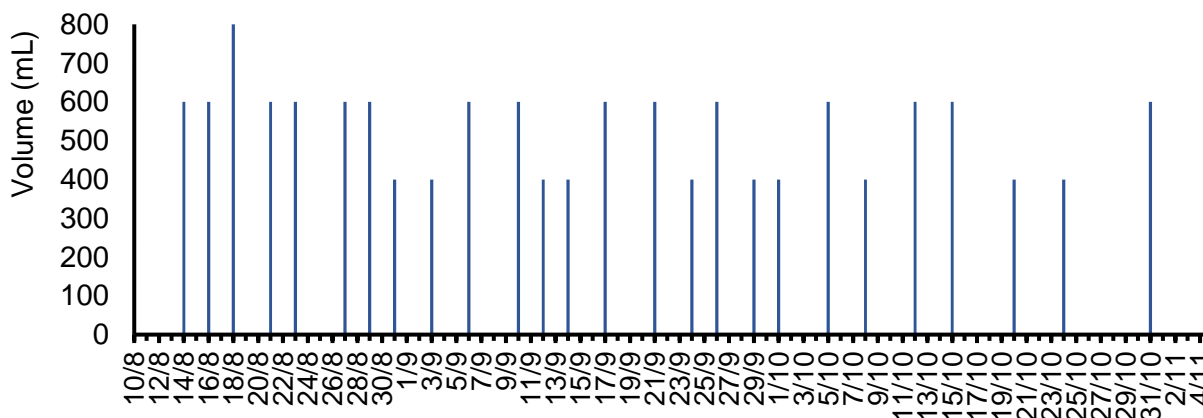


Figure A2-2. Irrigation frequency by date and nominal quantity of each water portion

Table A2-11. Measured concentrations of PFAAs in the spiked irrigation water by date and irrigation treatment

Date:	11/8/2018			20/8/2018			29/8/2018					
µg/L	W1	W10	W80	W1	W10	W80	W1	W10	W80			
PFBA	0.90	11.77	100.93	1.07	9.18	73.40	0.87	8.63	60.76			
PFPeA	0.96	13.07	105.34	0.99	10.92	72.82	0.88	9.09	58.59			
PFBS	0.84	13.36	83.12	1.14	10.41	76.22	0.95	8.73	68.04			
PFHxA	1.23	13.25	102.37	1.23	9.28	83.82	1.18	11.72	69.12			
PFHpA	0.82	10.73	82.83	0.89	8.27	81.29	0.79	8.25	79.00			
PFOA	0.86	11.01	72.94	0.99	8.82	75.04	0.86	8.87	81.52			
PFNA	1.06	13.36	103.04	1.08	8.63	78.18	0.86	7.62	123.22			
PFDA	0.71	11.35	106.52	0.95	7.42	76.58	0.96	7.45	116.51			
PFOS	0.99	12.12	93.45	1.00	8.97	72.85	1.01	8.53	128.74			
Date:	10/9/2018			19/9/2018			1/10/2018			15/10/2018		
µg/L	W1	W10	W80	W1	W10	W80	W1	W10	W80	W1	W10	W80
PFBA	1.15	10.33	81.98	0.95	6.86	64.76	0.89	9.59	71.46	0.89	9.85	75.85
PFPeA	1.07	10.68	83.14	0.95	7.75	75.52	0.99	7.85	78.15	1.03	9.18	67.47
PFBS	1.27	9.42	61.01	1.08	9.06	79.37	1.11	10.52	71.89	1.01	10.55	78.86
PFHxA	1.28	10.11	82.85	1.21	9.50	90.64	1.23	10.87	90.06	1.25	14.10	95.59
PFHpA	1.09	10.50	75.84	0.87	9.08	87.00	1.05	9.43	68.07	1.01	11.07	80.05
PFOA	1.12	9.18	71.74	0.91	7.09	59.86	1.07	9.70	70.77	0.96	10.93	78.11
PFNA	0.94	9.87	76.87	1.04	9.26	89.12	1.01	9.38	81.12	1.11	10.45	76.69
PFDA	0.98	9.11	76.16	0.65	10.16	50.69	0.80	9.40	61.12	0.85	9.98	52.79
PFOS	1.08	9.72	77.55	0.80	7.91	60.05	1.03	9.73	77.52	0.76	8.77	64.72

A2-6. Measured concentrations of PFAAs in plant compartments and soil

Table A2-12. Measured concentrations of PFAAs in red chicory plant compartments. Concentrations are shown in the dry weight basis and as means with the standard error estimates of 3 replicate plats (n = 2 only for S100W10, due to problems with the spike homogeneity).

(ng/g d.w.)	S0W0		S100W0		S200W0		S0W1		S100W1		S200W1		S0W10		S100W10		S200W10		S0W80		S100W80		S200W80	
Roots	mean	st.err.	mean	st.err.	mean	st.err.	mean	st.err.	mean	st.err.	mean	st.err.	mean	st.err.	mean	st.err.	mean	st.err.	mean	st.err.	mean	st.err.	mean	st.err.
PFBA	<LOD	<LOD	20169.82	2696.29	42756.25	4195.93	<LOD	<LOD	19203.47	2470.03	29209.13	1923.80	2851.17	332.11	25169.03	3656.62	20632.57	1995.57	18394.25	3722.85	29100.73	4430.68	40037.31	3446.27
PFPeA	768.67	293.68	7053.92	1007.99	16934.67	487.45	<LOD	<LOD	7832.10	393.00	11546.12	2338.11	2289.24	560.37	11519.28	314.62	8894.18	1036.56	7956.04	988.26	11366.80	1108.75	18150.49	1299.70
PFHxA	<LOD	<LOD	3631.15	449.77	7246.01	812.34	<LOD	<LOD	3363.95	318.63	4164.89	363.53	<LOD	<LOD	4451.00	265.80	3817.73	434.84	4694.22	354.48	5190.63	658.79	7443.66	1265.59
PFHpA	<LOD	<LOD	1571.50	369.57	2732.90	497.08	<LOD	<LOD	1184.41	58.63	1603.52	241.40	<LOD	<LOD	2014.33	315.72	1699.78	350.45	1541.04	204.53	2102.60	279.08	3373.84	698.81
PFOA	<LOD	<LOD	771.51	110.88	1584.29	469.21	<LOD	<LOD	557.83	9.23	871.91	103.13	<LOD	<LOD	1147.57	201.99	750.48	120.40	995.58	375.82	950.25	139.01	1714.88	615.75
PFNA	<LOD	<LOD	747.54	25.23	884.50	180.87	<LOD	<LOD	<LOD	<LOD	<LOD	<LOD	<LOD	<LOD	<LOD	<LOD	<LOD	<LOD	830.37	136.56	<LOD	<LOD	850.27	109.36
PFDA	858.03	175.76	735.77	160.66	827.19	154.84	<LOD	<LOD	658.43	101.24	656.29	110.80	<LOD	<LOD	695.06	121.46	778.58	129.43	691.78	174.66	<LOD	<LOD	728.40	175.89
PFBS	1715.66	178.37	6243.13	557.16	18093.35	1074.58	<LOD	<LOD	6066.17	503.38	9737.53	2787.88	1979.21	141.23	6900.88	1714.02	9471.06	3561.96	8132.76	3002.76	13554.64	547.31	19125.80	1677.96
PFOS	<LOD	<LOD	864.68	57.45	1104.76	138.60	<LOD	<LOD	<LOD	<LOD	878.14	168.41	<LOD	<LOD	919.63	270.43	688.43	119.75	832.37	205.81	782.71	61.75	1064.19	197.73
(ng/g d.w.)	S0W0		S100W0		S200W0		S0W1		S100W1		S200W1		S0W10		S100W10		S200W10		S0W80		S100W80		S200W80	
Leaves	mean	st.err.	mean	st.err.	mean	st.err.	mean	st.err.	mean	st.err.	mean	st.err.	mean	st.err.	mean	st.err.	mean	st.err.	mean	st.err.	mean	st.err.	mean	st.err.
PFBA	<LOD	<LOD	5997.17	2548.60	9373.03	2577.35	<LOD	<LOD	10009.30	1779.36	12290.66	2370.82	2148.01	404.55	14245.22	747.05	9475.34	2435.88	9124.45	2268.05	15155.73	2661.77	25873.33	5962.63
PFPeA	<LOD	<LOD	2619.21	1059.08	4080.97	757.57	<LOD	<LOD	4141.83	592.00	4619.39	971.18	677.58	395.57	7506.87	402.23	4636.90	864.78	4600.98	921.77	7125.94	982.08	10787.38	2651.46
PFHxA	<LOD	<LOD	425.24	161.39	644.43	124.43	<LOD	<LOD	962.98	324.19	1034.68	353.52	<LOD	<LOD	1321.49	109.49	1162.26	335.68	1005.88	134.46	1708.52	525.58	3287.83	876.36
PFHpA	<LOD	<LOD	<LOD	<LOD	<LOD	<LOD	<LOD	<LOD	590.23	22.84	<LOD	<LOD	<LOD	<LOD	<LOD	<LOD	<LOD	<LOD	<LOD	<LOD	<LOD	<LOD	<LOD	<LOD
PFOA	<LOD	<LOD	<LOD	<LOD	<LOD	<LOD	<LOD	<LOD	337.43	20.15	<LOD	<LOD	<LOD	<LOD	<LOD	<LOD	<LOD	<LOD	<LOD	<LOD	<LOD	<LOD	<LOD	<LOD
PFNA	<LOD	<LOD	<LOD	<LOD	<LOD	<LOD	<LOD	<LOD	<LOD	<LOD	<LOD	<LOD	<LOD	<LOD	<LOD	<LOD	<LOD	<LOD	<LOD	<LOD	<LOD	<LOD	<LOD	<LOD
PFDA	<LOD	<LOD	<LOD	<LOD	<LOD	<LOD	<LOD	<LOD	370.59	46.94	<LOD	<LOD	<LOD	<LOD	<LOD	<LOD	<LOD	<LOD	<LOD	<LOD	<LOD	<LOD	<LOD	<LOD
PFBS	<LOD	<LOD	906.55	310.15	1880.96	451.75	<LOD	<LOD	1706.84	239.79	2384.17	373.05	1159.86	356.75	2954.01	62.21	2323.62	740.35	2283.76	535.40	3512.01	771.23	6653.09	2141.61
PFOS	<LOD	<LOD	<LOD	<LOD	<LOD	<LOD	<LOD	<LOD	359.64	11.19	333.11	49.98	<LOD	<LOD	<LOD	<LOD	<LOD	<LOD	<LOD	<LOD	<LOD	<LOD	<LOD	<LOD
(ng/g d.w.)	S0W0		S100W0		S200W0		S0W1		S100W1		S200W1		S0W10		S100W10		S200W10		S0W80		S100W80		S200W80	
Heads	mean	st.err.	mean	st.err.	mean	st.err.	mean	st.err.	mean	st.err.	mean	st.err.	mean	st.err.	mean	st.err.	mean	st.err.	mean	st.err.	mean	st.err.	mean	st.err.
PFBA	<LOD	<LOD	2938.49	223.41	3687.25	201.56	<LOD	<LOD	2554.00	55.41	3936.06	536.08	538.26	78.08	2594.70	449.95	3300.61	190.93	5615.81	602.28	8625.72	1090.54	9835.75	599.56
PFPeA	<LOD	<LOD	1422.96	42.80	2286.87	444.15	<LOD	<LOD	1321.65	110.37	1689.15	174.12	395.98	73.92	1402.05	118.01	1897.05	97.92	3580.21	496.00	4296.47	485.00	5345.02	129.78
PFHxA	<LOD	<LOD	648.05	71.47	1477.01	245.62	<LOD	<LOD	600.70	55.37	804.42	101.47	<LOD	<LOD	806.98	61.42	714.84	45.73	1946.06	335.54	3482.51	508.86	4757.41	822.71
PFHpA	<LOD	<LOD	280.76	63.97	560.72	129.33	<LOD	<LOD	211.46	8.06	310.88	58.38	<LOD	<LOD	366.10	63.22	316.41	54.22	611.07	30.92	1411.90	216.49	2138.99	407.14
PFOA	<LOD	<LOD	138.49	20.49	327.31	110.76	<LOD	<LOD	99.68	1.10	168.89	26.70	<LOD	<LOD	208.61	39.99	140.00	16.32	372.32	96.75	635.68	99.95	1075.88	360.84
PFNA	<LOD	<LOD	133.79	2.34	180.61	45.03	<LOD	<LOD	<LOD	<LOD	<LOD	<LOD	<LOD	<LOD	<LOD	<LOD	<LOD	<LOD	328.54	24.11	<LOD	<LOD	538.63	57.71
PFDA	<LOD	<LOD	133.19	32.49	205.67	25.06	<LOD	<LOD	118.26	20.19	127.59	26.48	<LOD	<LOD	126.38	24.07	145.25	17.88	268.59	37.79	<LOD	<LOD	459.19	100.00
PFBS	<LOD	<LOD	1115.44	83.65	3663.70	433.71	<LOD	<LOD	1081.60	75.10	1896.83	608.06	345.97	19.76	1257.02	330.95	1723.60	553.54	3311.10	1191.96	9051.46	385.22	12201.49	1178.81
PFOS	<LOD	<LOD	155.51	14.12	224.64	39.43	<LOD	<LOD	<LOD	<LOD	169.65	37.37	<LOD	<LOD	167.71	51.71	127.89	14.19	321.27	39.84	521.43	33.22	672.32	109.09

Table A2-13. Measured concentrations in the soil on the end of the experiment. Concentrations are expressed as means (n = 3) with standard error estimates.

(ng/g d.w.)	S0W0		S100W0		S200W0	
	mean	st.err.	mean	st.err.	mean	st.err.
PFBA	0	0	83.62	18.08	183.49	26.41
PFPeA	0	0	106.40	19.46	212.31	18.17
PFHxA	0	0	118.08	21.46	293.55	29.56
PFHpA	0	0	161.18	19.18	226.52	13.85
PFOA	0	0	115.30	3.84	223.73	23.51
PFNA	0	0	115.80	15.83	246.82	12.20
PFDA	0	0	118.47	19.86	187.30	4.76
PFBS	0	0	130.38	31.99	294.00	30.56
PFOS	0	0	84.52	3.86	145.74	10.45
(ng/g d.w.)	S0W1		S100W1		S200W1	
	mean	st.err.	mean	st.err.	mean	st.err.
PFBA	1.10	0.10	103.01	7.70	160.46	24.71
PFPeA	1.39	0.33	146.00	16.32	217.60	23.02
PFHxA	2.12	0.25	159.67	29.06	235.21	30.62
PFHpA	1.18	0.05	145.60	27.67	199.44	20.98
PFOA	0.88	0.13	129.95	16.07	170.26	7.80
PFNA	0.96	0.45	124.15	17.01	157.84	6.22
PFDA	0.69	0.24	137.08	15.13	167.71	9.86
PFBS	1.26	0.22	120.42	11.30	258.70	41.05
PFOS	0.52	0.19	112.49	17.93	166.87	7.57
(ng/g d.w.)	S0W10		S100W10		S200W10	
	mean	st.err.	mean	st.err.	mean	st.err.
PFBA	9.18	1.09	74.71	43.51	204.87	10.26
PFPeA	15.13	2.77	115.99	61.37	237.17	21.71
PFHxA	18.09	3.00	133.53	64.70	257.28	64.01
PFHpA	14.10	3.91	134.76	69.65	291.87	44.47
PFOA	6.41	2.57	125.74	70.47	226.54	11.51
PFNA	9.26	5.19	126.99	75.96	314.92	61.12
PFDA	6.34	3.50	133.42	79.03	250.20	28.10
PFBS	17.85	5.20	113.39	58.65	276.26	23.22
PFOS	9.01	4.63	102.81	59.39	266.19	38.89
(ng/g d.w.)	S0W80		S100W80		S200W80	
	mean	st.err.	mean	st.err.	mean	st.err.
PFBA	90.85	26.19	142.95	9.36	258.47	22.54
PFPeA	108.61	10.36	279.78	44.82	418.93	77.28
PFHxA	165.58	32.66	264.58	14.04	364.53	5.88
PFHpA	105.23	24.52	219.54	39.17	297.67	24.22
PFOA	90.09	19.88	213.80	22.62	341.21	13.82
PFNA	84.98	17.79	216.03	32.42	300.11	21.74
PFDA	82.19	20.27	200.49	26.43	286.75	21.27
PFBS	137.75	27.39	250.70	51.71	354.71	40.39
PFOS	85.48	19.70	172.88	25.38	254.80	9.69

A2-7. Percentage distributions of PFAAs in different plant compartments

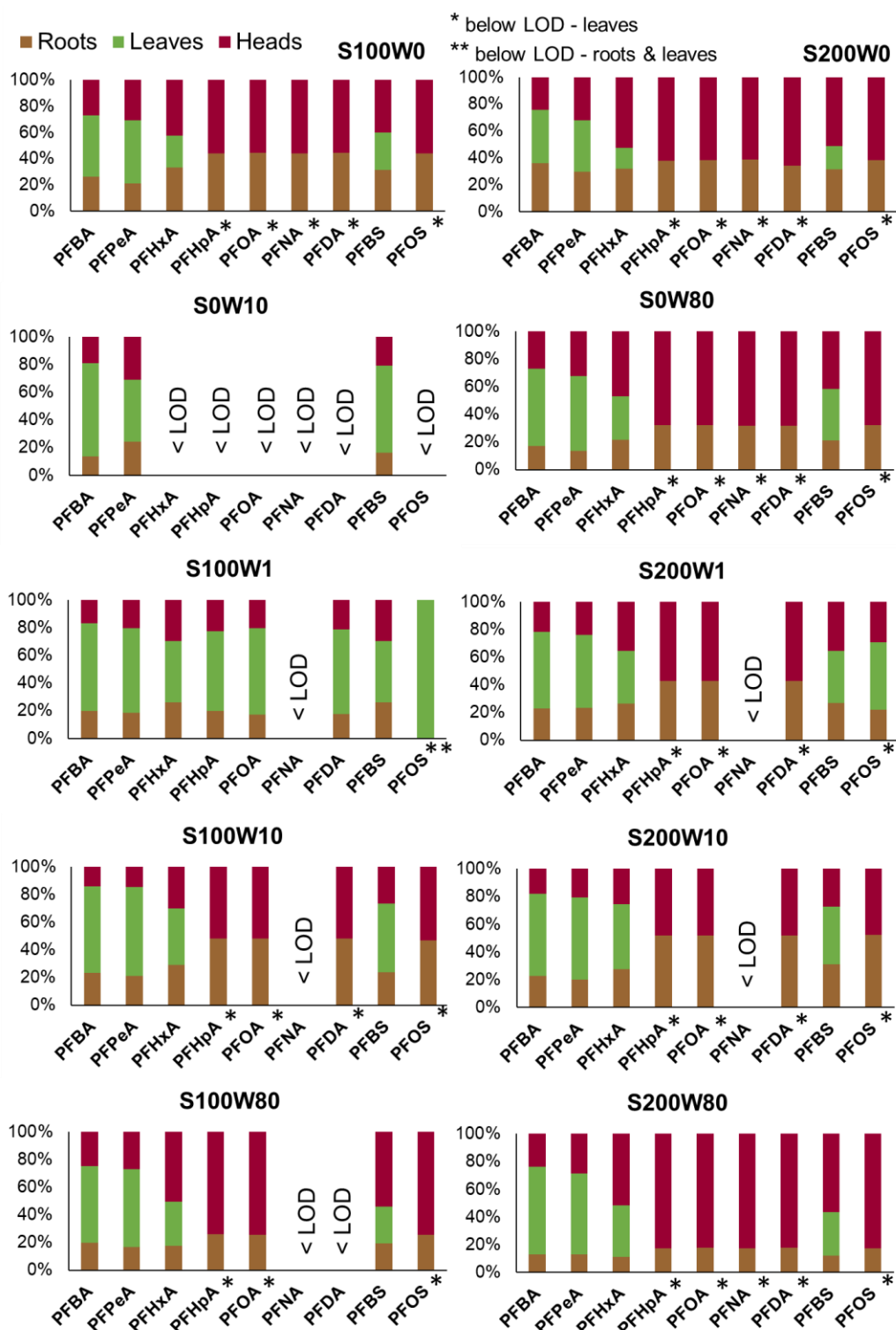


Figure A2-3. Inter-compartmental mass balances for 10 treatments (S0W0 and S0W1 were < LOD for all PFAAs) and expressed as % of total mass in each compartment: roots, leaves and heads. For all treatments and all PFAAs

A2-8. Bioconcentration metrics

Roots concentration factor:

$$RCF (g/g) = \frac{PF\text{AA concentration in roots (ng/g d.w.)}}{PF\text{AA concentration in soil (ng/g d.w.)}} \quad (\text{A2-1})$$

Leaves concentration factor:

$$LCF (g/g) = \frac{PF\text{AA conc in leaves (ng/g d.w.)}}{PF\text{AA conc in soil (ng/g d.w.)}} \quad (\text{A2-2})$$

Head concentration factor:

$$HCF(g/g) = \frac{PF\text{AA conc in heads (ng/g d.w.)}}{PF\text{AA conc in soil (ng/g d.w.)}} \quad (\text{A2-3})$$

Shoots concentration factor as:

$$SCF(g/g) = \frac{PF\text{AA concentration in shoots (ng/g d.w.)}}{PF\text{AA concentration in soil (ng/g d.w.)}} \quad (\text{A2-4})$$

Where shoots concentrations were calculated as:

$$c_{shoots} = \frac{m_{head} * c(PF\text{AA})_{head} + m_{leaves} * c(PF\text{AA})_{leaves}}{m_{head} + m_{leaves}} \quad (\text{A2-5})$$

For this purpose only and due to problems with most of PFAAs being > LOD in all the treatments in leaves, in the cases where PFAAs were also detected in heads (>LOD), concentrations in leaves were approximated as ½ LOD.

Table A2-14. Bioconcentration factors for all the treatments, calculated on the basis of nominal soil concentration (equation (3-2) of the manuscript). Factors are expressed as means (n = 3) with standard error estimates. All measured concentrations for S0W1 were <LOD, hence, BCFs column was not shown for this treatment.

RCFs (g/g _{dw})	S100W0		S200W0		S100W1		S200W1		S0W10		S100W10		S200W10		S0W80		S100W80		S200W80		Treatments average RCF (g/g _{dw})
	Mean	St.err.	Mean	St.err.	Mean	St.err.	Mean	St.err.	Mean	St.err.	Mean	St.err.	Mean	St.err.	Mean	St.err.	Mean	St.err.	Mean	St.err.	
PFBA	207.2	27.7	284.8	28.0	256.5	33.0	213.8	14.1	323.5	37.7	245.9	35.7	135.3	13.1	201.2	40.7	163.5	24.9	179.9	15.5	221.2
PFPeA	83.0	11.9	130.4	3.8	98.3	4.9	98.8	20.0	199.6	48.9	127.4	3.5	57.6	6.7	80.8	10.0	60.6	5.9	79.0	5.7	101.5
PFHxA	44.0	5.5	39.6	4.4	51.9	4.9	27.2	2.4	<LOD		42.6	2.5	20.5	2.3	47.8	3.6	27.9	3.5	30.0	5.1	36.8
PFHpA	16.8	4.0	17.0	3.1	15.4	0.8	11.4	1.7	<LOD		19.9	3.1	9.7	2.0	13.2	1.8	9.6	1.3	12.4	2.6	13.9
PFOA	8.4	1.2	11.4	3.4	7.0	0.1	7.2	0.8	<LOD		11.7	2.1	5.0	0.8	9.3	3.5	4.9	0.7	7.2	2.6	8.0
PFNA	7.7	0.3	4.7	1.0	<LOD		<LOD		<LOD		<LOD		<LOD		8.4	1.4	<LOD		3.2	0.4	6.0
PFDA	8.3	1.8	5.3	1.0	7.7	1.2	4.7	0.8	<LOD		6.7	1.2	4.8	0.8	5.7	1.4	<LOD		2.7	0.6	5.7
PFBS	70.1	6.3	113.9	6.8	70.4	5.8	72.8	20.8	163.2	11.6	61.0	15.1	57.8	21.7	77.5	28.6	68.7	2.8	71.8	6.3	82.7
PFOS	11.1	0.7	6.1	0.8	0.0	0.0	5.4	1.0	<LOD		10.8	3.2	4.2	0.7	7.4	1.8	4.0	0.3	3.6	0.7	5.9
LCFs (g/g _{dw})	S100W0		S200W0		S100W1		S200W1		S0W10		S100W10		S200W10		S0W80		S100W80		S200W80		LCF (g/g _{dw})
	Mean	St.err.	Mean	St.err.	Mean	St.err.	Mean	St.err.	Mean	St.err.	Mean	St.err.	Mean	St.err.	Mean	St.err.	Mean	St.err.	Mean	St.err.	
PFBA	61.6	26.2	62.4	17.2	133.7	23.8	90.0	17.4	243.7	45.9	139.2	7.3	62.1	16.0	99.8	24.8	85.2	15.0	116.2	26.8	109.4
PFPeA	30.8	12.5	31.4	5.8	52.0	7.4	39.5	8.3	59.1	34.5	83.1	4.4	30.1	5.6	46.7	9.4	38.0	5.2	46.9	11.5	45.8
PFHxA	5.2	2.0	3.5	0.7	14.8	5.0	6.8	2.3	0.0	0.0	12.7	1.0	6.2	1.8	10.2	1.4	9.2	2.8	13.3	3.5	8.2
PFHpA	<LOD		<LOD		7.7	0.3	<LOD		<LOD		<LOD		<LOD		<LOD		<LOD		<LOD		7.7
PFOA	<LOD		<LOD		4.2	0.3	<LOD		<LOD		<LOD		<LOD		<LOD		<LOD		<LOD		4.2
PFNA	<LOD		<LOD		<LOD		<LOD		<LOD		<LOD		<LOD		<LOD		<LOD		<LOD		<LOD
PFDA	<LOD		<LOD		4.3	0.5	<LOD		<LOD		<LOD		<LOD		<LOD		<LOD		<LOD		4.3
PFBS	10.2	3.5	11.8	2.8	19.8	2.8	17.8	2.8	95.7	29.4	26.1	0.5	14.2	4.5	21.8	5.1	17.8	3.9	25.0	8.0	26.0
PFOS	<LOD		<LOD		4.7	0.1	2.1	0.3	<LOD		<LOD		<LOD		<LOD		<LOD		<LOD		3.4
HCFs (g/g _{dw})	S100W0		S200W0		S100W1		S200W1		S0W10		S100W10		S200W10		S0W80		S100W80		S200W80		HCF (g/g _{dw})
	Mean	St.err.	Mean	St.err.	Mean	St.err.	Mean	St.err.	Mean	St.err.	Mean	St.err.	Mean	St.err.	Mean	St.err.	Mean	St.err.	Mean	St.err.	
PFBA	30.2	2.3	24.6	1.3	34.1	0.7	28.8	3.9	61.1	8.9	25.3	4.4	21.6	1.3	61.4	6.6	48.5	6.1	44.2	2.7	38.0
PFPeA	16.7	0.5	17.6	3.4	16.6	1.4	14.5	1.5	34.5	6.4	15.5	1.3	12.3	0.6	36.4	5.0	22.9	2.6	23.3	0.6	21.0
PFHxA	7.9	0.9	8.1	1.3	9.3	0.9	5.3	0.7	<LOD		7.7	0.6	3.8	0.2	19.8	3.4	18.7	2.7	19.2	3.3	11.1
PFHpA	3.0	0.7	3.5	0.8	2.7	0.1	2.2	0.4	<LOD		3.6	0.6	1.8	0.3	5.2	0.3	6.4	1.0	7.8	1.5	4.0
PFOA	1.5	0.2	2.3	0.8	1.2	0.0	1.4	0.2	<LOD		2.1	0.4	0.9	0.1	3.5	0.9	3.3	0.5	4.5	1.5	2.3
PFNA	1.4	0.0	1.0	0.2	<LOD		<LOD		<LOD		<LOD		<LOD		3.3	0.2	<LOD		2.0	0.2	1.9
PFDA	1.5	0.4	1.3	0.2	1.4	0.2	0.9	0.2	<LOD		1.2	0.2	0.9	0.1	2.2	0.3	<LOD		1.7	0.4	1.4
PFBS	12.5	0.9	23.1	2.7	12.6	0.9	14.2	4.5	28.5	1.6	11.1	2.9	10.5	3.4	31.5	11.4	45.9	2.0	45.8	4.4	23.6
PFOS	2.0	0.2	1.2	0.2	<LOD		1.0	0.2	<LOD		2.0	0.6	0.8	0.1	2.9	0.4	2.7	0.2	2.3	0.4	1.9
SCFs (g/g _{dw})	S100W0		S200W0		S100W1		S200W1		S0W10		S100W10		S200W10		S0W80		S100W80		S200W80		SCF (g/g _{dw})
	Mean	St.err.	Mean	St.err.	Mean	St.err.	Mean	St.err.	Mean	St.err.	Mean	St.err.	Mean	St.err.	Mean	St.err.	Mean	St.err.	Mean	St.err.	
PFBA	43.3	9.4	38.0	5.6	82.6	15.4	55.6	4.9	145.8	19.8	55.7	0.5	43.3	8.7	82.0	11.5	67.6	7.0	81.0	15.2	69.5
PFPeA	22.6	4.8	22.2	1.1	33.7	5.1	25.4	2.5	45.4	17.7	34.2	0.8	21.8	3.1	41.8	3.5	30.8	1.3	35.2	5.7	31.3
PFHxA	6.3	0.6	6.0	0.7	12.0	1.9	5.9	1.4	<LOD		8.1	0.4	5.1	0.8	14.4	2.1	13.1	2.5	16.2	3.3	9.7
PFHpA	2.2	0.2	2.8	0.3	5.1	0.3	2.0	0.3	<LOD		3.9	0.1	0.8	0.1	4.8	0.6	4.0	0.4	4.8	0.7	3.4
PFOA	1.2	0.1	1.8	0.3	2.6	0.2	1.3	0.1	<LOD		1.8	0.1	2.2	0.1	2.9	0.2	2.1	0.3	2.8	0.7	2.1
PFNA	1.2	0.1	1.0	0.0	<LOD		<LOD		<LOD		<LOD		<LOD		3.5	0.2	<LOD		1.7	0.1	1.9
PFDA	1.2	0.3	1.2	0.1	2.8	0.4	0.9	0.1	<LOD		1.5	0.0	1.3	0.0	2.2	0.1	<LOD		1.3	0.2	1.5
PFBS	11.1	1.3	17.9	1.4	16.1	1.2	15.6	3.2	59.3	11.5	15.1	0.8	12.4	1.6	26.4	8.1	29.8	2.3	35.3	5.6	23.9
PFOS	1.5	0.2	1.1	0.0	2.2	0.2	1.5	0.3	<LOD		2.3	0.1	1.2	0.1	2.7	0.2	2.0	0.2	1.6	0.2	1.8

A2-9. Percentage distribution for the top and bottom soil samples for the S0W80, S200W0, S200W80 treatments

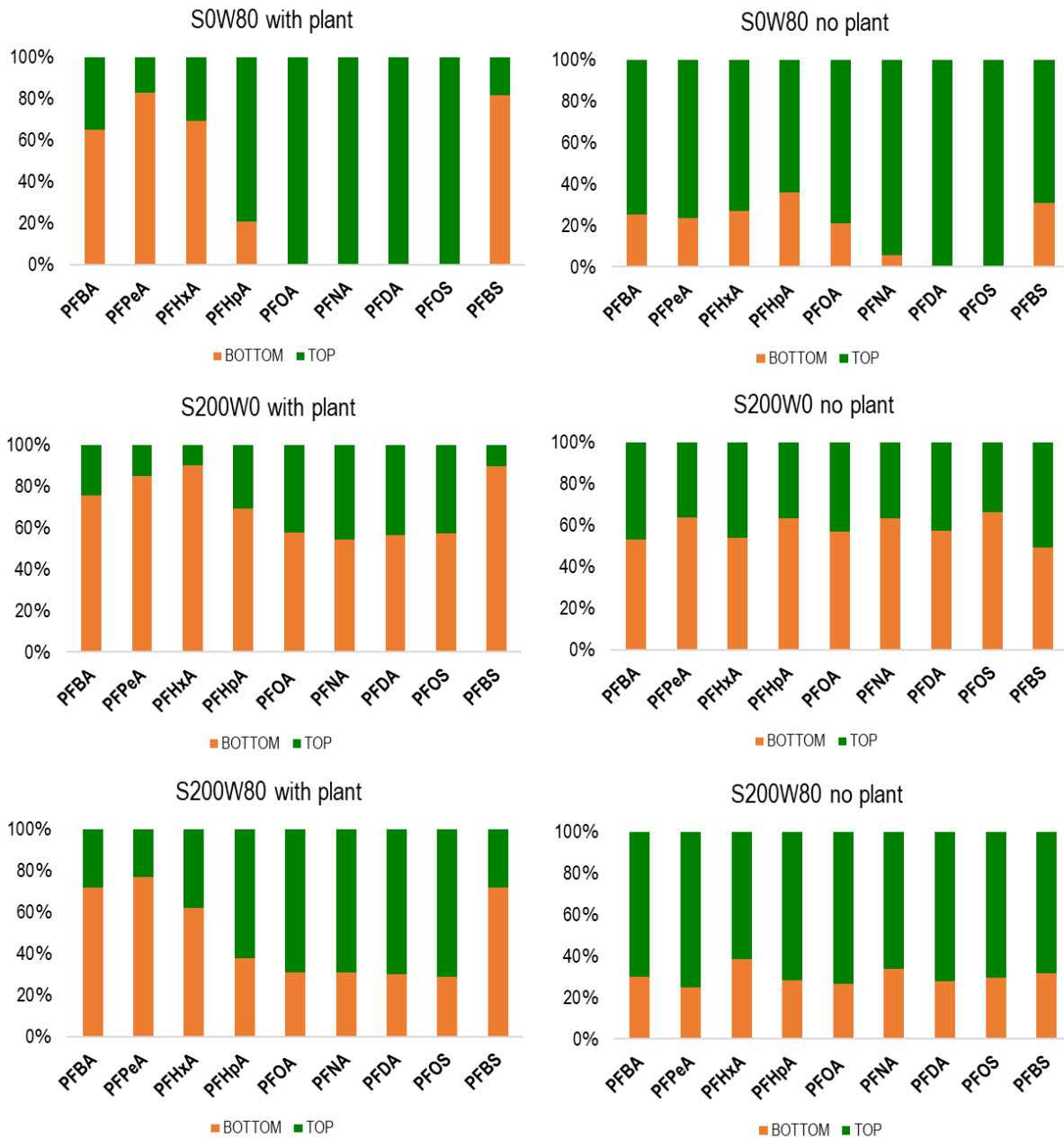


Figure A2-4. Mass balances of the soil in pots by depth. For the pots containing plants, means of 2 replicates are shown.

A2-10. Soil-water adsorption and desorption coefficients

a) Data analyses

Solid-liquid distribution coefficient for adsorption (K_d^{ads}) and desorption (K_d^{des}) were determined by fitting the data from the adsorption-desorption equilibrium experiment to the linear and Freundlich isotherm models, where K_d^{ads} is defined as the ratio between the substance concentration in the soil phase and the mass concentration of the substance in the aqueous solution after the adsorption equilibrium has been achieved (Chen et al., 2016; Milinovic et al., 2015; OECD, 2000):

$$K_d^{ads} = \frac{c_s^{ads}(eq)}{c_{aq}^{ads}(eq)} \quad (mL/g) \quad (A2-6)$$

C_s^{ads} (ng/g) is the content of the substance (PFAA) adsorbed on the soil at adsorption equilibrium and c_{aq}^{ads} ($\mu\text{g/L}$) is mass concentration of PFAA in the aqueous phase at adsorption equilibrium, that was determined analytically, while C_s^{ads} was calculated based on the aqueous loss (OECD, 2000):

$$c_s^{ads} = \frac{(c_0 - c_{aq}^{ads}(eq)) * V_0}{m_{soil}} \quad (ng/g) \quad (A2-7)$$

where C_0 ($\mu\text{g/L}$) is the initial mass concentration of PFAA in the test solution at the beginning of the experiment (calculated based on the analyses of PFAAs concentrations in the stock spike solution), V_0 (mL) is a volume of the solution in the test vial and m_{soil} (g) mass of the soil on a dry weight basis.

Equilibrium adsorption and desorption data were plotted as c_s^{ads} against c_{aq}^{ads} for all tested initial concentration points and were fitted to the linear adsorption isotherm model:

$$c_s^{ads}(eq) = K_d^{ads} * c_{aq}^{ads}(eq) \quad (ng/g) \quad (A2-8)$$

by a least squares linear regression with the intercept set to zero, neglecting the background soil PFAAs contamination.

Data were also fitted to the Freundlich power model:

$$c_s^{ads}(eq) = K_F * c_{aq}^{ads}(eq)^{\frac{1}{n}} \quad (ng/g) \quad (A2-9)$$

by the least squares non-linear regression. K_F is the Freundlich constant reflecting the magnitude of sorption, whose units depend on the $1/n$, dimensionless empirical parameter describing the degree of non-linearity of the isotherm. Isotherm will appear convex if $1/n > 1$, K_d decreasing with the c_s increase, while if $1/n < 1$, Freundlich isotherm is concave and K_d increases with c_s . When

1/n approaches value of 1, Freundlich isotherm is becoming linear ($K_F = K_d$ and is valid through all the concentration range) (Milinovic et al., 2015; OECD, 2000; Qian et al., 2017).

For the adsorption kinetics experiment, adsorption percentage A (%) was calculated in every time step, while for the adsorption equilibrium experiment it was determined by the least square linear regression (OECD, 2000):

$$A_{t,i} = \frac{m_s^{ads}(t,i)}{m_0} * 100 = \frac{m_0 - c_{aq}^{ads}(t,i) * V_0}{C_0 * V_0} * 100 \quad (\%) \quad (A2-10)$$

as ratio of the mass of PFAA adsorbed to soil at the i-th time point t and the initial mass of PFAA at the time of spiking the aqueous solution. For the adsorption equilibrium data, time t was determined equilibration time.

The apparent desorption coefficient (K_d^{des}) is given as:

$$K_d^{des} = \frac{c_s^{des}(eq)}{c_{aq}^{des}(eq)} \quad (mL/g) \quad (A2-11)$$

where C_s^{des} (ng/g) is the content of the substance (PFAA) adsorbed on the soil at desorption equilibrium and c_{aq}^{des} ($\mu\text{g/L}$) is the mass concentration of PFAA, desorbed from the soil and consequently present in the aqueous phase at desorption equilibrium, both of which were determined analytically. All measured concentrations were accounted for the aqueous residual in soil by weighing, both after sorption and desorption, as soil was extracted immediately and without drying. After plotting the data of C_s^{des} (ng/g) against c_{aq}^{des} ($\mu\text{g/L}$), linear desorption isotherm and Freundlich desorption model were fitted to the data by the least squares linear and non-linear regression, respectively:

$$c_s^{des}(eq) = K_d^{des} * c_{aq}^{des}(eq) \quad (ng/g) \quad (A2-12)$$

$$c_s^{des}(eq) = K_F^{des} * c_{aq}^{des}(eq)^{\frac{1}{n}} \quad (ng/g) \quad (A2-13)$$

b) Results

Kinetics

Adsorption equilibration time was determined after plotting the adsorption percentages A (%) for each time-step against time. As the typical kinetically increasing behavior was absent for all PFAAs, even after the interpolation of the time points between 0 and 2h (but for PFNA), it was concluded that the apparent equilibrium has been reached instantaneously at the used soil to liquid (S/L) ratio and that the present variation can be ascribed to the experimental error (which was unavoidable due to the use of parallel method and sacrificial samples). Standard deviations of A (%) for all PFAAs were lower than 5% while evaluating adsorption percentages at all time-points between 2h and 72h. In the end, 72h was accepted as the equilibration time for both equilibrium adsorption and desorption experiments.

Adsorption/desorption isotherms

Concentrations of the PFAAs adsorbed on the soil at the equilibrium, c_s^{ads} (eq) (ng/g), were calculated according to the equation (A2-7), and were plotted against measured aqueous phase equilibrium concentrations c_{aq}^{ads} (eq). Linear and Freundlich models were fitted as described previously. Measured adsorption points are reported in the Table A2-16, while the sorption parameters and curve fitting statistics are reported in the Table A2-15.

Both linear and Freundlich models are proved to be a good fit for the short-chain PFAAs adsorption on the agricultural soil. Among the long-chain PFAAs, adsorption of PFOA to soil can still be sufficiently well described by linear isotherm and constant value of K_d . However, PFNA, PFDA and PFOS have shown very high sorption affinity for the Agripolis soil, having very high values of Freundlich's sorption coefficient K_F , and high deviation from linearity that would lead to underestimation of the K_d at the low concentrations.

However, since the concentration in soil in the pot experiment did not exceed 400 ng/g_{dw} for these PFAAs and very high concentrations being the one introducing non-linearity, for the purpose of easier calculations and to avoid erroneous estimates for a very low concentrations that were the case in some treatments, all calculations were repeated for only first 3 isotherm points for PFNA, PFDA and PFOS and then these linear K_d s were used in further calculations (Table A2-15).

Table A2-15. Adsorption isotherms parameters for all PFAAs with standard errors (SE) of the regression coefficients

	Linear			Freundlich					1/n = N			
	$c_s^{ads} (eq) = K_d^{ads} * c_{aq}(eq)$			$c_s^{ads} (eq) = K_F^{ads} * c_{aq} (eq)^{(1/n)}$								
	K_d (mLg ⁻¹)	SE	R ²	K_F (ug ^(1-N) LNg ⁻¹)	SE	N	SE	n	R ²			
PFBA	0.85	0.02	1.00	0.42	0.15	1.12	0.06	0.89	1.00			
PFPeA	0.58	0.03	0.99	1.48	1.05	0.84	0.12	1.19	0.98			
PFBS	0.80	0.06	0.98	0.44	0.69	1.10	0.27	0.91	0.96			
PFHxA	0.96	0.08	0.97	2.55	2.88	0.83	0.19	1.20	0.96	Linear, low range		
PFHpA	1.64	0.09	0.98	0.29	0.13	1.30	0.08	0.77	1.00	(isotherm points 1-3)		
PFOA	1.16	0.08	0.96	4.29	3.44	0.77	0.14	1.29	0.98	K_d (mLg ⁻¹)	SE	R ²
PFNA	1.56	0.37	0.56	54.66	31.29	0.39	0.10	2.56	0.93	5.11	0.17	1.00
PFDA	7.04	1.80	0.79	199.29	77.84	0.37	0.08	2.71	0.95	40.09	0.89	1.00
PFOS	25.09	4.29	0.90	245.82	57.43	0.48	0.06	2.10	0.99	93.56	1.05	1.00

Table A2-16. Measured concentrations in the aqueous solution for the all adsorption points after the adsorption equilibrium and calculated adsorbed concentrations (means of 3 replicate reactors with standard error estimates). Adsorption points are named as: “Ad initial concentration in the solution in $\mu\text{g/L}$ ”

	PFBA		PFPeA		PFBS		PFHxA		PFHpA	
	C_{aq} (eq) ($\mu\text{g/L}$)	$C_{\text{s}}^{\text{ads}}$ (eq) (ng/g)	C_{aq} (eq) ($\mu\text{g/L}$)	$C_{\text{s}}^{\text{ads}}$ (eq) (ng/g)	C_{aq} (eq) ($\mu\text{g/L}$)	$C_{\text{s}}^{\text{ads}}$ (eq) (ng/g)	C_{aq} (eq) ($\mu\text{g/L}$)	$C_{\text{s}}^{\text{ads}}$ (eq) (ng/g)	C_{aq} (eq) ($\mu\text{g/L}$)	$C_{\text{s}}^{\text{ads}}$ (eq) (ng/g)
Ad1-mean	1.22	0.00	0.79	0.90	0.76	1.05	0.92	0.36	0.72	1.36
Ad10-mean	8.41	5.96	7.70	10.01	6.92	13.77	8.34	7.91	7.04	14.54
Ad100-mean	82.21	69.18	87.73	45.27	77.50	95.49	87.22	59.61	84.69	72.42
Ad250-mean	208.39	158.54	211.91	151.31	215.70	127.00	196.67	258.35	191.28	285.54
Ad500-mean	408.44	358.40	436.20	238.02	413.06	346.26	420.57	376.45	369.84	634.70
Ad1-st.err	0.02	0.00	0.06	0.29	0.03	0.13	0.02	0.10	0.08	0.40
Ad10-st.err	0.44	2.27	0.28	1.40	0.12	0.74	0.50	2.53	0.05	0.27
Ad100-st.err	3.08	15.66	1.31	6.78	1.74	8.92	1.75	8.86	4.70	23.95
Ad250-st.err	18.07	92.34	3.46	17.74	14.92	76.08	7.53	38.67	13.73	69.92
Ad500-st.err	23.54	120.09	24.98	127.91	11.31	57.94	17.54	89.95	33.96	173.53
	PFOA		PFNA		PFDA		PFOS			
	C_{aq} (eq) ($\mu\text{g/L}$)	$C_{\text{s}}^{\text{ads}}$ (eq) (ng/g)	C_{aq} (eq) ($\mu\text{g/L}$)	$C_{\text{s}}^{\text{ads}}$ (eq) (ng/g)	C_{aq} (eq) ($\mu\text{g/L}$)	$C_{\text{s}}^{\text{ads}}$ (eq) (ng/g)	C_{aq} (eq) ($\mu\text{g/L}$)	$C_{\text{s}}^{\text{ads}}$ (eq) (ng/g)		
Ad1-mean	0.47	2.56	0.37	3.07	0.13	4.33	0.05	4.87		
Ad10-mean	4.83	24.81	3.72	30.52	0.80	45.94	0.43	47.30		
Ad100-mean	68.17	146.63	48.56	247.34	11.09	443.55	4.94	462.01		
Ad250-mean	204.30	221.92	148.77	478.90	45.24	1019.57	18.83	1140.89		
Ad500-mean	394.94	456.39	408.26	524.16	219.33	1380.96	87.35	2027.99		
Ad1-st.err	0.03	0.14	0.04	0.18	0.01	0.03	0.00	0.08		
Ad10-st.err	0.17	0.86	0.38	1.92	0.05	0.28	0.06	0.33		
Ad100-st.err	1.69	8.58	2.08	10.65	1.29	6.57	0.25	1.31		
Ad250-st.err	5.58	28.71	16.47	83.88	11.29	57.53	2.95	15.02		
Ad500-st.err	29.78	152.12	25.77	132.45	53.71	274.64	21.38	109.21		

Measured desorption equilibrium concentrations in the soil and aqueous solution were plotted after the correction for the residual PFAAs mass in aqueous solution remained in the soil after the sorption experiment (that would otherwise falsely contribute to the measured concentration in the solution at the desorption equilibrium) and in the soil extract (that would lead to overestimation of the sorbed PFAAs concentrations at the desorption equilibrium). After the initial evaluation of desorption equilibrium data, it was observed that concentrations of PFBA, PFPeA, PFBS and PFHxA could not be quantified precisely enough, considering their very low adsorption to soil and consequently low availability in the desorption reactors, so desorption isotherms were not calculated for this PFAAs. Linear and Freundlich models were fitted as described by the equations (A2-12) and (A2-13). The sorption parameters and curve fitting statistics are presented in the Table A2-18 and Table S2-17. For desorption, linear model was applicable (and even better fit in the cases of PFOA and PFOS) for all the PFAAs evaluated, but PFHpA, where Freundlich model for desorption must be used instead. Due to good overall linear fit, linear K_{des} values were used for the long-chain PFAAs in all further calculations.

Table A2-17. Desorption isotherm parameters for all PFAAs with quantifiable aqueous concentrations, with standard errors (SE) of the regression coefficients

	Linear			Freundlich					
	$c_s^{des} (eq) = K_d^{des} * c_{aq}^{des}(eq)$			$c_s^{des} (eq) = K_F^{des} * c_{aq}^{des}(eq)^{(1/n)}$					
	$K_{des} (mLg^{-1})$	SE	R ²	K_F ($ug^{(1-N)}L^N g^{-1}$)	SE	N	SE	n	R ²
PFHpA	0.67	0.16	0.56	3.25	0.65	0.39	0.09	2.57	0.89
PFOA	1.96	0.05	1.00	1.70	0.47	1.05	0.09	0.96	0.99
PFNA	5.34	0.27	0.98	1.93	1.34	1.26	0.17	0.80	0.99
PFDA	42.50	3.10	0.96	12.05	13.51	1.39	0.34	0.72	1.00
PFOS	59.77	3.95	0.98	91.96	41.15	0.83	0.17	1.20	0.97

Table A2-18. Measured concentrations in the aqueous solution after the desorption equilibrium and calculated adsorbed concentrations (mean of 3 replicate reactors with standard error estimates). Desorption points are named as: "De initial adsorption concentration in the solution in $\mu g/L$ "

	PFHpA		PFOA		PFNA		PFDA		PFOS	
	c_{aq}^{des} (eq) ($\mu g/L$)	c_s^{des} (eq) (ng/g)	c_{aq}^{des} (eq) ($\mu g/L$)	c_s^{des} (eq) (ng/g)	c_{aq}^{des} (eq) ($\mu g/L$)	c_s^{des} (eq) (ng/g)	c_{aq}^{des} (eq) ($\mu g/L$)	c_s^{des} (eq) (ng/g)	c_{aq}^{des} (eq) ($\mu g/L$)	c_s^{des} (eq) (ng/g)
De1-mean	0.02	0.08	0.13	0.18	0.15	1.09	0.05	2.79	0.00	2.27
De10-mean	0.16	0.56	0.92	2.10	1.11	10.87	0.40	26.47	0.00	19.61
De100-mean	0.67	2.96	7.82	16.62	17.73	90.34	4.77	260.34	2.00	249.50
De250-mean	3.87	6.72	16.58	29.58	43.23	197.13	19.58	650.34	8.18	443.18
De500-mean	14.76	8.68	27.36	55.02	62.27	356.80	29.42	1361.72	15.47	931.97
De1-st.err	0.01	0.01	0.01	0.03	0.01	0.10	0.01	0.12	0.00	0.13
De10-st.err	0.07	0.05	0.11	0.15	0.15	0.65	0.01	0.29	0.00	0.41
De100-st.err	0.41	1.56	0.79	1.46	2.79	13.94	0.16	9.76	0.08	30.01
De250-st.err	0.99	0.48	1.41	2.16	5.88	17.39	1.06	39.89	0.26	7.61
De500-st.err	0.29	1.37	4.29	5.02	17.06	20.82	13.01	40.14	1.73	45.71

c) QC

No significant loss to the PP tubes was present during the experiments and all variations were ascribed to the spiking variability. Also, there was no background contamination of the soil.

Mass balances of all reactors were calculated after the soil extraction on the end of the desorption test and expressed as recovery:

$$R = \frac{m_{aq}^{ads}(eq) + m_{aq}^{des}(eq) + m_s^{des}(eq, soil\ w.w.)}{m_0} * 100 \quad (\%) \quad (A2-14)$$

Where $m_{aq}^{ads}(eq)$ and $m_{aq}^{des}(eq)$ were masses present in the aqueous solution at the adsorption and desorption equilibrium, while $m_s^{des}(eq, soil\ w.w.)$ was the mass of PFAA present in the soil extract at the end of the desorption and experiment.

Full adsorption-desorption experiment recoveries were between 85-115% for most PFAAs and batch reactors, while several existing outliers (present for PFDA, PFNA and PFOS) were discarded from the triplicates of corresponding isotherm points. Lower recoveries were present only for PFOS, where they varied between 61% and 103% and can be explained by some the non-quantifiable concentrations in aqueous phase after both adsorption and desorption in the lower nominal concentrations reactors (< LOD). However, this was taken into account while calculating the equilibrium concentrations and did not affect the final results. Average recoveries across all reactors, per each PFAA are shown at the Figure , and were considered satisfactory (according to EPA, recoveries from the decant-refill adsorption/desorption experiment between 70-130% are considered satisfactory (Zhi and Liu, 2018)).

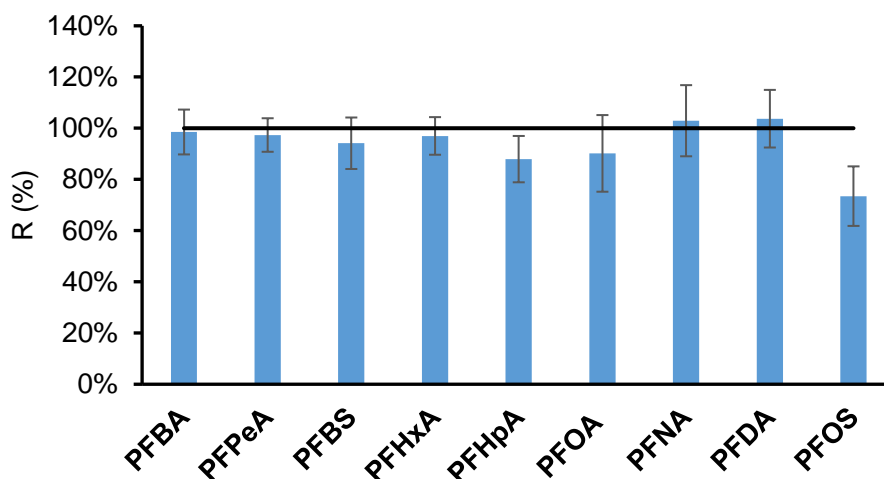


Figure A2-5. Average recoveries (\pm standard deviation) of the adsorption/desorption experiment, for each PFAA, across all reactors.

pH values through all the tests were constant and changed negligibly before and after the adsorption/desorption.

References:

- Chen, H., Reinhard, M., Nguyen, V.T., Gin, K.Y.H., 2016. Reversible and irreversible sorption of perfluorinated compounds (PFCs) by sediments of an urban reservoir. *Chemosphere* 144, 1747–1753. <https://doi.org/10.1016/j.chemosphere.2015.10.055>
- Milinovic, J., Lacorte, S., Vidal, M., Rigol, A., 2015. Sorption behaviour of perfluoroalkyl substances in soils. *Sci. Total Environ.* 511, 63–71. <https://doi.org/10.1016/j.scitotenv.2014.12.017>
- Northcott, G.L., Jones, K.C., 2000a. Spiking hydrophobic organic compounds into soil and sediment: a review and critique of adopted procedures. *Environ. Toxicol. Chem.* 19, 2418–2430. <https://doi.org/10.1002/etc.5620191005>
- Northcott, G.L., Jones, K.C., 2000b. Developing a standard spiking procedure for the introduction of hydrophobic organic compounds into field-wet soil. *Environ. Toxicol. Chem.* 19, 2409–2417. <https://doi.org/10.1002/etc.5620191004>
- OECD, 2000. Test No. 106: Adsorption - Desorption Using a Batch Equilibrium Method, OECD Guideline for the Testing of Chemicals. <https://doi.org/https://doi.org/10.1787/9789264069602-en>
- Qian, J., Shen, M., Wang, P., Wang, C., Hou, J., Ao, Y., Liu, J., Li, K., 2017. Adsorption of perfluorooctane sulfonate on soils: Effects of soil characteristics and phosphate competition. *Chemosphere* 168, 1383–1388. <https://doi.org/10.1016/j.chemosphere.2016.11.114>
- Zhi, Y., Liu, J., 2018. Sorption and desorption of anionic, cationic and zwitterionic polyfluoroalkyl substances by soil organic matter and pyrogenic carbonaceous materials. *Chem. Eng. J.* <https://doi.org/10.1016/j.cej.2018.04.042>

APPENDIX 3: Supplementary information for Chapter 4

Model-based analysis of the uptake of perfluoroalkyl acids (PFAAs) from soil into plants

Andrea Gredelj^{a,1}, Fabio Polesel^{a,b}, Stefan Trapp^a

^a Technical University of Denmark, Department of Environmental Engineering, Bygningstorvet 115, DK-2800 Kongens Lyngby, Denmark

^b Department of Industrial Engineering, University of Padova, via Marzolo 9, 35131 Padova, Italy

^c DHI A/S, Agern Allé 5, 2970 Hørsholm, Denmark

Table A3-1. Measured concentrations of PFAAs for selected treatments in red chicory compartments (fresh weight) and soil (dry weight) before planting (from (Gredelj et al., 2019a)). Results are shown as means of pots per treatment (n = 3) and respective estimated standard errors.

Soil concentration (ng/g_{dw})				
PFAA	S100W0		S200W0	
	MEAN	S.E.	MEAN	S.E.
PFBA	106.06	4.34	164.82	4.57
PFPeA	87.16	5.21	135.95	21.68
PFHxA	92.35	3.54	161.51	10.28
PFHpA	89.78	8.63	138.90	0.93
PFOA	95.25	6.45	188.36	15.80
PFNA	86.82	3.86	153.72	5.60
PFDA	87.04	6.23	157.95	3.15
PFBS	82.22	5.14	184.28	3.00
PFOS	76.21	6.32	179.93	22.64
Roots concentration (ng/g_{fw})				
PFAA	S100W0		S200W0	
	MEAN	S.E.	MEAN	S.E.
PFBA	1473.50	138.89	3342.11	352.24
PFPeA	514.41	53.47	1321.29	24.36
PFHxA	265.43	22.23	564.91	60.67
PFHpA	114.44	23.10	213.23	38.92
PFOA	56.86	7.83	123.79	37.10
PFNA	55.06	0.57	69.14	14.42
PFDA	55.40	14.78	64.80	12.58
PFBS	457.68	22.20	1411.69	78.68
PFOS	64.22	7.11	86.28	11.07
Leaves concentration (ng/g_{fw})				
PFAA	S100W0		S200W0	
	MEAN	S.E.	MEAN	S.E.
PFBA	442.40	114.05	559.42	77.57
PFPeA	194.85	46.86	250.66	9.12
PFHxA	31.77	6.81	39.56	1.72
PFHpA	11.17	0.07	20.58	0.20
PFOA	5.79	0.04	10.66	0.11
PFNA	7.92	0.05	14.59	0.14
PFDA	5.90	0.04	10.87	0.11
PFBS	68.62	12.64	114.19	11.67
PFOS	6.36	0.04	11.71	0.12
Heads concentration (ng/g_{fw})				
PFAA	S100W0		S200W0	
	MEAN	S.E.	MEAN	S.E.
PFBA	176.54	9.84	212.97	22.43
PFPeA	85.71	2.36	128.19	18.19
PFHxA	38.86	3.34	82.97	8.89
PFHpA	16.76	3.42	31.32	5.74
PFOA	8.32	1.15	18.19	5.47
PFNA	8.06	0.07	10.16	2.13
PFDA	8.10	2.15	11.63	0.66
PFBS	67.00	3.39	207.35	11.58
PFOS	9.40	1.03	12.68	1.64

Shoots concentration (ng/g _{fw}) ¹				
	S100W0		S200W0	
PFAA	MEAN	S.E.	MEAN	S.E.
PFBA	286.62	44.15	345.32	47.06
PFPeA	130.71	19.29	174.78	8.22
PFHxA	36.06	2.84	66.46	5.21
PFHpA	14.56	2.16	27.13	3.23
PFOA	7.30	0.71	15.14	3.07
PFNA	8.00	0.05	11.78	1.31
PFDA	7.16	1.24	11.35	0.39
PFBS	67.76	5.25	171.89	3.06
PFOS	8.13	0.58	12.25	0.91

¹Shoots concentrations were calculated as: $C_{shoots} = \frac{m_{head} * C(PFAA)_{head} + m_{leaves} * C(PFAA)_{leaves}}{m_{head} + m_{leaves}}$ where m denotes the fresh weight mass of a plant compartment and $C(PFAA)$ the concentration of a PFAA in the respective compartment.

Text A3-1. Calculation details for plant specific data of the red chicory

Exponential growth curves were fitted to the measured data and growth rates were calculated on the basis of the measured seedlings mass before planting and mass of red chicory compartments at harvest. Evapotranspiration volume was estimated between each irrigation session, when whole pots were weighed (usually every 2-3 days, before every irrigation). Pots without plants were present in every treatment to account for the evaporation, which was considered as the only way of water loss from the pot. In every i-th time step between irrigations, total mass (W) loss of water from the pot was a result of transpiration (T), evaporation (E) and leaching (L), while growth (G) of the plant increased the total pot mass. Using Δ for each i-th irrigation sessions, ΔW_i was equal to:

$$\Delta W_i = W_{i-1} + \Delta I_{i-1} - W_i \quad (\text{A3-1})$$

ΔI_i is the volume of irrigation water in the i-th irrigation session and W_i total mass of the pot including: the pot itself, dry soil mass, mass of the soil pore water and the plant mass, where pot and dry soil mass were considered constant. Considering leaching to be negligible since pots were closed at the bottom, the total volume of transpired water after a total of n irrigation sessions was calculated as:

$$\sum_{i=0}^n \Delta T_i = \sum_{i=0}^n (\Delta W_i - \Delta E_i + \Delta G_i) \quad (\text{A3-2})$$

Total volume that was transpired was divided by the number of days that were required for crop maturation afterwards to calculate the transpiration rate Q (L/d). Firstly, transpiration rate was calculated for shoots in total and afterwards for the chicory head and leaves separately. The exponential growth rate for head was calculated for the time of 33 days (as it was noticed that heads were starting to form), considering the initial mass of the head equivalent to the mass of 4 fully-grown leaves. Transpiration was accounted for heads for the last 33 days of growth with the assumption that only external head forming leaves are transpiring. Total measured transpiration volume was split between heads and leaves by calculating the transpiration coefficient T_c , as the water needed for produced shoots biomass (L/kg) and divided by the appropriate growth time (87 days for leaves and 33 for heads) to obtain Q_L and Q_H . All calculated red chicory specific constants and rates are given in the Table A3-2.

Table A3-2. Plant parameters for the red chicory per pot for evaluated treatments and non-contaminated control

Roots		Control	S100W0	S200W0
Parameter (unit)				
Transpiration stream	Q_R (L/d)	0.110	0.107	0.095
Roots mass	M_R (kg _{fw})	0.018	0.017	0.013
1st order growth rate for roots	k_R (1/d)	0.022	0.019	0.017
Roots water content	w_R (kg/kg)	0.923	0.926	0.922
Shoots		Control	S100W0	S200W0
Parameter (unit)				
Transpiration stream	Q_S (L/d)	0.110	0.107	0.095
Shoots mass	M_S (kg _{fw})	0.271	0.247	0.222
1st order growth rate for shoots	k_S (1/d)	0.037	0.034	0.034
Shoots water content	w_S (kg/kg)	0.933	0.930	0.933

Leaves				
Parameter (unit)		Control	S100W0	S200W0
Transpiration stream to leaves	Q_L (L/d)	0.061	0.064	0.054
Leaves mass	M_L (kg _{fw})	0.098	0.102	0.086
Growth rate for leaves	k_L (1/d)	0.026	0.024	0.023
Leaves water content	w_L (kg/kg)	0.919	0.915	0.934

Heads				
Parameter (unit)		Control	S100W0	S200W0
Transpiration stream to heads	Q_H (L/d)	0.122	0.114	0.107
Heads mass	M_H (kg _{fw})	0.155	0.146	0.137
Growth rate for heads	k_H (1/d)	0.064	0.062	0.060
Heads water content	w_H (kg/kg)	0.941	0.940	0.942

Table A3-3. Mean concentrations (in ng/g_{dw}) of PFAAs for crop compartments from (Blaine et al., 2014a)

	Tomato						Celery			
	Roots		Shoots		Fruit ¹		Roots		Shoots	
	MEAN	S.E.	MEAN	S.E.	MEAN	S.E.	MEAN	S.E.	MEAN	S.E.
PFBA	23.60	5.63	121.86	10.69	56.11	7.38	80.83	18.54	231.69	21.05
PFPeA	8.77	2.18	98.96	4.96	211.39	54.26	44.37	9.52	147.94	18.95
PFHxA	16.64	3.21	102.75	6.74	33.17	9.91	54.93	5.62	137.14	26.74
PFHpA	16.22	2.84	32.62	4.40	7.48	2.02	25.47	4.24	21.58	4.05
PFOA	75.00	7.72	190.24	39.40	8.81	0.67	111.35	28.79	55.40	16.79
PFNA	38.77	2.76	47.25	11.43	< 2.86	-	38.21	8.52	13.81	2.44
PFDA	173.30	18.46	134.05	32.53	< 2.86	-	99.41	15.69	30.14	2.58
PFBS	34.40	15.08	177.10	21.78	19.38	3.26	164.23	23.86	107.13	29.18
PFOS	225.14	21.53	210.65	46.87	< 0.14	-	185.52	19.14	69.27	5.07

	Pea				Radish					
	Root		Shoot		Fruit		Root		Shoot	
	MEAN	S.E.	MEAN	S.E.	MEAN	S.E.	MEAN	S.E.	MEAN	S.E.
PFBA	9.05	0.89	50.98	8.93	150.14	24.03	13.67	1.68	64.69	7.80
PFPeA	5.87	0.70	52.23	6.42	45.84	7.66	11.02	2.93	48.00	5.27
PFHxA	11.94	1.80	39.88	4.66	16.91	5.26	13.20	3.68	44.46	3.81
PFHpA	13.34	2.80	10.73	1.01	1.57	0.43	6.86	1.20	47.38	7.70
PFOA	62.23	17.40	41.03	3.09	2.65	0.76	66.89	13.36	596.76	119.26
PFNA	34.37	3.57	8.87	0.66	1.45	0.42	26.68	6.49	107.00	20.70
PFDA	133.53	19.30	13.84	1.19	< 0.14	0.00	40.91	13.19	103.01	19.30
PFBS	43.02	10.63	200.09	20.13	16.18	2.55	61.89	19.35	164.23	13.36
PFOS	118.65	16.77	61.57	3.84	1.28	0.30	34.86	12.05	185.52	38.93

¹ Data from (Blaine et al., 2013)

Table A3-4. Soil-water partition coefficients

	Soil – red chicory ¹		Soil - other crops ²
	K _{d,des} (L/kg)	K _{d,ads} (L/kg)	K _d (L/kg)
PFBA	-	0.85	1.70
PFPeA	-	0.58	0.53
PFHxA	-	0.96	0.46
PFHpA	-	1.64	0.96
PFOA	1.96	-	1.74
PFNA	5.34	-	5.13
PFDA	42.50	-	20.43
PFBS	-	0.80	1.38
PFOS	59.77	-	14.13

¹ (Gredelj et al., submitted), used for calculations with the red chicory

² Calculated from K_{oc} and f_{oc} for industrially impacted soil from (Blaine et al., 2014a), used for the uptake calculations of PFAAs in other crops

Table A3-5. Crop-specific parameters and default parameter values from the standard plant model (Trapp, 2015) used for the modeling of other crops

Default parameters for growth and transpiration based on 1m² of plant - standard plant model					
Roots					
Parameter (unit)		Tomato	Celery	Pea	Radish
Transpiration stream	Q _R (L/d)	1.2	1	1.2	1
Roots mass	M _R (kg _{fw})	1	1	1	1
1st order growth rate for roots	k _R (1/d)	0.1	0.1	0.1	0.1
Shoots					
Parameter (unit)		Tomato	Celery	Pea	Radish
Transpiration stream	Q _S (L/d)	1	1	1	1
Shoots mass	M _S (kg _{fw})	1	1	1	1
1st order growth rate for shoots	k _S (1/d)	0.035	0.035	0.035	0.035
Fruits					
Parameter (unit)		Tomato	Celery	Pea	Radish
Phloem and transpiration stream to fruits	Q _F (L/d)	0.2	-	0.2	-
Fruits mass	M _F (kg _{fw})	1	-	1	-
Growth rate for fruits	k _F (1/d)	0.035	-	0.035	-
Crop-specific parameters¹					
Parameter (unit)		Tomato	Celery	Pea	Radish
Growth time	t (d)	162	224	129	67
Roots					
Parameter (unit)		Tomato	Celery	Pea	Radish
Water content of roots	w _R (kg/kg)	0.88	0.82	0.74	0.90
Shoots					
Parameter (unit)		Tomato	Celery	Pea	Radish
Water content of shoots	w _S (kg/kg)	0.84	0.86	0.77	0.85
Fruits					
Parameter (unit)		Tomato	Celery	Pea	Radish
Water content of fruits	w _F (kg/kg)	0.94	-	0.82	-

¹ from (Blaine et al., 2014a)

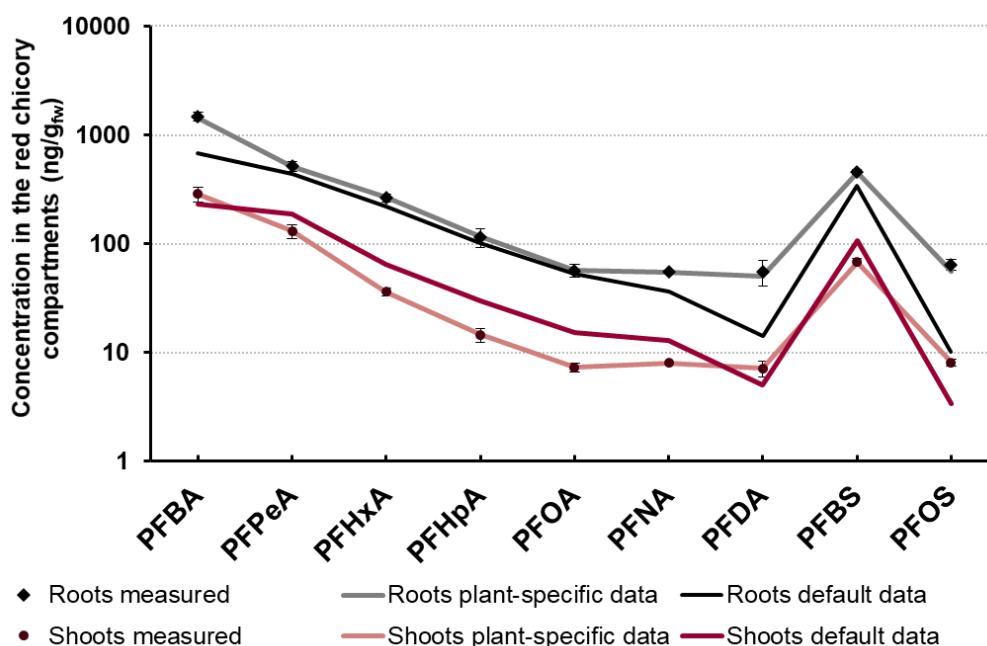


Figure A3-1. Comparison of measured and modeled roots and shoots concentrations using plant-specific and default plant parameters. Measured data are shown as means with standard error estimates (Gredelj et al., 2019a). To evaluate a significance of the use of plant-specific data compared to the default rules-of-thumb plant data (Trapp, 2015) for the red chicory, concentrations in the red chicory parametrized with the default data were calculated and compared with the model results when plant-specific data were employed, for the treatment S100W0 (Table S1 and Table S2). The use of default plant data resulted with significant under-prediction of PFBA, PFDA and PFOS concentrations in the chicory roots and shoots. On the contrary, in roots, modeled concentrations for all the other PFAAs, with both plant-specific and default data, were corresponding well to the measured concentrations. Modeled concentrations with the default plant data for all the PFAAs but PFBA, PFDA and PFOS were significantly over- predicted in shoots:

Table A3-6. Modeled concentrations in chicory roots and shoots with default and plant specific data

Roots (ng/g _{fw})	Default	Plant specific	MAPE ⁵ (%)	Shoots (ng/g _{fw})	Default	Plant specific	MAPE (%)
PFBA	680.62	1430.81	52%	PFBA	232.69	286.62	19%
PFPeA	440.96	514.63	14%	PFPeA	188.22	130.71	44%
PFHxA	219.52	265.74	17%	PFHxA	64.82	36.06	80%
PFHpA	101.60	115.31	12%	PFHpA	29.92	14.56	106%
PFOA	52.84	56.78	7%	PFOA	15.30	7.30	110%
PFNA	36.50	54.65	33%	PFNA	13.01	8.00	63%
PFDA	14.07	50.31	72%	PFDA	5.04	7.16	30%
PFBS	338.51	454.15	25%	PFBS	107.16	67.76	58%
PFOS	10.17	55.46	82%	PFOS	3.41	8.13	58%

⁵ Mean absolute percentage error (MAPE (%)), defined as: $MAPE = \left| \frac{x-y}{x} \right| * 100\%$ where x is the PFAA concentration calculated with the default plant parameters (Table S5) and y is the PFAA concentration calculated with the plant-specific data for red chicory.

Figure A3-2. Regression analyses for the relationships among $\log RCF$, $\log K_d$ and PFCA chain length for tomato, pea, celery and radish. Data for analyses were taken from (Blaine et al., 2014a) and are shown as means with standard errors.

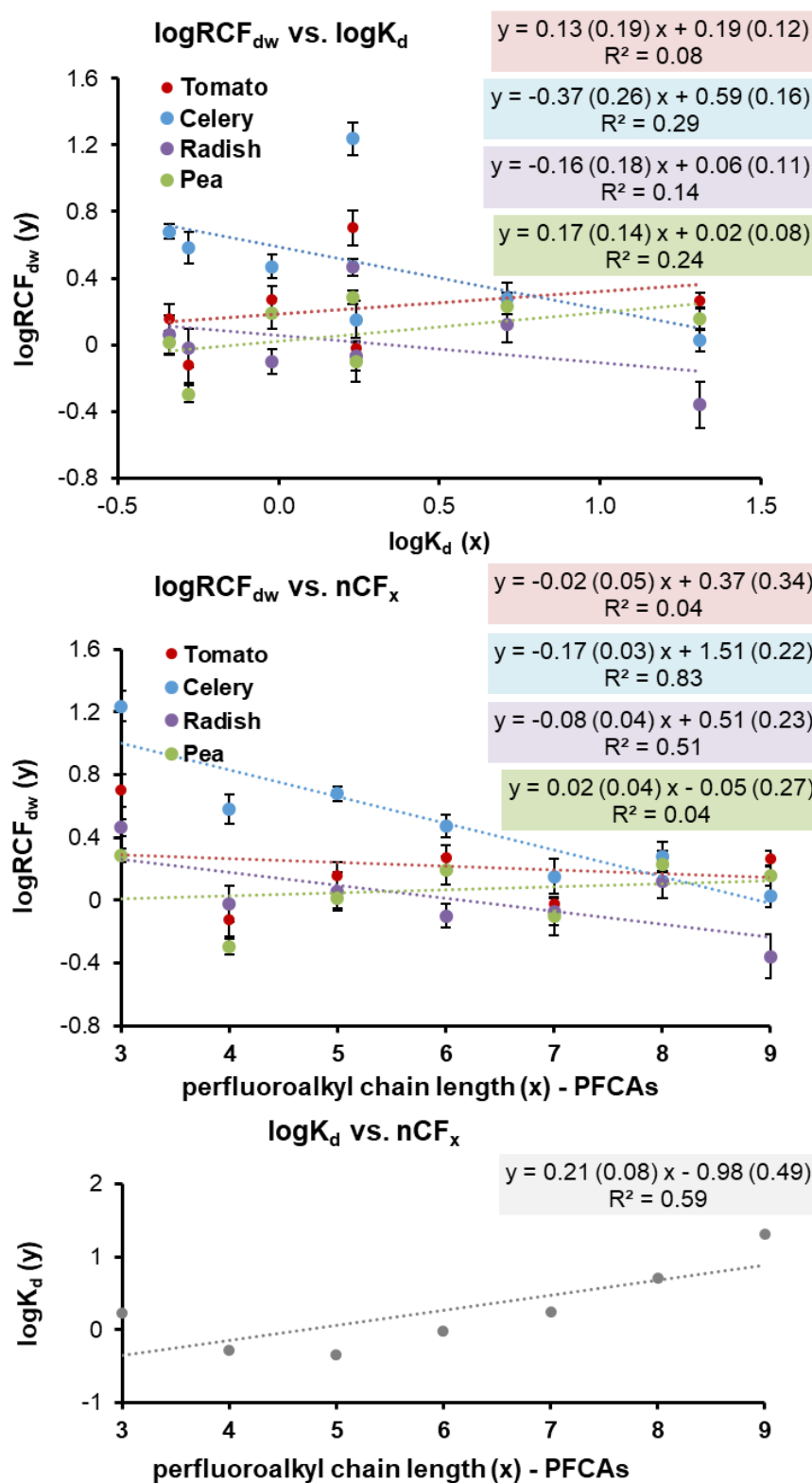


Table A3-6. Root-to-soil concentration factors on dry weight basis for PFOA and PFOS from published literature

PFAA	PLANT INFORMATION		Type of experiment	EXPOSURE INFORMATION			Root to soil concentration factor (g _{dw} /g _{dw})	REFERENCE
	PLANT NAME (COMMON)	PLANT NAME (SCIENTIFIC)		PFAA delivery	Treatment name	Exposure Duration (days)		
PFOA	Radish	<i>Raphanus sativus</i>	greenhouse	Biosolids application	Industrially impacted soil	67	0.85	(Blaine et al., 2014a)
PFOA	Celery	<i>Apium graveolens var, dulce</i>	greenhouse	Biosolids application	Industrially impacted soil	224	1.42	(Blaine et al., 2014a)
PFOA	Tomato	<i>Lycopersicon lycopersicum</i>	greenhouse	Biosolids application	Industrially impacted soil	162	0.96	(Blaine et al., 2014a)
PFOA	Sugar Snap	<i>Pisum sativum var, macrocarpon</i>	greenhouse	Biosolids application	Industrially impacted soil	129	0.79	(Blaine et al., 2014a)
PFOA	Wheat	<i>Triticum aestivum L.</i>	greenhouse/pot experiment	Spiked soil	Pot1	40	1.23	(Lan et al., 2018)
PFOA	Wheat	<i>Triticum aestivum L.</i>	greenhouse/pot experiment	Spiked soil	Pot2	40	2.66	(Lan et al., 2018)
PFOA	Tomato	<i>Solanum lycopersicum</i>	climate control rooms	Biosolids application (Sewage sludge)	Control	six months	2.25	(Navarro et al., 2017)
PFOA	Tomato	<i>Solanum lycopersicum</i>	climate control rooms	Biosolids application (Sewage sludge)	Treatment 1	six months	8.30	(Navarro et al., 2017)
PFOA	Tomato	<i>Solanum lycopersicum</i>	climate control rooms	Biosolids application (Sewage sludge)	Treatment 2	six months	1.54	(Navarro et al., 2017)
PFOA	Alfalfa	<i>Medicago sativa</i>	greenhouse	Biosolids application	biosolids amended soil	45	10.34	(Wen et al., 2016)
PFOA	Lettuce	<i>Lactuca sativa</i>	greenhouse	Biosolids application	biosolids amended soil	45	6.05	(Wen et al., 2016)
PFOA	Maize	<i>Zea mays</i>	greenhouse	Biosolids application	biosolids amended soil	45	1.69	(Wen et al., 2016)

PFOA	Mung bean	<i>Vigna radiata</i>	greenhouse	Biosolids application	biosolids amended soil	45	7.75	(Wen et al., 2016)
PFOA	Radish	<i>Raphnus sativus</i>	greenhouse	Biosolids application	biosolids amended soil	45	3.00	(Wen et al., 2016)
PFOA	Ryegrass	<i>Lolium multiflorum</i>	greenhouse	Biosolids application	biosolids amended soil	45	2.35	(Wen et al., 2016)
PFOA	Soybean	<i>Glycine</i>	greenhouse	Biosolids application	biosolids amended soil	45	3.21	(Wen et al., 2016)
PFOA	Lettuce	<i>Lactuca Sativa</i>	greenhouse	soil amended with compost spiked with PFOS and PFOA	Pot 1	4-5 weeks	4.19	(Bizkarguenaga et al., 2016)
PFOA	Lettuce	<i>Lactuca Sativa</i>	greenhouse	soil amended with compost spiked with PFOS and PFOA	Pot 2	4-5 weeks	4.87	(Bizkarguenaga et al., 2016)
PFOA	Wheat	<i>Triticum aestivum L.</i>	greenhouse	spiked soil	soil with PFASs	70	1.64	(Zhao et al., 2017)
PFOA	Rapeseed	<i>Brassica campestris L.</i>	greenhouse	spiked soil	soil with PFASs	70	4.96	(Zhao et al., 2017)
PFOA	Wheat	<i>Triticum aestivum L.</i>	field study	Biosolids application	Control	8 months (nov-june)	1.79	(Wen et al., 2014)
PFOA	Wheat	<i>Triticum aestivum L.</i>	field study	Biosolids application	Plot 1	8 months (nov-june)	4.94	(Wen et al., 2014)
PFOA	Wheat	<i>Triticum aestivum L.</i>	field study	Biosolids application	Plot 2	8 months (nov-june)	2.51	(Wen et al., 2014)
PFOA	Wheat	<i>Triticum aestivum L.</i>	field study	Biosolids application	Plot 3	8 months (nov-june)	1.94	(Wen et al., 2014)
PFOA	Wheat	<i>Triticum aestivum L.</i>	field study	Biosolids application	Plot 4	8 months (nov-june)	1.73	(Wen et al., 2014)
PFOS	Radish	<i>Raphanus sativus</i>	greenhouse	Biosolids application	Control	67	8.38	(Blaine et al., 2014a)
PFOS	Radish	<i>Raphanus sativus</i>	greenhouse	Biosolids application	Industrially impacted soil	67	0.70	(Blaine et al., 2014a)

PFOS	Radish	<i>Raphanus sativus</i>	greenhouse	Biosolids application	Municipal	67	0.07	(Blaine et al., 2014a)
PFOS	Celery	<i>Apium graveolens var, dulce</i>	greenhouse	Biosolids application	Industrially impacted soil	224	4.22	(Blaine et al., 2014a)
PFOS	Tomato	<i>Lycopersicon lycopersicum</i>	greenhouse	Biosolids application	Industrially impacted soil	162	4.53	(Blaine et al., 2014a)
PFOS	Sugar Snap	<i>Pisum sativum var, macrocarpon</i>	greenhouse	Biosolids application	Industrially impacted soil	129	2.39	(Blaine et al., 2014a)
PFOS	Wheat	<i>Triticum aestivum L.</i>	field study	Biosolids application	Control	8 months (nov-june)	1.52	(Wen et al., 2014)
PFOS	Wheat	<i>Triticum aestivum L.</i>	field study	Biosolids application	Plot 1	8 months (nov-june)	1.62	(Wen et al., 2014)
PFOS	Wheat	<i>Triticum aestivum L.</i>	field study	Biosolids application	Plot 2	8 months (nov-june)	1.19	(Wen et al., 2014)
PFOS	Wheat	<i>Triticum aestivum L.</i>	field study	Biosolids application	Plot 3	8 months (nov-june)	1.33	(Wen et al., 2014)
PFOS	Wheat	<i>Triticum aestivum L.</i>	field study	Biosolids application	Plot 4	8 months (nov-june)	1.36	(Wen et al., 2014)
PFOS	Wheat	<i>Triticum aestivum L.</i>	greenhouse/pot experiment	Spiked soil	Control	40	1.39	(Lan et al., 2018)
PFOS	Wheat	<i>Triticum aestivum L.</i>	greenhouse/pot experiment	Spiked soil	Pot1	40	1.47	(Lan et al., 2018)
PFOS	Wheat	<i>Triticum aestivum L.</i>	greenhouse/pot experiment	Spiked soil	Pot2	40	1.65	(Lan et al., 2018)
PFOS	Tomato	<i>Solanum lycopersicum</i>	climate control rooms	Biosolids application (Sewage sludge)	Control	six months	3.93	(Navarro et al., 2017)
PFOS	Tomato	<i>Solanum lycopersicum</i>	climate control rooms	Biosolids application (Sewage sludge)	Treatment 1	six months	2.49	(Navarro et al., 2017)

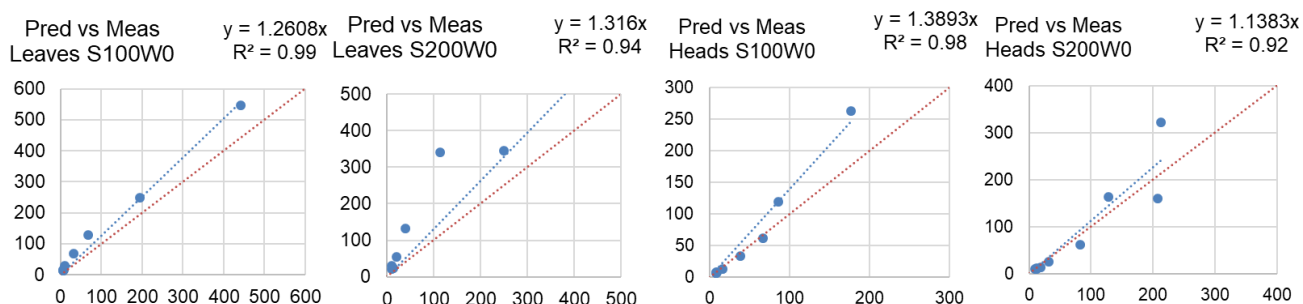
PFOS	Tomato	<i>Solanum lycopersicum</i>	climate control rooms	Biosolids application (Sewage sludge)	Treatment 2	six months	1.46	(Navarro et al., 2017)
PFOS	Maize	<i>Zea mays</i>	climate control rooms	Spiked soil	Treatment 1	28	6.60	(Navarro et al., 2017)
PFOS	Maize	<i>Zea mays</i>	climate control rooms	Spiked soil	Treatment 2	28	3.51	(Navarro et al., 2017)
PFOS	Alfalfa	<i>Medicago sativa</i>	greenhouse	Biosolids application	biosolids amended soil	45	3.12	(Wen et al., 2016)
PFOS	Lettuce	<i>Lactuca sativa</i>	greenhouse	Biosolids application	biosolids amended soil	45	3.89	(Wen et al., 2016)
PFOS	Maize	<i>Zea mays</i>	greenhouse	Biosolids application	biosolids amended soil	45	2.65	(Wen et al., 2016)
PFOS	Mung bean	<i>Vigna radiata</i>	greenhouse	Biosolids application	biosolids amended soil	45	4.15	(Wen et al., 2016)
PFOS	Radish	<i>Raphanus sativus</i>	greenhouse	Biosolids application	biosolids amended soil	45	2.61	(Wen et al., 2016)
PFOS	Ryegrass	<i>Lolium multiflorum</i>	greenhouse	Biosolids application	biosolids amended soil	45	1.38	(Wen et al., 2016)
PFOS	Soybean	<i>Glycine</i>	greenhouse	Biosolids application	biosolids amended soil	45	4.69	(Wen et al., 2016)
PFOS	Lettuce	<i>Lactuca Sativa</i>	greenhouse	soil amended with compost spiked with PFOS and PFOA	Pot 1	4-5 weeks	3.14	(Bizkarguenaga et al., 2016)
PFOS	Lettuce	<i>Lactuca Sativa</i>	greenhouse	soil amended with compost spiked with PFOS and PFOA	Pot 2	4-5 weeks	3.49	(Bizkarguenaga et al., 2016)
PFOS	Wheat	<i>Triticum aestivum L</i>	greenhouse	spiked soil	soil with pfas	70	3.95	(Zhao et al., 2017)
PFOS	Rapeseed	<i>Brassica campestris L.</i>	greenhouse	spiked soil	soil with pfas	70	5.14	(Zhao et al., 2017)

Table A3-8. Comparison of measured and modeled PFAAs concentrations in red chicory leaves and heads and statistical evaluation of model performance.

LEAVES					HEADS			
S100W0	MEAN	S.E.	MODEL	MAPE ⁶ (%)	MEAN	S.E.	MODEL	MAPE (%)
PFBA	442.40	114.05	546.77	53%	176.54	9.84	263.04	50%
PFPeA	194.85	46.86	249.34	52%	85.71	2.36	119.95	40%
PFBS	68.62	12.64	129.27	103%	67.00	3.39	62.19	7%
PFHxA	31.77	6.81	68.79	139%	38.86	3.34	33.09	14%
PFHpA	11.17	0.07	27.77	149%	16.76	3.42	13.36	19%
PFOA	5.79	0.04	13.92	141%	8.32	1.15	6.70	23%
PFNA	7.92	0.05	15.26	93%	8.06	0.07	7.34	9%
PFDA	5.90	0.04	13.66	131%	8.10	2.15	6.57	23%
PFOS	6.36	0.04	15.52	144%	9.40	1.03	7.46	19%
S200W0	MEAN	S.E.	MODEL	MAPE (%)	MEAN	S.E.	MODEL	MAPE (%)
PFBA	559.42	77.57	683.03	29%	212.97	22.43	321.46	54%
PFPeA	250.66	9.12	345.70	38%	128.19	18.19	162.70	32%
PFBS	114.19	11.67	339.98	203%	207.35	11.58	160.01	22%
PFHxA	39.56	1.72	131.46	233%	82.97	8.89	61.87	23%
PFHpA	20.58	0.20	53.65	161%	31.32	5.74	25.25	24%
PFOA	10.66	0.11	29.95	181%	18.19	5.47	14.10	27%
PFNA	14.59	0.14	23.30	60%	10.16	2.13	10.96	32%
PFDA	10.87	0.11	22.46	107%	11.63	0.66	10.57	31%
PFOS	11.71	0.12	24.23	107%	12.68	1.64	11.40	12%

Model evaluation - all PFAAs		
	R ²	slope
Leaves S100W0	0.99	1.26
Leaves S200W0	0.94	1.32
Heads S100W0	0.98	1.39
Heads S200W0	0.92	1.14

Model evaluation – only PFCAs		
	R ²	slope
Leaves S100W0	1.00	1.25
Leaves S200W0	0.98	1.26
Heads S100W0	0.99	1.44
Heads S200W0	0.97	1.36



⁶ Mean absolute percentage error (MAPE (%)), defined as: $MAPE = \frac{100\%}{n} \sum_{i=1}^n \left| \frac{x_i - y}{x_i} \right|$, where n is the number of replicate plants (n=3, from (Gredelj et al., 2019a)), x is the measured PFAA concentration and y is the PFAA concentration predicted by the model.

Table A3-9. Comparison of mean measured and modeled concentrations (ng/gfw) in crop compartments with default plant parameters and statistical evaluation of model performance.

	ROOTS				SHOOTS				FRUITS													
	Tomato	Celery	Pea	Radish	Tomato	Celery	Pea	Radish	Tomato	Pea												
Modeled concentrations																						
PFBA	2.59	9.29	2.19	1.30	PFBA	14.00	9.80	14.10	13.17	PFBA	2.80	2.82										
PFPeA	1.05	7.65	1.52	1.10	PFPeA	43.25	41.73	42.83	39.19	PFPeA	8.65	8.57										
PFHxA	1.98	9.42	3.06	1.31	PFHxA	21.11	20.34	20.86	19.19	PFHxA	4.22	4.17										
PFHpA	1.91	4.34	3.35	0.68	PFHpA	6.00	5.81	5.86	5.51	PFHpA	1.20	1.17										
PFOA	8.84	19.14	15.68	6.58	PFOA	16.40	15.98	16.05	14.90	PFOA	3.28	3.21										
PFNA	4.23	5.83	7.48	2.49	PFNA	3.87	3.62	3.54	3.61	PFNA	0.77	0.71										
PFDA	15.06	12.84	21.22	3.75	PFDA	27.34	27.18	22.90	31.43	PFDA	5.47	4.58										
PFBS	4.08	27.09	10.87	6.07	PFBS	64.33	59.76	62.72	57.88	PFBS	12.87	12.54										
PFOS	16.41	17.05	17.75	3.17	PFOS	29.49	24.87	27.73	40.04	PFOS	5.90	5.55										
Measured concentrations																						
	mean	s.e.	mean	s.e.	mean	s.e.	mean	s.e.		mean	s.e.	mean	s.e.	mean	s.e.	mean	s.e.		mean	s.e.	mean	s.e.
PFBA	2.83	0.68	14.55	3.34	2.35	0.23	1.37	0.17	PFBA	19.50	1.71	32.44	2.95	11.73	2.05	9.70	1.17	PFBA	3.37	0.44	27.03	4.33
PFPeA	1.05	0.26	7.99	1.71	1.53	0.18	1.10	0.29	PFPeA	15.83	0.79	20.71	2.65	12.01	1.48	7.20	0.79	PFPeA	12.68	3.26	8.25	1.38
PFHxA	2.00	0.39	9.89	1.01	3.10	0.47	1.32	0.37	PFHxA	16.44	1.08	19.20	3.74	9.17	1.07	6.67	0.57	PFHxA	1.99	0.59	3.04	0.95
PFHpA	1.95	0.34	4.58	0.76	3.47	0.73	0.69	0.12	PFHpA	5.22	0.70	3.02	0.57	2.47	0.23	7.11	1.16	PFHpA	0.45	0.12	0.28	0.08
PFOA	9.00	0.93	20.04	5.18	16.18	4.52	6.69	1.34	PFOA	30.44	6.30	7.76	2.35	9.44	0.71	89.51	17.89	PFOA	0.53	0.04	0.48	0.14
PFNA	4.65	0.33	6.88	1.53	8.94	0.93	2.67	0.65	PFNA	7.56	1.83	1.93	0.34	2.04	0.15	16.05	3.11	PFNA	0.17	0.00	0.26	0.08
PFDA	20.80	2.22	17.89	2.82	34.72	5.02	4.09	1.32	PFDA	21.45	5.20	4.22	0.36	3.18	0.27	15.45	2.90	PFDA	0.17	0.00	0.03	0.00
PFBS	4.13	1.81	29.56	4.29	11.19	2.76	6.19	1.94	PFBS	28.34	3.48	15.00	4.09	46.02	4.63	24.63	2.00	PFBS	1.16	0.20	2.91	0.46
PFOS	27.02	2.58	33.39	3.45	30.85	4.36	3.49	1.21	PFOS	33.70	7.50	9.70	0.71	14.16	0.88	27.83	5.84	PFOS	0.01	0.00	0.23	0.05

Model evaluation - all PFAAs			Model evaluation - short-chain PFAAs		
	R ²	slope		R ²	slope
Roots			Roots		
Tomato	0.97	0.68	Tomato	1.00	0.97
Celery	0.94	0.74	Celery	0.99	0.88
Pea	0.96	0.66	Pea	1.00	0.97
Radish	1.00	0.96	Radish	1.00	0.98
Shoots			Shoots		
Tomato	0.75	1.22	Tomato	0.86	1.82
Celery	0.52	1.32	Celery	0.51	1.19
Pea	0.86	1.57	Pea	0.89	1.51
Radish ¹	0.78	1.73	Radish	0.87	2.36
Fruits			Fruits		
Tomato	0.35	0.82	Tomato	0.43	0.80
Pea	0.15	0.24	Pea	0.18	0.24

¹ PFOA was eliminated from the evaluation, very high measured value strongly influencing the parameters of the regression line

References

- Bizkarguenaga, E., Zabaleta, I., Mijangos, L., Iparraguirre, A., Fernández, L.A., Prieto, A., Zuloaga, O., 2016. Uptake of perfluorooctanoic acid, perfluorooctane sulfonate and perfluorooctane sulfonamide by carrot and lettuce from compost amended soil. *Sci. Total Environ.* <https://doi.org/10.1016/j.scitotenv.2016.07.010>
- Blaine, A.C., Rich, C.D., Hundal, L.S., Lau, C., Mills, M.A., Harris, K.M., Higgins, C.P., 2013. Uptake of perfluoroalkyl acids into edible crops via land applied biosolids: Field and greenhouse studies. *Environ. Sci. Technol.* 47, 14062–14069. <https://doi.org/10.1021/es403094q>
- Blaine, A.C., Rich, C.D., Sedlacko, E.M., Hundal, L.S., Kumar, K., Lau, C., Mills, M.A., Harris, K.M., Higgins, C.P., 2014. Perfluoroalkyl acid distribution in various plant compartments of edible crops grown in biosolids-amended soils. *Environ. Sci. Technol.* 48, 7858–7865. <https://doi.org/10.1021/es500016s>
- Gredelj, A., Nicoletto, C., Valsecchi, S., Ferrario, C., Polesello, S., Lava, R., Zanon, F., Barausse, A., Palmeri, L., Guidolin, L., Bonato, M., 2019. Uptake and translocation of perfluoroalkyl acids (PFAA) in red chicory (*Cichorium intybus* L.) under various treatments with pre-contaminated soil and irrigation water. *Sci. Total Environ.* <https://doi.org/10.1016/j.scitotenv.2019.134766>
- Lan, Z., Zhou, M., Yao, Y., Sun, H., 2018. Plant uptake and translocation of perfluoroalkyl acids in a wheat–soil system. *Environ. Sci. Pollut. Res.* 25, 30907–30916. <https://doi.org/10.1007/s11356-018-3070-3>
- Navarro, I., de la Torre, A., Sanz, P., Porcel, M.Á., Pro, J., Carbonell, G., Martínez, M. de los Á., 2017. Uptake of perfluoroalkyl substances and halogenated flame retardants by crop plants grown in biosolids-amended soils. *Environ. Res.* 152, 199–206. <https://doi.org/10.1016/j.envres.2016.10.018>
- Trapp, S., 2015. Calibration of a plant uptake model with plant- and site-specific data for uptake of chlorinated organic compounds into radish. *Environ. Sci. Technol.* 49, 395–402. <https://doi.org/10.1021/es503437p>
- Wen, B., Li, L., Zhang, H., Ma, Y., Shan, X.Q., Zhang, S., 2014. Field study on the uptake and translocation of perfluoroalkyl acids (PFAAs) by wheat (*Triticum aestivum* L.) grown in biosolids-amended soils. *Environ. Pollut.* 184, 547–554. <https://doi.org/10.1016/j.envpol.2013.09.040>
- Wen, B., Wu, Y., Zhang, H., Liu, Y., Hu, X., Huang, H., Zhang, S., 2016. The roles of protein and lipid in the accumulation and distribution of perfluorooctane sulfonate (PFOS) and perfluorooctanoate (PFOA) in plants grown in biosolids-amended soils. *Environ. Pollut.* 216, 682–688. <https://doi.org/10.1016/j.envpol.2016.06.032>
- Zhao, S., Fan, Z., Sun, L., Zhou, T., Xing, Y., Liu, L., 2017. Interaction effects on uptake and toxicity of perfluoroalkyl substances and cadmium in wheat (*Triticum aestivum* L.) and rapeseed (*Brassica campestris* L.) from co-contaminated soil. *Ecotoxicol. Environ. Saf.* 137, 194–201. <https://doi.org/10.1016/j.ecoenv.2016.12.007>

APPENDIX 4: Supplementary information for Chapter 5

Uptake and translocation of perfluoroalkyl acids (PFAAs) in hydroponically grown red chicory (*Cichorium intybus L.*): PFAAs toxicity, comparison with the soil experiment and bioavailability implications

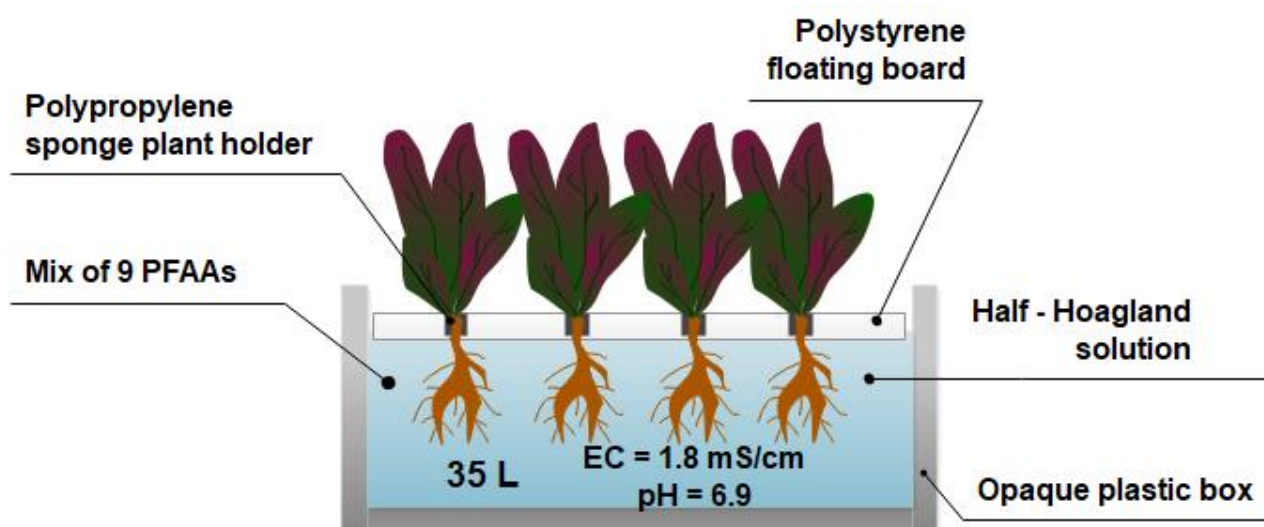


Figure A4-1. Hydroponic tank scheme.

Text A4-1. Preparation protocol for the spiking and nutrient solution

a) Spiking solution:

Spiking solution for irrigation water was prepared by solving 90 mg (nominal mass) of each PFAAs in 250 mL of MeOH/H₂O (v/v) 70:30. Firstly, 40 mL of H₂O LC/MS grade 80 mL of MeOH (both Fluka Analytical) PFAAs were added in the volumetric flask and then solved from longest to the shortest. Long-chain were weighted and short chain (< 6CF_x) were added by volume directly to the flask. After that, 35 mL of ultrapure water and remaining MeOH were added and flask was shaken and sonicated for 5 min (to dissolve remaining visible amounts of PFAAs). Solution was transferred to the plastic bottle afterwards and 1 mL was taken for the analyses to validate the spiking accuracy.

b) Nutrient solution (amounts and composition):

Target nutrients concentrations in the hydroponic tanks (half-concentrated Hoagland's nutrient solution) are accepted from (Felizeter et al., 2012).

To achieve the target nutrients amounts, 5L concentrated nutrient stock solutions were prepared and 350 mL (10 mL per each L of water) of each was added to every hydroponic tank. Two 5L stock nutrient solutions (A and B) were prepared as follows:

Table A4-1. Preparation of the stock nutrient solutions

SOLUTION A		
Substance		Mass [g]
Iron EDTA	Fe(EDTA)	2.154
Calcium nitrate tetrahydrate	Ca(NO ₃) ₂ ·4H ₂ O	290.593
Ammonium nitrate	NH ₄ NO ₃	171.769
SOLUTION B		

Substance		Mass [g]
Magnesium sulfate heptahydrate	MgSO ₄ *7H ₂ O	121.704
Sodium molybdate dihydrate	Na ₂ MoO ₄ *2H ₂ O	0.006
Zinc Sulfate Dihydrate	ZnSO ₄ *2H ₂ O	0.038
Boric acid	H ₃ BO ₃	0.715
Cooper sulfate pentahydrate	CuSO ₄ *5H ₂ O	0.02
Manganese chloride	MnCl ₂ *4H ₂ O	0.415
Potassium sulfate	K ₂ SO ₄	130.925
Added separately – 3 mL/L		
Phosphoric acid (45%)	H ₃ PO ₄	

Measured pH of the prepared hydroponic solutions was 6.9 and electrical conductivity 1.8 mS/cm.

Table A4-2. Target and resulting nutrients concentration in the hydroponic tanks

Concentration of nutrients in the hydroponic tanks		
Element	Target concentration [mg/L]	Final concentration [mg/L]
N (NO ₃ ⁻)	85	86.964
N (NH ₄ ⁺)	20	18.036
P	15.5	15.5
K	117.5	117.5
Mg	24	24
Ca	100	98.627
S	32	79.87
Fe	0.56	0.56
Zn	0.025	0.025
B	0.25	0.25
Mn	0.25	0.25
Cu	0.01	0.01
Mo	0.005	0.005
Na	0	0.002
Cl	0	0.161

Table A4-3. Measured concentrations in the red chicory shoots and roots. Different treatments are entitled as the nominal concentrations values in the nutrient solution. Measurements are expressed as means with standard error estimates.

Shoots (ng/g_{fw})	62.5 ug/L		125 ug/L		250 ug/L	
	Mean	St.err.	Mean	St.err.	Mean	St.err.
PFBA	447.9	86.4	711.8	39.0	1774.4	231.5
PFPeA	460.0	106.8	660.7	57.4	1577.1	268.1
PFHxA	452.7	113.5	514.6	47.1	1149.7	208.3
PFHpA	271.5	51.8	405.7	38.5	781.0	92.8
PFOA	230.7	55.0	369.7	60.7	659.9	54.2
PFNA	233.2	62.6	387.1	77.4	636.4	62.8
PFDA	204.1	67.1	375.6	49.8	666.4	64.7
PFBS	297.0	81.8	434.1	17.0	1187.2	279.9
PFOS	168.4	72.2	297.7	59.4	550.7	29.1

Roots (ng/g_{fw})	62.5 ug/L		125 ug/L		250 ug/L	
	Mean	St.err.	Mean	St.err.	Mean	St.err.
PFBA	130.4	19.0	195.9	11.3	433.0	42.8
PFPeA	105.8	4.3	190.2	7.9	340.7	21.1
PFHxA	158.5	9.6	284.4	3.8	442.2	25.1
PFHpA	268.7	38.7	559.2	6.2	748.6	66.4
PFOA	653.0	165.8	1585.2	36.8	2061.2	330.2
PFNA	1407.0	232.9	3868.7	210.7	7002.7	1670.4
PFDA	4945.9	1139.0	14017.5	593.9	23003.2	5466.9
PFBS	162.5	8.4	361.9	15.0	637.5	49.3
PFOS	3158.5	706.5	7972.7	251.5	14005.4	2618.9

Table A4-4. Total experimental recoveries. Calculated as percentage of the recovered PFAA mass (PFAA mass remained in nutrient solution + measured in plants/PFAA mass in the beginning), expressed as individual recoveries per each tank.

Treatment:	62.5 ug/L			125 ug/L			250 ug/L		
PFBA	87.7%	73.5%	77.2%	79.4%	77.9%	74.2%	79.4%	86.7%	92.9%
PFPeA	89.0%	73.9%	83.1%	84.0%	85.5%	77.1%	84.0%	79.8%	86.5%
PFHxA	118.2%	81.9%	108.2%	101.6%	96.7%	107.0%	97.6%	98.2%	110.3%
PFHpA	93.5%	58.3%	79.8%	84.1%	76.4%	77.4%	72.5%	83.0%	80.8%
PFOA	89.5%	68.7%	85.3%	89.2%	84.2%	87.5%	91.9%	92.6%	94.2%
PFNA	99.8%	79.5%	109.6%	96.7%	87.8%	114.3%	89.1%	85.2%	91.0%
PFDA	152.1%	130.2%	187.2%	238.1%	165.1%	267.5%	86.4%	93.2%	95.9%
PFBS	95.0%	73.9%	100.9%	88.6%	80.9%	84.1%	88.8%	91.0%	96.6%
PFOS	115.7%	104.0%	120.8%	146.4%	101.7%	176.2%	64.7%	71.5%	77.3%

Table A4-5. Measured concentration of PFAAs in the nutrient solution, data are shown as means (n = 3) with error estimates.

Date: 11/8/2018								
	Control		62.5 µg/L		125 µg/L		250 µg/L	
	Mean	St.err.	Mean	St.err.	Mean	St.err.	Mean	St.err.
PFBA	0.0	0.0	81.8	2.5	142.8	4.7	287.1	1.6
PFPeA	0.0	0.0	100.2	5.6	174.8	11.2	296.5	6.5
PFBS	0.0	0.0	69.8	3.7	135.5	2.0	258.2	12.9
PFHxA	0.0	0.0	97.9	4.4	187.2	7.0	338.0	9.6
PFHpA	0.0	0.0	55.2	2.8	119.0	4.1	239.9	6.9
PFOA	0.0	0.0	62.9	2.7	127.5	5.4	265.6	9.6
PFNA	0.0	0.0	80.8	6.1	197.8	19.4	381.8	41.9
PFDA	0.0	0.0	147.7	13.5	407.2	88.0	603.0	9.2
PFOS	0.0	0.0	104.5	5.8	250.8	39.8	465.2	36.7

Date: 20/8/2018								
	Control		62.5 µg/L		125 µg/L		250 µg/L	
	Mean	St.err.	Mean	St.err.	Mean	St.err.	Mean	St.err.
PFBA	0.0	0.0	78.6	4.3	147.3	12.9	278.6	2.8
PFPeA	0.0	0.0	85.0	5.4	169.1	1.7	285.0	11.4
PFBS	0.0	0.0	73.2	1.8	142.6	7.7	277.7	4.3
PFHxA	0.0	0.0	91.9	6.2	183.1	12.7	337.7	20.6
PFHpA	0.0	0.0	70.4	3.7	131.4	9.7	265.6	5.5
PFOA	0.0	0.0	70.9	4.3	136.3	9.6	289.3	11.8
PFNA	0.0	0.0	72.5	3.1	155.6	7.4	287.4	6.0
PFDA	0.0	0.0	68.6	3.3	150.5	4.1	271.6	15.9
PFOS	0.0	0.0	69.1	2.7	154.6	2.6	273.2	4.6

Date: 27/8/2018								
	Control		62.5 µg/L		125 µg/L		250 µg/L	
	Mean	St.err.	Mean	St.err.	Mean	St.err.	Mean	St.err.
PFBA	0.0	0.0	83.1	7.8	139.7	5.3	258.1	9.2
PFPeA	0.0	0.0	74.0	3.6	145.1	6.5	248.2	23.0
PFBS	0.0	0.0	77.7	3.9	132.7	3.5	291.3	14.7
PFHxA	0.0	0.0	83.9	4.2	155.5	6.6	283.7	18.7
PFHpA	0.0	0.0	76.0	3.2	140.6	4.1	265.9	8.0
PFOA	0.0	0.0	70.3	2.7	131.7	7.1	271.4	7.0
PFNA	0.1	0.1	70.3	1.5	137.7	4.1	287.3	3.5
PFDA	0.3	0.2	59.0	2.0	121.6	9.6	202.4	16.7
PFOS	0.1	0.1	67.6	4.5	130.5	3.2	250.2	13.0

Date: 3/9/2018								
	Control		62.5 µg/L		125 µg/L		250 µg/L	
	Mean	St.err.	Mean	St.err.	Mean	St.err.	Mean	St.err.
PFBA	0.0	0.0	79.3	8.6	147.5	5.7	266.1	18.7
PFPeA	0.0	0.0	81.4	1.3	147.4	2.5	305.4	5.6
PFBS	0.0	0.0	74.2	10.4	141.5	4.0	270.6	27.8
PFHxA	0.0	0.0	68.4	4.5	128.9	10.2	268.0	11.3

PFHpA	0.0	0.0	71.6	8.8	127.0	8.2	221.5	18.0
PFOA	0.0	0.0	66.9	9.8	126.5	8.4	269.9	3.7
PFNA	0.0	0.0	106.7	13.5	186.3	8.6	290.8	28.9
PFDA	0.0	0.0	228.6	38.7	380.4	10.5	386.6	42.9
PFOS	0.0	0.0	130.1	19.6	256.9	10.0	348.8	28.6

Date: 10/9/2018

	Control		62.5 µg/L		125 µg/L		250 µg/L	
	Mean	St.err.	Mean	St.err.	Mean	St.err.	Mean	St.err.
PFBA	0.0	0.0	61.4	3.0	112.1	2.3	240.1	2.6
PFPeA	0.0	0.0	69.4	2.3	135.6	7.5	279.1	18.4
PFBS	0.0	0.0	60.1	4.1	125.2	7.3	235.9	9.3
PFHxA	0.0	0.0	82.0	5.1	141.5	3.5	272.5	5.1
PFHpA	0.0	0.0	67.8	3.1	129.1	2.0	253.3	13.0
PFOA	0.0	0.0	69.9	7.9	120.6	5.0	252.3	15.0
PFNA	0.0	0.0	68.7	8.2	137.0	15.7	246.7	3.0
PFDA	0.0	0.0	99.0	23.3	157.7	13.0	372.8	36.4
PFOS	0.0	0.0	88.9	17.9	130.8	1.3	267.8	14.0

Date: 17/9/2018

	Control		62.5 µg/L		125 µg/L		250 µg/L	
	Mean	St.err.	Mean	St.err.	Mean	St.err.	Mean	St.err.
PFBA	0.0	0.0	47.3	2.2	95.0	3.1	217.6	9.1
PFPeA	0.0	0.0	48.5	2.4	101.4	4.0	210.0	6.8
PFBS	0.0	0.0	55.6	4.8	106.5	3.9	235.3	4.6
PFHxA	0.0	0.0	64.3	6.4	132.6	3.8	270.1	9.6
PFHpA	0.0	0.0	52.2	6.8	109.4	4.7	221.7	7.3
PFOA	0.0	0.0	48.2	3.3	104.4	3.2	230.3	1.4
PFNA	0.0	0.0	63.1	5.8	129.8	11.7	235.4	7.0
PFDA	0.0	0.0	101.5	11.1	290.2	46.7	220.5	15.6
PFOS	0.0	0.0	76.0	2.9	188.9	33.6	181.2	14.0

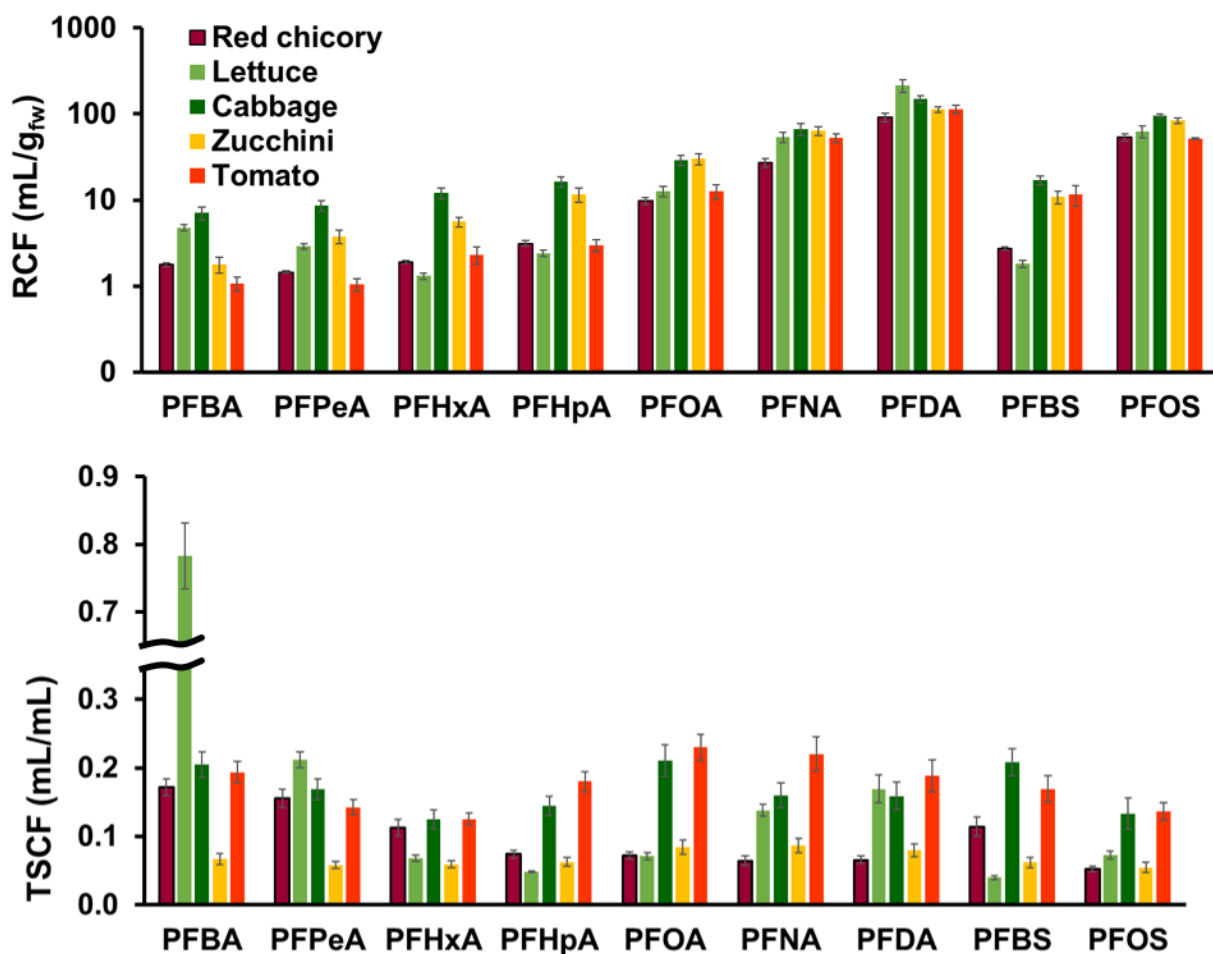


Figure A4-2. Comparison of the RCFS and TSCFs with other hydroponic experiments. Data for lettuce are taken from (Felizeter et al., 2012), cabbage, zucchini and tomato are from (Felizeter et al., 2014) and red chicory is from this study.

Table A4-6. Comparison of the equilibrium root concentration factor (RCF) from hydroponics (treatment with 62.5 $\mu\text{g/L}$), equilibrium soil-water partition coefficient (K_d), dry weight based RCF from hydroponics and soil to water partition coefficient normalized to organic matter content in soil (K_{om})

(mL/g)	$\text{RCF}_{\text{hydro}}$	$\text{RCF}_{\text{hydro}}(\text{dw})$	K_d	K_{om}
PFBA	2.4	29.8	0.9	34.7
PFPeA	1.7	21.2	0.6	23.4
PFHxA	2.4	30.0	1.0	39.0
PFHpA	3.5	44.0	1.6	66.5
PFOA	8.4	104.7	1.2	47.3
PFNA	18.5	231.1	5.1	207.8
PFDA	59.1	739.3	40.1	1629.9
PFBS	2.7	34.0	0.8	32.4
PFOS	37.2	464.9	93.6	3803.4

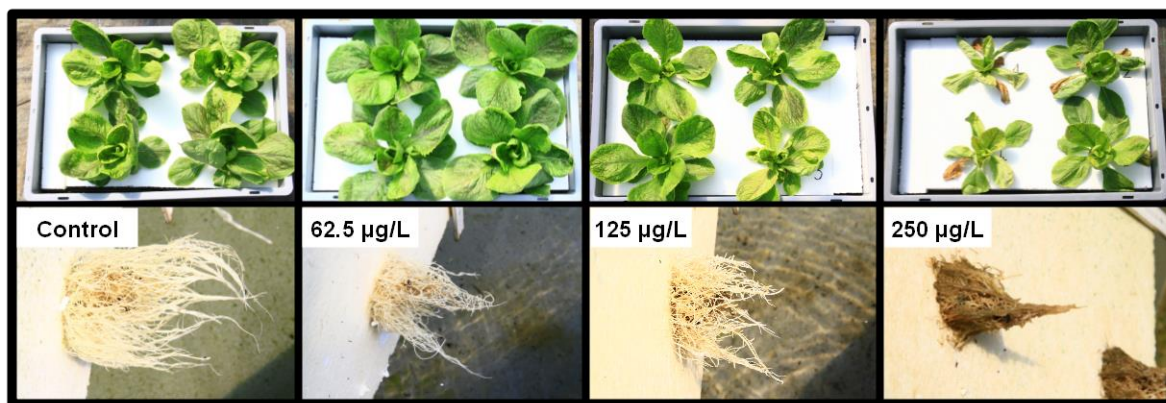


Figure A4-6. Photographs of chicory shoots and roots per treatments, 2 weeks after the initial exposure (27/08/2018)

References:

- Felizeter, S., McLachlan, M.S., De Voogt, P., 2014. Root uptake and translocation of perfluorinated alkyl acids by three hydroponically grown crops. *J. Agric. Food Chem.* 62, 3334–3342. <https://doi.org/10.1021/jf500674j>
- Felizeter, S., McLachlan, M.S., De Voogt, P., 2012. Uptake of perfluorinated alkyl acids by hydroponically grown lettuce (*Lactuca sativa*). *Environ. Sci. Technol.* 46, 11735–11743. <https://doi.org/10.1021/es302398u>

APPENDIX 5: Supplementary information for Chapter 6

Predicting the human exposure to perfluoroalkyl acids (PFAAs) through diet: A case of the Veneto Region, Italy

Text A5-1. Crop modelling framework details and parametrization

For every crop, growing area of 1 m² was established, with the rooting depth of 0.4 m typical for the most crops, but for the wheat and maize for which 1 m depth was used (FAO, 2004). Loam soil that was used in the experimental work from Chapter 3 was considered representative for the Veneto region agricultural soil and soil-water partition coefficients derived for the PFAA mixture were applied here as well. The same soil was sampled with the plastic corer (Chapter 3), showed that the long-chain PFAAs did not move towards the bottom pot part (approximately 20 cm depth) when irrigated with the spiked water. According to the study of (Sepulvado et al., 2011), where leaching potential of the set of PFAAs was studied in the soil cores (silt-loam) from the fields that received various biosolids loading, leaching decrease for the long-chain PFAAs was observed from the surface to the depth of 0.45 m. On the contrary, short-chain PFAAs, being very mobile, were always detected on the bottom of the cores (1.2 m depth). Hence, to calculate the nominal bulk soil concentration, based on the calculated soil volume and measured dry weight bulk density of the tested loam soil, depth of the 0.4 m was used for all the crops and long-chain PFAAs (including the maize and wheat), while for the short-chain PFAAs depth of 1 m was used for maize and wheat and 0.4 m for all the other crops. For the purpose of the worst-case scenario, it was assumed that all delivered water was from irrigation and that all water used for irrigation purposes was contaminated. Water needs for each crop were calculated based on the simple estimation equations given by (FAO, 1986), where daily water needs for grass in the certain climatic area are increased or decreased percentagewise, depending of the crop type. Daily crop water needs were then multiplied with the average growing period for each crop type to get the total water volume per 1m² (FAO, 1986).

The only studies, apart from (Gredelj et al., 2019a) (Chapter 3), providing the empirical root to soil concentration factors for the set of PFAAs (i.e. not only for PFOS and PFOA) were (Blaine et al., 2014a, 2013; Wen et al., 2014), providing the RCFs for tomato, celery, pea, radish (Blaine et al., 2014a, 2013) and wheat (Wen et al., 2014). The crop selection also depended on the food categories for consumed cereals and vegetables given in the dietary study (Leclercq et al., 2009). Selected cereal/vegetable crops were considered representative for every food category, as shown in Table A5-1.

Table A5-1. Representative crop models for the corresponding food and feed categories.

Food category (groups/subgroups)	Representative model	Water needed ¹ per crop per day (mm/day)	Growth time (day)
Cereals, cereal products and substitutes	Wheat	6.05	135 ¹
Pulses, fresh and processed	Peas	6.05	129 ²
Leafy vegetables, fresh	Red chicory	5.50	87 ³
Tomatoes, fresh	Tomato	6.05	162 ²
Other fruiting vegetables, fresh	Tomato	6.05	162 ²
Roots and onions, fresh	Radish	6.05	67 ²
Other vegetables, fresh	Celery	6.05	224 ²
Vegetables, processed	Tomato	6.05	162 ²
Potatoes, tubers and their products	Potato	6.05	125 ¹
Citrus fruits, fresh	Lemon (background concentration)	-	-

Exotic fruits,fresh	Banana (background concentration)	-	-
Other fruits,fresh	Strawberry	6.05	84 ¹
Animal feed:			
Forage	Grass	5.5	100 ¹
Silage	Alfalfa	5.5	100 ¹
Grains	Maize	5.5	150 ¹

¹(FAO, 1986)

² (Blaine et al., 2014a)

³ (Gredelj et al., 2019a)

Potato is the most consumed vegetable in the North-East Italian consumption region, with the 26% of the total intake (average population) among all the other vegetables (Leclercq et al., 2009). Potato is a tuber, a storage organ located at the end of a stem, that is not connected to the root system or transpiration stream (Lechner and Knapp, 2011; Trapp et al., 2007) and due to this physiological differences the same modelling approach (as for the other crops), based on the xylem transport, was not applicable. The literature data were not sufficient for developing the semi-empirical model in the same way as it was done for the red chicory (Chapter 4), only two studies investigating the transfer of PFOS and PFOA from the soil into potatoes (Lechner and Knapp, 2011; T. Stahl et al., 2009). In the study of (Lechner and Knapp, 2011) concentrations of PFOS and PFOA were measured in soil, potato peels, peeled tubers and the vegetative part. Based on the measured concentrations, peeled potato-soil bioconcentration factors (BCF_{PS}) for PFOS and PFOA were calculated and used in the model. For all the other PFAAs, having no data for potato, ratio between shoots concentration factors (SCF) for PFOA and other PFCAs and PFOS and PFBS, which were derived for the red chicory, were used to estimate the potential BCFs for the potato, based on the BCF_{PS} for PFOS and PFOA. The same chain-length dependency, with the short chain homologues being the most accumulating PFAAs in shoots, was expected also for the potatoes, considering that it was observed for all the other crop plants in the literature (Ghisi et al., 2019).

There is less research on the bioaccumulation of PFAAs in fruits than it is for vegetables, plant uptake studies on fruits being reduced to only one for strawberry from (Blaine et al., 2014b), considering the most grown fruits are perennial long-living woody plants, making this kind of experiments hardly feasible. The same modelling approach developed in Chapter 4 was applied for the strawberry. The modelled concentrations in strawberry fruits were two orders of a magnitude lower than the measured ones for PFBA, PFPeA and PFHxA, in contrast with the pea and tomato (having the same plant compartments), while concentrations in shoots and roots were well predicted (not shown). The reason for this could be the different experimental set-up for strawberry, that has been grown in the sandy-soil mix with the very low sorption capacity for PFAAs and irrigated with the contaminated water (Blaine et al., 2014b). The other reason for such high fruit uptake, as stated by the authors, was the low amount of water that was used for irrigation, which was preferentially used by plant for the fruit development, less water being transpired by shoots (and hence less PFAAs delivered to this compartment by xylem) (Blaine et al., 2014b). For this purpose and with the lack of other data, the model was used for strawberry fruit predictions regardless. Three fruit categories were provided in the Italian food consumption study (Leclercq et al., 2009): citrus fruits, exotic fruits and other fruits. Only fruits listed as the “other fruits” (e.g. apple, pear, cherry, strawberry, etc.) are commercially grown in the Veneto Region while no citrus nor exotic fruits are commonly cultivated (Veneto agricoltura, 2016). Hence, for the representative fruits from the “citrus” and “exotic” fruits categories, the concentrations detected in the study that included fruits, cereals

and vegetables sampled in the European retail stores were directly used (D'Hollander et al., 2015). From the study of (D'Hollander et al., 2015), lemon and banana sampled from Italy were chosen as the fruits representative for the categories of citrus and exotic fruits, respectively, both having very low concentrations of PFAAs (a few pg/g). In the lemon, among the PFAAs of interest, only PFOA was detected above LOD (2 pg/g) and in the bananas only PFNA (3 pg/g) and PFOS (7 pg/g).

Table A5-2. Bioconcentration parameters used in the crop modelling

RCFs (g/g _{dw})	Tomato ¹	Celery ¹	Pea ¹	Radish ¹	Red chicory ²	Wheat ³	Maize ³	Alfalfa ^{4,7}	Grass ^{4,7}	Strawberry ⁵	Potato ^{6,7}
					S200W80	Wheat RCFs		Alfalfa RCFs			BCF _{PS} (g/g _{dw})
PFBA	5.04	17.27	1.93	2.92	156.93	2.70	2.70	259.08	259.08	30.98	1.50
PFPeA	0.76	3.84	0.51	0.95	74.18	3.60	3.60	113.79	113.79	108.94	0.66
PFHxA	1.45	4.77	1.04	1.15	27.18	2.83	2.83	43.25	43.25	109.77	0.25
PFHpA	1.88	2.96	1.55	0.80	14.25	2.68	2.68	17.81	17.81	104.63	0.10
PFOA	0.96	1.42	0.79	0.85	6.57	1.73	1.73	10.34	10.34	74.11	0.06
PFNA	1.92	1.90	1.71	1.32	3.15	2.86	2.86	4.63	4.63	77.86	0.03
PFDA	1.85	1.06	1.43	0.44	2.77	1.99	1.99	3.84	3.84	27.52 ⁷	0.02
PFBS	0.71	3.38	0.89	1.27	75.63	1.91	1.91	61.55	61.55	74.86	0.27
PFOS	4.53	3.74	2.39	0.70	3.70	1.36	1.36	3.12	3.12	91.67	0.01

¹ (Blaine et al., 2014a)

² (Gredelj et al., 2019a)

³ (Wen et al., 2014), plot 4, with the highest rate of biosolids amendment

⁴ (Wen et al., 2016), RCFs for PFOS and PFOA in alfalfa

⁵ (Blaine et al., 2014b)

⁶ (Lechner and Knapp, 2011), BCFs calculated between peeled potato and soil for PFOS and PFOA

⁷ Extrapolated values for other PFAAs (but PFOS and PFOA), based on the PFCAs to PFOA and PFBS to PFOS ratio calculated for the red chicory (Gredelj et al., 2019a)

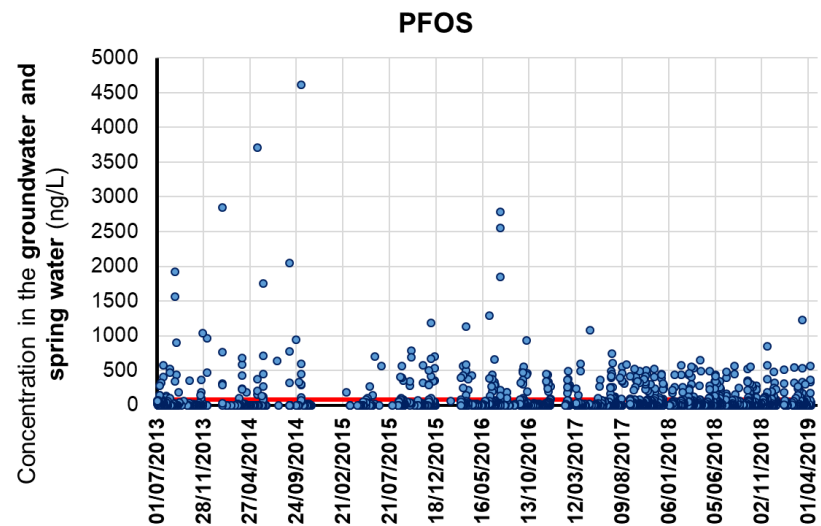
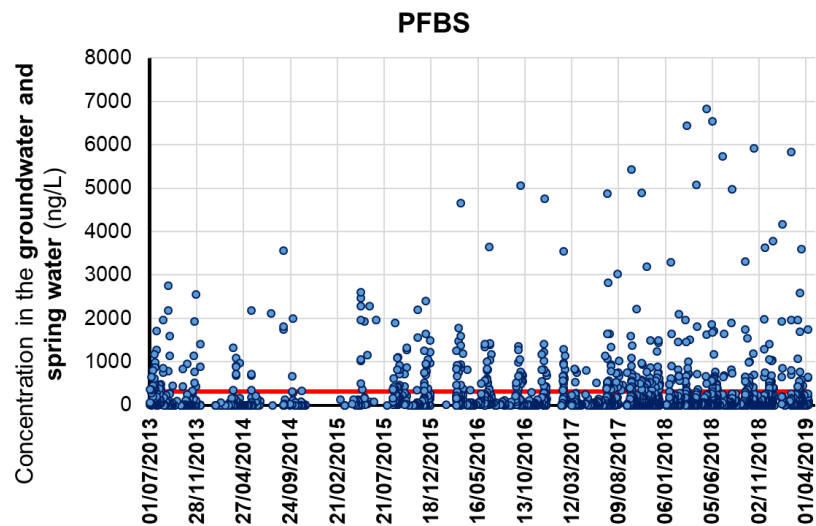
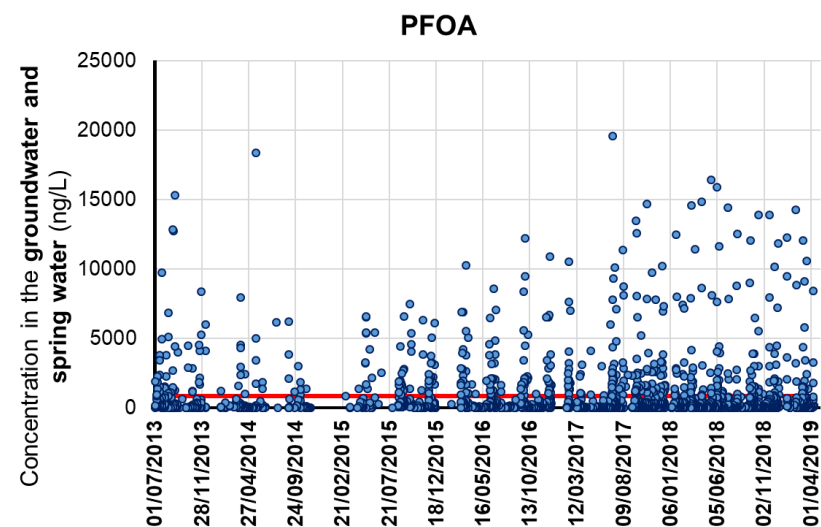
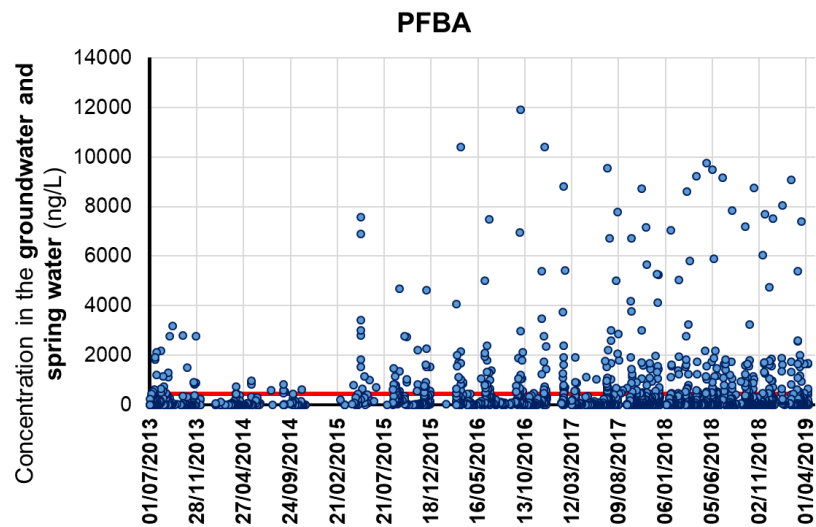


Figure A5-1. Concentration ranges of the most abundant PFAAs measured in the **groundwater and spring waters** of the Veneto region. Monitoring data from the Regional Environmental Protection Agency of the Veneto Region, from 02/07/2013 to 08/04/2019 (ARPAV, 2019). Average values are shown as the red line.

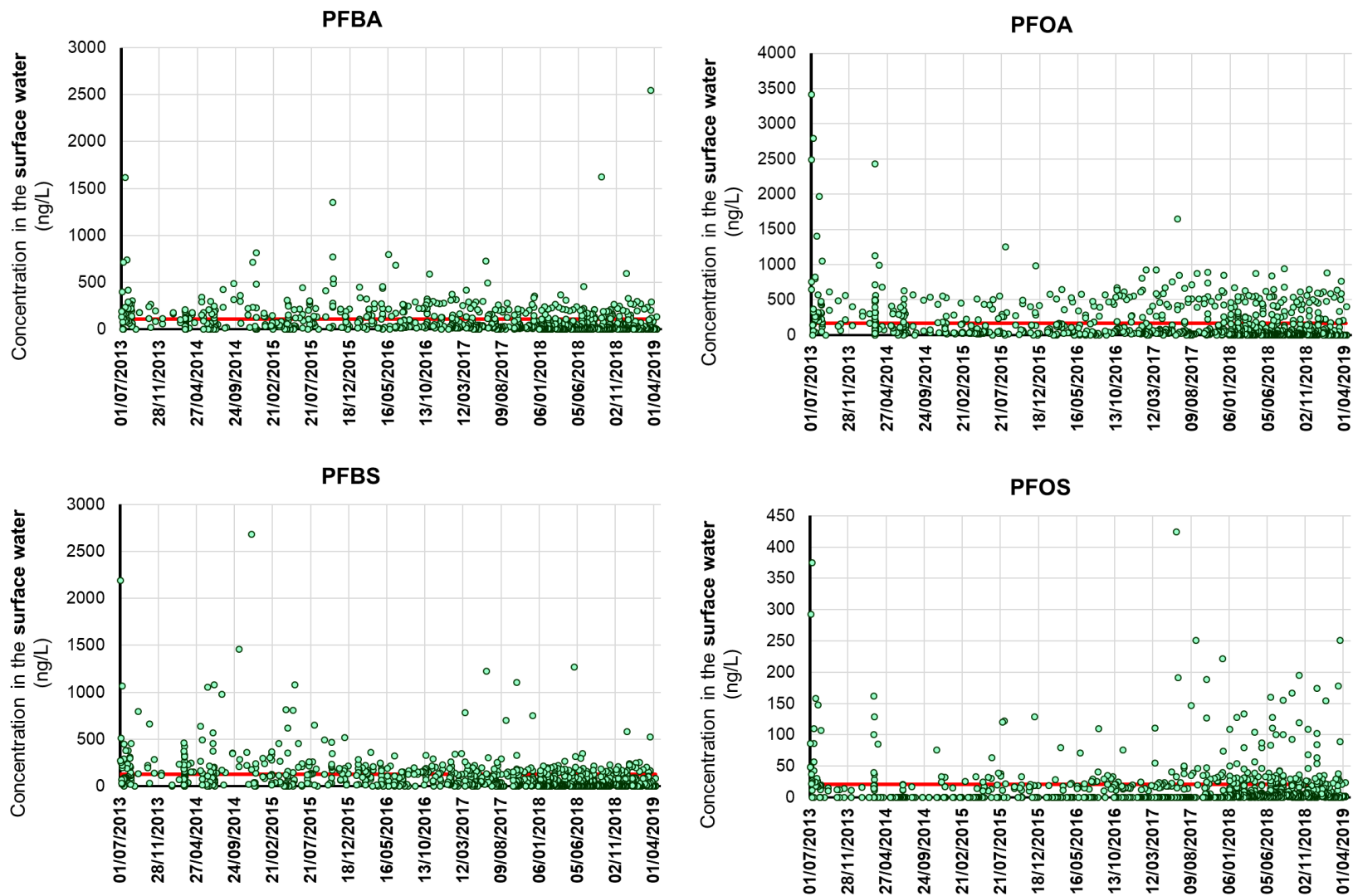
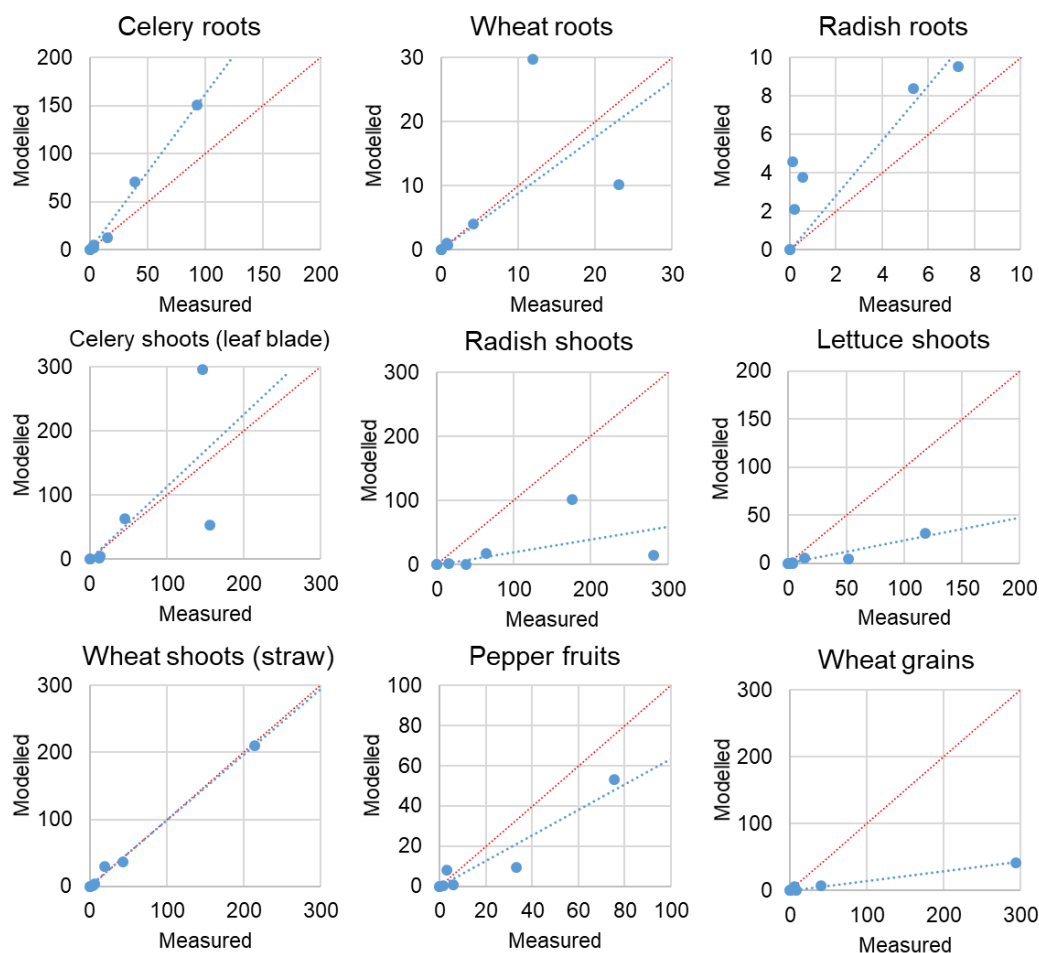


Figure A5-2 Concentration ranges of the most abundant PFAAs measured in the **surface waters** of the Veneto region. Monitoring data from the Regional Environmental Protection Agency of the Veneto Region, from 02/07/2013 to 08/04/2019 (ARPAV, 2019). Average values are shown as the red line.

Table A5-3. Crop models evaluation statistics when validated with the field data from (Liu et al., 2019, 2016). Linear regression lines are shown as the modelled concentrations vs. measured concentrations in various crop compartments. All concentrations are expressed on the fresh weight basis.

Models evaluation statistics		
	slope	R ²
Roots:		
Celery	1.62	0.99
Wheat	0.88	0.53
Radish	1.43	0.84
Shoots:		
Celery	1.13	0.65
Radish	0.20	0.42
Lettuce	0.24	0.93
Wheat	0.98	1.00
Fruits:		
Pepper	0.63	0.93
Wheat	0.14	0.98



References

- ARPAV, 2019. Concentrations of the Perfluoroalkyl substances in the waters of Veneto region, Open data on PFASs monitoring, from 02/07/2013 to 11/04/2019 [WWW Document]. URL <https://www.arpa.veneto.it/dati-ambientali/open-data/idrosfera/concentrazione-di-sostanze-perfluoroalchiliche-pfas-nelle-acque-prelevate-da-arpav> (accessed 9.7.19).
- Blaine, A.C., Rich, C.D., Hundal, L.S., Lau, C., Mills, M.A., Harris, K.M., Higgins, C.P., 2013. Uptake of perfluoroalkyl acids into edible crops via land applied biosolids: Field and greenhouse studies. *Environ. Sci. Technol.* 47, 14062–14069. <https://doi.org/10.1021/es403094q>
- Blaine, A.C., Rich, C.D., Sedlacko, E.M., Hundal, L.S., Kumar, K., Lau, C., Mills, M.A., Harris, K.M., Higgins, C.P., 2014a. Perfluoroalkyl acid distribution in various plant compartments of edible crops grown in biosolids-amended soils. *Environ. Sci. Technol.* 48, 7858–7865. <https://doi.org/10.1021/es500016s>
- Blaine, A.C., Rich, C.D., Sedlacko, E.M., Hyland, K.C., Stushnoff, C., Dickenson, E.R. V., Higgins, C.P., 2014b. Perfluoroalkyl Acid Uptake in Lettuce (*Lactuca sativa*) and Strawberry (*Fragaria ananassa*) Irrigated with Reclaimed Water. *Environ. Sci. Technol.* 48, 14361–14368. <https://doi.org/10.1021/es504150h>
- D'Hollander, W., Herzke, D., Huber, S., Hajslova, J., Pulkrabova, J., Brambilla, G., De Filippis, S.P., Bervoets, L., de Voogt, P., 2015. Occurrence of perfluorinated alkylated substances in cereals, salt, sweets and fruit items collected in four European countries. *Chemosphere* 129, 179–185. <https://doi.org/10.1016/j.chemosphere.2014.10.011>
- FAO, 2004. Scaling soil nutrient balances Enabling mesolevel applications for African realities, FAO Fertilizer and Plant Nutrition Bulletins (Book 15). Food and Agriculture Organization of the United Nations, Rome.
- FAO, 1986. Irrigation Water Management: Irrigation Water Needs. Food and Agriculture Organization of the United Nations, Rome.
- Ghisi, R., Vamerali, T., Manzetti, S., 2019. Accumulation of perfluorinated alkyl substances (PFAS) in agricultural plants: A review. *Environ. Res.* 169, 326–341. <https://doi.org/10.1016/j.envres.2018.10.023>
- Gredelj, A., Nicoletto, C., Valsecchi, S., Ferrario, C., Polesello, S., Lava, R., Zanon, F., Barausse, A., Palmeri, L., Guidolin, L., Bonato, M., 2019. Uptake and translocation of perfluoroalkyl acids (PFAA) in red chicory (*Cichorium intybus* L.) under various treatments with pre-contaminated soil and irrigation water. *Sci. Total Environ.* <https://doi.org/10.1016/j.scitotenv.2019.134766>
- Lechner, M., Knapp, H., 2011. Carryover of Perfluorooctanoic Acid (PFOA) and Perfluorooctane Sulfonate (PFOS) from soil to plant and distribution to the different plant compartments studied in cultures of carrots (*Daucus carota* ssp. *Sativus*), potatoes (*Solanum tuberosum*), and cucumber. *J. Agric. Food Chem.* 59, 11011–11018. <https://doi.org/10.1021/jf201355y>

- Leclercq, C., Arcella, D., Piccinelli, R., Sette, S., Le Donne, C., 2009. The Italian National Food Consumption Survey INRAN-SCAI 2005–06: main results in terms of food consumption. *Public Health Nutr.* 12, 2504–2532. <https://doi.org/10.1017/S1368980009005035>
- Liu, Z., Lu, Y., Song, X., Jones, K., Sweetman, A.J., Johnson, A.C., Zhang, M., Lu, X., Su, C., 2019. Multiple crop bioaccumulation and human exposure of perfluoroalkyl substances around a mega fluorochemical industrial park, China: Implication for planting optimization and food safety. *Environ. Int.* 127, 671–684. <https://doi.org/10.1016/j.envint.2019.04.008>
- Liu, Z., Lu, Y., Wang, T., Wang, P., Li, Q., Johnson, A.C., Sarvajayakesavalu, S., Sweetman, A.J., 2016. Risk assessment and source identification of perfluoroalkyl acids in surface and ground water: Spatial distribution around a mega-fluorochemical industrial park, China. *Environ. Int.* 91, 69–77. <https://doi.org/10.1016/j.envint.2016.02.020>
- Sepulvado, J.G., Blaine, A.C., Hundal, L.S., Higgins, C.P., 2011. Occurrence and fate of perfluorochemicals in soil following the land application of municipal biosolids. *Environ. Sci. Technol.* 45, 8106–8112. <https://doi.org/10.1021/es103903d>
- Stahl, T., Heyn, J., Thiele, H., Hüther, J., Failing, K., Georgii, S., Brunn, H., 2009. Carryover of Perfluorooctanoic Acid (PFOA) and Perfluorooctane Sulfonate (PFOS) from Soil to Plants. *Arch. Environ. Contam. Toxicol.* 57, 289–298. <https://doi.org/10.1007/s00244-008-9272-9>
- Trapp, S., Cammarano, A., Capri, E., Reichenberg, F., Mayer, P., 2007. Diffusion of PAH in Potato and Carrot Slices and Application for a Potato Model. *Environ. Sci. Technol.* 41, 3103–3108. <https://doi.org/10.1021/es062418o>
- Veneto agricoltura, 2016. IL VENETO ... CHE FRUTTA! (Map of the fruticultural products of Veneto). Padova.
- Wen, B., Li, L., Zhang, H., Ma, Y., Shan, X.Q., Zhang, S., 2014. Field study on the uptake and translocation of perfluoroalkyl acids (PFAAs) by wheat (*Triticum aestivum* L.) grown in biosolids-amended soils. *Environ. Pollut.* 184, 547–554. <https://doi.org/10.1016/j.envpol.2013.09.040>
- Wen, B., Wu, Y., Zhang, H., Liu, Y., Hu, X., Huang, H., Zhang, S., 2016. The roles of protein and lipid in the accumulation and distribution of perfluorooctane sulfonate (PFOS) and perfluorooctanoate (PFOA) in plants grown in biosolids-amended soils. *Environ. Pollut.* 216, 682–688. <https://doi.org/10.1016/j.envpol.2016.06.032>